

Thesis  
2354

**SOIL MICROMORPHOLOGY AND IMAGE ANALYSIS; A STUDY OF BRONZE AGE  
TO RECENTLY IMPROVED SOILS AT LAIRG, SUTHERLAND, SCOTLAND**

Timothy G. Acott, BSc (Hons)  
Department of Environmental Science  
University of Stirling

March 1993

Submitted for the Degree of Doctor of Philosophy



## Abstract

The applications of multispectral and morphometric image analysis to soil thin section descriptions is examined. It is shown that unsupervised classification and contrast stretching can be used to enhance and label features of interest. Morphometric measurements, allow the shape and abundance of features in thin sections to be compared and statistical relationships established. This method of analysis offers a precision beyond that which is possible using a qualitative approach.

Using soil micromorphology as the main analytical technique a case study was carried out to evaluate the applicability of image analysis to an investigation of an archaeological site at Lairg in northern Scotland. The interactions of anthropogenic activity and pedogenesis since the Bronze Age is examined. The condition of the soils prior to the Bronze Age is not known because no buried soils predated this period. Evidence suggests that in freely draining situations complete podzols might have formed by this time. During the Bronze and Iron Age intensive cultivation of soils occurred with associated erosion. In areas of the site, where human activity is dated to the Post Medieval period, deepening of A horizons is apparent and the soils are maintained as Brown Podzols. In many areas where human activity stops stagnopodzols are the dominant soil type.

The potential of image analysis to aid soil micromorphological descriptions is demonstrated. Contrast stretching aided a qualitative subdivision of thin section slides during the case study. Morphometric analysis confirmed a relationship between shape of voids and c/f ratios in an Iron Age buried A horizon, A PM buried A horizon and an undated deep topsoil. It is concluded that the full benefits of image analysis, when used as a routine tool to aid thin section descriptions, will only be realised when procedures become more interactive and processes can be speeded up.

## **Acknowledgements**

My sincerest thanks to Professor Donald Davidson for his unfailing support throughout my work. He always had time to listen for which I am very grateful. Nobody could wish for a better supervisor.

Many many thanks to Dr Stephen Carter for keeping me on track and assuring me things were not as bad as they seemed at the time. Thanks for always having time to talk. Thanks also to Joan and Kate for always making me so welcome.

This work would not have been completed without the tremendous help of Muriel Macleod. Thanks for all the help in the laboratory, I hope that you finally get rid of the green dye someday. Muriel was responsible for technical help preparing the thin sections and developing a useable method to measuring water in Acetone.

Thanks to all at AOC (Scotland) Ltd. for the continued support and financial assistance throughout my work.

Thanks to all the technical staff and academics in the Dept. of Env. Sci. at Stirling University, in particular Bill (bluesman) Jamison, John McArthur, Chris Anderson (rock on), Dave Harrison, Dave Gilvear and Alistaire Watson.

Thanks to the other postgrads in the Department for making my stay at Stirling a memorable one, in particular Rachel Marsden. Thanks also to Sandra Winterbottom, Sandra Vick and Tracy Grieve.

Last but not least thanks to my family, in particular to my Mum, Mrs Joan Acott, for always being there and to Kate Farr whose encouragement started off the whole Ph.D.

|   |    |
|---|----|
| CHAPTER 1   |    |
| SCIENCE AND PALAEOENVIRONMENTAL RECONSTRUCTION: THE OBJECTIVES OF THE STUDY . . . . .                             | 1  |
| 1.1 The present the key to the past? . . . . .  | 1  |
| 1.2 Methods of investigating the past . . . . .   | 5  |
| 1.3 Soil micromorphology . . . . .  | 6  |
| 1.4 Image analysis and soil micromorphology . . . . .   | 9  |
| 1.5 Objectives of the thesis . . . . .  | 9  |
| CHAPTER 2   |    |
| IMAGE ANALYSIS AND SOIL MICROMORPHOLOGY . . . . .   | 12 |
| 2.1 Introduction. . . . .   | 12 |
| 2.2 General applications of image analysis techniques. . . . .  | 13 |
| 2.3 Applications of image analysis to soil micromorphology. . . . .   | 15 |
| 2.4 Capture and processing of images derived from soil thin sections. . . . .                                     | 19 |
| 2.5 Hardware. . . . .   | 20 |
| 2.6 Image capture . . . . .   | 22 |
| 2.6.1 Image capture using an Olympus BH2 . . . . .  | 27 |
| 2.6.2 Image capture using a 50mm macro lens. . . . .  | 30 |
| 2.7 Multispectral image classification. . . . .   | 34 |
| 2.8 Supervised and unsupervised classification methods . . . . .  | 35 |
| 2.9 Supervised classification of a soil thin section. . . . .   | 36 |
| 2.10 Unsupervised classification . . . . .  | 40 |
| 2.11 Unsupervised maximum likelihood classification. . . . .  | 41 |
| 2.12 Assigning spectral classes to informational groups. . . . .  | 44 |
| 2.13 Classification of voids without staining using image Whit1 . . . . .   | 49 |
| 2.14 Results of assigning Whit1 spectral classes to informational categories corresponding to void area . . . . . | 52 |
| 2.15 Multispectral classification isolating 5 different soil features. . . . .                                    | 55 |
| 2.16 Calculation of classification accuracy. . . . .  | 59 |
| 2.17 Confusion matrix for Whit1b. . . . .   | 61 |
| 2.18 Interpretation of the confusion matrix . . . . .   | 62 |
| 2.19 Non parametric classification techniques. . . . .  | 66 |
| 2.20 Use of the Watershed classification routine to classify soil thin section images. . . . .                    | 67 |
| 2.21 Image quantification . . . . .   | 70 |
| 2.22 Morphometric analysis equipment at Stirling . . . . .  | 72 |
| 2.23 Stages in the automatic measurement of object area . . . . .   | 73 |
| 2.24 Post classification processing . . . . .   | 77 |
| 2.25 The use of image processing techniques to enhance features seen in thin section. . . . .                     | 82 |
| 2.26 Linear contrast stretch . . . . .  | 83 |
| 2.27 Histogram equalisation stretch (HES). . . . .  | 85 |
| 2.28 User defined contrast stretch. . . . .   | 86 |

|      |   |    |
|------|---|----|
| 2.29 | Applying contrast enhancement techniques to images of soil thin sections. . . . . | 87 |
| 2.30 | Summary . . . . .   | 88 |

CHAPTER 3

|   |    |
|---|----|
| DESCRIPTION OF LAIRG SITE AND THE THIN SECTION SAMPLING PROGRAMME . . . . . | 90 |
|---|----|

|      |   |     |
|------|---|-----|
| 3.1  | Introduction . . . . .  | 90  |
| 3.2  | Trends in upland soil development. . . . .                                | 91  |
| 3.3  | The effect of humans on the soil system. . . . .                          | 99  |
| 3.4  | Evidence for soil development with emphasis on sites in Scotland. . . . . | 104 |
| 3.5  | Description of the site at Lairg . . . . .                                | 109 |
| 3.6  | Block 1 (The southern block). . . . .                                     | 113 |
| 3.7  | Block 2 (The southern central block). . . . .                             | 114 |
| 3.8  | Block 3 (The northern central block). . . . .                             | 114 |
| 3.9  | Block 4 (The northern block). . . . .                                     | 114 |
| 3.10 | Thin section sampling strategy . . . . .                                  | 115 |
| 3.11 | Sampling strategy for buried soils. . . . .                               | 117 |
| 3.12 | Monuments chosen to examine buried soils. . . . .                         | 118 |
| 3.13 | Monument selected in group A. . . . .                                     | 119 |
| 3.14 | Monuments selected in group B . . . . .                                   | 119 |
| 3.15 | Monuments selected in group C . . . . .                                   | 121 |
| 3.16 | Sampling strategy for soil accumulations . . . . .                        | 121 |

Chapter 4

|  |     |
|--|-----|
| Thin section preparation techniques. . . . . | 125 |
|--|-----|

|     |   |     |
|-----|---|-----|
| 4.1 | Introduction . . . . .  | 125 |
| 4.2 | Sampling techniques. . . . .  | 125 |
| 4.3 | Removal of water. . . . .   | 127 |
| 4.4 | Equipment for acetone exchange. . . . .                                   | 129 |
| 4.5 | Measuring water in acetone using specific gravity. . . . .                | 131 |
| 4.6 | Sample impregnation. . . . .  | 133 |
| 4.7 | Preparing thin sections from blocks or Kubiena tins. . . . .              | 135 |
| 4.8 | Problems encountered during the thin section preparation process. . . . . | 136 |

Chapter 5

|  |     |
|--|-----|
| Results of the excavation and thin section analysis of monuments in group A. . . . . | 138 |
|--|-----|

|       |  |     |
|-------|--|-----|
| 5.1   | Introduction . . . . .                             | 138 |
| 5.2   | Results from EP and LP monuments . . . . .         | 138 |
| 5.2.1 | Excavation results of M64 a LP hut circle. . . . . | 139 |
| 5.2.2 | M64 thin section results. . . . .                  | 144 |
| 5.2.3 | M64, sample 1 . . . . .                            | 145 |
| 5.2.4 | M64, sample 5. . . . .                             | 145 |
| 5.2.5 | M64, sample 7 . . . . .                            | 146 |
| 5.2.6 | M64, sample 8. . . . .                             | 148 |
| 5.2.7 | M64, sample 6. . . . .                             | 149 |
| 5.2.8 | Discussion of samples 1, 5, 7, 8. . . . .          | 149 |
| 5.2.9 | Summary of M64 . . . . .                           | 153 |

|        |  |     |
|--------|--|-----|
| 5.3    | Excavation results of M62, an EP cross contour dyke. . . . .   | 153 |
| 5.3.1  | M62 thin section results . . . . .   | 157 |
| 5.3.2  | M62, sample 2. . . . .   | 157 |
| 5.3.3  | M62 sample 5. . . . .  | 157 |
| 5.3.4  | Discussion of M62. . . . .   | 158 |
| 5.4    | Results of the analysis of M86, an EP lynchet.   | 159 |
| 5.5    | Results of the thin section analysis of M86.   | 161 |
| 5.5.1  | M86, sample 162, c.5024 and c.5025. . .  | 161 |
| 5.5.2  | M86, sample 161. . . . .   | 162 |
| 5.5.3  | Discussion of M86. . . . .   | 163 |
| 5.6    | Results from M88, an EP clearance cairn. . .   | 164 |
| 5.6.1  | M88, results of thin section analysis.   | 166 |
| 5.6.2  | M88, sample 160, c.5020 . . . . .  | 166 |
| 5.6.3  | M88, sample 159, c.5020 and c.5021. . .  | 166 |
| 5.6.4  | Interpretation of M88. . . . .   | 167 |
| 5.6.5  | Results from M87, an EP clearance cairn  | 167 |
| 5.7    | Results from Post Medieval monuments. . . . .  | 170 |
| 5.8    | Excavation results of M127. . . . .  | 170 |
| 5.8.1  | M127 thin section results. . . . .   | 174 |
| 5.8.2  | M127, sample 1, c.8045. . . . .  | 174 |
| 5.8.3  | Spectral analysis and thin section description of M127 sample 1. . . . .                                   | 175 |
| 5.8.4  | Interpretation . . . . .   | 179 |
| 5.8.5  | M127, sample 2, c.8046. . . . .  | 180 |
| 5.8.6  | M127, sample 3, c.8046. . . . .  | 181 |
| 5.8.7  | M127, sample 4, c.8046. . . . .  | 182 |
| 5.8.8  | Interpretation of M127, samples 2, 3 and 4. . . . .  | 182 |
| 5.9    | Excavation results of M75/4, enclosure dyke.   | 185 |
| 5.9.1  | M75/4 thin section results. . . . .  | 188 |
| 5.9.2  | M75/4, sample 1, c.8029, c.8030, c.8026.   | 188 |
| 5.9.3  | M75/4, sample 4, c.8027. . . . .   | 189 |
| 5.9.4  | Interpretation of M75/4 . . . . .  | 190 |
| 5.10   | Results of the analysis of M164, a PM dyke. . . . .  | 192 |
| 5.10.1 | M164, thin section analysis. . . . .   | 193 |
| 5.10.2 | M164, sample 1, c.3032. . . . .  | 193 |
| 5.10.3 | M164, sample 2, c.3032. . . . .  | 195 |
| 5.10.4 | M164, sample 3, c.3032 . . . . .   | 196 |
| 5.10.5 | M164, sample 4, c.3032 and c.3033 . . .  | 197 |
| 5.10.6 | Interpretation of M164. . . . .  | 198 |
| 5.11   | Results of the analysis of an undated deep top soil accumulation and an underlying buried profile. . . . . | 200 |
| 5.11.1 | Results of M21. . . . .  | 200 |
| 5.11.2 | M21, thin section results. . . . .   | 204 |
| 5.11.3 | M21 sample 1, c.8000. . . . .  | 204 |
| 5.11.4 | M21 sample 2, c.8000 . . . . .   | 205 |
| 5.11.5 | M21, sample 3, c.8000. . . . .   | 205 |
| 5.11.6 | M21, sample 4, c.8000. . . . .   | 206 |
| 5.11.7 | M21, sample 5, c.8000. . . . .   | 206 |

|  |     |
|--|-----|
| 5.11.8 M21, sample 6, c.8000. . . . .                          | 207 |
| 5.11.9 Interpretation of M21, samples 1-6. . . . .             | 207 |
| 5.11.10 Thin section description, sample 7,<br>c.8002. . . . . | 211 |
| 5.11.11 M21, sample 8, c.8003. . . . .                         | 211 |
| 5.11.12 Interpretation of M21, samples 7 and 8. . . . .        | 212 |

## Chapter 6

|   |     |
|---|-----|
| Results of the excavation and thin section analysis of monuments<br>in group B. . . . . | 214 |
| 6.1 Introduction . . . . .  | 214 |
| 6.2 M648, an EP field boundary. . . . .   | 214 |
| 6.3 Results from thin section analysis . . . . .  | 215 |
| 6.3.1 M648, sample 1, c.7004. . . . .   | 215 |
| 6.3.2 M648, sample 2, c.7004. . . . .   | 218 |
| 6.3.3 M648, sample 3, c.7007. . . . .   | 218 |
| 6.3.4 M648 interpretation of thin section<br>results . . . . .                          | 219 |
| 6.4 Transect 7000. . . . .  | 221 |
| 6.4.1 Transect 7000, result of thin section<br>analysis. . . . .                        | 222 |
| 6.4.2 Interpretation of transect 7000. . . . .  | 223 |
| 6.5 M505, a LP field boundary. . . . .  | 224 |
| 6.6 Results of thin section analysis. . . . .   | 228 |
| 6.6.1 M505, sample 1, c.8064. . . . .   | 228 |
| 6.6.2 M505, sample 2, c.8064 and c.8065. . . . .  | 229 |
| 6.6.3 M505, sample 3, c.8067. . . . .   | 229 |
| 6.6.4 Interpretation of M505. . . . .   | 230 |
| 6.7 M504, a LP (Iron Age) hut circle. . . . .   | 232 |
| 6.7.1 M504, results of thin section<br>analysis. . . . .                                | 235 |
| 6.7.2 Summary thin section description,<br>M504, sample 1, c.8071 and c.8072. . . . .   | 236 |
| 6.7.3 Summary thin section description M504<br>sample 2, c.8072 and c.8074. . . . .     | 236 |
| 6.7.4 Description for context 8072, buried A<br>horizon. . . . .                        | 239 |
| 6.7.5 Description for context 8074, buried Bs<br>horizon. . . . .                       | 239 |
| 6.7.6 Summary thin section description M504<br>sample 3, c.8076 and c.8074. . . . .     | 239 |
| 6.7.7 Description of context 8076, buried A<br>horizon. . . . .                         | 240 |
| 6.7.8 Description of context 8074, buried Bs<br>horizon. . . . .                        | 240 |
| 6.7.9 Summary thin section description M504<br>sample 4, c.8076 and c.8074. . . . .     | 241 |
| 6.7.10 Summary thin section description M504<br>sample 5 . . . . .                      | 242 |
| 6.7.11 Interpretation of M504. . . . .  | 243 |

|   |     |
|---|-----|
| 6.8 M659, a LP hut circle . . . . .   | 247 |
| 6.9 M659, results of thin section analysis. . . . .   | 247 |
| 6.9.1 Sample 1, buried A horizon (C.F2300) . . . . .  | 247 |
| 6.9.2 Interpretation of the buried A horizon<br>under M659. . . . .   | 248 |
| 6.10 Monument 660, a LP hut circle . . . . .  | 248 |
| 6.11 Results of thin section analysis. . . . .  | 251 |
| 6.11.1 M660, sample 1, c.2132 and c.2184 . . . . .  | 251 |
| 6.11.2 M660 sample 2, c.2099, c.2136 and<br>c.2132. . . . .   | 252 |
| 6.11.3 M660, sample 3, c.2099. . . . .  | 253 |
| 6.11.4 Interpretation of M660. . . . .  | 253 |
| <br>Chapter 7   |     |
| Results of the excavation and thin section analysis of monuments<br>in group C. . . . .                                 | 256 |
| 7.1 Introduction . . . . .  | 256 |
| 7.2 Results from M975, the PM head dyke. . . . .  | 256 |
| 7.3 Results of the thin section analysis. . . . .   | 260 |
| 7.3.1 M975, sample 2, c.8101, c.8102,<br>c.8103. . . . .  | 260 |
| 7.3.2 M975/2, sample 3, c.8103. . . . .   | 261 |
| 7.3.3 M975, sample 6, c.8105. . . . .   | 262 |
| 7.3.4 Interpretation of M975. . . . .   | 262 |
| 7.4 Results from M1069, a PM rectangular house . . . . .  | 263 |
| 7.5 Results of the thin section analysis. . . . .   | 265 |
| 7.5.1 M1069, sample 1, c.8111. . . . .  | 265 |
| 7.5.2 M1069, sample 2, c.8112. . . . .  | 267 |
| 7.5.3 M1069, sample 3. c.8113. . . . .  | 268 |
| 7.5.4 Interpretation of M1069. . . . .  | 268 |
| <br>Chapter 8   |     |
| Morphological quantification of 3 buried A horizons. . . . .  | 270 |
| 8.1 Introduction . . . . .  | 270 |
| 8.2 Image capture . . . . .   | 271 |
| 8.3 Classification of voids coarse material and fine<br>material. . . . .   | 272 |
| 8.4 Result of quantification . . . . .  | 274 |
| <br>Chapter 9   |     |
| Interpretation of the thin section analysis and conclusion<br>applying image analysis to soil micromorphology . . . . . | 284 |
| 9.1 Introduction . . . . .  | 284 |
| 9.2 Analysis of glacial till. . . . .   | 284 |



|       |   |     |
|-------|---|-----|
| 9.3   | Development of Bs horizons . . . . .  | 289 |
| 9.3.1 | Morphology of Bs horizons . . . . .   | 290 |
| 9.3.2 | Morphology of Bs horizons at Lairg . . . . .  | 292 |
| 9.3.3 | Interpretation of the formation of Bs horizons . . . . .  | 298 |
| 9.4   | Formation of fragmented nodules and thin iron pans . . . . .                                      | 300 |
| 9.5   | Evidence for landuse and soil development at Lairg from prehistoric to recent times. . . . .      | 311 |
| 9.5.1 | Effect of human activity on the soils at Lairg based on field observations . . . . .              | 312 |
| 9.5.2 | Evidence from soil micromorphology . . . . .  | 315 |
| 9.7   | Summary of results from an analysis of buried soils . . . . .                                     | 323 |
| 9.8   | Summary of results from the analysis of soil accumulations . . . . .                              | 327 |
| 9.9   | The applicability of image analysis techniques to the description of soil thin sections . . . . . | 328 |

|           |  |     |
|-----------|--|-----|
| Fig. 8.8  | as fig. 8.7 but voids are coloured with a red overlay . . . . .                                | 282 |
| Fig. 8.9  | M1271, PTL, red 160-189, green 27-159, blue 44-162, voids are coloured red, FL 3.8mm . . . . . | 282 |
| Fig. 8.10 | M1272, PTL, red 49-175, green 25-161, blue 34-164, voids are coloured red, FL 3.8mm . . . . .  | 283 |
| Fig. 8.11 | M1273, PTL, red 47-167, green 25-156, blue 38-182, voids are coloured red, FL 3.8mm . . . . .  | 283 |
| Fig. 8.12 | M5041, PTL, red 62-158, green 37-142, blue 37-137, voids are coloured red, FL 3.8mm . . . . .  | 283 |
| Fig. 8.13 | M5042, PTL, red 66-157, green 45-154, blue 67-189, voids are coloured red, FL 3.8mm . . . . .  | 283 |
| Fig. 8.14 | M5043, PTL, red 66-157, green 45-154, blue 67-189, voids are coloured red, FL 3.8mm . . . . .  | 283 |

## CHAPTER 9

|           |   |     |
|-----------|---|-----|
| Fig. 9.1  | Undisturbed capping overlying a rock fragment M504, S5, PPL, X1, FL 8mm . . . . .                   | 286 |
| Fig. 9.2  | Undisturbed link capping within groundmass, M504, S5, PPL, X1, FL 8mm . . . . .                     | 286 |
| Fig. 9.3  | Orange pellets forming the infill of a channel, M75/4, S4, PPL, FL 8mm . . . . .                    | 293 |
| Fig. 9.4  | Orange pellets present forming areas of the groundmass, M75/4, S4, PPL, FL 8mm . . . . .            | 293 |
| Fig. 9.5  | Pelty microstructure in Bs horizon M1069, S3, PPL, FL 2mm . . . . .                                 | 296 |
| Fig. 9.6  | Pelty microstructure from Bs horizon, M62, S5, PPL, FL 2mm . . . . .                                | 297 |
| Fig. 9.7  | Pelty microstructure from Bs horizon, M504, S3, PPL, FL 2mm . . . . .                               | 297 |
| Fig. 9.8  | Thin iron pan below M127, S1, PPL, FL 8mm . . . . .   | 297 |
| Fig. 9.9  | Detail of fig. 9.8, PPL, FL 4mm . . . . .   | 302 |
| Fig. 9.10 | As fig. 9.9 except using OIL . . . . .  | 302 |
| Fig. 9.11 | Thin iron pan below M88, S162, PPL, FL 8mm . . . . .  | 303 |
| Fig. 9.12 | Thin iron pan below M88, S162, OIL, FL 7mm . . . . .  | 304 |
| Fig. 9.13 | Fragmented nodule found in the buried A horizon below M64, S1, PPL, FL 8mm . . . . .                | 305 |
| Fig. 9.14 | Fragmented nodule found in the buried A horizon below M505, S1, PPL, FL 8mm . . . . .               | 305 |
| Fig. 9.15 | Fragmented nodule at base of buried A horizon, M88, S159, PPL, FL 4mm . . . . .                     | 306 |
| Fig. 9.16 | Fragmented nodule at base of buried A horizon, M86, S161, PPL, FL 8mm . . . . .                     | 306 |
| Fig 9.17  | Detail of a fragmented nodule found in the buried A horizon under M505, S1, PPL, FL 0.8mm . . . . . | 307 |
| Fig 9.18  | Detail of a fragmented nodule found in the buried A horizon under M505, S1, XPL, FL 0.8mm . . . . . | 307 |
| Fig 9.19  | Detail of a fragmented nodule found in the buried A horizon under M505, S1, OIL, FL 0.8mm . . . . . | 308 |
| Fig. 9.20 | Ard marks in the top of a Bs horizon under a LP hut circle . . . . .                                | 314 |
| Fig 9.21  | Procedure for an image analysis study of a soil thin section . . . . .                              | 329 |

## LIST OF TABLES

### CHAPTER 2

|  |    |
|--|----|
| Table 2.1 Analysis of one pore space image after four different segmentation protocols (after Thompson <i>et al.</i> , 1992) . . . . . | 17 |
| Table 2.2 Fields of view using Olympus microscope . . . . .  | 27 |
| Table 2.3 Combinations of colour filters, light sources and magnifications using the Olympus microscope. . . . .                       | 29 |
| Table 2.4 Spectral classes of L164com produced by an unsupervised maximum likelihood classification . . . . .                          | 43 |
| Table 2.5 Spectral classes of Whit1 produced using an unsupervised maximum likelihood classification. . . . .                          | 51 |
| Table 2.6 Number of pixels belonging to spectral classes of Whit1. . . . .   | 54 |
| Table 2.7 Spectral classes of Whit1b produced using an unsupervised maximum likelihood classification . . . . .                        | 56 |
| Table 2.8 Spectral groups allocated to informational classes for the classified image of Whit1 . . . . .                               | 57 |
| Table 2.9 Confusion matrix for Whit1B . . . . .  | 61 |
| Table 2.10 Comparison of classified label and the ground truth class . . . . .   | 63 |
| Table 2.11 Details the errors of commission and omission for the classification of Whit1b. . . . .                                     | 64 |
| Table 2.12 Description of the spectral classes of l164com produced using the Watershed Classification. . . . .                         | 70 |

### CHAPTER 3

|   |     |
|---|-----|
| Table 3.1 Suggested effects of the influence of man on five classic factors of soil formation (Bidwel and Hole 1965, after Davidson 1982) . . . . . | 102 |
|---|-----|

### CHAPTER 5

|  |     |
|--|-----|
| Table 5.1 Comparison of micromorphological features from M64 . . . . .                     | 150 |
| Table 5.2 Comparison of microstructure and c/f ratios from M64 . . . . .                   | 151 |
| Table 5.3 Micromorphological features of samples taken from M62 . . . . .                  | 158 |
| Table 5.4 Micromorphological features of the layers which comprise M127 sample 1 . . . . . | 178 |
| Table 5.5 Micromorphological features of samples taken from M127 . . . . .                 | 183 |
| Table 5.6 Comparison of microstructure and c/f ratios from M127 . . . . .                  | 183 |
| Table 5.7 Micromorphological features of samples taken from M75/4 . . . . .                | 190 |
| Table 5.8 Comparison of microstructure and c/f ratios from M75/4 . . . . .                 | 190 |

|   |     |
|---|-----|
| Table 5.9 Micromorphological features of samples taken from M21 . . . . . | 208 |
| Table 5.10 Comparison of microstructure and c/f ratios from M21 . . . . . | 209 |

CHAPTER 6

|  |     |
|--|-----|
| Table 6.1 Micromorphological features of samples taken from M648 . . . . . | 219 |
| Table 6.2 Comparison of microstructure and c/f ratios from M648 . . . . .  | 220 |
| Table 6.3 Micromorphological features of samples taken from M504 . . . . . | 244 |
| Table 6.4 Comparison of microstructure and c/f ratios from M504 . . . . .  | 245 |

CHAPTER 8

|   |     |
|---|-----|
| Table 8.1 Comparison of void abundance and c/f ratios between A horizons of different ages. . . . .                         | 270 |
| Table 8.2 Abundance of coarse material, fine material and void in M127IA, M127IB and M127IC (PM buried A horizon) . . . . . | 274 |
| Table 8.3 Abundance of coarse material, fine material and void in M21IA, M21IB and M21IC . . . . .                          | 274 |
| Table 8.4 Abundance of coarse material, fine material and void in M504IA, M504IB and M504IC . . . . .                       | 275 |

CHAPTER 9

|  |     |
|--|-----|
| Table 9.1 Depth of undisturbed cappings . . . . .  | 287 |
| Table 9.2 Thickness of Prehistoric and Post Medieval buried A horizons . . . . .         | 312 |
| Table 9.3 Presence of features indicating mixing of Bs horizons and A horizons . . . . . | 316 |

## CHAPTER 1

### SCIENCE AND PALAEOENVIRONMENTAL RECONSTRUCTION: THE OBJECTIVES OF THE STUDY

#### 1.1 The present the key to the past?

During the past 12000 years the landscape in northern Scotland has undergone profound and extensive environmental change. A major challenge facing palaeoenvironmentalists is to determine the factors that have created modern landscapes. In trying to do this a distinction is often made between natural processes and human activity. To some extent this is a valid distinction because anthropogenic activity has had such an important effect on the environment. This is particularly true as the Holocene progresses and human activity becomes increasingly important in determining the composition of landscapes.

A negative aspect of dividing anthropogenic activity from the natural environment is that humans are regarded as somehow fundamentally different from the rest of nature. When trying to reconstruct the past it becomes clear that humans cannot be regarded as separate from other environmental processes. Throughout human evolution individuals, communities and societies have culturally interacted with each other and with the environment. This process continues today but many people in western societies do not directly perceive the influence they have on the environment because they are isolated by a layer of

technology. As humans have culturally evolved, so has their ability to alter aspects of the world they live in.

Studies of the past should regard humans as an integral component of the evolving environment. By breathing we are interacting with numerous physical systems including the atmosphere, the hydrological cycle, the biotic environment (if we inhale organic material), the geological cycle (if we inhale dust) and numerous elemental cycles. Positive and negative relationships exist between cultural systems, biotic and abiotic components of the environment.

Humans interact with the environment through many layers of acquired cultural practices. This is not a deterministic relationship as different cultures may be observed living in similar biomes. The environment does influence the development of particular cultures to some extent. For example Inuit tribes, living in polar regions, and African tribes living in tropical regions, have to adapt to completely different environmental conditions. The cultures that develop in each of these circumstances are, in part, affected by environmental conditions that are experienced. Studies of past physical environments should recognise that cultural activities of particular societies are part of a larger ecosystem and can be integral in the development of particular landscapes.

The scientific paradigm that is used to study the past is important because it makes assumptions about the relationships

that exist between different aspects of the environment and also affects the methodology that is used in the investigation. This is important in the context of this thesis because a central theme is examining the benefits of qualitative versus quantitative methodologies.

The emphasis of science since the scientific revolution has been to divide humans from the rest of nature. A cartesian dualistic approach was adopted and greater value placed on qualities that can be quantitatively measured. The philosophy known as positivism rejects metaphysics and theism and recognises only observed facts and phenomena (Pepper 1990). Classical rationalism is based on inductivism and is responsible for much of the knowledge acquired in the earth sciences today (Bell and Walker 1992).

There are some new ideas in science that may have important implications for reconstructing the past. Chaos theory suggests, for example, that a butterfly's wingbeat, by producing small perturbations in its localised environment, could over a period of time affect the course of global weather systems (Gleick 1987, Stewart 1990). The implications of this for the palaeo-environmentalist are profound. If it is possible that a butterfly in Australia could be effecting the weather patterns experienced over New York what possibility is there of reconstructing the history of the Holocene using a traditional empirical approach? Bell and Walker (1992) suggest that stochastic events might be as important as physical laws in explaining the operation of

environmental systems. This is a concept that many scientists have yet to come to terms with.

Despite these ideas and the important implications that they raise about the nature of scientific inquiry, and the role of humans in the global ecosystem, a methodological uniformitarian approach is adopted in this thesis. It is implicit in this study that changes which occurred in the past can be elucidated by studying features which compose the modern landscape. It is recognised that stochastic cataclysmic events might have had a profound influence on landscape development.

Human impact on the environment has altered with time although the intensity of the impact has not always been known. For instance, to what extent did hunter gatherers or early agriculturalists modify the landscape using fire? Despite this uncertainty the potential of humans to modify the environment has increased in accordance with technological advances. Perhaps one of the most profound influences of prehistoric human activity, on the physical environment, was the change from a society based on hunting and gathering to one based on sedentary agriculture (Bell and Walker 1992).

It is beyond doubt that interactions occur between humans and the environment. A more contentious issue is whether humans are somehow fundamentally different from other aspects of the environment or are an integral component. This issue has pervaded western scientific thought since the development of formalised



scientific hypothesis in the 17<sup>th</sup> century. What is of particular relevance to palaeoenvironmentalists, and to anybody concerned with the way human behaviour has affected the world, is how the environment has developed and the effects of human activity on this development. This theme forms a central part to the background of the thin section analysis undertaken as part of this thesis.

## **1.2 Methods of investigating the past**

To reconstruct the physical environment at periods in time, a systems approach can be utilised which provides spatial and temporal frameworks for studying interactions between physical, biotic and cultural domains. Palaeoenvironmentalists can use numerous methods for reconstructing the past. Radiometric dating techniques, including <sup>14</sup>C, thermoluminescence, Lead - 210 and Caesium - 137 (Roberts 1991) can be used to provide temporal frameworks. Palaeoreconstruction techniques, including pollen analysis, diatom analysis, tephrochronology, the study of plant macrofossils and the study of Mollusca, can be used to investigate the physical environment.

The geographical location of sites provides a spatial framework for analysis to be carried out. If studies of the past combine dating techniques and archaeological investigation, cultural and temporal aspects can be included in the investigation. Cognitive-processual approaches emphasise the importance of linking evidence for past physical environments with the environmental

perceptions of cultural groups living in those environments (Bell and Walker 1992, Butzer 1982).

To study the history of soil development in an area the analysis of buried soil profiles can yield important information. A profile can be regarded as an evolving pedo-sedimentary complex in which palaeoenvironmental change can be discerned (Lautridou, 1977, in Fedoroff and Goldberg 1982). Soil micromorphology is rapidly being developed as a palaeoenvironmental analytical tool.

### 1.3 Soil micromorphology

An important technique that is used to study undisturbed soils and sediments associated with archaeological sites is soil micromorphology. Since 1938, after the publication of Micropedology by W.L.Kubiena, soil micromorphology has developed into a distinct branch of soil science. Applications are varied and include agricultural and engineering studies, particularly the effects of stress on the soil, soil genesis, soil classification, Quaternary studies and archaeology.

A number of developments since Kubiena's work have stimulated the advancement of soil micromorphology as an analytical technique. These developments include the instigation of international working meetings on soil micromorphology, the first one was held in 1958. The nomenclature used to describe thin sections has undergone many changes and revisions. Two important events are the publication of a system of description and classification by

Brewer in 1964 and the production of an international system of description and interpretation (Bullock et al., 1985). The international system attempts to standardise the terminology used by researchers and provide a routine method for the analysis of soil thin sections. Fitzpatrick has made numerous contributions to soil micromorphology particularly the publication of a book titled Soil Micromorphology in 1974.

Apart from some early work by Dalrymple (1958) there was little research concerned with archaeology until the 1970s and early 1980s. The last decade has seen a gradual increase in the use of soil micromorphology as a diagnostic technique for the description and interpretation of soils and sediments found on archaeological sites. A major synthesis of work was the publication of Soils and Micromorphology in Archaeology (Courty et al. 1989). A number of review papers have also been produced detailing recent work and the benefits of using soil micromorphology as an analytical technique (Goldberg 1983, Macphail et al. 1990b, Davidson et al. 1992).

Micromorphology has been used in numerous ways to help archaeological site investigation. Examples include the analysis of Dark Earth (Macphail 1981, Macphail 1983, Macphail and Courty 1985), the study of deposits in prehistoric caves (Wattez, Courty and Macphail 1990), the analysis of tree subsoil hollows (Macphail and Goldberg 1990), the reconstruction of cultivation techniques and anthropogenic soil disturbance (Macphail, Romans and Robertson 1987, Slager and Van Der Wetering 1977, Courty and

Fedoroff 1982, Cornwall 1963, Romans and Robertson 1983a, Romans and Robertson 1983b) and the study of Holocene soil development (Macphail, Romans and Robertson 1987). Micromorphology has also been used to study environmental changes and pedosedimentary sequences (Courty and Federoff 1982, Fedoroff and Goldberg 1982, Macphail 1986, Federoff, Courty and Thompson 1990).

Soil micromorphology has the advantage over other analytical techniques in that it can be used to study the spatial arrangements of features in the soil (Fisher and Macphail 1985). This is of particular relevance to archaeology when deposits can consist of complex sedimentary sequences. Using soil thin sections and physio-chemical analysis, Courty and Federoff (1982) differentiated between two types of pedogenesis that took place simultaneously in archaeological layers and the fill of a pit.

Despite recent advances in soil micromorphology, the discipline has remained largely qualitative although greater use is now made of submicroscopic techniques to investigate features not resolvable with the optical microscope. Methods of analysis include SEM, TEM and microprobe analysis. The use of staining to isolate soil features, primarily organic components, has been successful (Altmuller and Van Vliet 1990, Van Vliet et al. 1983, Tippkotter 1990). However for the majority of studies, particularly where the analyst does not have access to expensive equipment, a qualitative description, possibly backed up with the use of point counting, remains the only practical method of analysis.

#### **1.4 Image analysis and soil micromorphology**

An area of rapidly increasing interest is the application of image analysis techniques to soil micromorphology. Research started in this area during the 1970s but recent years have seen an increase in the number of research papers published in this area. Despite this, the author is not aware of any studies specifically relating to the study of archaeological material. The emphasis has been on the morphological and spatial quantification of voids in the soil.

This study examines 3 types of image analysis techniques, multispectral classification, morphometric quantification and image enhancement using contrast stretch. Multispectral classification and morphological quantification are two methods of increasing the objectivity of the analysis. Image enhancement is a method to increase the spectral differences making a qualitative analysis more reliable.

#### **1.5 Objectives of the thesis**

There are four main objectives to the thesis as follows;

1. To evaluate the way different types of digital image analysis techniques can be applied to the study of soil thin sections.

2. To carry out a detailed thin section analysis of soils and sediments on a multiperiod archaeology site at Lairg in northern Scotland using image analysis wherever applicable.

3. To investigate the history of pedogenesis and effects of human activity on the soil at the Lairg site.

4. To evaluate the benefits, if any, of a quantitative approach, provided by image analysis, to the description of soil thin sections.

Based upon these objectives the thesis is divided into the following chapters.

Chapter 2 is entirely methodological. An overview of the image analysis process is given followed by a description of how image analysis is used in other disciplines. A brief literature review of image analysis and soil micromorphology is presented. The equipment needed for the analysis of multiband imagery is then described, followed by the results of applying multispectral classification to soil thin sections. A technique for the morphological quantification of binary images using IDRISI GIS software is given. The last sections in chapter 2 describe post classification processing and image enhancement procedures.

Chapter 3 describes the Lairg site and the rationale behind the thin section sampling programme. Different ideas about anthropogenic impact in the uplands are presented. Modifications

to the traditional thin section sampling technique were necessary to sample from all the contexts excavated at Lairg. Chapter 4 details changes in laboratory procedures that were necessary to make thin sections from stony contexts.

The monuments sampled at Lairg are divided into 3 groups. Chapters 5, 6 and 7 detail excavation results in these three groups and the results of the thin section analysis. Stratigraphic interpretations of individual monuments are presented after the appropriate thin section results. Chapter 8 describes a quantitative morphometric analysis of 2 buried A horizons and a deep topsoil not buried by a monument.

Chapter 9 is divided into two parts. Firstly, the evidence for anthropogenic impact on pedogenesis is evaluated. The micromorphological evidence for the development of glacial till, Bs horizons and A horizons is considered and the development of brown podzols and podzols is discussed. Secondly the final section of the thesis considers the usefulness of image analysis as an analytical technique to aid a micromorphological investigation based on the experiences and results of this study.

## CHAPTER 2

### IMAGE ANALYSIS AND SOIL MICROMORPHOLOGY

#### 2.1 Introduction.

Image analysis is a large subject area and includes many types of algorithms for processing digital images. There are numerous ways images can be manipulated, the specific routines used will depend on the purpose of the analysis. This study examines three image analysis routines;

1. Spectral classification
2. Morphometric analysis
3. Spectral enhancement

Of these only morphometric analysis has been widely used in soil micromorphology. The main objective of this chapter is to investigate the way these 3 types of image analysis can be applied to soil micromorphology. The chapter is therefore technique orientated, the results do not correspond to any field study. Applications of techniques are presented in subsequent chapters.

This chapter is divided into 8 main sections. Firstly an overview of how image analysis has been applied to other scientific disciplines is given. The different ways image analysis has been applied to soil micromorphology is then considered. The results of this study are then presented beginning with a description of



equipment available in the Department of Environmental Science at Stirling University. The following sections are divided into multispectral classification, morphological quantification, post classification processing, and finally, spectral enhancement.

## **2.2 General applications of image analysis techniques.**

Image analysis is used in different ways in many subjects. The purpose of the study influences the specific image analysis techniques that are used. For instance, the most important criteria in remote sensing is often the spectral enhancement and quantification of regions, in an image, which correspond to a specific property. Examples are varied and include relating spectral values to water quality, vegetation type, soil types, rock types etc. Many types of spectral classification routines and image enhancement techniques can be used to define homogeneous areas. Combinations of image bands can be classified using mathematical algorithms and multispectral data to achieve results not possible using single band imagery.

In other subjects the purpose of the image analysis can be quite different. Morphological quantification of objects might be of primary importance. For instance if cells or regions of cells are dyed using a staining technique, they can be discriminated based upon their grey level difference in one spectral band. Morphometric measurements can then be made of the isolated feature. Morgan et al. (1991) developed a fully automated image analysis method to determine fungal biomass in soils. This method

uses staining to isolate the fungal material allowing hyphal length and biovolume to be calculated.

Industrial uses include object recognition. This consists of many diverse applications including optical character recognition of letters and numbers to the identification of objects in real time to help navigate a robot or drive a car. Geologists use image analysis to perform porosity and structural analysis of building materials in different weathering states (Fitzner 1990, Meng 1990). The main result of this type of investigation is pore size distribution or structural characteristics rather than the specific optical properties of the pores.

Meng (1990) isolated pores in building material specimens using a soluble dye added to the resin used for impregnation. Morphometric measurements were calculated to analyse the samples. The size of features were used to differentiate sand grains from a microcrystalline matrix of the same colour. The shape of voids distinguished between spherical air pores and microcracks in a hardened cement paste.

The recrystallization process of rhombohedral camphor was studied using results from a combination of morphometric and grey level analysis (Janssen et al. 1991). Increasing uniformity of grey level values is interpreted as indicating a crystallographic preferred orientation developed during shear deformation. Grain size and frequency are related to grain boundary migration. The

shapes of grains are shown to change immediately after the shear deformation started.

The previous examples illustrate a number of applications of image analysis. The specific routines used depend on the purpose of the study. Image analysis techniques used to analyse soil thin sections have concentrated mainly on morphometric measurements of different soil features, in particular developing methods for the quantification of voids in the soil.

### **2.3 Applications of image analysis to soil micromorphology.**

In the 1970s purpose built image analysis systems were used for investigating void space. Some of the earliest work was done in the Department of Soil Micromorphology of the Netherlands Soil Survey Institute using the Quantimat B image analyser and later the Quantimat 720. Jongerius et al. (1972) describe a number of problems relating to the isolation of features in soil thin sections. Single band monochrome images were used for analysis and soil features were differentiated using various illumination techniques. The problems and possible solutions for digitising humic microaggregates, ferruginous accumulations, faecal pellets of mites, pyritic bodies, clay accumulations and porosity are discussed.

Murphy et al. (1977a) describe the measurement and characterisation of voids in thin section using image analysis. Voids were discriminated using staining techniques and high

contrast photographs to obtain grey level discrimination in a single band. The results of their analysis was a series of measurements which could be used to describe orientation, irregularity and form separation of different voids. They applied these measurements to an analysis of two sets of soils (Murphy et al. 1977b). One was from a gley soil of the Deighton Series and another was from a compaction experiment. They used the measurements of voids to quantify morphological changes to a soil after compaction and confirm the impervious nature of the Deighton subsoil.

Most research, in image analysis and soil micromorphology, during the 1970s and 1980 was concerned with measuring the shape and distribution of soil pores. Bouma et al. (1977) quantified the hydraulic function of three types of macropore using the Quantimat 720. Bullock and Thomasson (1979) measured and characterised macroporosity in soil thin sections. Bullock and Murphy (1980) discussed quantification of aggregated and non aggregated soil material. Walker and Trudgill (1983) examined the relationship between two dimensional image analysis of soil thin sections and tracer breakthrough curves. They suggested that caution is needed when trying to relate two-dimensional images to a three-dimensional pore system. A system called Anopor is described by Ringrose-Voase and Bullock (1984) and Ringrose-Voase (1987). They use the Quantimat 720 to characterise fissures, channels, packing pores and vughs. McKeague et al. (1987) compared macro and microstructural properties of soils under different cropping systems. McBratney and Moran (1990) used

various depth functions to study pore geometry between different soil types. Data were obtained from a tillage trial to illustrate an application of the technique. Ringrose Voase (1990) used a one-dimensional image analysis system called Anosol to measure the distances of test lines in a random direction across and between pore spaces. The use of 1-D parameters as structural indices and their relationship to 3-D parameters was discussed. Ringrose-Voase and Nys (1990) used the Anosol system to analyse horizontal sections of pore space in four forest soil profiles with impeded drainage.

Thompson et al. (1992) discussed some of the problems associated with quantitative image analysis. Firstly it is suggested that the protocols used to create a segmented binary image significantly affected resulting measurements even though the operator might not be aware of any differences (table 2.1).

|   | Protocol |      |      |      | Mean<br>n=4 | Standard<br>deviation |
|---|----------|------|------|------|-------------|-----------------------|
|   | A        | B    | C    | D    |             |                       |
| Number of pores                         | 499      | 501  | 579  | 620  | 550         | 60                    |
| Pore area (mm <sup>2</sup> )            | 869      | 681  | 909  | 739  | 799         | 107                   |
| Area of largest pore (mm <sup>2</sup> ) | 18.5     | 14.5 | 19.4 | 15.7 | 17.0        | 2.3                   |

Table 2.1 Analysis of one pore space image after four different segmentation protocols (after Thompson et al., 1992)

Their results show that an understanding of the effects post classification processing is essential before the results of any image analysis are accepted.

Apart from Jongerius et al. (1972) there is little work concerned with measuring features in the soil other than voids. Exceptions to this include the characterisation (Pawluk 1987) and counting (Bui 1991) of faunal faecal pellets. Both of these studies relied on discrimination of features using a single grey level image.

With the publication of a special edition of Geoderma in 1992, entirely devoted to image analysis and soil thin sections, some important new developments were reported. Protz et al. (1992) suggested that feature colour is an important diagnostic property and should not be neglected from computer aided soil micromorphological investigations. Using supervised spectral analysis on multiband imagery Protz et al. (1992) were able to classify features including skeletal grains, void space, mottles, organic material, manganese concretions, carbonates and depletion zones.

Terribile and Fitzpatrick (1992) compared supervised and unsupervised multispectral classification techniques for the isolation of soil features. They found the most useful technique for the isolation of soil features was supervised maximum likelihood classification and suggested that future research should examine other classification techniques including the incorporation of nonspectral features. Specific problems

encountered included the misclassification of quartz grains which had been cut perpendicular to their basal section. These quartz grains have the same appearance as voids using circularly polarised light and could not be differentiated.

In summary in the 1970s and most of the 1980s research, in image analysis and soil micromorphology, was mainly concerned with distributions and morphometric measurements of soil pores. The optical properties of the pores were not usually of interest providing they could be discriminated from other components in the soil. In the early 1990s research started to be concerned with examining the spectral properties of different soil features using multi-dimensional image classification techniques. The following sections in this chapter describe how different image classification techniques, morphometric analysis and image enhancements can be used in soil micromorphology.

#### **2.4 Capture and processing of images derived from soil thin sections.**

To study soil thin sections using image analysis it is necessary to capture optical information from the thin section slide and store this as digital information in a computer. The specific method of capturing data varies with the equipment being used. In the Department of Environmental Science, at Stirling University, image analysis had not been previously used to study images of soil thin sections. The first task included an

evaluation of the equipment available for image analysis within the department.

## 2.5 Hardware.

The following hardware facilities were available. There were 2 PCs, a Hewlett Packard 386DX, with maths co-processor, connected to a 32 bit N° 9 graphics board (N° Nine corporation) and separate high resolution monitor, and an Opus IV 286. The Hewlett Packard used MS.DOS version 5 and the Opus used MS.DOS version 3.1. There was also a Hewlett Packard Vectra workstation running under Unix and a MicroVAX running under VMS. Initially a system called Diad, which operated using a Motorola 68000 CPU, was used.

The sensor used for digitising images was a monochrome phototube Hamatsu camera. There are two basic types of video digitisers, those using a picture tube and those using a solid state sensor (Russ 1990). Picture tube cameras work by light striking a photosensitive coating in the camera. Electrons are used to charge the layer which functions as a capacitor. A current, that varies with the intensity of the initial illumination, is produced which is used as the video signal. Solid state sensing devices, like CCD cameras, are also used to capture images. A voltage is produced when light strikes a photosensitive plate within the camera. The strength of this voltage is dependant on the intensity of the incoming light.



Whichever type of camera is used the voltage produced has to be converted to a digital value for storage and manipulation on a computer. An analogue to digital converter, sometimes referred to as a frame grabber, is used to convert the analogue signal to a digital value. The value is stored as part of an array of numbers in the computer. The size of the array depends on the resolution of the camera. The upper and lower limits that the values can be assigned to depends on the radiometric resolution. A binary image only needs 2 values but most modern cameras can digitise images with up to 256 values. These values are often referred to as grey scales or grey levels. The Hammatsu camera at Stirling could operate at a maximum radiometric resolution of 256 grey levels and 1024 x 1024 spatial resolution.

The software available at Stirling included 2 packages running under MS.DOS called R-Chips (ITS Reading) and IDRISI. R-Chips ran on the Hewlett Packard 386DX and was written to operate with the 32 bit N° Nine graphics board. This permitted a three band colour composite image and 8 overlay planes to be displayed at resolutions up to 512 x 512. IDRISI operated using a conventional VGA monitor allowing the package to be used with any IBM compatible PC. IDRISI, although being designed primarily for GIS, included a number of image processing functions not available on the R-Chips package. R-chips used the fast N° Nine graphics board allowing rapid processing as operations could be performed in video RAM. Consequently IDRISI was only used when the program did not exist on R-Chips. Numerous programs were available on the MicroVAX written by Dr A. Watson, Stirling University. These

included unsupervised Maximum-likelihood Classification and Watershed Classification.

## 2.6 Image capture

Between September 1989 and February 1991 images were captured via a frame grabber using a system called Diad. There were numerous problems using this equipment, mainly caused by faulty connections within the computer. The unreliability of the equipment resulted in considerable delays capturing and processing images. Owing to faults with the Diad no processing was attempted on this particular computer. Images were transferred to separate systems to allow classification or enhancement operations. The data lines used while the Diad was operating are illustrated in figure 2.1.

Images were captured on the Diad and transferred to the Microvax via a Kermit link. The transfer of images took approximately 5 minutes. Another Kermit line connected the MicroVAX to the Hewlett Packard PC where R-Chips was running. Classification of images could be performed on the MicroVAX although transfer to R-Chips was necessary for visual examination and enhancement of the images. Data transfer between the MicroVAX and R-chips took 5 minutes. The Diad stopped working in February of 1991 and a new image capture system set up.

The system used after February 1991 is illustrated in fig 2.2 Software was written by B. Bullen (Stirling University) to

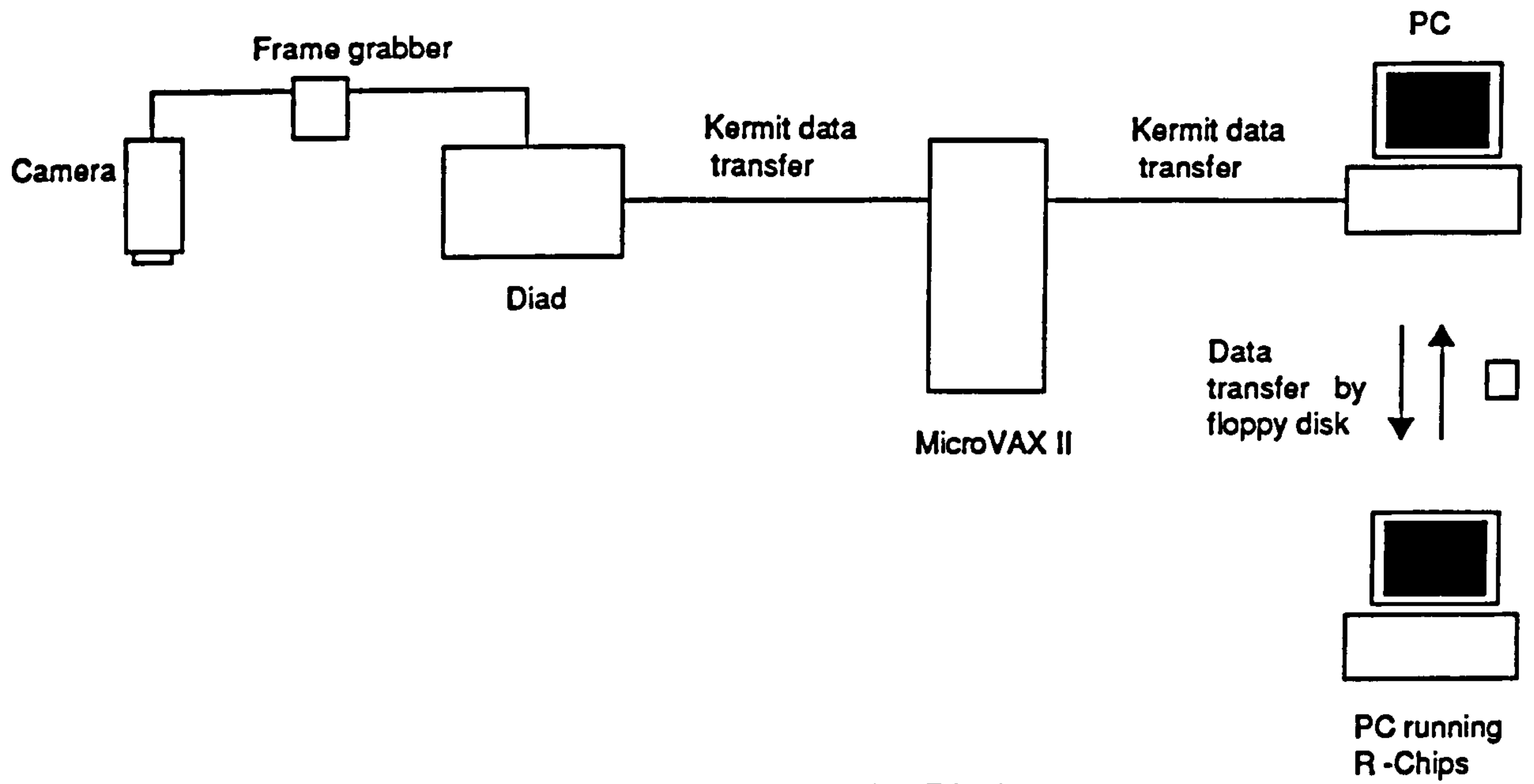


Fig 2.1 Image capture system used with Diad

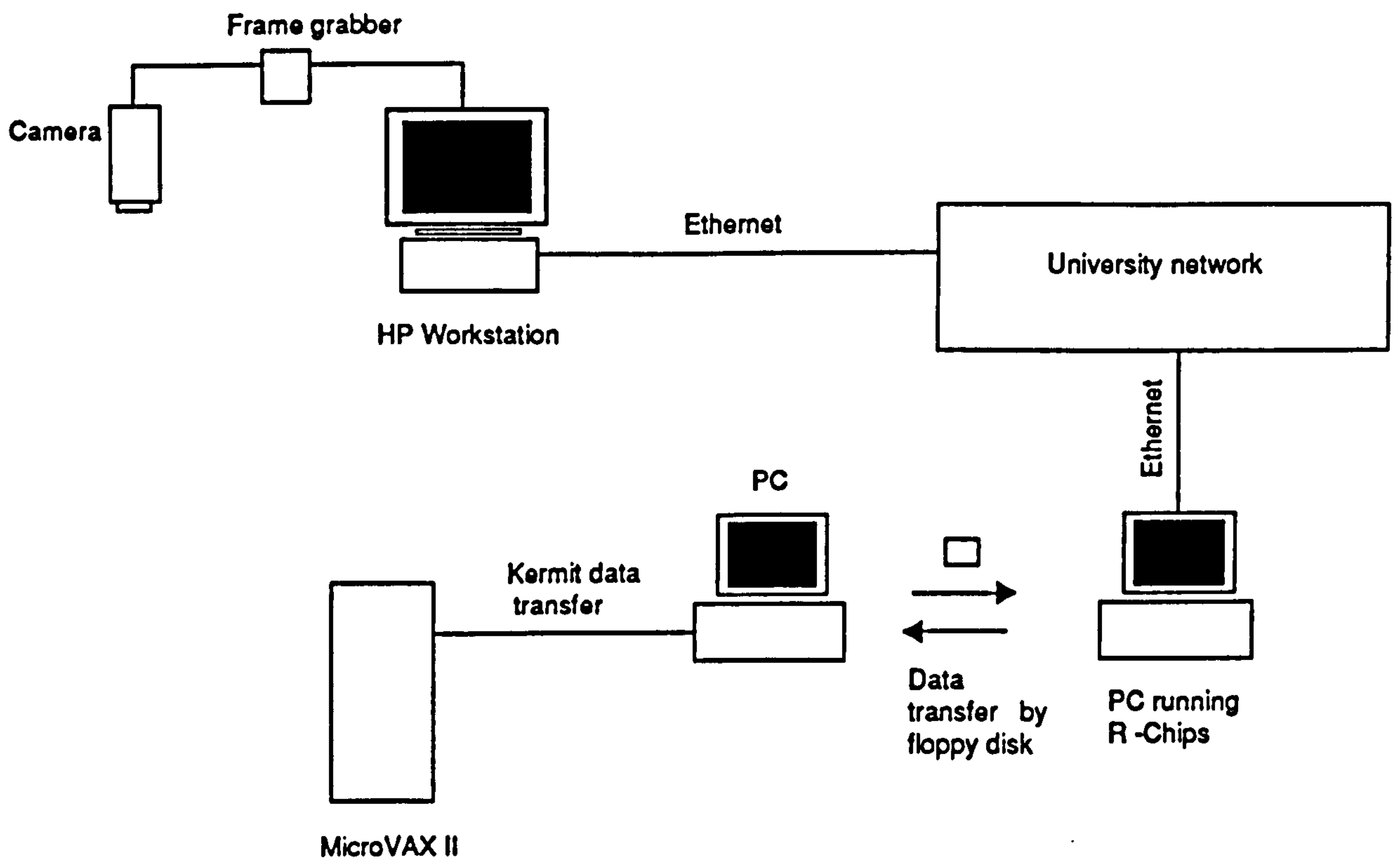


Fig. 2.2 Image capture system used when connected to University network

interface the Hamatsu camera with a Hewlett Packard workstation running under Unix. The Hewlett Packard workstation and the PC running R-Chips were connected to the university Ethernet network. This provided large areas to store images and rapid transfer of data. There was no display on the Hewlett Packard workstation but images could be transferred in seconds to R-Chips. Initially R-Chips would not work while connected to the network, so the computer had to be rebooted to reset the operating parameters each time data transfer had been completed. This problem was solved allowing images to be viewed and manipulated immediately they had been captured. To transfer data to the Microvax, images were copied to floppy disk and then copied onto a PC (fig 2.2). The PC was connected via Kermit to the Microvax. As before data transfer took approximately 5 minutes for a single image band. Once the images were stored on the Microvax they had to be reformatted using software written by Dr A. Watson.

Images captured at a resolution of 1024 x 1024 could not be sent to the MicroVAX via Kermit. Each 1024 x 1024 image had to be split into 4, transferred individually, each one reformatted, and then recombined on the VAX. The reason for this is not known but it was suggested that the Dos Kermit buffer could not hold enough data to allow transfer from the PC to the VAX.

Soil thin sections are composed of microscopic and macroscopic features. This means that thin sections have to be viewed at numerous magnifications if all the components of the slide are

to be recorded. For instance features that measure  $40\mu\text{m}$  across are not seen if the slide is observed without the use of a microscope. Conversely it is not possible to observe the distribution of macrovoids while observing the slide microscopically. To enable images to be captured from soil thin section at different magnifications, two separate image capture systems were constructed (sections 2.61 and 2.62).

As well as observing the slide at numerous magnifications, it is also necessary to capture images using various light sources and colour filters. For instance to differentiate quartz mineral grains and voids it is necessary to compare their spectral properties using plane polarised light (PPL) and crossed polarised light (XPL). Using PPL quartz and voids have the same appearance. When XPL is used the voids remain black and the quartz grains, being anisotropic, are white when observed at their maximum interference colour.

Reflected light is also used to differentiate between features. For instance ferruginous and amorphous organic material might have a similar appearance using PPL. When the materials are observed using oblique incident light (OIL), the ferruginous material is strongly reflective and the amorphous organic material has a dull appearance. The importance of using specific illumination techniques to differentiate between soil features is discussed by Jongerius et al. (1972).

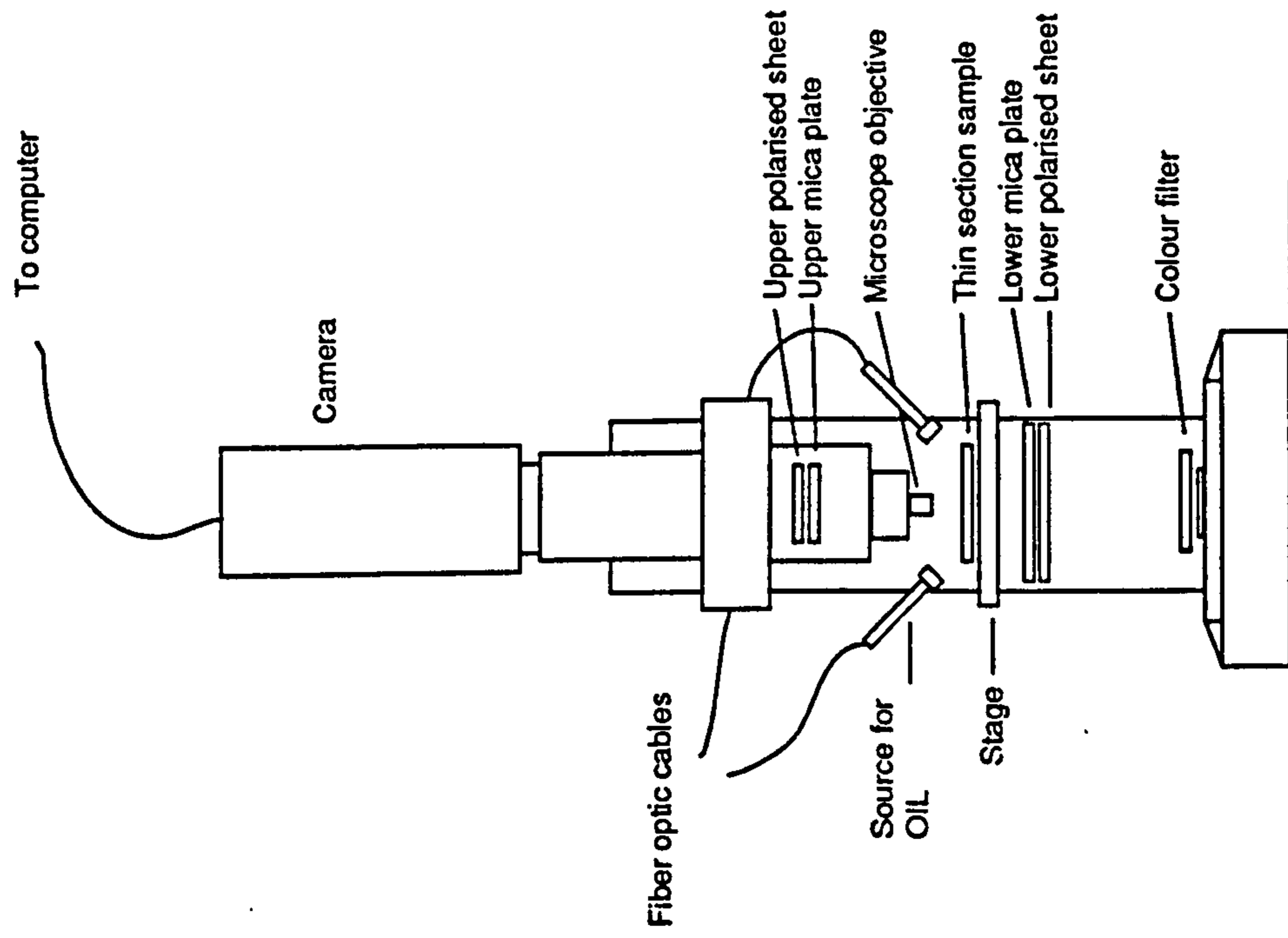


Fig 2.3 Image capture using microscope

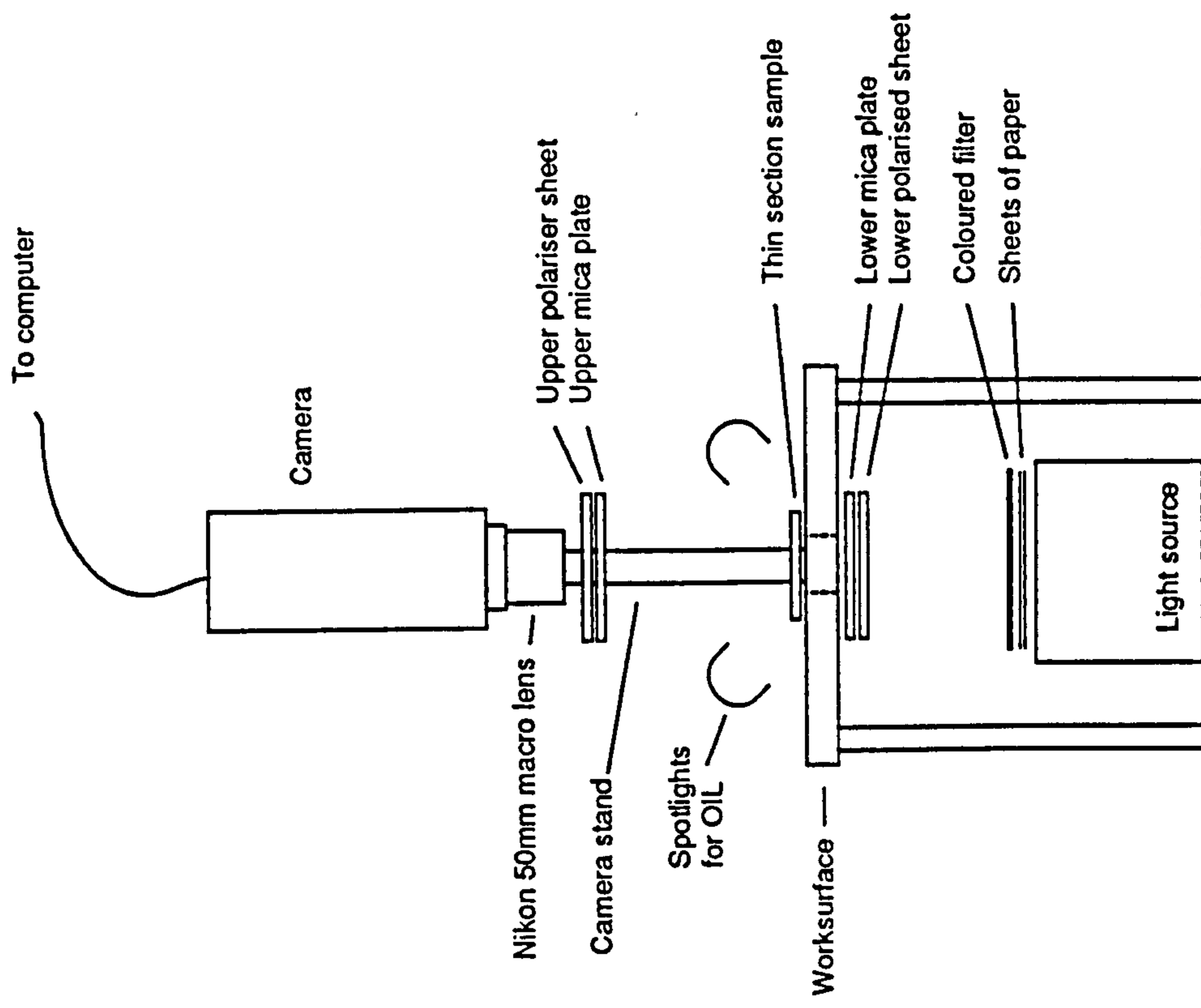


Fig 2.4 Image capture using 50mm Nikon lens

### 2.6.1 Image capture using an Olympus BH2

The Hamamatsu digitising camera was mounted on top of an Olympus BH2 microscope (fig 2.3). Images were captured using x2, x4 and x10 objectives. Although a x1 objective was fitted to the Olympus microscope it caused a slight blurring at the edges of images and consequently was not used. Each objective resulted in the following field of view;

| Objective | Field of view ( $\mu\text{m}$ ) |
|-----------|---------------------------------|
| x 2       | 3800                            |
| x 4       | 1900                            |
| x 10      | 760                             |

Table 2.2 Fields of view using Olympus microscope

Light sources available for use with the microscope included circularly polarised light (CPL), crossed polarised light XPL, plane transmitted light (PTL), plane polarised light (PPL) and oblique incident light (OIL). Colour images were generated by using red, green and blue filters placed between the lower polariser and the specimen. This was the only position with enough room to house the filters.

Circularly polarised light was used to enable all features, within a field of view, to be observed at their maximum interference colours. This was particularly useful when trying to discriminate voids from quartz, although there was still a problem with quartz grains cut close to their basal sections.

Circularly polarised light was created using a mica plate and polarising filter between the specimen and the camera (Fitzpatrick 1984, Pape 1974). A slight diffraction of the light was caused by placing a polarising filter and mica plate between the sample and the camera. This meant that if multiple images were captured, using a combination of light sources, the individual bands were no longer in perfect registration.

The same problems were reported by Terribile and Fitzpatrick (1992). They attempted to rectify the problem using image processing techniques. It was found that the complex nature of the distortion could not be successfully rectified even using high order polynomial equations. In this study the problem was overcome by leaving in place any filters positioned between the sample and the camera during the capture of multiband imagery. Images were captured using CPL and then the lower polariser and mica plate removed for capture using PTL.

Using the Olympus microscope and a fibre optic light source to generate OIL it was not possible to use colour filters. The light source was situated in a protective case and there was no room between the sample and the camera to place colour filters. Consequently only monochrome images were captured using reflected light.

A limiting factor during image capture was the amount of light entering the camera. The mica plates, polarisers, colour filters and the use of high magnification objectives all reduced the



level of illumination. This limited the combination of different images that could be captured.

The optical properties of different thin sections also affected the combinations of light sources that were possible. For instance if OIL was used with a sample that was highly reflective a bright image was created. If a sample was not particularly reflective a dull image was created. This meant the features in a thin section affected the way that they could be digitised. Combination of light sources are presented in table 2.3 and are subject to the variations discussed.

| Light source | Colour filter | Objective |     |      |
|--------------|---------------|-----------|-----|------|
|              |               | x 2       | x 4 | x 10 |
| OIL          | Red           |           |     |      |
|              | Green         |           |     |      |
|              | Blue          |           |     |      |
|              | Monochrome    | *         | *   |      |
| CPL          | Red           | *         | *   |      |
|              | Green         | *         | *   |      |
|              | Blue          | *         | *   |      |
|              | Monochrome    | *         | *   |      |
| PTL          | Red           | *         | *   | *    |
|              | Green         | *         | *   | *    |
|              | Blue          | *         | *   | *    |
|              | Monochrome    | *         | *   | *    |

Table 2.3 Combinations of colour filters, light sources and magnifications using the Olympus microscope.

The light source generated by the Olympus microscope appeared evenly distributed, so no correction for uneven illumination was necessary.

#### **2.6.2 Image capture using a 50mm macro lens.**

A second system was set up to allow images to be captured from larger areas of the slide than was possible using the microscope (fig 2.4). A 50mm macro Nikon lens was attached to the front of the Hamatsu camera. This allowed fields of view to be captured between 1.9cm and the whole of the slide.

A light source was needed that evenly illuminated the whole of the slide. It was found that a halogen bulb inside an overhead projector (OHP) provided the most suitable illumination. Although this light source was bright, there were problems with uneven illumination. Sheets of cartridge paper and tracing paper were placed directly on top of the OHP to diffuse the light. Despite this, a hot spot remained in the centre of the image (fig 2.5). The intensity of illumination across the image varied by approximately 20 grey levels.

The uneven illumination could not be rectified before image capture, so it was decided to correct using image processing techniques. When an image was captured of a thin section, a second image was captured with the thin section removed. This created a blank which could be used to correct the original.

A blank was captured for each combination of filter and light source.

The type of light source affected the processing that was used to correct the images. If the illumination was transmitted, the original image was divided by the blank and multiplied by a scaling factor. The scaling factor was used to keep the grey level values between 1 and 255. If the illumination was reflected, the blank was subtracted from the original and multiplied by a scaling factor. The effects of uneven illumination were not noticed to such an extent if only a monochrome image was captured.

Protz et al. (1992) and Terribile and Fitzpatrick (1992) showed that it was possible to generate colour images by placing colour filters between the specimen and the camera with no apparent effect on registration of the images. When this approach was used in this study, it was found that the filters used did cause refraction of light. When the separate bands were combined as a composite they were no longer in perfect registration. To solve this problem, the filters were placed between the light source and the sample. When placed in this position relative to the sample and the light source, the filters did not effect the registration of images.

The colour filters used with the microscope were too small to be placed below the sample. Their size meant they would have had to be placed in close proximity to the bulb in the OHP which would

have resulted in damage caused by the heat of the bulb. Instead, large sheets of coloured acetate were placed on top of the OHP at a safe distance from the bulb. Although the spectral properties of the acetate were not known, a visual inspection of the images suggested the data were satisfactory.

The thin section slide was mounted above a 6 x 6cm hole cut in a worktop. This allowed the OHP to be placed underneath the thin section slide. The filters used were mounted around the slide using a combination of retort and copy stands. 10 x 10cm linear polarising sheets and 10 x 10cm mica plates were used to create circularly polarised light. As with the microscope, any filter placed between the specimen and the camera was left in place during capture of multiband images.

Four spot lights were used to generate OIL but this caused a number of problems. Reflections from the colour filters, polarising filters and the edge of the hole created stray light which effected digitisation. It was not possible to eliminate this stray light with the equipment available. The equipment was extremely delicate and could not be set up with precision. During image capture, filters could be accidentally moved creating delays in capturing sets of images. It was not possible to ensure that the filters were completely parallel with the specimens and the camera, or filters were placed in precisely the correct position. This introduced some variability in the quality of the images.

## 2.7 Multispectral image classification.

Multispectral classification allows features of interest to be discriminated based upon differences in numerous spectral bands. There are many types of classification routines. When this work was started there was no published work which used multispectral classification techniques to classify features observed in soil thin sections. An evaluation was made to determine the classification technique most applicable to soil micromorphological studies. Three classification routines were chosen;

1. Supervised maximum likelihood multispectral classification
2. Unsupervised maximum likelihood multispectral classification
3. Unsupervised non-parametric watershed classification

In general multispectral classification operates by taking data from many spectral bands and producing a single image with homogenous areas labelled as spectral classes. Further analysis of identified features is then possible. Binary images can be created which allow morphological measurements of features to be calculated.

It is important to distinguish between spectral classes and informational classes. An informational class is a component of the image which is of interest to the analyst and normally contains an amount of spectral variation. For example in a remote sensing application forest might be characterised by variations

in age, species composition and density. All these factors contribute to spectral variation although the analyst might only be interested in the informational category of forest (Jensen 1986). Spectrally distinct sub-classes can be identified which when combined form a single informational class. A spectral class is a label produced by the classifier that corresponds to a homogeneous spectral region. Informational classes and spectral classes seldom match exactly.

## **2.8 Supervised and unsupervised classification methods**

Supervised classification operates interactively with the analyst. Groups of pixels representing known features, referred to as training areas, are identified by the analyst. Unknown pixels are assigned to classes based upon statistical parameters of values in the training areas. The statistical estimates used vary between classification processes. For instance one of the simplest classification procedures is the parallelepiped classifier. Estimates are made about the maximum and minimum values in each band which correspond to specific features. Using these values, as upper and lower limits, a box is constructed in the data set. Any points that fall within this box are assigned a classification label.

The maximum likelihood method uses a larger number of statistical parameters to assign labels to classes. The location of each class in Euclidean space is calculated by reference to the class means. Estimates of the variance and covariance are used to

calculate the spread of the class in feature space. A specific n-dimensional vector is assigned to the class for which its probability of membership is highest (Mather 1987). The accuracy of supervised classification depends on the size, location and representativeness of the training areas drawn by the analyst. Any anomalous data values included in the training areas reduces the accuracy of the classified image.

Unsupervised classification requires a minimal amount of intervention by the analyst, although this will depend on how the program being used has been written. Often the analyst decides the number of output classes to be produced. The classification operates by building clusters of pixels each associated with a mean vector. Pixels are then assigned to each cluster using a maximum likelihood algorithm (Jensen 1986). When the classification is completed, the spectral classes must be assigned to informational classes by the analyst.

## **2.9 Supervised classification of a soil thin section.**

A soil thin section slide was chosen to investigate the applicability of different classification procedures to isolate soil pores. The results were used to determine if multispectral classification was a suitable technique to discriminate features of interest. For this reason the context the slide was derived from is not of great importance. The first procedure used was a supervised maximum likelihood classification. An image was captured using a high magnification and 3 bands of data.

A slide was chosen where the voids had been dyed green using fluorescent Epo Dye (Struers). Red, green and blue bands were captured using PPL and labelled L164red, L164green and L164blue respectively. The bands were displayed as a colour composite image on R-Chips, called l164com (fig 2.6), and contrast stretched (section 2.25) to enhance features to be classified. Training areas, representing quartz, void space and groundmass, were interactively delimited. The data within the training areas were used to create a spectral signature for each component. A maximum likelihood classification of the entire image was carried out creating classes based upon these spectral groups. The result of the classification is illustrated in fig 2.7. Despite obvious spectral variation in the groundmass and in the dye, the image is classified satisfactorily although some problems are apparent.

The edges of the quartz grains are often classified as void space. This is attributed to a combination of mixed pixels and a phenomenon known as the Becke line. The Becke line appears as a halo between areas of different refractive index. The brighter area around the edges of quartz grains might have contributed to the misclassification.

Many small specks of carborundum, a residue from the preparation process, occur within the void area (fig 2.6). The carborundum is spectrally different to void and is not assigned to the same class. Thus the informational class of void does not correspond to a single spectral category. This is an example of an informational class not matching a spectral class.





Fig. 2.9 Binary image depicting voids after 4 median filtrations, FL 760µm

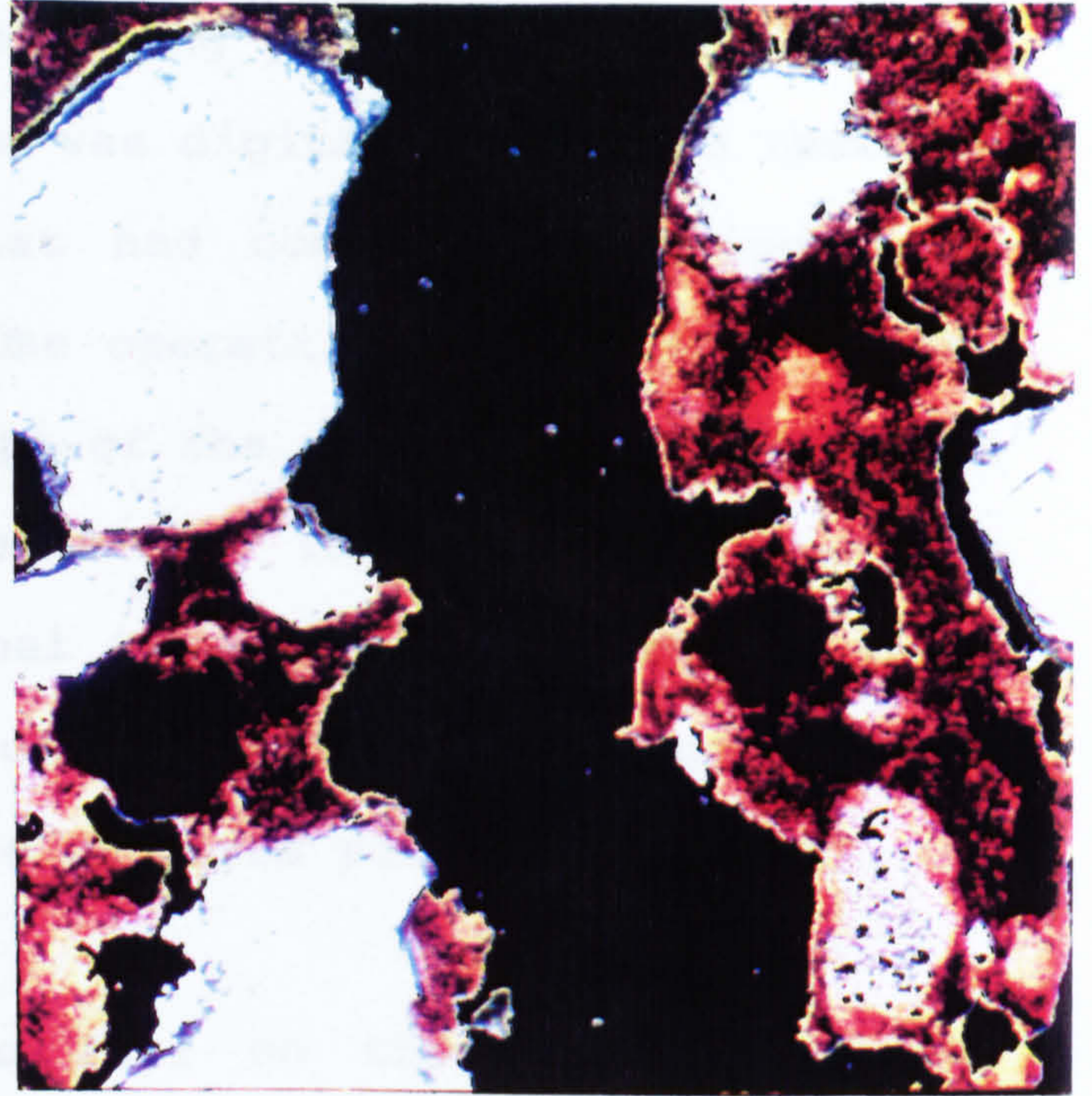


Fig. 2.10 Voids displayed as a black overlay covering L164com, FL 760µm

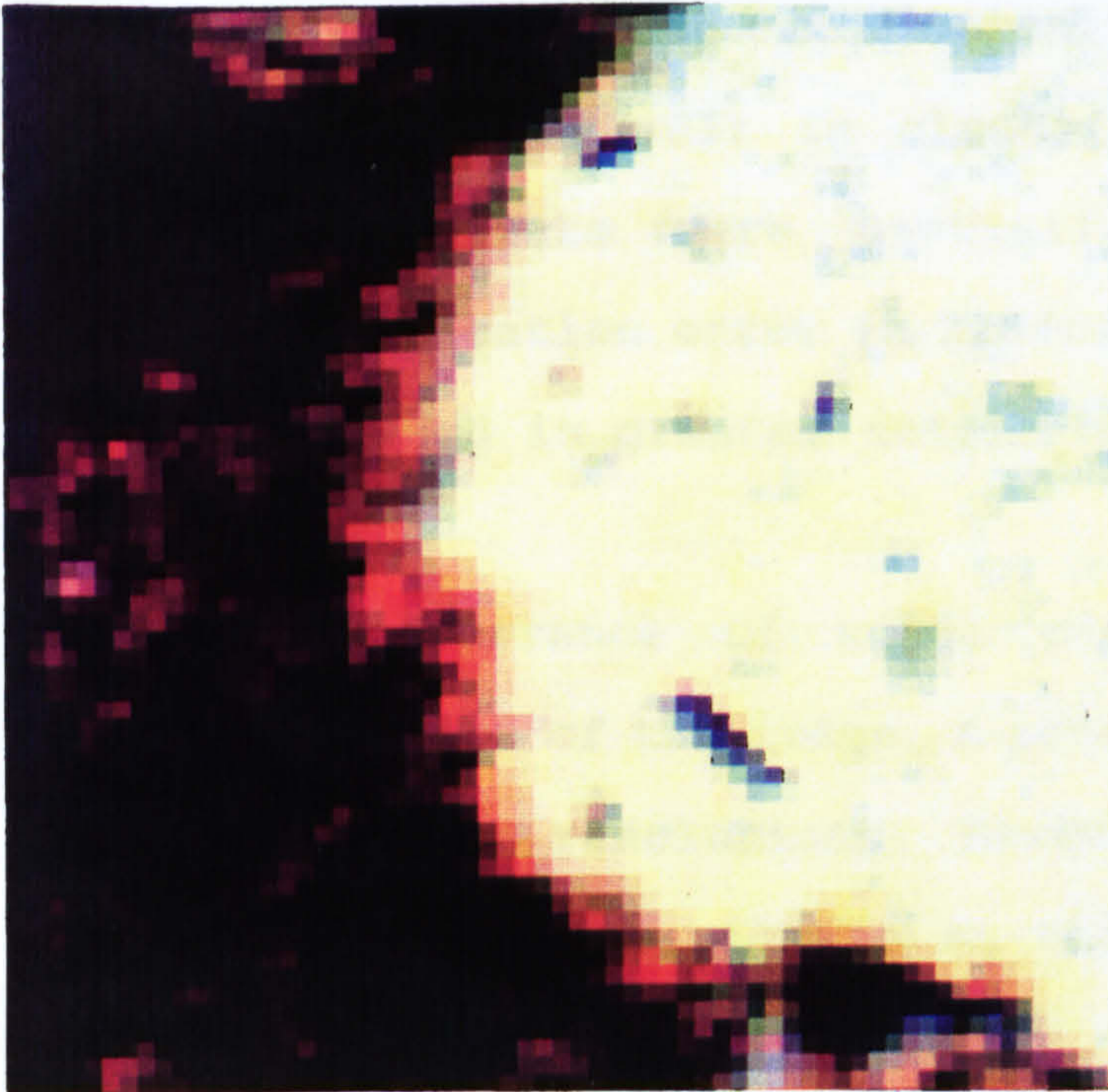


Fig.2.11 Detail of L164com showing regions of mixed pixels at the boundary of void and groundmass

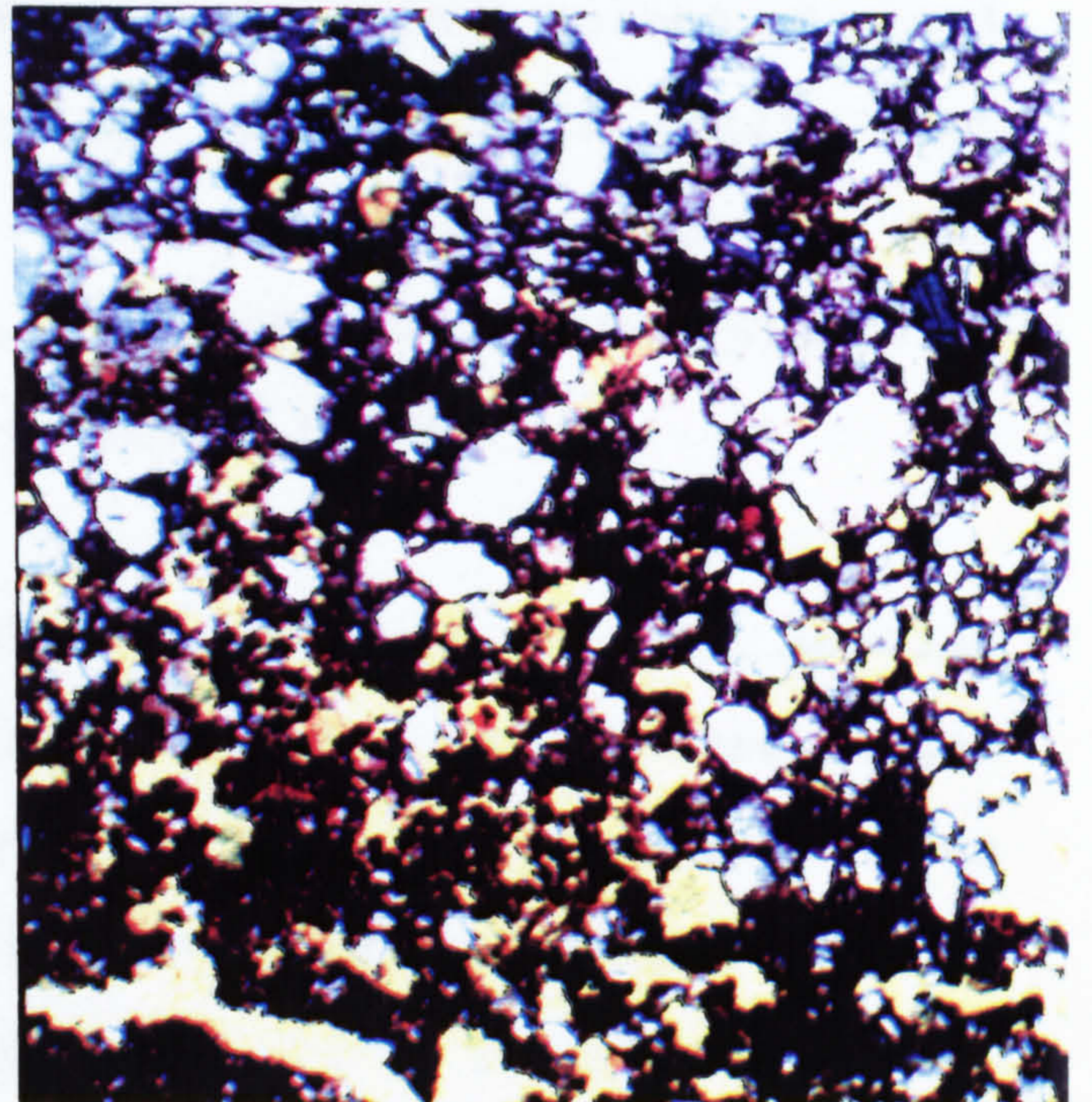


Fig. 2.12 Colour composite image of L1644, PTL, ACS, red 53-167, green 50-174, blue 37-165, FL 3.8mm

A binary image was produced depicting just the area of void in image 1164 (fig 2.8). The image was digitally filtered (section 2.24) to remove the noise that had occurred as a result of misclassification (fig 2.9). The operation removed most of the noise in the image and the shape of the voids were not affected to a great extent. The filtered binary image was displayed, as an overlay covering the original 3 band colour composite image (fig 2.10). An area approximately 3 pixels wide, present at the edges of the voids, is composed of mixed pixels (fig 2.11).

Mixed pixels occur if pixels fall on the boundary of two spectrally different areas. Pure pixels have intensities that correspond to the brightness of the image at one location. The intensity of a pixel that spans the boundary of two areas does not correspond to either area. The anomalous data values of mixed pixels can result in classification error. It is likely that mixed pixels were partially responsible for some of the classification error in L164com. The problems of mixed pixels is discussed in greater detail by Campbell (1987).

The occurrence of mixed pixels is related to the spatial resolution of the image. A possible solution is to capture images at higher resolutions. However this does not always work as detail becomes visible at the higher resolution which was not present previously. Sadowski and Sarno (1976, in Campbell 1987) found that classification accuracy decreased as spatial resolution became finer. Changing the magnification of the

optical microscope has the same effect as increasing the resolution of the sensor.

In summary two problems are identified using the supervised classification approach.

1. Voids are not spectrally homogeneous so it is difficult to accurately delimit training areas.

2. Mixed pixels, at the edges of voids, result in classification errors.

The supervised classification was used on an image captured at a high magnification in order to simplify the classification process and enable errors to be easily recognised. The results indicate that there are problems trying to delimit training areas that accurately describe the spectral information of voids. To overcome this difficulty an unsupervised approach was used.

## **2.10 Unsupervised classification**

A second set of images was captured to introduce more complexity into the classification. Bands of data were captured using PTL and CPL. Each light source was captured using red, green and blue filters (fig 2.12 and 2.13) producing six bands of data in total labelled 11644. The field of view measures 3800 $\mu$ m.

Only 3 bands of data can be displayed at one time using the R-Chips system. To make an assessment of the spectral information present in all six bands the data was compressed using a principal component transformation (Jensen 1986). The first three components were displayed as a colour composite image (fig 2.14). The voids are dark red, the colour of the minerals vary between white and pink and the groundmass is blue and green. The strong colour variation between different components of the image suggests that there is enough information present in the data set to differentiate between the various features. An unsupervised maximum likelihood classification was carried out.

#### **2.11 Unsupervised maximum likelihood classification.**

The unsupervised maximum likelihood classification routine, written by Dr. A. Watson (Stirling University), ran on the MicroVAX. The only interaction necessary was for the analyst to decide the number of output classes to be produced. The original 6 bands of data were transferred to the MicroVax, reformatted and submitted to the classification. Thirty classes were specified for output. This created a single grey scale image which was transferred to R-Chips for visual analysis. Each label, corresponding to a spectral class, was assigned a label (Table 2.4). Mineral refers to quartz and feldspar unless otherwise stated.

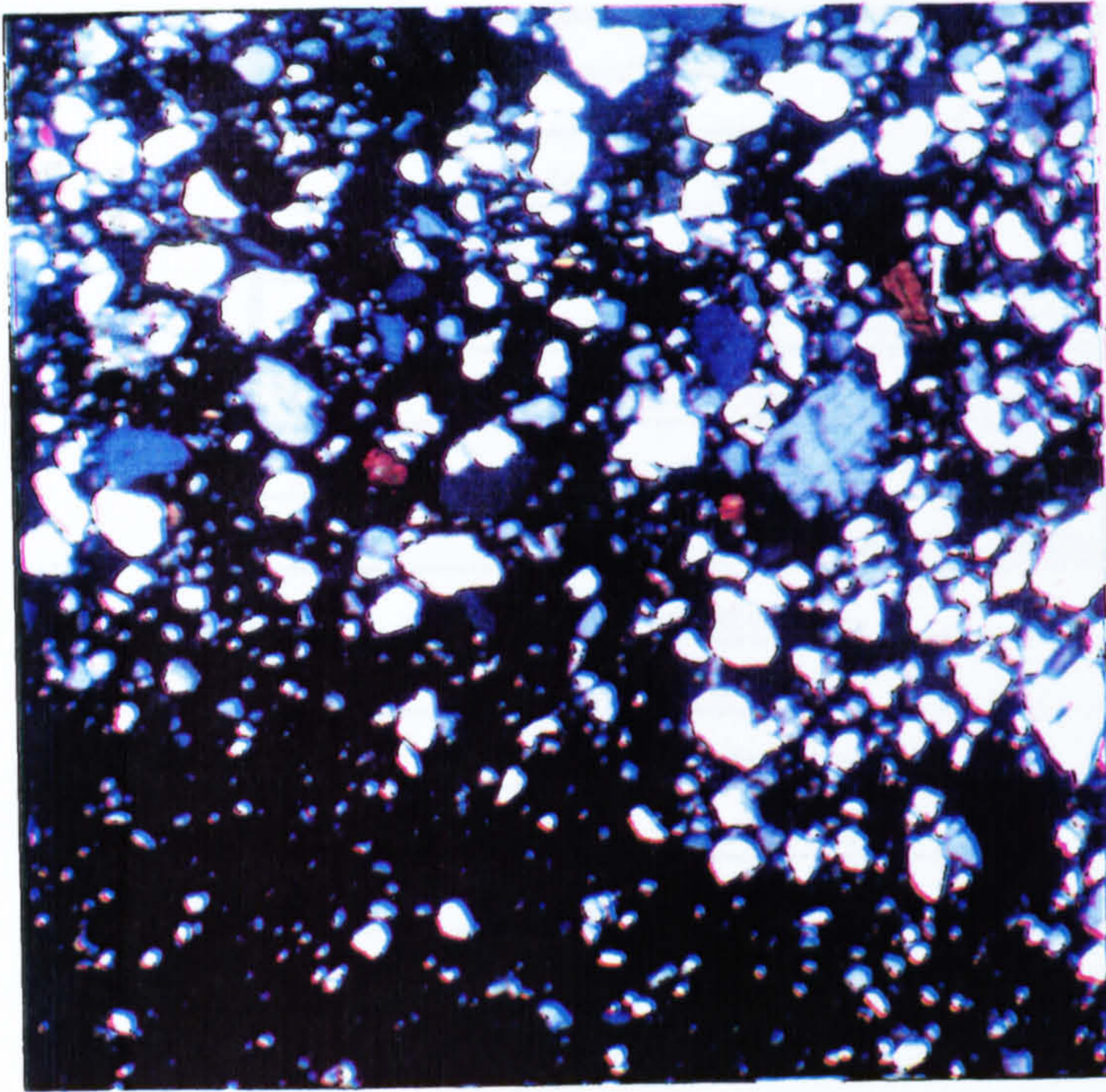


Fig. 2.13 Colour composite of L1644, CPL, ACS, red 43-182, green 19-164, blue 22-160

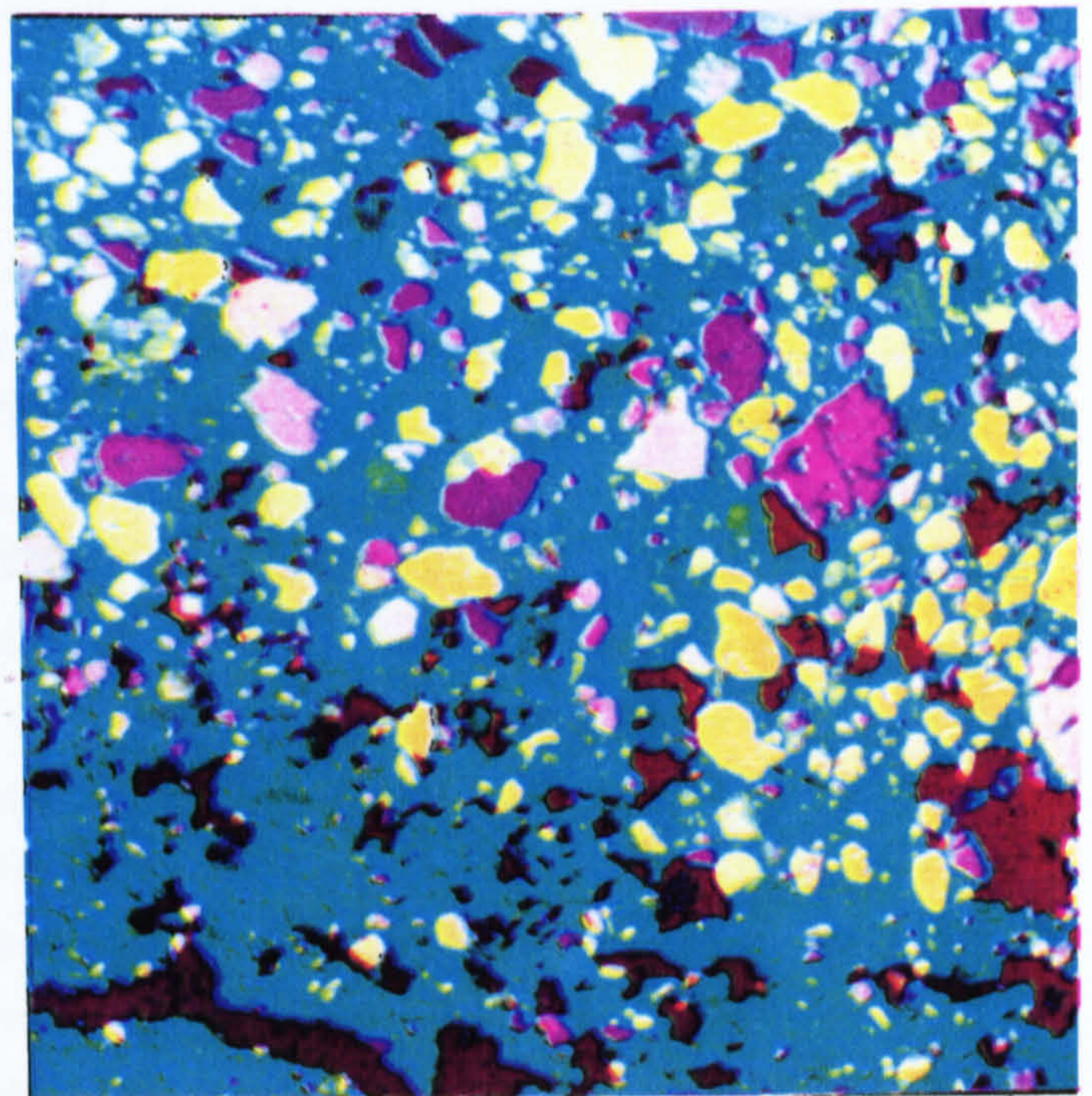


Fig. 2.14 Principal component transformation of L1644, ACS, 1st com. 43-182, 2nd com. 19-164, 3rd com. 22-160

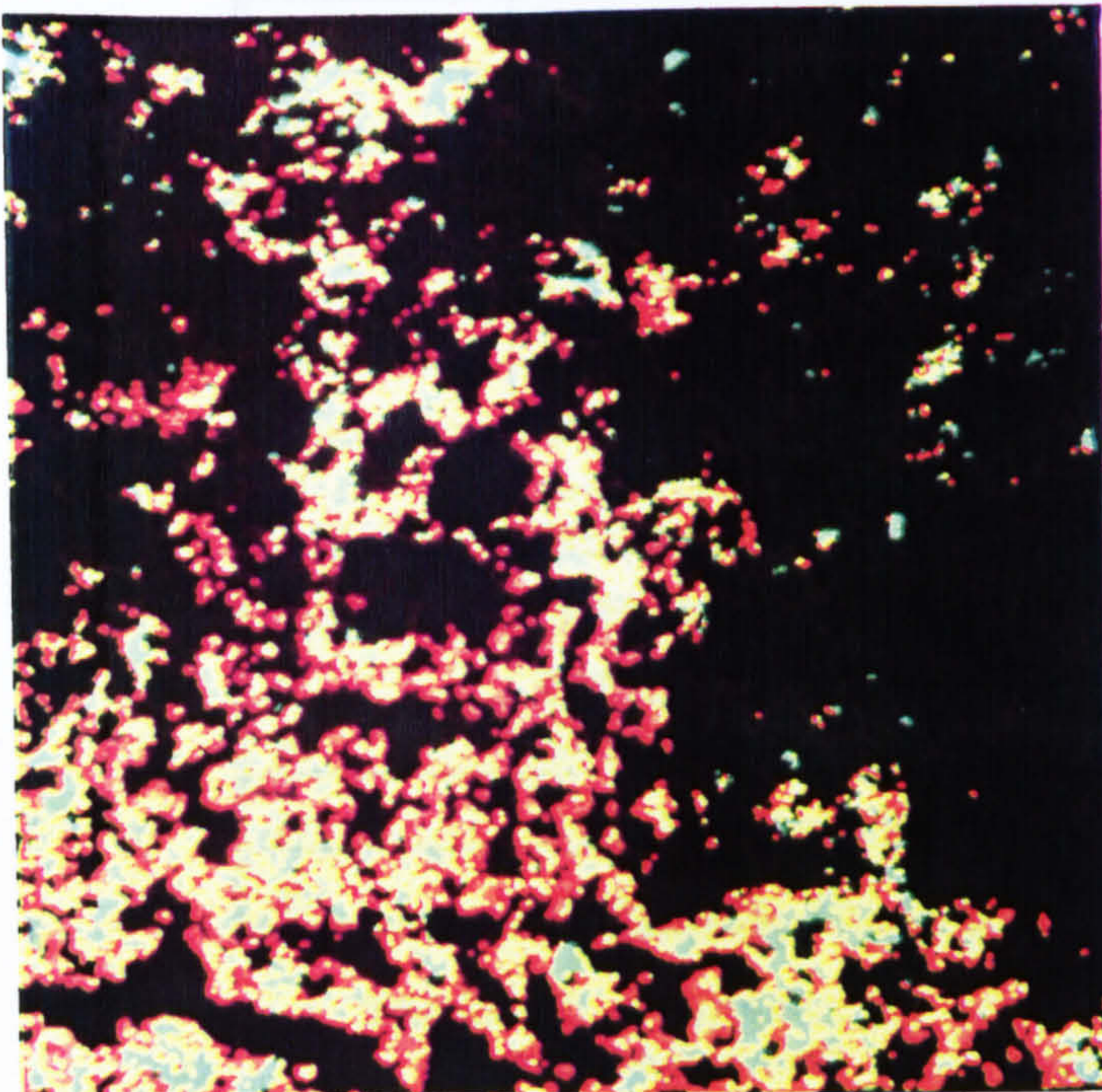


Fig.2.15 Classified image of a vertically orientated fabric pedofeature in L1644, FL 3.8mm

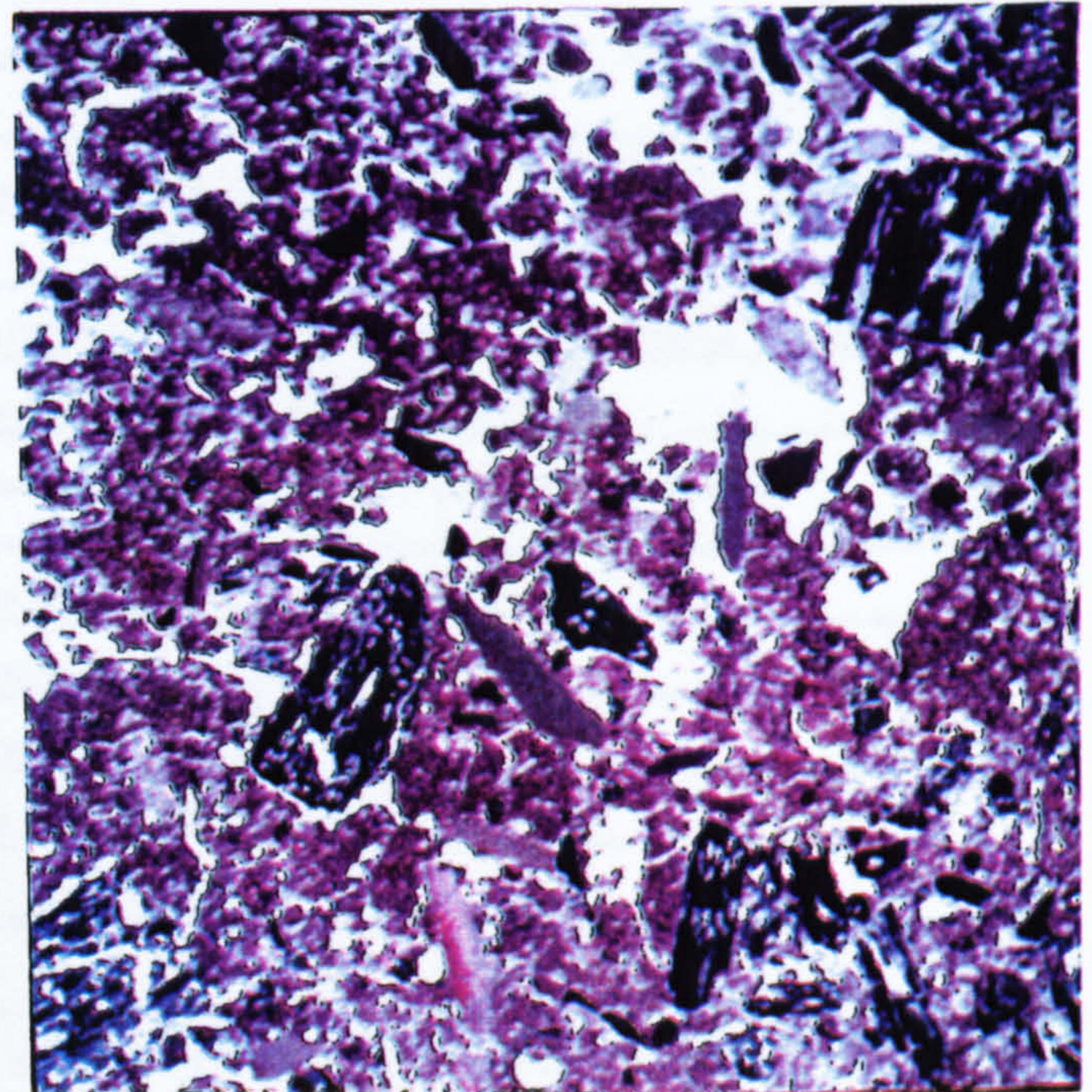


Fig. 2.16 Colour composite image of Whit1, PTL, ACS, red 47-138, green 48-159, blue 60-141, FL 4cm

| Spectral Class | Description  |
|----------------|--|
| 1              | Internal area of minerals  |
| 2              | Outer area of minerals   |
| 3              | Outer area of minerals   |
| 4              | Internal area of some minerals, edges of others                                      |
| 5              | Edges of minerals  |
| 6              | Internal area of some minerals, edges of minerals                                    |
| 7              | Edges of minerals  |
| 8              | Edges of minerals  |
| 9              | Edges of minerals  |
| 10             | Edges of minerals  |
| 11             | Edges of minerals  |
| 12             | Central area of minerals   |
| 13             | Edges of minerals  |
| 14             | Edges of minerals  |
| 15             | Central area of voids and edges of some minerals                                     |
| 16             | Void edge and mineral edge   |
| 17             | Void edge  |
| 18             | Void edge and narrow voids   |
| 19             | Void edge  |
| 20             | Void edge  |
| 21             | Central area of green amphibole, weathered mineral and edges of mineral              |
| 22             | Edges of mineral   |
| 23             | Edges of void and some material within voids including amorphous organic material    |
| 24             | Edges of void, edges of green amphibole, some groundmass material                    |
| 25             | Unidentified weathered mineral, part of green amphibole and some groundmass material |
| 26             | Weathered mineral, green amphibole and some groundmass material                      |
| 27             | Edge of groundmass, some amorphous organic material                                  |
| 28             | Groundmass, particularly at the top of the slide                                     |
| 29             | Groundmass, particularly at the bottom of the slide                                  |
| 30             | Large central area of groundmass   |

Table 2.4 Spectral classes of L164com produced by an unsupervised maximum likelihood classification

The spectral classes that had been identified were then assigned to informational groups.

#### **2.12 Assigning spectral classes to informational groups.**

The minerals with the highest interference colours, quartz and feldspar, are assigned the lower spectral classes. Classes 1, 2, 6 and 12 represent the internal areas of mineral material. Classes 2, 3, 7, 8, 9, 10, 11, and 14 represent the edges of minerals. A visual inspection of these areas using the microscope reveals no observable differences so the reasons for the classification results are not clear. The classes representing the internal areas of minerals and the edges of minerals are combined into one informational group.

It is difficult to allocate the classes that represent the edges of minerals. If all the classes are assigned to one informational group some of the minerals that are close to each other end up touching. This may or may not be important depending on the reason of the original classification. If the purpose of the study is to identify features for object measurements a small number of pixels linking different objects might considerably affect the result.

The central area of a green amphibole is assigned to the same spectral class as some weathered mineral material. Their optical characteristics are similar using CPL. When viewed using PTL the green amphibole is green and the weathered mineral is brown

yellow. A close inspection shows that the green amphibole is not homogeneous. Fractures within the mineral remain black using PTL and CPL. Although the mineral appears to be a reasonable size for classification when the fractures are considered as another class, the remaining homogeneous area is quite small and is composed of mixed pixels.

There are other spectral classes that do not correspond exactly to informational classes. For instance, class 16 includes edges of voids and also edges of minerals. If the class is assigned to voids then over-classification of voids results. If the spectral class is assigned to minerals then under classification of voids results. Other examples of different informational categories belonging to one spectral group include class 15, 21, 23, 24, 25, 26 and 27.

In an attempt to rectify the problem of overlapping informational and spectral classes, the 6 image bands were reclassified increasing the number of output classes. The classification was repeated twice, specifying output of 50 and 70 classes respectively. There is an improvement in discrimination using 50 classes although there is still some overlap. There is no improvement between 50 and 70 classes. As the number of classes is increased the time taken to label each spectral groups also increases. The subjective error of trying to assign smaller groups of pixels randomly scattered over the image to informational groups also becomes greater. A more suitable and



less time intensive way of reducing the classification error is to use post classification processing (section 2.24).

Using output from the unsupervised classification a digital filter was used to create an informational group depicting voids. Class 16, which contains information about voids and edges of minerals was processed using an averaging filter (section 2.24). The modified class could now be included in the informational group of voids without the problems of edge effects. Spectral classes 15, 17, 18 and 23 were grouped together and filtered in the same way as class 16. The final informational category of voids was then created.

The advantage of processing the spectral classes separately is that unwanted pixels are not combined into larger groups. Groups of pixels are only removed from the image if they are smaller than the critical size determined by the type of filter used. A problem with this approach is that it can take a considerable amount of time to sort the spectral groups in such detail. The time taken begins to approach the time taken for manual editing of the image. Attempts were made to isolate green amphibole using filters. This time the results were not successful because the groups of unwanted pixels were too large to be removed.

The last class considered in this example is the groundmass. Before classification the groundmass appeared reasonably homogeneous (fig 2.12). Spectral classes 29 and 30 represent areas of dark brown and brown material within the groundmass.

When the two classes are combined a vertically orientated fabric pedofeature is visible (fig 2.15).

Detailed observation of a small area of the image shows that class 30 represents darker material than class 29. Using the Olympus microscope and the original thin section slide small individual dark particles were observed. These correspond to the spatial locations of class 30. In the classification the particles are not discriminated individually but are amalgamated into larger groups owing to their small size.

In summary, as with the supervised classification, each informational category is not represented by individual spectral groups. Difficulties in classification are apparent because of the problems associated with mixed pixels. It is possible to correct most of the classification errors using some type of post classification processing. The unsupervised approach is more suitable for the study of thin sections for the following reasons;

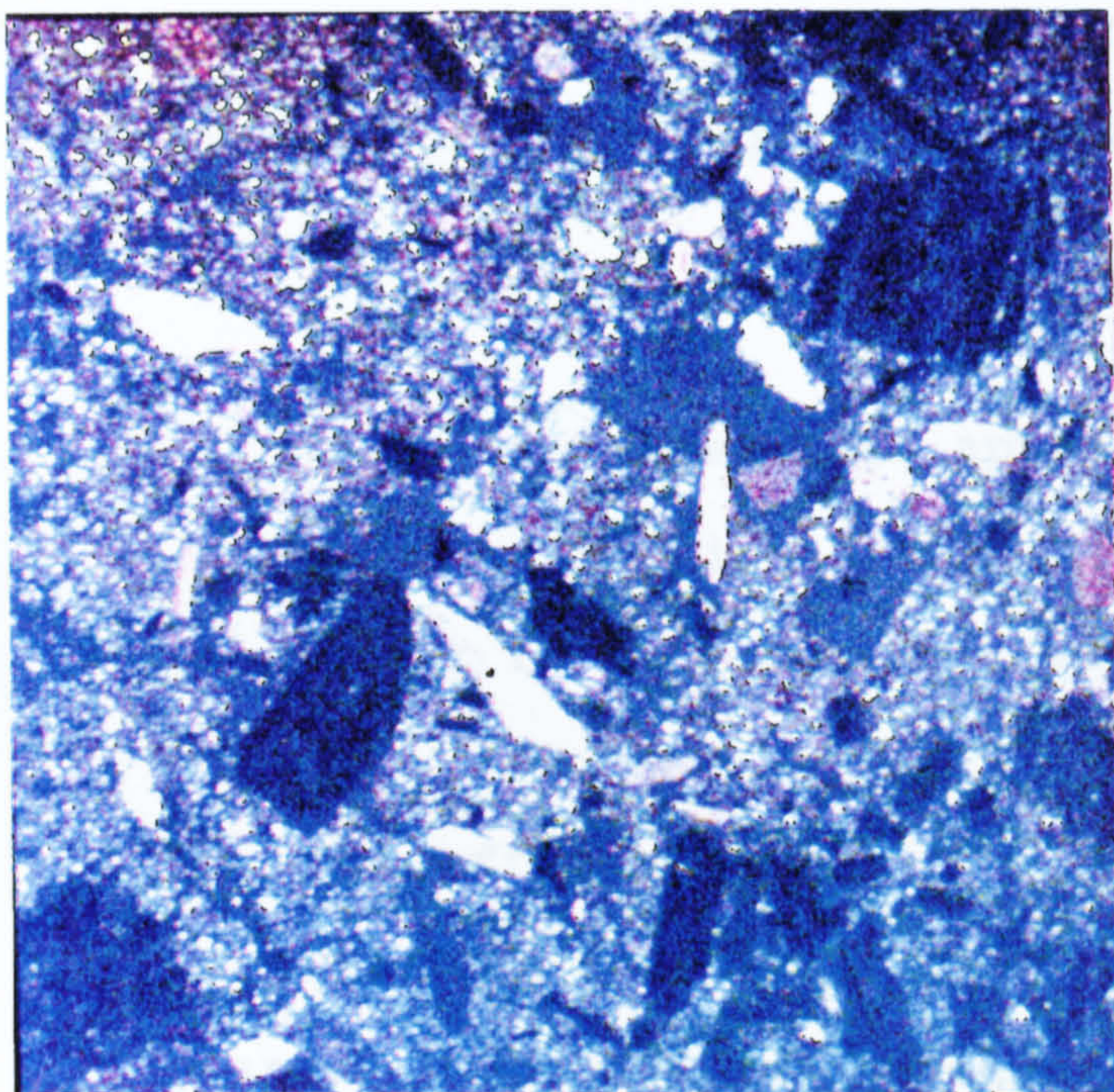


Fig. 2.17 Colour composite of Whit1, CPL, ACS, red 117-160, green 105-136, blue 98-115, FL 4cm

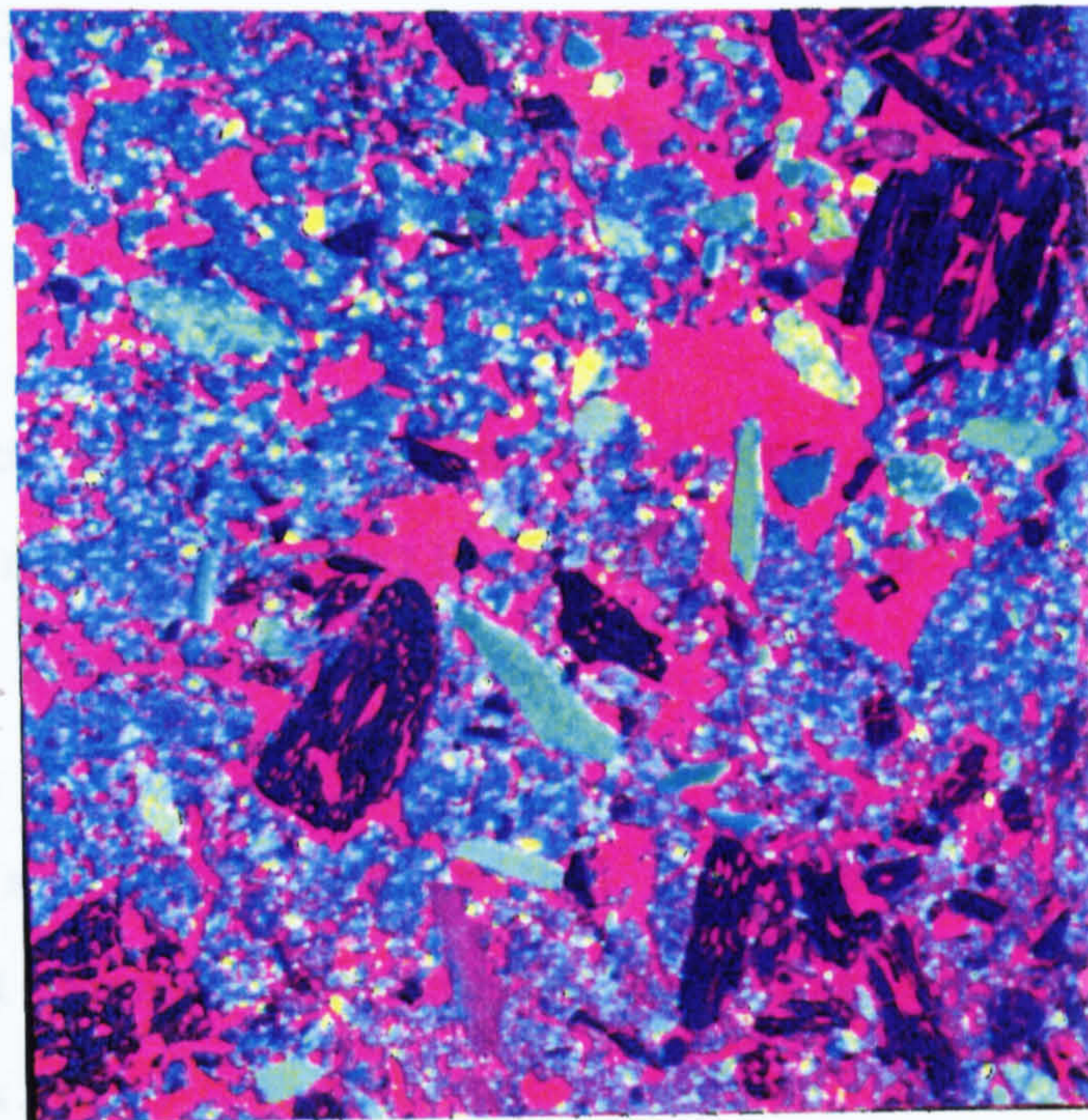


Fig. 2.18 Principal component transformation of Whit1, ACS, 1st com. 25-299, 2nd com. 18-88, 3rd com. 108-115

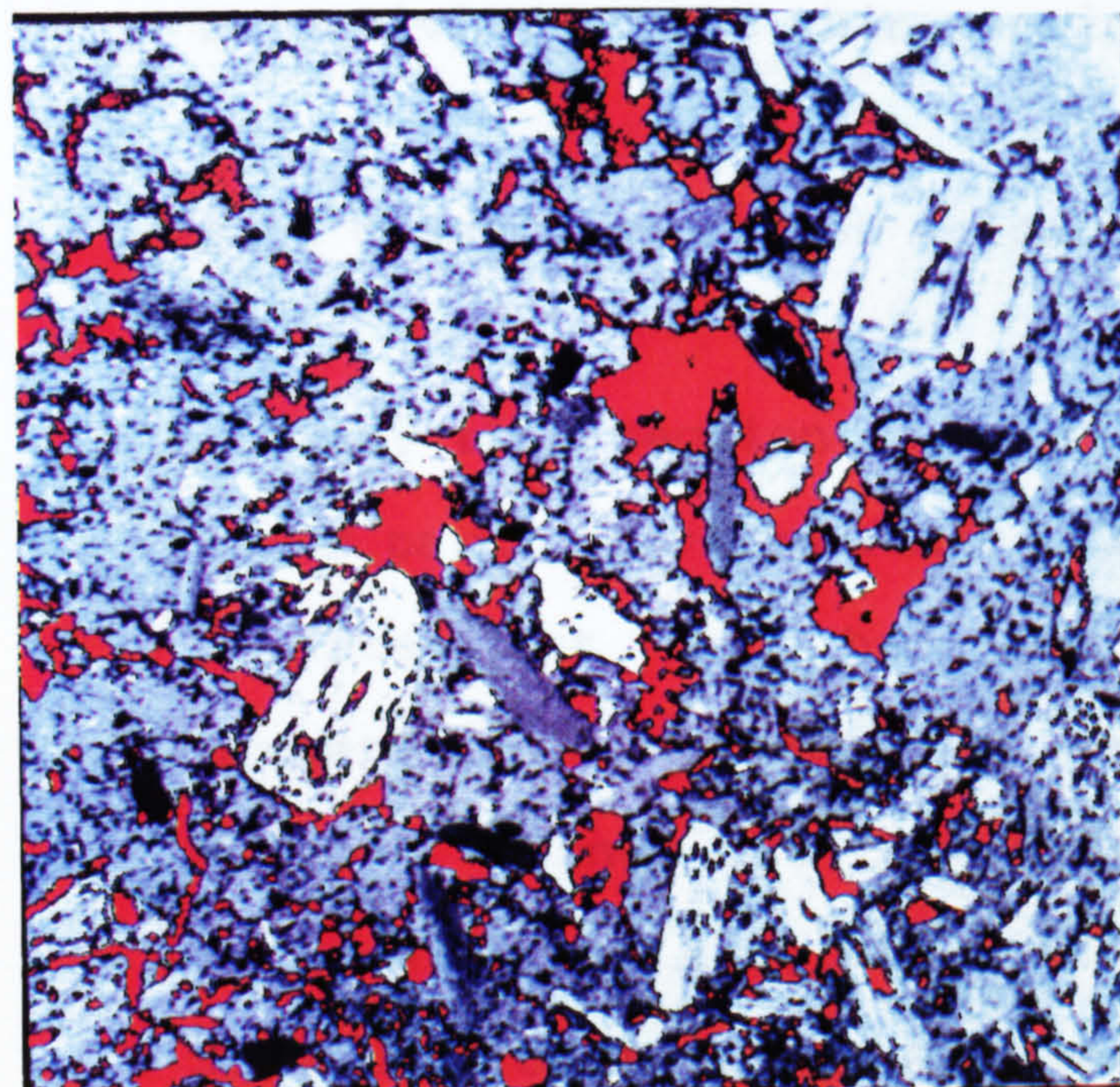


Fig.2.19 Unsupervised classification of Whit1, spectral class 3 shown as a red overlay, FL 4cm

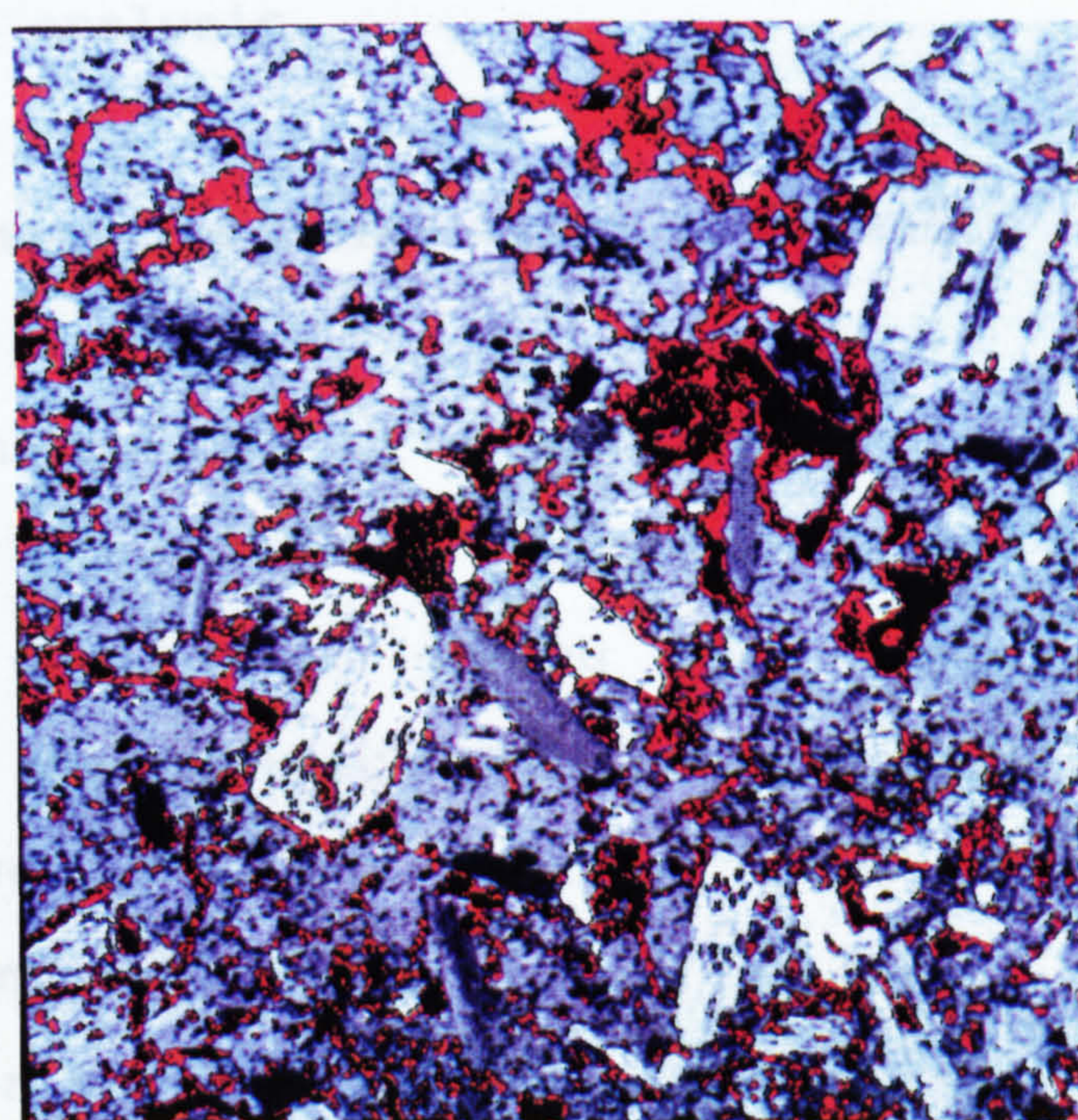


Fig.2.20 Unsupervised classification of Whit1, spectral class 4 shown as a red overlay, FL 4cm

1. It is easier to label spectral groups and amalgamate them into informational groups than try and interactively delimit training areas.

2. Using the supervised approach at lower magnifications means delimiting training areas for numerous small objects. This is difficult to do accurately and is time consuming.

3. The effects of mixed pixels can be minimised by removing errors from individual spectral groups and combining them into larger informational categories.

4. Unsupervised classification can find spectral variation in an image that is not expected by the analyst. This increases the objectivity of the thin section analysis.

### **2.13 Classification of voids without staining using image Whit1**

In many thin section studies the ability to measure soil pores is of particular importance. In the preceding example voids are isolated but they had been dyed green during the sample preparation. Another slide was chosen which had been prepared without using the green dye. A thin section from an archaeological site at Whithorn, S.W. Scotland, was selected. This particular slide was chosen for two reasons;

1. Green dye had not been used in the sample preparation.

2. The structure could be observed macroscopically allowing a larger area of the thin section to be captured compared to the previous example.

Six bands of data were captured using the 50mm Nikon lens and the free standing equipment. The resulting image is labelled Whit1. The light source was corrected by rationing each band by a blank (section 2.6) to produced the results illustrated in fig 2.16 and 2.17. The image captured using CPL is not of a high quality. This was caused by low light levels entering the camera. This is the best that could be achieved with the equipment available.

As before (section 2.11) a principal component transformation was done on the images to visually asses the differentiation between features. The first three components were displayed as a colour composite image (fig 2.18). The voids are very distinct from other features which suggests that there is enough spectral information present to classify the voids. An unsupervised maximum likelihood classification was performed on all 6 bands. Labels were attached to each of the spectral classes produced (Table 2.5).

| Spectral Class | Description   |
|----------------|---|
| 1              | Quartz minerals   |
| 2              | Quartz and weathered material   |
| 3              | Central area of voids   |
| 4              | Voids, including the edges and narrow voids                             |
| 5              | Some weathered material and fine grained Schist                         |
| 6              | Edges of voids  |
| 7              | Edges of voids  |
| 8              | Fine grained Schist and weathered rock fragments                        |
| 9              | Edges of voids and areas of bone showing interference colours using CPL |
| 10             | Edges of Schist and weathered rock fragments                            |
| 11             | Bone and edges of voids   |
| 12             | Pixels scattered throughout the groundmass and some bone                |
| 13             | Bone and pixels scattered throughout the groundmass                     |
| 14             | Pixels scattered throughout the groundmass and weathered rock fragments |
| 15             | Weathered rock fragments and fine grained Schist                        |
| 16             | Pixels scattered throughout the groundmass and some bone                |
| 17             | Bone and some edge pixels   |
| 18             | Fine grained schist and groundmass                                      |
| 19             | Groundmass and edge pixels  |
| 20             | Bone and groundmass, mainly in the lower half of the slide              |
| 21             | Groundmass and Schist   |
| 22             | Groundmass and bone   |
| 23             | Edges of charcoal   |
| 24             | Edges of charcoal and scattered pixels in the groundmass                |
| 25             | Edges of charcoal and scattered pixels in the groundmass                |
| 26             | Edges of charcoal and scattered pixels in the groundmass                |
| 27             | Edges of charcoal and scattered pixels in the groundmass                |
| 28             | Scattered pixels  |
| 29             | Edges of charcoal   |
| 30             | Central area of charcoal  |

Table 2.5 Spectral classes of Whit1 produced using an unsupervised maximum likelihood classification.

## **2.14 Results of assigning Whit1 spectral classes to informational categories corresponding to void area**

An informational group depicting soil pores was created by grouping together the relevant spectral classes. Classes 3, 4, 6, 7, 9, and 11 depict soil pores. Each of these classes was displayed as a red overlay covering the classified image. Figures 2.19 to 2.23 illustrate the difficulty of assigning spectral classes to informational groups. When there is only a small number of pixels in a spectral class it is difficult to be sure what that group represents. The difficulty is increased if the spectral class includes more than one informational group.

Classes 3 and 4 (figs. 2.19 and 2.20) are composed entirely of void space and were incorporated into the void informational group with no modification. These two classes do not describe all of the void area. Classes 6 and 7 were added to the group and no misclassification occurred (figs. 2.21 and 2.22). If class 9 and class 11 are added to the same category, features which are not void are included in the informational group. In particular, fragments of bone begin to be incorporated (the large area of red overlay at the bottom of the image depicted in fig. 2.23 and 2.24). A filtration of the binary classes 9 and 11 did not remove the unwanted pixels because the groups are too large. In this case the analyst must decide between under-classification and over-classification or manual editing of the image.

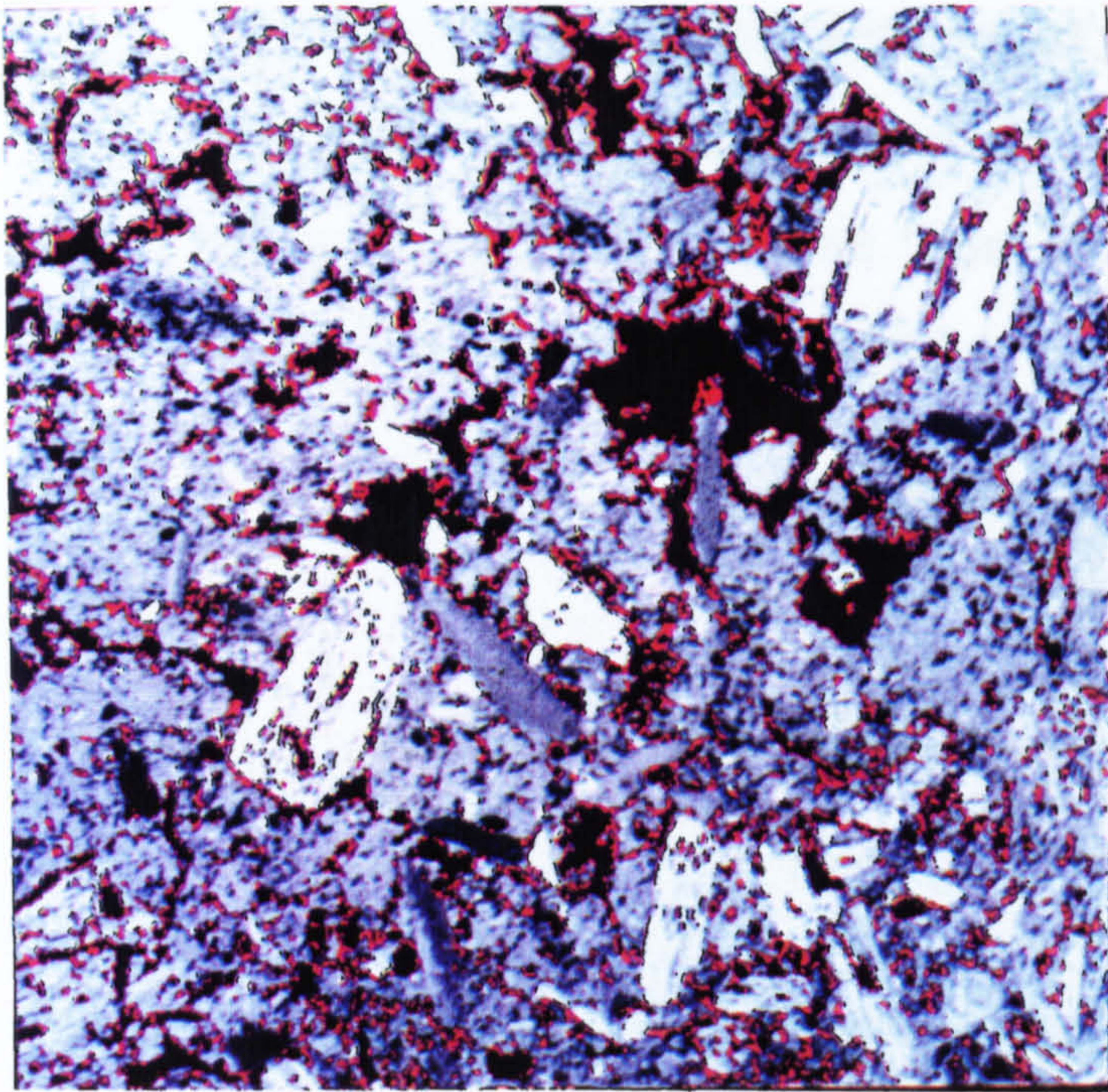


Fig.2.21 Unsupervised classification of Whit1, spectral class 6 shown as a red overlay, FL 4cm

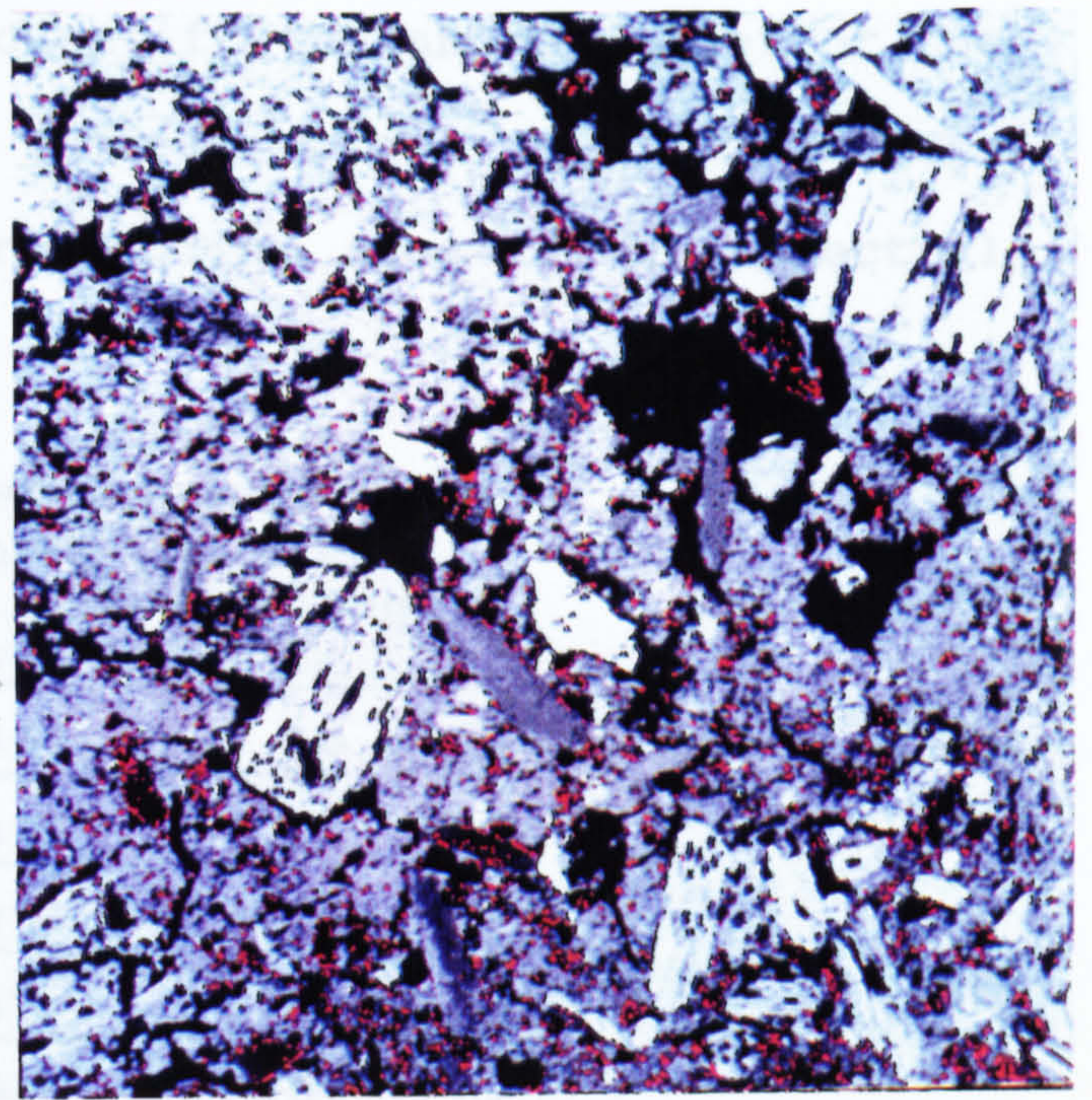


Fig.2.22 Unsupervised classification of Whit1, spectral class 7 shown as a red overlay, FL 4cm

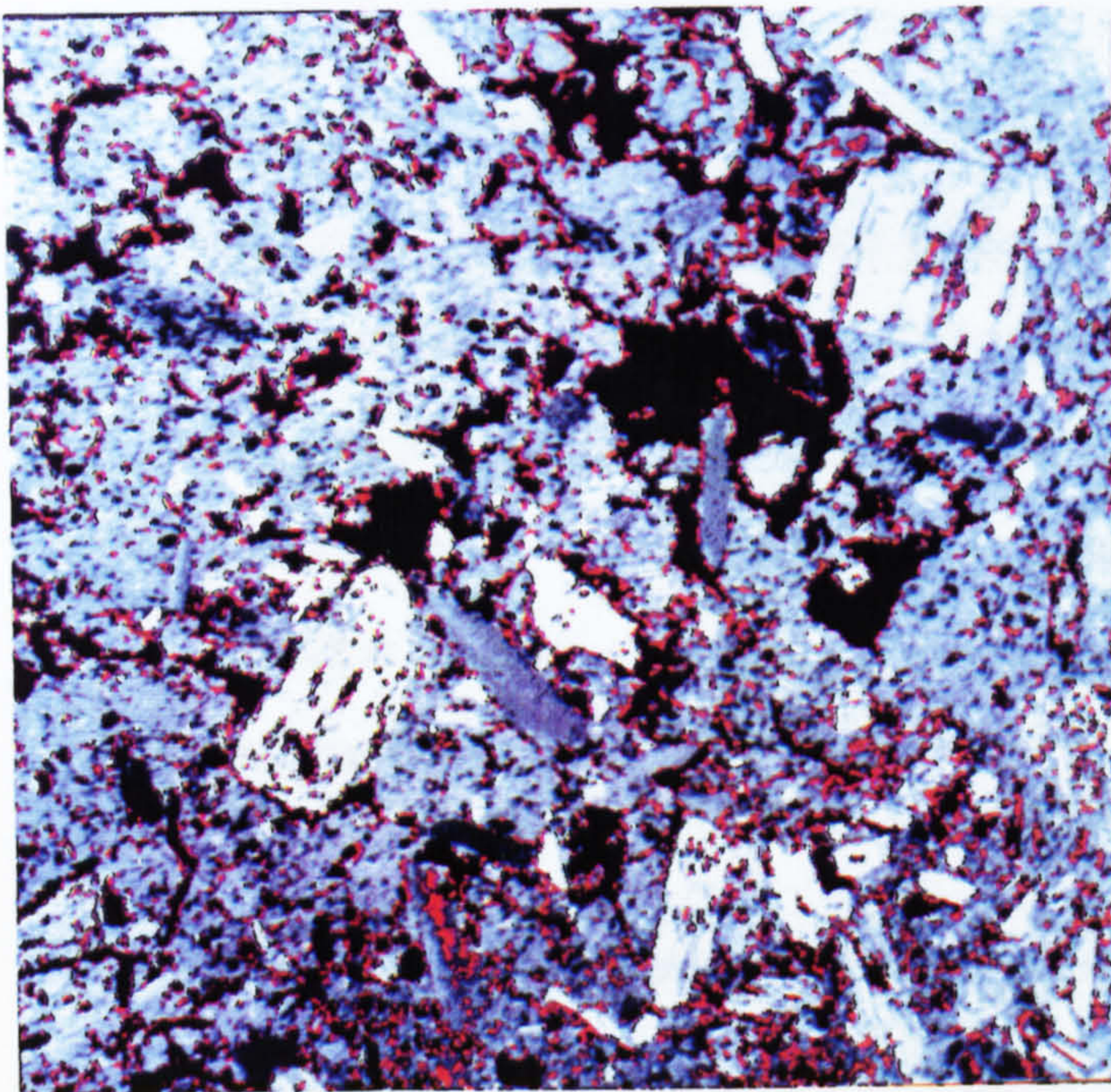


Fig.2.23 Unsupervised classification of Whit1, spectral class 9 shown as a red overlay, FL 4cm

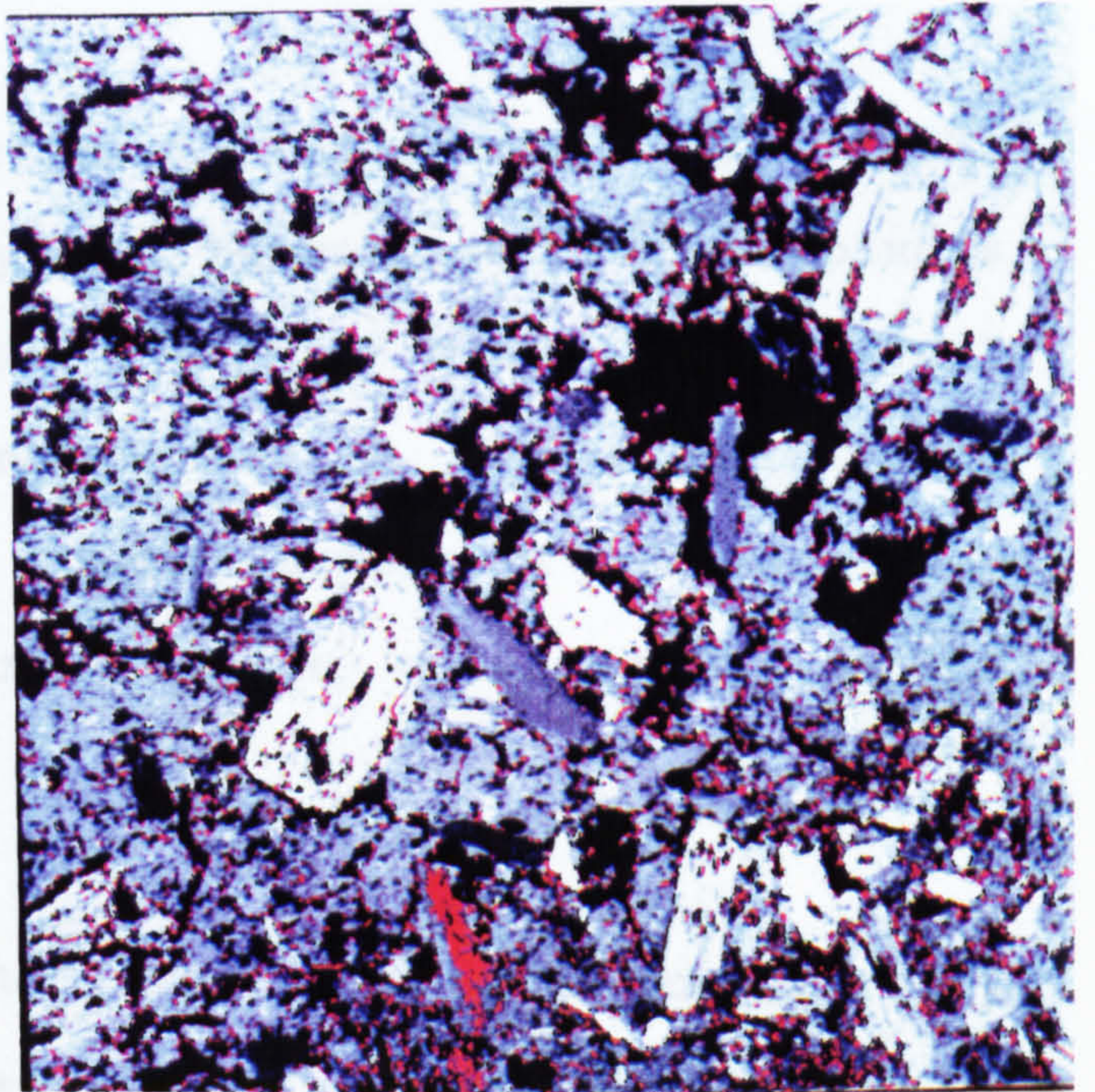


Fig.2.24 Unsupervised classification of Whit1, spectral class 11 shown as a red overlay, FL 4cm



It is difficult to accurately quantify the amount of error the incorporation or exclusion of classes 9 and 11 creates. The number of pixels and the corresponding area of the spectral classes is shown in table 2.6.

| Spectral class number | Number of pixels | % area of image |
|-----------------------|------------------|-----------------|
| 3                     | 18603            | 7.10            |
| 4                     | 13400            | 5.11            |
| 6                     | 10957            | 4.18            |
| 7                     | 4187             | 1.60            |
| 9                     | 12048            | 4.60            |
| 11                    | 8958             | 3.48            |

Table 2.6 Number of pixels belonging to spectral classes of Whit1.

Class 9 represents 4.60% and class 11 represents 3.48% of the image. It is not known precisely what percentage of these pixels are voids. It is likely that the amount of error in the final calculation of void area would not exceed 5%. This might seem an acceptable level of error but a small number of misclassified pixels can cause large errors when calculating object measurements.

In summary, voids which are not stained can be successfully discriminated using unsupervised classification. Correction of some spectral groups using post classification processing is often necessary. The amount of error caused by the these groups

is unlikely to exceed 5%. Even this small level of error has important implications for subsequent object measurements.

#### **2.15 Multispectral classification isolating 5 different soil features.**

It is shown, in preceding sections, that voids can be identified using multispectral classification without prior staining of the sample. The correlation of red, green and blue bands captured using PPL are highly correlated as are the red, green and blue bands captured using CPL. In view of this high correlation it was decided to see if a region of a thin section slide could be classified using three bands of data.

The thin section from the Whithorn site was used again, (section 2.13) and three monochrome bands were captured, one using PTL, one using CPL and one using OIL. PTL and CPL were chosen to differentiate between voids and minerals. OIL was used to differentiate charcoal from the rest of the groundmass. An unsupervised maximum likelihood classification was used and an output of thirty spectral classes specified. The spectral classes are presented in table 2.7.

| Spectral Class | Description  |
|----------------|--|
| 1              | The internal area of single grain quartz fragments, and quartz within quartz dominated rock fragments  |
| 2              | Edges of quartz single mineral grains and part material forming part of a quartz dominated rock fragment   |
| 3              | Material within the quartz dominated rock fragments and the internal area of fine grained elongated rock fragments   |
| 4              | The internal area of elongated fine grained rock fragments. Material within the quartz dominated rock fragment. Isolated single mineral grains within the groundmass |
| 5              | Internal region of fine grained elongated rock fragment, edges of fine grained elongated rock fragments. Internal area of quartz dominated rock fragments            |
| 6              | Edges of quartz dominated rock fragments, starting to include a mixture of quartz and groundmass in one small area   |
| 7              | Edges of groundmass around rock fragments and some internal areas of bone  |
| 8              | Edges of voids and areas of voids associated with carborundum  |
| 9              | Main internal area of larger voids   |
| 10             | Edges of elongated and quartz dominated rock fragments and some internal areas of fine grained rock fragments. This class causes linkages between some features      |
| 11             | Some internal areas of burnt bone. Some edges of groundmass and rock fragments   |
| 12             | Edges of groundmass and rock fragments, starting to include areas of groundmass  |
| 13             | Internal area of smaller voids and some edges of larger voids  |
| 14             | Edges of voids   |
| 15             | Edges of voids and groundmass  |
| 16             | Internal areas of some fine grained and quartz dominated rock fragments  |
| 17             | Groundmass   |
| 18             | Internal areas of rock fragments and some groundmass   |
| 19             | Groundmass, bone and edges of bone   |
| 20             | Groundmass   |
| 21             | Groundmass, some bone, some charcoal edges   |
| 22             | Edges of charcoal, some void edges and groundmass  |

Table 2.7 Spectral classes of Whit1b produced using an unsupervised maximum likelihood classification

| Spectral class cont. | Description cont.                              |
|----------------------|--|
| 23                   | Groundmass                                     |
| 24                   | Groundmass                                     |
| 25                   | Groundmass and some internal charcoal material |
| 26                   | Edges of charcoal                              |
| 27                   | Groundmass                                     |
| 28                   | Edges of charcoal                              |
| 29                   | Edges of charcoal                              |
| 30                   | Internal area of charcoal                      |

Table 2.7 cont.

Using the spectral classes listed above the spatial distribution of each spectral class was examined and subjectively assigned to informational groups (table 2.8, fig 2.25).

| Spectral classes                      | Informational group             |
|---------------------------------------|---------------------------------|
| 1, 2, 3, 4, 5, 6, 10, 16, 18          | Mineral material (blue overlay) |
| 7, 12, 17, 19, 20, 21, 23, 24, 25, 27 | Groundmass (yellow overlay)     |
| 28, 29, 30                            | Charcoal (red overlay)          |
| 8, 9, 13, 14, 15, 22, 26              | Voids (green overlay)           |
| 11                                    | Bone (pink overlay)             |

Table 2.8 Spectral groups allocated to informational classes for the classified image of Whitlb

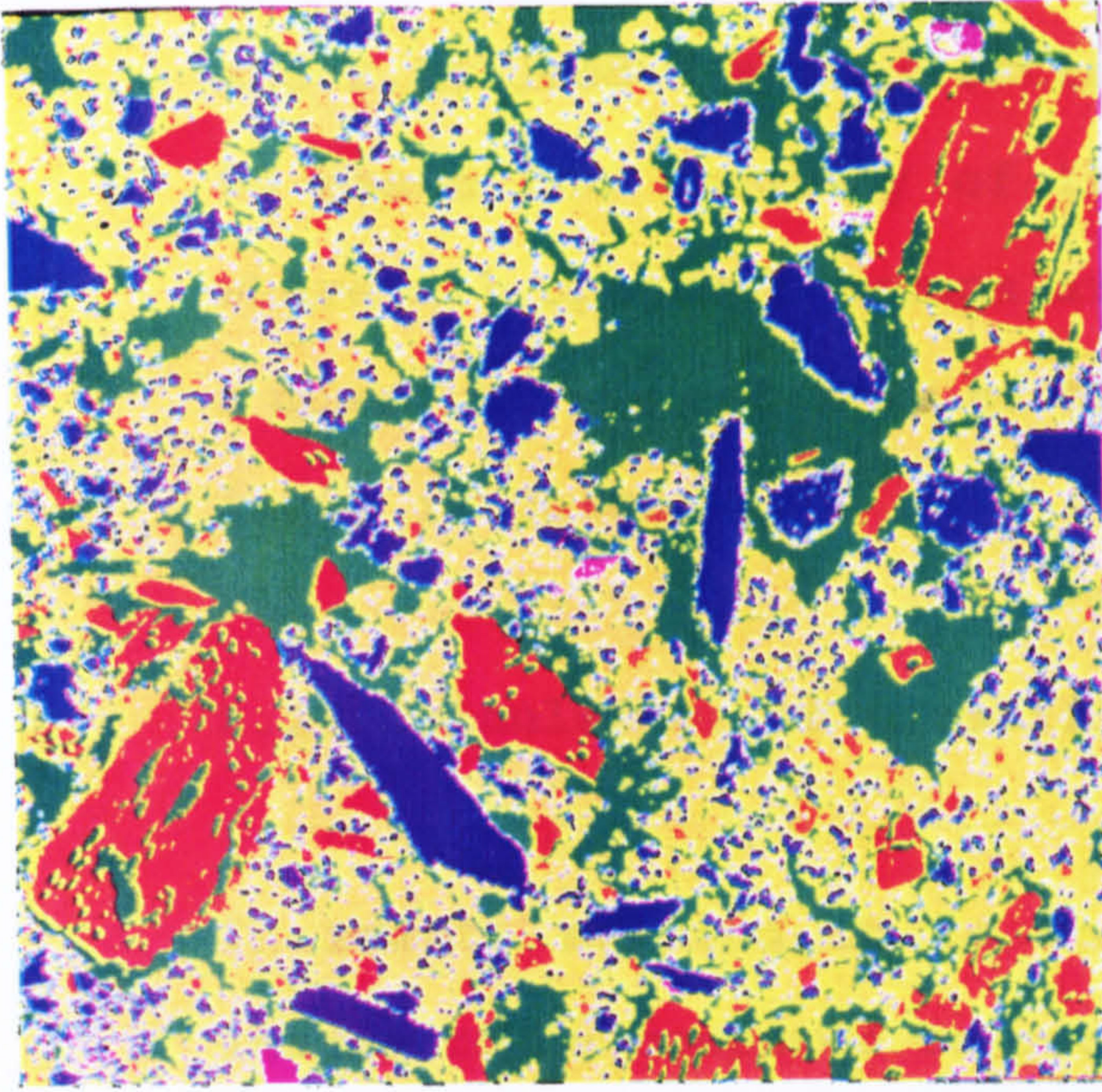


Fig.2.25 Classified image of Whit1b, FL 2.2cm

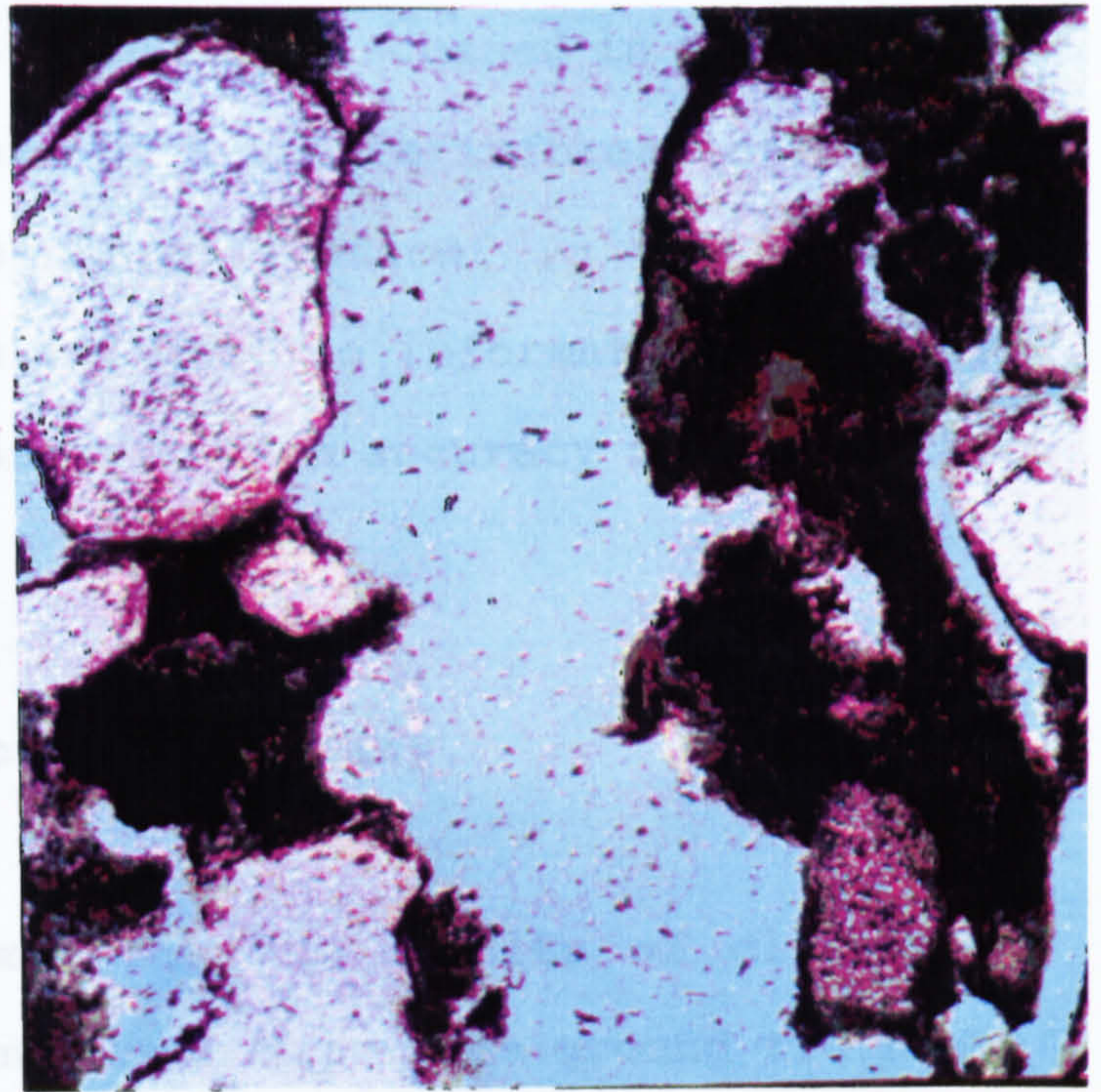


Fig.2.26 Watershed classification of L164com, FL760µm

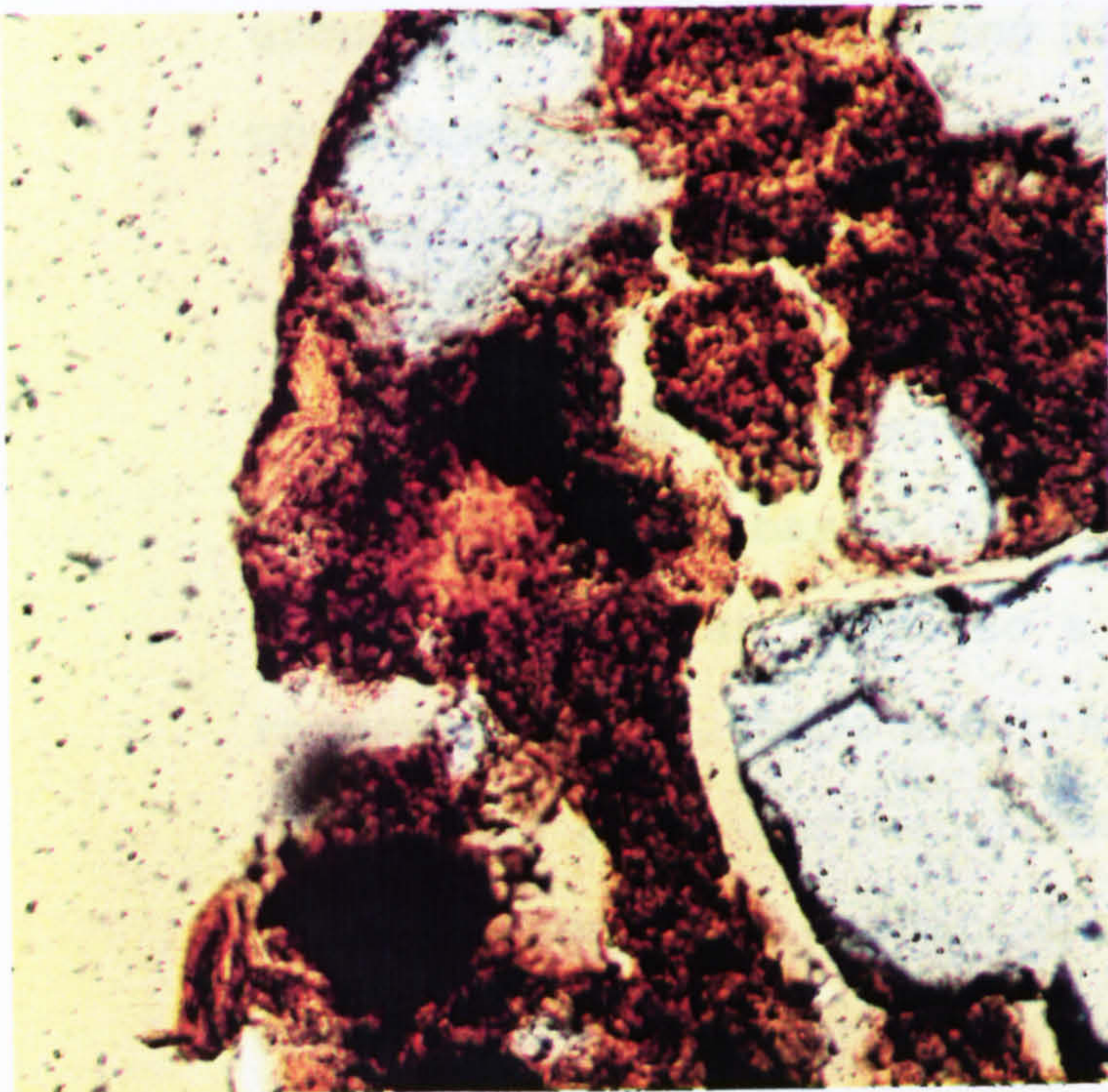


Fig.2.27 Detail of L164com taken using the Olympus microscope, FL 400µm

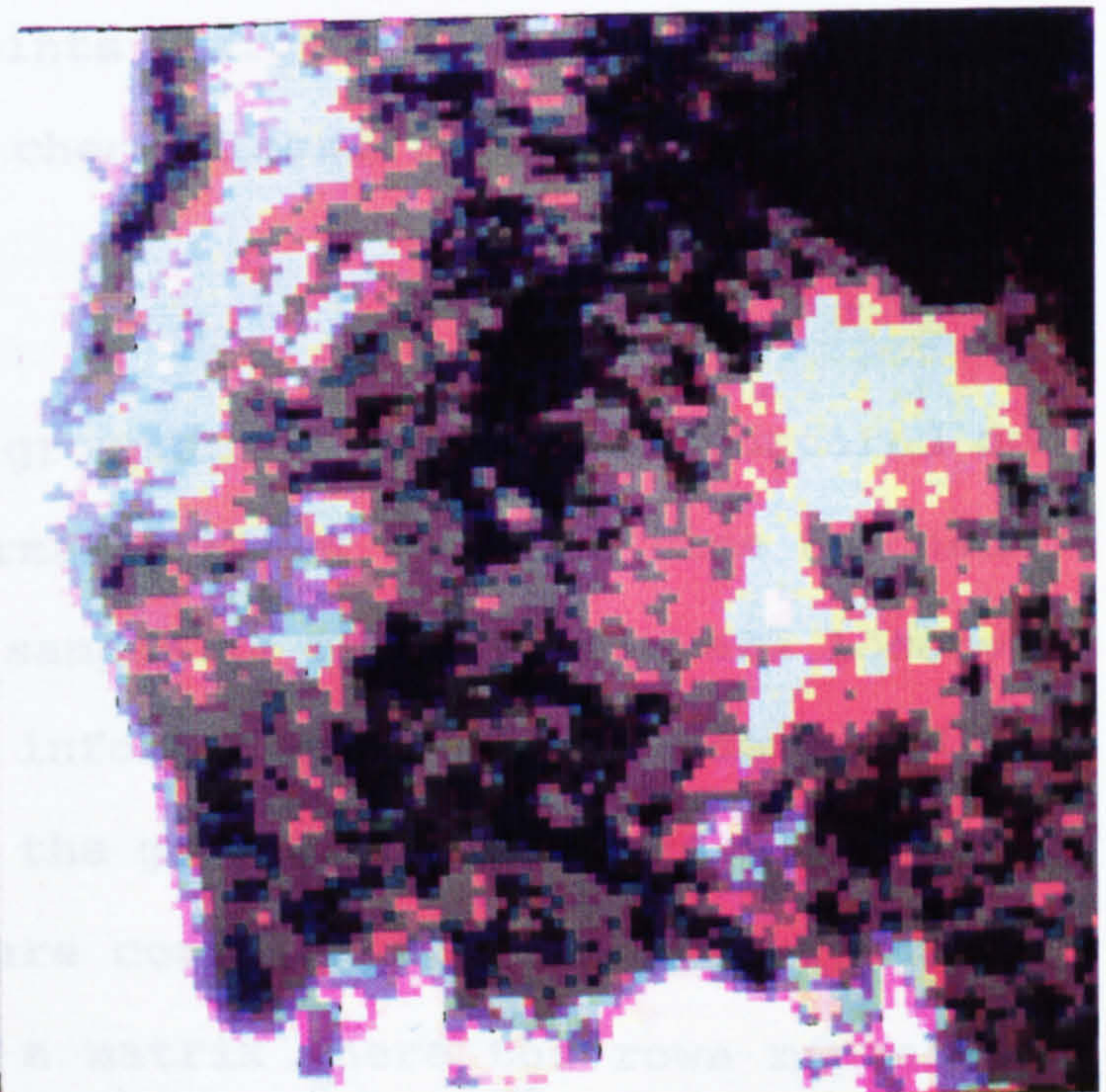


Fig.2.28 Detail of an area of L164com after a watershed classification

The examples of spectral classification discussed in section 2.12 and 2.14 used a visual estimate of a single informational group to assess the accuracy of the classification. In this example, where all spectral groups are assigned to informational groups, a quantitative estimate of classification accuracy for the entire image is calculated.

#### **2.16 Calculation of classification accuracy.**

In remote sensing it is common for the results of classified images to be compared to ground truth maps. The ground truth map can be derived from a number of different sources including images that are obtained at a higher resolution than the classified image, aerial photographs or observations on the ground at selected sampling points. Large scale (1:20,000) aerial photographs are often used to check classifications derived from Landsat images (Jensen 1986).

The classified image and the groundtruth map can be compared on a pixel by pixel basis. It normally takes too much time to check every pixel in an image so a sample is used. Pixels are located randomly on the image and the informational group is compared to the actual class derived from the ground truthing exercise. Data derived from this operation are compiled to form a contingency or confusion matrix. This is a matrix where the rows represent the ground truth classes and the columns the informational groups. Jensen (1986) suggests that one of the most useful attributes of contingency tables is the ability to be able to

define errors of commission and omission. Errors of omission are spectral groups of class (i) being labelled as members of another class. Errors of commission are pixels that belong to members of another class being labelled as members of class (i) (Mather 1987).

Mather (1987) states that the actual percentages derived from a confusion matrix should not be treated literally. They are results based upon a sample of a finite population. It is necessary to evaluate confidence limits to calculate the amount of error that might have resulted from the placement of random samples.

Mather (1987) suggests that the distribution of accuracy values can be summarised by a binomial probability distribution which allows the evaluation of confidence limits. The probability employed and the sample size affect the upper and lower confidence limits. A formula for the evaluation of a lower confidence limit for a specific classification accuracy obtained from N samples is;

$$s = P - \left[ z \sqrt{\frac{PQ}{N}} + \frac{50}{N} \right]$$

z is the (100 - r) / 100 th point of the standard normal distribution. P is the apparent classification accuracy, Q is 100 - P, N is the number of samples (Jensen 1986, p.228 in Mather 1987, p.326).

A ground truthing exercise was carried out to check the classification accuracy of Whit1b. The classified image represents a 2.2cm field of view. A random number generator was used to create the x and y co-ordinates of pixel locations. Observations through the Olympus microscope were used to determine what feature was present at each location. This information was then compared to the classified image. This procedure is directly analogous to checking the classification accuracy of satellite imagery using ground observations or aerial photographs.

#### 2.17 Confusion matrix for Whit1b.

A confusion matrix was constructed to examine the classification of Whit1b (table 2.9). The row labels represent the information obtained from the ground truthing exercise. The column labels are the results of the classification. For example, in the first row, labelled groundmass, there are 100 points which are correctly identified. However 4 points, which should have been groundmass, are labelled mineral and 3 points are labelled charcoal.

| class label/ G.T. | Gmass | Min | Void | Bone | Char | Total Points | % cor. |
|-------------------|-------|-----|------|------|------|--------------|--------|
| Gmass             | 100   | 4   | 0    | 0    | 3    | 107          | 96.40  |
| Min               | 0     | 36  | 0    | 0    | 0    | 36           | 90.00  |
| Void              | 8     | 0   | 58   | 1    | 0    | 67           | 86.57  |
| Bone              | 1     | 0   | 0    | 2    | 0    | 3            | 100    |
| Char              | 2     | 0   | 0    | 0    | 35   | 37           | 97.37  |
| Total             | 111   | 40  | 58   | 3    | 38   | 250          |        |

Table 2.9 Confusion matrix for Whit1B



## 2.18 Interpretation of the confusion matrix

The overall classification accuracy is 92.4%. Using the method for calculating classification accuracy described in section 2.16 the lower 95% confidence limit is 89.44%. A more detailed inspection of the confusion matrix shows that voids are being under classified. Of the total number of groundtruth classes that are actually void only 86.6% are accurately identified. Using this sample of 250 points there is no feature incorrectly labelled void.

Initially the classification accuracy of voids appears quite low. This does not take into account the reasons for the misclassifications. Table 2.10 shows each misclassified pixel with the corresponding groundtruth class. Four examples are the result of voids which are small compared to the resolution of the image. Four examples are the result of pixels located at the edge of objects. There is only one example of a void being properly misclassified.

These results suggest that before any classification is carried out the analyst should be aware of the size of feature that can be recognised for a given magnification and resolution. Features only visible at the limits of the sensor resolution are likely to be misclassified owing to mixed pixels. It is suggested that checking should be restricted to those areas which are separated from the road edge or any other similar clearly non-homogenous

ground cover classes by at least 1 and preferably 2 pixels (Thomas et al 1987).

There are obvious disadvantages to not including mixed pixels in the final classification result. If the image includes a large amount of detail, and objects are small, ignoring misclassifications will greatly increase the final classification accuracy. A better method might be to record all the instances of samples falling on mixed pixel classes in a separate column, but do not include these in the final classification results. If the amount of samples located on areas of mixed pixels is large with respect to the number of samples taken it might be concluded that the resolution of the image is unsuitable for the differentiation of selected features.

| co-ordinate | Class      | Ground truth label | Description                               |
|-------------|------------|--------------------|---|
| 55, 502     | Groundmass | Void               | Void measuring 40 $\mu$ m across.         |
| 396, 448    | Bone       | Void               | Edge pixel.                               |
| 290, 242    | Groundmass | Void               | Narrow neck of void, 60 $\mu$ m wide.     |
| 507, 91     | Groundmass | Void               | Edge pixel.                               |
| 144, 81     | Groundmass | Void               | Edge of void and mineral.                 |
| 194, 460    | Groundmass | Void               | Void 40 $\mu$ m wide.                     |
| 464, 187    | Groundmass | Void               | Edge pixels.                              |
| 453, 205    | Groundmass | Void               | Edge of void measuring 20 $\mu$ m across. |
| 361, 82     | Groundmass | Void               | Void                                      |

Table 2.10 Comparison of classified label and the ground truth class

| G. T.  | Errors of omission |      | Errors of commission |      |
|--------|--------------------|------|----------------------|------|
|        | Total              | %    | Total                | %    |
| G.mass | 7/107              | 6.5  | 11/107               | 10.3 |
| Min    | 0/36               | 0    | 4/36                 | 11.1 |
| Void   | 9/67               | 13.4 | 0/67                 | 0    |
| Char   | 2/37               | 5.4  | 3/37                 | 8.1  |

Table 2.11 Details the errors of commission and omission for the classification of Whitlb.

Of the 250 random samples 107 are classified as groundmass (table 2.11). 11 observations are errors of commission and 7 observations errors of commission indicating that the groundmass is overclassified. Minerals are also overclassified, there are 4 errors of commission and no errors of omission. Bone is not included in this table as only 3 of the random points actually fell on the class that is bone. This is not a high enough sample number to base any valid conclusions on.

This technique of assessing classification accuracy has not been applied before to classification of soil thin section images. It is useful because it provides a method of making a statistical evaluation of the classification results. Using the errors of commission and omission it is also possible to determine the reasons for misclassification. There are two main drawbacks to using this method.

1. The method is very time consuming. This may or may not be a problem depending on the reasons for the initial investigation. If the object of the analysis is to examine the spectral variability of a limited number of thin sections then this method

of checking might be useful. A statistical evaluation of classification accuracy is particularly useful if different classification techniques are compared. If, however, the purpose of the investigation is to determine object measurements of features in a large number of images then the length of time it takes to prepare a confusion matrix might be prohibitive. An important advantage of using image analysis is the speed that operations can be carried out. If the procedures devised include lengthy manual checking of the results then other methods of analysis might be more suitable.

2. This technique does not give any information about the effect of misclassification on object measurements. For instance a small increase in the number of pixels wrongly classified could have a large effect on an object measurements.

Misclassifications tend to occur for one of two reasons. Firstly, there is not enough spectral information to discriminate the object of interest. Secondly, mixed pixels at the edges of objects create new spectral groups. Misclassification of object edges is important because it can result in separate objects being joined together invalidating an object measurement analysis. If the purpose of the investigation is to measure the morphological characteristics of features in the thin section, a visual checking of the classified results followed by post classification processing is a more appropriate way of checking the classification.

## 2.19 Non parametric classification techniques.

There are many types of classification techniques. Distinctions can be made between supervised and unsupervised routines (section 2.8). Another distinction is to consider the algorithms that are used to carry out the classifications. The maximum likelihood classification is an example of a parametric classification technique.

The basis of parametric methods is the use of a probability distribution to assign specific  $n$  dimensional vectors to spectral classes. The data that represents the spectral classes can be derived from either training areas or a clustering algorithm. Each pixel, represented by a vector  $\underline{x}$ , is assigned to a class for which its probability of membership is highest. Statistical measures normally used include mean, standard deviation and variance / covariance. It is assumed that the training data can be represented by multi-normal distributions in  $n$  dimensional data space (Watson 1987). It is suggested that;

'No attempt is ever made to justify either theoretically or empirically the validity of such an assumption. The normal assumption is most certainly always wrong, both a priori and empirically', (Watson 1987, pg. 15).

Watson also states that the presence of mixed pixels will blur the edges of the normal distribution and he suggests a pattern

recognition approach is necessary that does not make any a priori assumptions about the data.

A program called the Watershed classification, written by Dr. Watson (Stirling University) is such an approach. It does not make any assumptions about the original data in the image. Pixels are assigned to classes based on the property of connectivity using the watershed algorithm of Lantuejoul (1978) and Beucher and Lantuejoul (1979). The classification works in 2 dimensions but it is suggested that the classification can either be applied to all possible pairs of bands and the results combined, or a data reduction transformation be used prior to analysis (Watson 1990). The first method was applied in this study.

#### **2.20 Use of the Watershed classification routine to classify soil thin section images.**

The three bands described in section 2.9 were assigned to an unsupervised watershed classification. An output of 20 classes was specified. The watershed classified each pair of bands separately resulting in an output of 3 images each classified to 20 classes. The 3 classified images were displayed as a composite image (fig 2.26). The data was contrast stretched to allow a visual analysis of the results.

An inspection of fig 2.26 shows that the quartz material and voids do not consist of pure spectral classes. There are many flakes of material within the void space and there is uneven

staining of the voids. The edges of many quartz grains are classified as pink. The classification differentiated much detail in the groundmass. Fig 2.27 shows a detail of the classified image taken using the Olympus microscope and an Olympus OM4 35mm format camera. A comparison of the classified image and the photograph shows that the classification has accurately isolated humified organic material (classified as black), two types of organic fine material, (classified as green and orange), and the majority of the groundmass material (brown).

This result shows benefits of using classification to discriminate fine detail in the image. Although there was not time in this study, it would have been of considerable interest to see how an analysis using a microprobe correlated with the results of the spectral classification.

The main problem with using this classification method is the result is based on the analysis of a 3 band composite image so each pixel is described by a 3 dimensional vector. For instance the orange material in fig 2.28 is composed of two vectors, (11,7,4) and (11,7,5). In this case it is relatively easy to isolate the individual vectors. This is not the case where there is more spectral variation within the informational groups. Although the recognition of spectral variation is an important result itself, it becomes difficult for the analyst to create binary images of specific features in preparation for further morphometric analysis. The watershed classification did not reduce the number of bands during the classification but it

produced three images each displaying 20 classes. If the three classified images are displayed as a colour composite numerous combinations of values at each pixel location are possible. It is difficult to identify single discrete classes using the classified composite image because each pixel label is unique and is independent of the value of its neighbour. This means small variations in the colour of the image might represent different classes.

The individual classified images were examined to see how much information was represented in one band. The classification of the red and blue bands produced the best discrimination of the groundmass and a classification of red and green bands the worst. Each spectral class was examined using the results from a classification of the red and blue bands (table 2.12).

Some of the classes visible on the classified composite image are not differentiated using this single band. For instance the central green and orange areas, visible on the composite image, are allocated to just one class. This means that the best discrimination is present when the 3 band classified composite image is used.

In summary, there is maximum differentiation of features when a composite classified image is displayed. This agrees with conclusions by Watson (1987). However if the purposes of the investigation is morphometric analysis, it is difficult to determine the vectors that correspond to specific features,



making the production of binary images difficult. It might have been possible to reduce the dimensionality of the data prior to classification but there was not time to fully investigate this possibility.

| Spectral class | Description   |
|----------------|---|
| 1              | Central area of humified material                             |
| 2              | Main edges of humified material                               |
| 3              | Edges of humified material                                    |
| 4              | Groundmass  |
| 5              | Groundmass type 1   |
| 6              | Groundmass  |
| 7              | Groundmass type 2   |
| 8              | Carborundum and some areas of groundmass                      |
| 9              | Carborundum   |
| 10             | Lighter orange areas in the groundmass                        |
| 11             | Quartz  |
| 12             | Quartz  |
| 13             | Carborundum within void, edges of void and weathered material |
| 14             | Void  |
| 15             | Edges of quartz   |
| 16             | Quartz  |
| 17             | Quartz  |
| 18             | Void  |
| 19             | Quartz  |

Table 2.12 Description of the spectral classes of 1164com produced using the Watershed Classification.

## 2.21 Image quantification

In image analysis, image classification might only be part of the overall study. After an image has been accurately classified, a binary image can be produced that corresponds to a specific feature. The feature might be labelled 1 and the background 0.

Morphological measurements can then be applied to measure specific attributes.

Measurements of attributes can generally be divided into two categories. Firstly field measurements are calculations based on the whole of the image. If voids are represented as 1 and groundmass as 0 in a binary image, a field measurement of area would calculate the total area of void in the image. Secondly object measurements recognise individual objects and will measure each one separately. The number of attributes that can be measured depends on the software that is available to the analyst.

With the advent of relatively low cost powerful P.Cs. image analysis software is becoming available to a wider range of users. For example PC\_Image is an image analysis software package produced by Foster Findlay. It contains a wide range of field and object measurements including area, centre of area, perimeter, circularity, length, breadth, orientation, and feret diameters at angles of 0, 45, 90 and 135°. Any range of measurements can be applied to a set of objects. The results can then be used to classify the objects on the basis of morphological criteria.

Object measurements can be further subdivided into basic measurements and derived measurements. Basic measurements are the result of a direct analysis of the objects in an image, for example area and perimeter. Derived measurements are combinations of basic measurements which can be used to analyse objects in

more detail. For instance, measurements of area and perimeter can be combined to create an index of shape. Russ (1990) describes comprehensive procedures for the measurement and analysis of images.

The spatial distribution of features can also be studied if binary images are created. 1-D measurements including length and intercept density can be made along test lines (Ringrose-Voase 1991). McBratney and Moran (1990) and Moran et al. (1990) developed an imaging system called Solicon. This system was used to generate depth functions of structural parameters in surface soils (Ringrose-Voase 1991).

## **2.22 Morphometric analysis equipment at Stirling**

In February 1991 a software package called Hips was purchased from the Turing Institute, Glasgow. This package had extensive shape classification utilities. In Glasgow the package runs on a Sun workstation under Unix. Ten months were spent trying to run the software on Hewlett Packard machines at Stirling University without success. As an alternative, R-Chips was used to measure total area of features and IDRISI was used for object measurement of area and perimeter.

An automated procedure was written for IDRISI that measures certain morphological criteria. The results were output to an Ascii file format allowing manipulation in spreadsheets and statistical packages. Before the procedure could be used a binary

image had to be created depicting the feature of interest. This image was created using an unsupervised maximum likelihood classification routine followed by manually editing to remove noise and any features touching the border of the image.

The automated routine was written to process the binary image, fill holes in any of the objects, delete any objects smaller than 5 pixels, count the number of objects remaining and finally calculate area measurements on an object by object basis. A separate program was run to measure perimeters of objects. When this program was operating IDRISI was run in the background using Windows (version 3.0). This allowed the computer to be used for other purposes during the 5 hours it took for the procedures to be completed.

### **2.23 Stages in the automatic measurement of object area**

1. The binary image was processed using a module called reclass. This was used to produce an image with all the voids labelled with an integer value of 1 and the background an integer value of 0. The image was given a name BBB.

2. At a later stage in the processing an image was needed with voids labelled 0 and background 1. This was created using reclass and called CCC.

3. A program called Group was used to identify all those areas in the image that constituted contiguous groupings of pixels,

i.e. all those labelled with 1, and assigned each one a unique integer identifier. This also labelled holes in voids with integer identifiers. Point 5 explains how holes in voids were removed. The input to this program was an image called BBB and the output DDD.

4. It was necessary to make the void labels start from 2 rather than 1. A scaler module was used to add one to DDD and the results were saved into ADD1. This was necessary because the overlay module used in point 5 reset the background value to 1. If the void labels had started from 1, then the first void would have been lost.

5. An Overlay module was used to remove all the holes from voids in the image. The Cover operation from the Overlay module was used. Two images had to be specified. If the value in the first image was 0, the value in the second image remained unaltered. Any other value in the first image replaced the value in the second image. The image CCC was specified as the first image and ADD1 was specified as the second image. This produced an image called EEE where all the holes in the voids and the background had been labelled with the integer 1.

6. All the voids were now removed which had a value of 5 pixels or less. A module called Area was used to measure the number of pixels in each cell. This was stored as an image file called FFF where each cell was identified by an integer corresponding to area. As the holes were measured separately their value had to

be reset to 1. This was done using the Overlay and Cover options as before and result was saved into FFF.

7. Reclass was then used to assign all labels with a value 0 - 5 to the value 1 so removing all cells with an area of less than 5 pixels. The results were stored in GGG.

8. Each area was then given an integer code. The results were saved in HHH. Overlay was used again to remove any holes and the results saved in III. The areas and perimeters of the remaining cells could now be measured and the results output to an Ascii file allowing incorporation into other spreadsheet or statistical packages.

Basic measurements of area and perimeter can be combined using the statement;

$$\frac{4\pi AREA}{PERIMETER^2}$$

This produces a dimensionless number called formfactor (Russ 1990). A perfect circle has a formfactor of 0 (fig 2.29). Any other shape has a greater perimeter for the same area. The formfactor describes this relationship. A square has a formfactor of 0.785. As the shape being measured becomes more irregular the value for the formfactor gets lower. Russ (1990) cites the example of a many petalled flower having a formfactor of 0.05 or less.

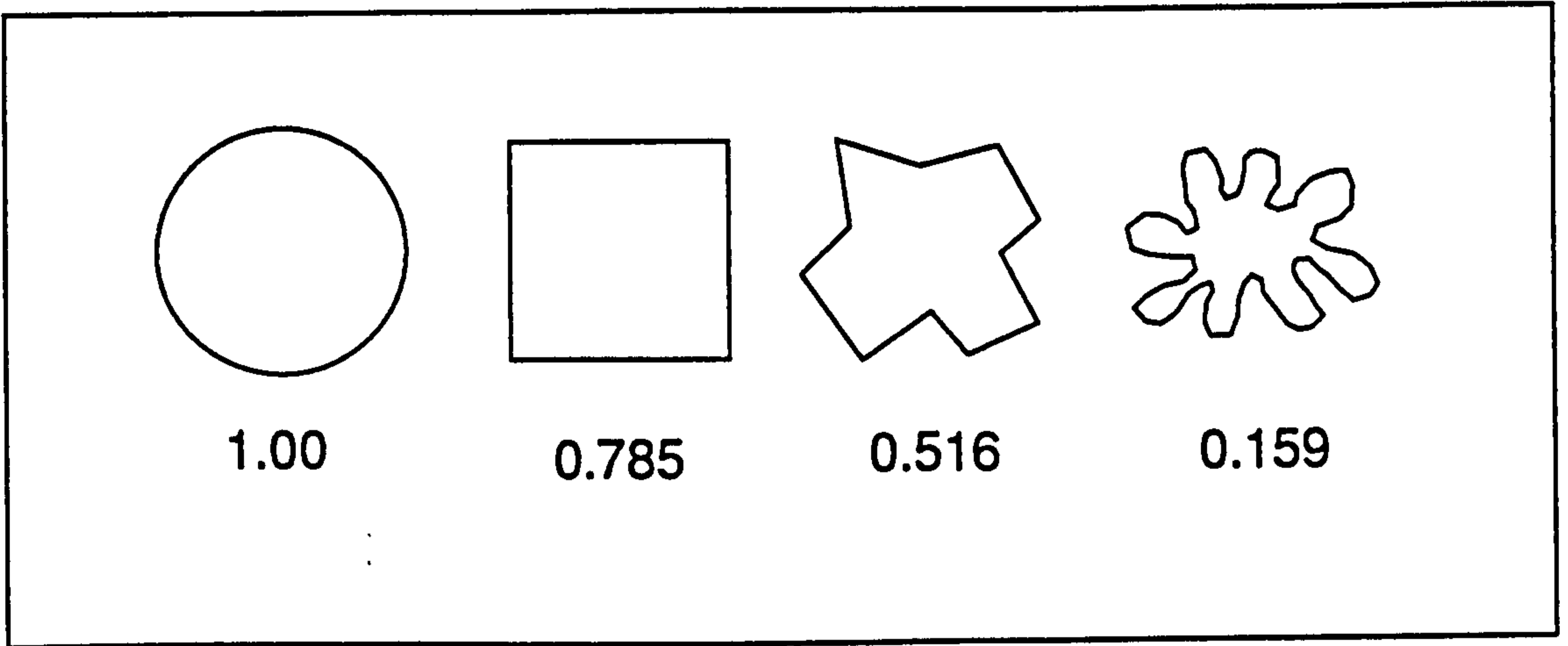


Fig. 2.29 Formfactors of 4 basic shapes  
(after Russ 1990)

Spatial variation in features could be quantitatively analysed. A 512 x 512 binary image was converted to an Ascii file format using the data conversion facility in IDRISI. The data was then imported into a statistical analysis package called Minitab running on the university mainframe under Unix. The data could then be manipulated on a row by row basis. For instance the sum of each row was calculated plotted on a graph to show the vertical distribution of void area. This technique of spatial analysis could be extended to any feature described by a binary image.

#### **2.24 Post classification processing**

Post classification processing is the removal of unwanted effects that occur as a result of classification. The methods used, in any study, depend on the software that is available to the analyst and the specific problems caused by the classification process. The simplest technique is for the analyst to interactively edit the classified image. A 32 bit graphics board allows accurate editing of classified features. A binary image can be produced, overlaid onto the original colour composite image, which is used as reference data, and manually edited. Accurate results can be produced in this way but the process is time consuming. The technique is only suitable if the features that have been classified are clearly visible on the colour composite image.



Another method is to use digital filters to automatically remove unwanted effects from classified images. Grey scale images contain a parameter called spatial frequency. This is defined as;

'The number of changes in brightness value per unit distance for any particular part of an image,' (Jensen 1986, pg.138).

High frequency detail occurs when there are large changes in brightness values over a given area. A low frequency area occurs when there are few changes in brightness. Digital filters operate by passing a kernel over the image (fig 2.30).

|    |    |    |
|----|----|----|
| C1 | C2 | C3 |
| C4 | C5 | C6 |
| C7 | C8 | C9 |

Fig. 2.30 3 X 3 digital filter

C<sub>1</sub> to C<sub>9</sub> represent values that can be set by the analyst. The brightness value of the pixel located in the centre of the kernel is modified by a function of its neighbours. The image produced is affected by the function defined by the analyst. For instance an averaging filter gives equal weight to each value within the kernel and replaces the value of central pixel with the average of all 9 neighbours.

$$\frac{\sum a, b, c, d, e, f, g, h, i}{9}$$

where a to i represent the brightness values of pixels located in a 9 x 9 kernel as follows

|   |   |   |
|---|---|---|
| a | b | c |
| d | e | f |
| g | h | i |

Fig. 2.31 Co-ordinates in a 9 x9 kernel

The end product of a filtration is a new image in which the spatial frequencies have been altered. Features that remove high frequency detail are referred to as low frequency filters and those that emphasise the high frequency detail are high frequency filters. A hypothetical example is described to illustrate the effect a low frequency filter has on an object in a binary image.

Fig 2.32 illustrates 6 rows and 6 columns of a hypothetical binary image. The 1s in the image indicate the location of an object. The result of an averaging filtration, with each position in the kernel set to 1 and a scaling factor of 1, is the complete removal of the object (fig 2.33).

|   |   |   |   |   |   |
|---|---|---|---|---|---|
| 0 | 0 | 0 | 0 | 0 | 0 |
| 0 | 0 | 0 | 0 | 0 | 0 |
| 0 | 0 | 1 | 1 | 0 | 0 |
| 0 | 0 | 1 | 1 | 0 | 0 |
| 0 | 0 | 0 | 0 | 0 | 0 |
| 0 | 0 | 0 | 0 | 0 | 0 |

Fig 2.32 Grid representing a sample of pixels within a binary image

|   |   |   |   |   |   |
|---|---|---|---|---|---|
| 0 | 0 | 0 | 0 | 0 | 0 |
| 0 | 0 | 0 | 0 | 0 | 0 |
| 0 | 0 | 0 | 0 | 0 | 0 |
| 0 | 0 | 0 | 0 | 0 | 0 |
| 0 | 0 | 0 | 0 | 0 | 0 |
| 0 | 0 | 0 | 0 | 0 | 0 |

Fig. 2.33 Sample of pixels after a low pass filtration

If the object was larger (fig 2.34) only the corners are effected by the filtration (fig 2.35).

|   |   |   |   |   |   |   |
|---|---|---|---|---|---|---|
| 0 | 0 | 0 | 0 | 0 | 0 | 0 |
| 0 | 0 | 0 | 0 | 0 | 0 | 0 |
| 0 | 0 | 1 | 1 | 1 | 0 | 0 |
| 0 | 0 | 1 | 1 | 1 | 0 | 0 |
| 0 | 0 | 1 | 1 | 1 | 0 | 0 |
| 0 | 0 | 0 | 0 | 0 | 0 | 0 |
| 0 | 0 | 0 | 0 | 0 | 0 | 0 |

Fig 2.34 Sample of 7 x 7 pixels of a binary image

|   |   |   |   |   |   |   |
|---|---|---|---|---|---|---|
| 0 | 0 | 0 | 0 | 0 | 0 | 0 |
| 0 | 0 | 0 | 0 | 0 | 0 | 0 |
| 0 | 0 | 0 | 1 | 0 | 0 | 0 |
| 0 | 0 | 1 | 1 | 1 | 0 | 0 |
| 0 | 0 | 0 | 1 | 0 | 0 | 0 |
| 0 | 0 | 0 | 0 | 0 | 0 | 0 |
| 0 | 0 | 0 | 0 | 0 | 0 | 0 |

Fig 2.35 Sample of 9 x 9 pixels after a low pass filtration

Although the larger object has not been removed the shape of the object has been effected to some extent. To restore the original

shape the filtered image could be filtered again increasing the scaling factor so the product of the nine values is greater than 1 when the central pixel is over one of the old edges. In this case the a scaling factor of two would work (fig 2.36).

$$\frac{\sum a, b, c, d, e, f, g, h, i}{9} \times 2$$

Fig 2.36 An averaging filter and a scaling factor of 2.

It is possible to use filtration techniques in this way to modify the informational groups derived from the classification. The output of the filtration depends on the type and size of filter used. If the purpose of the analysis is the morphometric measurement of objects then care must be taken to ensure that the filtration does not cause any significant morphological changes. The shape created by a group of pixels influences object shape to a greater extent the smaller the object is. The results presented in this study have relied on a visual assessment of the effect of digital filters. Clearly there is need for quantification of this possible source of error.

## **2.25 The use of image processing techniques to enhance features seen in thin section.**

Most research, concerned with soil micromorphology and image analysis, has concentrated on applying quantitative morphological measurements to soil thin section slides. Another approach is to use contrast enhancement techniques to clarify features that are

normally indistinct, thus improving the qualitative information available to the analyst.

Enhancing an image generally means altering its appearance in such a way that the analyst can interpret the image with greater confidence. This implies that the results are judged subjectively. Specific enhancements will depend on the requirements of the analyst and will be affected by the distribution of data in the image. Consequently the use of a particular technique for a given situation will often be arrived at by trial and error. This section begins with a brief description of contrast enhancement techniques and then examine how these can be applied to images of soil thin sections.

#### **2.26 Linear contrast stretch**

One of the most basic enhancement techniques is the linear contrast stretch. An image is represented by a finite number of grey levels, the number depending on the hardware and software being used. Many image capture facilities are 8 bit allowing 256 grey levels to be distinguished. Although image data can have any value between 0 and 255 the actual digitised values are normally well within these limits.

If the data does not occupy the complete displayable range the result is a dark image lacking in contrast. Small differences in grey levels are not visible. Pixel values can be reassigned so that the entire range (0-255) is used for display. This process

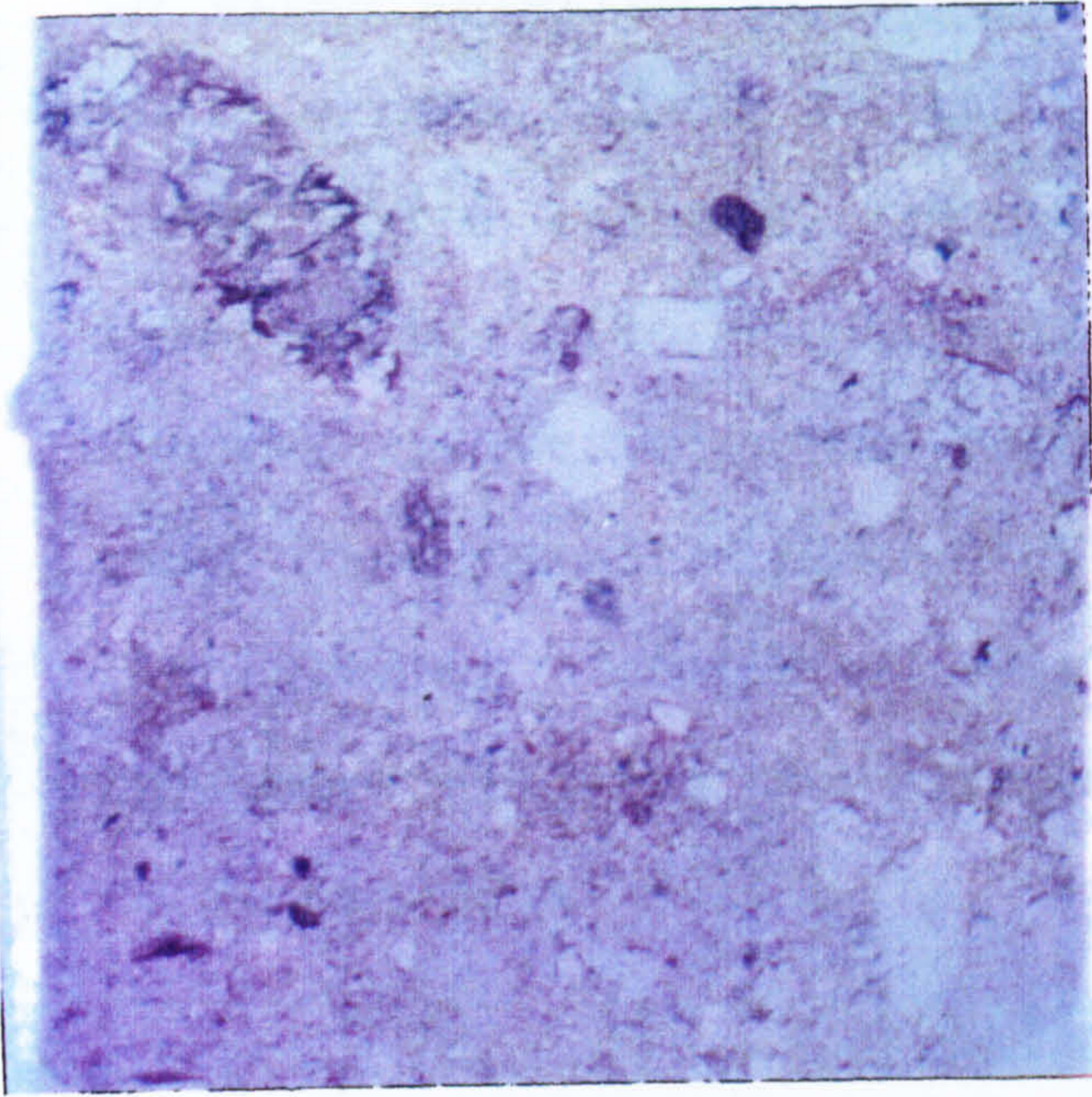


Fig.2.37 Colour composite of M505, S3, no contrast stretch, whole slide

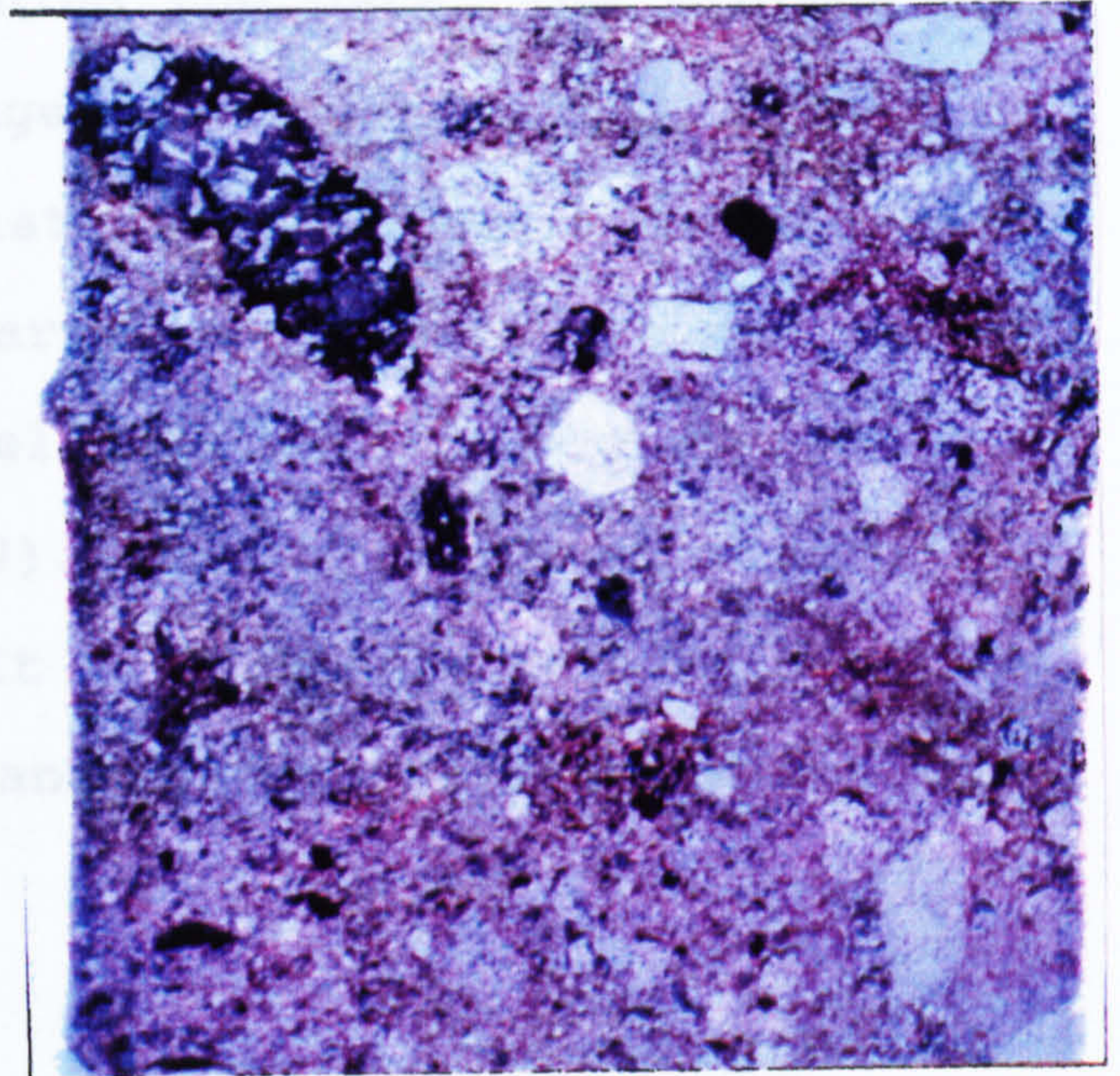


Fig.2.38 Colour composite of M505, S3, ACS, whole slide

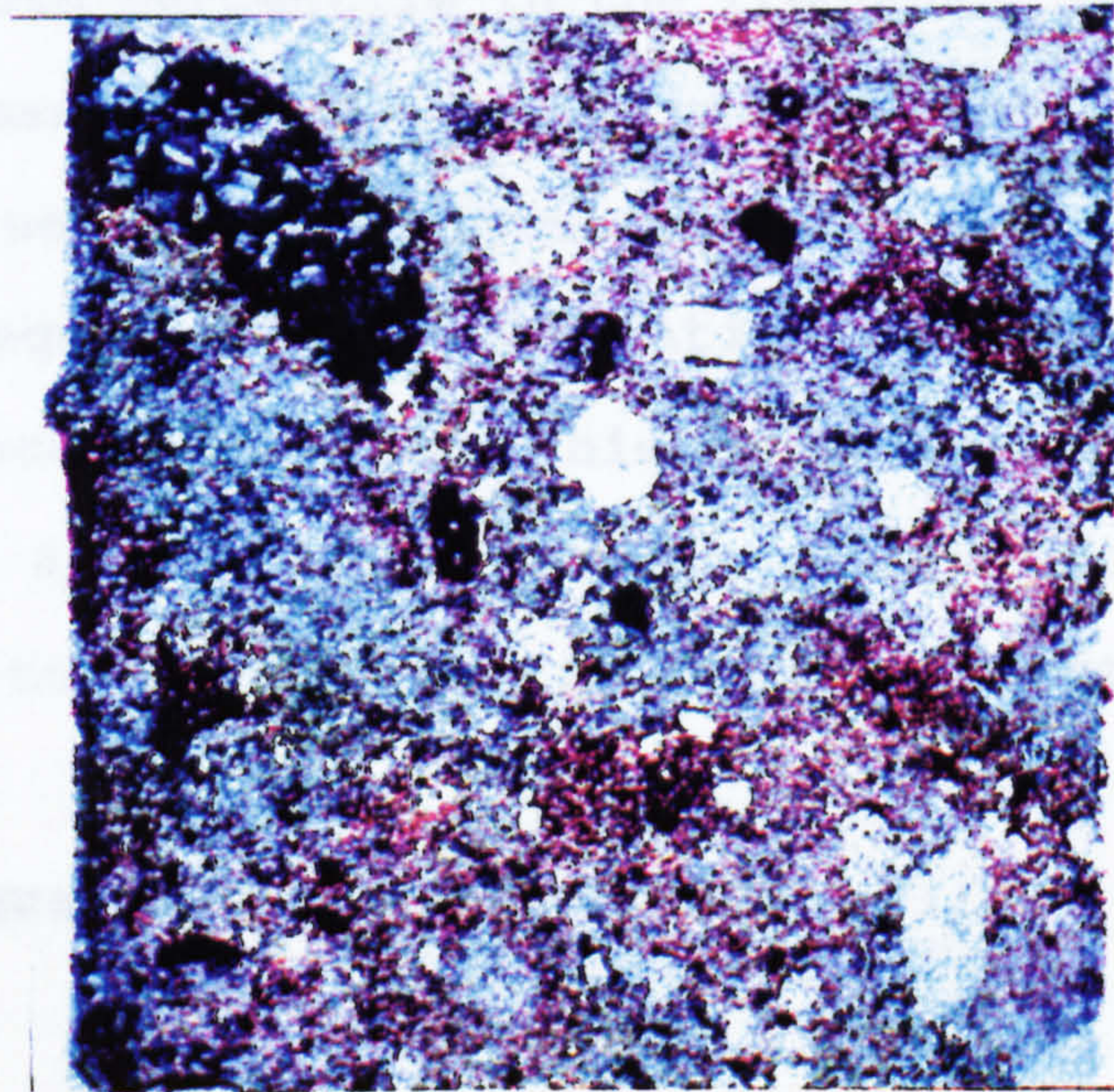


Fig.2.39 Colour composite of M505, HES, S3, whole slide

is often referred to as stretching the data. The minimum and maximum data values in the image are reset, using a look up table, to 0 and 255. Intermediate values remain in the same relative position, but are linearly mapped onto the new range. The central value in the original data will now be mapped to a grey level of 127 (Mather 1987). Colour images are normally displayed as 3 separate bands. It is necessary to consider each band separately as the minimum and maximum values are unlikely to be the same.

Digitised images can contain stray values located away from the main body of data. In such a case, if only the maximum and minimum values are considered, a less than optimum contrast stretch will result. A method of overcoming this problem is to use the 5th and 95th percentile in the frequency distribution of the data as the maximum and minimum values. The data that lies between these values is linearly mapped to 0 and 255 as before. This operation requires more computation than the maximum and minimum method because the image histogram must be calculated. R-Chips includes an automated version of the linear contrast stretch referred to as an automatic contrast stretch (ACS).

### **2.27 Histogram equalisation stretch (HES).**

A HES uses a cumulative frequency distribution of the input data values to create a new look up table. The target number of output pixels in each class is determined by dividing the total number of pixels in the image by the number of grey levels. Using a



cumulative frequency of the number of pixels in each input class the first value to exceed the target number is found. All values less than this are then assigned to zero. All values less than the target number multiplied by 2 but greater than the target number are set to 1. This process continues until all the classes have been assigned. Using this technique it is possible to have less classes in the output image than in the input image because input classes can be set to the same output value. The effect of this procedure is to reduce the contrast in input classes which have small numbers of pixels and increase contrast where there are large numbers of pixels in the input classes. If the input data are normally distributed then the contrast will be enhanced in the centre of the data range

#### **2.28 User defined contrast stretch.**

The effects of the contrast stretches described previously have been to generally enhance an image. If specific spectral regions of interest can be identified, this approach may not prove satisfactory. An alternative is to apply a user defined stretch to the image. For instance, the analyst might be interested in emphasising the fine spectral differences in darker regions of the image i.e. the areas that correspond to low spectral values. By specifying upper and lower values to be mapped to 0 and 255, narrow spectral regions can be enhanced.

## 2.29 Applying contrast enhancement techniques to images of soil thin sections.

As an example of the way that contrast enhancement techniques can benefit the qualitative interpretation of thin section slides, images were captured of a slide from a buried B horizon. The slide was from the Lairg site and was chosen because it contained complex lenses of material, silt cappings, and translocated ferruginous compounds. All these features are difficult to observe at the macro scale but are readily identified using the microscope. The microscope only gives a relatively small field of view making it difficult to relate visible features to their overall distributions.

Red, green and blue images were captured from the whole of the slide using PTL and the free standing equipment described in section 2.6.2. Blank images were captured for each separate band and the images corrected for uneven illumination. The three bands were then displayed as a colour composite image with no contrast stretch (fig. 2.37). An automatic linear contrast stretch and a histogram equalisation stretch were applied to the image (fig. 2.38 and 2.39).

A visual examination of the results shows that histogram equalisation is the most successful contrast stretch. Different regions on the slide are immediately visible. The red regions indicate areas where the translocation of amorphous compounds has

occurred, and often correspond to areas with inwashes of finer material and the formation of link cappings.

Using R-Chips, ACS and HES can be performed in a few seconds. This makes this technique useful where a quick visual assessment of the slide is necessary and a full classification of the image is not warranted.

### 2.30 Summary

This chapter discusses ways that image analysis can be applied to the study of thin sections. Three areas of interest are identified;

1. Multispectral classification
2. Morphological quantification
3. Spectral image enhancement

The unsupervised maximum likelihood classification is found to be the most suitable for the identification of features, particularly if the object of the analysis is further morphological measurements. The watershed classification is successful at isolating fine detail in the image but feature extraction is difficult owing to the composite nature of the classified image.

The software available, at Stirling University in the Department of Environmental Science, for morphological measurements is

described and procedures for removing noise from classified images discussed. The technique of contrast stretching images to improve the visual appearance of thin section features is considered and applied to one example.

To evaluate the applicability of these techniques, to a real world situation, a case study was carried out. The following 8 chapters describe the thin section analysis on an archaeological site at Lairg in Northern Scotland. The image analysis techniques described in this chapter are used whenever applicable. The final chapter is divided into two halves. Firstly the thin section analysis is concluded and then the usefulness of image analysis evaluated.

## CHAPTER 3

### DESCRIPTION OF LAIRG SITE AND THE THIN SECTION SAMPLING PROGRAMME

#### 3.1 Introduction

The thin section analysis was carried out on a multi-period archaeological site near Lairg in northern Scotland and forms part of a larger palaeoenvironmental study conducted in the area. Other research on the site includes pollen analysis and tephra analysis, as well as extensive excavations undertaken by AOC (Scotland) Ltd.. The thin section sampling programme was devised in close collaboration with AOC using results from previous exploratory excavations.

The study area is a multiperiod site with a chronology of monuments and associated landuse dating from the Neolithic to present day. The diversity of monuments offered the potential for sampling many types of archaeological contexts. The sampling strategy was designed with two main objectives;

1. To answer hypothesis concerned with the origin and development of archaeological contexts (section 3.10).
2. To assess the applicability of the image analysis techniques, described in chapter 2, to an archaeological site investigation.

This chapter is divided into 5 main sections. The first three sections discuss trends in soil development and the effects of anthropogenic activity on pedogenesis. The first section examines general ideas about soil development while the second section considers some ideas about the effects of humans on the soil system. The third section examines evidence for soil development in Scotland. In the fourth section a site description is presented. A discussion of the thin section sampling strategy forms the last part of this chapter.

### **3.2 Trends in upland soil development.**

Soils develop as a result of interactions between environmental factors, these factors include climate, organisms, parent material, topography and time (Keeley 1982, Fitzpatrick 1983, Brady 1990). The effect of humans is considered to be included with organisms. The first four factors interact through time to produce a variety of soil profiles and soil horizons. Some people, including Jenny (1941, in Fitzpatrick 1983), have suggested that the soil forming factors operate as independent variables. Fitzpatrick (1983) disagrees with this and claims that the only true independent variable is time, the others are interrelated to a lesser or greater extent. This is an important point for two reasons. Firstly it affects the way that humans perceive how ecosystems function and secondly it recognises that small disturbances might have effects larger than their magnitude suggests. The relative importance of each soil forming factor varies between localities, in specific areas it might be possible

to recognise those factors that are of greater importance than others (Fitzpatrick 1983).

Consideration of processes are important when examining soil genesis. Duchaufour (1982) identifies three fundamental processes;

1. The formation of surface humus horizons by the incorporation of organic matter.
2. Mineral weathering.
3. The movement of material in a soluble or pseudo-soluble state, or as suspensions, through the profile.

Soil development can be explained by the interaction of these processes and associated controlling environmental conditions (Duchaufour ibid.). Five trends of soil development in the British Isle can be recognised (Keely 1982), these include podzolisation, clay movement, gleying, peat formation and erosion. The importance of these processes during the Holocene has varied with time and geographical location.

The trends in post glacial soil development in the British Isles has been discussed by Keely (1982), Limbrey (1975), Evans (1975), Bridges (1978), Simmons and Tooley (1981) and Askew et al. (1985). There is much debate about the direction of soil development in the uplands. Askew et al (ibid.)

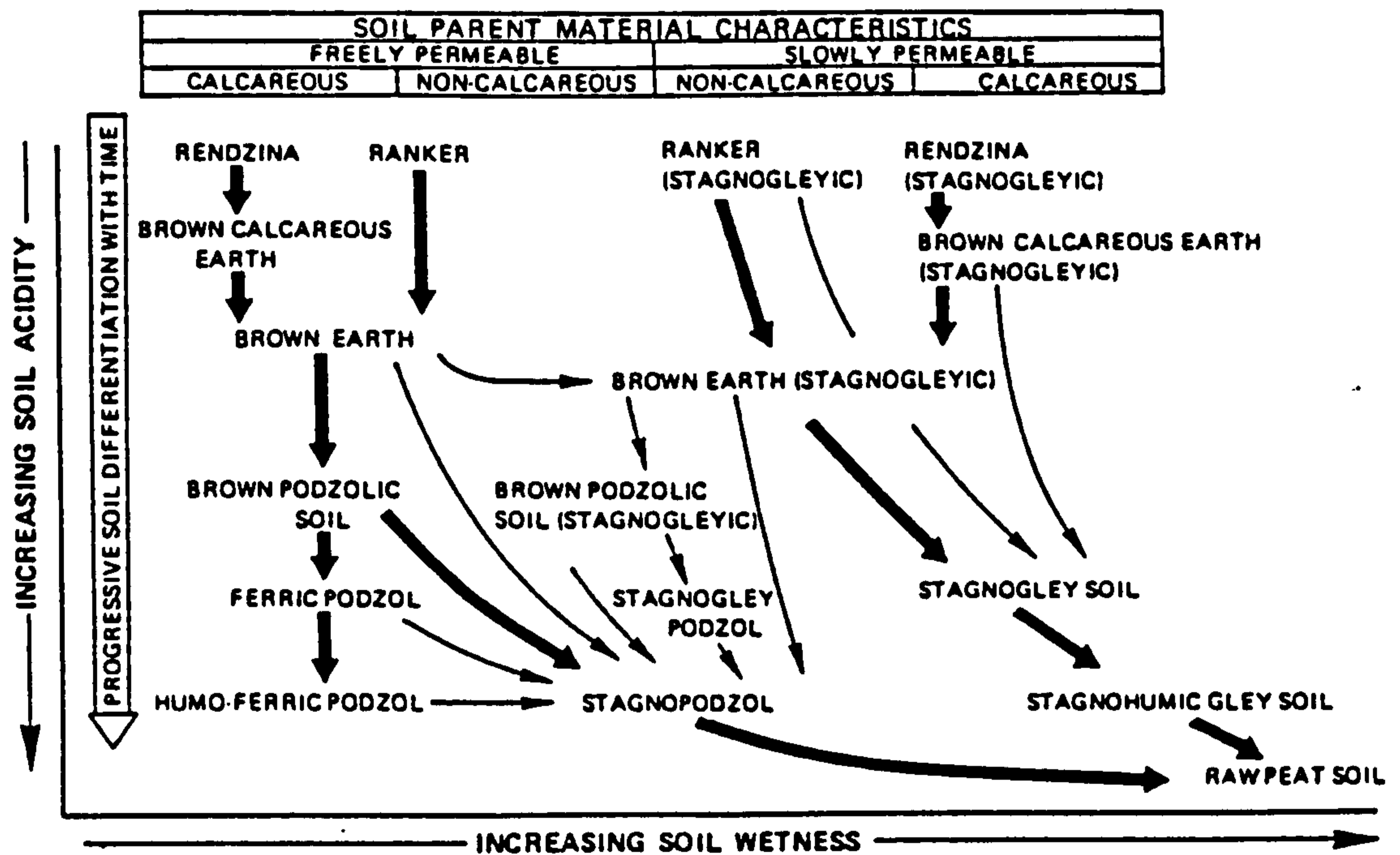


Fig. 3.1 Potential pathways of soil evolution in the British Uplands (after Askew *et al* 1985)



suggests that soils can be considered as entities that evolve along developmental pathways. Soil properties alter through time maintaining dynamic equilibrium with environmental conditions.

Potential pathways of soil evolution are illustrated in fig 3.1. Two distinct pathways can be recognised. Firstly, in freely draining situations, increasing acidification results in mull humus forms being replaced by mor and the development of podzol profiles. Secondly in areas of increased wetness gleying can occur resulting in stagnohumic profiles and the development of peat. Stagnopodzols develop where there is initially a freely draining profile but surface waterlogging results in the development of a peaty surface. An idealised sequence of soil development, described by Bridges (1978) and summarised in fig 3.2, indicates that brown soils had developed by the Mesolithic. On coarse textured soils leaching contributes to the formation of acid brown soils which eventually resulted in the formation of Podzols. This was followed by gleying leading to the development of Stagnopodzols. Bridges (*ibid.*) emphasises that this is an idealised soil sequence and is subject to many local variations.

Podzolisation is undoubtedly an important soil process in the uplands and is closely influenced by climate and vegetation. For example during the post glacial period soils in the conifer zone were susceptible to podzolisation (Limbrey 1975). Conifers are low base demanding species with few bases returned to the surface

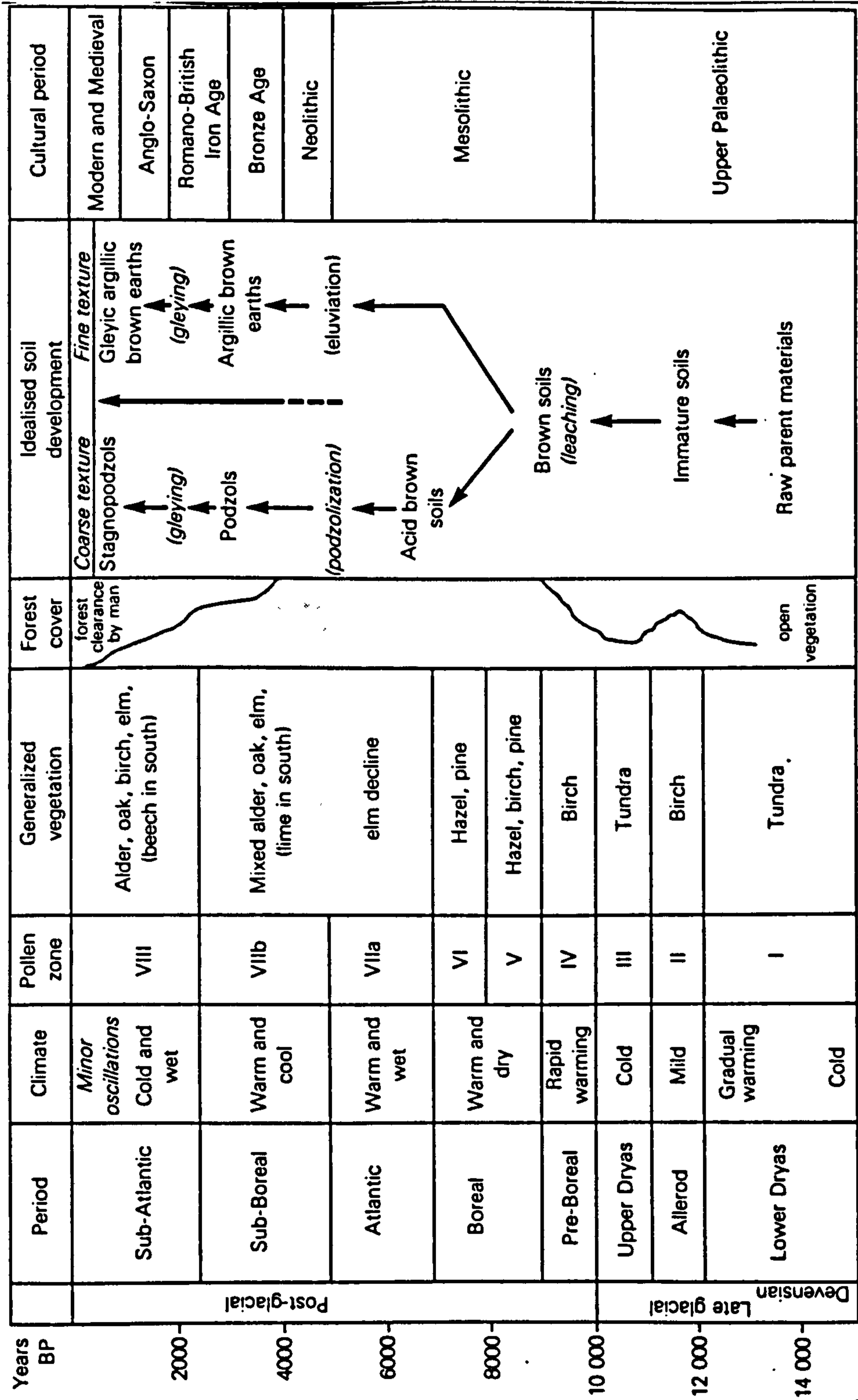


Fig. 3.2 Relationship between climate, pollen zones, vegetation and soils in the post-glacial period (after Bridges 1978)

from depth. This property is particularly significant in areas where there are coarse grained parent materials which were originally base poor and easily leached.

The litter below coniferous vegetation comprises leaves with resistant cuticles and high polyphenol content which limits micro-organism activity. As water passes through the layer of mor humus into the underlying mineral soil it is charged with CO<sub>2</sub> derived from the atmosphere and organic compounds, such as polyphenols (Fitzpatrick 1983). The acid soil solution encourages weathering of primary minerals. Mobile complexes of sesquioxides and humus are created which are subsequently washed down the profile. A characteristic feature of many podzolised soils is a bleached E horizon, where material has been removed, and a strongly coloured Bs horizon, where material has been illuviated. The translocation of organic material to form Bh horizons is a characteristic feature of many podzols. The result of podzolisation is a soil profile with surface horizons depleted in bases and concentrations of sesquioxides and humus at depth.

The main cause of widespread podzolisation during the Holocene is not known. Climatic factors have been suggested as the main determinant (Romans 1970). The impact of humans on the landscape is suggested as another cause (Barber 1984, Barret et al 1976, Bradley 1978 and Turner 1981). Coles and Harding (1979) suggest that podzolisation occurred as a result of Bronze Age clearances. Lynch (1981) suggests that the great variability in dates for the initiation of podzolisation indicates an anthropogenic influence.

However Barber (1984) states that natural factors could quite easily account for all the variation observed. If podzolisation occurs when a system crosses a threshold then climatically induced podzolisation might result in different dates from different sites. Local pedological and environmental factors, by influencing the susceptibility of the soil system to change, determine when the threshold is crossed.

Waterlogging of the soil profile has affected many upland soils and, like podzolisation, is closely linked to climate and vegetation. A product of soil waterlogging is the development of organic horizons resulting in the development of peat. Fig 3.3 illustrates the factors that influence waterlogging and the consequences this is likely to have on the soil system. There is debate concerning the initiation of moorlands in the British uplands (Moore 1988). An important factor to be resolved is the relative importance of climatic and anthropogenic factors in determining changes in vegetation and soils recorded during the Holocene.

It is useful to study soils that have not been affected by anthropogenic activity to evaluate the impact of humans on pedogenesis. It is likely that the majority of soils present today have been modified by anthropogenic activity to some extent. However it is possible to make assumptions about soil development during the Holocene using Pleistocene interglacials as an analogue (Roberts 1991). If this method is adopted then 5 phases can be identified, protocratic, mesocratic, oligocratic,

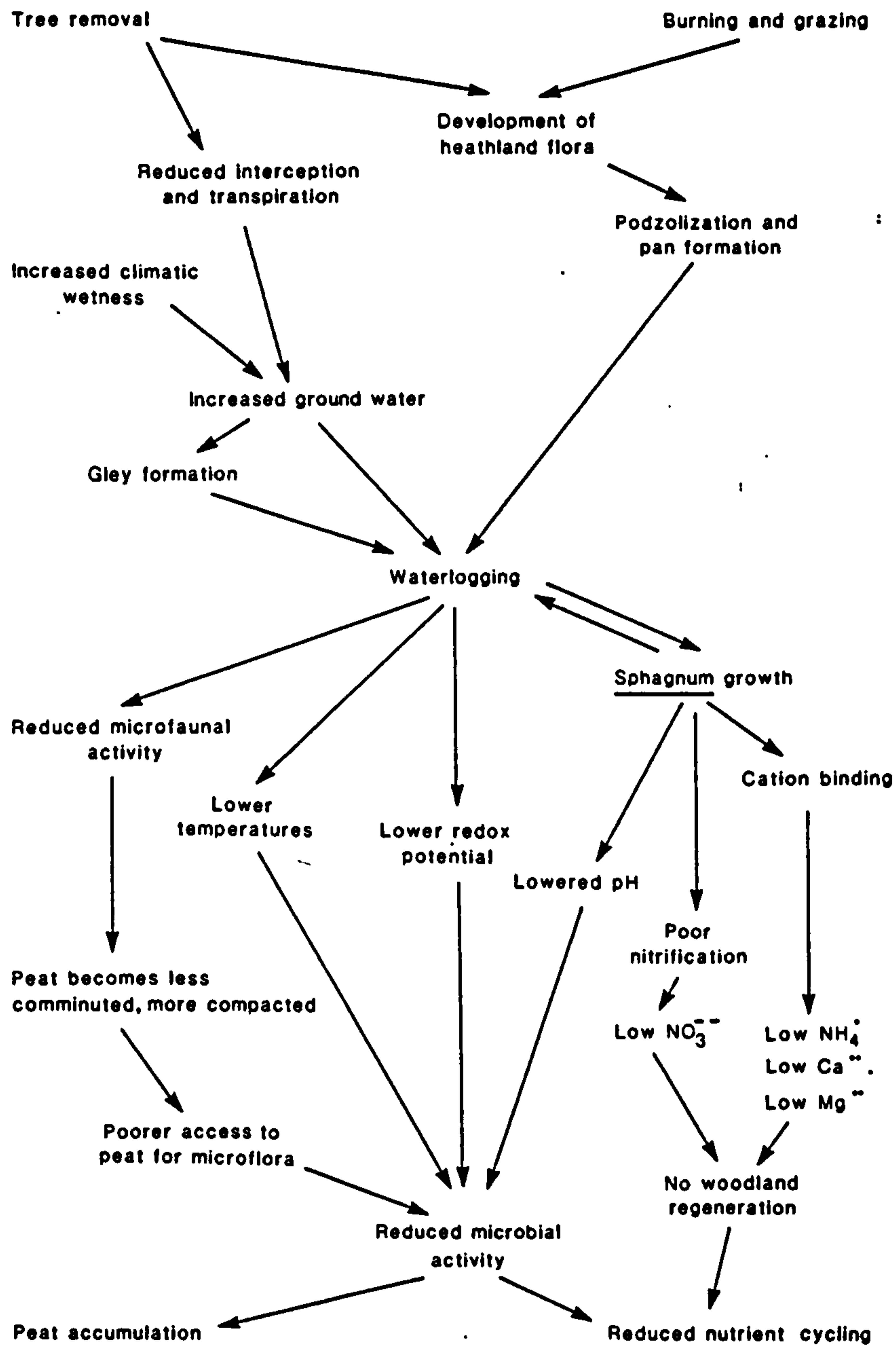


Fig. 3.3 Factors affecting the upland ecosystem (after Moore 1988)

telocratic and cryocratic (Iverson 1958, Roberts 1991). In summary this represents a transition from open woodland to mixed deciduous woodland, with brown forest soils, to heath and conifer vegetation, with leaching of soils and the formation of podzols. As glacial conditions return arctic mineral soils develop. This sequence suggests that soil development can be considered in terms of cyclical changes. Duchafour (1982) uses the terms progressive and retrogressive to describe different parts of a soil development cycle. An important feature of this cycle is that podzolisation is a natural result of pedogenesis in upland situations.

Given the complexity of interactions between soils and environment it is difficult to isolate specific mechanisms causing change. In a particular space and time there is no one factor operating independently from all the others. This makes it difficult for the palaeoenvironmentalist to distinguish changes in the environment that were specifically caused by humans.

### **3.3 The effect of humans on the soil system.**

Any discussion about the effects of human impact on the environment, often involves the use of terms like beneficial and detrimental. However these terms imply certain anthropocentric value judgements (Davidson 1982). For instance it is generally regarded that podzolisation is a degradational effect and manuring of the soil to improve fertility is a positive effect.

It should be remembered that all soil types are part of a larger ecosystem. An increase in the nutrient status of the soil might be an improvement in terms of soil as a resource for humans, but for fragile plant and animal communities, that have developed on infertile soil, it represents a removal of their habitat. The terms detrimental and beneficial will be used in this thesis to refer to the potential of the soil as a resource for human use. It does not imply anything about the intrinsic properties of soil.

Human activity can cause both beneficial and detrimental effects to the soil system (Bidwell and Hole 1965). Beneficial effects include addition of material that results in increased nutrient status. This balances the effect of leaching, as well as the reduces the possibility of erosion. Draining liming, manuring and controlled grazing can stop increasing acidity and wetness, and in some cases reverse it (Askew et al. 1985).

Plaggen soils are an example of the soil system being improved by anthropogenic activity. A plaggen soil can be created by the addition of turf, peat and seaweed to sandy soils, or the addition of sea sand to peat. Soil taxonomy describes a plaggen horizon as "a manmade surface layer that has been produced by long continual manuring. Sods or other material used for bedding livestock in Medieval times were spread with the manure on the fields being cultivated. Commonly the epipedon contains artifacts such as bits of brick and pottery throughout its depth" (U.S.D.A. 1975). The recognition of such horizons is not always obvious

although enhanced phosphate levels are associated with these types of soils. There is evidence to suggest that anthropogenic activity, since ca. 1200 AD, resulted in the formation of plaggen soils on Orkney (Simpson 1985).

In an arable system detrimental effects can include the removal of nutrients by crops or stock at a faster rate than which they are replaced. This process can result in an increase in acidity and leaching resulting in podzolisation. Human activity can also have an indirect impact on soils through the manipulation of vegetation. Forest clearance can completely alter the soil ecosystem resulting in loss of nutrients and acidification. The removal of the trees affects the hydrological balance of the soil water system. Evapotranspiration rates decrease encouraging the initiating of gley soils and the development of peat (Moore 1988).

Removal of surface vegetation increases the potential of soil erosion. A dramatic example of agricultural mismanagement resulting in soil erosion is the 'Dust Bowl' of the 1920s and 1930s in the mid-latitude prairie grasslands of the U.S.A.. Although this was a catastrophic event it is likely that early agricultural practises faced their own soil erosion problems. Other beneficial and detrimental effects are described by Bidwell and Hole (1965) and summarised by Davidson (1982, table 3.1).

In the early part of the Holocene anthropogenic activity would probably have modified the soils indirectly through the



**Table 3.1 Suggested effects of the influence of man on five classic (though arbitrary) factors of soil formation (after Bidwell and Hole 1965, summarised by Davidson 1982)**

|                           | Beneficial effects*   | Detrimental effects*  |
|---------------------------|---|---|
| <b>1. Parent Material</b> | (a) Adding mineral fertilizers; (b) accumulating shells and bones; (c) accumulating ash locally; (d) removing excessive amounts of substances such as salts; (e) marling; (f) warping   | (a) Removing through harvest more plant and animal nutrients than are replaced; (b) adding materials in amounts toxic to plants or animals; (c) altering soil constituents in a way to depress plant growth                                       |
| <b>2. Topography</b>      | (a) Checking erosion through surface roughening, land forming, and structure building; (b) raising land level by accumulation of material; (c) land levelling   | (a) Causing subsidence by drainage of wetlands and by mining; (b) accelerating erosion; (c) excavating  |
| <b>3. Climate</b>         | (a) Adding water by irrigation; (b) rain-making by 'seeding' clouds; (c) release of CO <sub>2</sub> to atmosphere by industrial man, with possible warming trend in climate; (d) heating air near the ground; (e) subsurface warming of soil, electrically, or by piped heat; (f) changing color of surface of soil to change albedo; (g) removing water by drainage; (h) diverting winds | (a) Subjecting soil to excessive insolation, to extended frost action, to exposure to wind, to compaction; (b) altering aspect by land forming; (c) creating smog; (d) clearing and burning off organic cover                                     |
| <b>4. Organisms</b>       | (a) Introducing and controlling populations of plants and animals; (b) adding organic matter (including 'nightsoil') to soil directly or indirectly through organisms; (c) loosening soil by plowing to admit more oxygen; (d) fallowing; (e) removing pathogenic organisms, as by controlled burning   | (a) Removing plants and animals; (b) reducing organic matter content of soil through burning, plowing, overgrazing, harvesting, accelerating oxidation, leaching; (c) adding or fostering pathogenic organisms; (d) adding radioactive substances |
| <b>5. Time</b>            | (a) Rejuvenating the soil through additions of fresh parent material or through exposure of local parent material by soil erosion; (b) reclaiming land from under water   | (a) Degrading the soil by accelerated removal of nutrients from soil and vegetative cover; (b) burying soil under solid fill or water   |

manipulation of vegetation. Later, as cultivation increased, soils and geochemical environments would have been directly affected.

There were still many areas of the UK with Brown soils as late as the Bronze Age (Macphail, Romans and Robertson 1987). It is possible that increased human activity during this period led to widespread podzolisation (Dimbleby 1962, Romans and Robertson 1983b, Scaife and Macphail 1983, Macphail 1986).

It is suggested that human activity has tended to direct pedogenesis towards leaching, acidity, podzolisation, gleying and peat formation through post glacial times (Ball 1975). This trend, similar to the suggested cycle of events during a Pleistocene interglacial, implies the effect of human impact has been mainly one of accelerating a natural process.

In summary, there is much uncertainty about the effect of human impact on the soil system. Soil development, during the Holocene, can be placed in a theoretical framework in which progressive and retrogressive stages of development can be observed. Given the tendency for soils to podzolise and gley, under certain climatic conditions, it is difficult to be certain about the impact of anthropogenic activity on the soil system. Examples, discussed previously, show that anthropogenic activity can, potentially, have positive and negative effects on pedological development. This section has been concerned with general ideas about soil development, the following section describes specific evidence

for soil development with particular reference to sites in Scotland.

### **3.4 Evidence for soil development with emphasis on sites in Scotland.**

Generally the impact of humans on the upland soil system is associated with accelerating soil development towards podzolisation, gleying and peat formation. The construction of monuments approximately 5000 years ago in Scotland began to bury fragments of contemporary soils. These soils can now be studied facilitating reconstruction of pedological conditions in the past.

Any discussion about soil development, based upon evidence in the literature, immediately encounters problems of chronology. Authors refer to periods of time in different ways. Systems include using culturally derived time scales like Neolithic and Mesolithic, pollen based time scales like boreal and sub-boreal, absolute and relative time scales including BP, bp and BC. The dates referred to in this discussion will be those quoted by the original author. Fig. 3.2 shows an approximate comparison of each of the different systems, although it should be remembered that the cultural divisions can not be applied directly to Scotland.

Different soil terminologies are used by various researchers to refer to pedological horizons. Elsewhere in the thesis the England and Wales soil classification system is used wherever

possible. This discussion will mainly use this system, although where a direct conversion is ambiguous, for instance brown forest soils used in the Scottish classification, the quoted source will be used.

The lack of any buried soils older than about 5000 BP makes it difficult to assess the condition of the soils before this date. Whittington (1980) suggests that the effect of Neolithic activity on vegetation became important during the Sub-Boreal period. Neolithic settlement of Scotland involved the gradual clearance of woodland and the establishment of arable and mixed farming areas (Ritchie and Ritchie 1981).

Neolithic sites at Edzell and Fochabers showed buried brown forest soils with oak charcoal present in A horizons (Romans and Robertson 1975b). The exact profile characteristics of a brown forest soil are slightly ambiguous as this label is used to describe a broad group of soils which include brown podzolic soils. A modern podzol profile was present in a gravel pit close to the Edzell site suggesting a degredational sequence of soil development. At Fochabers the modern profile is a humus podzol. A podzol profile, contemporary with the brown forest soil at Edzell, was found at Monamere Chambered Cairn near Lamlash on the Isle of Arran (Mackie 1963-64).

The evidence from Edzell, Fochabers and Monamere shows that, as expected, there was regional variation in the development of soils approximately 5000 years ago. The soils from all three

sites had podzolised to some extent. The sites at Edzell and Fochabers both had small amounts of orientated clay present in the profile which was used to imply slash and burn cultivation. If the soils were being cultivated then it is also possible that they were truncated. A truncated podzol profile can have the same characteristics as a brown podzol.

Acid brown soils were identified from sites on Shetland dated to 4000 years ago (Whittle et al. 1986). An acid brown soil was also found under the stone circle at Raigmore, Inverness (Romans and Robertson 1983a). Evidence from a multi period site at North Mains, Strathallan, Perthshire shows there was a brown forest soil under mixed deciduous woodland present before the site was cleared and cultivated (Barclay 1983). Monuments on the site dated from the 3rd millennium BC to the 1st millennium AD.

Romans and Robertson (1975b) suggest that podzolisation was widespread by the Iron Age and Roman period. At Dalnaglar in north east Perthshire, at an altitude of 325m, a buried soil below a circular enclosure was identified as a podzol or brown podzolic soil (Stewart, 1961-62). At Kilphedir in the Strath of Kildonan, Sutherland, at an altitude of 130m, an indurated B<sub>3</sub> horizon with a thin iron pan on its upper surface formed the floor of an excavated hut circle (Fairhurst, 1970-71). Romans (in Fairhurst, 1970-71) suggests that this settlement, dating to the 5th century BC, was established on a soil transitional between a podzol and podzol with thin iron pan.

A buried podzol was identified at a Roman marching camp at Kirkbuddo in Angus (Romans 1962). The camp is located at an altitude of 145m and was probably constructed between AD 140 and 211. Thin section analysis of the podzol indicates that an acid brown soil was present prior to the onset of podzolisation. It is thought that the podzol profile might have been developing for hundreds or thousands of years (Romans and Robertson 1975b).

It is suggested that it was not until the monastic era that there was any significant change in agricultural practice in Scotland (Romans and Robertson 1983a). The result of activity during this time was a replenishment of soil organic matter and the deepening of cultivated topsoils. It is thought that Christian monastic orders brought agricultural techniques to Scotland which were latter used by a greater number of people (ibid.).

In summary, the evidence presented above does not indicate any obvious trends in pedogenesis. Brown forest soils, which might be truncated podzols, are present 5000 years ago. During Iron age and Roman periods acid brown soils and podzols are identified. Romans and Robertson (1983a) suggest that a major change in agricultural practice is brought about by activities of the monasteries. The following section describes the site used for the present study. The broad temporal distribution of monuments offers the potential of studying buried soils from Bronze Age to recent times.

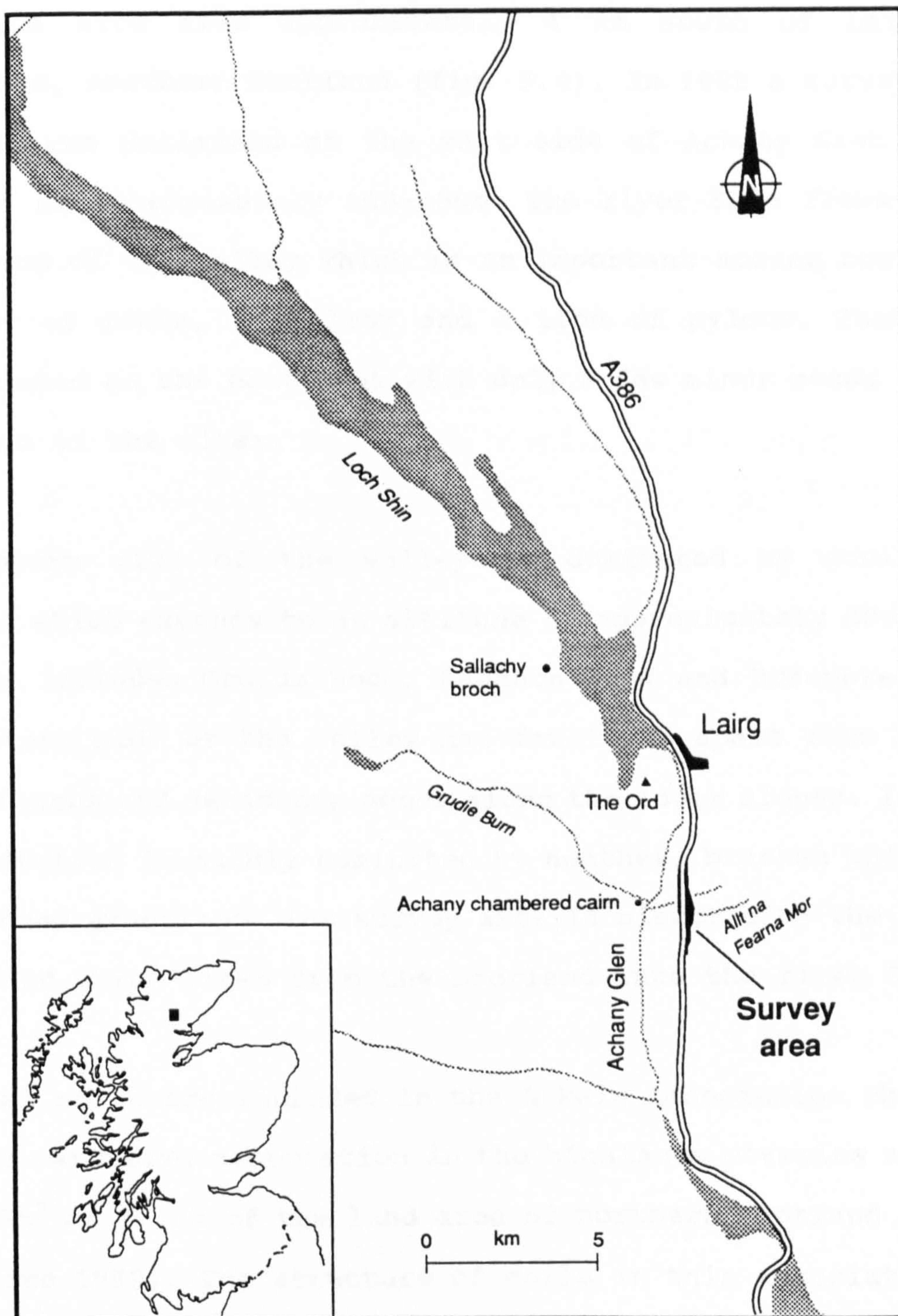


**FIG. 3.4** Location of survey area at Lairg, Sutherland

### 3.5 Description of the site at Lairg

The field site lies approximately 4 km south of Lairg in Sutherland, northern Scotland (fig. 3.4). In 1988 a survey area of 59 ha was delimited on the east side of Achany Glen at an altitude of approximately 100-150m. The river Shin flows along the bottom of the valley which is an important access route for a number of roads, a railway and a line of pylons. These are concentrated on the east bank with only a few minor roads on the west side of the river.

The western side of the valley is dominated by coniferous woodland which extends to an altitude of approximately 200m. The woodland includes Gruids Wood, Raemore Wood and Braemore Wood. The eastern side of the valley has few trees apart from a band of coniferous and deciduous woods along the lower slopes. Instead the vegetation is mainly dominated by heather, bracken and areas of improved grassland. The survey area is bisected by the Alt na Fearn Mor which flows from the moorland into the river Shin.

The local soils are included in the Arkaig Association which is the most extensive association in the highlands covering an area of 6130km<sup>2</sup> or 37.3% of the land area of northern Scotland (Futty and Towers 1982). The structure of soils in this association is generally weak. The soils exhibit complex variations over small regions. Along the valley sides there are areas of enclosed and semi enclosed mires (Futty and Towers 1982) and encroaching unenclosed hill peat. Within the survey area the soils are



dominated by peaty podzols, gleys and freely draining brown podzols.

The solid geology is dominated by siliceous granulites of the Precambrian Moine series. Owing to glacial processes, the dominant soil parent material is glacial till. The till is composed of material derived from the Precambrian Moine series and some granite and hornblende schists (Futty and Towers 1982). There are limited areas of fluvio-glacial gravels and river alluvium in the valley bottom. The glacial till is generally very stony with textures varying between loamy sand and sandy loam. Gleys, which occur over a coarse textured stony till, are common. Towards the higher slopes of the valley and on the moorland the soils are dominated by peat, peaty gleys and some peaty podzols. Thin iron pans are present in some areas. Where the land has not been reclaimed heather moors dominate.

An initial survey of the site, carried out in 1989 by AOC (Scotland) Ltd., identified 653 archaeological features. These represent 4000-5000 years of landuse. Evidence of human activity spans the Neolithic period to the Post Medieval period. The survey area is divided into 4 blocks (figs. 3.5 and 3.6). The following information is taken from unpublished reports produced by AOC and gives a brief description of each block.

Block 2

A286

Fig. 3.5 Lairg survey area,  
position of monuments sampled  
for thin section analysis, map 1

Scale 1:5000

Block 1

Group A monuments

M127  
PM rectangular structure

M62  
EP Dyke

M21  
Unburied accumulation  
of soil

M164 PM Dyke

M75/4 PM Dyke

M86 EP Lynchet

M88 EP Clearance cairn

M87 EP Clearance cairn

M64  
LP Hut circle



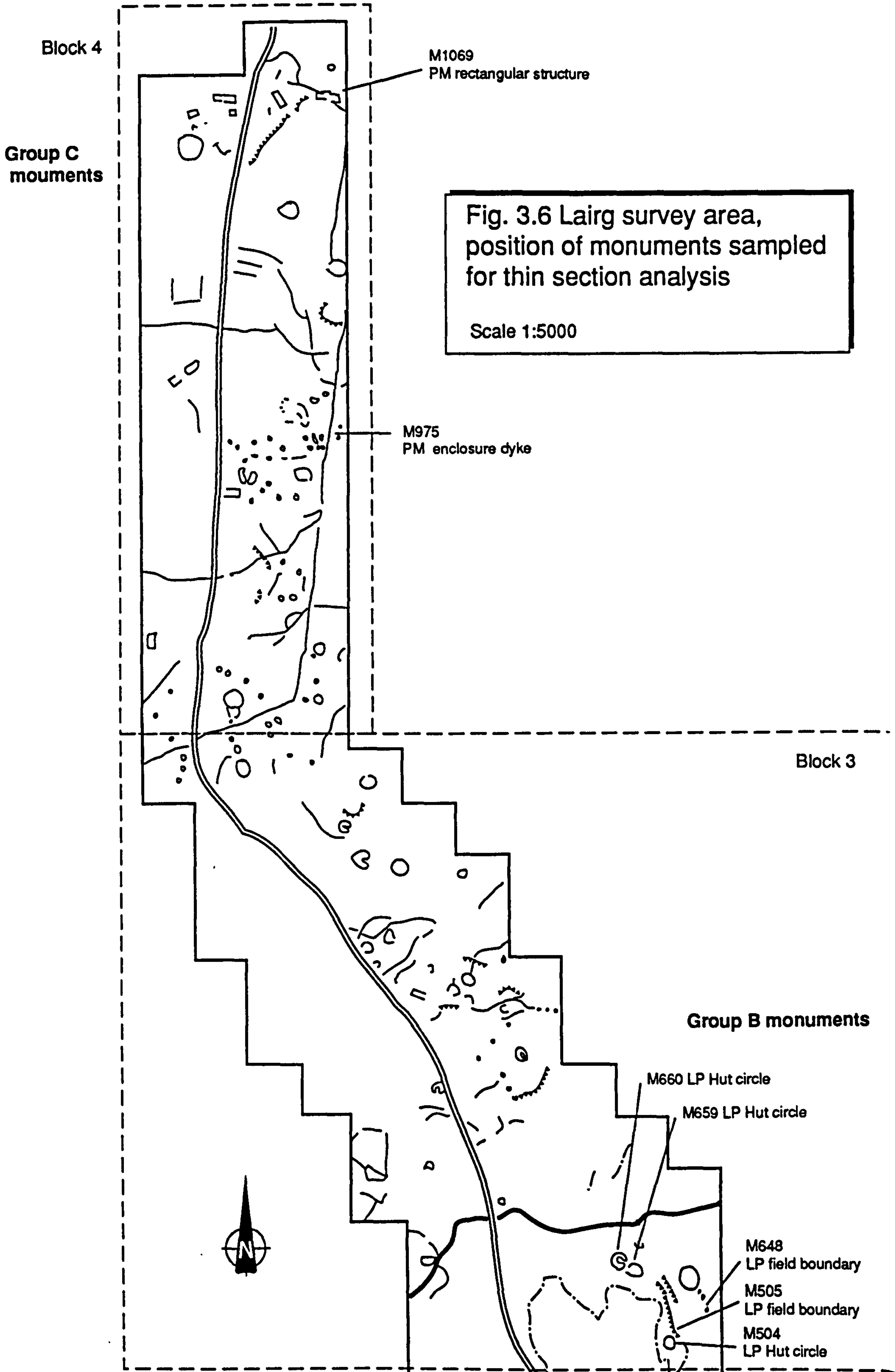


**Fig. 3.6 Lairg survey area,  
position of monuments sampled  
for thin section analysis**

Scale 1:5000

### 3.6 Block 1 (The southern block).

The vegetation gradually changes from grassland in the south to heather covered rough grazing in the north. The topography is gentle with fairly well drained slopes. A croft which was deserted earlier this century lies just outside the survey area. The density of archaeological monument decreases towards the croft. This decrease is attributed to the more recent landuse in the immediate vicinity of the building. The road, cutting the block along its north-south axis, acts as a division between different landuses and densities of archaeological monuments. On the improved land to the west of the road there is a marked reduction in sites.

The largest monument in this area is the stone and earth Post Medieval enclosure dyke. All rectangular structures are within or abut the dyke and are thought to be associated with it. Earlier monuments are present within the dyke and also spread out over the slopes above it. Examples of early signs of occupation in the area include clearance cairns, hut circles and smaller dykes.

The construction of the large enclosure represents many episodes of rebuilding. The surviving dyke has replaced earlier wall lines. At several points the dyke has been built around hut circles and cairns. At one point a rectangular building overlies the dyke. The forms of the hut circles vary from massively embanked and platformed structures (greater than 10m diameter)

to smaller structures (5m diameter or less). Parallel banks, approximately 50-60m, apart represent the field system which is probably associated with the hut circles.

### **3.7 Block 2 (The southern central block).**

This area is almost completely devoid of any archaeology. Exceptions include a few cairns and possibly the site of a water mill in the gorge of Alt na Fearna Mor. A series of soil pits showed that the land had probably always been poorly drained and that little soil development took place before the growth of the peat began. This would indicate that this area is genuinely sparse in archaeological monuments.

### **3.8 Block 3 (The northern central block).**

This area contains numerous platforms, embanked hut-circles, relict dykes and clearance cairns. Unlike blocks 1 and 4, block 3 shows no evidence of later occupation. The vegetation is predominantly heather with areas of improved grassland further north.

### **3.9 Block 4 (The northern block).**

This area has many similarities to Block 1. A Post Medieval dyke encloses a large area. It cross-cuts several denuded dykes, which run east-west, and encloses several substantial hut circles. Evidence of later occupation includes a number of rectangular

structures found on both sides of the road. Large parts of this area are covered by bracken and improved grassland.

### **3.10 Thin section sampling strategy**

The Lairg site offered an opportunity to conduct an intensive thin section sampling programme. The diversity of monuments, combined with their temporal and spatial distribution, presented the possibility of collecting samples that could be used to test specific hypothesis and to assess the usefulness of the image analysis techniques described in chapter 2.

It is common for thin section samples on archaeological sites to be taken only from horizons of potential archaeological significance. This does not reflect the fact that pedogenesis occurs throughout the entire soil profile. It was not feasible to sample from every horizon in every profile examined, so representative thin section samples were taken from specific contexts, for instance A horizons, B horizon and glacial till.

Samples for thin section analysis were obtained from three field seasons. In September 1989 AOC (Scotland) Ltd. undertook a prospective sampling season. A small number of samples for thin section analysis were taken at this time. In July 1990 four weeks were spent collecting the majority of the material for the thin section study. The main excavation took place in late 1990. Monuments were excavated in plan for the first time. This offered

a last opportunity to collect any additional samples that were needed to complement the thin section analysis.

As the thin section analysis was designed prior to the main excavation, it was necessary to identify contexts that could be sampled using a trench dug through upstanding monuments. The majority of samples were taken to study buried soils, soil accumulations and walls of structures. These samples were derived from contexts that could be interpreted without the need for open plan excavation.

To compare and contrast soils of different ages derived from different areas of the site, an understanding was needed of the effects of pedogenesis on present day profiles. In selected monuments trenches were extended so that samples could be taken from soils that had not been buried.

During the 1989 survey, trenches were generally excavated at the edges of monuments to minimise any damage prior to the main excavation. Many of the soils described were not particularly well sealed. This might have been caused by the location of the trenches. In the excavation to obtain samples for thin section analysis in 1990, trenches were dug through substantial parts of monuments to try and find examples of buried soils that were sealed and thus not subject to modern pedogenesis.

### 3.11 Sampling strategy for buried soils.

The 1989 survey, identified numerous buried soils of varying age which were distributed over the site. Nine questions were formulated that could potentially be answered by the use of thin section analysis;

1. Do buried soils with a temporal distribution exhibit specific characteristics?
2. Can temporal variation be isolated from spatial variation?
3. Can former landuse be inferred from buried soils?
4. Can changes in landuse be identified using evidence from buried soils?
5. Can differences in landuse be observed in buried soils of the same age?
6. Can differences in landuse be observed in buried soils of different ages?
7. Can specific pedogenetic / sedimentary events be established using a chronological sequence of buried soils?
8. Can types of vegetation be identified from the remains of organic matter in buried soils?
9. Can the study of pollen, diatoms, and phytoliths in thin section be used for palaeoenvironmental reconstruction purposes?

To resolve these various questions it was necessary to consider the following;

- a. The results of previous surveys indicated that many of the buried soils at Lairg were poorly sealed. This meant that post depositional change (PDC) might have resulted in the loss of important diagnostic information. Assessing the amount of PDC and the way that it varied across the site was considered important.



b. A knowledge of the morphological variability of buried soils across the site was necessary to ensure that diagnostic features were representative of specific soils.

c. Some buried soils were sampled along transects in order to understand how soils are modified by continuing pedogenesis.

d. The preservation of biological remains in the soil was unknown. Well preserved, identifiable organic fragments potentially offer useful information about inputs to the soil and past vegetation. A detailed analysis of the coarse organic fraction might provide useful palaeoenvironmental information.

### **3.12 Monuments chosen to examine buried soils.**

The results of the 1989 field survey allowed specific monuments to be selected for further excavation. The following section describes the monuments that were chosen and the reasons for choosing them. The monuments selected are located in 3 areas, group A, group B and group C (figs. 3.5 and 3.6). Group A is located in block 1 and has LP and PM monuments. The monuments in area B are situated in block 3 and date to the prehistoric. Group C, situated at the northern end of the survey area in block 4, includes only PM monuments.

Monuments were dated either directly by radiocarbon analysis, or by inference from monuments of known date. They were then assigned to the following broad temporal classification;

Early Prehistoric (EP), monuments predating 3500 BP.

Later prehistoric (LP), monuments dating to 3500-2000 BP, (in group B LP is further subdivided into Bronze Age and Iron Age monuments).

Post medieval (PM), monuments dating from 500-0 BP.

The gap between 2000 BP and 500 BP represents a lack of evidence for human activity during this period.

### **3.13 Monument selected in group A.**

Samples were taken from two EP cairns, M86 and M87 and EP lynchet M88. Thin section samples were taken from soils accumulating on the upslope sides of these monuments. Monuments 62, an EP dyke and M64, an LP hut circle, were sampled to provide thin sections of prehistoric buried soils. Monument 64 was excavated for a number of reasons;

- a. To sample a well sealed buried soil extending laterally from under the monument into the surrounding surface soil.
- b. To sample an accumulation of material against the upslope side of the monument (section 3.16).
- c. To examine the buried soil itself.

Samples were taken from monuments 75, 127 and 164 as examples of PM buried soils.

### **3.14 Monuments selected in group B**

Samples were taken from this area during both 1990 field seasons. M504 is an Iron Age hut circle sealing a well preserved buried

brown podzol. The A and B horizons and the underlying glacial till were sampled for thin section analysis. Samples were also taken laterally along the trench to examine the A horizon where it had not been buried.

M505 is a revetment, again overlying what appears to be a cultivation layer. Samples were taken from the buried soil despite the poor sealing by the overlying stones.

During the excavation by AOC in 1990, additional samples were collected from contexts where the type of agricultural activity could be inferred from field evidence. Samples were taken from a buried A horizon and overlying soil accumulation abutting M648 (a lynchet). Evidence of ridge and furrow cultivation was preserved in the upper part of the soil profile. There are ard marks in the top of the Bs horizon at the base of the buried A horizon. The ridge and furrows are only preserved in the upper part of the soil profile because of the development of a layer of peat. The thin section samples were taken to determine if these two layers had developed as a result of different agricultural techniques or a continuation of the same cultivation method.

A single sample was taken from transect 7000. This sample was taken from the middle of a field lying between two lynchets, where large areas of ridge and furrow was present. A buried soil below a LP hut circle (M660) was sampled. The buried soil was overlain by a layer of charcoal which was overlain by a turf

bank. Both of these contexts were sampled. Samples were also taken from the A and B horizons below another Bronze age hut circle, M659.

### **3.15 Monuments selected in group C**

The last group of sites was at the northern end of the survey area. The monuments in this area were better preserved and tended to be of a later date than the monuments situated around the quarry.

Samples were taken from M975, a large enclosure dyke. This was constructed of turf and stone. Samples were taken from the wall of the monument and the buried profile below it.

The second monument in this group was the remains of a PM house, M1082. Samples were also taken from the buried profile below M1062, a PM house.

### **3.16 Sampling strategy for soil accumulations**

During the 1989 survey a number of sites were identified where soils had accumulated against upstanding monuments. In group A this included sites adjacent to prehistoric hut circles and large cairns (also thought to be prehistoric). One location was identified where the A horizon, on the edge of a field, exceeded 1m in depth. Although these accumulations could not be dated it was decided that they warranted investigation to discover why they were formed. In many cases the angle of the slope on which

they were situated did not appear steep enough to indicate soil movement as the only mechanism responsible for their depth. Importation of material was considered a possibility. Thin section samples were taken to try and answer the following questions;

1. Can the source of the deposit be identified i.e. is it natural or anthropogenic?
2. Can the process leading to the formation of the soil be identified, for instance hillwash or fluvial?
3. Can different sedimentary and pedogenic phases be identified in the soil? Can these be correlated with pedogenic sequences observed in buried soils?
4. If separate phases can be identified what palaeoenvironmental information can be determined from the biological remains?
5. Can a sequence of landuse change be inferred from the soil accumulations?

To answer these questions it was necessary to consider the following;

- a. How has pedogenesis affected the soil accumulations, in particular have any diagnostic micromorphological features been lost?
- b. Can regions of homogeneity and heterogeneity be identified in the accumulations?
- c. Are mineral and organic remains orientated?
- d. How do the shapes of soil constituents vary?
- e. How well preserved are the biological remains?

A number of monuments with soil accumulating against them were selected for the investigation. The principal monument was M21, in group A (fig 3.5). Although this was undated it was considered worthwhile to excavate for the following reasons:

1. The micromorphology of the soil was not known. Although field observation suggested the A horizon was homogenous, it was possible microstratigraphy was present which would enable formation processes to be identified. This examination was seen as a preliminary investigation to determine if a more detailed study was necessary.

2. If diagnostic information was present in soil, it might be possible to correlate stratigraphy within the accumulation to buried soils studied elsewhere in group A.

A number of other soil accumulations against upstanding monuments were also sampled. In group A samples were taken from the soil accumulation against the upslope side of the hut circle (M64). In the 1989 survey an EP cairn (M88), and a EP lynchet (M86) were excavated and samples taken from the soil accumulating against these monuments. Soil accumulations sampled in group B included monument 648.

In summary, this chapter discusses generalised ideas about pedogenesis in upland regions concluding that it is difficult to isolate any one environmental variable as a dominant factor initiating change in soil development. If the uplands are considered as a functioning open system, composed of many smaller interacting systems, then the search for any one dominant reason for change becomes unnecessary. The interactions between all environmental factors becomes more important than the effects of individual components. Thus the case study at Lairg is put into

perspective. The purpose of the soil thin section analysis is to discover how much information can be derived concerning pedological development and related environmental processes, human activity being of primary importance. The last section in this chapter describes the thin section sampling strategy that was designed to achieve this objective. The interpretations made from the thin section analysis form only part of a larger palaeoenvironmental investigation being carried out in the area. Combination of the results from all the studies will allow the soil study to be placed within the larger framework of an upland ecosystem.

## Chapter 4

### Thin section preparation techniques.

#### 4.1 Introduction

Samples for thin section analysis are normally taken using rigid metal boxes called Kubiena tins. These provide a convenient way of removing blocks of undisturbed soil material for thin section analysis. The boxes are not particularly suitable if the contexts being sampled have a high stone content. The stones prevent the Kubiena tins being placed in the soil. This chapter describes specific problems that were encountered during the first field season at Lairg and how these problems were resolved prior to the main thin section sampling programme.

#### 4.2 Sampling techniques.

During the 1989 field season, samples were taken for thin section analysis using the standard Kubiena tins measuring 8 x 5cm. The large abundance of stones in many of the soils and sediments at Lairg made the use of such small, inflexible, containers very difficult since the stones often prevented the tins being pushed into the soil. Such failures meant it was necessary to repeat the operation in a location where the soil had not been disturbed. Many of the trenches were quite small restricting the number of times a particular context could be sampled. A method of sampling was needed that would not be affected by the stone content of the



soil and would maximise the chance of removing a sample from the position first tried.

One possible method involved cutting a small block from the soil face and trimming the edges so it would fit into a standard Kubiena tin. This was only of limited success at Lairg because samples easily cracked along lines of weakness caused by stones.

Another alternative was to cut blocks larger than the Kubiena tin such that the blocks would not crack or fall apart. The main limitation to this was the size of block that could be made into a thin section. Moran et al (1988) reports that blocks of soil up to 12x12x12cms could be successfully impregnated with resin. Murphy (1986 pg. 16) states;

"The maximum size of thin sections that can be made is limited by the machinery available to saw and grind impregnated blocks".

It was decided that the most appropriate method of taking undisturbed samples from contexts at Lairg would be to cut large blocks from the soil. The maximum size of block that could be impregnated was determined by the size of the desiccator. The internal diameter of the desiccator used in this study measured 24cm. This was the first time that samples other than Kubiena tins had been processed in the Stirling laboratory. It was decided that the method should first be tried on some test blocks to ensure that the central areas of the blocks had impregnated properly.

Two large soil blocks, measuring approximately 12x12x12cm, were taken from the A horizon of a podzolic sandy loam soil. They were cut from the ground using a trowel and a sharp knife. The blocks were wrapped in a sheet of thin aluminum foil and then in a sheet of thicker foil. The foil was carefully moulded around the sample to give it maximum support. The sample was then placed in a plastic bag and sealed to prevent loss of moisture which would cause structural damage. Finally masking tape was wrapped around the plastic bag. The orientation and sample number could be easily written on the outside of the masking tape. The samples were then transported back to the laboratory where they were placed in a fridge and stored until processing.

#### **4.3 Removal of water.**

During the manufacture of thin sections all the water must be removed from the sample without causing structural modification to the block of soil. Common techniques include freeze drying, air drying or acetone replacement. Blackburn et al. (1988) published a method describing a water exchange method using an almost saturated sodium chloride solution. Freeze drying, air drying and acetone replacement are all described in Murphy (1986). The main disadvantage using freeze drying is the possibility of structural deformation caused by the growth of ice crystals (Murphy 1986, Thompson et al., 1985, Jongerius and Heitzberger 1975) and the modification of some organic material (Fitzpatrick and Gundmundsson 1977). Acetone replacement is the most widespread water replacement method although some problems

have been encountered using this technique on samples with a high organic or clay content. Approximately 6-8 weeks is required to remove the water from blocks of soil using acetone replacement. Not all people have found acetone replacement completely reliable. Chartres (1989) found samples from an A horizon of a swelling grey clay were prone to disruption if treated with acetone.

Another option is the use of a resin that is miscible with water. This negates the need to remove moisture from the sample thus speeding up processing time and reducing the risk of causing damage to the sample during preparation. Moran et al. (1989b) report the use of a resin of this type and Thompson et al. (1992) suggests that this method needs further testing.

The resin used in this study was a crystic polyester resin. This type of resin is used in the majority of thin section laboratories. Acetone replacement was used to remove the water from the samples. The soil blocks were removed from their protective foil wrappings and any excess material trimmed off. The blocks were reasonably consolidated so this did not cause any problems. A new container was made to fit the block using a heavy gauge tin foil. Holes were punched in the bottom of the foil container to allow the free circulation of acetone around the sample.

#### 4.4 Equipment for acetone exchange.

The preferred method for exchange of acetone would have been the method described by Moran et al (1989a). This involves allowing the continuous circulation of acetone around the samples. The water is removed from the acetone using a desiccating filter and molecular sieve during circulation. Using this method, large numbers of samples can be processed at the same time. The quantity of acetone used is minimised as the water content is continually removed during circulation. The speed of acetone exchange is also greater than normal soaking because the acetone is in constant motion.

To use this method at Stirling University it was required that the equipment be set up in a fume cupboard in accordance with C.O.S.H.H. (Control of substances hazardous to health) regulations. There was no fume cupboard available that was large enough, so a different technique was used. The samples were placed in plastic bowls, half filled with acetone, and covered with a lid. The bowl was placed in a fume cupboard and the acetone changed every 3 or 4 days.

All the samples that had been made in the Stirling laboratory up to this time had been conventionally-sized blocks derived from Kubiena tins. The rate that the water is removed from the soil was estimated from the experiments conducted by Murphy (1985). Using samples taken in Kubiena tins (7.5 x 6.5 x 4cm deep) he

monitored the rate of acetone exchange using a Jeol PMX60 <sup>1</sup>H NMR spectrometer.

Murphy's experiments describe the rates of water exchange using conventionally sized blocks. The samples from Lairg are much larger than this and it was decided an independent method of measuring the water content of the acetone was needed. The method needed to be quick and reliable, so measurements could be calculated on a routine basis, and use inexpensive laboratory equipment.

Moran et al (1989a) suggests the use of enthalpimetry to measure small quantities of water in a solvent. The measurements are based upon the heat of dilution. The initial amount of water in the solvent affects the magnitude of temperature change on addition of water. The reaction is endothermic for water concentrations of less than 5.5% and exothermic for concentrations greater than this. Moran et al (ibid.) suggests that this is a useful method for determining the concentration of water in acetone because of its accuracy, economy and simple apparatus.

The following apparatus was used based upon the equipment described by Moran et al (ibid.) A silvered dewer flask was held in a retort stand. A 50ml standard solution of water and acetone was placed inside the flask. A 1.5ml sample of distilled water was placed in a small plastic beaker and floated on the surface of the sample. A thermistor, connected to an amp meter, was

placed through a sealing bung into the water/acetone sample. The apparatus was then left for 1 minute to allow the temperature of the water in the plastic beaker to equalise with the temperature of the sample in the dewer flask. The dewer flask was then agitated to upturn the beaker and the resultant reading taken from the amp meter. This was repeated 10 times for water concentrations of 0-10%. Although Moran et al (ibid.) reported that this method could be used for concentrations between 0-15%, it was found that the results were not consistent enough to be used with confidence. This inconsistency might have been caused by using a narrow necked dewer flask. This made it difficult to consistently add the 1.5ml sample of water in a controlled manner. The technique was cumbersome using this flask. A wide necked flask was not available. It was decided that specific gravity might be used to measure the amount of water in a sample of acetone (S. Carter pers. comm.).

#### 4.5 Measuring water in acetone using specific gravity.

Using figures published in a solvents guide (Marsden 1963) a curve was drawn for % w/w water in acetone against specific gravity. The published figures did not give enough detail in the range 1-10%. To increase the detail in this range standards of known concentrations were made. Specific gravity is temperature dependant so 3 sets of standards were mixed at 18, 20 and 22°C using distilled water and laboratory grade acetone. The standards were mixed v/v and then converted to w/w. The results were plotted to give 3 calibration curves. The curves were similar to

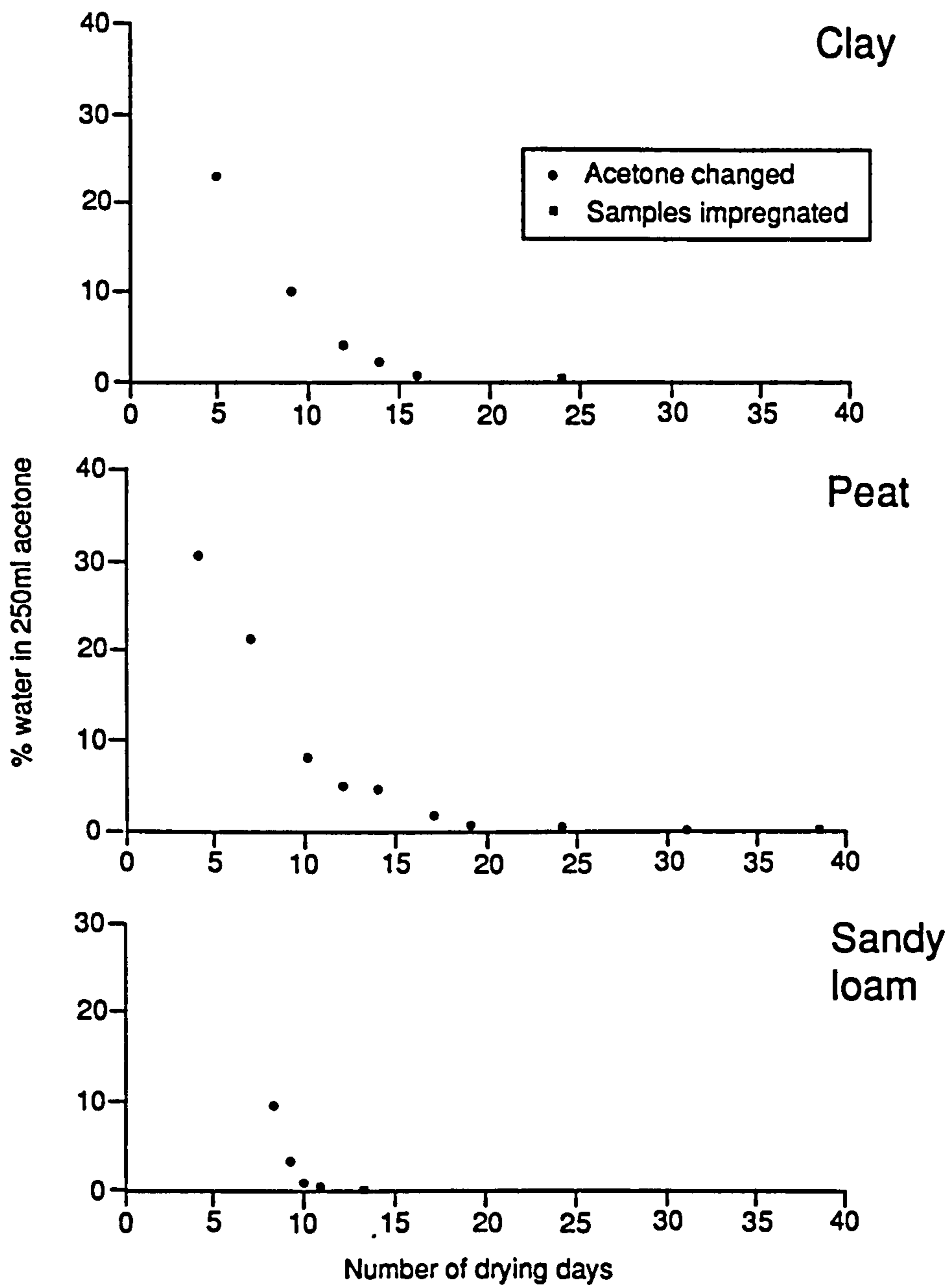


Fig. 4.1 Concentration of water in acetone measured by <sup>1</sup>H NMR spectrometer for clay, peat and sandy loam samples (after Murphy 1985)

graphs drawn by Murphy (1985, fig 4.1) indicating that this method could be used to make general estimates of the water content in acetone. There was not the time to check the standards against an independent method such as NMR spectrometry.

Using the specific gravity method the water content of the acetone was measured each time the acetone was changed. When the critical level of 0.5% water in acetone had been reached the samples were considered ready for impregnation. Having developed this method it became apparent that it was not necessary to use high grade acetone the whole time. A distillation facility was constructed by Mrs M.Macleod enabling the recovery of used acetone. This facility produced acetone that had a water content of 2%. The recovered acetone was used until the 2% level was attained. High grade acetone was then used for the last few changes. This resulted in a considerably saving on the use of fresh acetone.

#### **4.6 Sample impregnation.**

When the water content of the acetone had reached 0.5% the soil blocks were removed and placed in a desiccator ready for impregnation. The samples were transferred to containers made from aluminium foil and placed in the desiccator with the orientation recorded. The containers were made so that the samples would fit tightly but there was still room for the addition of resin between the sample and the foil. The resin was



mixed in plastic beakers, using magnetic stirrers, in the following proportions;

180ml Crystic polyester resin : 1.8ml catalyst : 25ml acetone

The ratios of the resin to catalyst to acetone were based on previous experience in the thin section laboratory. The resin mixture was carefully poured down the side of the samples and allowed to stand. After a few minutes the resin was added so the sample was completely immersed. Vaseline was spread around the lid of the desiccator to ensure a good seal and the lid fitted. A Speedivac 2 vacuum pump was used to create a vacuum in the desiccator.

The use of a polyester resin consisting of 40% styrene and thinned with acetone produced a large amount of volatile material during outgassing. The vapours released were trapped before they reached the pump. This had the advantage of protecting the pump and preventing noxious gases being released into the atmosphere. The trap consisted of a 500ml flask placed inside a 1 litre dewer flask. The flask was modified to fit a Dreschel bottle head and filled with liquid nitrogen. The released gases condensed to a liquid as they passed through the flask.

The level of resin was continually monitored to ensure that it did not fall below the top of the sample. When the level started to get low, the vacuum was turned off, the lid of the desiccator removed and the resin topped up. It was not unusual to top up the

resin 3 or 4 times in one day. The sample was left under vacuum for approximately 7-8 hours after which it was removed and placed in a fume cupboard where it was left to cure for approximately 6-8 weeks. For the first couple of weeks, in the fume cupboard, the level of resin was continually checked to ensure that the sample remained immersed.

#### **4.7 Preparing thin sections from blocks or Kubiena tins.**

At the end of the curing period the large blocks were removed from the fume cupboard and cut open using a diamond circular saw. The block was cut in half and the internal faces examined. There was complete impregnation of the central area and no significant cracking or shrinkage. It was decided that this method was suitable for preparing large blocks, so all the Lairg samples that had not been taken in Kubiena tins were prepared using this method. The experimental blocks were not made into thin sections because a macro examination showed that the impregnation had been successful. The following method was used to make thin sections from the impregnated blocks.

The impregnated sample was taken and a slice approximately 1-2cm thick removed using the circular saw. This slice was then lapped using Logitech equipment and silicon carbide powder mixed with water in the ratio 100ml silicon carbide to 1.5l of water. If the sample was particularly peaty, then ethanediol was used instead of water. The sample was lapped until the surface was completely smooth and then cleaned using trichloroethane. A glass slide was

lapped, the sample was bonded to the slide using an epoxy resin which was then placed in a bonding jig and left overnight to harden.

The following day the excess sample was removed using the diamond circular saw and the remainder lapped down to a standard 30 $\mu$ m thickness. A cover slip was then placed over the sample and left overnight. The slide was then ready for analysis. The total procedure took approximately 12 weeks to produce a block and another 2-3 days to produce a slide.

#### **4.8 Problems encountered during the thin section preparation process.**

The manufacture of the large blocks took much longer than had been estimated. Using conventional sized samples up to 6 blocks can be placed in the desiccator and impregnated simultaneously. The large blocks could only be impregnated 1 or 2 at a time.

The diamond saw used was not powerful enough to cope with the large blocks being made. Blocks were cut very slowly to reduce the possibility of the saw overheating. The block had to be trimmed before the final slice for lapping could be produced. This took more time than slicing a conventional block.

The resin in many of the early blocks made did not set properly. It is thought that a catalyst, that had gone past its shelf life, had been used by accident . This meant that the resin took longer

to set than had been anticipated. In some cases the resin around the edges of the blocks did not set at all. These two factors increased the time that it took to produce the finished number of thin sections.

## Chapter 5

### Results of the excavation and thin section analysis of monuments in group A.

#### 5.1 Introduction

Group A monuments are located at the southern end of the survey site in area 1 on the block location plan (fig 3.5). Within the Medieval enclosure on improved land the soils are freely draining and dominated by brown podzols with localised gleying in areas of wet flushes. The vegetation consists mostly of grass and bracken. Outside the enclosure the vegetation is dominated by heather and the soils by stagnopodzols.

#### 5.2 Results from EP and LP monuments.

Five prehistoric monuments suitable for sampling were identified in group A. M64 is a LP prehistoric hut circle and M62 is an EP cross contour dyke. To the east of the medieval enclosure (M75) there is an area with numerous small cairns. Although these cairns were not dated they are believed to represent EP activity on the site. Two of these cairns were excavated, M88 and M87. Situated in the same area as the cairns is a lynchet, M86. This is again undated but believed to be associated with an early period of activity on the site.

### 5.2.1 Excavation results of M64 a LP hut circle.

M64, situated within the enclosure dyke (M75), is a large embanked and platformed hut circle. It is set within a parallel cross contour field system. The field boundaries consist of alignments of short segments of dykes, linear cairns and lines of cairns. The vegetation immediately around M64 is dominated by grass and bracken. Within the centre of the hut circle there are rushes growing indicating localised waterlogged conditions associated with the interior of the structure.

In the 1989 field season a trench was cut through the monument on the down-slope side of the hut circle wall on the north west side of the structure. Results show a well preserved buried A horizon overlying a buried B horizon. The B horizon extends some way beyond the foot of the wall and is then truncated. Beyond the wall the modern A horizon is situated directly on glacial till or residual pockets of darker soil.

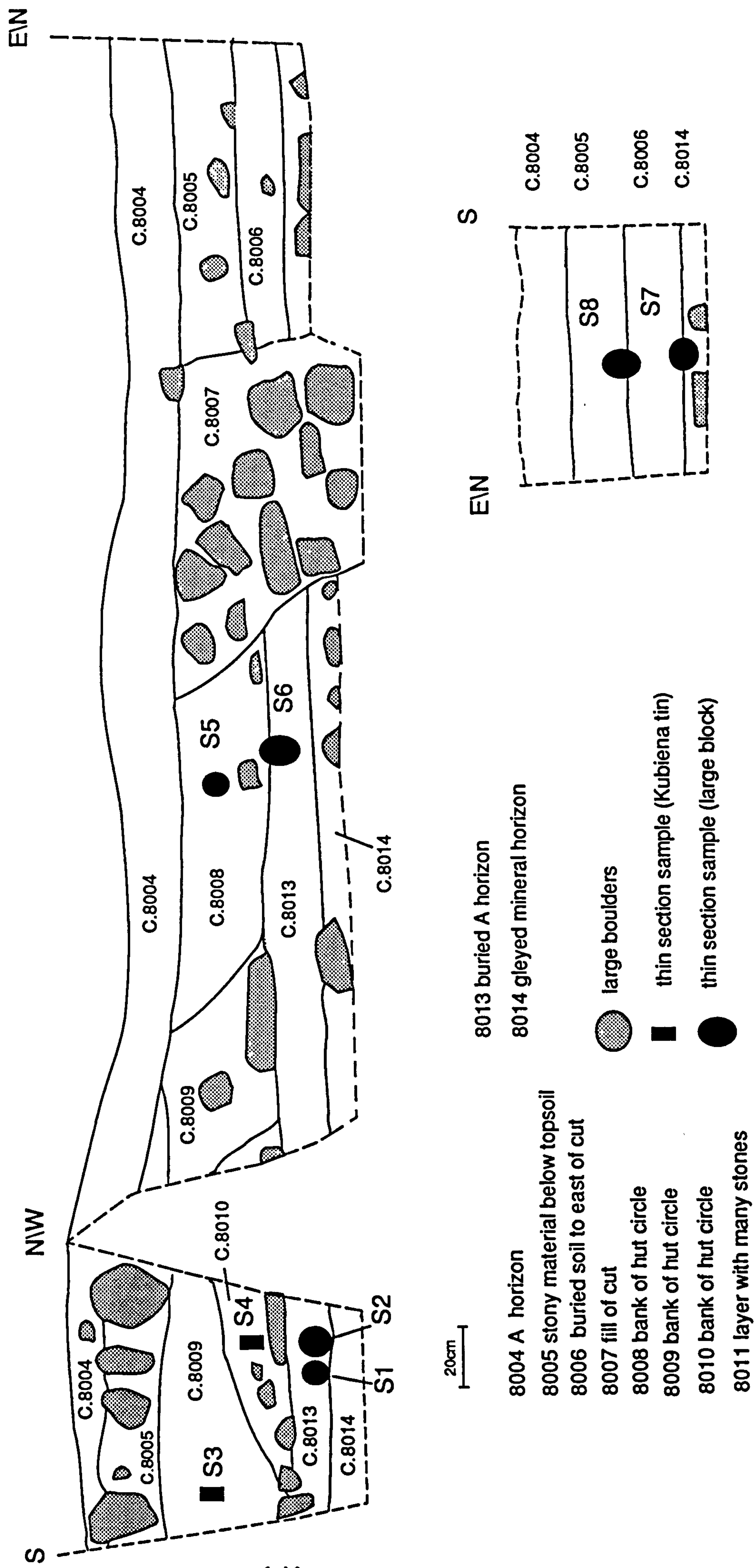
During the 1990 field season, a trench was cut through the eastern bank of the hut circle to allow the sampling of a buried soil as it extended out from underneath the monument to an area where it was no longer buried. A section drawing was produced (fig. 5.1), section photographs taken (figs. 5.2 and 5.3) and soil descriptions written for each context identified.

The base of the trench reached the surface of a Bg horizon (C.8014). Water accumulated in the bottom of the trench

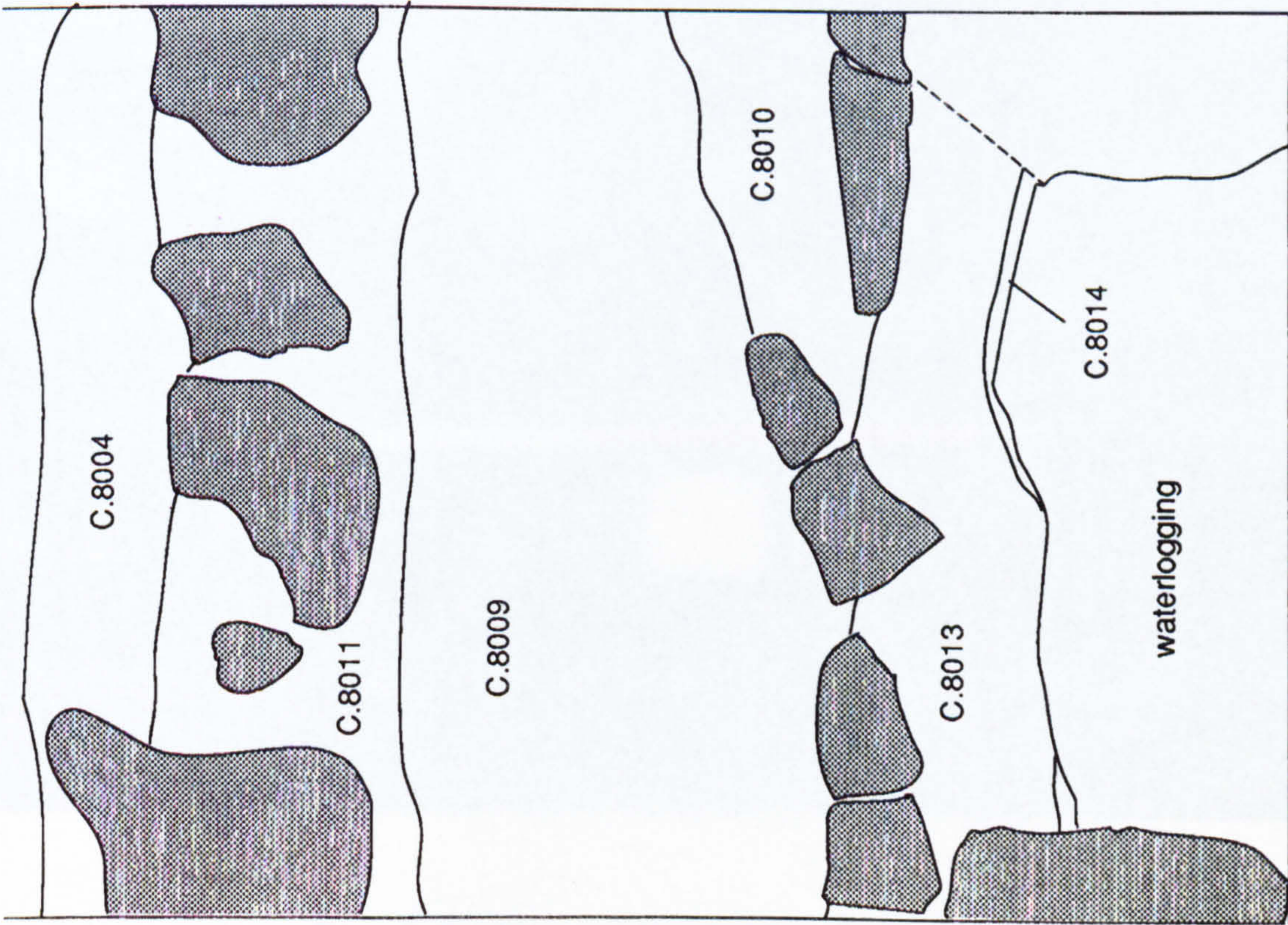
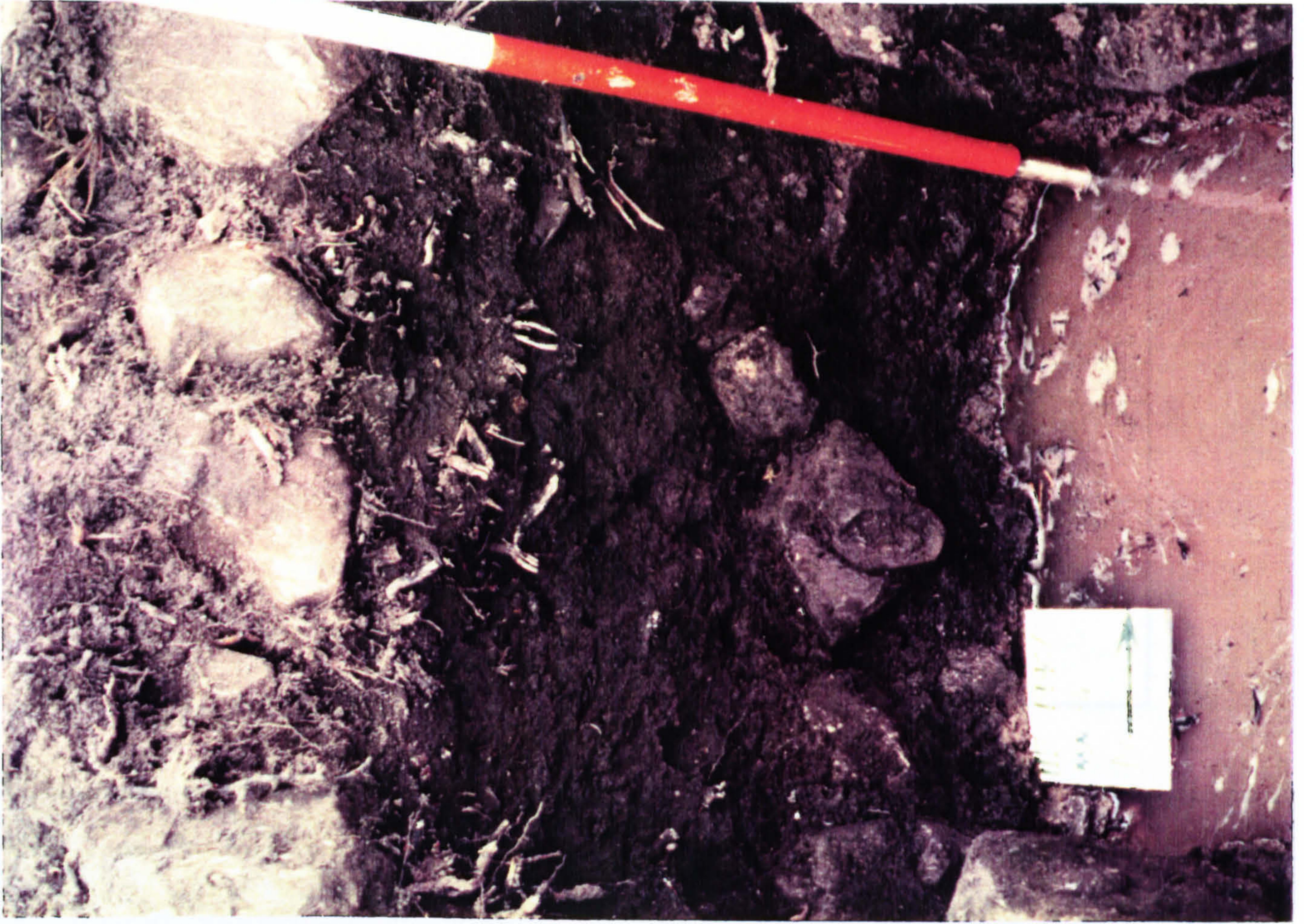
preventing it from being excavated any deeper. The extent of waterlogging can be seen in figures 5.2 and 5.3. A buried A horizon, approximately 20cm thick, is present below the monument but is not continuous. Approximately 2m from the western end of the trench, the buried A horizon is cut by an archaeological feature, context 8007, packed with large and very large boulders. The base of the feature was not reached because of waterlogging at the bottom of the trench. The cut postdated the construction of the hut circle. On the west of the cut the buried soil is sealed by bank material (C.8008) and on the east by an accumulation of soil (C.8004, 8005 and 8006). The colour and structure of the buried soil is very dark brown (10YR 3/2), apedal massive, and remains the same along its length.

To the east of the cut the buried soil has a stone content of abundant medium to large subangular/subrounded stones, to the west the stone content is many medium subangular stones. The amount of root penetration is greater to the east of the cut, suggesting that the accumulation of soil had not sealed the soil as effectively as the construction of the hut circle bank. Bracken rhizomes had not penetrated any deeper than 30cm

Fig. 5.1 M64, LP hut circle








 Large boulders

Fig. 5.2 M64, LP hut circle, east facing section

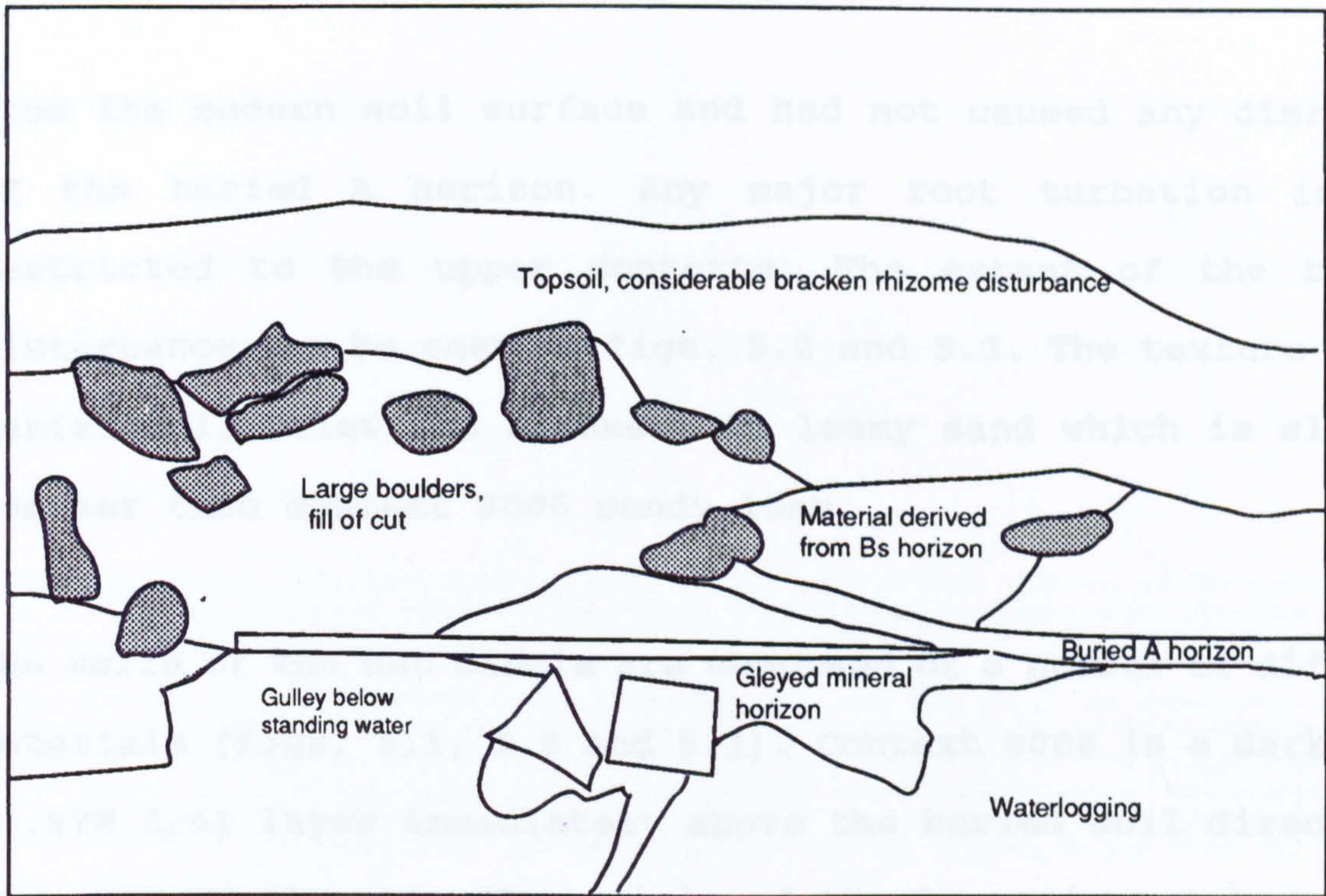


Fig. 5.3 M64, gully and bank material of a LP hut circle, north facing section

from the modern soil surface and had not caused any disruption of the buried A horizon. Any major root turbation is thus restricted to the upper contexts. The extent of the bracken disturbance can be seen in figs. 5.2 and 5.3. The texture of the buried soil below the monument is loamy sand which is slightly coarser than context 8006 sandy loam.

The walls of the hut circle are composed of a number of different materials (figs. 5.1, 5.2 and 5.3). Context 8008 is a dark brown (7.5YR 3/4) layer immediately above the buried soil directly to the west of the cut. The origin of the layer is not known, but the colour suggests that it is derived from a Bs horizon. The rest of the bank material is formed by two more contexts 8009 and 8010. A dark black layer (10YR 2/1, C.8009), is sandwiched between two layers with abundant stones. Context 8010 is a pocket of material within the stone free layer with a greater concentration of orange colour than the surrounding material. Contexts 8008, 8009 and 8010 probably represent different phases of material being added to the bank of the hut circle during construction.

#### **5.2.2 M64 thin section results.**

Eight thin sections were taken for analysis from M64 (fig. 5.1) and 5 of these were analyzed.

### 5.2.3 M64, sample 1

Sample 1 is from the most completely sealed part of the buried A horizon below the monument at the west end of the trench (fig. 5.1).

The microstructure is intergrain micro aggregate and intergrain channel. Channels are the dominant type of void although complex packing voids are also present. Channel diameter varies between 200-800 $\mu$ m and complex packing voids measure 40-800 $\mu$ m. The abundance of voids is common.

Single mineral grains are dominated by quartz which compose more than 70% of the coarse mineral material. There are also smaller quantities of muscovite biotite and feldspar. The larger rock fragments are quartz dominated with variable amounts of feldspar. Some fragments have quantities of biotite approaching 50%. The fragments with the greatest amounts of biotite had undergone the most alteration. In some places, where the alteration of minerals is strongest, intra-mineral material is completely removed leaving single mineral grains with faces that accommodated each other. The fine material is brown to grey brown and composed of organo mineral material.

There is little coarse organic material, just a few remains of roots found in channels. The average root diameter is approximately 400 $\mu$ m which suggests that root growth caused many of the channels seen in the section.

There are fine black irregularly shaped particles randomly distributed throughout the groundmass, abundance is rare. Using just the optical microscope identification of the smallest of these particles is not possible but they are probably a mixture of fine charcoal and amorphous pedofeatures. Some phytoliths are also present. The c/f related distribution is chitonic to enaulic and the c/f ratio is 60:40. The coarse and fine material is poorly sorted.

Strongly impregnated nodules occupy approximately 20% of the thin section area. Large fragments of charcoal are sometimes embedded within a ferruginous matrix. The areas of the nodules that are dark in PPL are also dark using OIL suggesting an organic component to the amorphous material.

There are two fabric pedofeatures present, these differ from the surrounding groundmass only because of their slightly light brown colour. They have sharp boundaries and in places appear disrupted.

### 5.2.4 M64, sample 5.

Sample 5 is from the buried A horizon to the west of the cut (C. 8013).

The microstructure is complex consisting of intergrain channel and microaggregate structure. Voids include channels and complex packing voids. Channel diameter measures 400-800 $\mu$ m. The abundance of total void space as a percentage of the thin section is common.

The ratio of coarse to fine material is 60:40. The coarse mineral material is dominated by quartz rich metamorphic fragments. There are very few remains of roots in channels and occasional charcoal fragments measuring 50-400 $\mu$ m randomly distributed. There are also rare fragmented diatoms and phytoliths randomly distributed. The fine material is organo mineral with a variable c/f related distribution including chitonic and enaulic. The material composing the slide is poorly sorted.

Pedofeatures include many fragmented ferruginous nodules and mottles. Most of the nodules are large measuring 400 $\mu$ m to 2mm. Large rock fragments and fragments of charcoal are impregnated within the ferruginous matrix. Using OIL the nodules are quite reflective however dark brown to black colours are also

present. The nodules are generally isotropic, however some areas show interference colours which seem to be associated with areas of less reflective material.

Rare very faint fabric pedofeatures, 400-600 $\mu$ m in diameter, form passages running through the soil of variable length. They are very faint with little difference in colour to the adjacent groundmass but the boundaries are sharp. They have a strong basic orientation and are referred parallel to the surface.

There are some indications of large ovoid excrement pedofeatures measuring 2mm across. These are organo mineral and have an enaulic internal composition. These features are very faint and strongly coalesced.

### 5.2.5 M64, sample 7

This sample is from the buried A horizon (c.8006), to the east of the cut (c.8007), which is buried by an accumulation of soil (c.8005). The lower half of the sample included c.8014 but this was lost during the preparation of the thin section.

The microstructure is dominantly intergrain microaggregate. The microaggregates are composed of weakly developed ultrafine granules. Voids present include complex packing voids and channels. The diameter of channels measure 200-800 $\mu$ m. The total void space as a percentage of the thin section is common.

Coarse mineral material is dominated by quartz rich metamorphic fragments. Alteration of the minerals is generally light to moderate. Coarse organic components include the remains of roots in channels with a diameter of approximately 800 $\mu$ m, rare fragments of charcoal, measuring 800 $\mu$ m, and occasional fragments of charcoal measuring 40-400 $\mu$ m. There are rare fragmented diatoms and phytoliths randomly distributed throughout the groundmass.

The fine material is grey brown to brown, using PPL, organo mineral. There are occasional black, PPL and OIL, particles randomly distributed measuring 2-50 $\mu$ m. The material is poorly sorted.

The related distribution between the coarse and the fine material is variable including chitonic, enaulic with isolated examples of porphyric.

There are very abundant prominent ferruginous nodules in the lower 3cm of the slide. These are irregularly shaped and strongly impregnated. The impregnating material is composed of two types. Firstly black (PPL), black grey (OIL), isotropic, strongly impregnated amorphous material forms the central area. The impregnation is so strong it was not possible to determine if the nodule is orthic or anorthic. Around this material, within the void space but also impregnating the groundmass, is orange (PPL), dark brown (OIL), material. The edges are weakly anisotropic. In the lower part of the slide the nodules are irregularly shaped and measure from 800 $\mu$ m to 1.5cms. The maximum size found in the upper half of the slide is 2mm.

Dark lines running through the soil, approximately 400 $\mu$ m wide, are clearly seen using image analysis (fig 5.4 to 5.7). They are strongly orientated perpendicular to the surface. The internal fabric is the same as the surrounding groundmass apart from a slight alteration in colour.

A macro and microscopic examination of the slide indicates an abundance of fabric pedofeatures throughout the groundmass. The faint morphology of these made them difficult to distinguish. Images were captured from two different areas of the slide using

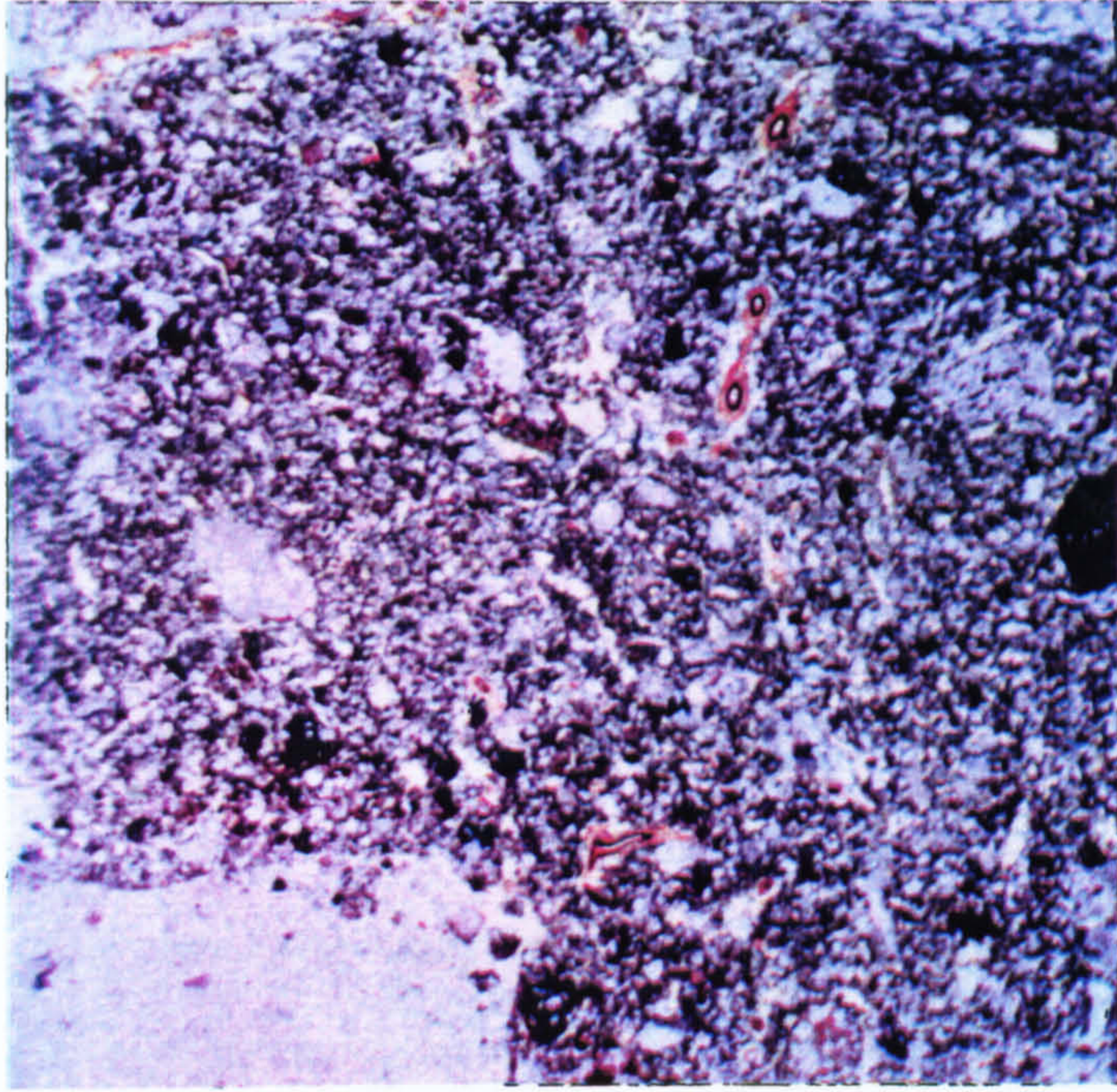


Fig. 5.4 M64, S71, ACS, red 51-84, green 44-86, blue 41-78, FL 31mm

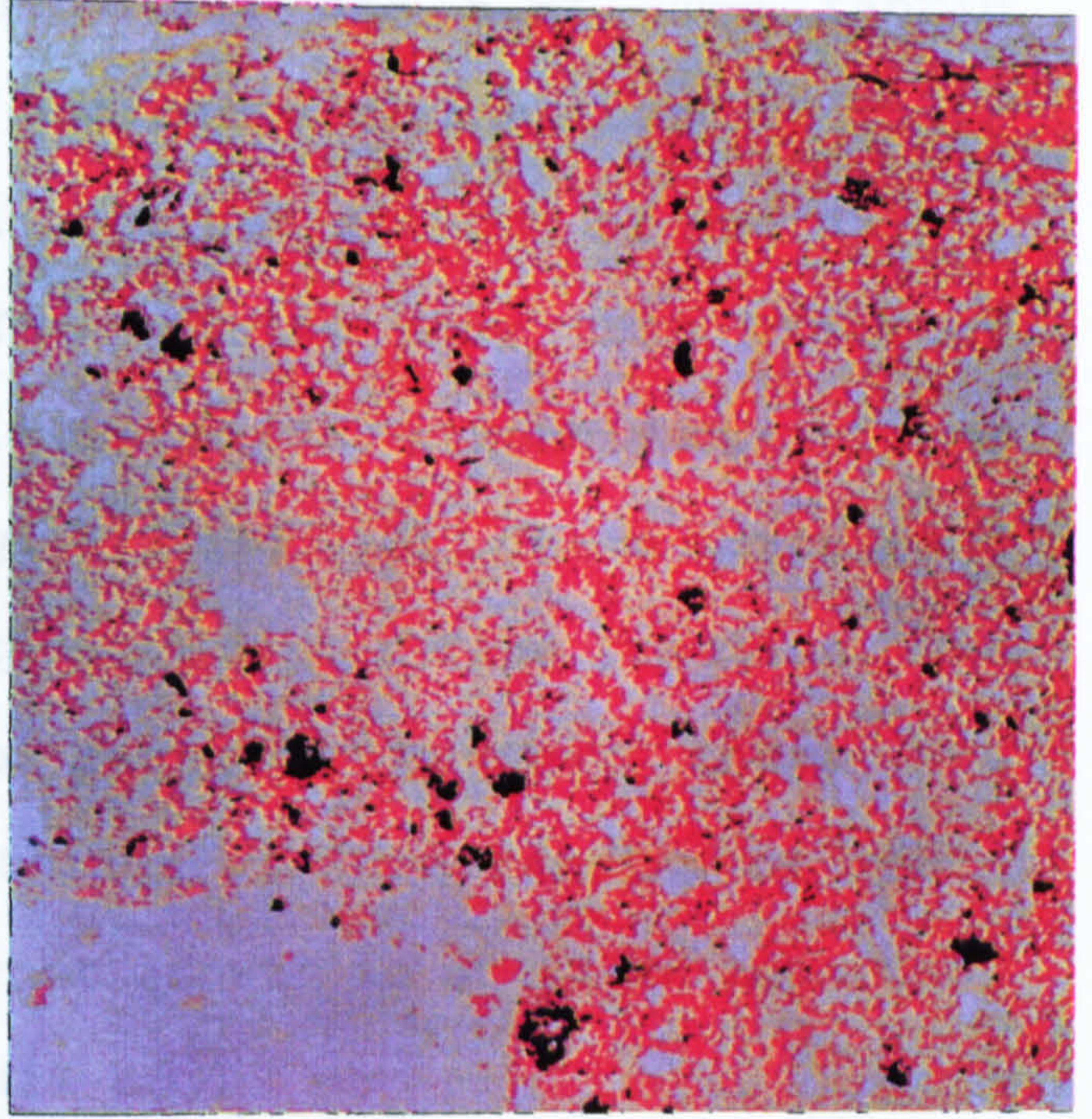


Fig. 5.5 M64, S71, red 55-56, green 50-70, blue 40-80, FL 31mm

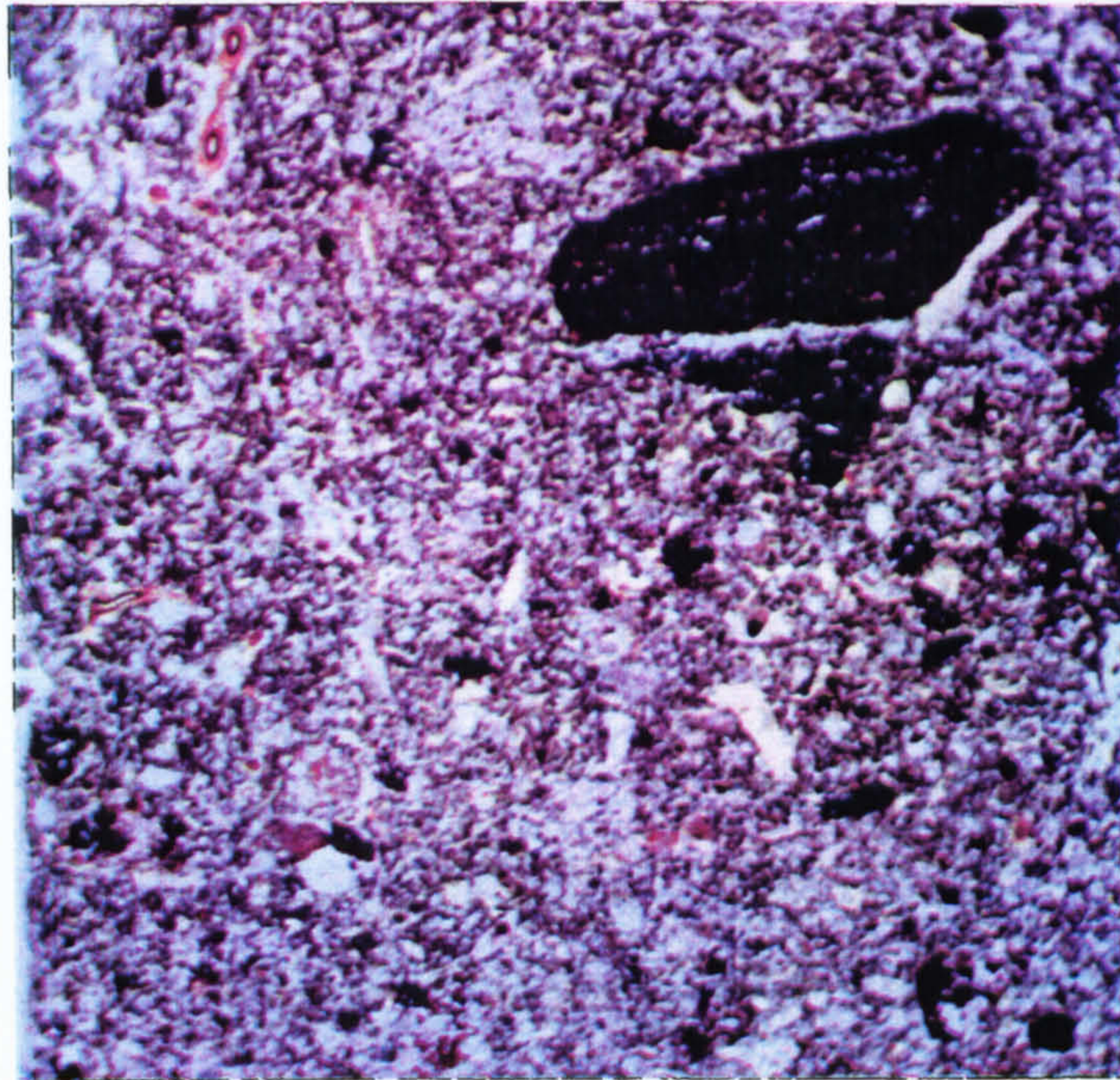


Fig. 5.6 M64, S72, ACS red 38-80, green 36-85, blue 42-91, FL 31mm

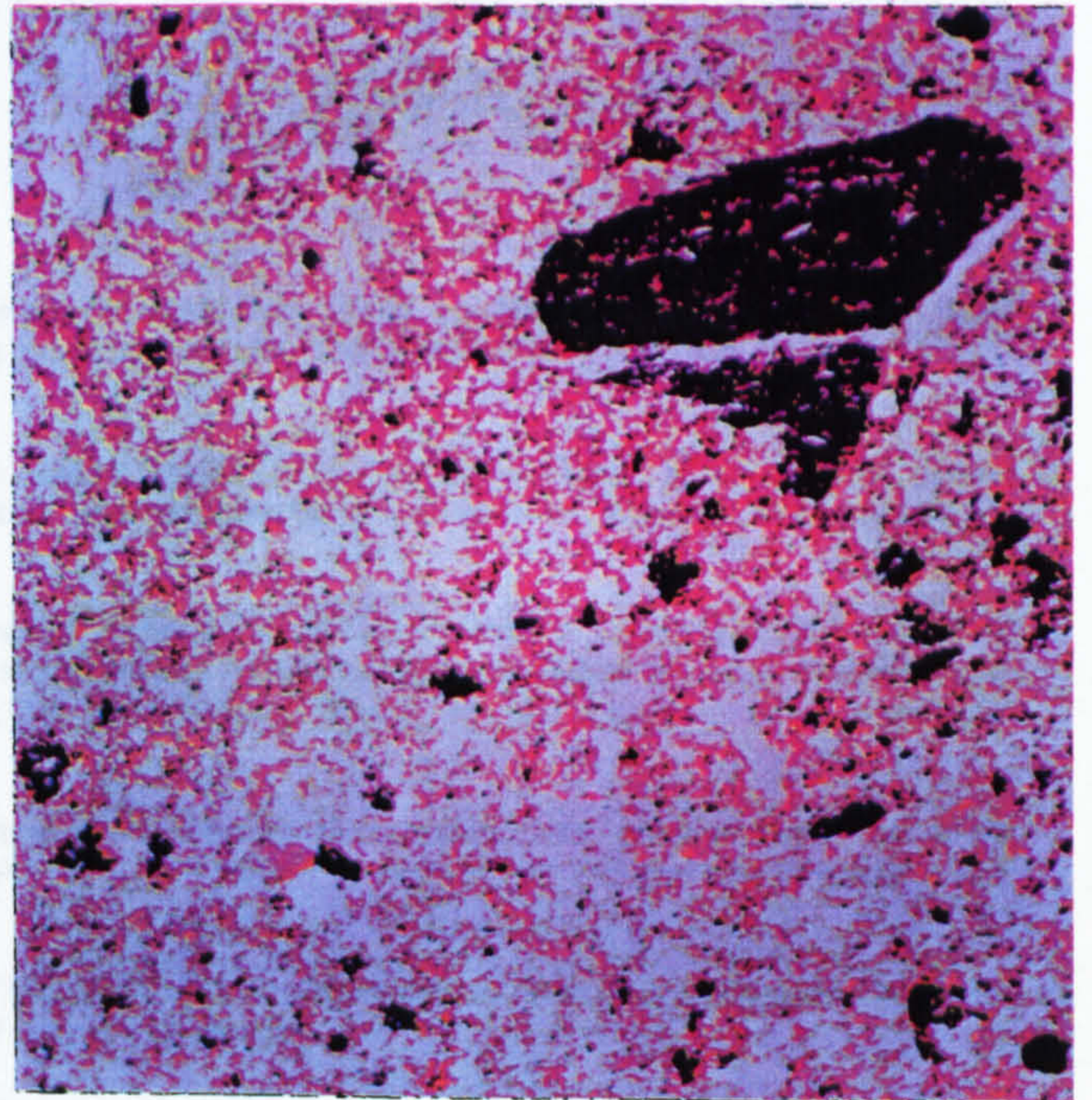


Fig. 5.7 M64, S72, red 55-56, green 50-70, blue 40-80, FL 31mm

red, green and blue filters (fig. 5.4 and 5.6). The fabric pedofeatures were enhanced and a macroscopic assessment of their distribution made using a manual contrast stretch of red 55-56, green 50-70 and blue 40-80 . The results show that lines of darker material are present within the slide, strongly orientated perpendicular to the surface (fig. 5.5 and 5.7). These correspond to areas on the slide with a slightly greater fine fraction. The orientation and width of the features suggest there are associated with root growth. Although visible remains of roots in the thin section is limited, root growth is still an important component in the formation of this soil.

#### 5.2.6 M64, sample 8.

This sample is from the lower part of the soil accumulation above the buried A horizon (C.8005).

The microstructure is dominantly intergrain microaggregate although there is some tendency to localised massive. The main void types are channels and complex packing voids. The area of void space as a total of the thin section is frequent.

Single mineral grains are dominated by quartz with small quantities of muscovite, biotite and green amphibole. Rock fragments are mainly quartz dominated and metamorphic. Light to strong alteration is present.

The coarse organic material includes rare black charcoal fragments (OIL) randomly distributed, very few remains of roots in channels, rare, blackened, humified spherical rings measuring 240 $\mu$ m across. These might represent the outer epidermis of a fungal residue like sclerotium, there is one example of a complete sclerotium.

There are fragments of diatoms and phytoliths randomly distributed throughout the groundmass. The fine material is organo-mineral and randomly distributed rare black fragments, measuring 2-50 $\mu$ m are present. The material is poorly sorted.

The related distribution between the coarse and the fine material is dominantly enaulic although there is some tendency to chitonic where localised bridging of material occurs.

Pedofeatures are dominated by very abundant strongly impregnated ferruginous nodules. These are fragmented resulting in sharp boundaries and variable size and shape. The morphology of the nodules suggests they once formed a pan approximately 4mm wide which was disrupted. Many of the fragments are elongated. Colours vary between orange to red to black, (PPL). Using OIL much of the material is very dark brown. This darker material seems to be found mainly in old void areas but the strong impregnation of the groundmass makes identification difficult. The amorphous material impregnates a matrix consisting of dominantly quartz mineral grains, fine material and in some cases fragments of charcoal.

There are faint loose discontinuous infillings present composed of ultrafine granules measuring approximately  $40\mu\text{m}$ . These are difficult to observe owing to the coarse nature of the material being analyzed.

#### **5.2.7 M64, sample 6.**

This sample is from part of the bank of the hut circle (C.8008, fig 5.1). The field interpretation suggested that this material was derived from a Bs horizon.

The dominant structure is intergrain microaggregate although there is some bridging of coarse material in places. The microaggregates are composed of moderately to strongly developed ultrafine granules. The main types of voids are complex packing voids and channels.

The mineral component of the soil consists of mainly metamorphic quartz dominated fragments. There is only light to moderate alteration of any of the minerals. There are no inorganic residues of biological origin and little charcoal in the sample. There are some remains of roots in channels. The material is poorly sorted to unsorted. The related distribution between the fine and the coarse material is dominantly enaulic with local tendencies to chitonic.

Pedofeatures include the fragmented remains of silt cappings, and strongly ferruginised nodules measuring  $400\mu\text{m}$  to  $2\text{mm}$ . The nodules consist of a dark strongly reflective material and an orange duller material associated with old void spaces. This orange material also forms much smaller nodules measuring  $100\text{-}200\mu\text{m}$  which are randomly distributed throughout the groundmass. These are sometimes associated with channel shapes.

#### **5.2.8 Discussion of samples 1, 5, 7, 8.**

In all the sections taken from the buried A horizon, there are abundant irregularly shaped ferruginous nodules. Rock fragments and large fragments of charcoal are often embedded in a strongly impregnated ferruginous matrix. The matrix is composed of two types of material. The first is orange (PPL), dull (OIL), and found most often in voids. This is weakly anisotropic and shows some signs of layering. The second material is generally found impregnating the groundmass and is more reflective using OIL. The sharp boundaries and irregular shape of the nodules suggest that they are fragmented.



| Sample No | Context                                  | Coarse charcoal | Black particles <50 $\mu$ m | Phytoliths | Diatoms |
|-----------|--|-----------------|-----------------------------|------------|---------|
| 1         | Buried A horizon                         | No              | Rare                        | Yes        | No      |
| 5         | Buried A horizon                         | Occasional      | Occasional                  | Yes        | Yes     |
| 7         | Buried A horizon                         | Occasional      | Occasional                  | Yes        | Yes     |
| 8         | Soil accumulation above buried A horizon | Rare            | Rare                        | Yes        | Yes     |
| 6         | Wall material                            | Rare            | No                          | No         | No      |

Table 5.1 Comparison of micromorphological features from M64

The occurrence and abundance of coarse charcoal, fine black particles less than 50 $\mu$ m, phytoliths and diatoms in samples taken from M64 are given in table 5.1. A positive identification of the smallest black particles is not always possible using the optical microscope. However unidentified fragments often occur with many fragments that are slightly larger and identified as charcoal.

Sample 1, taken from a part of the soil that is well sealed by the overlying monument has fewer coarse and fine charcoal fragments than samples 5 and 7, which are from different lateral positions along the buried A horizon (fig 5.1 and 5.3). Fragmented diatoms and phytoliths are present in samples 5, 7 and 8, but in sample 1, only phytoliths are observed.

The microstructures of samples 1, 5 and 7 are all identical (table 5.2).

| Sample N <sup>o</sup> | Context             | Dominant c/f related distribution, c/f ratio | Sorting            | Total voids TTS    | Microstructure                                 |
|-----------------------|---------------------|--|--------------------|--------------------|--|
| 1                     | Buried A            | Chitonic, local enaulic, 60:40               | Poorly             | Common             | Intergrain channel and microaggregate          |
| 5                     | Buried A            | Chitonic, local enaulic, 60:40               | Poorly             | Common             | Intergrain channel and microaggregate          |
| 7                     | Buried A            | Chitonic, local enaulic and porphyric, 60:40 | Poorly             | Frequent to common | Intergrain microaggregate                      |
| 8                     | Soil above buried A | Enaulic, localised chitonic, 60:40           | Poorly             | Frequent           | Intergrain microaggregate, localised massive   |
| 6                     | Wall material       | Enaulic, localised chitonic, 70:30           | Poorly to unsorted | Common             | Intergrain microaggregate, local bridged grain |

Table 5.2 Comparison of microstructure and c/f ratios from M64

The microstructure of sample 8 is similar to samples 1, 5 and 7 except for a slight tendency to massive structure in some areas of the slide. The lowest abundance of voids and the greatest amount of fungal material are present in sample 8. It is possible that the differences in sample 8 are related to the organic component of the slide. Any increase in the amount of organic material would create conditions more suited to fungal activity. In slides from other parts of the site (section 6.8) where there is an increase in the organic material within the soil, for instance above an iron pan, the porosity of the soil gets lower and the structure tends towards massive. These changes are consistent with those observed in sample 8.

The results from the 1989 field season show a well developed buried Bs horizon below the buried A horizon on the north west side of the structure. There is no E horizon present indicating that this is a buried brown podzol. The bottom of the 1990 trench

represents the top of a Bg horizon. The trench could not be excavated any deeper because of waterlogging.

Sample 6 was taken to determine if context 8008 is derived from a Bs horizon. There are fragmented silt cappings present throughout the context. Evidence from other contexts on the site show that silt cappings are characteristic of glacial till (section 9.2) and are often found incorporated into Bs horizons (section 9.3). The presence of fragmented silt cappings within context 8008 combined with the strong orange colour observed in the field indicates that this material is derived from a Bs horizon. The orange colour is derived from the colour of the ultrafine granules found throughout the slide showing the Bs horizon was polymorphic (section 9.3).

The presence of diatoms and phytoliths throughout an A horizon indicates mixing of surface organic material and underlying mineral material. This mixing could be anthropogenic or biological. There are no diatoms present in sample 1 so it is possible that the diatoms present in samples 5 and 7 are the result of material added to the soil after the construction of the monument. This observation is only speculative. The abundance of diatoms in any of the slides is rare. It is only possible to observe diatoms using high magnifications. This makes it difficult to assess abundance in an area as large as a thin section slide. Recording presence or absence is also difficult when abundance is rare. If diatoms are considered an important diagnostic feature then it is best to isolate them using more

suitable techniques, for instance acid digestion of the soil to leave only silica.

#### **5.2.9 Summary of M64**

M64, a hut circle constructed during the LP period, was probably initially built on a freely draining podzolic soil. Sometime during occupation of the hut circle waterlogging occurred, probably caused by a modification in drainage after monument construction, and a drainage gully was dug. There was still a Bs horizon present at this time. The construction of the gully moved material from the Bs horizon and incorporated it into the bank of the hut circle. Gleying subsequently removed any indications of a podzolic B horizon below the A horizon.

#### **5.3 Excavation results of M62, an EP cross contour dyke.**

M62 is an early prehistoric cross contour dyke. It forms the lowest part of a number of features which are interpreted as a cross contour boundary. The dyke belongs to a cross contour prehistoric land use phase thought to represent an early period of human activity on the site.

The vegetation immediately around the position of the 1990 trench is dominantly grass with some bracken and moss. The vegetation suggests freely draining conditions. The 1989 survey revealed a buried A horizon below the dyke directly overlying glacial till. The monument was excavated again in 1990.

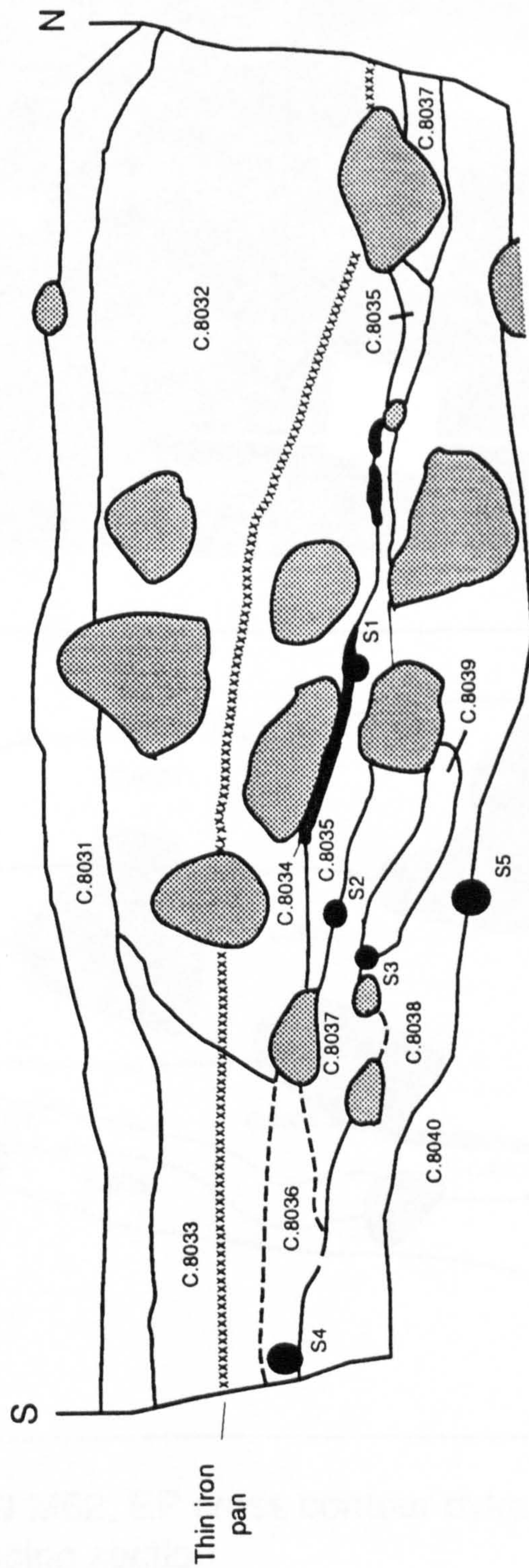
A layer of topsoil 20cms deep covers the monument (fig. 5.8 and 5.9). Soil had accumulated to the south of the main dyke burying a brown podzol below it. Considerable disturbance by bracken was noted in the top of context 8033 and within the monument itself. The main part of the dyke is 50 to 70cm deep and composed of very abundant large to very large subangular stones. The massive structure of the monument completely seals a buried soil profile.



Directly below the dyke there is a dark black (7.5YR 2/0) organic layer, (C.8034, fig 5.8 and fig. 5.9). This is interpreted as the original turf line that the monument was constructed on. Below the turf line is a buried A horizon (8035) approximately 20cms thick. The colour varies between dark brown (10YR 3/3) and dark brown (7.5YR 3/4). The texture is loamy sand and the structure apedal massive. There is very little recent disturbance of this layer with few very fine fibrous roots recorded.

Underlying context 8035 on the southern edge of the monument is a pale brown (10YR 3/3) context (8037), apedal massive with few very fine fibrous roots indicating little disturbance. This is interpreted as a buried E horizon (figs 5.8 and 5.9).

Below the entire monument and extending beyond it is a buried Bs horizon. There is some colour variation present throughout this context, dark brown (7.5YR 4/4) present directly under the monument and, strong brown (7.5YR 4/6) to the south.

Fig 5.8 Monument 62, EP cross contour dyke



- Contexts:
- 8031 Topsoil
  - 8032 Matrix of the monument
  - 8033 Accumulation to south of the monument
  - 8034 Buried organic layer
  - 8035 Buried A horizon sealed by monument
  - 8036 Buried A horizon to south of monument
  - 8037 Buried E horizon
  - 8038 Bs horizon
  - 8039 Colour variation within Bs horizon
  - 8040 Glacial till
-  Large boulders
  -  Samples for thin section (wrapped block)

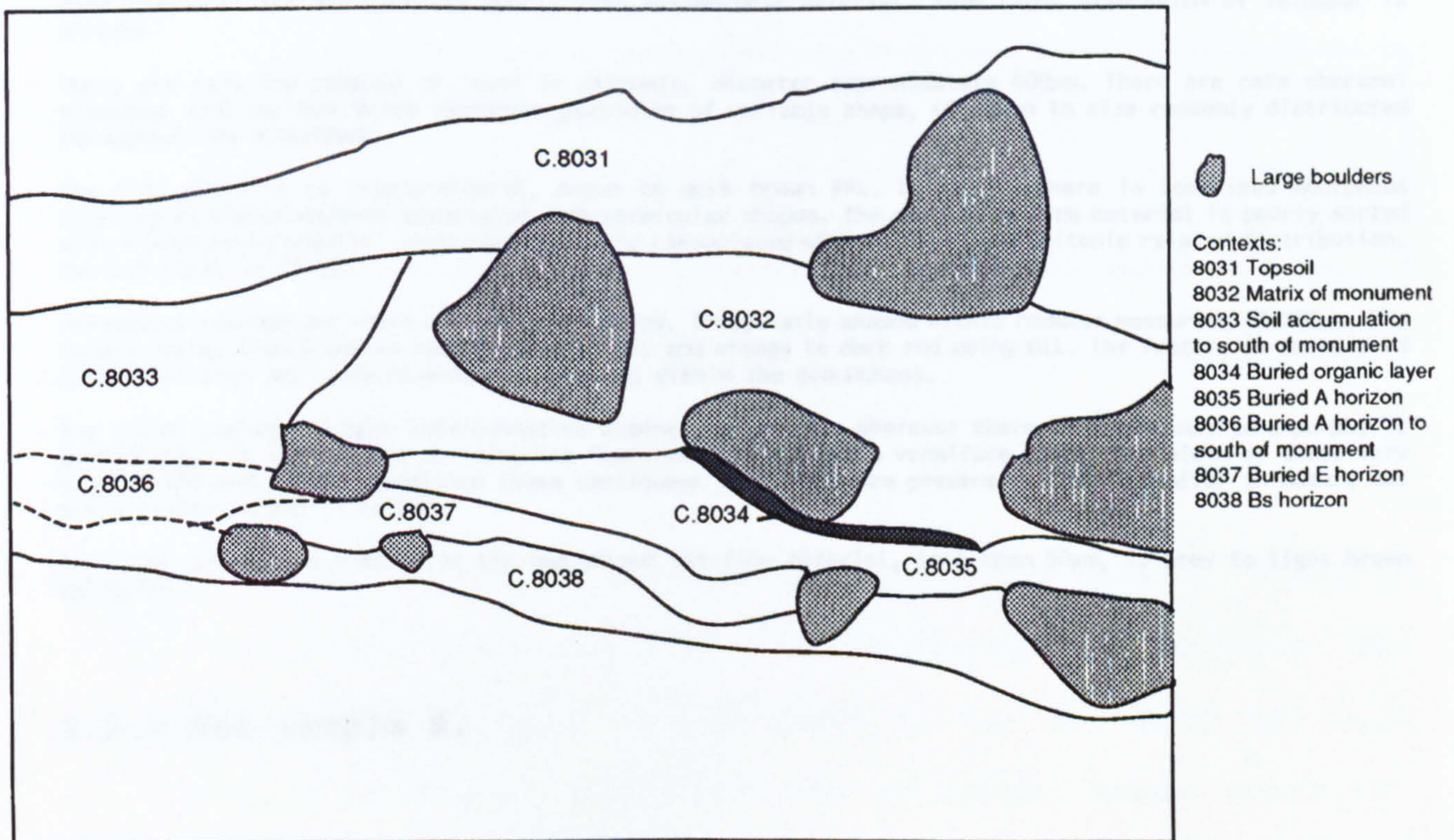
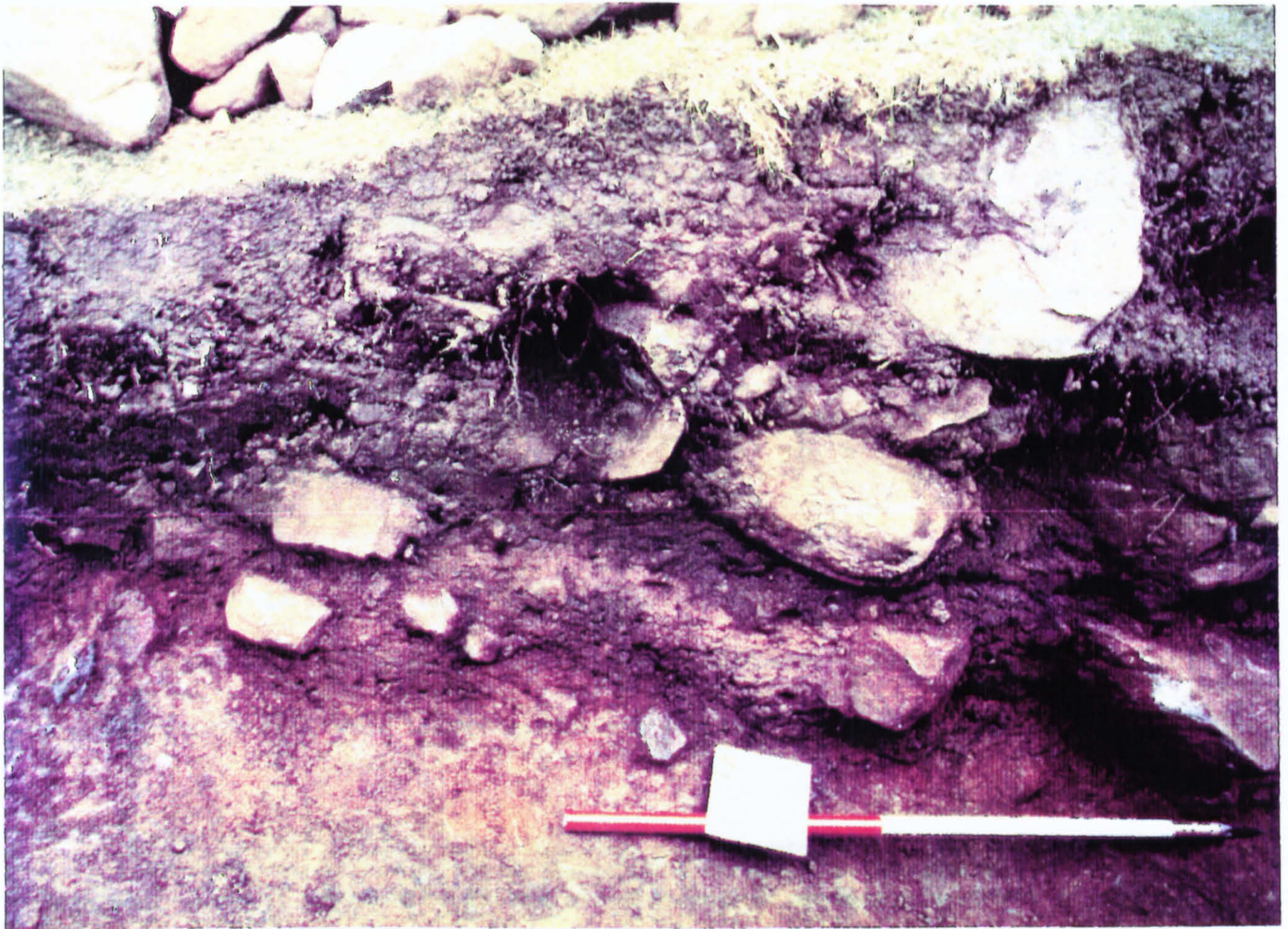


Fig. 5.9 M62, EP cross contour dyke east facing section

### **5.3.1 M62 thin section results**

Five thin sections were taken for analysis and 2 were analysed.

### **5.3.2 M62, sample 2.**

Sample 2 is from the boundary between the buried A horizon and the buried E horizon. The upper context is the buried A horizon (c.8035) and the lower context is the buried E horizon (c.8037).

Apedal soil material with a dominantly intergrain microaggregate structure with some localised tendency to a bridged grain. The main types of voids are complex packing voids and channels. Channels are approximately 400 $\mu$ m in diameter. The abundance of voids as a percentage of the context is frequent.

Single mineral grains are dominated by quartz in the size range 50 to 800 $\mu$ m. There are few green amphiboles, few feldspars, very few biotite and muscovite all found in the same size range. Compound mineral grains and rock fragments are dominated by quartz rich metamorphic material. Some light alteration of feldspar is present.

There are very few remains of roots in channels, diameter approximately 400 $\mu$ m. There are rare charcoal fragments and few dark black amorphous particles of variable shape, 40-400 $\mu$ m in size randomly distributed throughout the groundmass.

The fine material is organo-mineral, brown to dark brown PPL. Using OIL there is localised amorphous staining of the groundmass associated with vermicular shapes. The coarse and fine material is poorly sorted with a dominantly enaulic, localised porphyric (associated with infills) and chitonic related distribution. The c/f ratio is 65:35.

Throughout the context there are small, 40-500 $\mu$ m, irregularly shaped orthic nodules measuring 40-500 $\mu$ m. The colour varies from black to red/brown using PPL and orange to dark red using OIL. The feature is associated with infillings and vermiform fabric features within the groundmass.

The slide consists of many interconnected channel infillings. Wherever there is a tendency to a porphyric distribution it is possible to recognise features that exhibit a vermiform shape. The width of these vary between 800 and 1000 $\mu$ m. Sometimes loose continuous infillings are present which are similar in nature but are a lighter brown in colour.

The lower context is similar to the top except the fine material, less than 50 $\mu$ m, is grey to light brown using PPL.

### **5.3.3 M62 sample 5.**

The sample is from the boundary between the Bs horizon and the underlying glacial till. During sampling the bottom of the sample was disrupted so only the Bs horizon (c.8038) is described.



The microstructure is intergrain microaggregate with some disturbance by channels. The groundmass consists of many small ovoid pellets measuring 40µm across in various stages of coalescing and forming aggregates in some places. Between these pellets the main types of voids are compound and complex packing voids. These have an irregular shape and measure 20-40µm. Larger voids are generally caused by channels and measure 100-400µm. The abundance of voids as a percentage of the thin section is few.

Single mineral grains are dominated by quartz with smaller quantities of green amphibole, feldspar, muscovite and biotite.

Compound mineral grains and rock fragments are dominated by metamorphic fragments. The mineralogy is dominantly interlocking quartz grains but also includes biotite, feldspar, muscovite and green amphibole, some of the feldspar and green amphibole has banded distributions. There is generally light alteration of the feldspar although some stronger alteration is present.

Coarse organic material includes very few remains of roots in channels and one dark ring. The fine material is orange using PPL and organo mineral. The c/f ratio is 70:30 and the material is poorly sorted.

The slide is divided into areas based upon variability in the colour of the groundmass. The lower part of the slide is less variable than the upper, is dominantly orange using PPL, and has an enaulic c/f related distribution. The upper part of the slide has a variable colour, dark brown, dark grey brown to orange. In places coatings of the darker material is present around some of the larger rock fragments. The c/f related distribution of both of the contexts is dominantly enaulic.

Textural pedofeatures include fragmented silt cappings on stones and fragmented silt cappings incorporated into the general groundmass. The silt cappings on rock fragments are layered with coarser material overlying finer material. Generally the colour of the silt cappings is grey. At the top of the slide a capping is present which had been impregnated by ferruginous material colouring it red. Lying on top of the same fragment is a thin orientated clay coating. The abundance of cappings as a percentage of the section is few.

There are occasional ferruginous coatings and few ferruginous nodules. The coatings are brown red PPL, very dark brown OIL, mainly isotropic but some orientation at the edges is visible.

#### 5.3.4 Discussion of M62.

| Sample No     | Context  | Coarse charcoal | Black particles <50µm | Phytoliths | Diatoms |
|---------------|----------|-----------------|-----------------------|------------|---------|
| M62, sample 2 | Buried A | Rare            | No                    | No         | No      |
| M62, sample 5 | Buried B | No              | No                    | No         | No      |

Table 5.3 Micromorphological features of samples taken from M62

The soil profile buried below the monument is a podzol. There is a well developed E horizon (fig 5.9) overlying a Bs horizon. The E horizon is not present to the south of the monument and does not extend completely underneath the monument. Human activity, post dating the construction of the dyke, could have truncated the profile creating a brown podzol. The absence of the E horizon

from below the dyke might reflect a period when the dyke was much smaller than its present size.

The thin section analysis showed there are rare coarse charcoal fragments present in the buried A horizon below the monument but no fine black particles (table 5.3) or fragmented diatoms or phytoliths. This absence of these features might reflect minimal anthropogenic use (section 9.5).

Disturbance in the Bs horizon is indicated by the presence of fragmented silt cappings (section 9.3). Some of the cappings are impregnated with ferruginous material at the top of the slide suggesting formation of the podzolic B horizon after disturbance of glacial till. A major constituent of the Bs horizon is the abundance of ultrafine granules. These have a similar appearance to the polymorphic organic material described by De Coninck and D. Righi (1983) and De Coninck et. al (1974). The formation and different types of B horizon are discussed in greater detail in section 9.3.

#### **5.4 Results of the analysis of M86, an EP lynchet.**

A trench was cut in an east west direction through M86 (fig 5.10). This is a lynchet to the north of the head dyke in an area of modern stagnopodzols. Overlying the monument is a peaty layer measuring up to 25cms thick. Below this is a bleached mineral horizon, very dark greyish brown (10YR 3/2, C.5023). Context 5024 is a mineral horizon, in part below the peat and in part below

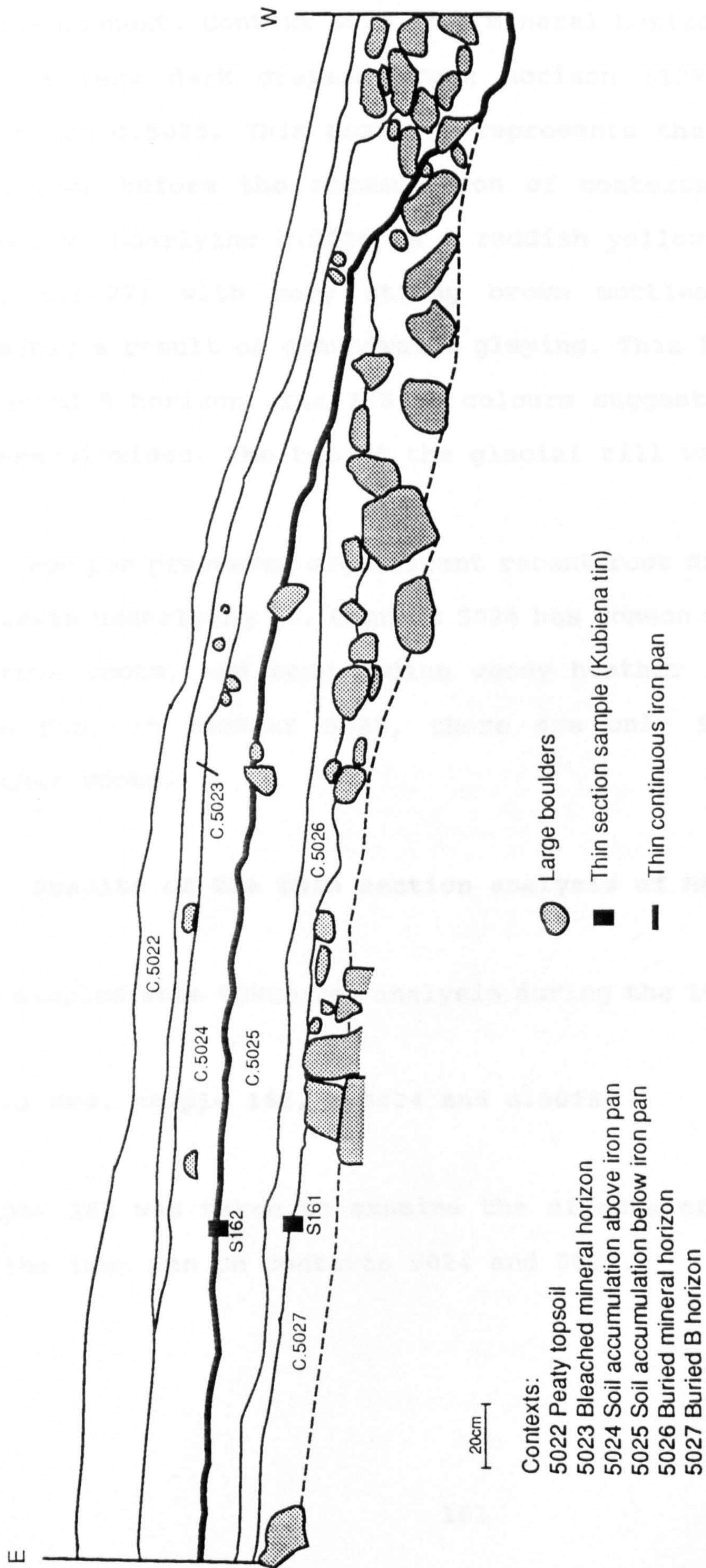


Fig. 5.10 M86, undated lynchet located in an area of stagnopodzols,  
north facing section

the bleached layer, with a thin continuous iron pan at the base of the context. Context 5025 is a mineral horizon below the iron pan. A very dark greyish brown horizon (10YR 3/2, C.5026), underlies c.5025. This possibly represents the original buried A horizon before the accumulation of contexts 5025 and 5024. Directly underlying c.5026 is a reddish yellow horizon (7/5 YR 6/6, c.5027) with many strong brown mottles (7/5 YR 5/6), possibly a result of groundwater gleying. This is interpreted as a buried B horizon. The 7/5 YR colours suggest some enrichment of sesquioxides. The top of the glacial till was not reached.

The iron pan prevented significant recent root disturbance in the contexts underlying it. Context 5024 has common very fine to fine fibrous roots, and many medium woody heather roots. Below the iron pan, in context 5025, there are only few fine fibrous heather roots.

#### **5.5 Results of the thin section analysis of M86.**

Two samples were taken for analysis during the 1989 field season.

##### **5.5.1 M86, sample 162, c.5024 and c.5025.**

Sample 162 was taken to examine the effects of the development of the iron pan on contexts 5024 and 5025.

## **1. Soil above Fe pan (C.5024).**

This context has a dense groundmass and abundant roots. Root growth is impeded by the iron pan. The microstructure is channel and massive. The channels are irregularly shaped reflecting the coarse grained nature of the groundmass. Many of the channels have decomposing remains of roots within them. At the top of the slide channels are moderately referred perpendicular to the surface while closer to the iron pan channels are moderately referred parallel to the pan. The abundance of voids as a percentage of this context is few.

Coarse organic components include very abundant roots in various stages of decomposition. They form a root mat along the top of the iron pan. Using OIL the roots are generally dark although greater reflectance is observed in some areas. There are rare fragments of charcoal measuring 50-800 $\mu$ m, randomly distributed. The fine material is organo mineral, brown PPL. There are one or two black particles measuring 2-50 $\mu$ m randomly distributed. The related distribution between the coarse and the fine material is porphyric and the c/f ratio is 40:60.

Pedofeatures comprise rare ferruginous nodules measuring 400 $\mu$ m across, red brown (PPL), red orange (OIL), randomly distributed, strongly impregnated, prominent, sharp boundary, internal fabric composed of mineral fragments, mainly quartz and ferruginous material, isotropic.

## **2. Iron pan.**

The top of the pan is the most strongly impregnate area. The colour is dominantly black with some dark red areas (PPL), dark red to strong orange (OIL). The boundary at the top of the pan is sharp and diffuse below. The top part of the pan incorporates dominant quartz grains with some green amphibole and biotite. There is one charcoal fragment which measures 2mm across. The area below the pan is moderately to strongly impregnated with ferruginous material. This forms coatings on voids and impregnates the groundmass. The coatings on the voids are generally orange (PPL), brown orange (OIL), isotropic, approximately 20-40 $\mu$ m thick. They occasionally fill entire void spaces.

## **3. Lower soil sealed by the iron pan (C.5025).**

The microstructure is intergrain microaggregate structure with very limited bridging of fine material between coarse mineral grains. The abundance of voids as a percentage of this context is frequent. There are no coarse organic components. The fine material is organo mineral, grey brown (PPL), pale brown (OIL). There are one or two black particles measuring 2-50 $\mu$ m. The material is well sorted although there is not much present on the slide to make a reliable estimate. The c/f related distribution is enaulic.

Pedofeatures comprise abundant strongly impregnated, probably orthic, ferruginous nodules. These are strong red to black (PPL), red brown to strong orange (OIL). The matrix consists of dominant quartz with some green amphibole. The size varies from small (200 $\mu$ m) fragmented particles of dominantly amorphous ferruginous material to large examples measuring 8mm across.

There are occasionally silt sized coatings on some of the larger voids. This is the result of disturbance during sampling. In the disturbed areas the groundmass has formed into ovoid, 800 $\mu$ m to 4mm, organo mineral granules. The morphology of these are similar to the larger organo mineral excrements seen in other slides.

### **5.5.2 M86, sample 161.**

Sample 161 is from the interface between the possible buried A and buried B horizon. Although the sample is from the interface of two horizons the slide appears homogenous apart from a concentration of ferruginous nodules in the lower part.

The microstructure is intergrain microaggregate and channel. There is some bridging of the fine material between the mineral grains. The abundance of voids as a percentage of the section is frequent. The material is poorly sorted.

Coarse organic components consist of occasional fragments of charcoal measuring 50-400 $\mu$ m and rare remains of roots in channels, in places forming almost amorphous material. Inorganic residues of biological origin include rare phytoliths. The fine material is organo mineral, brown to grey brown (PPL), pale orange brown (OIL). There are occasional black particles measuring 2-50 $\mu$ m present throughout the slide, many are probably charcoal. The c/f related distribution varies between enaulic and chitonic.

There are very abundant, strongly impregnated, ferruginous nodules, dark red to black (PPL), orange red to dark red (OIL), isotropic present in the bottom 2cm of the slide. Amorphous ferruginous material impregnates a matrix of dominantly quartz grains but small quantities of other minerals are also present. The nodules measure 100 $\mu$ m to 5mm. The larger examples tend to be fragmented with angular edges although subrounded fragments are also observed. The nodules have the same appearance as fragmented iron pan features seen in other early contexts except they are not found with any charcoal.

### 5.5.3 Discussion of M86.

There is evidence from M86 to suggest three episodes of soil development and pedogenesis. Context 5026 is a buried A horizon. There is occasional coarse and fine charcoal fragments present throughout this layer suggesting a period when the soil was disturbed. Context 5026 is buried by an accumulation of soil (contexts 5025 and 5024). The abundance of carbonised residues is minimal in the soil accumulation. There are only one or two fine black particles present.

At some point during the development of the soil accumulation an iron pan formed. This created an almost complete barrier against any root penetration. A root mat formed along the top of the iron pan and caused abundant decomposing roots to accumulate in context 5024. There are considerable structural and organic matter differences between the contexts 5024 and 5025. Above the iron pan the structure is massive with a porphyric c/f related distribution caused by the addition of organic material from decomposing roots. The microstructure of context 5025 is dominantly intergrain microaggregate with an enaulic c/f related

distribution. Once the iron pan had formed the low porosity and dense groundmass contributed to surface waterlogging promoting the development of a peaty topsoil (context 5022).

There is no micromorphological difference between the base of the buried A and the top of the buried B apart from an abundance of fragmented ferruginous nodules in the latter. The morphology of the nodules is very similar to those seen in buried A horizons under M64 and M505. It is possible that the nodules either represent disturbance of iron pan during the later prehistoric or are associated with groundwater gleying. The formation and distribution of fragmented ferruginous nodules is discussed in section 9.4.

#### **5.6 Results from M88, an EP clearance cairn.**

M88 is one of several large vacuous cairns (see also M87) to the east of the main enclosure in an area of modern stagnopodzols. It is situated in an area with numerous other cairns of comparable size. The cairns are considered to represent early prehistoric activity. A layer of peat (C.5016) is present overlying a bleached layer (C.5017, fig 5.11). Underlying these horizons there is approximately 0.5m of mineral soil that has accumulated on the upslope side of the cairn. This accumulation is divided into two components, contexts 5028 and 5029, and incorporates an iron pan. Below the soil accumulation is a buried A horizon (context 5020). The B horizon (context 5021) appears

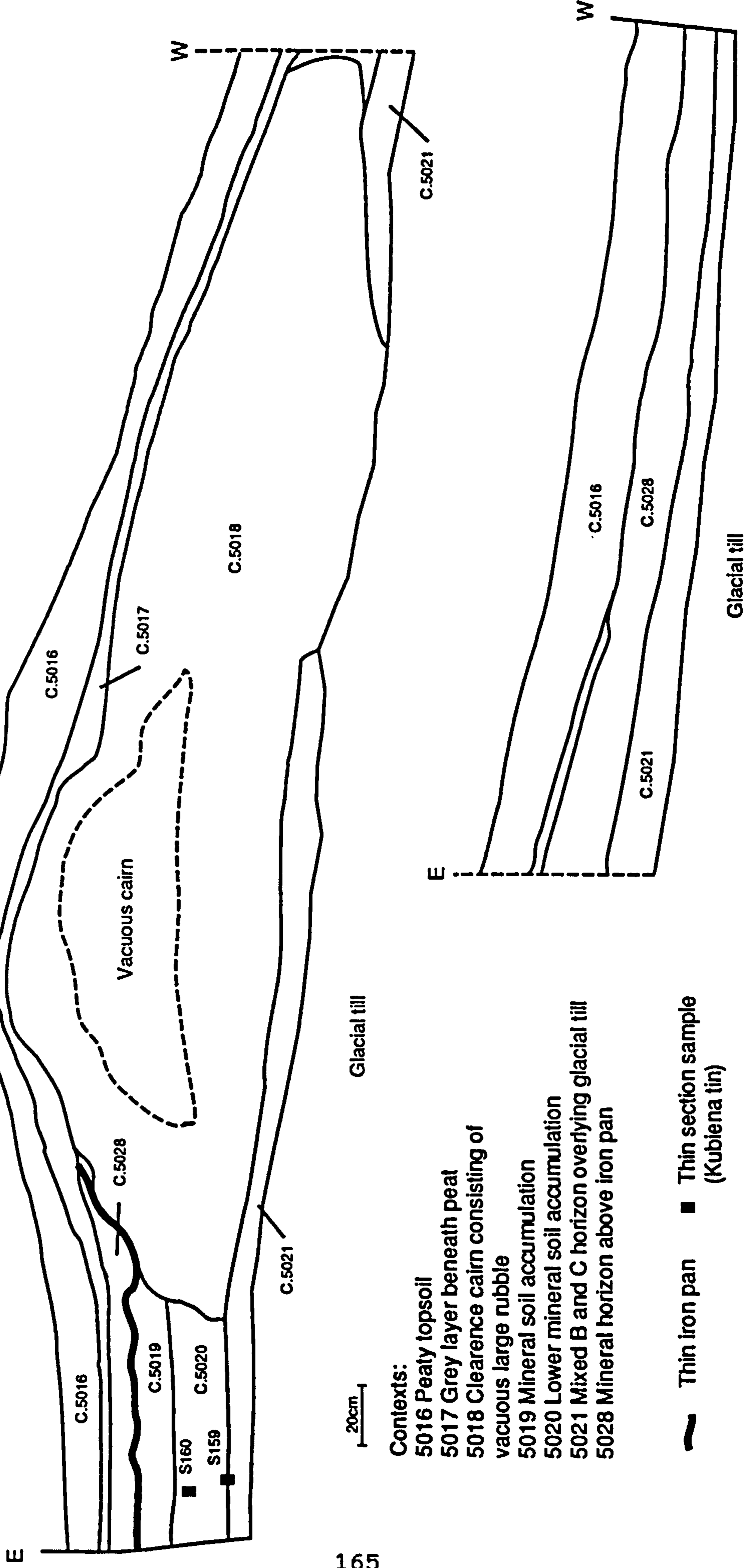


Fig. 5.11 M88, soil accumulation against an EP cairn



disturbed, colours included brown (10YR 4/3) and strong brown (7.5YR 5/6).

#### **5.6.1 M88, results of thin section analysis.**

Two samples were taken for thin section analysis.

#### **5.6.2 M88, sample 160, c.5020**

Sample 160 was taken to examine the morphology of context 5020.

The microstructure is intergrain microaggregate tending towards bridged grain. The abundance of voids as a percentage of the thin section is frequent. Coarse organic components include rare sclerotium, rare charcoal fragments measuring 20 $\mu$ m to 1.5mm, rare dark rings, diameter 80 $\mu$ m and rare unidentified humified organic remains measuring 0.5mm across. There are very few remains of roots in channels. Inorganic residues of biological origin include rare fragmented phytoliths randomly distributed. The fine material is organo mineral, brown (PPL) and orange brown (OIL). There are rare black particles measuring 2-50 $\mu$ m, randomly distributed. The material is well sorted. The c/f ratio is 60:40.

The groundmass is randomly dotted with many small typic ferruginous nodules with a diameter measuring 20-100 $\mu$ m, brown orange OIL dark red to black PPL, sharp boundary. There are also rare strongly impregnated ferruginous nodules, sphericity 2-3, black to dark red PPL, orange red to red OIL, measuring 2mm across, internal fabric consists of quartz and fine material.

Fabric pedofeatures include rare loose discontinuous infillings of channels. The internal material is light brown (PPL), ovoid, moderately to strongly coalesced, ultrafine granules measuring approximately 40 $\mu$ m, irregularly shaped, organo mineral. These are probably coalesced excrement features.

#### **5.6.3 M88, sample 159, c.5020 and c.5021.**

This sample is from the interface between 5020 and 5021 to determine the cause of the disturbance seen at the bottom of the profile.

The microstructure is intergrain microaggregate with some tendency towards bridged grain. The abundance of voids, as a percentage of the thin section, are frequent. Coarse organic components include rare remains of roots, one sclerotium 600 $\mu$ m diameter, the internal material had been almost completely removed, one or two charcoal fragments measuring 100-200 $\mu$ m. There are no inorganic residues of biological origin. The fine material is brown (PPL) and pale orange brown (OIL), organo mineral. There are no fine black particles. The material is well sorted. The related distribution between the coarse and the fine material includes enaulic bridged grain and porphyric. The c/f ratio is 70:30.

Pedofeatures include rare manganese nodules, black (PPL and OIL), 40 $\mu$ m to 400 $\mu$ m randomly distributed. There are also rare orthic ferruginous nodules, orange red (OIL), brown red (PPL), isotropic, 400 $\mu$ m to 1mm. Amorphous ferruginous material impregnates a coarse mineral material matrix consisting of dominantly quartz. These are generally found at the base of the section.

#### **5.6.4 Interpretation of M88.**

The microstructure of context 5020 is dominantly intergrain microaggregate. There are rare fragments of coarse and fine charcoal present. Excremental infillings of some channels suggest reworking of roots. There are no features present that suggest mixing of material between horizons, for instance fragmented cappings or relict B horizon material. This might reflect the loss of features caused by pedogenesis or the absence of features originally.

The top of context 5021 is morphologically different to B horizons observed elsewhere. There are no fragmented cappings or indications of the formation of a Bs horizon. There are rare ferruginous and manganese nodules in this context but these do not have the morphological characteristics of fragmented iron pan. The presence of nodules in this context at approximately the same stratigraphic point as M88 suggests that the two sets of features might be associated. This is discussed in section 9.4.

#### **5.6.5 Results from M87, an EP clearance cairn**

M87 is a large clearance cairn situated to the east of the head dyke in an area of modern stagnopodzols. It forms part of the same group of monuments as M86 and M88. Morphologically it is very similar to M88. It was excavated to discover if the cairn was built on top of an A horizon.

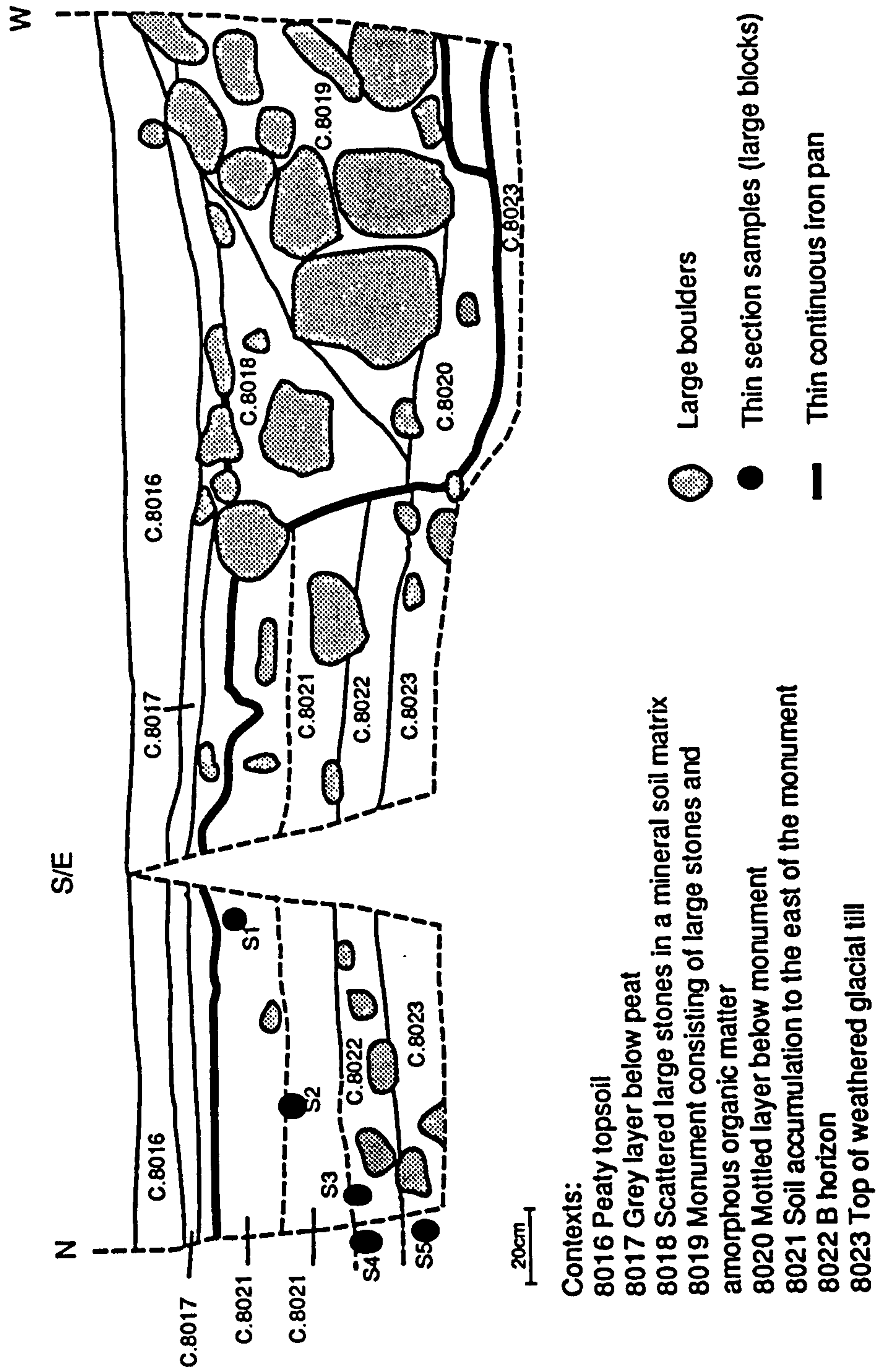
The dominant vegetation around the monument is heather with a low abundance of moss. A trench was dug in an east west direction through the monument. The monument, and a soil accumulation to the east, are sealed by a layer of semi fibrous peat (fig 5.12). The monument, consisting primarily of very abundant large to very large subangular stones, is mostly vacuous although cells of organic material, formed by the decomposition of roots around the large stones, are present.

To the east of the monument there is a series of horizons, approximately 80cm deep in places, representing an accumulation of soil behind the cairn. A thin continuous iron pan is present in the accumulation at a depth of approximately 25cm. Below the monument the iron pan is at a depth of approximately 1m (fig 5.12). Context 8021 is approximately 40cm deep and apart from a slight colour change from dark brown (10YR 4/3) at the top to 10YR 3/3 at the bottom the horizon appeared homogenous. Few very fine fibrous roots below the iron pan indicate little root disturbance in this area. Stone abundance is common with medium to large subangular stones.

Below context 8021 is a dark brown horizon (7.5YR 4/4, C.8022) thought to represent a B horizon. Directly below this is the weathered top of the glacial till. At the west end of the trench where the iron pan rises concretions are present.

There is no buried soil below the monument despite the fact the trench was dug through a massive part of the structure. The

Fig. 5.12 M87, soil accumulation against an EP cairn



profile is similar to that found under M88 except the B horizon is enriched in sesquioxides. Thin sections from M88 had already been made when M87 was excavated. The similarities in the contexts of M88 and M87 resulted in the samples from M87 not being made into thin sections.

#### **5.7 Results from Post Medieval monuments.**

There are 4 monuments identified in group A, dated to the Post Medieval period, that were excavated for sampling. M127 is a rectangular structure, M75 is the head dyke that encloses most of group A and M164 is a dyke which forms an addition to M75. M21 is a deep accumulation of soil in the southern part of group A. This accumulation is not buried by any monument and thus has been subject to pedogenesis and effects of human activity for the longest period of the soils chosen for study.

#### **5.8 Excavation results of M127.**

M127 is a rectangular hut which forms part of a group of rectangular huts built on a platform. Several dykes appear to be either truncated or buried by the platform. In the 1989 season a buried A horizon was identified below the structure. To the east of the monument there are rushes growing indicating waterlogging. Immediately surrounding the monument the vegetation is dominated by grass.

In the 1990 field season a trench was dug in a north - south direction perpendicular to the wall of the structure. A section drawing was produced (fig. 5.13), a section photograph taken (figs. 5.14) and samples taken for thin section analysis.

The bank is composed mainly of decomposing turves with a concentration of large stones on its west side (fig. 3.11),. The colour varies between dark brown (10YR 3/3), where the texture is loamy sand, to black (10YR 2/1) where there is a greater amount of organic material. Organic matter content varies between amorphous organic and humose. The cells of orange loamy sand material (c.8043) within the wall of the structure probably represent material derived from a Bs horizon.

A black layer of amorphous organic material (C.8044), approximately 2cm thick, is present directly below the wall of the monument. The layer is thickest below the concentration of stones. This feature is interpreted as an O horizon. Below context 8046 is a layer with many small to medium subangular stones (C.8045). This layer appears to be caused by human activity although no clear interpretation could be made without further excavation. Close to the base of context 8045 is a thin iron pan. This is continuous at the western end of the trench, the interior of the monument, but gradually become less distinct towards the northern end of the trench, eventually disappearing (fig. 5.13).

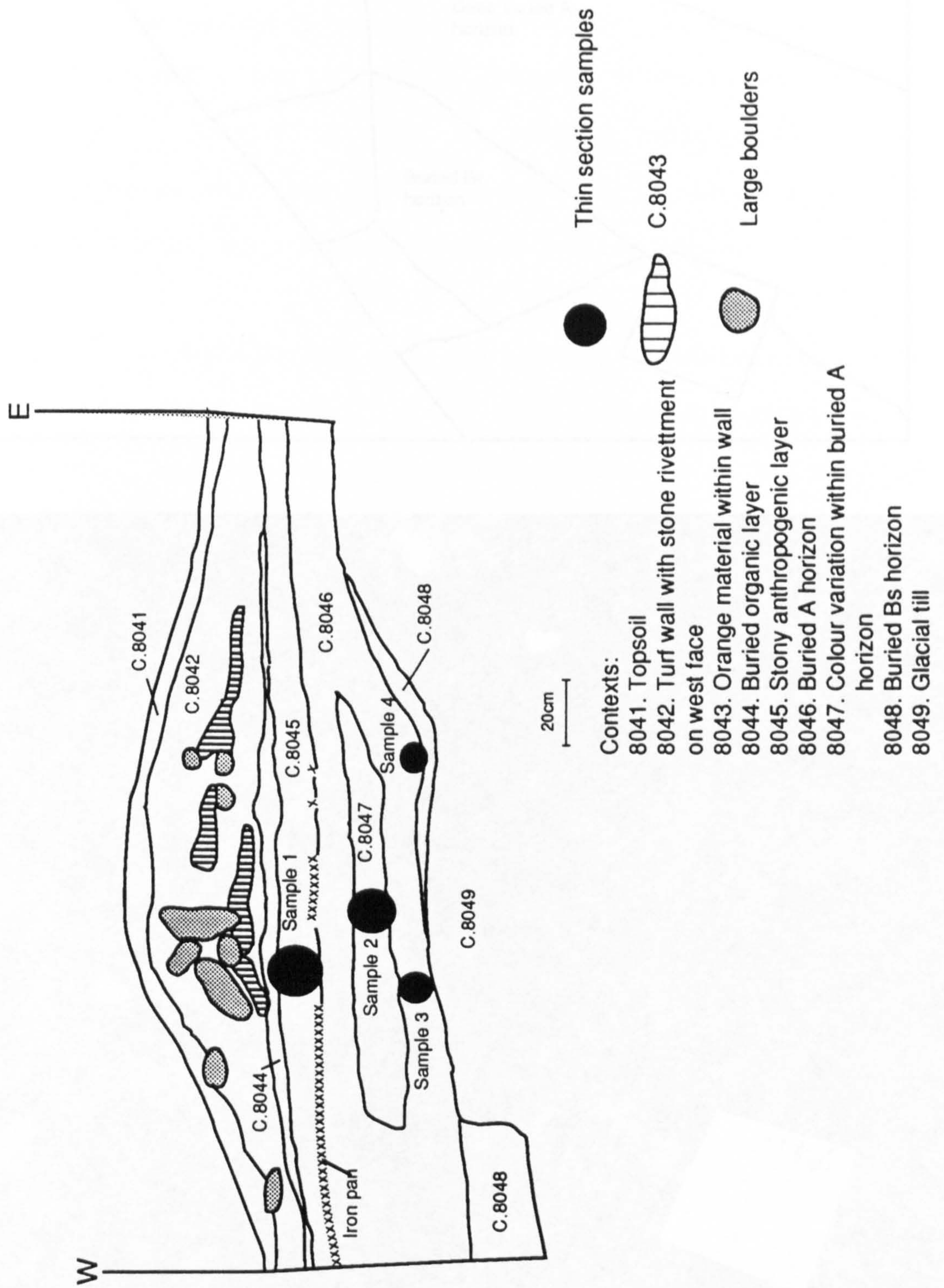


Fig. 5.13 M127, PM rectangular structure

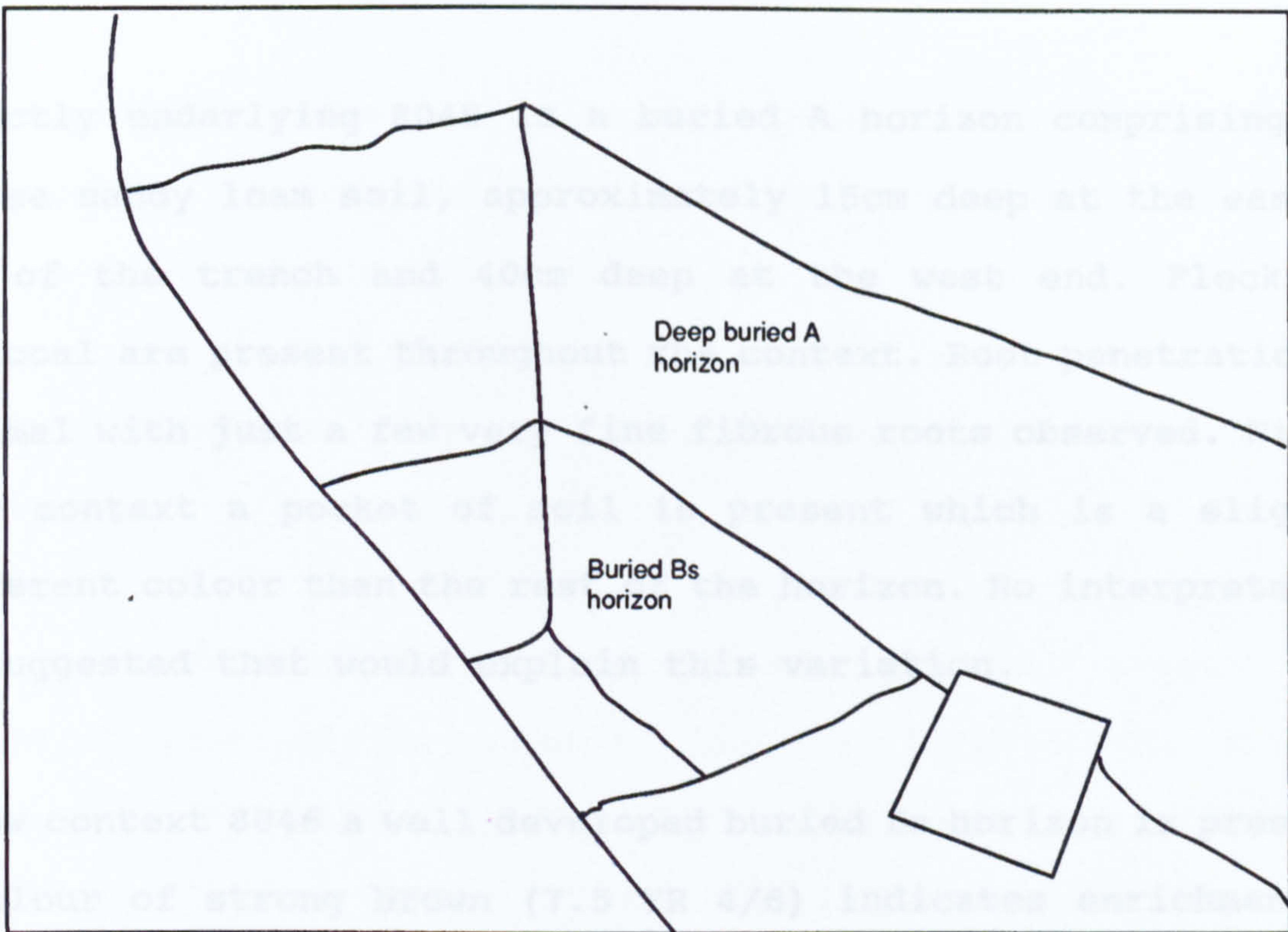


Fig. 5.14 Buried A horizon and buried Bs horizon under M127



Directly underlying 8045 is a buried A horizon comprising non humose sandy loam soil, approximately 15cm deep at the eastern end of the trench and 40cm deep at the west end. Flecks of charcoal are present throughout the context. Root penetration is minimal with just a few very fine fibrous roots observed. Within this context a pocket of soil is present which is a slightly different colour than the rest of the horizon. No interpretation is suggested that would explain this variation.

Below context 8046 a well developed buried Bs horizon is present. A colour of strong brown (7.5 YR 4/6) indicates enrichment of sesquioxides. The bottom of the Bs horizon is only revealed at the west end of the trench. At this point it is approximately 20cm deep.

#### **5.8.1 M127 thin section results.**

Four samples were taken for thin section analysis. Image analysis was used to describe the complex layering seen in sample 1, and morphometric analysis used to quantify voids, minerals and groundmass in sample 2.

#### **5.8.2 M127, sample 1, c.8045.**

This sample is from context 8045, a layer of stony material underlying the old ground surface (C.8046). The morphology of the slide at a macro scale is very complex, being composed of numerous layers of material. To enable the slide to be divided

into homogenous areas for a micromorphological description the stratigraphy was studied using spectral enhancement techniques described in chapter 2.

### 5.8.3 Spectral analysis and thin section description of M127 sample 1.

Red, green and blue images were captured from M127 sample 1 and displayed as a colour composite image on R-chips. The spatial resolution of the images was 512 x 512 and the radiometric resolution 256 grey levels. Figure 5.15 shows an image displaying the whole slide using an ACS. Figure 5.16 shows the same image using a histogram equalisation stretch (HES). The HES differentiates between the various layers more effectively than the automatic contrast stretch. This is because of the boundary around the picture, caused by digitising a rectangular slide using a square picture format. Within this boundary there are some data values that are much higher and lower than the values within the useful part of the image. Although the ACS uses 5% cut off points, it is still stretching data values that are not of use to the analyst, consequently the area including the thin section does not get fully enhanced. The outer area of the image could have been masked and only the unmasked area included in the contrast enhancement. This was considered unnecessary as a HES gave good results and was quicker to implement. Using the image produced with the HES, a diagram was manually drawn depicting the different layers observed macroscopically (fig 5.17).

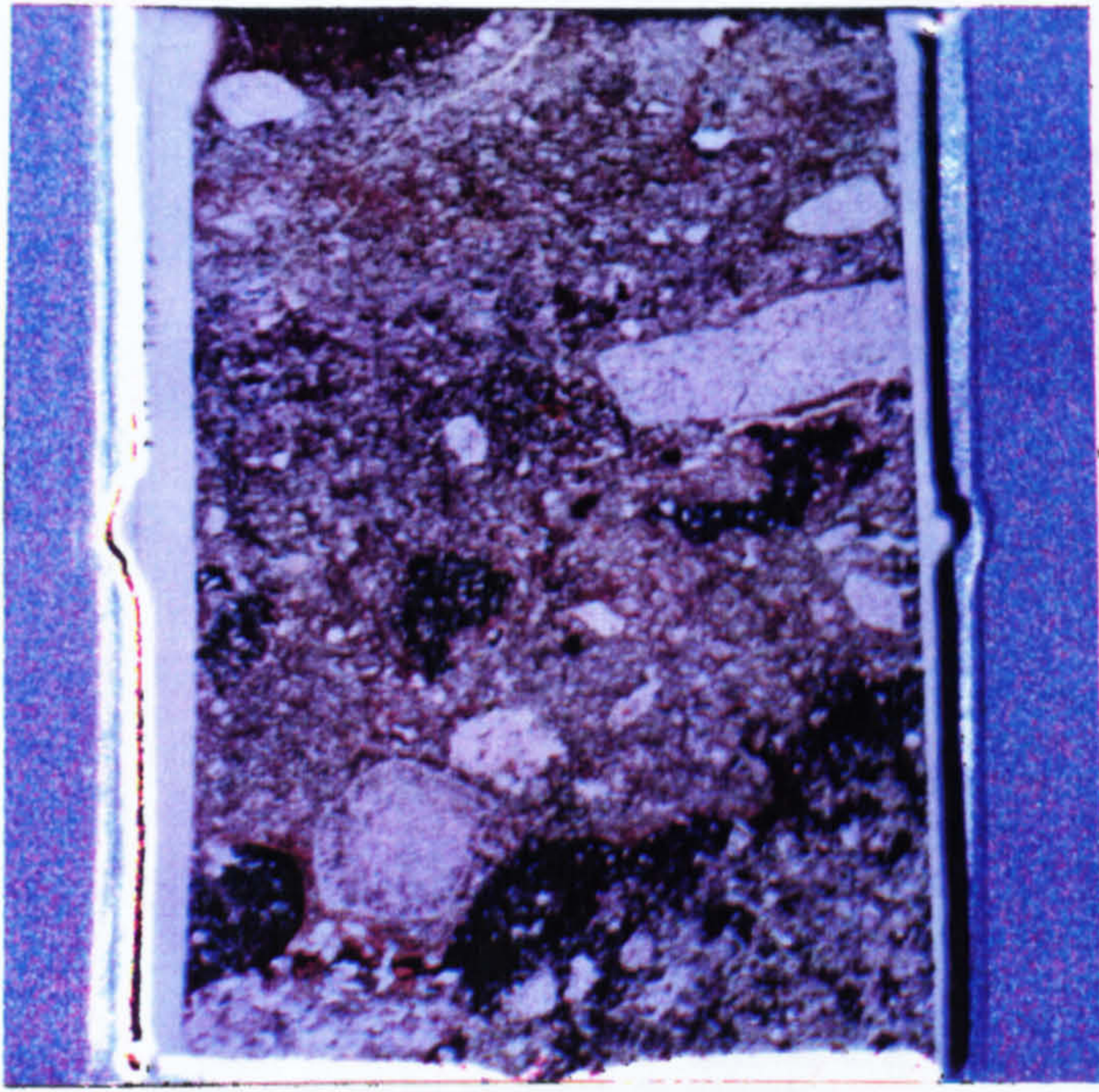


Fig. 5.15 M127, S1, ACS, red 31-109, green 28-120, blue 36-135, whole slide

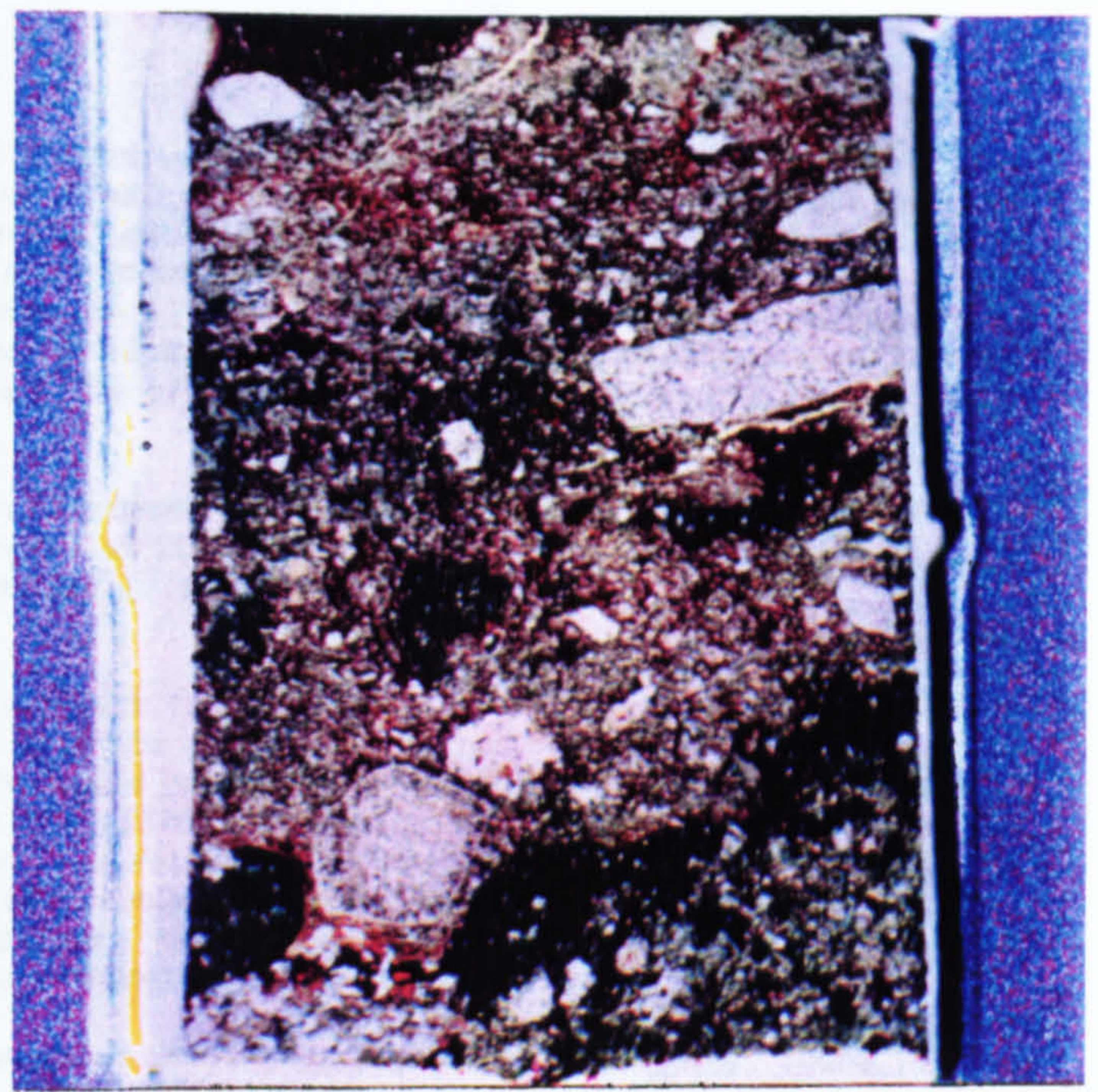
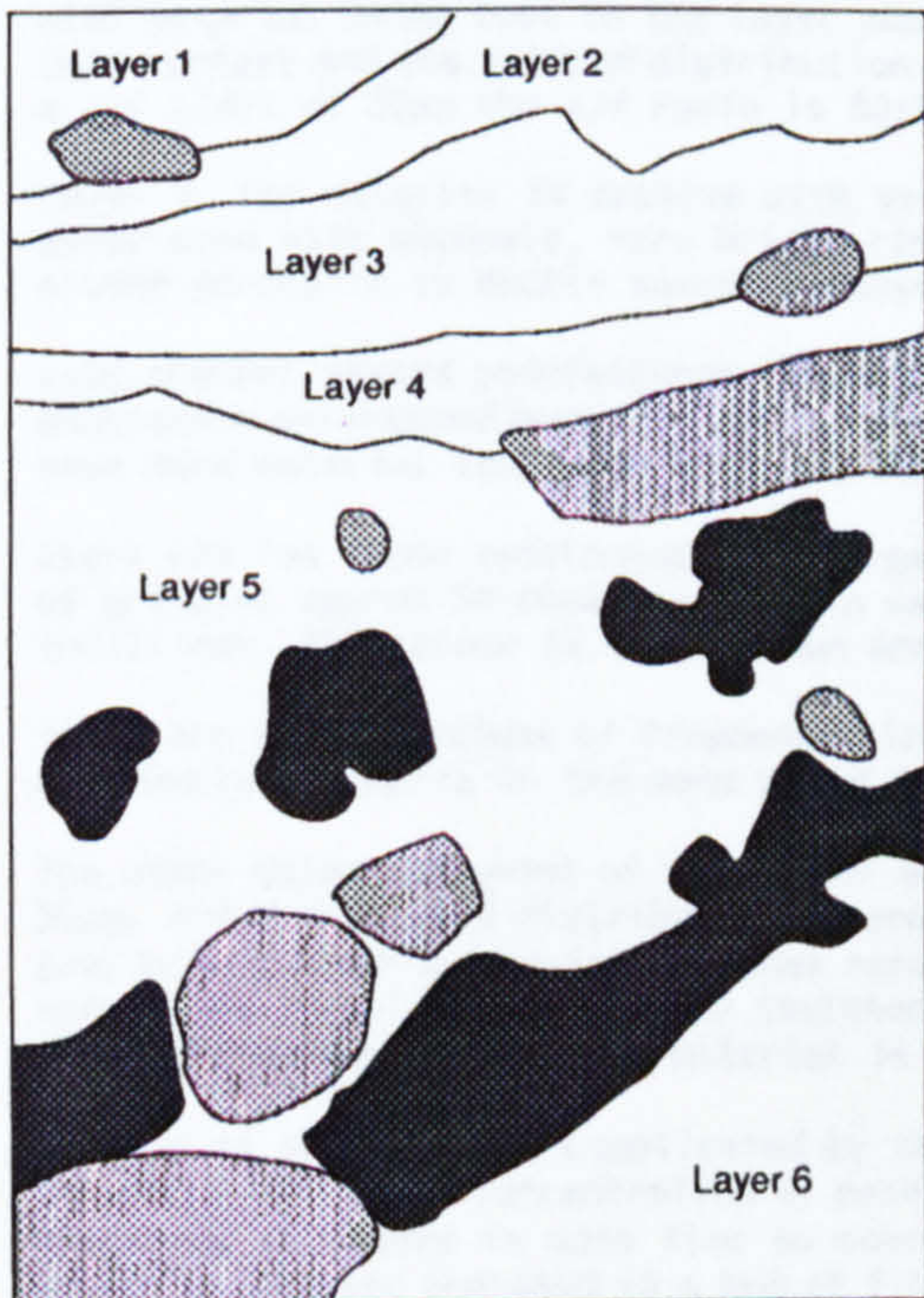


Fig. 5.16 M127, S1, HES, whole slide



● Iron pan    ● Mineral fragments

Fig. 5.17 Stratigraphy in M127, S1

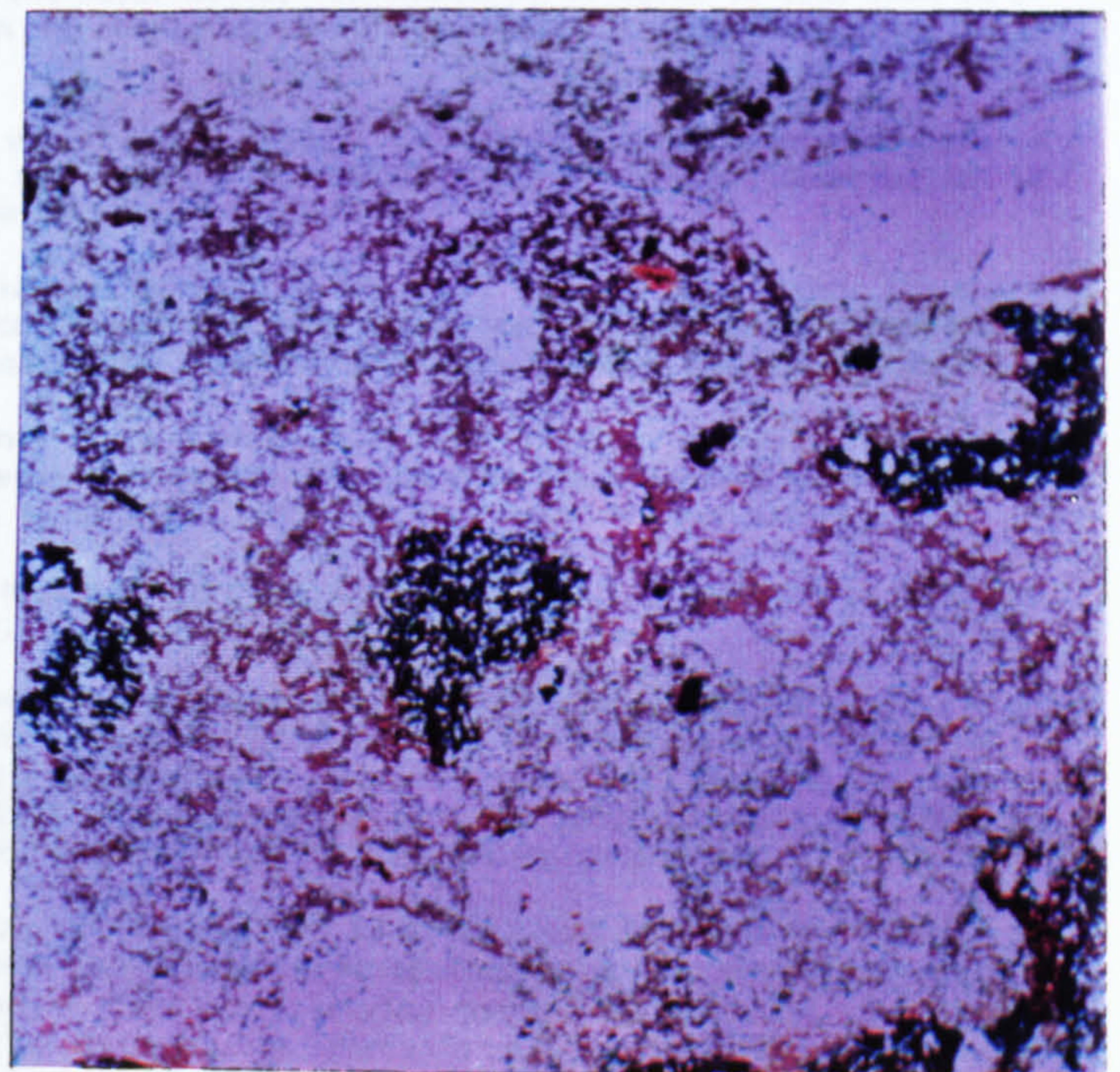


Fig. 5.18 M127, S1, red 32-93, green, 27-90, blue 31-85, FL 36mm

**Layer 1.** Layer 1 includes material that is dominantly massive with some localised tendency towards crumb. There is little mineral material with most of the organic material humified and strongly orientated parallel to the surface. There are occasional sclerotia, rare bright rings and rare phytoliths and diatoms. Many black particles and cell residues measuring 2-50 $\mu$ m are randomly distributed throughout the context. There are common loose continuous to dense incomplete channel infillings. The infilling material is lighter than the surrounding groundmass and composed of granules 30-40 $\mu$ m diameter. Textural pedofeatures include few amorphous organic coatings. These are situated on the sides of voids and continue into layer 2. The coatings are orange brown using PPL and isotropic.

**Layer 2.** In places there is a layer approx 2mm thick between layer 1 and layer 2. The structure of this layer is massive with a c/f limit of 50 $\mu$ m and c/f ratio of 20:80. The colour of the fine material is grey brown, the same colour as the interaggregate fine material in layer 2.

Layer 2 consists of intergrain microaggregate structure with few channels. There are 2 areas where the voids are much larger and material has been incorporated from the overlying horizon. The abundance of voids as a percentage of this layer is frequent to common. The ratio between the coarse and fine material is 60:40. There are few remains of roots in channels, 1 dark ring (120 $\mu$ m diameter) and 2 squashed dark rings. The colour of the fine material is generally grey brown. The related distribution between the coarse and the fine material is enaulic. Pedofeatures include loose continuous infillings strongly orientated perpendicular to the surface, the infills are a stronger orange red colour than the surrounding groundmass. There are also orange red amorphous organic coatings which have been translocated from the overlying layer.

**Layer 3.** Layer 3 is almost massive with local abundances of small (40 $\mu$ m) granular aggregates. There is also disruption by channels in places.

There are very few remains of roots in channels, rare dark rings and rare fungal remains (possibly one fragment of sclerotia), one sclerotia could be positively identified. Rare fragmented diatoms and phytoliths are randomly distributed throughout the groundmass. The colour of the fine material is orange red using PPL. There are occasional black particles measuring 2-50 $\mu$ m randomly distributed. The c/f ratio is 40:60 and the related distribution is enaulic in areas of faunal disruption but approached porphyric in other areas.

Textural pedofeatures include very few amorphous fragmented organic coatings associated with channels. Fabric pedofeatures consist of lenses of material where the ratio of coarse to fine material is higher than stated. There are also few loose continuous infillings of channels.

**Layer 4.** Immediately underlying layer 3 there are lenses of material with a very high coarse mineral component. This layer may once have formed a continuous layer across the slide but has now become fragmented with material being lost to the layer above and the layer below. The abundance of voids is less than 1% of this context and the related distribution between the coarse and the fine material is close porphyric. Using a c/f limit of 20 $\mu$ m the c/f ratio is 80:20.

**Layer 5.** The material is massive with very few voids. Basic organic components include rare root remains associated with channels, rare bright rings and rare remains of charcoal. The c/f related distribution is closed porphyric to double spaced porphyric. The material is unsorted.

Long channel shaped pedofeatures 400 $\mu$ m to 2mm wide are present in the upper half of this layer. These are moderately orientated perpendicular to the surface. They differ from the surrounding groundmass because they have more material less than 50 $\mu$ m. In very few cases the material is also a stronger red in colour.

There are few loose continuous infillings (channel width approx 400 $\mu$ m). The internal material is composed of granules approx 50-60 $\mu$ m that are in various stages of coalescing, in some cases forming dense complete infillings. The colour is light brown and seems to be associated with root remains (see before).

There are large sections of fragmented iron pan approximately 2mm thick. The internal material is composed dominantly of quartz in the sand sized fraction.

The other major component of this layer are lenses of fine material where 90% of the material is less than 50 $\mu$ m, and a clustered distribution of coarse mineral grains. The colour of the fine material using PPL is grey brown. Organic material includes rare bright rings and dark rings. Some local iron staining was present around the fungal material (very isolated examples). Pedofeatures include few dense incomplete infillings where the colour of the fine material is slightly lighter than the surrounding groundmass.

The top of the layer is complicated by the mixing of layers 4 and 5. At approx 3.8cm from the surface of the slide there is a concentration of material where the groundmass is more red than the context immediately overlying it. There is more fine to coarse material than the overlying context with some of the mineral grains completely enclosed in a bed of fine material with a close porphyric related distribution. There are frequent channels with loose continuous infillings to dense complete infillings. The infillings are a lighter colour than the surrounding material and have lost some of their redness. In places the infillings are associated with channels containing the remains of roots.

The boundary between layers 5 and 6 is a heavily impregnated iron pan approximately 2-4mm thick. The top of the pan has a sharp boundary while the lower boundary is more diffuse. The amorphous iron rich compounds have cemented sand sized mineral grains, rock fragments and a large fragment of charcoal.

The colours of the pan vary from black/red, PPL, where it is most heavily impregnated to red/brown where it is diffuse. Using OIL the material at the top of the pan is bright orange to red this changes to dark brown and black as the material becomes diffuse. The lower diffuse side of the pan appears to extend into layer 6 in vermiform tongues of material.

Layer 6. Layer 6 consists of material with an intergrain microaggregate structure. The abundance of voids as a percentage of this layer is frequent. Coarse organic components include randomly distributed rare fragments of charcoal measuring 800µm to 2mm. The related distribution of the coarse and fine material is enaulic consisting of a c/f ratio of 60:40.

Pedofeatures include common ferruginous nodules with variable shape but generally in the size range 1-2mm. They are orthic, red/brown PPL and brown/black OIL. The darker blacker material is found in the old void spaces. Few faint elongated fabric pedofeatures were recognised by their arrangement and slightly greater abundance of fine material.

Layers 2, 4 and 6 on the HES image have a greater green component than the other layers. In layers 2 and 6 this corresponds to a greater abundance of voids (table 5.4). In layer 4 the green colour is caused by the dominance of mineral material and the lack of fine organic material. The darker redder colours, layers 1, 3, 5 and the iron pan, corresponds to areas with a greater fine fraction and ferruginous content.

| Layer | c/f ratio,<br>50µm limit | Abundance of<br>voids, % of<br>layer |
|-------|--------------------------|--------------------------------------|
| 1     | (20µm) limit<br>10:90    | Very few                             |
| 2     | 60:40                    | Frequent to<br>common                |
| 3     | 40:60                    | Few                                  |
| 4     | (20µm limit)<br>80:20    | Very few                             |
| 5     | 40:60                    | Few                                  |
| 6     | 60:40                    | Frequent                             |

Table 5.4 Micromorphological features of the layers which  
comprise M127 sample 1

The ACS image (fig. 5.15) divided the areas of organic material and ferruginous material more effectively than the HES (fig.

5.16). To examine the distribution of vermiform passages in the groundmass in more detail, images were captured from a smaller section of the image (fig 5.18). Using a contrast stretch of red 32-93, green 27-90 and blue 31-85, the organization of these features became easily recognisable. At the top of layer 5 there is a concentration of material with a greater fine component. Vermiform passages of the material extend downwards into layer 5 between the fragments of iron pan. These passages represent bioturbation of the sample. It is possible that the top of layer 5 once formed a ground surface which has had mineral material added above it.

#### 5.8.4 Interpretation

The slide is composed of complex layers of material. The field description described context 8045 as being a stony layer below an organic rich horizon. The thin section analysis shows that the horizon can be sub-divided into a number of layers representing variations in coarse and fine material and abundance of voids. This layering probably resulted from human activity prior to the development of the organic rich horizon. The exact type of activity is difficult to determine. Dumping of material, animal trampling and periods of disuse, could have resulted in deposit formation of this type. The iron pan developed after the formation of the layered deposits. The fragmented pan within layer five might have been caused by biological activity given the level of vermiform features in this area. The iron pan then reformed below its original level. However the possibility of the

pan being disrupted allowing biological activity to take place can not be discounted.

The dark organic band overlying context 8045 formed during a period post-dating the anthropogenic layers and predating the construction of the rectangular structure. The massive structure of some of the underlying layers and the resulting low porosity could have contributed to impeded soil water movement and possibly caused waterlogging, thus creating anaerobic conditions and allowing the accumulation of organic material.

#### **5.8.5 M127, sample 2, c.8046.**

This slide is from the buried A horizon spanning contexts 8046 and 8047. The slide was homogeneous and treated as one layer.

The microstructure is complex and consisted of bridged grain, channel structure and some localised intergrain microaggregate. The abundance of voids as a percentage of the thin section are frequent. Single mineral grains are dominated by quartz in the size range 50-500 $\mu$ m. There are smaller quantities of mica, biotite and feldspar (narrow twins). Green amphiboles as a percentage of the slide is few. Compound mineral grains and rock fragments are generally dominated by quartz although fragments with greater abundances of green amphibole and biotite are present.

Coarse organic material includes occasional to many charcoal fragments measuring 400-800 $\mu$ m randomly distributed. There are also very few remains of roots in channels. There are no inorganic residues of biological origin.

The fine material is organo-mineral, brown to dark brown (PPL). There are abundant, dark brown to dark red brown, equidimensional to elongate, amorphous at x400, particles. These include fragments of organic material and ferruginous compounds, set in an amorphous brown to orange brown matrix. There are also occasional black fragments measuring 2-50 $\mu$ m randomly distributed. The coarse and fine material is moderately sorted.

The related distribution between the coarse and the fine material is chitonic and the c/f ratio is 50:50.

Pedofeatures include occasional orthic ferruginous nodules, sphericity 3, measuring 400 $\mu$ m to 1mm, sharp boundaries, unreferred and unorientated. These are sometimes fragmented. The colours using PPL are black with some dark red areas, dark grey to dark orange (OIL). The type of groundmass is difficult to determine owing to the strength of the impregnation. Mineral material including quartz and biotite are present within the matrix. There is medium variability between different nodules. Other less strongly impregnated examples are present. The colours of these vary from black to red with more brown reds than before (PPL), very dark brown to orange brown (OIL). The darker colours are associated with material in the old voids.

Textural pedofeatures include rare amorphous orange (PPL), dark brown to black (OIL), material forming coatings of voids less than 20-40 $\mu$ m thick. There is weak birefringence along the edges of the coatings. In places these coatings form weak mottling of the groundmass.

There is one example of silt capping located on a rock fragment orientated perpendicular to the surface. The capping is highly ferruginised and measured 400 $\mu$ m wide.

There are unidentified crystalline pedofeatures located throughout the slide. These are rare, orange (PPL), sharp boundaries and spherical to half circle to irregularly shaped. Completely spherical examples measure approximately 80 $\mu$ m. There are also larger irregularly shaped examples. The internal segments are weakly anisotropic (XPL) which emphasise the segmented fabric.

Fabric pedofeatures include loose continuous infillings containing small granules measuring approximately 40 $\mu$ m across. The infillings are located in channels approximately 400 $\mu$ m wide. The abundance of this feature is difficult to ascertain owing to assimilation into the groundmass.

#### **5.8.6 M127, sample 3, c.8046.**

This sample is from the base of the buried A horizon (C.8046) and was taken to examine the vertical variation in the context.

The microstructure is complex consisting of intergrain microaggregate and bridged grain structure. The abundance of voids as a percentage of the thin section is frequent to common. Single mineral grains are dominated by quartz with smaller amounts of feldspar, muscovite, green amphibole and biotite. Compound mineral grains and rock fragments measured 400 $\mu$ m - 3mm, the mineralogy is mixed, sometimes quartz is dominant in other cases feldspar is dominant. The feldspars tended to show light to moderate weathering.

Coarse organic material includes rare remains of roots in channel, rare unorientated, unrefracted fragments of charcoal, measuring 800-1200 $\mu$ m. Two examples of unidentified organic remains are present and one dark ring with a diameter of 100 $\mu$ m.

The fine material is organo-mineral brown to light brown (PPL). There are rare black particles randomly distributed measuring 2-50 $\mu$ m. The material is moderately sorted. The c/f related distribution between the coarse and the fine material is chitonic and the c/f ratio is 60:40.

Pedofeatures include occasional orthic moderately impregnated nodules, in some cases these had halos. Using PPL the central area is dark red to red and the outer area is orange. There is only a very slight difference between the orange areas and the surrounding groundmass. Using OIL the darker areas (PPL) have a low reflectance and are generally dark in colour. The size of these nodules varies between 600 $\mu$ m to 1mm.

The distribution of the fine material indicates channel shaped fabric features throughout the slide. These have a diameter of approximately 400 $\mu$ m and are characterised by their porphyric c/f related distribution. They are difficult to distinguish making any estimate of their frequency unreliable.

Loose discontinuous infillings are rare with an internal morphology composed of loose granular material. These are moderately to strongly coalesced with the groundmass. An area of material approximately 2mm wide differed from the surrounding groundmass because of its orange yellow colour and sharp boundary.

Crystalline pedofeatures. Clusters of orange (PPL) unidentified crystalline pedofeatures are present. Their structure and shape varies depending on preservation. They are found in void spaces, including channels or complex packing voids, or enclosed within the groundmass. Where the structure is present the outer rim is a darker orange than the rest. They are mainly isotropic although weak birefringence along the internal segments also occurs. Using OIL the reflectance is weak to moderate although the outer rim is generally more highly reflective than the internal area.



### 5.8.7 M127, sample 4, c.8046.

This sample is from the interface of the buried A horizon and the buried Bs horizon. During sample preparation there was some disruption and the Bs horizon soil was lost.

The microstructure is intergrain microaggregate. The microaggregates consist of ultrafine granules measuring approximately 20-40 $\mu$ m. The abundance of voids as a percentage of the thin section is common. The coarse mineral material is the same as sample 3 (section 3.2.7).

Coarse organic material includes rare fragments of charcoal measuring 50 $\mu$ m to 1.5mm randomly distributed. There is one fragment that measures 5mm across. Phytoliths are randomly distributed throughout the groundmass, their abundance is rare.

The fine material is organo mineral, brown using PPL. There are rare black particles measuring 2-50 $\mu$ m randomly distributed. The material is poorly sorted. The related distribution between the coarse and the fine material is enaulic with localised geric and the c/f ratio is 60:40.

Pedofeatures include abundant orthic nodules measuring 400 $\mu$ m, irregularly shaped. The fabric is dark red to black (PPL), dark brown to black (OIL), embedded with quartz grains measuring 20-80 $\mu$ m. There are many to abundant mottles, dark brown to black (OIL), red to black (PPL), 40-400 $\mu$ m.

In places there are unidentified crystalline pedofeatures similar to those described in section 3.2.7, abundance is occasional. Rare loose discontinuous infillings with internal material consisting of ultrafine granules measuring 40 $\mu$ m are randomly distributed. These also include reworking of translocated amorphous orange material.

There are textural pedofeatures consisting of coatings of amorphous material, orange (PPL), dark brown (OIL), weakly anisotropic on the edges, generally no thicker than 40 $\mu$ m. These seem to be forming orange crystalline pedofeatures in places.

### 5.8.8 Interpretation of M127, samples 2, 3 and 4.

These 3 thin sections were taken to examine the vertical variation of features within the buried A horizon.

| Sample No | Context          | Coarse charcoal | Black particles <50 $\mu$ m | Phytoliths | Diatoms |
|-----------|------------------|-----------------|-----------------------------|------------|---------|
| 2         | Buried A horizon | Occasional      | Occasional                  | No         | No      |
| 3         | Buried A horizon | Rare            | Rare                        | No         | No      |
| 4         | Buried A horizon | Rare            | Rare                        | Yes        | No      |

Table 5.5 Micromorphological features of samples taken from

M127

The abundance of coarse and fine charcoal is greatest at the top of the profile (Table 5.5). The coarse fine ratio is also greatest at the top of the profile (Table 5.6).

| Sample No | Context  | Dominant c/f related distribution, c/f ratio | Sorting  | Total voids TTS    | Dominant Microstructure                     |
|-----------|----------|--|----------|--------------------|---|
| 2         | Buried A | Chitonic, 50:50                              | Moderate | Frequent           | Bridged Grain                               |
| 3         | Buried A | Chitonic, 60:40                              | Moderate | Frequent to common | Intergrain microaggregate and bridged grain |
| 4         | Buried A | Enaulic, gefuric, 60:40                      | Poor     | Common             | Intergrain microaggregate                   |

Table 5.6 Comparison of microstructure and c/f ratios from M127

There are no inorganic residues of biological origin in the top two samples but phytoliths are present in sample 4. There is a decrease in the c/f ratio down the profile accompanied by a change in the c/f related distribution from chitonic in sample 2 to enaulic in sample 4. The abundance of voids increases down the profile from frequent in sample 2 to common in sample 4. These changes are reflected in a bridged grain microstructure in sample 2 becoming intergrain microaggregate and bridged grain in sample 3 and purely intergrain microaggregate in sample 4. The soil becomes less well sorted with depth (table 5.6).

The changes in the microstructure and void space can be related to a change in the ratio of the coarse and fine material (section 9.5). The vertical distribution of features in this profile

suggest a greater input of carbonised material at the top of the profile, but no inorganic residues of biological origin.

There is indication of translocated material forming nodules and mottles in all the samples. They all contain less reflective material in old voids suggesting an organic component to the translocated material. These features might relate to the development of context 8044, the organic layer. Without a more detailed elemental analysis this observation is only speculative.

The fragmented remains of a silt capping in sample 2 suggests mixing materials within the profile (section 9.2). Silt cappings were formed in the glacial till as periglacial features. The rarity and small size of the capping in sample 2 suggests that the mixing occurred at an earlier stage in the development of the profile rather than later.

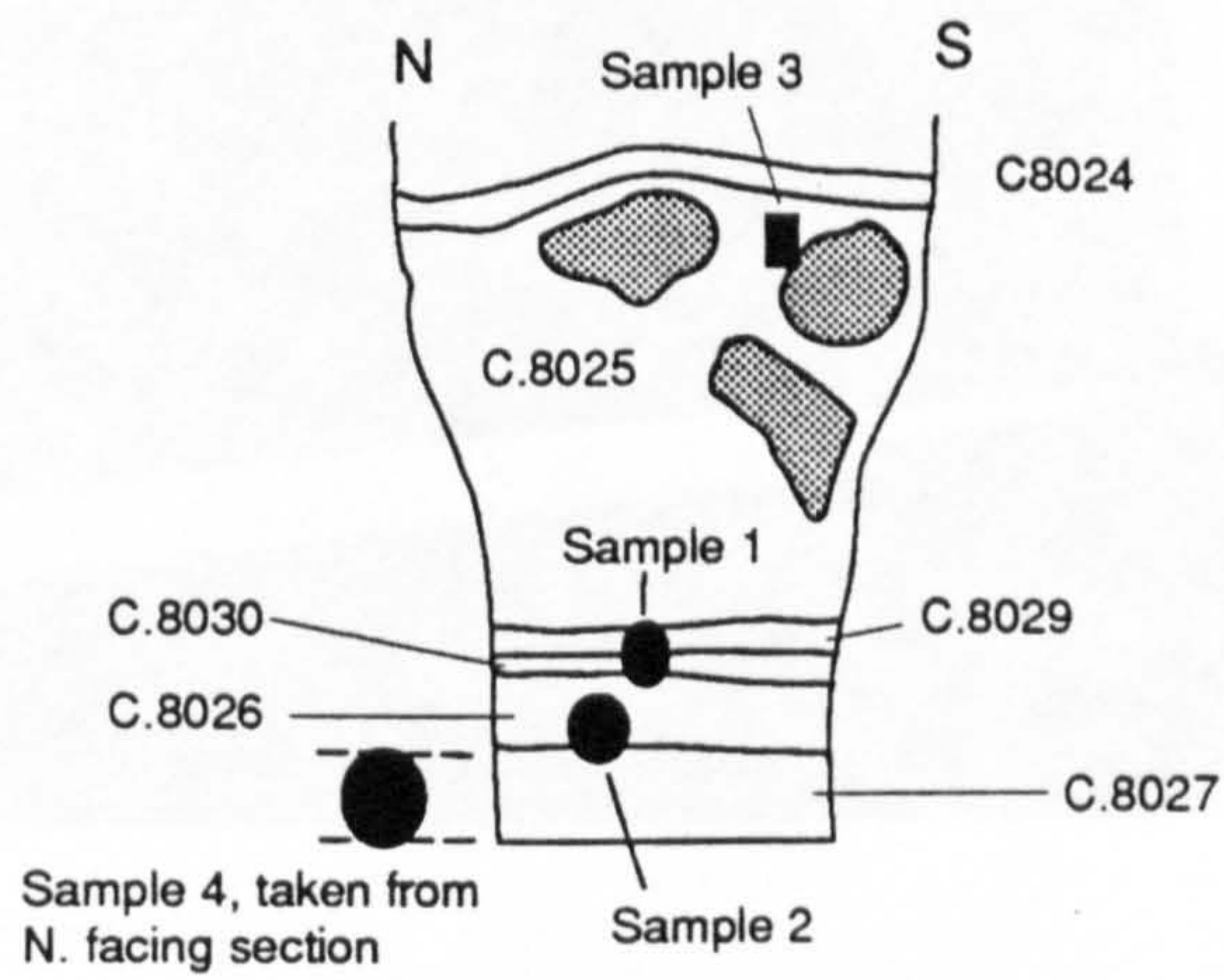
In all the samples there are unidentified crystalline features. In sample 4 intermediate stages between textural coatings and the crystalline pedofeatures are present. This suggests that these are formed by precipitation from soil solution. This feature is not present in any of the Bronze Age soils in group A. The features are not positively identified.

## 5.9 Excavation results of M75/4, enclosure dyke.

M75 is the main enclosure dyke at the southern end of the site. It is a multi phase structure constructed during the Post Medieval period. There is standing water just to the north of the 1990 trench. The area around the trench is dominated by mosses, grass and rushes. The monument was excavated in an east west direction where the structure was most substantial. A thin layer of topsoil covered the monument (fig. 5.19). The bank of the dyke was constructed using turves and stone. Organic lenses are present within the matrix of the dyke which can be interpreted in two ways. Firstly they are the remnant of turves that had been used to build the dyke. Secondly they are the result of the growth and decomposition of roots around the edges of large stones.

Directly underlying the monument is a series of contexts that are the result of different periods of pedogenesis affecting the buried profile (fig. 5.19 and 5.20). Context 8029 is a thin very dark grey (10YR 3/1), buried humose A horizon. Below this (C.8030) there are weak signs of eluviation. Contexts 8026 is very dark brown (10YR 3/2) and context 8027 is dark brown (10YR 3/3) with strong brown mottles (7.5YR 5/8). The mottles were interpreted in the field as indications of gleying in the buried A horizon. This is consistent with the standing water observed to the north of the monument.

Fig. 5.19 M75/4, PM turf and stone dyke



20cm

Contexts:

- 8024. Topsoil
- 8025. Turf and stone dyke
- 8026. Buried A horizon
- 8027. Buried A, weakly gleyed
- 8028. Weathered mineral horizon
- 8029. Thin buried humose A horizon
- 8030. Area of weak eluviation

- Sample for thin section (Kubienna tin)
- Sample for thin section (wrapped block)
- Large boulders

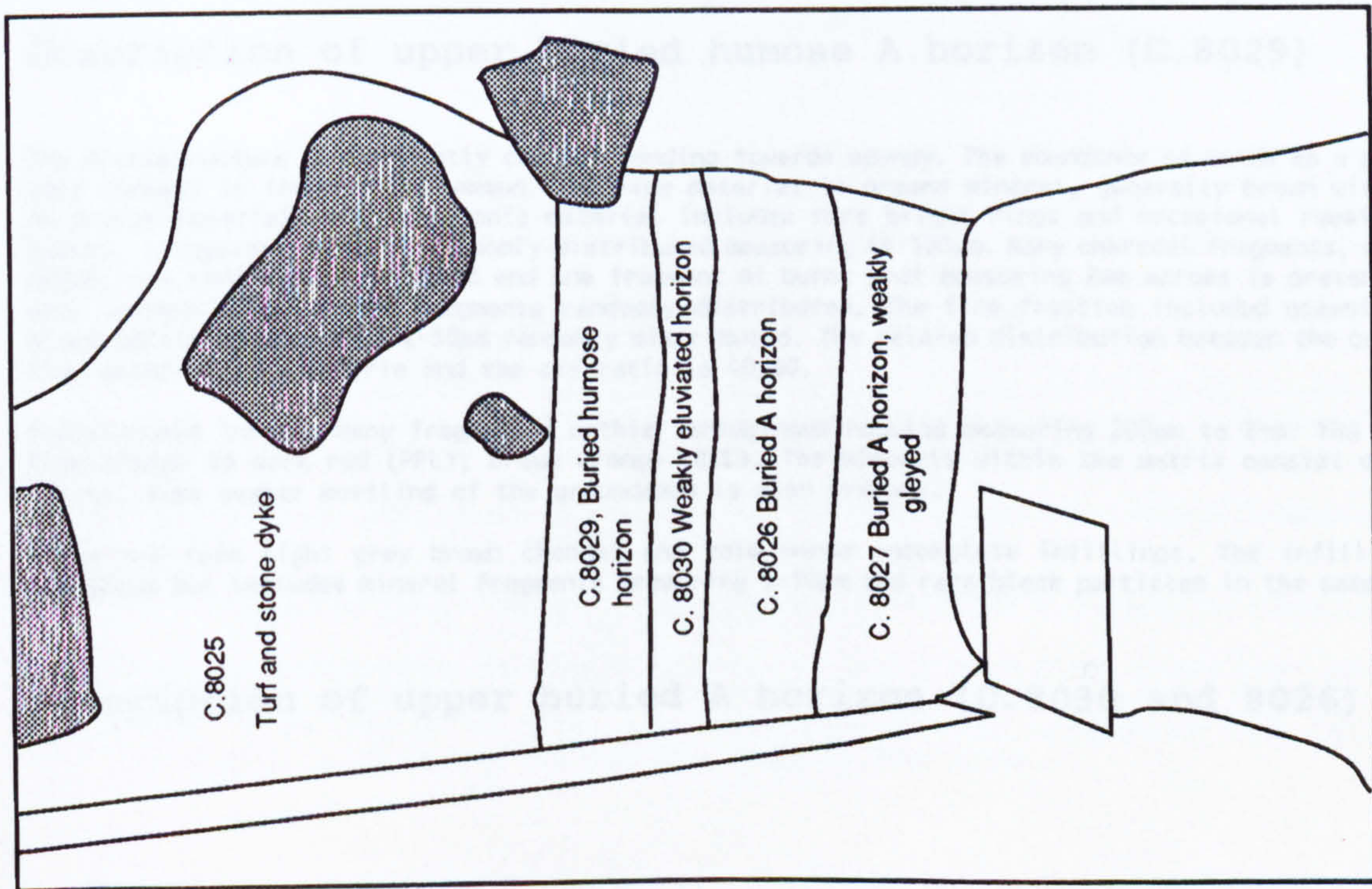


Fig. 5.20 M75/4, PM turf and stone dyke

There is no Bs horizon below the monument where the 1990 trench was excavated. However two trenches were dug through M75 in the 1989 field season. In one of these trenches there is a well developed Bs horizon and in the other there is not. It is likely that the presence or absence of a Bs horizon can be correlated to gleying of the B horizon.

#### 5.9.1 M75/4 thin section results.

Four samples were taken for thin section analysis but only 2 analysed.

#### 5.9.2 M75/4, sample 1, c.8029, c.8030, c.8026.

Sample 1 is from the interface between the buried humose A horizon (C.8029), and the top of the underlying buried non humose A horizon (C.8030, 8026).

#### Description of upper buried humose A horizon (C.8029)

The microstructure is dominantly channel tending towards spongy. The abundance of voids as a percentage of this context is frequent to common. The fine material is organo mineral, generally brown with rare areas of orange material. Coarse organic material includes rare bright rings and occasional remains of fungal spores, irregularly shaped, randomly distributed measuring 40-100 $\mu$ m. Many charcoal fragments, measuring 20-400 $\mu$ m, are randomly distributed and one fragment of burnt peat measuring 2mm across is present. There are many unidentified organic fragments randomly distributed. The fine fraction included occasional to many black particles measuring 2-50 $\mu$ m randomly distributed. The related distribution between the coarse and the fine material is porphyric and the c/f ratio is 40:60.

Pedofeatures include many fragmented orthic ferruginous nodules measuring 200 $\mu$ m to 2mm. The colours vary from orange to dark red (PPL), brown orange (OIL). The minerals within the matrix consist dominantly of quartz. Some weaker mottling of the groundmass is also present.

There are rare light grey brown channel and void dense incomplete infillings. The infill material is amorphous but includes mineral fragments measuring 5-10 $\mu$ m and rare black particles in the same size range.

#### Description of upper buried A horizon (C.8030 and 8026)

The dominant microstructure is spongy, locally almost channel. The abundance of voids as a percentage of the thin section is frequent. Coarse mineral material includes single mineral grains dominated by quartz showing some clustering. Compound mineral grains and rock fragments include quartz dominated metamorphic fragments. There are rare fragmented phytoliths and diatoms randomly distributed throughout the sample. The fine fraction is organo mineral with a variable composition consisting of orange (PPL) and dull brown (OIL) material. The groundmass consists of very abundant, equidimensional to elongate pellets measuring 40-60 $\mu$ m, weakly to strongly coalesced, forming the infilling of channels but also incorporated into the groundmass. These are strong orange using PPL. There are many fragments of groundmass with grey brown colour and a porphyric c/f related distribution. The groundmass is generally chitonic to porphyric with a c/f ratio of 55:45. The material is poorly sorted.

Using a c/f limit of 20 $\mu$ m the ratio between coarse and fine organic components is 90-10. Fine organic material includes occasional black (PPL and OIL) particles randomly distributed measuring 8-20 $\mu$ m. Coarse organic material includes rare cell residues clustered in areas of grey brown material. The rest of the coarse organic fragments are randomly distributed and include rare bright rings, rare isotropic rings, 40-50 $\mu$ m diameter, rare groups of cells, possibly the internal spores from a sclerotium, occasional charcoal fragments measuring 20-200 $\mu$ m and rare elongate organ residues 20-40 $\mu$ m wide, probably the remains of roots.

Pedofeatures includes many to abundant loose continuous, weakly to strongly coalesced void and channel infillings.

Context 8030, the area identified as having weak indications of eluviation, is not identified in thin section.

### 5.9.3 M75/4, sample 4, c.8027.

Sample 4 was taken from the context 8027 to examine the lower part of the buried A horizon and the top of the context 8028.

The microstructure is spongy with localised bridged grain. The abundance of voids as a percentage of this context is frequent.

Coarse mineral material includes single mineral grains dominated by quartz, some clustering of quartz caused by channels. There are also small amounts of green amphibole, muscovite, biotite and feldspar. Compound mineral grains and rock fragments are composed mainly of interlocking quartz grains with varying amounts of feldspar showing moderate to strong weathering. There is strong alteration of material between quartz grains.

Coarse organic material includes one bright ring, located in the central area of an orange infilling, rare remains of roots in channels and rare fragments of charcoal measuring 3-10mm. The groundmass is randomly dotted with rare black fragments measuring 20-400 $\mu$ m which consist dominantly of charcoal although there are also some small amorphous nodules. Inorganic residues of biological origin include rare phytoliths which are randomly distributed.

There are two types of fine material present

1. Orange (PPL), dull brown (OIL), irregularly shaped pellets forming the infillings of many channels (see pedofeatures) but also incorporated into the groundmass. Organo mineral but large amounts of organic material particularly in the areas with the brightest orange colours.

2. Brown to grey brown (PPL) organo mineral material. Composed of many small mineral fragments and organic fine material.

There are rare black particles randomly distributed measuring 2-50 $\mu$ m throughout the whole slide.

The c/f related distribution is chitonic to porphyric and the c/f ratio 50:50. Pedofeatures include abundant channel infillings. In the top of the 1.5 to 2cms of the slide these are strongly referred parallel with the surface, in the rest of the slide they are strongly referred perpendicular with the surface. The infilling material is composed of ovoid pellets measuring 40 $\mu$ m across.



In the lower part of the slide there are occasional disturbed cappings and link cappings, grey, composed of mineral material. Cappings on rock fragments are not greater than 400µm wide. Two layers are visible, a finer grey mineral material overlying a coarser grey mineral material.

#### 5.9.4 Interpretation of M75/4

| Sample No | Context                             | Coarse charcoal | Black particles <50µm | Phytoliths | Diatoms |
|-----------|-------------------------------------|-----------------|-----------------------|------------|---------|
| 74/5 S1   | Buried humose A horizon, C.8029     | Many            | Occasional            | No         | No      |
| 75/4 S1   | Buried non humose A horizon, C.8026 | Occasional      | Occasional            | Yes        | Yes     |
| 75/4      | Buried A horizon, upper             | Rare            | Rare                  | Yes        | No      |

Table 5.7 Micromorphological features of samples taken from M75/4

Context 8029 is the remnant of a thin humose horizon. There are many coarse charcoal fragments and occasional black particles in this layer and one fragment of burnt peat. The abundance of carbonised remains in the surface horizon indicates an input possibly related to burning of surface vegetation or manuring (section 9.5). The amount of carbonised residues decrease vertically down the profile (table 5.7). There are phytoliths and diatoms present throughout the lower part of the buried A horizon.

| Sample No | Context                   | Dominant c/f related distribution, c/f ratio | Sorting | Total voids TTS    | Microstructure          |
|-----------|---------------------------|--|---------|--------------------|-------------------------|
| 75/4 S1   | Buried Ao, C.8029         | Porphyric, 40:60                             | -       | Frequent to common | Channel                 |
| 75/4 S1   | Buried A, C.8030 and 8026 | Chitonic to porphyric, 55:45                 | Poor    | Frequent           | Channel to spongy       |
| 75/4 S4   | Buried A, C.8027          | Chitonic to porphyric 50:50                  | -       | Frequent           | Spongy to bridged grain |

Table 5.8 Comparison of microstructure and c/f ratios from M75/4

The buried profile had been modified by channels, this was most noticeable in context 8029. The effect was to increase the porosity (table 5.8) while leaving fragments of the original massive structure and porphyric c/f related distribution still present between the channels.

The abundance of fungal material, particularly bright rings and clusters of spores suggests a soil environment more suited to these organisms, possibly relating to the organic content of the soil (section 9.5).

The majority of the groundmass in contexts 8026 and 8027 is composed of many ultra fine pellets. In context 8027 there are two types of groundmass (section 3.2.4.2). Type 1 is interpreted as the result of post depositional root development and subsequent faunal reworking creating many small pellets which were then incorporated into the general groundmass. Type 2 is the fine material present before the post depositional alteration.

Determination of the precise elemental composition of the pellets is only possible with the use of submicroscopic microprobe techniques. The strong orange colour of the pellets, combined with field evidence indicating illuviation, does suggest an enrichment of sesquioxides.

At the base of sample 4 there are disturbed cappings. The cause of the disturbance of the glacial till is unclear using evidence from this one profile. There is no remnant of cappings in the

buried A horizon suggesting no significant mixing of the profile. However biological activity within the A horizon might have caused the loss of these features. In sample 2, from M127, there is only one small fragment of a silt capping in the buried A horizon. This suggests that these features are susceptible to reworking and turbation.

#### **5.10 Results of the analysis of M164, a PM dyke.**

M164 is a dyke or field boundary, probably constructed in the later Medieval period, which forms part of an addition to the head dyke (M75). The monument was excavated and sampled for thin sections in the 1989 field season.

A modern A horizon (C.3031) covers the main turf and stone dyke (fig 5.21). The monument (C.3032) consists of an outer cladding of large stones over a stone free turf core. Bands of horizontally aligned black (10YR 2/1) organic material are visible within the matrix. These probably represent the remnants of turves used to build the dyke.

Directly below the main structure is a black (10YR 2/1) band of amorphous organic material, which is interpreted as a buried O horizon. Underlying this is a dark brown (7.5 YR 3/2) buried A horizon. Disturbance of this layer is minimal with few very fine fibrous roots. Below C.3033 there is a thin continuous iron pan.

The context underlying the buried A is interpreted as a buried B horizon (C.3034). Disturbance of this layer is minimal with few very fine fibrous roots. The colour is dark brown (7.5 YR 3/4) at the top of the context which changes to dark yellowish brown (10YR 3/4) at the bottom. Context 8035 represents a soil accumulating against the side of the dyke.

#### 5.10.1 M164, thin section analysis.

Four samples were taken from this monument to examine the buried A horizon and the overlying turf dyke.

#### 5.10.2 M164, sample 1, c.3032.

This sample is from context 3032, approximately 39cm below context 3031 (fig 5.21). The slide has an organic rich band running horizontally 1cm below the top of the slide which is described separately.

The microstructure is intergrain microaggregate. The abundance of voids as a percentage of the thin section is common.

Coarse mineral material includes single mineral grains dominated by quartz measuring 50-800 $\mu$ m. There are almost no other types of minerals present. Only 1 fragment of biotite is present. Compound mineral grains and rock fragments are found in the size range 200 $\mu$ m to 1cm. A distinctive feature is that most of the rock fragments are no larger than 250 $\mu$ m. The material is well sorted.

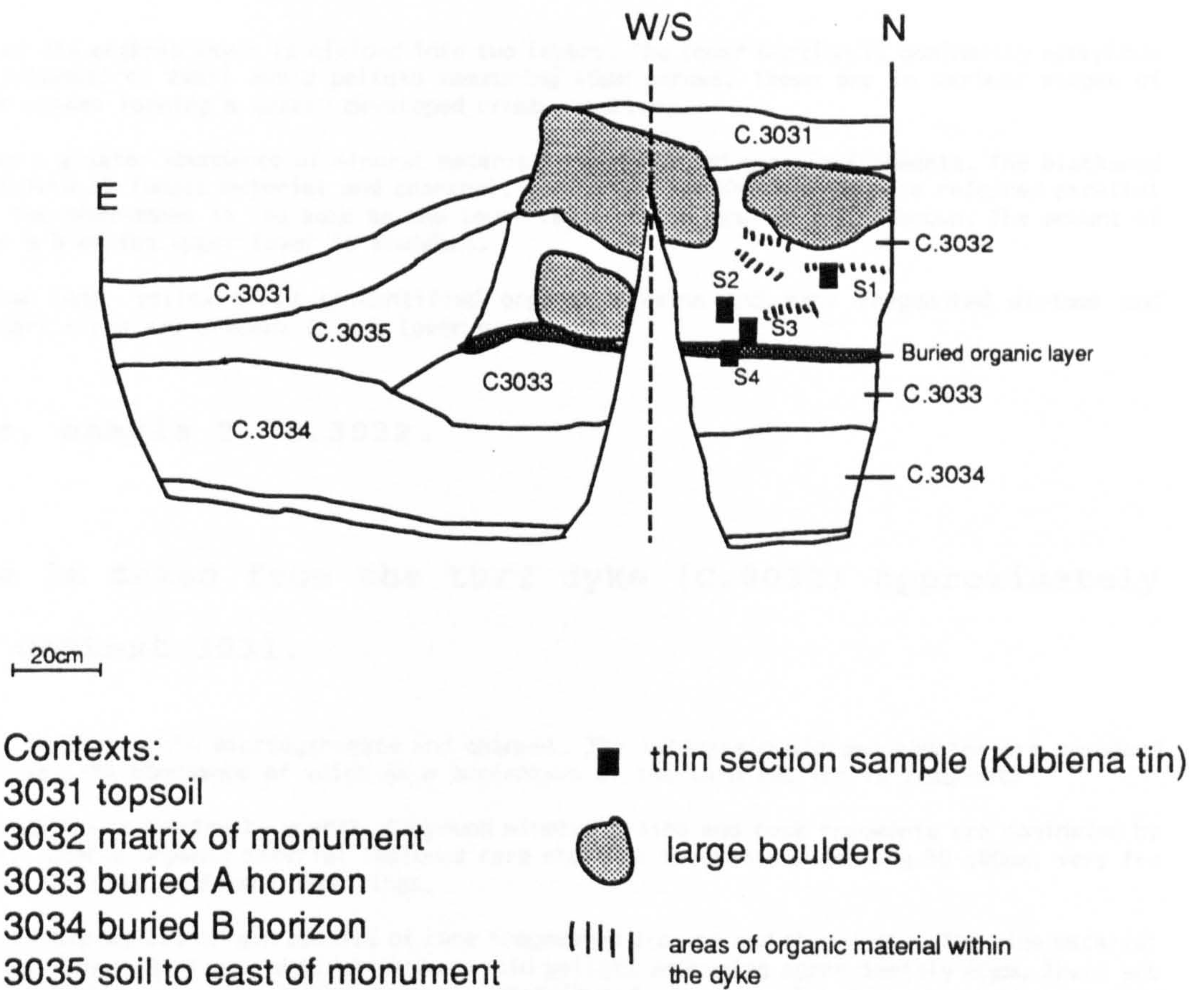
Coarse organic components comprise rare remains of roots in channels, rare dark rings, diameter 100-200 $\mu$ m, rare charcoal fragments measuring 50-100 $\mu$ m randomly distributed, rare fragments of peat, randomly distributed (see pedofeatures). Inorganic residues of biological origin include occasional fragmented phytoliths and diatoms randomly distributed.

The fine material is composed of almost completely ovoid pellets measuring 40 $\mu$ m across with only very light coalescing occurring. They are brown to slightly red brown. There are one or two black particles measuring 2-50 $\mu$ m randomly distributed.

The related distribution between the coarse and the fine material is enaulic with some localised tendency to chitonic where bridging occurred. The c:f ratio is 45:55.

Excrement pedofeatures consist of rare earthworm excrements, ovoid 900 $\mu$ m long, brown matrix (PPL), organo mineral. Some examples found in a large channel are fragmented. There is one example of a feature which is composed of a much higher quantity of organic material.

Fig. 5.21 M164, PM turf and stone dyke



There are two examples of a compound ferruginous nodule. The size of one fragment is 2 x 2mm. This consists of an upper strongly humified organic layer, orange to red (PPL), dark brown (OIL), and a lower strongly impregnated ferruginous layer, dark red to black (PPL), bright orange (OIL). This is the remnant of an iron rich layer directly below a peat layer. The fragment is subrounded and equidimensional although there are some irregularities. There are also other examples of strongly impregnated iron rich nodules which are probably relict iron pan, abundance very few.

Fabric pedofeatures include very few fragments of highly humified organic material. These are equidimensional, subangular, 600 $\mu$ m x 600 $\mu$ m. The internal fabric is composed almost entirely of organic material although 6 quartz grains measuring 40-60 $\mu$ m were counted. Blackened highly humified organic residues are present within the generally brown red matrix. The remains measured 20-200 $\mu$ m. The larger examples look like the internal area of a sclerotia. Phytoliths and very few fragmented diatoms are present.

There are very few spherical, 900 $\mu$ m diameter, remnants of organic material. These are possibly excrements. A fragmented diatom is on the sharp boundary of one.

One poorly preserved incomplete crescent fabric features is visible. This is about 200 $\mu$ m wide and 1mm long. The crescents consist of red brown amorphous material.

### **Description of the organic layer.**

A central section of the organic layer is divided into two layers. The lower section is dominantly amorphous organic material composed of small ovoid pellets measuring 40 $\mu$ m across. These are in various stages of coalescing in some places forming a weakly developed crumb structure.

The top section has a greater abundance of mineral material and blackened organic fragments. The blackened fragments are a mixture of fungal material and charcoal. They measured 20-200 $\mu$ m and are referred parallel with the surface. The groundmass is the same as the lower layer except predominantly brown. The amount of black fragments as a % of the upper layer is abundant.

There are very few long, yellow (PPL) unidentified organic remains and many fragmented diatoms and phytoliths. Rare dark rings are present in the lower band.

### **5.10.3 M164, sample 2. c.3032.**

This sample is taken from the turf dyke (C.8032) approximately 46cm below context 3031.

The microstructure is intergrain microaggregate and channel. The intergrain microaggregates are composed of ultrafine granules. The abundance of voids as a percentage of the thin section is frequent.

Single mineral grains are dominated by quartz. Compound mineral grains and rock fragments are dominated by feldspar and quartz. Coarse organic material includes rare charcoal fragments measuring 50-400 $\mu$ m, very few remains of roots in channels, and rare dark rings.

Inorganic residues of biological origin consist of rare fragmented diatoms and phytoliths. The fine material is organo mineral and composed of very dominant brown ovoid pellets measuring approximately 40 $\mu$ m. There are one or two black particles measuring 2-50 $\mu$ m randomly distributed. The material is moderately to poorly sorted. The c/f related distribution is enaulic with a c/f ratio of 50:50.

Fabric pedofeatures include channel infillings, 400 $\mu$ m diameter, 8mm long but broken and fragmented in places. There is a weak crescent arrangements of internal features. Colours are orange red (PPL) and brown red (OIL).

There are many weakly impregnated mottles measuring 20-200 $\mu$ m, randomly distributed, orange to brown orange (OIL), brown (PPL).

#### 5.10.4 M164, sample 3, c.3032

This sample is taken from the turf dyke (C.3032) approximately 51cm below context 3031. Different layers identified within the slide are emphasised within the overall description.

The microstructure is generally intergrain microaggregate, some areas of the groundmass are composed completely of ultrafine granules. Towards the base of the slide there is an area with a more dense fabric with a porphyric c/f related distribution. Voids are frequent to common (about 30%) in areas with a greater abundance of coarse material and frequent in areas with a greater abundance of fine material.

Coarse organic components consist of rare remains of roots in channels. Rare charcoal fragments, measuring 50-300 $\mu$ m, are generally present towards the top of the slide. One fragment measures 3mm across. In one place a large fragment, 2 x 2mm, of black (PPL) organic material is present, probably a fragment of burnt wood but might be charred peat. Near the base of the slide some larger fragmented remains of charcoal are present. These are generally elongate, angular and measured 2-4mm along the long axis. One fragment is incorporated into a nodule (see pedofeatures).

In two places there are clusters of 3 dark red and black unidentified organ residues lying in a chamber. The abundance of dark rings is very few and the abundance of sclerotia is rare.

Inorganic remains of biological origin include rare fragmented phytoliths randomly distributed. The colour of the fine material is generally brown (PPL), and consists of ovoid (40 $\mu$ m) pellets in various stages of coalescing.

There are generally only one or two fine black particles but this abundance increases towards the top of the slide as the amount of fine material increases. The material is moderately sorted.

The c/f related distribution varies between enaulic (pure intergrain microaggregate) to chitonic (where the aggregates are becoming more connected and bridging mineral grains). The c/f ratio is also variable, 20:80 in areas dominated by fine material, 50:50 elsewhere. Using OIL some dark brown to slightly orange brown mottling of the groundmass is visible. This is particularly evident in the top 1cm of the slide. At the bottom of the slide there is a porphyric c/f related distribution.

Pedofeatures include one compound ferruginous nodules measuring 1 x 2mm. This is strongly impregnated, red to dark red (PPL), bright orange (OIL). The matrix is dominated by quartz grains in the size range 20-200 $\mu$ m. A large fragment of charcoal has been incorporated into the matrix of the nodule. Other nodules include very few orthic nodules, subrounded to subangular, equidimensional measuring 3mm x 3mm.

A fabric pedofeature consists of an area of groundmass incorporating voids, coarse and fine mineral material. Minerals are dominated by quartz but also included biotite and feldspar. One small 100 $\mu$ m fragment of charcoal is present.

One area of the groundmass is strongly impregnated with ferruginous material. The colours are dark red to black (PPL), strong orange (OIL) in 30% of the area. 70% of the area is composed of amorphous orange (PPL), dull brown (OIL), material that forms as amorphous coatings in old void areas. This sometimes completely fills void areas but other times is present as coatings. This is probably a fragment of iron pan derived from below an organic rich layer.

An area 3mm x 4mm has amorphous orange (PPL), brown (OIL), isotropic, coatings in void spaces. The coatings are 20-40 $\mu$ m thick. Small, 100-200 $\mu$ m diameter, typic iron rich nodules are present with small 20-40 $\mu$ m amorphous black fragments and small ovoid pellets measuring 40 $\mu$ m across. This feature occurs at the end of an area with more fine to coarse material than in most of the slide and is characterised by greater than normal dark brown mottling (OIL).

### 5.10.5 M164, sample 4. c.3032 and c.3033

This sample is taken from the boundary between the buried A horizon (C.3033) and the buried A<sub>0</sub> horizon. This slide is divided into three layers.

#### Layer 1 buried A horizon:

The characteristic feature of this layer is the variation in the distribution of coarse and fine material across the slide. Areas with a porphyric related c/f related distribution, c/f ratio 40:60 (limit 50 $\mu$ m), are in close proximity to areas where single mineral grains are bridged by areas of fine material, c/f ratio 80:20. In many areas with a porphyric distribution vermiform shapes criss-cross the slide. The microstructure consists of vughy, channel and massive areas. The abundance of voids as a percentage of this layer are few.

The mineral material greater than 50 $\mu$ m is clustered and separated by areas of porphyric material. Coarse organic components include rare charcoal fragments measuring 300-400 $\mu$ m and rare dark rings, 100 $\mu$ m diameter. Inorganic residues of biological origin consist of rare fragmented phytoliths. The fine material is organo mineral, brown to dark brown (PPL). Some limited areas of staining by red amorphous material is present (see pedofeatures). There are one or two black particles, randomly distributed, probably not charcoal. The material is moderately sorted.

An important feature of this layer is the concentration of fine material showing a porphyric c/f related distribution. These areas varied from fairly large, 3-4mm, irregularly shaped areas to areas thinner than 400 $\mu$ m wide which look like fabric features crossing the soil.

There are rare mottles, orange red (PPL), measuring 16-40 $\mu$ m randomly distributed.

The boundary between layer 1 and layer 2 varies between sharp and diffuse. Layer 2 corresponds to the buried organic layer and consists of dominantly fine material where the organic material is the least disrupted. In disturbed areas there are greater concentrations of coarse mineral material. This description refers to the area of intact organic material.

The microstructure is massive with few cracks about 40 $\mu$ m wide. Coarse organic components include rare bright rings, rare sclerotia and the decomposing remains of organic material. There are many organic fragments consisting of charcoal and cell residues, randomly distributed, 50-500 $\mu$ m, black to dark red (PPL). Inorganic residues of biological origin comprised occasional diatoms and phytoliths randomly distributed. The fine material is mainly organic, orange brown, red brown to light brown (PPL) material. There are abundant cell residues, randomly distributed and many black particles measuring 2-50 $\mu$ m randomly distributed. The c/f related distribution is open spaced porphyric with an undifferentiated b-fabric and a 10:90 c/f ratio.

Excrement pedofeatures are present within the large cracks that ran vertically through the organic rich material. They are ovoid, measured a maximum of 800 $\mu$ m across, organo-mineral and weakly to moderately coalesced. Using OIL they are a light grey brown. Some areas of light grey brown material are also present within the more massive areas suggesting faunal activity.



Layer 3 represented the turf dyke (C.3032) which is analysed in samples 1-3.

#### **5.10.6 Interpretation of M164.**

The organic rich band of material at the top of sample 1 is the remnant of a turf added to the dyke. The darker colour observed in the field corresponds to a layer consisting almost completely of organic material. The top of this layer has a greater abundance of mineral material than the bottom suggesting that the turf is inverted. There are many fragmented diatoms within the organic layer and an abundance of fungal material mixed with charcoal.

There are rare coarse charcoal fragments within the mineral part of sample 1 but only one or two fine black particles. This is surprising considering the abundance of charcoal within the organic layer. This suggests there was little mixing of the mineral A and the organic layer above it. A similar distribution of black particles is seen in the buried O horizon the buried A horizon. There are many coarse carbonised residues and fine black particles throughout the buried O horizon but only rare coarse charcoal in the buried A horizon. There are occasional phytoliths and diatoms in the buried O horizon and only rare fragmented phytoliths in the buried A horizon again indicating little mixing of the two horizons. There is some layering of mineral material between the top of the buried O horizon and the base of the dyke. This is probably the result of monument construction.

In sample 1 there is a compound nodule, consisting of an organic fragment directly overlying ferruginous material, within the mineral groundmass. A similar feature is present in sample 3. These features might have been present in the soil prior to the construction of the dyke, or be a result of disturbance during construction. They are not present in the underlying buried A horizon. It is possible that they originate from a location where an iron pan had formed below organic material. In sample 3 there are fragments with abundant amorphous orange coatings. The morphology of these areas are very similar to the accumulation of organic material seen above iron pans elsewhere on the site (M86, transect 7000).

Faunal reworking had resulted in almost completely biological fabrics in samples 1, 2 and 3. In sample 2 this is indicated by the abundance of ultrafine granules. Channel infillings are also present with an internal crescent arrangement. Elongate crescent features running through the soil are characteristic of faunal activity where the organism backfills its channel as it passes through the soil matrix (West et al. 1991, Shipitalo and Protz, 1987).

Reworking of the buried O horizon is indicated by the presence of many ultrafine granules. Large excrement pedofeatures are present in the vertically orientated cracks. These are possibly derived from earthworms. This is the only area where significant mixing of organic and mineral material had occurred. Apart from this, there did not seem to be any major displacement of material

between layers. The microstructure of the buried A (C.8033) horizon is intergrain micro aggregate, caused by biological reworking of the groundmass.

At the time when M164 was constructed, an organic layer had developed on the ground surface. The turves were probably derived from close to the dyke given the micromorphological similarity between them and the buried A horizon. There had been minimal incorporation of carbonised residues with the buried A horizon prior to the formation of the organic layer. This suggests little cultivation or anthropogenic disturbance for a period of time (section 9.5). Where an organic layer is preserved, as in the dyke wall, a layering of carbonised residues is present. This suggests surface burning of vegetation.

#### **5.11 Results of the analysis of an undated deep top soil accumulation and an underlying buried profile.**

M21, a deep accumulation of soil, is located in the southern part of group A. The soil is unburied and represents an area where human activity and pedogenesis has continued to effect soil development to the present day.

##### **5.11.1 Results of M21.**

M21 is located at the edge of a field on gently sloping ground. An accumulation of soil, approximately 1m deep, buried a revetment. Below this is a buried A horizon and buried A/B

horizon. Given the angle of slope, the depth of the deep topsoil seemed to be greater than could be accounted for by colluvial movement alone. Manuring of the profile was suggested as a reason for the deepening of the soil.

A trench was excavated in 1990 (fig 5.22) to allow a thin section analysis of the deep topsoil and any buried soil that present below the revetment. The vegetation on top of the field boundary is grass while rushes and Iris pseudacorus are present to the west of the monument.

A deep accumulation of topsoil (C.8000, fig 5.22 and fig. 5.23) is located above a stone revetment (C.8001). Context 8000 is homogenous with no apparent stratigraphy. The colour is dark reddish brown (5 YR 3/2), humose with few small angular/subangular stones, few medium to large subangular stones. The texture is loamy sand and the structure is apedal massive. There are many very fine fibrous grass roots in the top 5-10cms with few fine fibrous roots below this. Faunal activity includes earthworms and unidentified arthropods.

Context 8001 consists of very abundant large to very large subangular to subrounded stones. These form a revetment perhaps fronting an original field. Further excavation upslope is needed to make a more precise archaeological interpretation. Below context 8001 there are two contexts which represent the original pre-revetment soil. The upper context, 8002, is greyish brown (10 YR 4/2), non humose sandy loam with abundant small to large

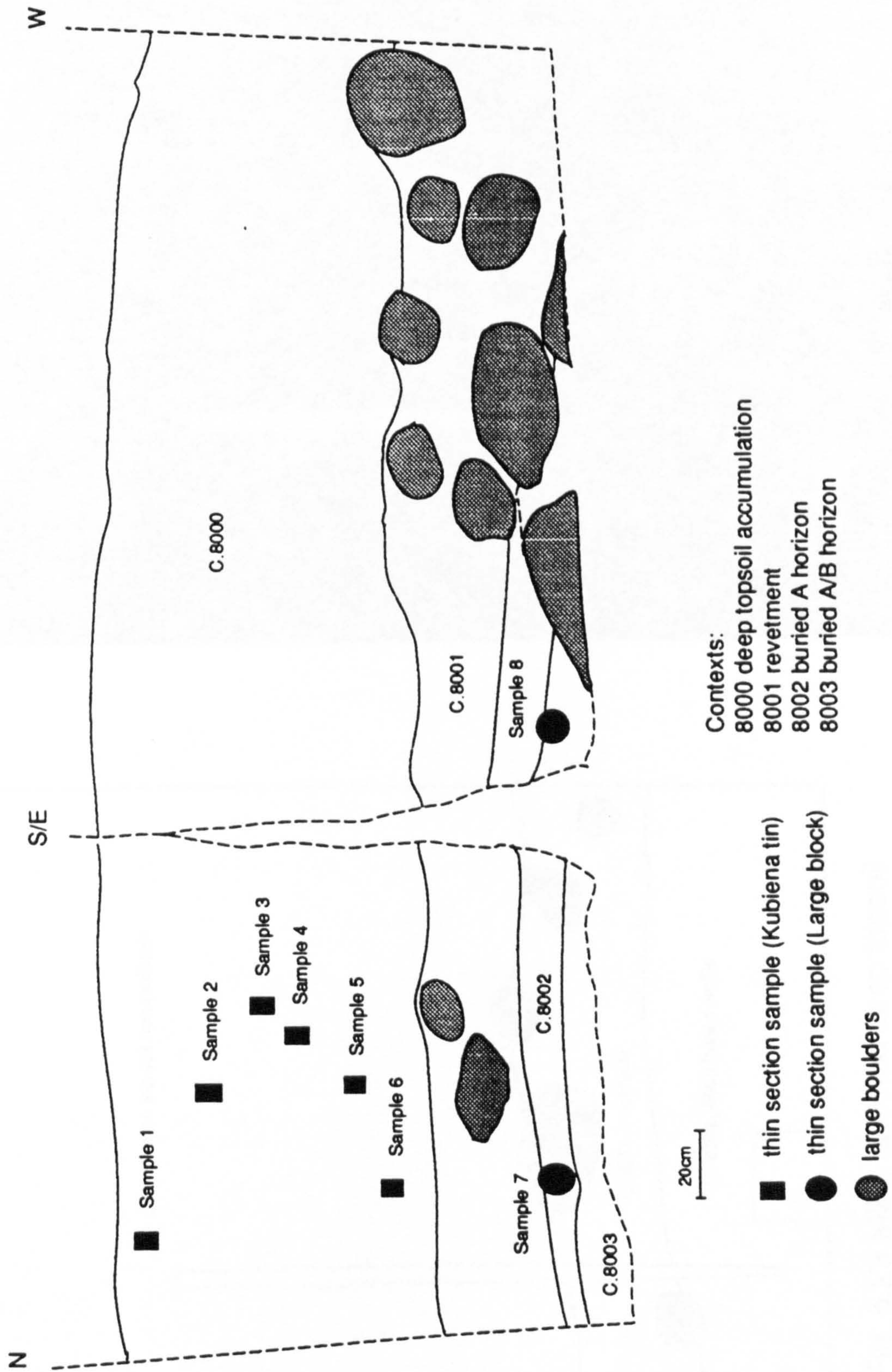


Fig. 5.22 M21, undated deep top soil accumulation

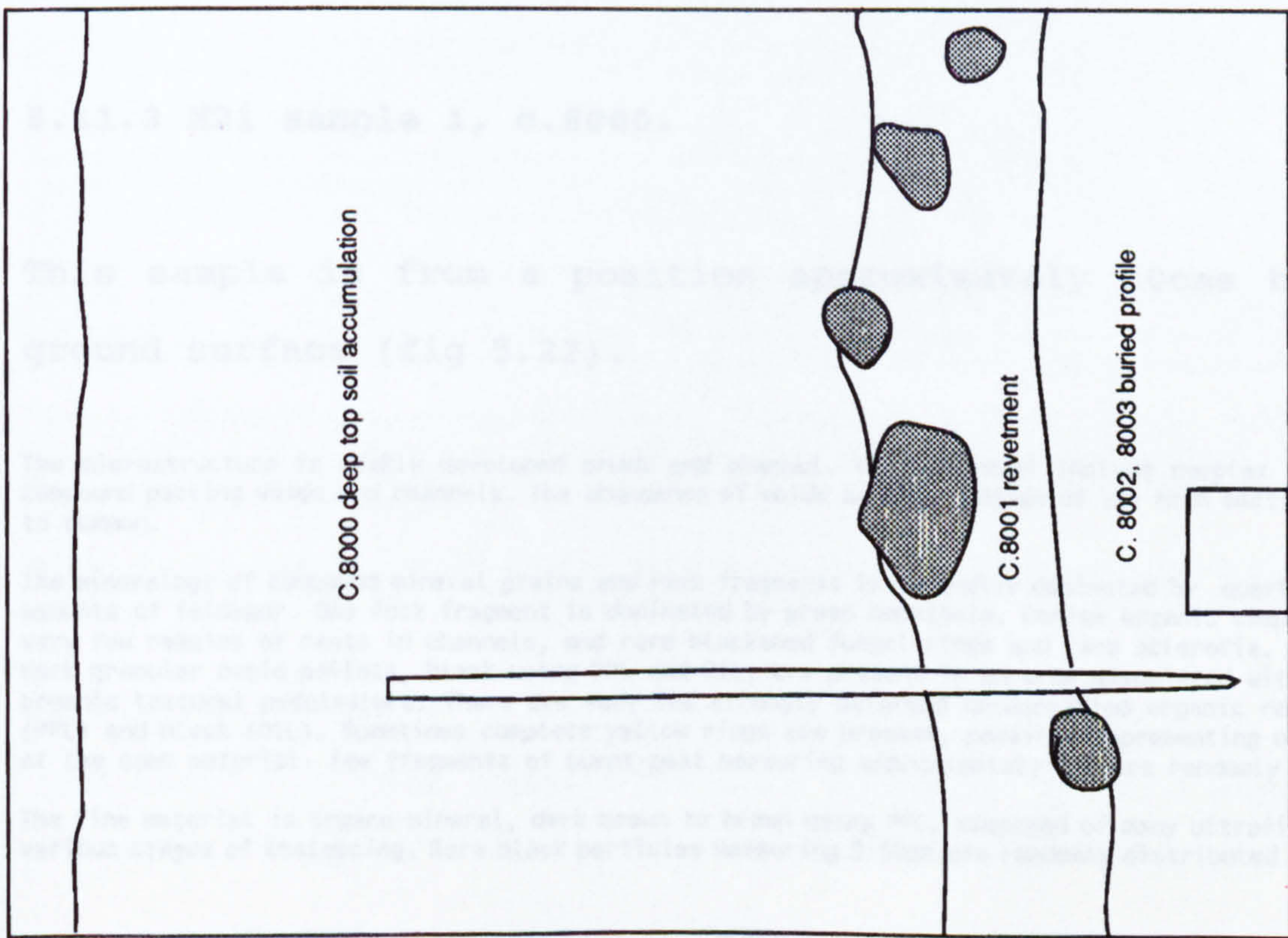
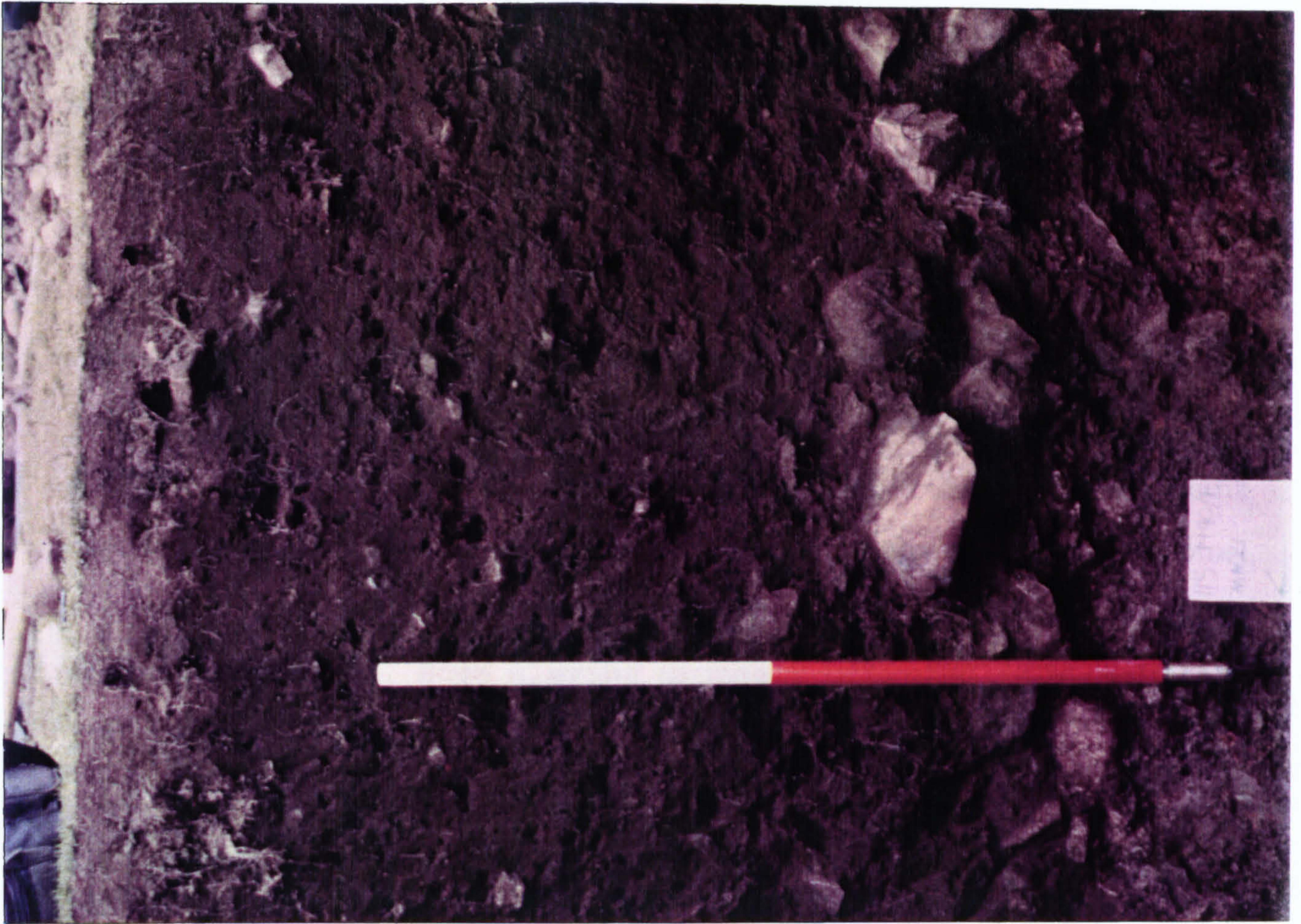


Fig. 5.23 M21, undated deep topsoil accumulation, west facing

subrounded to angular equidimensional stones. The structure is apedal single grain with few fine fibrous roots. This is interpreted as the remnants of a buried A horizon. The greyish colours suggest some waterlogging has occurred.

Underlying context 8002 is the buried A/B horizon (C.8003). The colour is brown (10 YR 4/3) with many, fine distinct, clear mottles 7.5 YR 4/4 brown. The texture is loamy sand with abundant small to very large subangular and angular equidimensional stones. The structure is apedal single grain. The lower boundary was not excavated. some gleying probably occurred as a result of groundwater gleying.

#### **5.11.2 M21, thin section results.**

Eight thin sections were taken for analysis. Six from the main accumulation (C.8000) and 2 from the underlying buried soils.

#### **5.11.3 M21 sample 1, c.8000.**

This sample is from a position approximately 10cms below the ground surface (fig 5.22).

The microstructure is weakly developed crumb and channel. Voids present include complex packing voids, compound packing voids and channels. The abundance of voids as a percentage of the thin section is frequent to common.

The mineralogy of compound mineral grains and rock fragments is generally dominated by quartz with varying amounts of feldspar. One rock fragment is dominated by green amphibole. Coarse organic components include very few remains of roots in channels, and rare blackened fungal rings and rare sclerotia. A cluster of 8 dark granular ovoid pellets, black using PPL and OIL, are present in an area associated with an amorphous organic textural pedofeature. There are very few strongly deformed unidentified organic residues, yellow (PPL) and black (OIL). Sometimes complete yellow rings are present, possibly representing unaltered types of the same material. Few fragments of burnt peat measuring approximately 4mm are randomly distributed.

The fine material is organo-mineral, dark brown to brown using PPL, composed of many ultrafine granules in various stages of coalescing. Rare black particles measuring 2-50 $\mu$ m are randomly distributed throughout the

groundmass. These probably include fragments of charcoal and burnt peat. The related distribution between the coarse and the fine material is variable, some areas are open porphyric other areas are enaulic to gefuric. The c/f ratio is 45:55. The material is moderately to well sorted.

Excrement pedofeatures include rare, brown yellow, ovoid, equidimensional organic material measuring 200-500 $\mu$ m. There are also some smaller examples measuring 10-80 $\mu$ m. They consist of fragmented diatoms and phytoliths and organic residues. The variability between individuals is moderate. In some of the red brown examples fragmented diatoms and fibrous organic material are present. Not all of the examples include fragmented diatoms.

There are many typic nodules with sharp boundaries measuring between 20 $\mu$ m and 1mm, black to dark red PPL, orange to dark grey OIL. There is one example of a nodule that is larger than the rest. This is red using PPL and OIL, elongate, 2mm long. It is almost completely typic apart from one fragment of quartz. The boundary to the adjacent groundmass is sharp.

Fabric pedofeatures include rare faint loose continuous infillings. Long fabric pedofeatures approx 400 $\mu$ m wide criss cross the slide. There is one area 2mm x 1mm composed of humified organic material. Laminations within the material are present but no mineral material. This is a residue of peat added to the soil.

#### **5.11.4 M21 sample 2, c.8000**

This sample is from a position approximately 30cm below the top of context 8000 (fig. 5.22). Features are only described if they are different from sample 1.

The microstructure is channel and weakly developed crumb structure. The fine material is composed of ultrafine granules in various stages of coalescence. The abundance of voids as a percentage of the thin section is common. Coarse organic components include very few remains of roots in channels, rare sclerotia randomly distributed, and occasional fragments of charcoal measuring 40 $\mu$ m to 1mm, also randomly distributed. Inorganic residues of biological origin consist of rare fragmented phytoliths and diatoms.

The fine material is organo-mineral, brown to dark brown (PPL) with occasional black particles measuring 2-50 $\mu$ m including fine charcoal. The material is well sorted. The c/f related distribution is variable, some areas are porphyric, others gefuric. The c/f ratio is 45:55. In the bottom left hand corner of the slide there is a local tendency towards porphyric. This is probably a result of the slide being thicker in this area. Throughout the slide there are small fabric pedofeatures of variable size that consist of 90% amorphous organic material. The size of these areas varies between 80 and 1200 $\mu$ m. They are slightly irregularly shaped but approximately equidimensional. The internal fabric is composed of almost entirely of organic residues. The fragmented remains of diatoms are present. In some of the examples there is a weak lamination of the organic residues. The variability between individuals is moderate, the colour varying from brown yellow to red brown. Their abundance as a percentage of the thin section is rare TTS.

Much of the groundmass consists of faint fabric pedofeatures about 400 $\mu$ m wide. These resemble passages through the soil. Single mineral grains are embedded within the fine material (porphyric related distribution). It is difficult to estimate the abundance of these features owing to their indistinct composition. However > 50% of the slide would seem to include these features to some extent.

There are rare typic strongly impregnated nodules. Deep red to black (PPL), isotropic, red brown to orange (OIL), measuring approx 1mm x 1.5mm, subrounded. There are also smaller nodules measuring 20-200 $\mu$ m, randomly distributed, orange brown to grey black (OIL), very dark red brown to black (PPL), isotropic, sharp boundary distinct to prominent, abundance is rare.

Much of the groundmass is composed of small ovoid pellets varying in size between 20 and 40 $\mu$ m. They are in various states of coalescing with the surrounding groundmass and probably represent excrement pedofeatures.

#### **5.11.5 M21, sample 3, c.8000.**

This sample is from a position 40cm below the ground surface (fig 5.22).



The microstructure is channel with localised intergrain microaggregate. The abundance of voids as a percentage of the thin section is frequent. Coarse organic components include rare remains of roots in channels, rare charcoal and burnt peat fragments measuring 80 $\mu$ m to 1mm, randomly distributed. Inorganic residues of biological origin comprise rare fragmented phytoliths. The fine material is organo-mineral, in small areas impregnated by iron compounds. Using PPL these appear as small red areas 80 $\mu$ m across. The colour of the fine material is brown to dark brown. There are rare black particles measuring 2-50 $\mu$ m, randomly distributed. The material is well sorted. The related distribution between the coarse and the fine material is variable including porphyric and enaulic areas. The c/f ratio is 50:50.

Pedofeatures include rare nodules measuring 20-200 $\mu$ m. These are randomly distributed, orange brown to grey black (OIL), very dark red brown to black (PPL), isotropic, sharp boundary distinct to prominent.

Fabric pedofeatures comprise faint vermiform shaped features, 400 $\mu$ m wide, single mineral grains are embedded in a matrix of finer material, porphyric c/f related distribution.

#### **5.11.6 M21, sample 4, c.8000.**

This sample is from a position approximately 48cm below the top of context 8000 (fig 5.22).

The microstructure is channel and localised intergrain microaggregate. The abundance of voids as a percentage of the thin section is frequent. Coarse organic components include rare charcoal fragments measuring 50 $\mu$ m to 1mm, randomly distributed, very few remains of roots in channels and one fragmented remain of a bright ring. Inorganic residues of biological origin include rare phytoliths randomly distributed. The fine material is brown to dark brown (PPL), organo mineral. There are rare black particles measuring 2-50 $\mu$ m randomly distributed. The material is well sorted. The related distribution of the coarse and the fine material is porphyric to enaulic. Small areas of the slide have a completely porphyric related distribution. The c/f ratio is 40:60.

When the slide is viewed macroscopically dark lines, moderately orientated perpendicular to the surface, can be observed within the groundmass. Using a microscopic scale of observation the dark lines are composed of areas with a porphyric c/f related distribution and a darker brown fine material than the surrounding groundmass. There are some areas of the groundmass, abundance rare, composed of ultrafine granules in various stages of coalescence.

Occasional nodules measuring 20-200 $\mu$ m are randomly distributed. These are black (PPL), orange, brown red and dark grey (OIL).

#### **5.11.7 M21, sample 5, c.8000.**

Sample 5 is from a position approximately 65cm below the surface of context 8000 (fig 5.22).

Variable microstructure which consists of channel structure with a high c/f related distribution approaching open porphyric. Areas of the slide are also intergrain microaggregate structure composed of ultrafine granules, probably created by biological activity. In places there are indications of a very weakly developed crumb structure. Coarse organic components include rare sclerotia, one bright ring, very few remains of roots in channels, rare fragments of charcoal measuring 50-80 $\mu$ m. The fine material is organo-mineral, brown (PPL). In the areas with the greatest biological activity colours are generally a darker brown. There are rare black particles measuring 2-50 $\mu$ m randomly scattered throughout the groundmass. The material is moderately sorted. The c/f related distribution is porphyric with areas of gefuric and enaulic. The c/f limit and the c/f ratio vary but are generally 35:65.

Some areas of the groundmass are composed of ultrafine granules which consist of many ovoid shaped pellets approx 40µm along the long axis. These sometimes form channel infillings but also comprise large areas of the groundmass.

Fabric pedofeatures approximately 1600µm wide are present. These are composed of material which is sometimes slightly darker than the surrounding groundmass, with higher ratios of coarse to fine material and a stronger tendency towards a porphyric c/f related distribution.

There are occasional nodules randomly distributed. These measured 20-200µm, black (PPL), orange, brown red and dark grey (OIL).

#### **5.11.8 M21, sample 6, c.8000.**

This sample is from a position approximately 82cm below the surface of context 8000 (fig 5.22).

The microstructure is variable consisting of spongy to channel material. In areas with the highest fine to coarse ratios the structure is dominantly channel with some vughs. Where the % of void space increases, and the voids become more interconnected, the structure is spongy. Where the groundmass is disrupted numerous aggregates ranging in size between 40-800µm are present (see excrement pedofeatures). In other areas the groundmass is composed of numerous ultrafine granules, probably excrement features. The smallest recognisable structural unit within these measures approximately 40µm along the long axis. The abundance of voids is variable, few in the areas dominated by channels, common in the disturbed areas.

Coarse organic components include very few remains of roots in channels, one dark ring and rare charcoal fragments, randomly distributed measuring 50-400µm. Inorganic residues of biological origin consist of rare phytoliths which are randomly distributed. The fine material is brown (PPL) organo-mineral material. There are rare black particles measuring 2-50µm randomly distributed. The material is moderately sorted. The related distribution between the coarse and the fine material is porphyric with some areas of gefuric and enaulic. The c/f ratio is 40:60. In some areas of the groundmass there are many small ovoid pellets measuring 40µm. These are densely packed and separated by compound packing voids.

Fabric pedofeatures approximately 800µm wide are present in areas of the slide. They are organo-mineral and tend towards a porphyric c/f related distribution.

In disturbed areas of the slide aggregates measuring 1mm across are present. These are organo-mineral and are partially fragmented. Positive identification is not possible but they might be earthworm excrements.

Textural pedofeatures include rare orange red, amorphous, limpid coatings. They are generally no thicker than 20µm, isotropic but some orientation using XPL is visible.

There are occasional nodules randomly distributed, 20-200µm, black (PPL), orange, brown red and dark grey (OIL).

#### **5.11.9 Interpretation of M21, samples 1-6.**

The thin section analysis confirms that manuring had contributed to the formation of context 8000. Residues of burnt peat and unburnt peat are present in samples 1 and 2. Some of the peat residues had been reworked resulting in excrement pedofeatures. There are abundant diatoms and phytoliths present in fragments

of peat. The addition of organic material alone does not explain the deepening of the profile, it is possible that turves were also being used as manure, thus increasing the fine mineral content of the soil.

The addition of peat to the soil resulted in a number of micromorphological characteristics. There is a greater abundance of coarse organic fragments and residues in the top 40cm of the soil than in any prehistoric context. These are fungal and organic residues probably derived from the peat. Phytoliths are present throughout most of context 8000 but diatoms are only identified in surface layers (table 5.9).

| Sample No     | Context   | Coarse charcoal | Black particles <50µm | Phytoliths | Diatoms |
|---------------|---|-----------------|-----------------------|------------|---------|
| M21, sample 1 | Deep soil accumulation, 10cm from surface, C.8000 | Occasional      | Rare                  | Yes        | No      |
| M21, sample 2 | Deep soil accumulation, 30cm from surface, C.8000 | Occasional      | Occasional            | Yes        | Yes     |
| M21, sample 3 | Deep soil accumulation, 40cm from surface, C.8000 | Rare            | Rare                  | Yes        | No      |
| M21, sample 4 | Deep soil accumulation, 48cm from surface, C.8000 | Rare            | Rare                  | Yes        | No      |
| M21, sample 5 | Deep soil accumulation, 65cm from surface, C.8000 | Rare            | Rare                  | No?        | No?     |
| M21, sample 6 | Deep soil accumulation, 82cm from surface, C.8000 | Rare            | Rare                  | Yes        | No      |

Table 5.9 Micromorphological features of samples taken from M21

At the top of the profile the coarse to fine ratio is 45:55. This gradually increases towards the base of the deep soil accumulation. This trend is matched by a reduction in the coarse organic components and by changes in microstructure, c/f related distribution and sorting (table 5.10).

| Sample No     | Context   | Dominant c/f related distribution, c/f ratio | Sorting          | Total voids TTS    | Microstructure                               |
|---------------|---|--|------------------|--------------------|--|
| M21, sample 1 | Deep soil accumulation, 10cm from surface, C.8000 | Porphyric, gefuric 45:55                     | Moderate to well | Frequent to common | Weakly developed crumb & channel             |
| M21, sample 2 | Deep soil accumulation, 30cm from surface, C.8000 | Porphyric, gefuric, 45:55                    | Well             | Frequent           | Channel & weakly developed crumb             |
| M21, sample 3 | Deep soil accumulation, 40cm from surface, C.8000 | Porphyric, enaulic, 50:50                    | Well             | Frequent           | Channel, localised intergrain microaggregate |
| M21, sample 4 | Deep soil accumulation, 48cm from surface, C.8000 | Porphyric to enaulic, 40:60                  | Well             | Frequent           | Channel, localised intergrain microaggregate |
| M21, sample 5 | Deep soil accumulation, 65cm from surface, C.8000 | Porphyric to gefuric and enaulic, 35:65      | Moderate         | Frequent to common | Channel, localised intergrain microaggregate |
| M21, sample 6 | Deep soil accumulation, 82cm from surface, C.8000 | Porphyric to gefuric and enaulic             | Moderate         | Frequent to common | Spongy to channel                            |

Table 5.10 Comparison of microstructure and c/f ratios from M21

The c/f related distribution within any single slide is very variable. The results in table 5.10, and the thin section descriptions for M21, refer to the dominant c/f related distribution. More than one type is included if it forms an important constituent of the matrix.

Table 5.10 shows a change in microstructure within context 8000. Samples 1 and 2 are weakly developed crumb and channel, sample 3, 4, and 5 include intergrain microaggregate structures and have lost any development of a crumb. There is minimal vertical variation in sorting and c/f ratio.

The changes in the profile are in part a response to variable organic matter content and abundance of fine material. The exact composition of the fine fraction cannot be determined using light microscopy but the composition probably includes a combination of fine mineral and organic material.

The structure of the soil at different depths is partly related to biological activity. The top two samples include a weakly developed crumb structure. The aggregates are partially the result of faunal reworking of the soil. Samples 3-5 include large areas of the groundmass composed of ultrafine granules, a result of biological activity.

The crumb structure at the surface indicates larger organisms are operating close to the surface, probably earthworms, reworking fresh organic material. Deeper in the profile smaller organisms continue the process of comminution producing ultrafine granules which coalesce, to varying amounts, and form geric to enaulic c/f related distributions.

#### **5.11.10 Thin section description, sample 7, c.8002.**

This section was taken from context 8002 which, using field evidence, is interpreted as the remnants of a buried A horizon.

The microstructure is channel with some areas of weakly developed granular microstructure. The peds are granular measuring 1600-2000 $\mu$ m (see excrement pedofeatures). The total abundance of voids as a percentage of the thin section is common.

Coarse organic material includes very few remains of roots in channels. Inorganic residues of biological origin consist of one or two phytoliths randomly distributed. The fine material is organo mineral, brown to dark brown (PPL). Rare black particles are randomly distributed throughout the groundmass. These are not necessarily charcoal because there are no larger particles of charcoal present. The material is moderately sorted. The c/f related distribution is porphyric, where ped development is strongest, with localised tendencies to chitonic.

Pedofeatures include many rounded strongly impregnated typic nodules with a sphericity of 1-2. The colour is mainly black (PPL), dark grey to orange (OIL), and the size is 8-200 $\mu$ m.

#### **5.11.11 M21, sample 8, c.8003.**

This sample is from context 8003 which was interpreted as a buried A/B horizon using field evidence.

The microstructure consists of a weakly developed spongy structure and intergrain microaggregates. The abundance of voids as a percentage of the thin section is common. Coarse organic material includes rare sclerotia. Inorganic residues of biological origin consist of rare phytoliths. These are more abundant in the orange porphyric areas. The fine material is organo-mineral, orange brown to brown (PPL). There are rare black particles measuring 2-50 $\mu$ m randomly distributed. The material is poorly sorted. Related distributions between coarse and fine material include enaulic, gefuric and porphyric. The porphyric areas consist of brighter orange areas where there is greater concentrations of fine material. The c/f ratio is generally 50:50.

Fabric pedofeatures include few loose discontinuous infillings with a moderate referred orientation perpendicular to the surface. The internal material consists of ovoid microaggregates measuring approximately 40 $\mu$ m in varying stages of coalescence. Some areas of the groundmass, with stronger orange colours than other areas, tend towards a porphyric c/f related distribution. Some areas of the groundmass have a compact grain structure, with some coatings, which have the same appearance as glacial till seen elsewhere.

There are rare, orthic halo nodules, black to dark red (PPL), in the central impregnated area fading to orange in the halo, orange red, OIL, 400 $\mu$ m diameter.

Textural pedofeatures include rare amorphous coatings. Orange (PPL), isotropic (XPL) and brown (OIL). These are only found in the orange areas of the groundmass.

#### 5.11.12 Interpretation of M21, samples 7 and 8.

Much of sample 7 consists of a groundmass composed of moderately to strongly coalesced granules. These are probably coalesced excrement pedofeatures formed by faunal activity. These features measured 1.6 - 2mm which is a similar size to the excrement features seen in sample 6. There is no indication of fine or coarse charcoal which suggests little or no manuring of the soil (although see section 9.5). There are only one or two phytoliths present.

In sample 8 there are areas of the groundmass that include orange, moderately coalesced, ultrafine granules which form infillings. It is likely that these are the remnants of roots as seen under M75/4 (section 5.9) and indicate enrichment of iron. The surrounding soil is probably partially gleyed. Textural coatings are also present in the orange areas of the groundmass which indicates translocation of material in decomposing root channels.

There are greater concentrations of biotite in context 8003 than seen in other similar contexts. Initially it was thought that this represented incorporation of material from the underlying glacial till. However there are no fragmented cappings as seen in B horizons elsewhere on the site.

Samples 7 and 8 represent the buried pre-revetment profile. There is no indication of cultivation and the soil appears to

have been able to support faunal activity possibly including earthworms. The morphology of the buried profile is similar to the profiles buried by Post Medieval monuments.

In summary, this chapter has presented the results of the field excavation and the thin section analysis of samples from monuments in group A. Results from a range of archaeological contexts are discussed. The individual contexts are placed into a wider perspective in chapter 9 when the evidence from the entire site is considered.



## Chapter 6

### Results of the excavation and thin section analysis of monuments in group B.

#### 6.1 Introduction

Group B monuments are located in the block 3 (fig. 3.6). The two main soil types in this area are freely draining brown podzols and stagnopodzols. The vegetation is dominantly grass and heather. All the monuments sampled in group B are late prehistoric.

Excavation by AOC (Scotland) Ltd. identified two possible phases of cultivation in the area. The first is associated with ard marks cut into the top of Bs horizons. The ard marks are sometimes found beneath the wall of structures, thus predating them. A later phase of ridge and furrow overlies the earlier arded soils and, in places, overlies the walls of monuments. It was suggested that the ridge and furrow was produced by a later episode of cultivation than that which produced the ard marks. Thin section samples were taken from both types of cultivated soil to enable a comparison of their micromorphological features.

#### 6.2 M648, an EP field boundary.

M648 is an early prehistoric field boundary. Context 7000 and 7005 are organic layers, with very abundant roots, approximately

20cm deep (fig. 6.1 and 6.2). A soil had accumulated (context 7007) against the field boundary (context 7003). There is an undulating boundary between context 7007 and the overlying organic layer indicating ridge and furrow cultivation. The field boundary itself is constructed on top of context 7004, an earlier tilled surface. There are ard marks present in the top of the Bs horizon (context 7001).

Two methods of tillage were suggested based on field evidence. Thin section were taken to try and determine if the two horizons (contexts 7007 and 7004) were produced as a result of different agricultural practises or a continuation of the same technique.

### **6.3 Results from thin section analysis.**

Three samples for thin section analysis were taken from below M648.

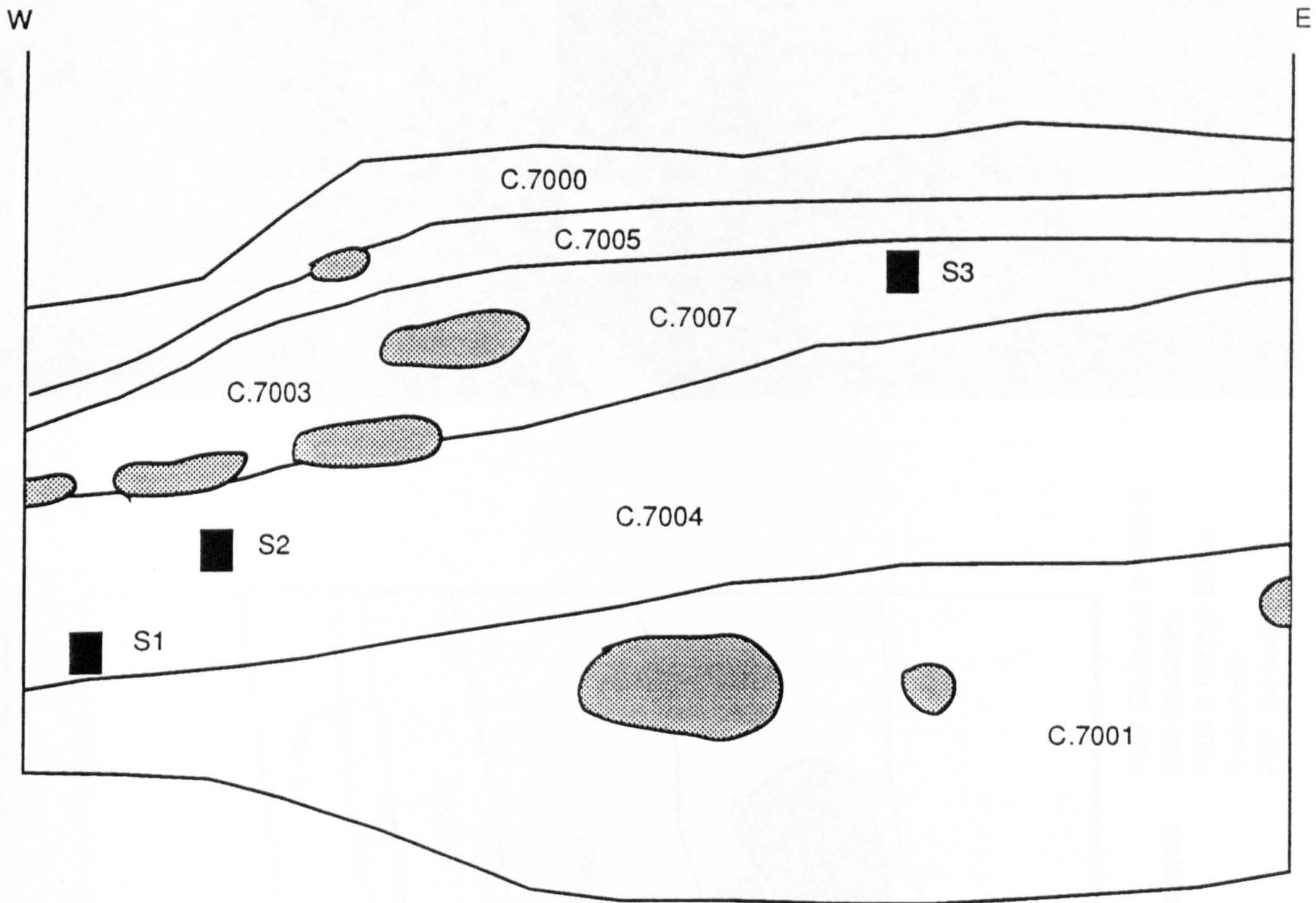
#### **6.3.1 M648, sample 1, c.7004.**

This sample is from the boundary between the buried A horizon (context 7004) and the Bs horizon (context 7001, fig 6.1). In thin section the two contexts appeared similar so they were described as one with any variation emphasised in relevant sections.

The microstructure is intergrain microaggregate. Voids are complex packing voids and channels. Both contexts are composed in part by ultrafine granules although these are more noticeable in the lower context. The abundance of voids as a percentage of the thin section is common.

The basic mineralogy is quartz dominated single mineral grains and metamorphic rock fragments. Coarse organic components include rare charcoal fragments measuring 50 $\mu$ m to 2.5mm in the upper context and only 1 or 2 fragments in the lower context. There are rare remains of roots in channels.

Fig. 6.1 Monument 648, LP field boundary

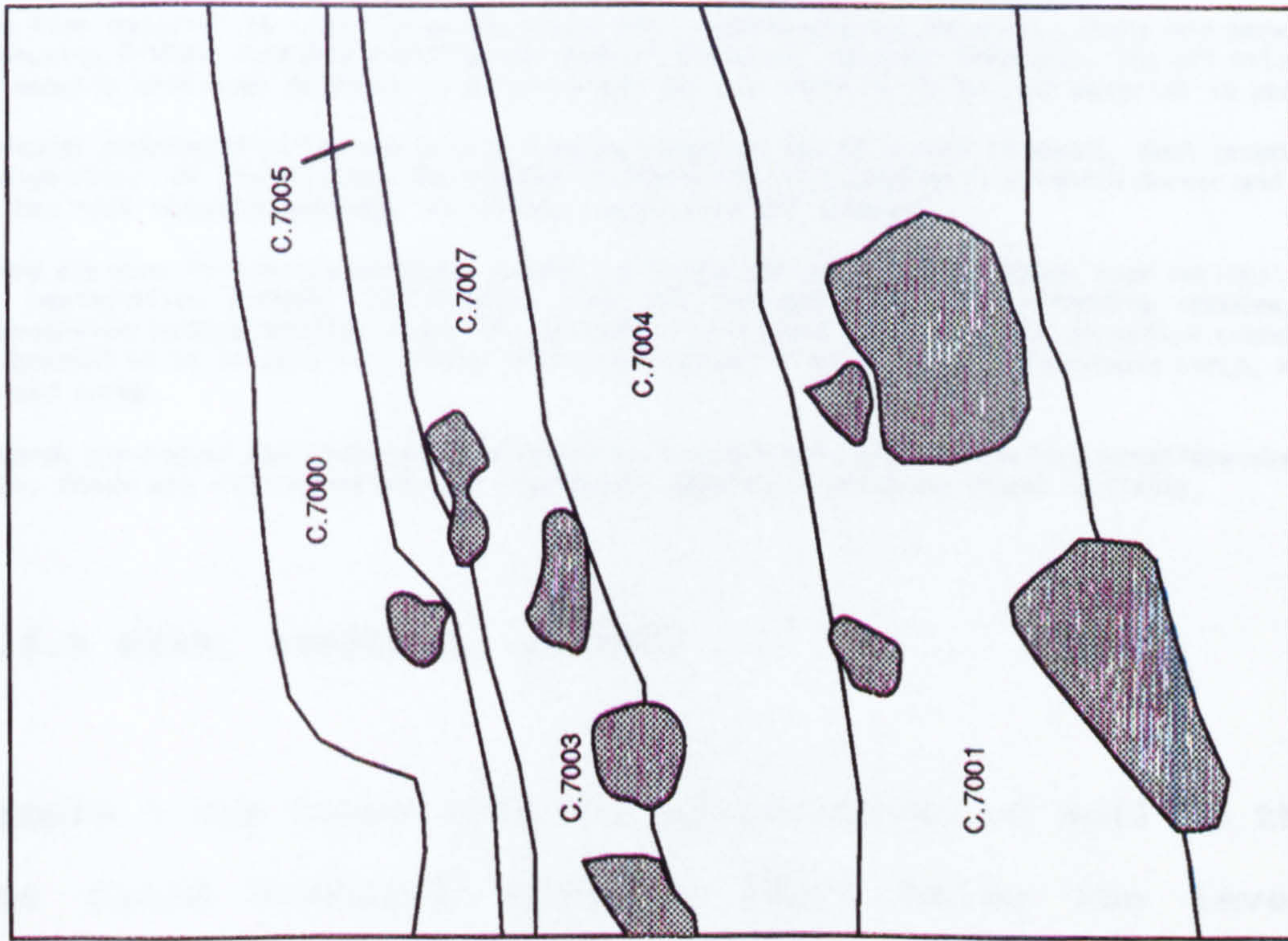


20cm

Contexts :  
 7000 and 7005 Layers of peat  
 7001 Bs horizon  
 7003 Scarp edge of the field boundary  
 7004 A horizon extending below monument  
 7007 Sediment on east of field boundary

○ Large boulders  
 ■ Thin section samples (Kubiena tins)

Fig. 6.2 Monument 648, LP field boundary, south facing section



- Contexts :
- 7000 and 7005 Peaty layers overlying monument
  - 7003 Scarp edge of field boundary
  - 7007 Sediment to east of field boundary
  - 7004 A horizon below monument
  - 7001 Bs horizon
- Large boulders



The fine material is organo-mineral, light brown to brown red (PPL). In the upper context there are occasional black particles measuring 2-50 $\mu$ m, randomly distributed, and in the lower context there are rare black particles measuring 2-50 $\mu$ m, randomly distributed. Inorganic residues of biological origin include rare phytoliths randomly distributed. The material is poorly sorted. The related distribution between the coarse and the fine material is enaulic with some tendency to chitonic. The c/f ratio is 65:35. The colour of the groundmass varies from dark brown to brown at the top of the slide to orange brown at the bottom.

Pedofeatures include many to abundant ferruginous mottles randomly distributed measuring 100 $\mu$ m to 1mm. There is high variability between mottles, some examples having much stronger impregnation and forming nodules. The colours vary from orange red to black (PLL), generally orange to black (OIL). Some of the strongly coloured orange material in old void spaces had anisotropic characteristics. This is generally correlated with darker colours using OIL.

Fabric pedofeatures 400 $\mu$ m wide criss crossing the slide are present particularly in the upper context.

### **6.3.2 M648, sample 2, c.7004.**

This sample is from context 7004. Stratigraphically this is the lower of the cultivated soils and the one associated with arid cultivation.

The microstructure is intergrain microaggregate. The abundance of voids as a percentage of the thin section is common. The basic mineral material includes quartz dominated single mineral grains and metamorphic rock fragments. Coarse organic components comprise occasional to many charcoal fragments measuring 50 $\mu$ m to 1.5mm, randomly distributed, very few remains of roots in channels, rare strongly decomposed organ residues measuring >1mm, randomly distributed. There are rare carbonised residues which might have been burnt peat. Inorganic residues of biological origin include rare fragmented phytoliths and diatoms randomly distributed.

The fine material is light brown to brown (PPL) organo-mineral material. There are many black particles measuring 2-50 $\mu$ m, randomly distributed. Many of these are charcoal fragments. The c/f related distribution is enaulic with some tendency to chitonic and the c/f ratio is 70:30. The material is poorly sorted.

Textural pedofeatures include a silt capping lying on top of a rock fragment, dark brown to black (PPL), orange (OIL). At its thickest the capping is 200 $\mu$ m wide. The capping is slightly darker and more orange next to the rock fragment although no obvious laminations are present.

There are many ferruginous mottles, randomly distributed, measuring 40-800 $\mu$ m, high variability in the degree of impregnation between individuals, some are strongly impregnated forming nodules, others weakly impregnated forming mottles. Some are the result of mineral alteration but in others translocated material is present which is generally orange (PPL), dark brown to black (OIL), anisotropic (XPL), and occurs mainly in old voids.

Towards the top of the slide the fine material is sometimes concentrated into vermiform shapes approx 200 $\mu$ m wide. These are interconnected and fragmented, possibly indicating faunal activity.

### **6.3.3 M648, sample 3, c.7007.**

Sample 3 was taken from the accumulation of soil to the east of the field boundary (context 7007) below the level of the

overlying peat. The slide is homogeneous and described as one context.

The microstructure is complex consisting of vughs and channels. There are some complex packing voids where the material has been disturbed creating fragments. The abundance of voids as a percentage of the thin section is frequent.

The basic mineral material consists of quartz dominated single mineral grains and metamorphic rock fragments. Coarse organic components include many remains of roots in channels with a diameter that varies between 80-800 $\mu$ m. There are occasional charcoal fragments measuring 50-400 $\mu$ m and rare fragments of burnt peat randomly distributed. There is a greater abundance of coarse organic components in this sample than in many of the other slides from early soils. Inorganic residues of biological origin consist of rare phytoliths and diatoms randomly distributed.

The fine material is light brown to very dark brown organo mineral. The lightest material is associated with channels and void infillings. There are occasional black particles measuring 2-50 $\mu$ m randomly distributed. The c/f related distribution is variable consisting of geric and porphyric regions and the c/f ratio is 55:45. The material is moderately to poorly sorted.

Fabric pedofeatures include faint vermiform shaped features, 400 $\mu$ m diameter with a porphyric c/f related distribution. There are loose continuous to loose discontinuous channel infills. The infilling material is composed of light brown, ovoid pellets. These are generally amorphous and isotropic although mineral fragments are also present. These features are probably the result of the biological reworking of roots.

There are many brown to dark red brown (PPL), dull (OIL) ferruginous nodules. These are strongly impregnated and consist of mineral, mainly quartz, and amorphous material. There is rare randomly distributed orange mottling of the groundmass. The mottles are no larger than 80 $\mu$ m.

#### 6.3.4 M648 interpretation of thin section results.

| Sample No | Context                                    | Coarse charcoal    | Black particles <50 $\mu$ m | Phytoliths | Diatoms |
|-----------|--|--------------------|-----------------------------|------------|---------|
| 1         | C.7004 Buried A horizon                    | Rare               | Occasional                  | Yes        | No      |
| 2         | C.7004 Buried A horizon                    | Occasional to many | Many                        | Yes        | Yes     |
| 3         | C.7007 Soil accumulation east of revetment | Occasional         | Occasional                  | Yes        | Yes     |

Table 6.1 Micromorphological features of samples taken from M648

| Sample N <sup>o</sup> | Context  | Dominant c/f related distribution, c/f ratio | Sorting          | Total voids TTS | Microstructure            |
|-----------------------|--|--|------------------|-----------------|---------------------------|
| 1                     | C.7004, Buried A horizon                       | Enaulic, chitonic, 65:35                     | Poor             | Common          | Intergrain microaggregate |
| 2                     | C.7004, Buried A horizon                       | Enaulic to chitonic, 70:30                   | Poor             | Common          | Intergrain microaggregate |
| 3                     | C.7007, soil accumulation to east of revetment | Gefuric to porphyric, 55:45                  | Moderate to poor | frequent        | Vughy and channel.        |

Table 6.2 Comparison of microstructure and c/f ratios from  
M648

The lowest abundance of carbonised residues is in sample 1 at the base of the lower buried A horizon (table 6.1). However even at the point the sample was taken, there are enough residues to suggest homogenisation of the horizon. There is a fragment of silt capping present in sample 2 which indicates mixing of the underlying Bs horizon into the A horizon.

It is not possible to determine if the carbonised residues were the result of in situ burning followed by tillage or of the application of manure followed by tillage. This is discussed in more detail in section (9.5).

There are many to abundant ferruginous nodules and mottles in samples 1 and 2. These are smaller than the fragments of iron pan seen in group A and are not associated with any charcoal. They probably indicate periodic waterlogging of the soil. The coatings in old void spaces are partly anisotropic.

The abundance of fine material is greatest in sample 3 and the material is better sorted. The abundance of finer material results in a reduction in void space and creates a c/f related distribution between geric and porphyric. The microstructure in samples 1 and 2 are intergrain microaggregate and vughy and channel in sample 3. There are many remains of decomposing roots in channels. Sample 3 is slightly better sorted than samples 1 or 2 (table 6.2). It is likely that the greater abundance of fine material in sample 3 is the result of soil movement on sloping ground.

In summary the differences between sample 3 and samples 1 and 2 can be explained in terms of soil movement and pedogenesis rather than techniques of tillage. There are no micromorphological features that indicate these two soils have been formed as the result of different methods of tillage. Two conclusions can be made. Firstly, in the soils sampled, any tillage method produces the same structure so different cultivation methods can not be differentiated. Secondly ard cultivation was occurring simultaneously with the ridge and furrow. Evidence of ridge and furrow is preserved in the top of context 7007 because this was the last method of tillage before the land was abandoned.

#### **6.4 Transect 7000.**

Transect 7000 is a long strip of land that was excavated by AOC (Scotland) Ltd. in 1990. M505 and M648 form field boundaries at either end of the transect. Both M505 and M648 have buried A



horizons preserved beneath them and soils accumulating against them. A thin section sample was taken from the mid point between the two field boundaries. Along most of the transect there is a dark peaty topsoil overlying a mineral A horizon. An iron pan is present within the A horizon. At intermittent points along the transect there are cells of paler material between the A horizon and the underlying Bs horizon.

#### **6.4.1 Transect 7000, result of thin section analysis.**

The sample is from the interface of the A horizon and the underlying Bs horizon. The slide is divided into an upper and a lower context.

In the upper context, the buried A horizon, the groundmass is most dense in the central area of the slide. In this area the microstructure is a-pedal massive. Elsewhere there are few channels and vughs that break up the continuity of the fine material. The abundance of void space as a percentage of this context is few. At the top of the context the percentage of void space is greater and the microstructure tends towards channel and vughy. In the lower context the microstructure is bridged grain. In some places quartz grains are completely surrounded by fine material in other areas the quartz grains are isolated. The abundance of voids as a percentage of this context are common.

The basic mineral material consists of quartz dominated single mineral grains and metamorphic rock fragments. The main type of coarse organic components are roots which have penetrated both contexts. Remains of roots often fill entire channels. The degree of root preservation varies between very good, where the original cellular material is still identifiable and the cell walls still show interference colours, to poor where the material is reworked to form orange amorphous pellets, ovoid approx 40 $\mu$ m. Roots are abundant as a percentage of the slide.

There are also very few bright rings with a diameter of approximately 200 $\mu$ m, rare charcoal fragments measuring 50-800 $\mu$ m randomly distributed, rare humified organic residues, black PPL. In some cases cellular structure containing brown residues are present. The cellular structure is more clearly seen in the larger examples. The smaller fragments tend to be more spherical with a diameter of approximately 200-400 $\mu$ m. The largest example is 2.3mm long and 800 $\mu$ m wide. Inorganic residues of biological origin consist of rare phytoliths randomly distributed.

The fine material is dark brown to black organo-mineral (PPL). Where the decomposing root material is incorporated into the groundmass orange brown amorphous areas are present. These tend to be confined to small 40-80 $\mu$ m irregularly shaped areas. The fine material in the lower context is lighter brown grey than the upper context. There are rare black fragments measuring 2-50 $\mu$ m randomly distributed. The material in the slide is poorly sorted. In the upper context the c/f related distribution is porphyric with a c/f ratio of 45:55. In the lower context the related distribution is chitonic with a c/f ratio of 55:45.

Pedofeatures include a heavily impregnated area of groundmass. This is irregularly shaped and associated with 2 large rock fragments. The impregnation is very strong with black to very dark red colours (PPL), orange red (OIL). The internal fabric is composed of dominant quartz in the size range 40-400 $\mu$ m with 3 fragments of green amphibole. The pedofeature has a sharp boundary and appears fragmented. The morphology is similar to fragments of iron pan seen elsewhere. One other smaller example of this feature is also present.

Textural pedofeatures consist of orange, isotropic coatings of amorphous organic material resulting from the decomposition of roots coating void walls.

Fabric pedofeatures include loose continuous to loose discontinuous infillings derived from the reworking of roots, composed of small ovoid 40 $\mu$ m pellets. These are in various stages of coalescence and are bright orange in colour. Fabric features criss crossing the soil are also present.

#### 6.4.2 Interpretation of transect 7000.

The groundmass of the A horizon has a porphyric c/f related distribution and a dominantly massive microstructure, the abundance of voids are few. There are abundant decomposing roots throughout the slide. Many of the roots have been reworked to form orange pellets measuring approximately 40 $\mu$ m across. The size of the pellets indicates that small organisms were active in the soil, perhaps enchytraeid worms or mites, but not larger organisms like earthworms. There are coatings of amorphous organic material on some of the void walls which appears to be the result of the decomposition of roots. Although there is a high abundance of roots in this context the amount of void space is low. The roots have been reworked to form orange pellets rather than being completely decomposed. There is no evidence to suggest that the rooting has increased the porosity of the soil.

There are rare coarse and fine carbonised remains throughout the A horizon. There may have been greater amounts of carbonised material present in the profile at some time. Faunal activity is indicated by the reworking of roots. There are fragmented nodules in the slide which might have been fragments of iron pan or the result of localised gleying (section 9.4).

There are lenses of pale soil between the A horizon and the Bs horizon at intermittent points along this transect. The genesis

of this material is unclear. It might represent fragments of E horizon that have not been disturbed by cultivation.

#### **6.5 M505, a LP field boundary.**

A trench was dug in an east west direction across a terrace edge. The monument, a LP field boundary (fig. 6.3), is formed by a stone revetment. Immediately overlying the monument is a layer of amorphous organic material 5 to 10cm thick (C.8061). Below this (C.8063) is the matrix supported stone revetment. The matrix is composed of humose material, sandy loam in texture with common medium to large subangular stones. A thin discontinuous iron pan is present approximately 20-25cm below the surface of the monument. Some of the monument has been disturbed by burrows, probably caused by rabbits.

Directly below the monument is a buried A horizon (C.8064) 10-20cm deep. There were abundant fragments of charcoal and fine equidimensional manganese nodules observed in the field. The colour of the horizon is very dark greyish brown (10 YR 3/2). Biological activity is indicated by common very fine fibrous roots. The buried soil to the west of the monument is truncated, possibly as a result of cultivation post dating the construction of the field boundary.

Underlying the buried A horizon is a light brownish grey horizon (10YR 6/2, C.8065). To the west of the monument the colour changes to brown (10YR 4/3). Context 8065 is interpreted as a

buried E horizon. Below the buried E horizon is a buried Bsg horizon (fig. 6.4).

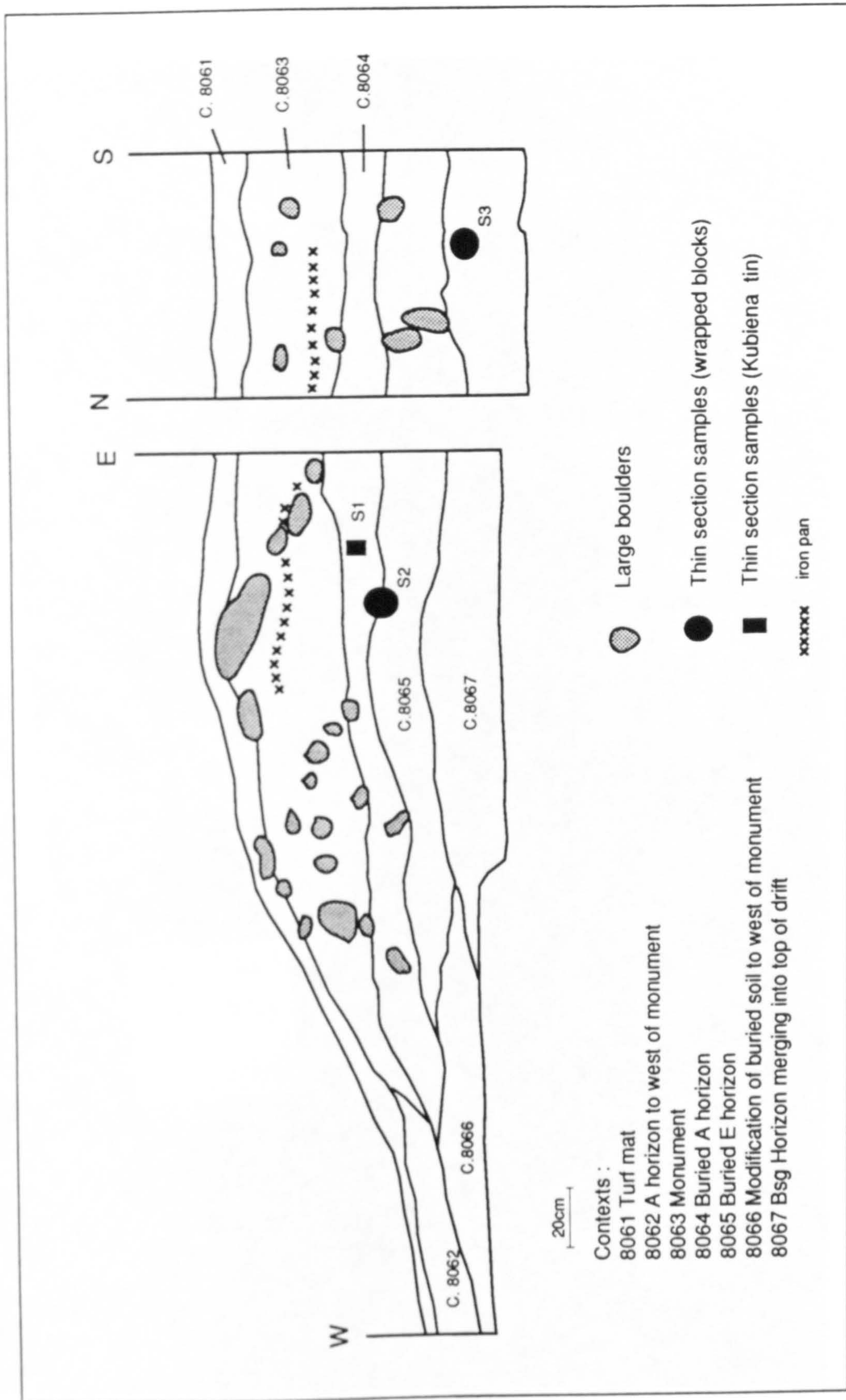


Fig. 6.3 M505, LP field boundary



Fig. 6.4 Buried podzol below M505, an EP field boundary

## 6.6 Results of thin section analysis.

Three samples were taken from M505 for thin section analysis.

### 6.6.1 M505, sample 1, c.8064.

Sample 1 is from context 8064, a LP buried A horizon, poorly sealed by a stone revetment (fig. 6.3) and located on the edge of a break of slope. The slide is homogeneous and described as one context.

The microstructure is complex consisting of intergrain microaggregates with channels. The abundance of voids as a percentage of the thin section is frequent to common.

The basic mineral material is quartz dominated single mineral grains and metamorphic rock fragments. Coarse organic components include occasional charcoal fragments, measuring 200-1000 $\mu$ m and one fragment measuring 2mm. Approximately 70% of the charcoal is part of a nodule (see pedofeatures). There are few remains of roots in channels, their internal cellular structure is still present and some browning of the outer epidermis has occurred. Inorganic residues of biological origin consist of rare fragmented phytoliths randomly distributed.

The fine material is brown grey to grey to dark grey to black (PPL) organo/mineral material. There are occasional to many black (OIL) particles measuring 2-50 $\mu$ m. These are probably charcoal or humified organic matter. The related distribution between the coarse and the fine material is chitonic with some tendency towards enaulic and porphyric. The c/f ratio is 60:40.

Pedofeatures include fragmented ferruginous nodules with a variable shape and measuring between 400 $\mu$ m and 4mm. The internal fabric is composed of strongly impregnated amorphous iron and organic material which is divided into 3 types.

1. Amorphous impregnation of the groundmass, isotropic and high reflectance (OIL).
2. Amorphous material in the old void space, low reflectance, weakly anisotropic.
3. Amorphous material in the old void space, isotropic, low reflectance.

Using PPL all three categories are red to dark brownish red.

The groundmass of the nodules consists of quartz with small fragments of feldspar and mica. Using a c/f limit of 20 $\mu$ m the ratio of coarse to fine material is 50:50. The nature of the fine fraction is obscured by the impregnating material. Large fragments, in some cases up to 2mm, of charcoal are frequently incorporated into the fabric of the nodules. The abundance of nodules is approximately 10% of the thin section area.

There is high variability in the colour of the nodules. Sometimes the amorphous material has much lighter yellow colours (PPL). An anisotropic layer approximately 8 $\mu$ m thick is sometimes associated with this material. The exact relationship of this layer to the amorphous material is unclear. Sometimes the material closest to the groundmass is anisotropic, other times the material bordering the void is anisotropic, laminations are occasionally present. The material in the old void space is darker and less reflective than the material in the surrounding groundmass.

Fabric pedofeatures include abundant loose discontinuous infillings associated with channels. These are composed of ovoid to irregularly shaped, strongly coalesced aggregates measuring 40 $\mu$ m which are a lighter brown material than the surrounding fabric.

Textural pedofeatures include a fragmented silt capping in which four layers are identified.

1. Coarse material 60-200 $\mu$ m embedded in a groundmass heavily impregnated with amorphous Fe.
2. Similar to layer 1 except the coarse mineral fraction is much finer, < 60 $\mu$ m.
3. Narrow band of amorphous translocated material.
4. Groundmass with a weaker impregnation of Fe than the rest of the pedofeature possibly resulting from impregnation from band 3. The underlying rock fragment shows some weathering in places.

#### **6.6.2 M505, sample 2, c.8064 and c.8065.**

This sample is from the interface of the buried A and the buried E horizon. The thin section is divided into 2 layers, the upper buried soil and the lower E horizon. Refer to the description of M505 sample 1 for a description of the upper layer. The boundary between the two layers is very sharp, approximately 200-400 $\mu$ m in width.

The microstructure is compact grain. The abundance of voids as a percentage of the thin section is frequent. The basic mineral material is quartz dominated single mineral grains and metamorphic rock fragments. There are no coarse organic components. Inorganic residues of biological origin include rare phytoliths randomly distributed. The fine material is mineral, composed of small fragments of the larger minerals present. The related distribution between the coarse and the fine material is Gefuric with local tendency to chitonic. The material is moderately sorted.

Pedofeatures include rare mottles which consist of iron/organic coatings within a poorly impregnated groundmass. These have low reflectance using OIL, yellow brown PPL, weakly anisotropic, size 3mm.

Few fragmented nodules measuring 1-2mm, similar to the mottles but a stronger impregnation of the groundmass is present. There are darker red colours (PPL) present in the fragmented nodules than in the mottles. The darker material is almost black using OIL.

#### **6.6.3 M505, sample 3, c.8067.**

This sample is taken from approximately 25cm below the old ground surface at the top of the Bsg horizon. There are many lenses of material associated with the translocation of amorphous iron compounds and silt sized material throughout the slide. The slide is described as one context but internal variation was enhanced using image analysis (section 2.29).



The microstructure is pellicular grain and compact grain. The abundance of simple packing voids is common and planar voids is few. The basic mineral material is dominated by quartz single mineral grains and quartz dominated metamorphic rock fragments. There is no coarse organic material present and the fine fraction is composed of mineral material.

Variation in the groundmass is illustrated in fig. 2.39. The green areas of the image indicate regions where the material is poorly sorted, c/f limit 50 $\mu$ m, c/f ratio 60:40 and had an enaulic c/f related distribution. The red areas have a chitonic c/f related distribution. The overall c/f ratio is 80:20. The material is moderately to poorly sorted.

Textural pedofeatures include silt cappings of varying size but approximately 4mm x 2mm. In the lower half of the slide they are moderately orientated parallel to the surface. Their internal composition shows some lamination.

Layer 1 is silt sized, bright orange red (OIL) and always found next to the surface the capping formed on. This layer is present in approximately one quarter of the cappings seen.

Layer 2 is composed of coarser material, still in the silt size range, but a greater proportion measures 40-50 $\mu$ m. Using OIL colours are an orange yellow. This layer is only well expressed in two of the silt cappings present.

Layer 3 sometimes overlies layer 1, sometimes layer 2 or sometimes forms the first layer.

Certain areas of the slide have an abundance of link cappings. These corresponded to the darker and redder areas in fig 2.39. The reflectance of the link cappings varies throughout the slide. They are brightest where they are disrupted. There is not any obvious lamination in the link cappings. The internal fabric closely corresponds to the last phase of the capping (ie silt sized material and orange yellow colours using OIL).

A dominant feature of this slide is the abundance of amorphous ferruginous coatings. The distribution of the material varied but is mostly concentrated in the red areas (fig 2.39). Coatings are few to frequent as a percentage of the thin section slide, and surround mineral grains and aggregates.

The coatings could be divided into 3 categories;

- a. Brown orange (PPL), yellow orange (OIL), isotropic.
- b. Amorphous brown material (PPL), dark brown under (OIL), weakly anisotropic.
- c. Orange (PPL), yellow brown to dark brown (OIL), isotropic.

Coating type a is much more abundant than type b. The coatings, especially type a, frequently coated the upper surfaces of both sorts of cappings. Sometimes the coatings travelled through the capping following voids.

An almost continuous band of translocated amorphous material is present running along one of the planer voids approximately 3/4 of the way down the slide. This is orientated approximately 30° to the surface. Colours are orange (PPL) and yellow brown to dark brown (OIL).

#### 6.6.4 Interpretation of M505.

A characteristic feature of the buried A horizon is the abundance of carbonised residues. There are occasional coarse charcoal fragments and occasional to many fine black particles. The carbonised residues are present throughout the context indicating homogenisation of the horizon. The source of the carbonised residues is unclear but might have included burning of surface vegetation followed by mixing of the profile or deliberate

manuring of the soil. There is a fragmented silt capping present in this context indicating mixing and incorporation of material derived from the B horizon. Biological activity is indicated by the abundant infillings of channels. All the excrements measure approximately  $40\mu\text{m}$  and there is no indications of larger faunal activity, for example earthworms.

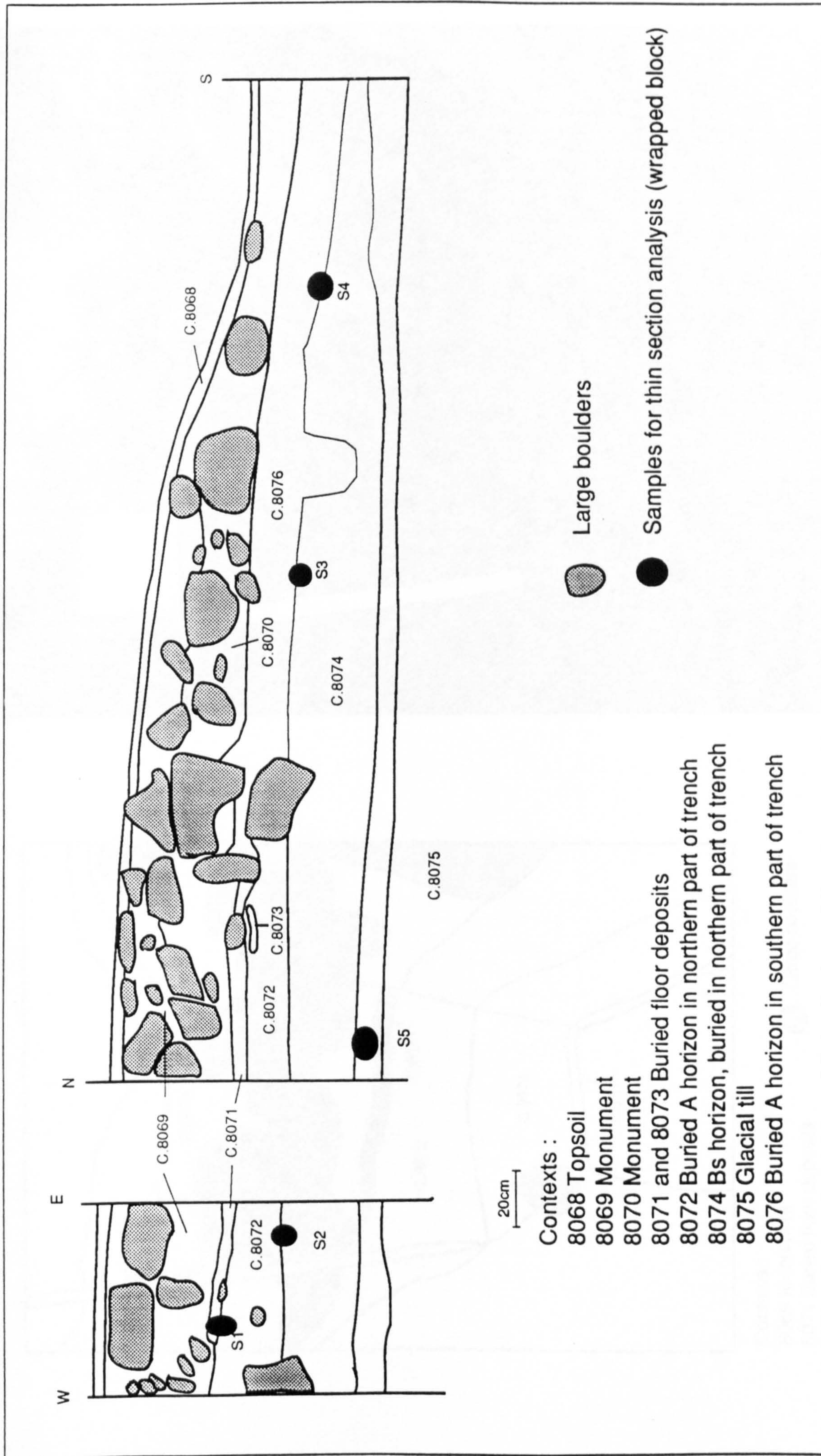
There are many fragmented ferruginous nodules throughout the buried A horizon. These have the same appearance as fragmented nodules seen elsewhere (M64, M86). Some of the ferruginous material which forms the nodules is weakly anisotropic (section 9.4). There are also ferruginous nodules present in the buried E horizon (context 8065). These have a similar morphology to the ones in the buried A horizon. There are no coarse or fine carbonised residues present in the E horizon. There are rare phytoliths, randomly distributed, and the material is moderately sorted.

Context 8067 is interpreted as a Bsg horizon on the basis of colours observed in the field (fig 6.4). The micromorphology of this B horizon is quite different to those under M127, M975, M1069, M62 and M504. In the lower half of the slide there is an abundance of undisturbed silt cappings. These are at a depth of 35 to 40cm below the top of the buried A horizon and mark the top of the glacial till. In the top half of the slide disturbed link cappings and silt cappings are present.

Translocated ferruginous material is present in the form of coatings throughout the slide forming a pellicular grain structure in some areas. The development of the profile buried below M505 is discussed in section 9.3.

#### **6.7 M504, a LP (Iron Age) hut circle.**

M504 is situated at the south western end of transect 7000. The vegetation immediately around the monument consists of mainly heather with some grass. Directly below a layer of thin humose topsoil (C.8068) is the wall of the hut circle which comprises abundant large to very large subangular to subrounded stones. The greatest concentration of stones, located at the northern end of the trench, are located directly above a black (10YR 2/1) layer of material (C.8071), interpreted as floor deposits (figs. 6.5 and 6.6). Minimal disturbance is indicated by few very fine fibrous roots. The stones at the southern end of the trench are thought to represent tumble from the main wall of the hut circle. Directly below context 8071 is a brown (10YR 3/3) buried A horizon 20-24cm thick (context 8072). This is non humose, apedal massive with few small to large stones. The presence of few very fine fibrous roots indicates minimal disturbance by roots. To the south of two large vertical stones the colour of the buried A horizon is dark brown (10YR 3/3, context 8076). There are many very fine fibrous roots, which is greater than in context 8072, which suggests the context is not as well sealed and pedogenesis should have continued to a greater extent in the southern area of the trench than in the northern.

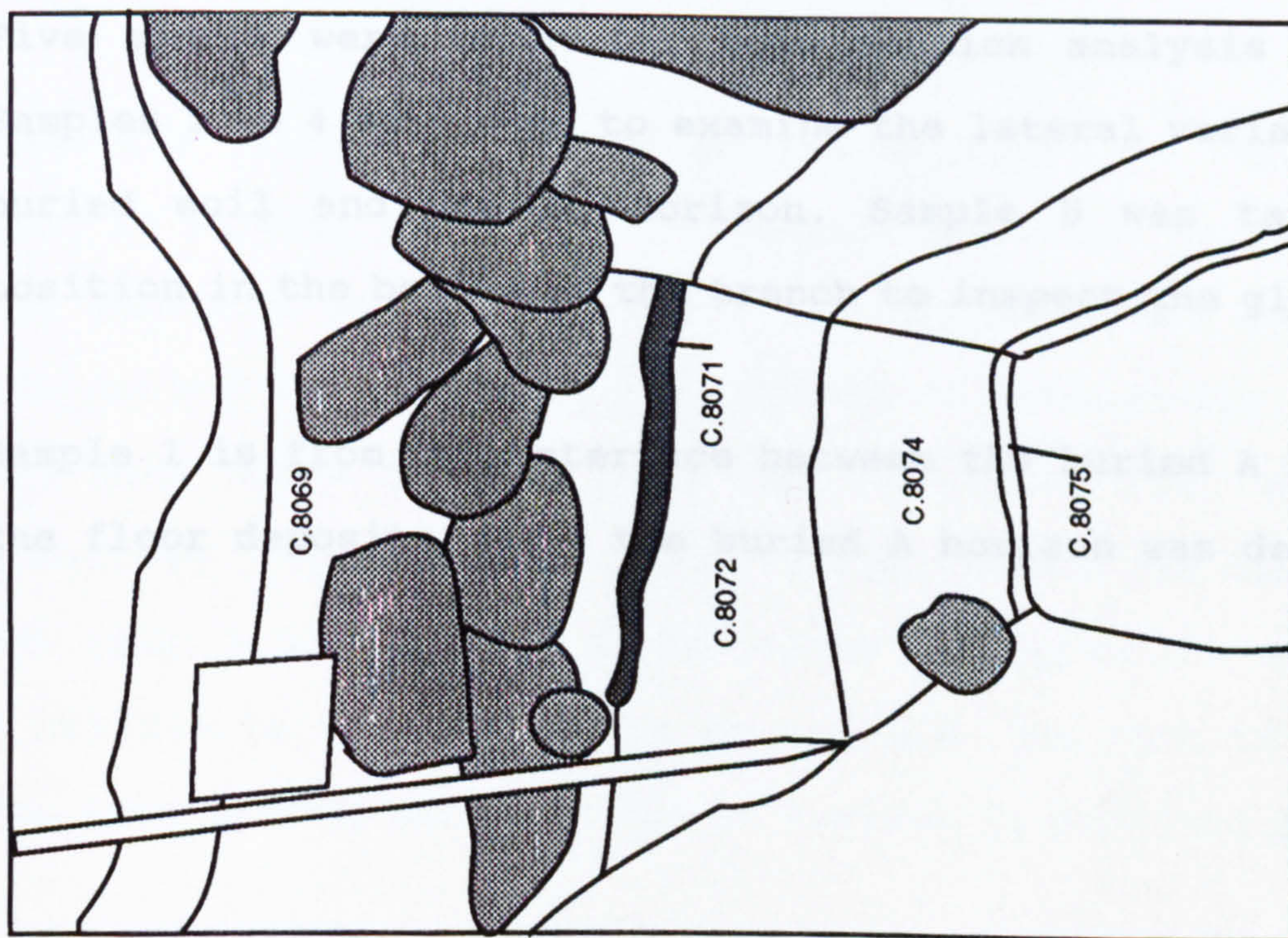


Contexts :

- 8068 Topsoil
- 8069 Monument
- 8070 Monument
- 8071 and 8073 Buried floor deposits
- 8072 Buried A horizon in northern part of trench
- 8074 Bs horizon, buried in northern part of trench
- 8075 Glacial till
- 8076 Buried A horizon in southern part of trench

Fig. 6.5 M504, LP Hut circle

Fig. 6.6 M504, LP hut circle



- Contexts :
- 8069 Monument
  - 8071 Buried floor deposits
  - 8072 Buried A horizon
  - 8074 Buried Bs horizon
  - 8075 Glacial till
- Large boulders



Underlying the buried A horizon is a buried Bs horizon. The Bs horizon is at least 30 to 40cm thick in the northern part of the trench. The buried profile is interpreted as a brown podzol truncated to the south of the monument by later episodes of cultivation. In the top of the Bs horizon there are shallow ardmarks orientated in a north west to south east direction. These are present inside and outside of the structure and therefore predate it. The buried A horizon is thought to represent an example of an early cultivated soil which did not show any evidence of later ridge and furrow cultivation. There are layers of orange and brown sandy loam sediment in the Bs horizon (context 8074) which are thought to indicate disturbance of the profile, possibly by cultivation given the presence of ardmarks in the area.

#### **6.7.1 M504, results of thin section analysis.**

Five samples were taken for thin section analysis (fig 6.5). Samples 1 to 4 were used to examine the lateral variation in the buried soil and the Bs horizon. Sample 5 was taken from a position in the bottom of the trench to inspect the glacial till.

Sample 1 is from the interface between the buried A horizon and the floor deposits. Only the buried A horizon was described.

### **6.7.2 Summary thin section description, M504, sample 1, c.8071 and c.8072.**

The microstructure is channel and bridged grain. The abundance of voids as a percentage of the thin section is frequent. Basic minerals include quartz dominated single mineral grains and metamorphic rock fragments. Coarse organic material includes rare remains of roots in channels, rare fragments of charcoal, randomly distributed and oval organic remains, 80 $\mu$ m long axis, dark to reddish brown PPL, outer epidermis, no internal structure, nipple at one end.

The fine material is brown (PPL) organo-mineral. There are rare black particles randomly distributed. There is a variable c/f related distribution including chitonic and porphyric material. The c/f ratio is 60:40.

Textural Pedofeatures includes one fragmented silt capping, 100 $\mu$ m wide, strongly impregnated with ferruginous material.

There are rare weakly impregnated mottles measuring 40-200 $\mu$ m randomly distributed, orange brown OIL, orange brown PPL.

Fabric pedofeatures includes an area measuring 2mm x 4mm, fine material is very dark brown to black PPL, orientated 45<sup>o</sup> to surface. A channel shape vertically orientated pedofeature is also present at intermittent intervals. This is interpreted as material being incorporated from the overlying context by biological activity.

### **6.7.3 Summary thin section description M504 sample 2, c.8072 and c.8074.**

Sample 2 was taken from a depth of approximately 20cm below the old ground surface at the interface of the buried A and the buried Bs horizon.

When the slide is observed macroscopically, on top of a light box, it is very difficult to identify any areas corresponding to the contexts recorded in the field. An image was captured from the entire slide to identify regions of homogeneity. Red, green and blue bands of data were captured using PTL, and contrast stretched (fig. 6.7). The best differentiation was obtained using HES (fig. 6.8). The area of the slide corresponding to the buried A horizon is much darker in colour than the rest of the slide. The area corresponding to the Bs horizon is depicted by red brown

colours. Two layers were identified on the basis of the image analysis results.



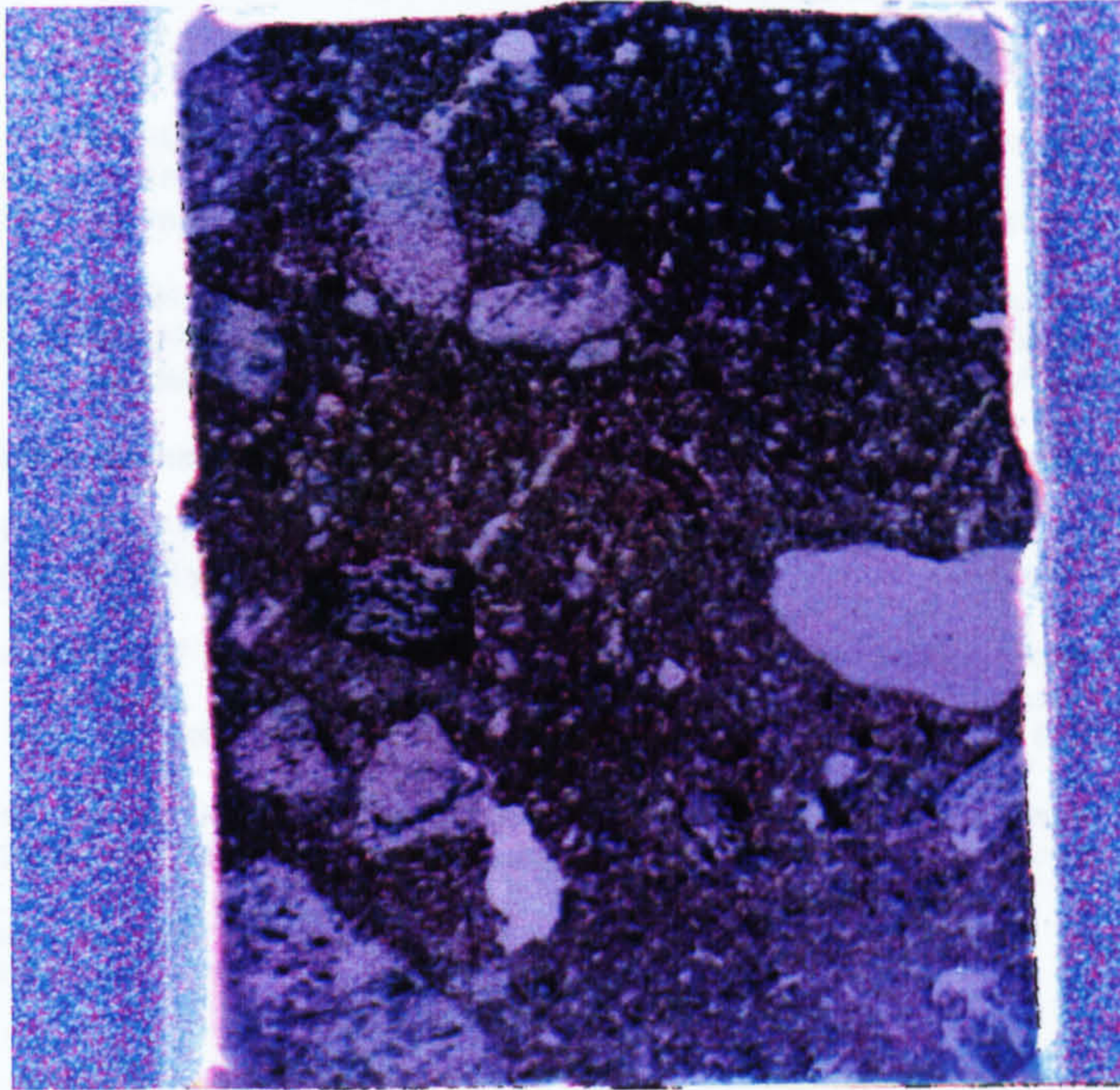


Fig. 6.7 M504, S2, ACS, red 48-88, green 52-108, blue 81-109

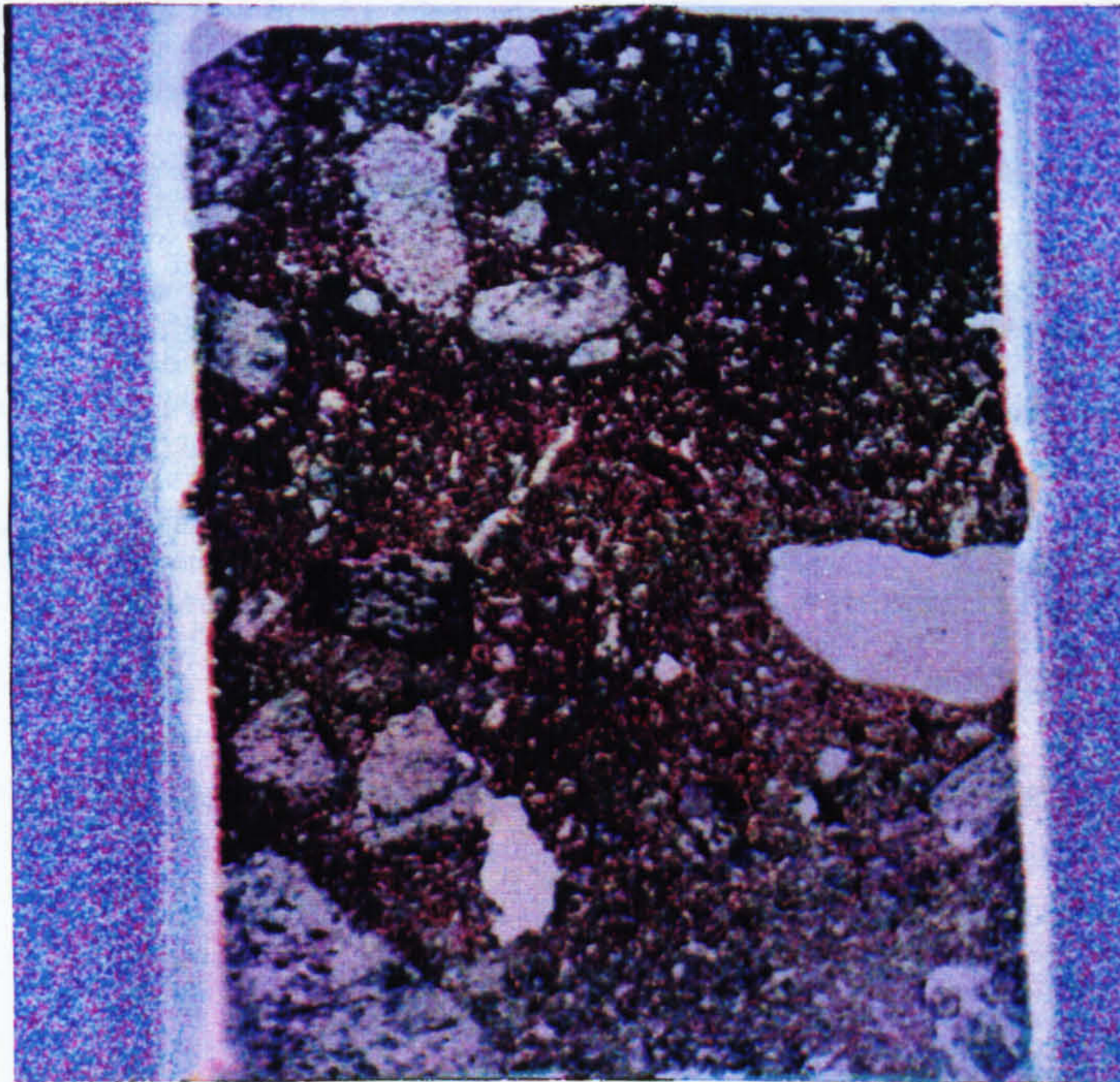


Fig. 6.8 M504, S2, HES

#### **6.7.4 Description for context 8072, buried A horizon.**

The microstructure is complex consisting of bridged grain with limited areas of intergrain microaggregate, channels are also present. The abundance of voids as a percentage of the thin section is common. Basic mineral material consists of quartz dominated single mineral grains and metamorphic rock fragments.

Coarse organic material includes rare charcoal fragments, randomly distributed and rare remains of roots. Inorganic residues of biological origin consist of rare fragmented phytoliths which are randomly distributed. There is one unidentified feature which might be a fragment of bone.

The fine material is light brown, organo mineral. There are rare black particles randomly distributed.

The dominant c/f related distribution is chitonic with localised porphyric. The c/f ratio is 60:40. The material is moderately to poorly sorted.

Textural pedofeatures consist of rare fragmented silt cappings. Some laminations are visible caused by bands of coarser and finer material. There had been some impregnation by ferruginous compounds. Only small examples, 300 $\mu$ m thick and 1mm long, of silt cappings are preserved in this horizon.

There are rare nodules measuring 20-200 $\mu$ m randomly distributed, red orange (PPL), orange red (OIL), isotropic. Sometimes these are typic but some examples include mineral material.

Excrement pedofeatures include rare strongly coalesced, ovoid, organo- mineral features measuring approximately 400 $\mu$ m diameter.

#### **6.7.5 Description for context 8074, buried Bs horizon.**

The microstructure is dominantly intergrain microaggregate and localised channel. Many of the microaggregates consist of irregularly shaped ultrafine granules. The abundance of voids as a percentage of the thin section is common. Many of the mineral grains are coated with fine material. A fragmented capping is located on top of a rock fragment below the rock fragment is an area of single grain structure.

Coarse organic material includes one bright ring, diameter 200 $\mu$ m, one organic residue, measures 80 $\mu$ m across, spherical, possibly part of a sclerotium. One or two fragments of charcoal are present which measure approximately 200 $\mu$ m and are randomly distributed.

The fine material is orange brown (PPL) organo mineral. The related distribution between the coarse and the fine material is enaulic and chitonic. The c/f ratio is 60:40.

Textural pedofeatures consist of many fragmented silt cappings on the surface of rock fragments. The best preserved cappings have laminations of coarse and fine material. Some of the cappings have layers coloured with ferruginous material closest to the rock fragment and uncoloured layers at the top. Some of the cappings have weakly anisotropic coatings covering fragmented surfaces. These coatings are orange (PPL), 16-20 $\mu$ m thick, in places they had penetrated the cappings along voids.

There are two strongly impregnated nodules, dark red brown to black (PPL), dark brown to black (OIL), isotropic, prominent, sharp boundary. The fabric is composed dominantly of quartz and some green amphibole single mineral grains. One example measures 1mm equidimensional the other 200 $\mu$ m equidimensional.

#### **6.7.6 Summary thin section description M504 sample 3, c.8076 and c.8074.**

This sample was taken to examine the lateral variability in the buried A horizon and the Bs horizon (fig 6.5). The slide consists

of two layers. The upper layer corresponds to context 8076 and the lower to context 8074.

### **6.7.7 Description of context 8076, buried A horizon.**

The microstructure is complex including intergrain microaggregate with localised channel and bridged grain. The abundance of voids as a percentage of this context is frequent to common.

The basic mineral material consists of quartz dominated single mineral grains and metamorphic rock fragments. Coarse organic material includes rare charcoal fragments which measure 300-500 $\mu\text{m}$  although 3 fragments are in the size range 800-1400 $\mu\text{m}$ . There is rare fungal material, possibly sclerotium, and rare remains of roots in channels. Inorganic residues of biological origin includes rare fragmented phytoliths which are randomly distributed.

The fine material is yellowish brown (PPL), and brownish yellow (OIL), organo mineral. There are rare black particles measuring 2-50 $\mu\text{m}$  randomly distributed. These probably include charcoal.

The related distribution between the coarse and the fine material is dominantly chitonic and the c/f ratio is 55:45. The material is poorly sorted.

There is one fabric pedofeature which is equidimensional, abrupt boundary and measures 1600 x 1600 $\mu\text{m}$ . Using a c/f limit of 20 $\mu\text{m}$  the c/f ratio is 50:50. The coarse material comprises quartz, green amphibole and biotite. The fine material is orange yellow (PPL) organo-mineral. This is interpreted as a fragment of Bs horizon.

There are rare few to frequent loose discontinuous infillings composed of weakly to moderately coalesced ultrafine granules. These are ovoid to irregularly shaped, 16-40 $\mu\text{m}$ , strong brown (PPL), clustered in channels. Much of the fine material might be composed of these coalesced granules.

There are rare randomly distributed typic reddish yellow (OIL) ferruginous nodules, 200-1200 $\mu\text{m}$ , equidimensional with sharp boundaries and pure impregnation.

In an area associated with fragmented ferruginous material there are rare typic aggregated nodules. These are dark reddish brown (OIL), yellow red to dark reddish brown (PPL) and randomly distributed.

Excrement pedofeatures includes rare strongly coalesced, ovoid, organo-mineral material measuring 400-500 $\mu\text{m}$ .

### **6.7.8 Description of context 8074, buried Bs horizon.**

The microstructure is complex which consists of dominantly channel structure with localised bridged grain. The abundance of voids as a percentage of the thin section slide is frequent. There are some areas, very rare, which are almost single grain microstructure.

Coarse mineral material includes quartz dominated single mineral grains and metamorphic rock fragments. Coarse organic components comprise very few remains of roots in channels and one group of cells, 100x200 $\mu\text{m}$ . These cells are encased by very dark red (PPL), black (OIL), amorphous material. This is possibly the remnant of a sclerotium.

The fine material is organo-mineral, orange yellow (PPL), reddish yellow (OIL). The related distribution, between the fine and the coarse material, is dominantly chitonic with localised enaulic. The material is poorly sorted.

Fabric pedofeatures include an elongated area almost vertically orientated. This is channel shaped, 1mm wide and impregnated by orange yellow (PPL), orange (OIL), isotropic, translocated ferruginous material. The internal composition is the same as the surrounding groundmass and consists of rare, 40-80 $\mu\text{m}$ , strongly coalesced equidimensional pellets with a sharp boundary. This feature is interpreted as part of a fragmented indurated B horizon.

Textural pedofeatures comprise very few disturbed fragmented silt cappings with no layering present.

There is one orange (PPL), orange (OIL) mottle present. This is irregularly shaped and measures approximately 400 $\mu$ m. The mottle appears to be composed of the same material as the larger fabric pedofeature described above.

#### **6.7.9 Summary thin section description M504 sample 4, c.8076 and c.8074.**

Separate descriptions are to be given for two layers, firstly the upper A horizon and secondly the lower contexts. The lower contexts are treated as one although they are composed of many lenses of material with different mineral assemblages.

#### **Description of context 8076, A horizon.**

The microstructure is dominantly channel with some localised tendency to bridged grain, particularly with depth. The abundance of voids as a percentage of this context is frequent.

Coarse minerals include quartz dominated single mineral grains and metamorphic rock fragments. Coarse organic components comprise occasional fragments of charcoal, 50 $\mu$ m to 2mm, which are randomly distributed. There are also rare remains of roots. Inorganic residues of biological origin consist of rare phytoliths randomly distributed.

The fine material is brown (PPL) organo mineral. There are rare black particles, 2-50 $\mu$ m, which are randomly distributed. The related distribution between the coarse and the fine material has a chitonic to porphyric c/f related distribution and a c/f ratio of 50:50.

There are rare, moderately to strongly coalesced, ovoid, organo mineral excrements, measuring 300 $\mu$ m to 1.2mm. Amorphous and cryptocrystalline pedofeatures include rare mottles, orange brown (OIL), brown orange (PPL). One example measures 1mm across otherwise they measure approximately 200 $\mu$ m.

#### **Description of context 8074, interface of Bs horizon and top of glacial till.**

This consists of complex lenses of material composed dominantly of mineral material. The microstructure is compact grain. The main type of mineral is quartz with banded layers of biotite also present. The elongated biotite fragments are strongly orientated parallel to the surface. Orange fine material is present in the lower part of the layer, the abundance is rare.

#### **6.7.10 Summary thin section description M504 sample 5, c.8076.**

This sample was taken at the interface of the Bs horizon and the glacial till at a depth approximately 45cm below the old ground surface.

The slide is divided into two contexts, above and below a layer of translocated ferruginous material.

#### **Description of the base of the Bs horizon, c.8074.**

The microstructure includes channel with areas of bridged grain. In some areas there are greater concentrations of fine material where there is a tendency to a massive structure. The abundance of voids as a percentage of this context is frequent.

Coarse minerals include quartz dominated single mineral grains and metamorphic rock fragments. Coarse organic components includes one fungal body, possibly sclerotia, located in the top part of the slide, that had split in half. There are also rare roots in channels and one bright ring with a diameter of 200 $\mu$ m.

The fine material is grey (PPL) and generally composed of mineral material. Towards the top of the layer there is orange amorphous isotropic material incorporated into the groundmass. This corresponds to the base of the Bs horizon. Some organo mineral material is also present at this point. The related distribution between the coarse and the fine material includes enaulic and porphyric. At the base of the Bs horizon there is only an enaulic c/f related distribution. The c/f ratio is 60:40. The material is moderately sorted.

Textural pedofeatures consist of amorphous, isotropic, orange (PPL), dark grey (OIL), material which is incorporated into the groundmass. This is most abundant at the top of the slide.

In the lower part of the upper context there are common link cappings which are weakly disturbed, possibly by roots.

There are frequent cappings on stones showing the dark grey colours that correspond to layer 1 (see description of lower context). The other layers are not distinct. Using OIL the grey layer varies between orange (possibly because of the alteration of the underlying rock) and white.

#### **Description of the top of the glacial till material, c.8075.**

The characteristic feature of this layer is the abundant undisturbed silt cappings and link cappings. In some areas large rock fragments have protected the groundmass below them from any silty inwash, thus preserving a single grain structure.

The microstructure is variable depending on the amount of fine material. Where there is the greatest concentrations of silt and link cappings there is a tendency towards a vesicular or massive structure. In areas protected from a finer input of material, the structure is single grain. The abundance of voids as a percentage of this context is few to frequent.

Coarse minerals are dominated by quartz single mineral grains and metamorphic rock fragments. There is no coarse organic material present. The fine material is grey (PPL) and consists of mineral material. Close to the boundary with the upper context the fine material is coloured orange by translocated ferruginous material. The related distribution between the fine and the coarse material is very variable. In some areas the groundmass is very dense, porphyric c/f related distribution, in other areas enaulic is present. In some areas movement of ferruginous material, into areas with single grain structure, has created coatings and a chitonic c/f related distribution. The material is unsorted.

Textural pedofeatures consist of common to dominant silt cappings and link cappings. In areas laminations within the fine material is present forming continuous undisturbed link cappings. There is moderate tendency for the silt and link cappings to form on the upper right hand side of fragments (The sample may have been rotated slightly during preparation).

In some link cappings a sequence of laminations are present.

1. A band of fine material, c/f limit 20 $\mu$ m, c/f ratio 5:95. Very dark grey to black under (PPL). This layer often forms the first layer on rock fragments.
2. Finer brown grey material (PPL), c/f limit 20 $\mu$ m, c/f ratio 10:90.
3. A band of coarser material, grey brown, slightly brown red in some areas, more orange, using OIL, than the underlying area, c/f limit 20 $\mu$ m, c/f ratio 65:35. The largest quartz grain measures 200 $\mu$ m across.
4. Fine brown grey material (PPL), dominantly smaller than 9 $\mu$ m. Very few quartz grains measuring up to 40 $\mu$ m are present, c/f limit 20 $\mu$ m, c/f ratio 5:95.

In an area close to the layer of translocated ferruginous material, cappings are coloured by the translocated material. Using PPL they are brown to red brown. Using OIL the colours vary from orange to strong orange (see textural pedofeature - coatings).

Approximately 3 to 4.5cm below the top of the slide there is a layer with dominant ferruginous coatings. These coatings line and sometimes fill void spaces. The colours vary from light orange to dark orange (PPL), orange to dark strong orange (OIL). Where the coatings have impregnated the groundmass, the colours are lighter away from the source area.

The coatings lining voids are isotropic and vary in thickness between 40-180 $\mu$ m. Laminations are present which consist of lighter orange layers (PPL) and darker orange layers (OIL). The majority of the coatings (see exception below) are confined to an area 4mm wide running at angle of about 140° across half the slide.

Below some large rock fragments, where the groundmass is protected from translocated fine material, amorphous ferruginous coatings are present surrounding mineral grains. These coatings are approximately 20 $\mu$ m thick, weak orange to orange (PPL), dark orange (OIL).

Fabric pedofeatures consist of very few loose discontinuous infillings in some of the larger voids. They appear to be parts of amorphous coatings forming small ovoid pellets measuring 40 $\mu$ m across. They are only seen in areas with amorphous coatings. These are darker orange (OIL) than the surrounding coatings.

### 6.7.11 Interpretation of M504.

Sample 1 was taken at the interface of the old ground surface and the overlying floor deposits. Sample 2 was taken almost directly below sample 1 at a depth of approximately 20-25cm at the interface of the buried A and Bs horizons. One fragmented silt capping is present at the surface of the buried A horizon but lower in the context the abundance increases to rare. These

fragmented remains of cappings indicate mixing of different horizons. A greater abundance of fragmented cappings are present in the Bs horizon while undisturbed examples are present in the glacial till at a depth of approximately 45cm below the old ground surface.

The greatest abundance of coarse charcoal fragments occurs where the buried A horizon is sealed by tumble from the hut circle wall (Table 6.3). There is no significant lateral variation in the distribution of fine black particles.

| Sample No | Context                        | Coarse charcoal      | Black particles <50µm | Phytoliths | Diatoms |
|-----------|--------------------------------|----------------------|-----------------------|------------|---------|
| 1         | 8072, buried A horizon.        | Rare                 | Rare                  | No         | No      |
| 2         | 8072, buried A horizon.        | Rare                 | Rare                  | Yes        | No      |
|           | 8074, buried Bs horizon        | One or two fragments | No                    | No         | No      |
| 3         | 8076, buried A horizon         | Rare                 | Rare                  | Yes        | No      |
|           | 8074, buried Bs horizon        | No                   | No                    | No         | No      |
| 4         | 8076, buried A horizon         | Occasional           | Rare                  | Yes        | No      |
| 5         | 8074, base of Bs horizon       | No                   | No                    | No         | No      |
|           | 8075, undisturbed glacial till | No                   | No                    | No         | No      |

Table 6.3 Micromorphological features of samples taken from M504

At the surface of the Bs horizon the morphology is friable (section 9.3) and is composed of polymorphic organic matter. At the base of the Bs horizon the morphology changes to monomorphic

with some cementation occurring. The type and formation of Bs horizons is discussed in greater detail in section 9.3.

There was not any significant variation in the c/f related distribution along different points of the buried A horizon although there is a slight increase in the fine fraction where the soil is not as well buried (Table 6.4).

| Sample No | Context                   | Dominant c/f related distribution, c/f ratio | Sorting          | Total voids TTS    | Microstructure   |
|-----------|---------------------------|--|------------------|--------------------|--|
| 1         | 8074, buried A horizon    | Chitonic and porphyric, 60:40                |                  | Frequent           | Channel and bridged grain                                      |
| 2         | 8072, buried A horizon    | chitonic, localised porphyric, 60:40         | Moderate to poor | Common             | Bridged grain localised intergrain microaggregate              |
|           | 8074, buried Bs horizon   | Enaulic and chitonic, 60:40                  | -                | Common             | Intergrain microaggregate, localised channel                   |
| 3         | 8076, buried A horizon    | Chitonic, 55:45                              | Poor             | Frequent to common | Intergrain microaggregate, localised bridged grain and channel |
|           | 8074, buried Bs horizon   | Chitonic, localised enaulic, 50:50           | Poor             | Frequent           | Channel, localised bridged grain                               |
| 4         | 8076, buried A horizon    | Chitonic and porphyric, 50:50                | -                | Frequent           | Channel, localised bridged grain                               |
| 5         | 8074, base of Bs horizon  | Enaulic, localised porphyric, 60:40          | Moderate         | Frequent           | Channel, localised bridged grain                               |
|           | 8075, top of glacial till | Variable                                     | Unsorted         | Few to frequent    | Variable, vesicular to massive                                 |

Table 6.4 Comparison of microstructure and c/f ratios from

M504

Undisturbed glacial till was identified by the presence of unfragmented silt and link cappings. Translocation of material into the surface of the till resulted in void coatings and infillings. Despite the general absence of any biological activity some of the coatings form small ovoid pellets in varying



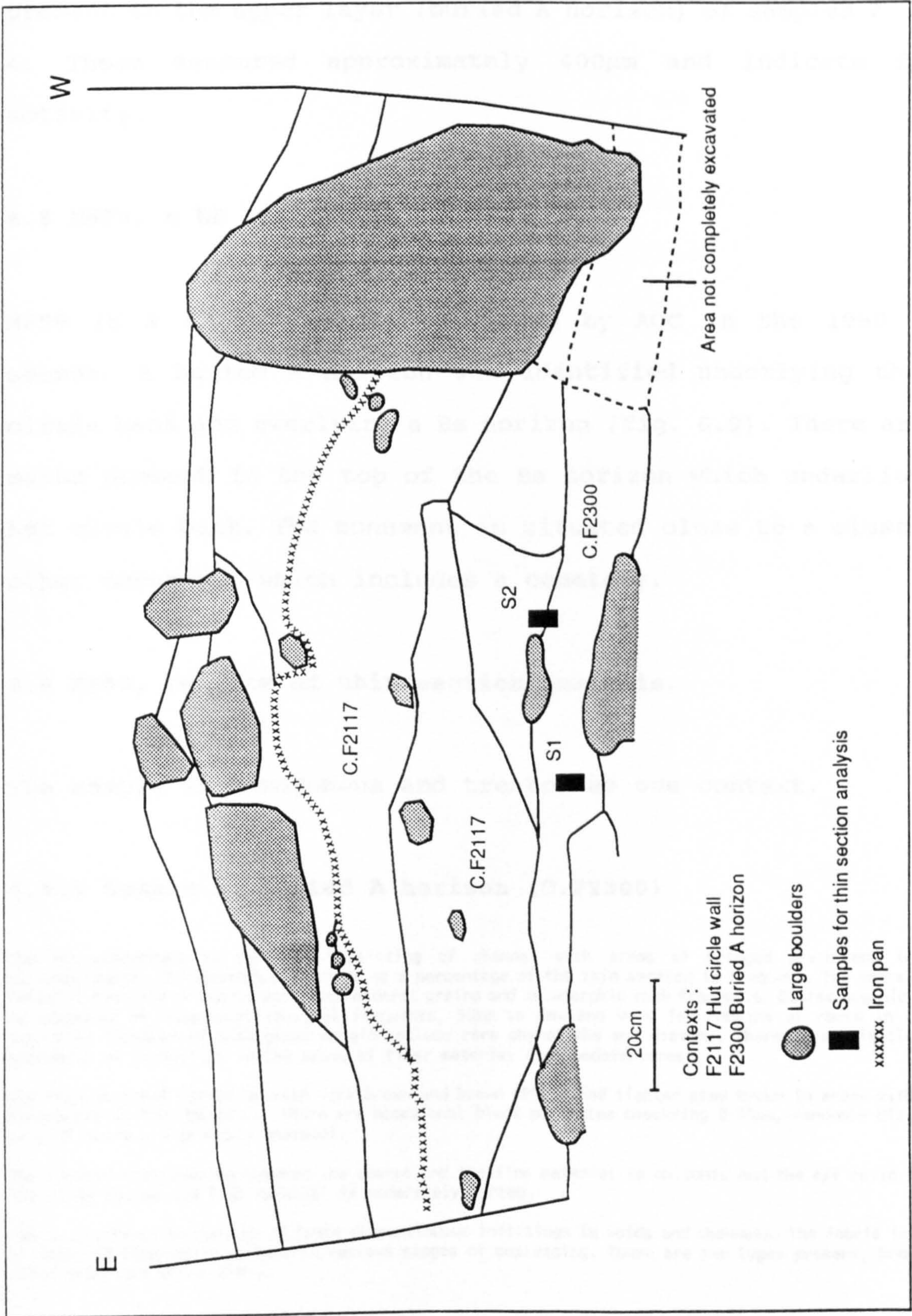


Fig. 6.9 M659, LP hut circle

degrees of coalescence. It is possible that small soil fauna used the same channels as the translocated material to move through the soil profile. There are strongly coalesced excrement features present in the upper layer (buried A horizon) of samples 2, 3 and 4. These measured approximately 400 $\mu$ m and indicate faunal activity.

### **6.8 M659, a LP hut circle**

M659 is a LP hut circle excavated by AOC in the 1990 field season. A buried A horizon was identified underlying the hut circle bank and overlying a Bs horizon (fig. 6.9). There are ard marks present in the top of the Bs horizon which underlies the hut circle bank. The monument is situated close to a cluster of other monuments which includes a cemetery.

### **6.9 M659, results of thin section analysis.**

The sample is homogenous and treated as one context.

#### **6.9.1 Sample 1, buried A horizon (C.F2300)**

The microstructure is variable consisting of channel with areas of bridged grain and intergrain microaggregate. The abundance of voids as a percentage of the thin section is frequent. The coarse mineral material consists of quartz dominated mineral grains and metamorphic rock fragments. Coarse organic material is composed of occasional charcoal fragments, 50 $\mu$ m to 3mm and very few remains of roots in channels. Inorganic residues of biological origin include rare phytoliths and diatoms. There is a slightly greater abundance of phytoliths in the areas of finer material (see pedofeatures).

The fine material varies between dark brown and brown (PPL), and lighter grey brown in areas with greater abundances of fine material. There are occasional black particles measuring 2-50 $\mu$ m, randomly distributed. Many of these are probably charcoal.

The related distribution between the coarse and the fine material is chitonic and the c/f ratio is 60:40. The slide coarse and fine material is moderately sorted.

Fabric pedofeatures consist of loose discontinuous infillings in voids and channels. The fabric is composed of small 40-80 $\mu$ m ovoid pellets in various stages of coalescing. There are two types present, brown orange (PPL) and light brown (PPL).

In one area there is a greater concentration of light brown fine material which has a greater concentration of phytoliths than the surrounding groundmass. The area of fine material is in part composed of ultrafine granules moderately to strongly coalesced. This is possibly the result of the crossing of two channel infillings.

In one part of the groundmass there is an area measuring 3 x 8mm. This is generally strong orange (PPL), orange (OIL), prominent with a sharp boundary. There is some amorphous orange to pale orange yellow (PPL), orange (OIL), generally isotropic coatings of voids present. There are small regions of the coatings which are weakly anisotropic.

#### **6.9.2 Interpretation of the buried A horizon under M659.**

The groundmass is variable incorporating material from different horizons. The strong orange fabric pedofeature is interpreted as a fragment of Bs horizon. This confirms the field interpretation that there had been mixing of Bs and A horizons. The distribution of phytoliths throughout the soil is not homogenous, some clustering is present. The areas of groundmass with the highest concentrations of phytoliths might be fragmented remnants of imported material or reflect the mixing of material from surface layers.

#### **6.10 Monument 660, a LP hut circle**

Directly below the hut circle wall is a thin red layer interpreted as ash (figs. 6.10 and 6.11). Three samples were taken spanning the underlying buried soil, the ash material and the overlying hut circle wall.

Fig. 6.10 M660, LP hut circle

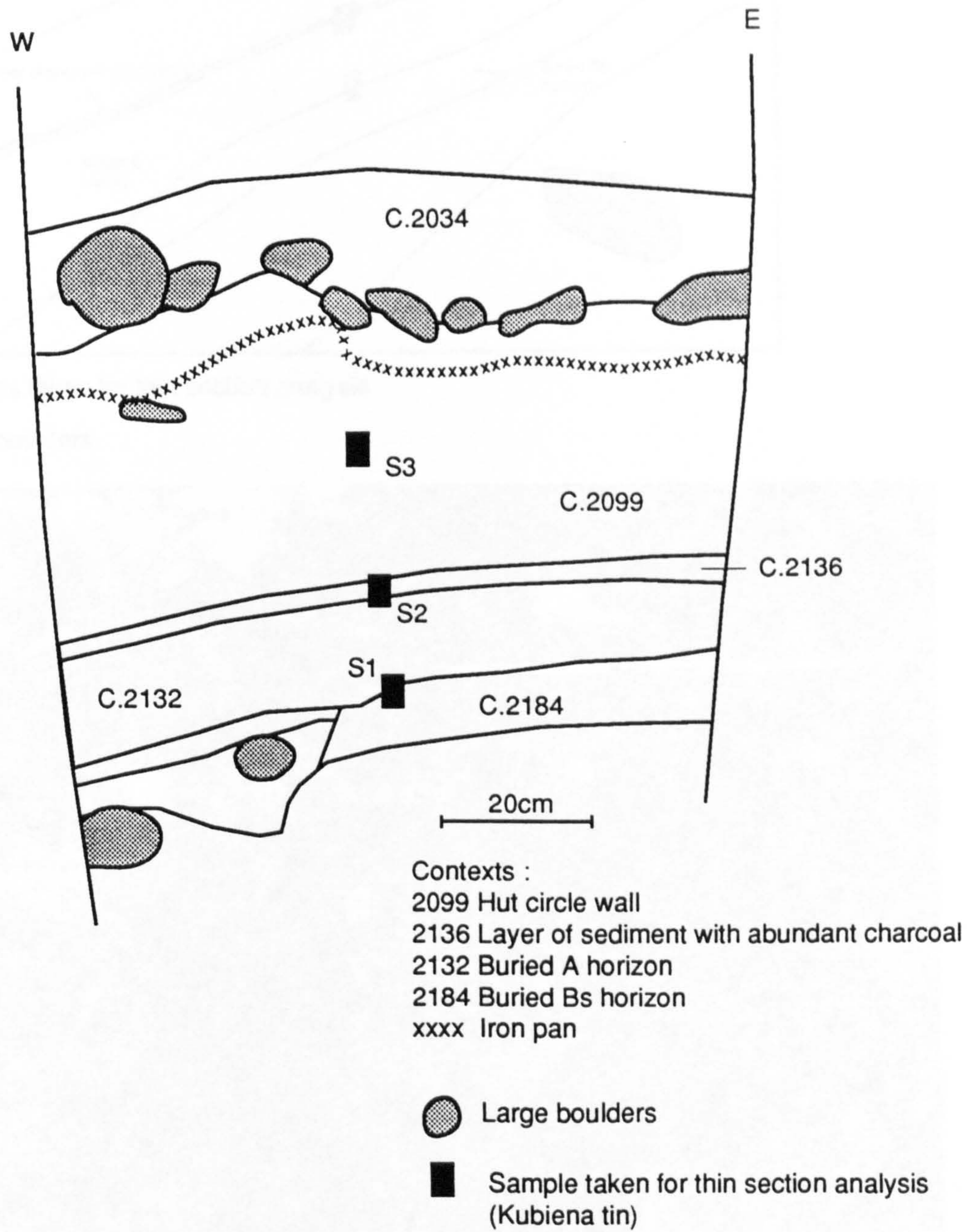
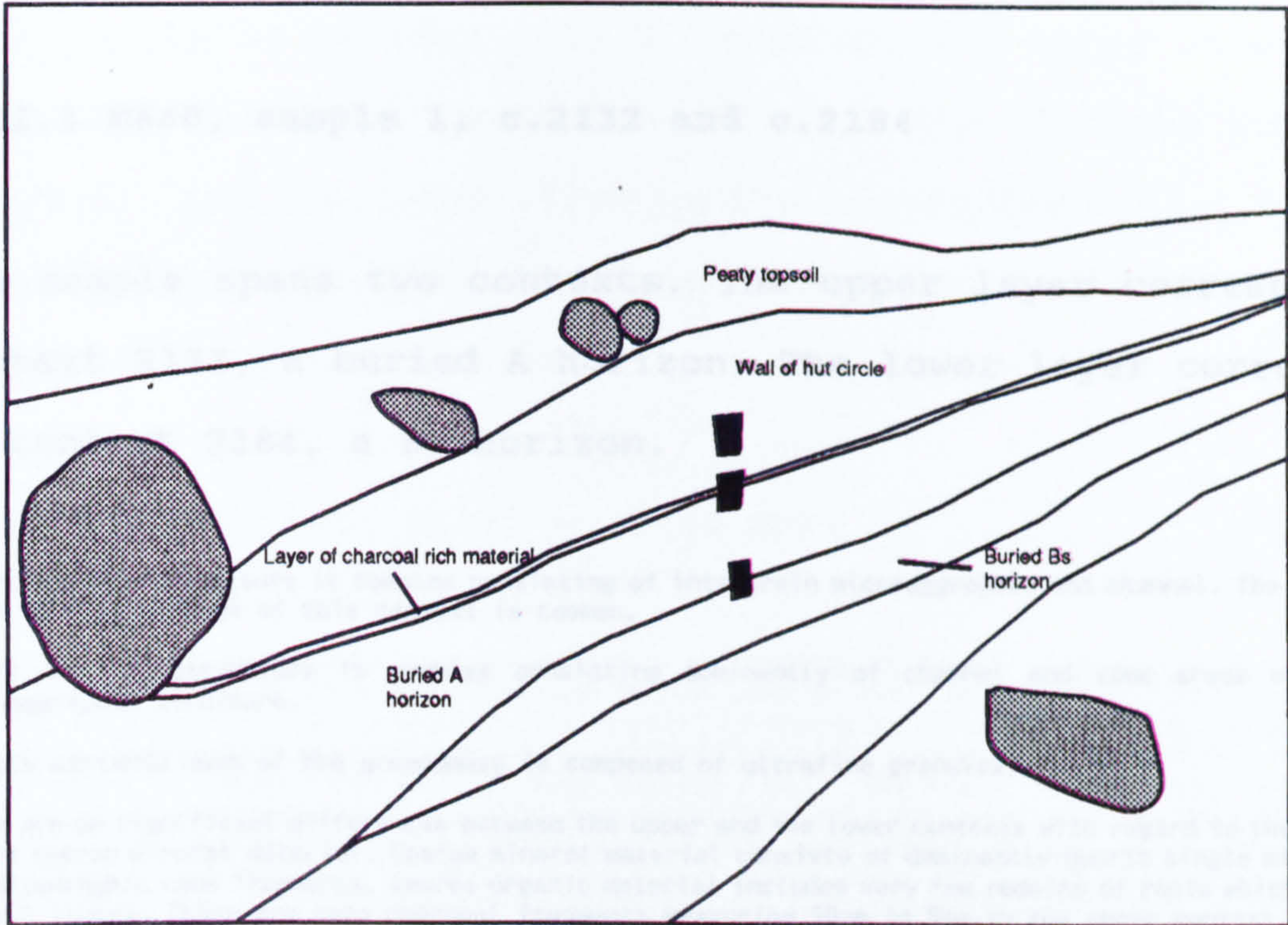


Fig. 6.11 M660, LP hut circle



## 6.11 Results of thin section analysis.

### 6.11.1 M660, sample 1, c.2132 and c.2184

The sample spans two contexts. The upper layer corresponds to context 2132, a buried A horizon. The lower layer corresponded to context 2184, a Bs horizon.

Upper; the microstructure is complex consisting of intergrain microaggregate and channel. The abundance of voids as a percentage of this context is common.

Lower; The microstructure is complex consisting dominantly of channel and some areas of intergrain microaggregate structure.

In both contexts much of the groundmass is composed of ultrafine granules.

There are no significant differences between the upper and the lower contexts with regard to the composition of the coarse mineral material. Coarse mineral material consists of dominantly quartz single mineral grains and metamorphic rock fragments. Coarse organic material includes very few remains of roots which are present in both layers. There are rare charcoal fragments measuring 50 $\mu$ m to 5mm in the upper context. No charcoal fragments are present in the lower context. Inorganic residues of biological origin consist of rare phytoliths and are randomly distributed.

In the upper layer the fine fraction is dark brown (PPL), organo mineral. The lower context is essentially the same as the upper except the fine material has an orange colour and in a few places examples of amorphous ferruginous compounds are present (see pedofeatures). There are rare black fragments measuring 2-50 $\mu$ m randomly distributed in the upper layer. There are no significant number of these in the lower layer. The c/f ratio is 60:40 in both layers. The material in the upper layer is moderately sorted and the material in the lower layer is poorly sorted.

Upper layer; There is one example of a rock fragment with an orange coating of fine material derived from the Bs horizon. This coating covers at least  $\frac{3}{4}$  of the perimeter of the fragment and is between 40-160 $\mu$ m thick. In one area the coating overlies a small remnant of a silt capping.

A small fragment of groundmass impregnated by ferruginous material is present. This is interpreted as a fragment of B horizon material.

There are many orange brown (OIL), dark red brown to black (PPL), faint to distinct mottles, randomly distributed, measuring 20-400 $\mu$ m. Sometimes dull (OIL) thin coatings are present within voids and form part of the mottles. These coatings are sometimes weakly anisotropic.

Lower layer; There are many mottles showing a high variability in degree of impregnation. Where the impregnation is the strongest irregular to rounded nodules are present. Colours vary from orange to very dark red to black (PPL), dark brown to black (OIL). They are generally isotropic although areas of anisotropic material are also present. Sizes range from 20 $\mu$ m to 1mm. Other examples groundmass impregnation are present. Sometimes coatings form part of the mottles. These coatings are orange (PPL), dark brown to black (OIL), sometimes weakly anisotropic.

There is one example of the remains of a small fragmented silt capping lying on a rock fragment. The fragment is in a vertical position and the silt capping is on the vertical face. The composition of the silt capping is coarse grained quartz and green amphibole the sizes of which vary between 20-120 $\mu$ m. These are set in a porphyric groundmass.

Coatings of fine material are present on many of the fragments throughout this section. These coatings are approximately 40 $\mu$ m wide. These are possibly the result of disturbance. In both the upper and lower layers channel shaped fabric pedofeatures with a 400 $\mu$ m diameter are present.

### **6.11.2 M660 sample 2, c.2099, c.2136 and c.2132.**

This sample is divided into 3 contexts. The upper layer is the turf bank (C.2099), the middle layer is the charcoal rich layer (C.2136), and the lower layer is the underlying buried A horizon (C.2184). Both the top layer and the bottom layer are included in either sample 1 or sample 3.

#### **Lower part of turf wall, context 2099**

The microstructure is intergrain microaggregate with bridging of the minerals by fine material in many places. The abundance of voids as a percentage of this layer is few. The c/f ratio is 50:50 and the related distribution between the coarse and the fine material is dominantly chitonic with localised enaulic. There are few to frequent remains of charcoal measuring 20 $\mu$ m to 6mm. The abundance of charcoal is slightly greater at the top of the context. There is one large partially burnt wood fragment. There are some fragments of blackened fungal material also present. The fine material is brown grey and grey brown (PPL) organo mineral. There is one fabric pedofeature that consists of closely packed quartz mineral grains measuring 1.5mm x 2.4mm, rounded. The fine material is orange red (PPL), strong orange (OIL). This is probably a fragment of ferruginised glacial till. There are very few 40 to 120 $\mu$ m ferruginous nodules randomly distributed.

#### **Charcoal rich occupation layer (C.2136)**

The central layer is composed of dominant charcoal fragments measuring 50 $\mu$ m to 7mm. The fragments are moderately referred parallel to the surface. The microstructure is intergrain microaggregate with some bridging between mineral grains. The c/f ratio is 50:50. The fine material is black to brown (PPL) organo mineral. There are abundant fine black particles randomly distributed throughout the central layer and one or two fragmented phytoliths. There are few ferruginous nodules (may be mineral alterations) 80-200 $\mu$ m, mostly equidimensional.

#### **Buried A horizon.**

The microstructure is dominantly intergrain microaggregate and channel with some bridging between the mineral grains. The abundance of voids as a percentage of this context are frequent. The c/f ratio is 60:40. There is some impregnation of the groundmass by amorphous ferruginous compounds and rare equidimensional nodules measuring 40-500 $\mu$ m. The nodules have sharp boundaries.

There is one example of a moderately to strongly impregnated, orange to red to black (PPL), dark brown to dull orange (OIL), mottle measuring 1.5mm across. This is composed dominantly of quartz with some green amphibole and muscovite. Smaller fragmented examples are also present. There is weak anisotropic material in voids. This corresponds to darker colours using (OIL). Smaller mottles, abundance rare, are randomly distributed.

There is one example of a fabric pedofeature with a porphyric c/f related distribution. This measures 2.5mm across, has a sphericity of 2 and is subrounded. The colour of the fine material is pale brown (PPL). The dominant mineralogy is quartz with small quantities of green amphibole and some muscovite. Two small areas

within the pedofeature show signs of mottling. Other examples of areas with a porphyric c/f related distribution are present. The abundance of these as a percentage of this layer is very few.

### **6.11.3 M660, sample 3, c.2099.**

Sample 1 was taken from the wall of the hut circle. The slide is homogenous and treated as one context.

The microstructure is variable, generally composed of an intergrain microaggregate and channel structure. In these areas the c/f ratio is approximately 50:50 with an enaulic to chitonic related distribution. This accounts for 70% to 80% of the slide. Approximately 5% to 10% of the slide has a microstructure that tends towards massive. In these area vughs are present and the c/f related distribution is porphyric with a c/f ratio of 45:55. The abundance of voids as a percentage of the thin section is frequent.

The coarse mineral material includes dominantly of quartz single mineral grains and metamorphic rock fragments. Coarse organic material includes occasional fragments of charcoal, randomly distributed, rare bright rings, diameter 200 $\mu$ m, rare remains of roots in channels and one organ residue, almost spherical but with a nipple at one end strongly humified outer epidermis, diameter 1200 $\mu$ m. There is also one unidentified fragment of humified organic material that is probably a fragment of partially burnt wood. Inorganic residues of biological origin include rare fragmented phytoliths and diatoms randomly distributed. The coarse and fine material is well sorted.

The fine material is brown to grey brown (PPL) organo mineral material. There are rare black particles randomly distributed.

Fabric pedofeatures include faint 400-500 $\mu$ m wide vermiform shaped features. There is an area of the slide that is intergrain microaggregate structure with a c/f ratio of 80:20 and an enaulic c/f related distribution. The mineral grains are strongly referred perpendicular to the surface. The area is 4mm wide (horizontal) and 16mm long. The mineralogy is dominantly quartz with 5% green amphibole. There is a sharp boundary with material to the left and a diffuse boundary with material to the right. It is likely that this feature was created during the construction of the wall as it can not be explained by biological processes.

There are occasional orange (OIL), dark brown to black (PPL) mottles measuring 20-50 $\mu$ m, randomly distributed, and rare ferruginous nodules measuring 20-400 $\mu$ m across, dark brown (PPL), orange red (OIL), randomly distributed. There is one typic nodule, dark red to black PPL, bright red OIL. This may be the result of the mineral alteration.

Textural pedofeatures consist of a dark brown to black fragmented ferruginous capping lying beneath a rock fragment. The capping is composed of coarse grained material with quartz in the size range 20-300 $\mu$ m. The width of the capping is 400-500 $\mu$ m.

### **6.11.4 Interpretation of M660.**

The contexts below M660 are archaeologically complex consisting of sediment associated with periodic house construction. This activity resulted in some truncation of the soil profile. Results from the field excavation suggest the following sequence of events;



1. Earlier period of activity including a house construction and creation of cremation pits.
2. Demolition of the house and levelling.
3. Cultivation of the soil.
4. The construction of a later house (M660).

The turf wall of M660 is composed of material with variable c/f ratios and c/f related distributions. The variations in the c/f ratio and c/f distribution possibly relate to a sorting of the soil as it was being used to construct the wall. The material at the edges of large soil clods are more likely to become disturbed than material in the centre.

Field observations show that the wall of the hut circle is strongly mottled. The only micromorphological feature that might account for this are variations in the c/f ratio. There were no differences in basic components. There is one capping present in the sample described. This was probably already present in the soil which was used for construction. There is no evidence of Bs horizon material being incorporated directly into the hut circle wall as in M64.

There is no indication of any movement of material between the charcoal layer and the contexts on either side of it, this suggests little disruption by soil fauna. It is unlikely that the layer of charcoal was burnt in situ because there were no modifications of the underlying context. This area was archaeologically complex, so the burning might have related to

a period of occupation, perhaps the burning of a dwelling or the spread of ash derived from another source.

There is minimal mixing of the A and Bs horizon. The Bs horizon is an example of a friable Bs horizon composed of polymorphic organic material (section 9.3). Both the buried A and Bs horizons are composed of dominantly ultrafine granules. There is no charcoal present in the buried Bs horizon but there are rare fragments of coarse and fine charcoal present in the buried A horizon. There are no cappings present in the Bs horizon suggesting that no material has been directly incorporated from the underlying glacial till.

## Chapter 7

### Results of the excavation and thin section analysis of monuments in group C.

#### 7.1 Introduction

Group C monuments are located in the northern area of the survey site within block 4 (fig. 3.6). The vegetation is dominantly grass and bracken. Three trenches were excavated and samples were described from two monuments. Freely draining brown podzols and gleys are the main types of soil in the area. The gleys are located mainly in flushes.

#### 7.2 Results from M975, the PM head dyke.

M975 is an enclosure dyke of recent origin, possibly 18<sup>th</sup> century (figs. 7.1 and 7.2). The vegetation surrounding the dyke consists dominantly of bracken with some grass. The dyke is composed of 2 components, an upper section with few small to medium stones and a lower section with abundant large subangular to subrounded stones. Below the dyke is an intermittent layer of very dark greyish brown (10YR 3/2) material (C.8102) with a thin discontinuous iron pan above and below it. This is interpreted as the result of localised reduction of a buried humose horizon. Decomposition of organic matter resulted in reducing environment which created the conditions for the mobilisation of iron. When

Fig. 7.1 M975, PM head dyke

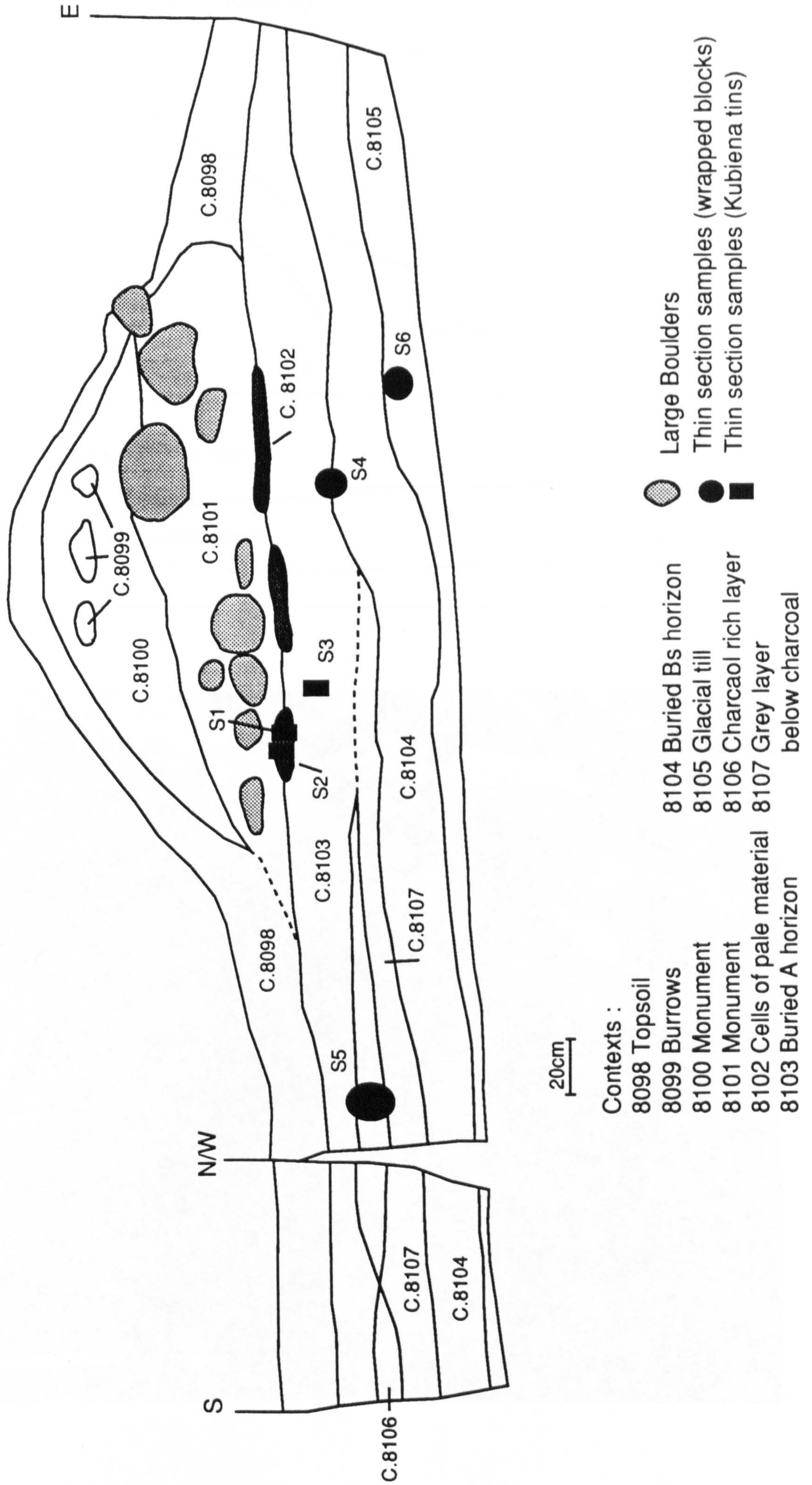
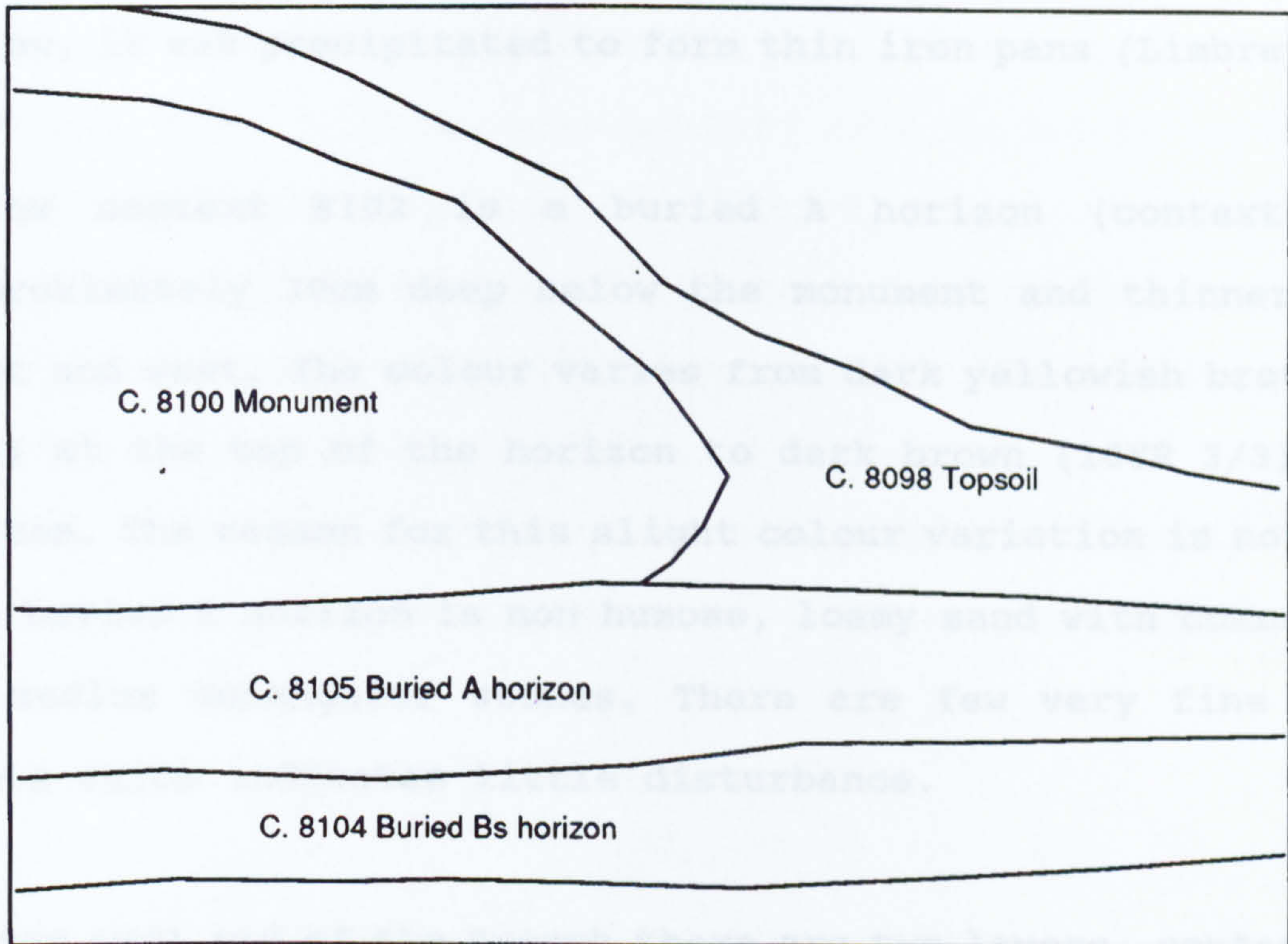


Fig. 7.2 M975, PM head dyke, south facing section



the iron came into contact with the oxygen rich soil above and below, it was precipitated to form thin iron pans (Limbrey 1975).

Below context 8102 is a buried A horizon (context 8105), approximately 30cm deep below the monument and thinner to the east and west. The colour varies from dark yellowish brown (10YR 3/3) at the top of the horizon to dark brown (10YR 3/3) at the bottom. The reason for this slight colour variation is not known. The buried A horizon is non humose, loamy sand with common small to medium subangular stones. There are few very fine fibrous roots which indicates little disturbance.

At the west end of the trench there are two layers, contexts 8106 and 8107, that are stratigraphically below the buried A but above the buried Bs (fig 7.1). Context 8106 is rich in charcoal. Context 8017 is dark greyish brown (10YR 4/2), non humose and sandy loam with many small subangular to subrounded stones. These two contexts only extend for a short distance under M975.

Underlying contexts 8013, 8016 and 8017 is the buried Bs horizon. The colour varies from yellowish brown (10YR 5/8) to 7.5YR 4/6 strong brown with many small to medium subangular to subrounded stones, and common large subangular to subrounded stones. The depth of the Bs horizon is fairly constant along the width of the trench.

The profile was interpreted in the field as follows. Context 8106 represents a buried A horizon overlying a buried E horizon

(8107). The formation of these layers might include a colluvial component building up against the wall of a hut circle just to the west of M975. Below context 8107 is a buried Bs horizon. The horizon sequence represents a buried podzol. Below M975 the podzol profile is truncated, probably by human activity pre-dating the construction of the head dyke. The A horizon buried by M975 (c.8105) is approximately 30cm deep and is a brown podzol. After the head dyke was constructed some erosion of the soil to the north and south of the monument occurred.

### **7.3 Results of the thin section analysis.**

#### **7.3.1 M975, sample 2, c.8101, c.8102, c.8103.**

This sample consists of 3 contexts. Layer 1 is located below the lower iron pan, layer 2 is the grey layer and layer 3 is located above the upper iron pan. Only layers one and two are described.

#### **Layer 1, context 8103.**

The microstructure is complex and consists of a channel and vughy structure. In some parts of the slide a localised bridge grained structure is present. There are areas of massive material and places where weakly developed aggregates are present. The abundance of voids as a percentage of this layer is frequent.

Coarse mineral material consists of quartz dominated single mineral grains and metamorphic rock fragments. Coarse organic material includes rare fragments of charcoal and rare remains of roots in channels. There is one unidentified elongate organic fragment. Inorganic residues of biological origin consists of rare phytoliths randomly distributed.

The fine material is grey brown with a slight indication of orange (PPL). There are occasional black particles measuring 2-50 $\mu$ m, probably charcoal or humified organic material. The related distribution between the coarse and the fine material is dominantly porphyric with localised chitonic. The c/f ratio is 40:60.

Pedofeatures include occasional orange, (PLL and OIL), weakly to moderately impregnated ferruginous orthic mottles. These are generally equidimensional varying in diameter between 40 $\mu$ m and 500 $\mu$ m. There are very few equidimensional nodules. The impregnation is strong so it is difficult to determine if they are orthic or not. They have sharp boundaries and appear separate from the surrounding groundmass. The diameter varies between 200 $\mu$ m and 400 $\mu$ m.

The boundary between layer 1 and layer 2 is a thin iron pan approximately 2.5mm thick. The colours of the pan vary between orange and dark red to black (PPL) in the areas of the strongest impregnation. Some

disruption of the pan is visible. There is some layering of the areas that are weakly and strongly impregnated.

## **Layer 2, context 8102**

The microstructure is weakly developed channel. The abundance of voids as a percentage of this layer is few. Approximately 70% of the coarse mineral material is single mineral grains which consist of quartz dominated material.

Coarse organic material includes rare charcoal fragments, randomly distributed, measuring 50-200 $\mu$ m, one larger fragment is also present. There are 6 bright rings with a diameter of approximately 200 $\mu$ m and rare fungal material, possibly sclerotium, 100 $\mu$ m to 200 $\mu$ m diameter. There is one unidentified organic component with a blackened outer epidermis with 2 nipples at either end. There are two areas, 0.5 x 0.5mm, of slightly layered humified organic material. There is one orange elongate unidentified organic fragment. Inorganic components of biological origin consists of occasional phytoliths randomly distributed.

The fine material is light orange brown to grey brown (PPL) organo mineral material. The related distribution between the coarse and the fine material is generally porphyric tending towards chitonic in some areas. The c/f ratio is 40:60. The material is perfectly sorted.

Within some channels and voids a pale amorphous material is present. This might have been the result of the almost total decomposition of roots. This material is also present coating the sides of some rooting material.

Fabric pedofeatures comprise rare loose discontinuous infillings of some channels. These are also present where root penetration is impeded. In places the infillings are ovoid pellets, measuring 40 $\mu$ m across, in various states of coalescing.

There is one strongly dark red (PPL) impregnated subrounded nodule, 300 $\mu$ m x 400 $\mu$ m. The internal fabric consists of quartz mineral grains and ferruginous amorphous material.

Excrement pedofeatures include rare moderately coalesced ovoid excrements, measuring approximately 400 $\mu$ m, slightly more orange than the surrounding groundmass. The orange colour is probably influenced by the iron pan above.

### **7.3.2 M975/2, sample 3, c.8103.**

This sample is taken from the buried A horizon, context 8105 (fig. 7.1), at a depth of approximately 10cm below the old ground surface. The slide is homogenous and described as one context.

The microstructure is channel structure tending towards intergrain microaggregate owing to the amount of infilling material (see excremental pedofeatures). The abundance of voids as a percentage of this layer is frequent.

The coarse mineral material is dominated by quartz single mineral grains and metamorphic rock fragments. Coarse organic components includes two bright rings, diameter approximately 100 $\mu$ m, very few remains of roots in channels, occasional charcoal fragments measuring 50 $\mu$ m to 3mm and two fragments of burnt peat measuring approximately 1mm across. Inorganic residues of biological origin include rare phytoliths randomly distributed.

The fine material is grey brown to orange brown (PPL) organo mineral material. There are occasional black, (PPL and OIL), particles measuring 2-50 $\mu$ m randomly distributed. These are probably charcoal fragments.

The related distribution between the fine and the coarse material is chitonic with undisturbed areas of porphyric and enaulic infills. The c/f ratio is 45:55 and the material is moderately sorted.



Excremental pedofeatures consist of many loose discontinuous infillings, sometimes infilling channels or irregularly shaped voids. The infillings are composed of small ovoid pellets measuring approximately 40µm, pale brown to orange brown (PPL).

There are occasional black (PPL), isotropic, generally equidimensional strongly impregnated, possibly orthic, nodules. Some less strongly impregnated examples are also present orange (PPL), generally measuring 50µm to 1mm. In places the impregnated areas are more elongate as if they are associated with channels.

In places the nodules are less well impregnated and appear as mottles. These are orthic, orange (PPL), brown (OIL). The internal composition includes 1 orientated, microlaminated, limpid clay coating. In one place mottling occurs around lignified epidermal material.

### 7.3.3 M975, sample 6, c.8105.

This sample is derived from the top of the glacial till below the Bs horizon. The sample is homogenous and treated as one context.

The microstructure is intergrain microaggregate with some areas of single grain. There are abundant cappings present (see pedofeatures). The abundance of voids as a percentage of this slide is generally frequent although there is variability in different areas of the slide.

There is a band of material approximately 1cm thick below the top of the slide. The concentration of fine material in this area is greater than elsewhere on the slide. The material above and below this reverts to an almost single grain structure.

The coarse mineral material consists of quartz dominated single mineral grains and metamorphic rock fragments. Coarse organic material includes rare remains of roots in channels. There are no inorganic residues of biological origin present. The fine material is generally grey brown (PPL) but also includes areas which are more orange and are associated with translocated amorphous material. The fine material is generally mineral.

The related distribution between the fine and coarse material is very variable. It is possible to distinguish all types of related distributions. The c/f ratio is generally 70:30 and the material is poorly sorted.

Textural pedofeatures includes very abundant silt and link cappings which are generally undisturbed although some disruption by small channels is present. Two layers are distinguished in the cappings lying on top of rock fragments;

(a). Next to the rock fragment the matrix consists of a fine grey mineral material. Set into this are quartz grains that varied in size from 50-200µm.

(b). Overlying layer (a) is a layer of fine brown material.

In the top right hand corner of the slide there is abundant dense incomplete infillings of large void areas. These are orange (PPL), dull brown (OIL). In places the material is composed of strongly coalesced, ovoid to irregularly shaped pellets. The material is almost entirely organic with occasional mineral grains smaller than 50µm.

### 7.3.4 Interpretation of M975.

The buried profile below the monument is a brown podzol. The depth of the buried A horizon is approximately 30cm. The abundance of coarse and fine charcoal is occasional in the buried

A horizon. Two of the larger carbonised fragments were identified as burnt peat. There are no textural pedofeatures suggesting material derived from the Bs horizon or glacial till.

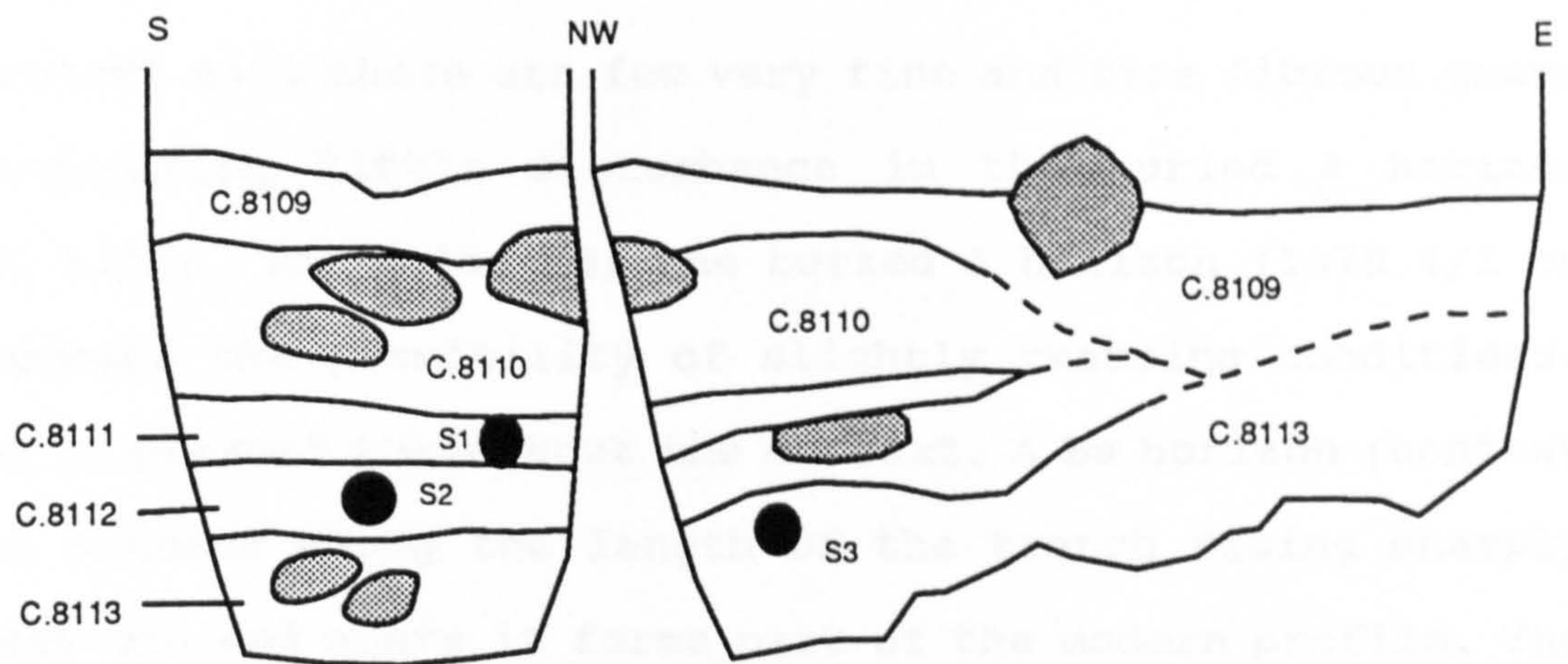
There are undisturbed cappings in sample 6 indicating that the profile is not disturbed at a depth of approximately 50cm below the old ground surface. The interface of the disturbed and undisturbed material can not be measured exactly because it is not included in a thin section sample.

#### **7.4 Results from M1069, a PM rectangular house.**

A trench was dug in an east to west direction through the inner wall of a Post Medieval rectangular structure. This wall is thought to be part of the original house thus burying a soil that pre-dates construction. The archaeological interpretation of this structure suggests it is a dwelling built in the 18<sup>th</sup> century and possibly associated with the main enclosure dyke (M975). Within the outer walls of the structure the dominant vegetation is grass. Along the walls, outside the walls and in the lower section of the monument there is abundant bracken.



The wall of the house (fig 7.3), context 8110, consists of abundant medium to large subangular equidimensional stones. The area covered by the stones marks the position of the original wall and an area covered when the wall collapsed. Contexts 8111 and 8112 represent a buried profile truncated to the east of the monument. An annex was added sometime after the main structure

Fig. 7.3 M1069, PM structure



40cm

- Contexts :
- 8109 Topsoil
  - 8110 Matrix of monument
  - 8111 Grey surface horizon
  - 8112 Buried A horizon
  - 8113 Bs horizon

-  Large boulders
-  Thin section samples (wrapped block)

had been completed. Disturbance during the construction of this annex probably truncated the profile to the east of the monument.

Context 8111 is dark grey to dark greyish brown (10YR 4/1 to 4/2) material. A thin continuous iron pan is present above and below this layer. Few very fine and fine fibrous grass roots indicate little disturbance. Context 8111 is interpreted as the original ground surface (see M975).

Below context 8111 there are few very fine and fine fibrous grass roots indicating little disturbance in the buried A horizon (context 8112). The colour of the buried A horizon (10YR 4/1 to 4/2) suggests the possibility of slightly reducing conditions. Charcoal is present throughout the context. A Bs horizon (context 8113) is present along the length of the trench rising sharply at the eastern end where it forms part of the modern profile. The buried soil is a brown podzol.

### **7.5 Results of the thin section analysis.**

Three samples were taken for thin section analysis (fig. 7.3).

#### **7.5.1 M1069, sample 1, c.8111.**

This sample is from context 8111, the grey surface horizon thought to represent the old ground surface. The sample consists of two iron pans running across the slide moderately parallel to the surface. Only the layer between the iron pans and below the

lower iron pan are described. The layer above the iron pan is part of the wall of the monument.

### **Layer between double iron pan.**

The microstructure is complex consisting of channel, spongy, intergrain microaggregate and bridged grain. The abundance of voids as a percentage of this layer is few to frequent. Coarse mineral material consists of quartz dominated single mineral grains and metamorphic rock fragments. Coarse organic components include rare remains of roots in channels, rare fragments of charcoal measuring between 100 $\mu$ m and 500 $\mu$ m. One elongate charcoal fragment 1mm long is present. Inorganic residues of biological origin include rare fragmented phytoliths and diatoms randomly distributed.

The fine material is brown to orange (PPL). In areas where the structure tends towards intergrain microaggregate many small ovoid 40 $\mu$ m pellets are present. There are rare black particles, measuring 2-50 $\mu$ m, randomly distributed.

The related distribution between the coarse and the fine material varies between chitonic, enaulic and porphyric. The c/f ratio is 45:55 and the material is moderately sorted.

Pedofeatures include rare orange orthic nodules, orange/red (PPL), generally equidimensional, measuring about 800 $\mu$ m.

The fine material is sometimes concentrated into 800-1000 $\mu$ m wide vermiform fabric features.

### **Layer below the iron pan, the buried A horizon.**

There is not much of this material left on the slide so abundances of some coarse features are not estimated.

The microstructure is intergrain microaggregate to bridged grain. The abundance of voids as a percentage of this context is frequent.

Coarse mineral material consists of quartz dominated single mineral grains although there is a greater abundance of green amphibole fragments than seen in other contexts. Coarse organic material includes one or two charcoal fragments measuring 100-200 $\mu$ m, randomly distributed.

The fine material is brown and light brown organo mineral material. Much of the fine material occurs as ovoid pellets approx 40 $\mu$ m across. There are rare black particles measuring 2-50 $\mu$ m randomly distributed.

The related distribution between the coarse and the fine material is variable including enaulic and bridged grain. There are also aggregates of porphyric material present.

In an area just below the lower iron pan few fragmented and unfragmented ferruginous nodules are present. There is strong central impregnation, often surrounded by a halo. Shape is variable possibly caused by fragmentation. Colours vary between dark red black in the central area to orange in the halo (PPL).

Fabric pedofeatures include an area of orange material about 2mm wide and 3mm long, almost vertically orientated. This has a porphyric c/f related distribution and a large abundance of biotite. This is interpreted as fragmented Bs horizon material.

There is a loose discontinuous infilling of a channel. The filling consisted of small ovoid, orange/brown pellets (40 $\mu$ m), moderately degree of coalesced.

The boundary between layer 2 and layer 3 is an iron pan which is described in two parts.

A double pan extends across the slide. Lying on the upper surface of both pans are the remains of rooting material. The pans are orthic with colours including brown to red/brown to strong orange (PPL) colours. The pans are both 1 to 2mm thick. Towards the right hand side of the slide the orientation of the pan changes from being parallel with the surface to 80° from the surface. In this area the pan is more strongly impregnated.

The material between the pans consists of a brown groundmass dominated by quartz single mineral grains. The c/f related distribution in this area is approaching porphyric.

On the left hand side of the slide there is an area of orthic pan where stronger impregnation is present. Colours vary between deep dark red and black (PPL). At its maximum this pan is about 5mm thick.

### 7.5.2 M1069, sample 2, c.8112.

This sample is from the buried A horizon at a depth of 10cm below the original ground surface. The slide was homogenous and treated as one context.

The microstructure is complex consisting of channel, intergrain microaggregate and bridged grain. The abundance of voids as a percentage of the slide is frequent. Coarse organic material consists of quartz dominated single mineral grains. There are slightly greater abundances of biotite than seen in other buried A horizons. Coarse organic components include rare remains of roots in channels. In some cases the central areas of the roots have been replaced by small microaggregates measuring 40µm. The colour of the groundmass surrounding these areas is strong orange (PPL).

There are rare elongate organic residues, 20-100µm thick and 2mm long, pale yellow PPL, in part completely surrounded by groundmass in part surrounded by void space. Weak interference colours are present in the form of parallel lines.

There are rare bright rings some of which are deformed, rare fungal material, possibly sclerotium, and rare fragments of charcoal measuring 50-100µm. There is one larger fragment measuring 2mm long. When the edges of this fragment is observed using OIL, some red colouring is apparent.

Inorganic residues of biological origin generally consist of only 1 or 2 phytoliths. However there are greater concentrations found in areas with a porphyric c/f related distribution and a greater concentration of fine material (see pedofeatures).

The fine material is grey brown, dark brown and orange brown (PPL). The variations in colour corresponds to changes in the c/f related distribution and to some extent to a change in the microstructure. The fine material is organo mineral. There are rare black particles measuring 2-50µm, randomly distributed.

The related distribution between the coarse and the fine material is generally chitonic although there are also areas of porphyric and enaulic. In areas of porphyric the material is matrix supported. In areas the colour of the groundmass varies. Where there are stronger orange colours or much darker brown colours the c/f related distribution tends towards porphyric. The c/f ratio is generally 55:45 and the material is moderately to well sorted.

There are many orange (OIL), red brown to black (PPL) mottles measuring 20-200µm randomly distributed. There are also mottles in the size range 200-800µm. The strength of impregnation is variable, sometimes forming nodules. Occasionally the mottling is present next to decomposing root remains.

The areas of groundmass with more fine to coarse material are fabric pedofeatures. The voids consist of compound packing voids and vughs, porphyric c/f related distribution. There are no single mineral grains larger than 200µm.

There are large areas of orange, (PPL), groundmass. These areas generally have a porphyric c/f related distribution, and a greater abundance of green amphibole and biotite than the surrounding groundmass. The features have a prominent, sharp boundary. These areas are interpreted as fragmented and transported Bs horizon material. There had been some post deposition disruption of this material by channel activity.

### **7.5.3 M1069, sample 3. c.8113.**

This sample is from the Bs horizon, context 8113. The slide is homogenous and treated as one context.

The microstructure is complex consisting of intergrain microaggregate and channels. The spacing between the mineral grains is greater than seen in other contexts. The abundance of voids as a percentage of this section is frequent.

Coarse mineral material is composed of single mineral grains dominated by quartz and biotite. There is a greater abundance of biotite than seen in similar contexts elsewhere. The ratio of quartz to biotite is 55:45. There are smaller amounts of muscovite and feldspar. The quartz grains are less densely packed than seen in other examples of B horizon material.

Coarse organic components include rare remains of roots, one fungal body, possibly sclerotium, and one or two charcoal fragments measuring 40-100 $\mu$ m. Inorganic residues of biological origin consist of one or two fragmented phytoliths. The fine material is orange brown (PPL), organo mineral and composed of many small ovoid pellets (50 $\mu$ m) in various stages of coalescing.

The related distribution between the coarse and the fine material is between chitonic and porphyric. The c/f ratio is 60:40 and the material is moderately sorted.

There are rare equidimensional to slightly irregular mottles, varying in diameter between 100 $\mu$ m and 800 $\mu$ m, dark red to dark orange (PPL). In old void spaces the colour is dark orange brown (OIL), becoming slightly lighter into the groundmass, and weakly anisotropic. The internal fabric consists of ferruginous material cementing mineral grains including biotite, green amphibole and quartz.

Textural pedofeatures consist of rare coatings, composed of a similar material to the nodules just described, around rock fragments, approximately 40 $\mu$ m wide.

Pedofeatures composed of elongated, 800 $\mu$ m wide fabric features are present throughout the slide. In one area near the bottom of the slide mineral material, linked by dark brown fine material, is present. There is not enough of the fine material to describe its structure.

### **7.5.4 Interpretation of M1069.**

The buried A horizon is thinner than under M975 and M127. The groundmass is characterised by a variable c/f related distribution. There tends to be a greater abundance of phytoliths found in the areas of porphyric material. The darker colour of these areas suggests that they might have a greater organic content than the lighter areas. The darker groundmass might

represent imported material or material mixed from a part of the profile with a greater organic content.

There are rare coarse and fine charcoal fragments present and also some fungal material including bright rings. There are also large orange fabric pedofeatures which suggest areas of transported Bs horizon material. The morphology of the Bs horizon is different to any seen elsewhere. There are no fragmented cappings and the material was well sorted. The mineral material is dominated by quartz and biotite. The development of Bs horizons is discussed in section 9.3.



## Chapter 8

### Morphological quantification of 3 buried A horizons.

#### 8.1 Introduction

The results of the thin section analysis of buried A horizons indicate a relationship between the age of monuments, coarse / fine ratios and the abundance of voids in the soil (table 8.1).

|   | Monument        | Void Abundance     | c/f ratio |
|---|-----------------|--------------------|-----------|
| Later Prehistoric Monuments                   | M62, sample 2   | Frequent           | 65:35     |
|   | M64, sample 1   | Common             | 60:40     |
|   | M505, sample 1  | Frequent to common | 60:40     |
|   | M504, sample 1  | Frequent           | 60:40     |
|   | M659, sample 2  | Frequent           | 60:40     |
| Medieval and Post Medieval buried A horizons. | M1069, sample 2 | Frequent           | 55:45     |
|   | M975, sample 3  | Frequent           | 45:55     |
|   | M127, sample 2  | Frequent           | 50:50     |
|   | M75/4, sample 1 | Frequent           | 55:45     |
|   | M164, sample 4  | Few                | 40:60     |
| Recently improved soil                        | M21, sample 2   | Frequent           | 45:55     |

Table 8.1 Comparison of void abundance and c/f ratios between A horizons of different ages.

Table 8.1 shows that the abundance of voids, in LP buried A horizons is in the range frequent to common. The abundance in the Post Medieval to recent soils varies from few to frequent. The c/f ratios are higher in the older buried soils and lower in the more recent soils. The differences in the c/f ratios are large

enough to show a trend in the data despite being subjectively collected. The correlation is not so clear using the results of void abundance. A quantitative analysis of buried A horizons was carried out to measure void abundance, morphology of voids, amount of coarse material and amount of fine material present in 3 buried soils of different ages. The analysis was carried out using the techniques described in chapter 2. The following thin sections were selected for analysis;

1. Prehistoric buried A horizon, M504, sample 2, context 8072 (results are labelled M504I)
2. Post Medieval buried A horizon, M127, sample 2, context 8047 (results are labelled M127I).
3. Top of a soil accumulation not buried by a monument, M21, sample 1, context 8000 (results are labelled M21I).

## 8.2 Image capture.

The analysis was carried out on voids which measured  $40\mu\text{m}$  to a few mm. Voids which are significantly larger than this could be attributed to post depositional disturbance of the soil, probably a result of disturbance by bracken rhizomes. There is some limited macro-structural development in the slide from M21.

It was thought that the size distribution of voids chosen for the analysis would most likely reflect difference in the coarse / fine ratios. It was expected that the slides with the greatest abundance of fine material would have voids which were most

regular in shape. If small packing voids had been partially formed by the passage of roots through the soil, an increase in the amount of fine material would increase the likelihood of regular channel shapes being preserved. In soils with less fine material the irregularly shaped areas between mineral grains would not be filled leaving them as packing voids.

To measure micro voids in the slides images were captured using the Olympus microscope and a field of view of 3.8mm. This meant that each pixel represents approximately 7 $\mu$ m. This allowed voids in the specified size range to be accurately measured. Voids larger than the sizes required were excluded by subjectively choosing areas of the slide where the smallest amount of post depositional alteration had occurred.

### **8.3 Classification of voids coarse material and fine material.**

To allow quantification of the slides, a binary image was created of each feature using an unsupervised maximum likelihood multispectral classification (section 2.10). Six bands of data were used to describe the features in each image. Red, green and blue bands were captured using PTL and red, green and blue bands were captured using CPL.

The size of the voids are small in comparison to the area of the slide. Three images were captured from each slide to ensure that the results were representative of the whole thin section.

Voids, coarse material and fine material were assigned to informational classes. Voids were discriminated using their spectral properties in PTL and CPL. The fine material is brown and composed of mineral and organic material. The exact composition of the fine material could not be determined using only the optical microscope, however the brown colour allowed it to be discriminated from the rest of the material on the slide.

The images were classified and the spectral classes allocated to informational categories. The informational categories were checked for accuracy by displaying the binary images on top of the original colour composite image. As discussed in section 2.18 some misclassification had occurred. It was necessary to correct the images using post classification processing. A combination of filtration techniques and manual editing was used to correct the classes.

An averaging filter, a 3 x 3 kernel with each position set to 1 multiplied by a scaling factor of 6, was effective at reducing much of the background noise in the images. The convolution removed an area 1 pixel wide from around the edges of the images. Any subsequent field measurements of area were calculated from 260098 pixels rather than 262144 pixels. The use of filtration techniques to remove noise is discussed in greater detail in section 2.24.

Sometimes large features had not been properly discriminated. For instance quartz minerals which had been cut perpendicular to

their basal section were sometimes classified into the same category as voids. If the size of the feature meant it could not be removed using filtration techniques manual editing was used instead.

#### 8.4 Result of quantification

Field measurements were derived from each image. The results are presented in tables 8.2 to 8.4.

| Feature         | M127IA, % abundance | M127IB, % abundance | M127IC, % abundance | Average, % abundance |
|-----------------|---------------------|---------------------|---------------------|----------------------|
| Coarse material | 35.15               | 27.23               | 25.41               | 29.26                |
| Void            | 16.91               | 14.41               | 16.28               | 15.87                |
| Fine material   | 47.94               | 58.36               | 58.30               | 54.87                |

Table 8.2 Abundance of coarse material, fine material and void in M127IA, M127IB and M127IC (PM buried A horizon)

| Feature         | M21IA, % abundance | M21IB, % abundance | M21IC, % abundance | Average, % abundance |
|-----------------|--------------------|--------------------|--------------------|----------------------|
| Coarse material | 29.12              | 22.68              | 23.14              | 24.98                |
| Void            | 11.21              | 13.50              | 10.50              | 11.74                |
| Fine material   | 59.66              | 63.74              | 67.16              | 63.52                |

Table 8.3 Abundance of coarse material, fine material and void in M21IA, M21IB and M21IC (top of soil accumulation)

| Feature         | M504IA, % abundance | M504IB, % abundance | M504IC, % abundance | Average, % abundance |
|-----------------|---------------------|---------------------|---------------------|----------------------|
| Coarse material | 34.48               | 35.13               | 34.79               | 34.80                |
| Void            | 19.27               | 24.72               | 26.21               | 23.53                |
| Fine material   | 44.84               | 40.15               | 39.00               | 41.33                |

Table 8.4 Abundance of coarse material, fine material and void in M504IA, M504IB and M504IC (Iron Age buried A horizon)

The average abundance of coarse and fine material was changed into a c/f ratio by summing the abundances and calculating the percentage of the total. This gave the following results;

M21 c/f ratio 28:72

M127 c/f ratio 35:65

M504 c/f ratio 46:54

These ratios are not the same as the subjectively determined ratios. Discrepancy was expected because the field of view, used in the image analysis, excluded coarse material above a certain size. The results confirm that the higher c/f ratios are associated with the earlier soils.

The abundance of voids, in the size range measured, is highest in the prehistoric soil (M504), intermediate in the PM soil (M127) and lowest in the unburied soil (M21). This is the relationship expected but had not been clearly demonstrated using a subjective analysis.

A large number of individual voids were measured in each slide, 1394 from M21, 970 from M127 and 1088 from M504. The size distribution of voids in each sample was positively skewed (table 8.5).

| Sample | Skewness | Equation   |
|--------|----------|--|
| M21    | 0.76     | $\text{skewness} = \frac{3(\text{mean} - \text{median})}{\text{standard deviation}}$ |
| M127   | 0.82     |  |
| M504   | 0.75     |  |

Table 8.5 Skewness values for voids measured in M21, M127 and M504

Fig 8.1 illustrates the abundance of voids in different size ranges. The abundance of smaller voids makes it difficult to recognise any trends in the data. Another analysis of voids was carried out. The voids measured in each sample were divided into 2 components, voids with an area larger than 160 pixels and voids with an area less than 160 pixels.

Fig 8.2 shows the abundance of voids in each size range and the total number of voids measured. In all three samples there are fewer larger voids than small voids but the larger voids contribute more to the total porosity of the sample. In M21 there is very little difference between the two groups. However in the samples from M127 and M504 voids composed of more than 160 pixels contribute to over half the area of voids in the size range measured.

Fig. 8.1 Number of voids in different size categories in M21c, M127c and M504c

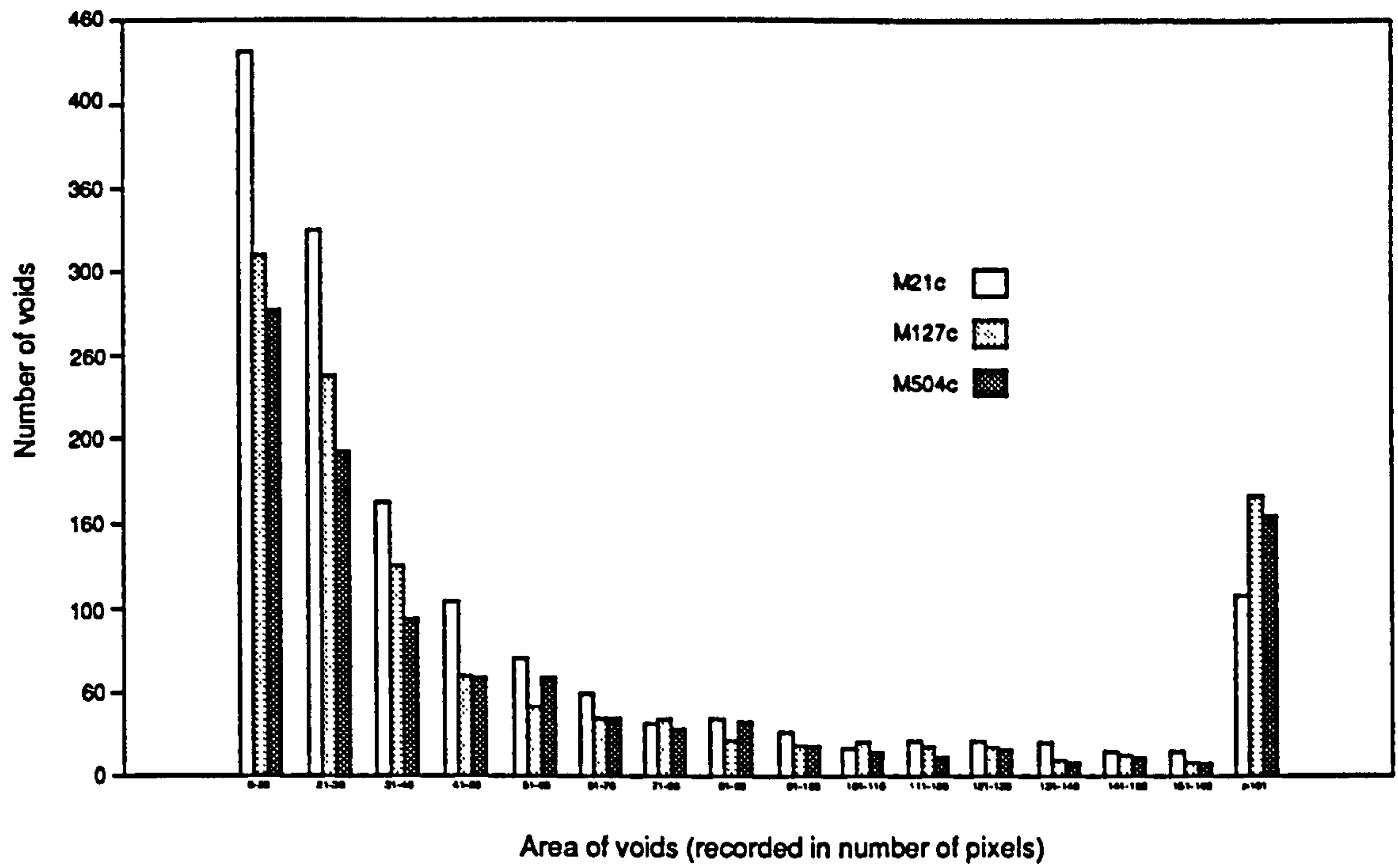
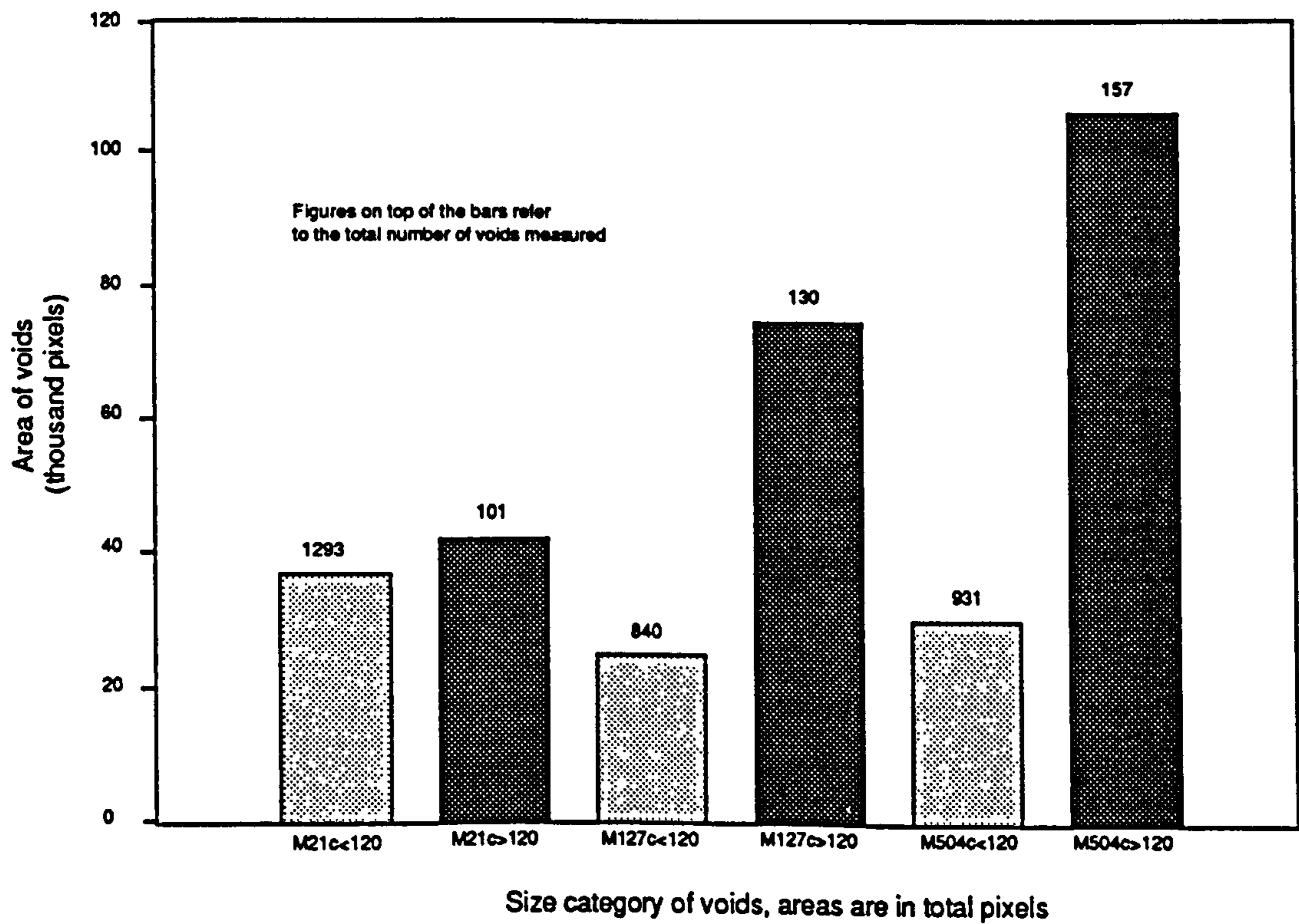


Fig. 8.2 Total area of voids measured above and below an area of 160 pixels





A formfactor was calculated for the individual voids. This used the following equation (discussed in section 2.22).

$$\frac{4\pi*Area}{Perimeter^2}$$

The data were divided as before and a separate analysis was carried out on voids which were smaller and greater than 160 pixels.

**Formfactor of voids with an area greater than 160 pixels.**

All the voids are highly irregular in shape with average values of 0.19 and 0.188 for M21 and M127 respectively. The average for M504 was slightly lower, 0.144. A Mann Whitney test was used to determine if these differences are significant. Using a 0.05 level of significance the test produced p values of 0.0028, for a comparison of M21 and M504, and 0.002, for a comparison of M127 and M504. In both these cases the null hypothesis could be rejected and significant difference between the samples accepted. The results of a Mann Whitney test carried out on M21 and M127 showed no significant difference could be determined between the samples.

**Formfactor of voids with an area less than 160 pixels.**

The voids in this group were irregular in shape although less so than the voids greater than 160 pixels. The mean values for M21, M127 and M504 are 0.38, 0.36 and 0.35 respectively. Using a Mann

Whitney test and 0.05 level of significance no significant difference between M127 and M504 was proved. There is a difference between M21 and the formfactor of voids measured in the other samples.

The results from this group of voids are not used in any interpretation because further research needs to be carried out to determine;

1. The effect of spatial image resolution on the results of shape measurement of objects.
2. The characteristics of void populations measured at different scales of observation.

The results of the morphometric analysis should be judged by making a comparison with results from a subjective analysis. Figs. 8.3, 8.5 and 8.7 show photographs of images from M21, captured using PTL and contrast stretched. It is difficult to distinguish between voids and coarse minerals, particularly quartz. Even with the use of polarised light it is often not possible to make accurate assessments of void abundance. The abundance categories used in the International Thin Section Handbook (Bullock et al. 1985) reflect this difficulty.

Figs. 8.4, 8.6 and 8.8 show the same images but this time with the voids highlighted as red overlays. This makes it easier to make accurate estimates of abundance but is still limited by the

accuracy of the analyst. A comparison of the images in figs. 8.3 to 8.14 illustrates the difficulties of using only a subjective approach to make detailed comparison of large numbers of thin sections.

The morphometric capabilities of image analysis allows more accurate measurements to be calculated for features of interest. This is of particular importance in a situation such as Lairg where contrasts between contexts of different age and location are of interest. The results of the study from Lairg are limited because of the time taken trying to get the specialised shape application software working. When this was abandoned the limited facilities offered by IDRISI were utilised. Consequently the results are not as comprehensive as they would have been if a software package like PC Image (Foster Findley) had been used.

The following chapter examines the results of the thin section analysis and discusses conclusions based upon results from the whole site. The quantitative results presented in this chapter are discussed as part of the evidence for environmental change since the prehistoric in section 9.5.

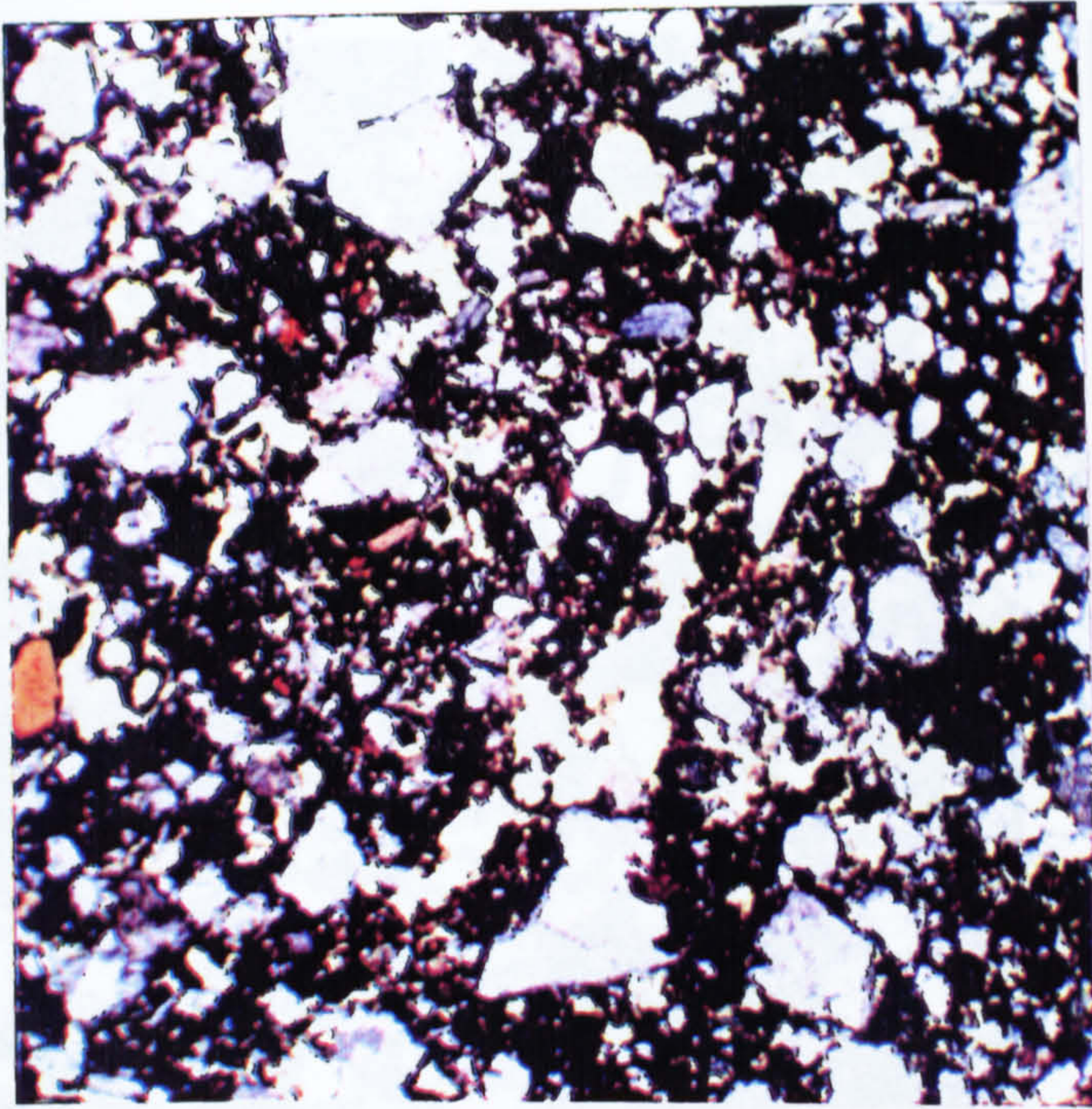


Fig. 8.3 M211, PTL, red 49-155, green 44-184, blue 34-150, FL 3.8mm

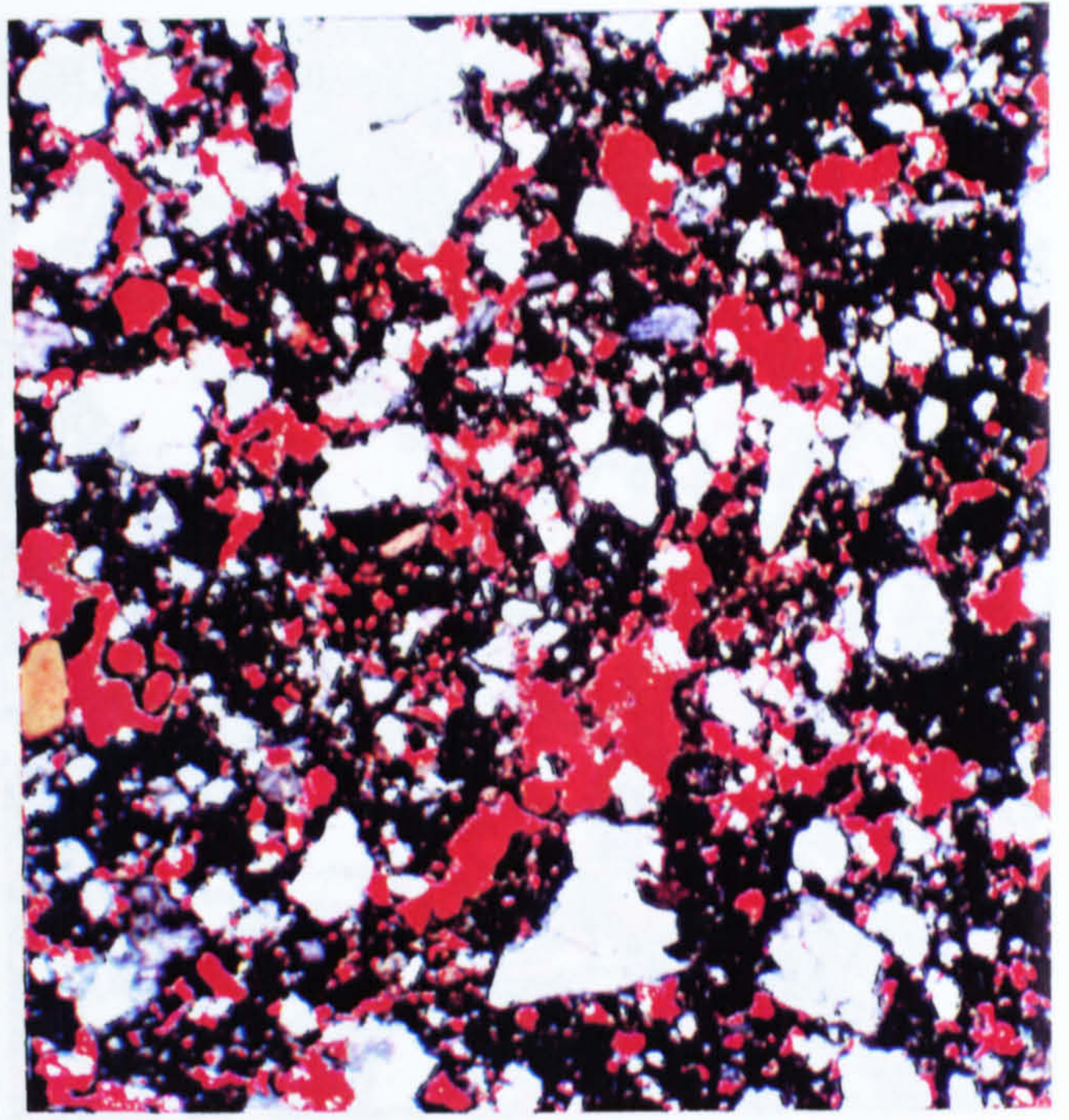


Fig. 8.4 as fig. 8.3 but voids are covered with a red overlay,

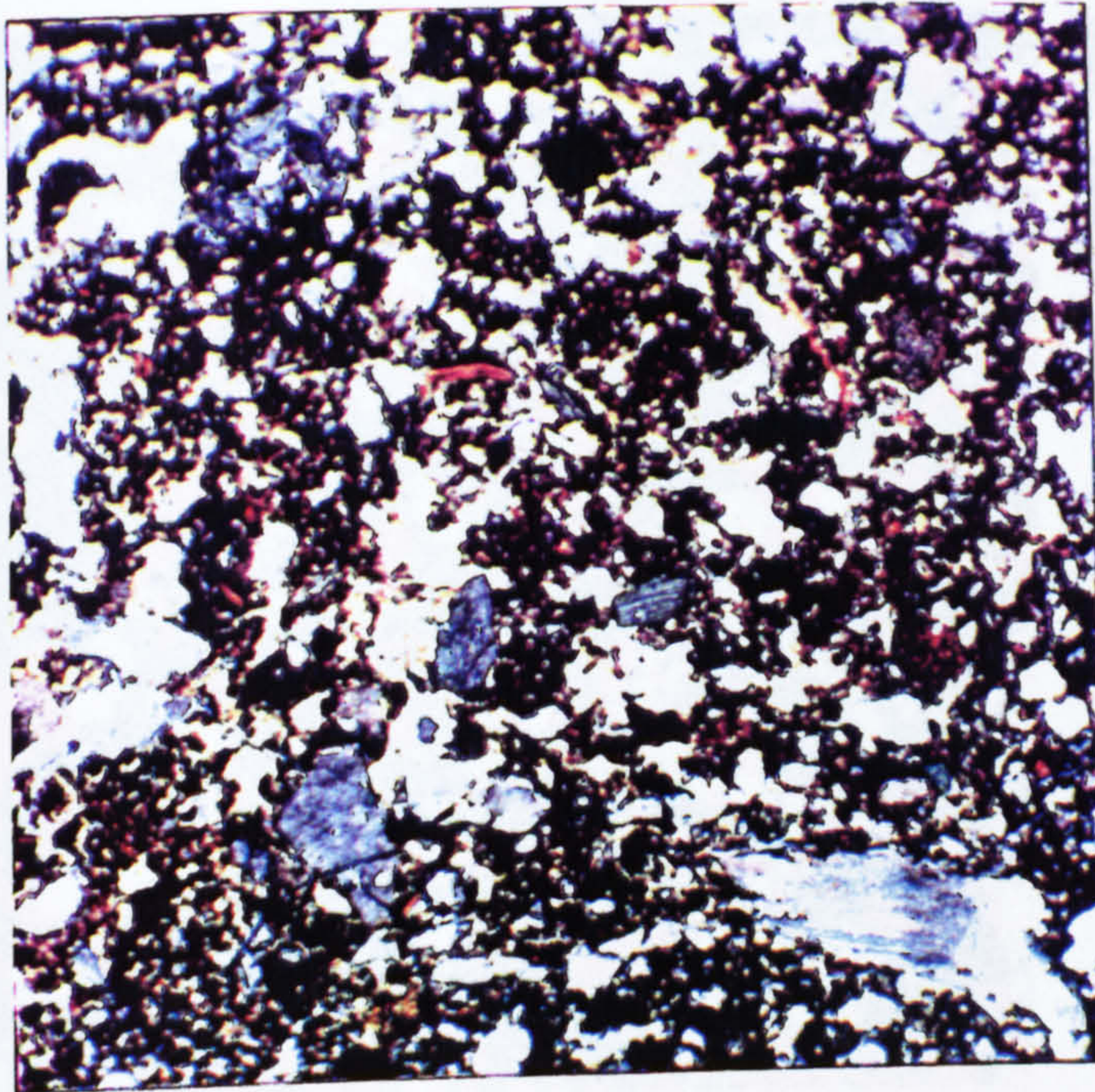


Fig. 8.5 M212, PTL, red 58-189, green 26-162, blue 33-156, FL 3.8mm

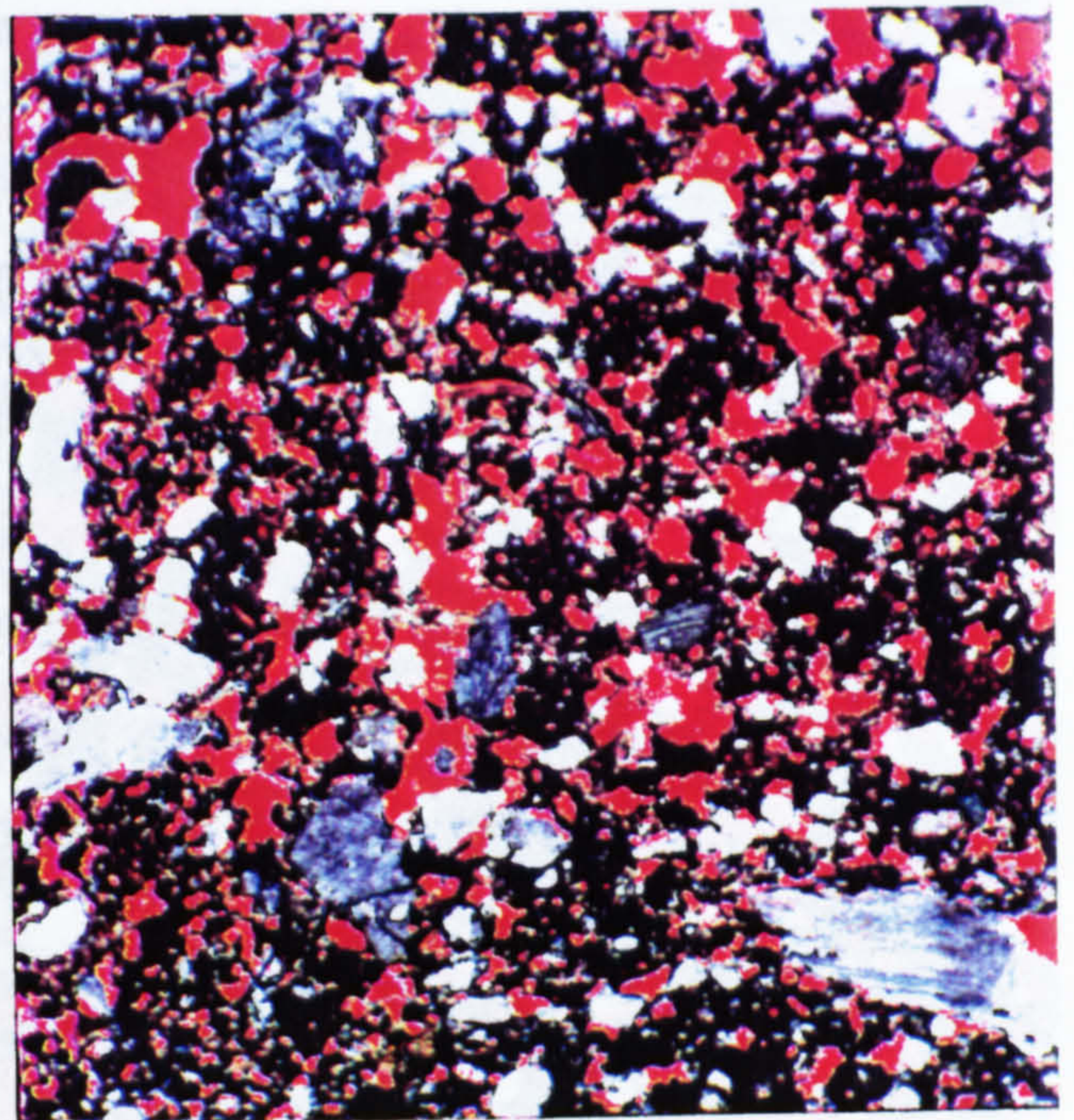


Fig. 8.6 as fig. 8.5 but voids are covered with a red overlay

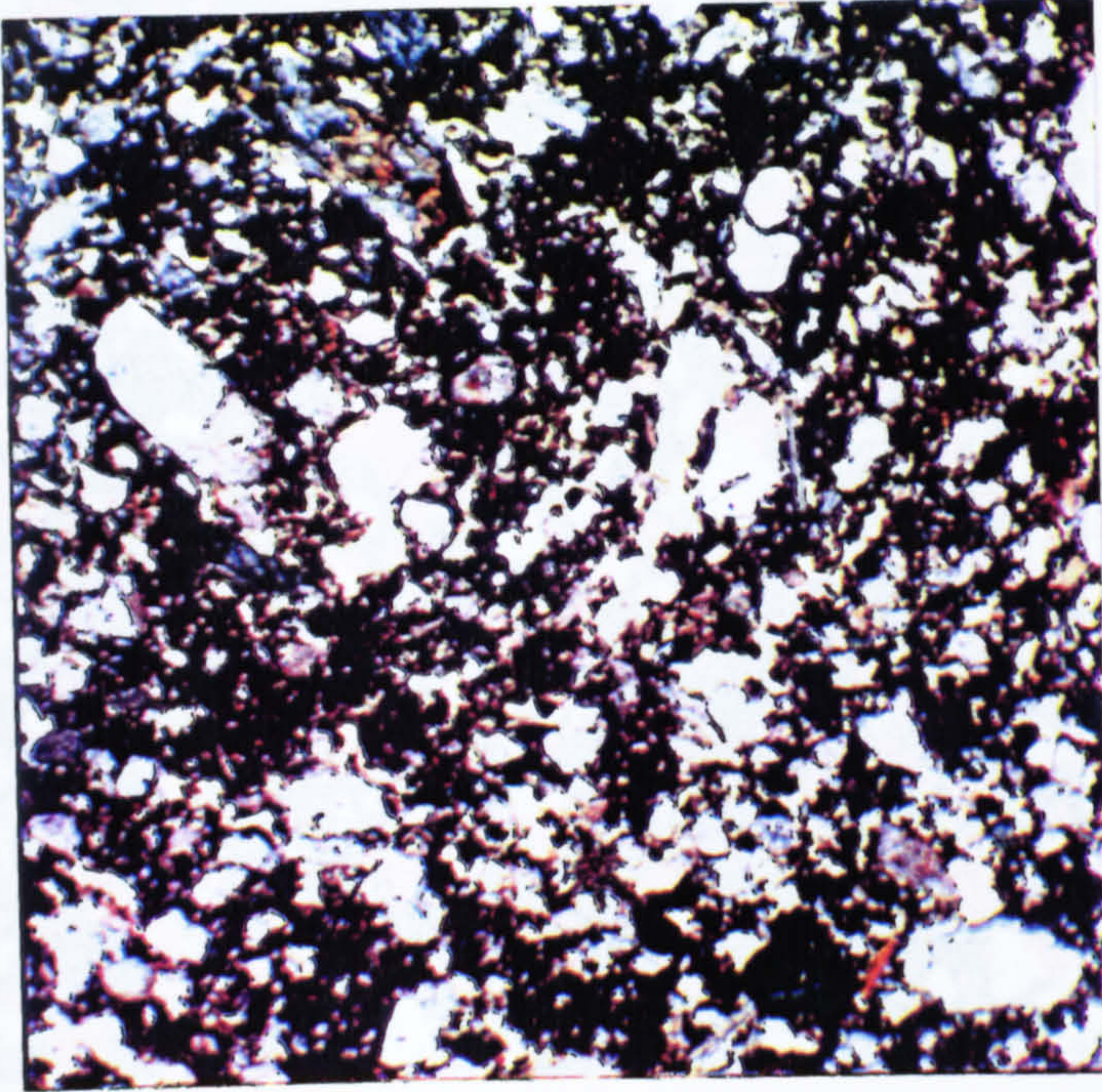


Fig. 8.7 M213, PTL, red 53-165, green 23-149, blue 42-160, FL 3.8mm

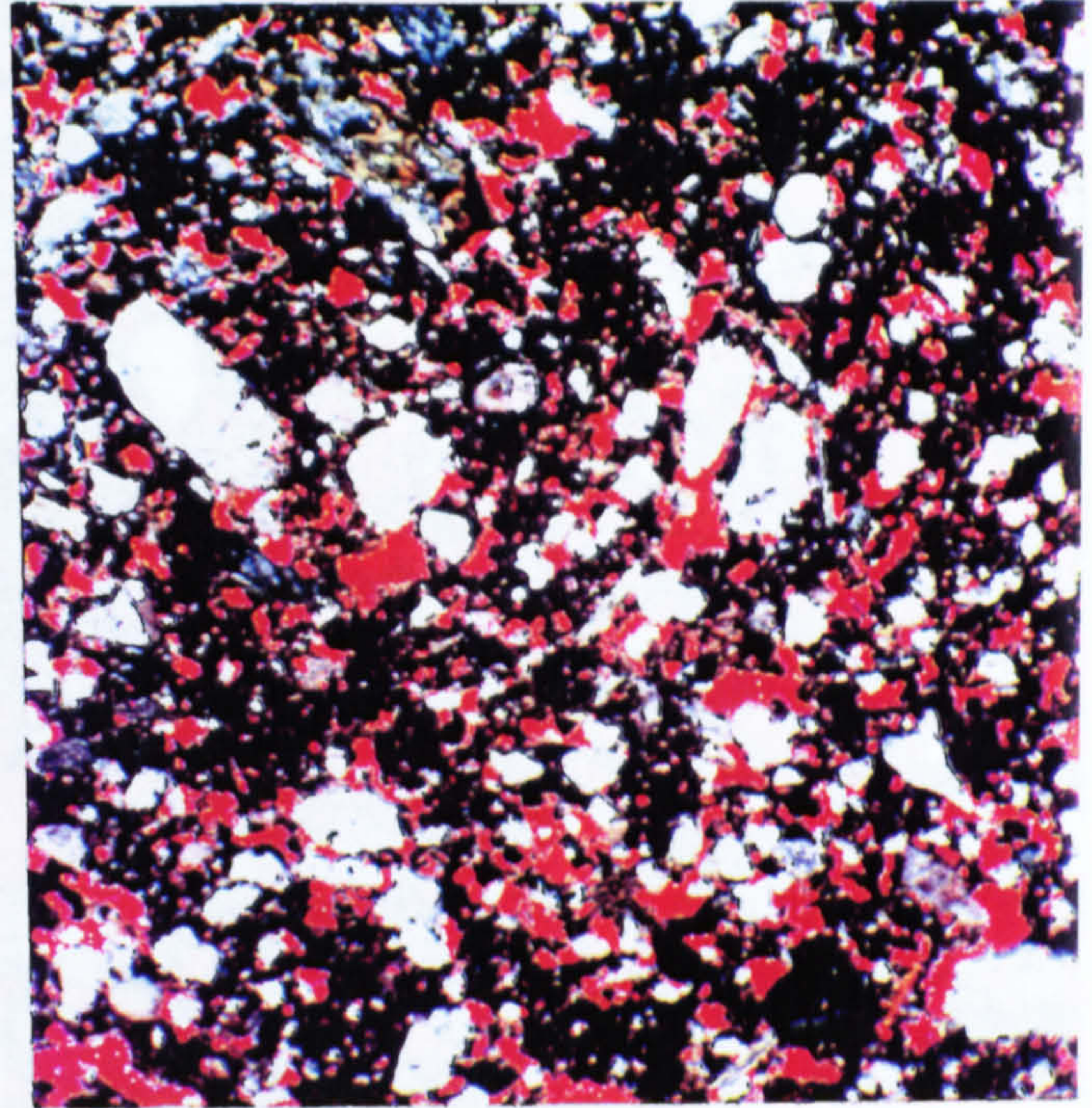


Fig. 8.8 as fig. 8.7 but voids are covered with a red overlay,

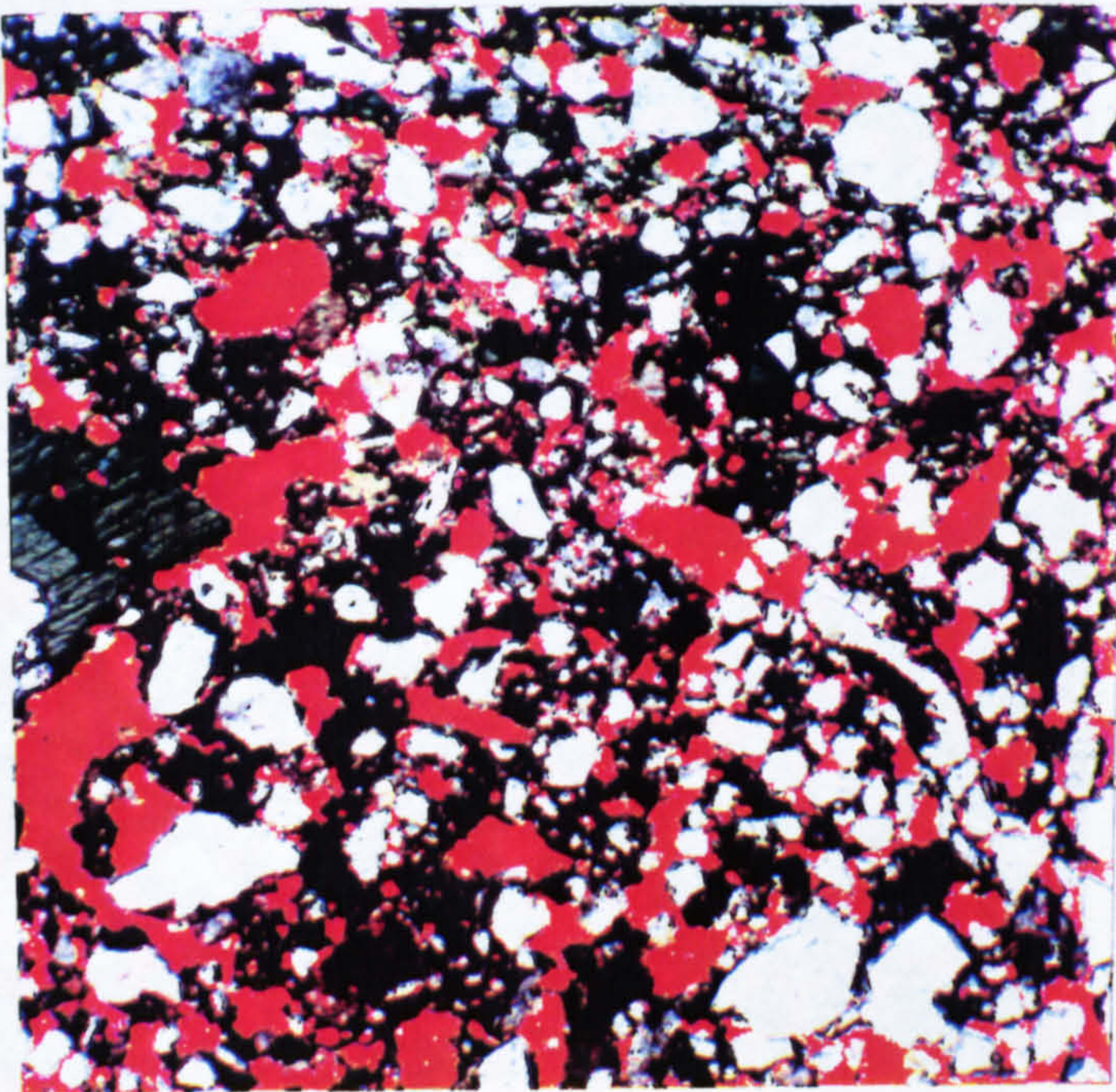


Fig. 8.9 M1271, PTL, red 60-189, green 27-159, blue 44-162, voids are covered by a red overlay, FL 3.8mm

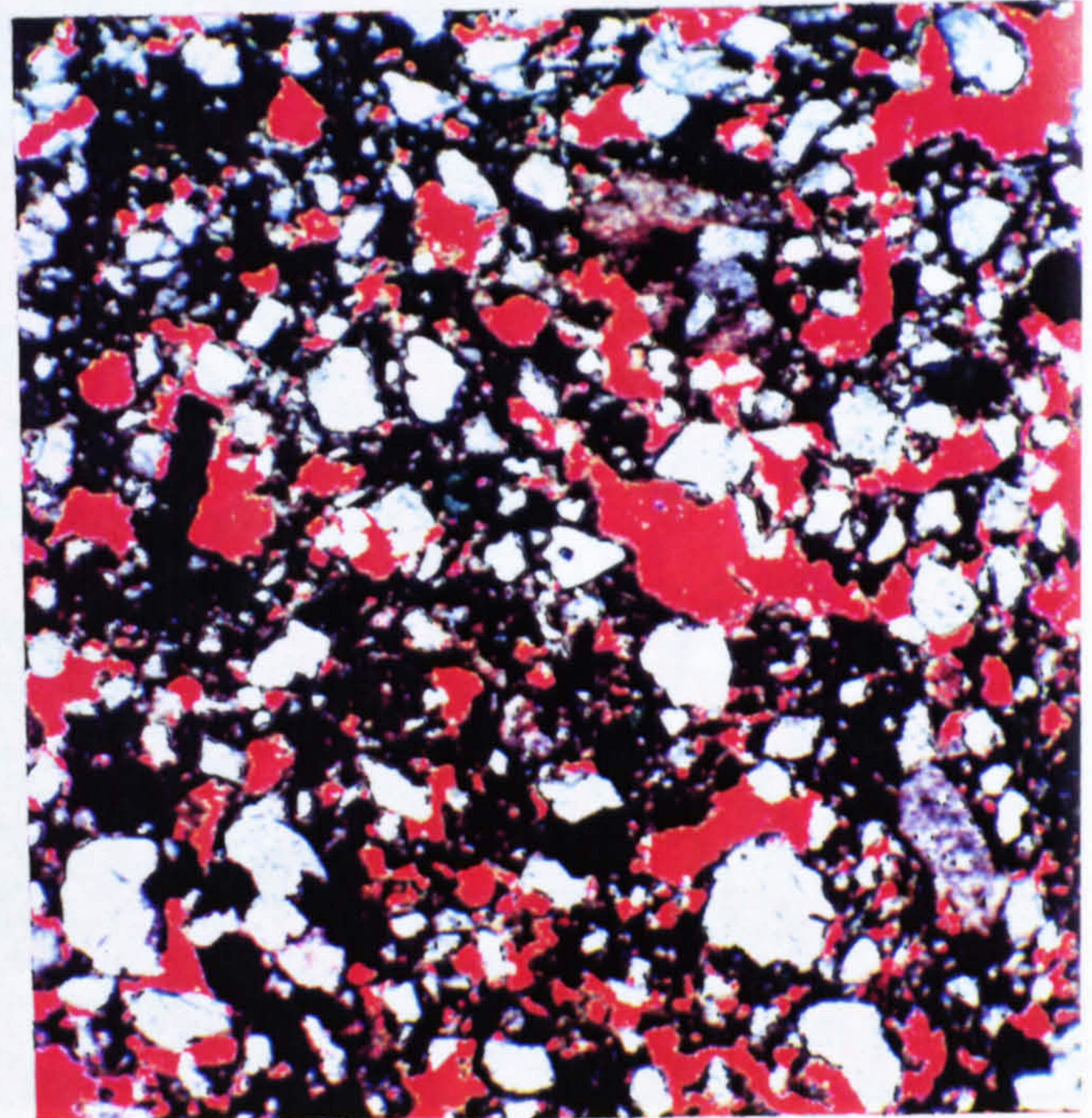


Fig. 8.10 M1272, PTL, red 49-175, green 25-161, blue 34-164, voids are covered by a red overlay, FL 3.8mm

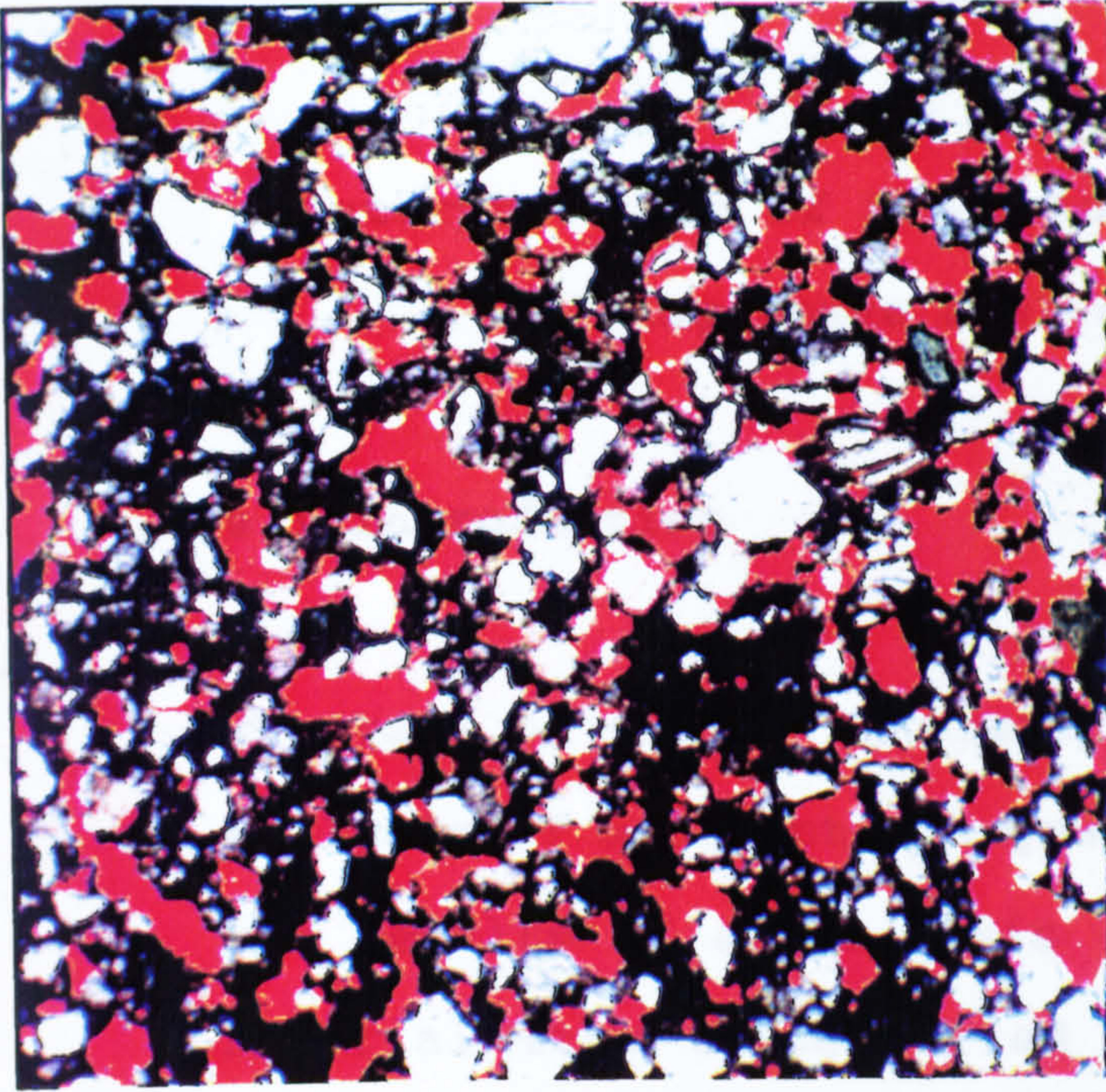


Fig. 8.11 M1273, PTL, red 47-167, green 25-156, blue 38-182, FL 3.8mm

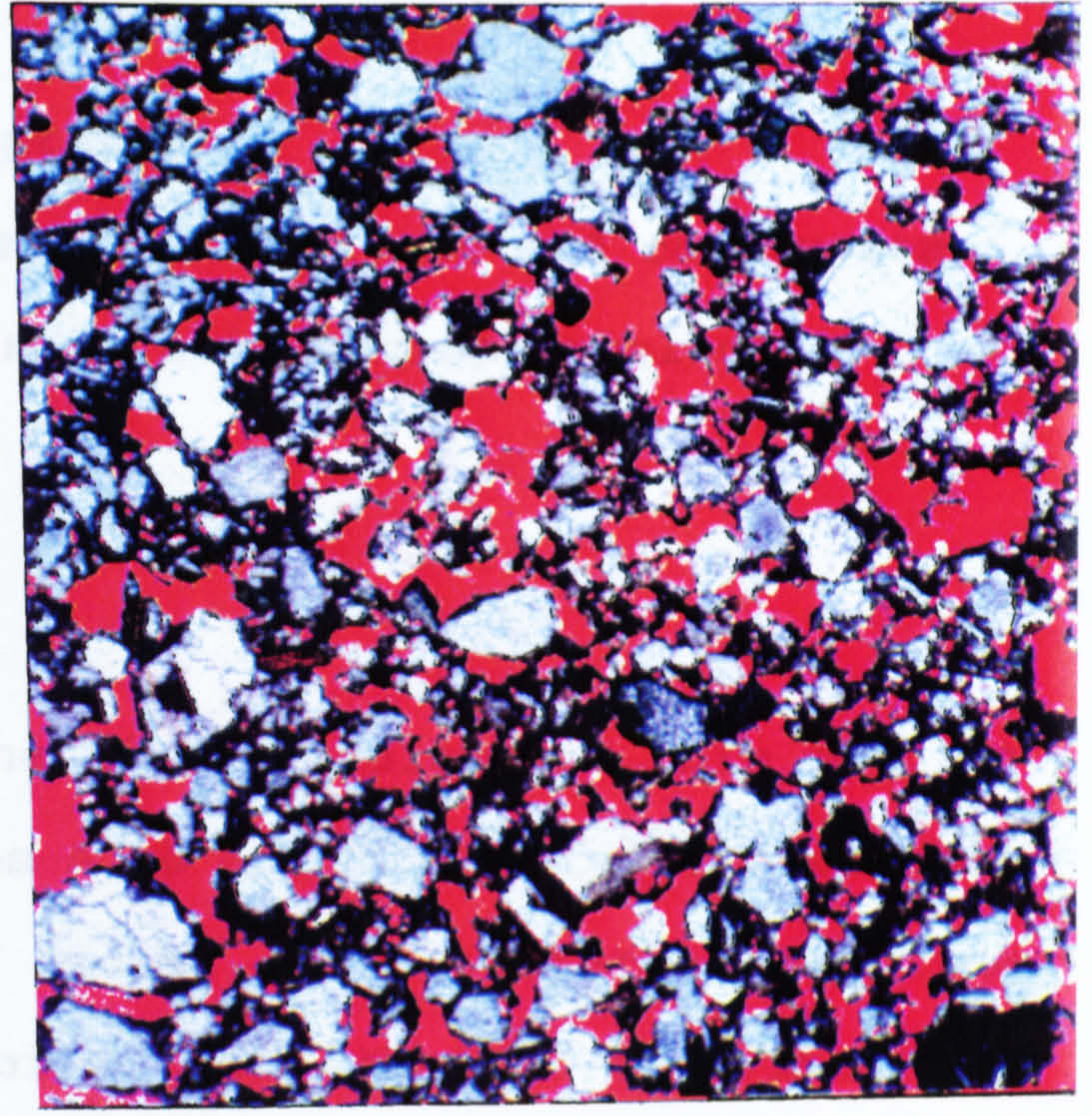


Fig. 8.12 M5041, PTL, red 62-158, green 37-142, blue 37-137, FL 3.8mm

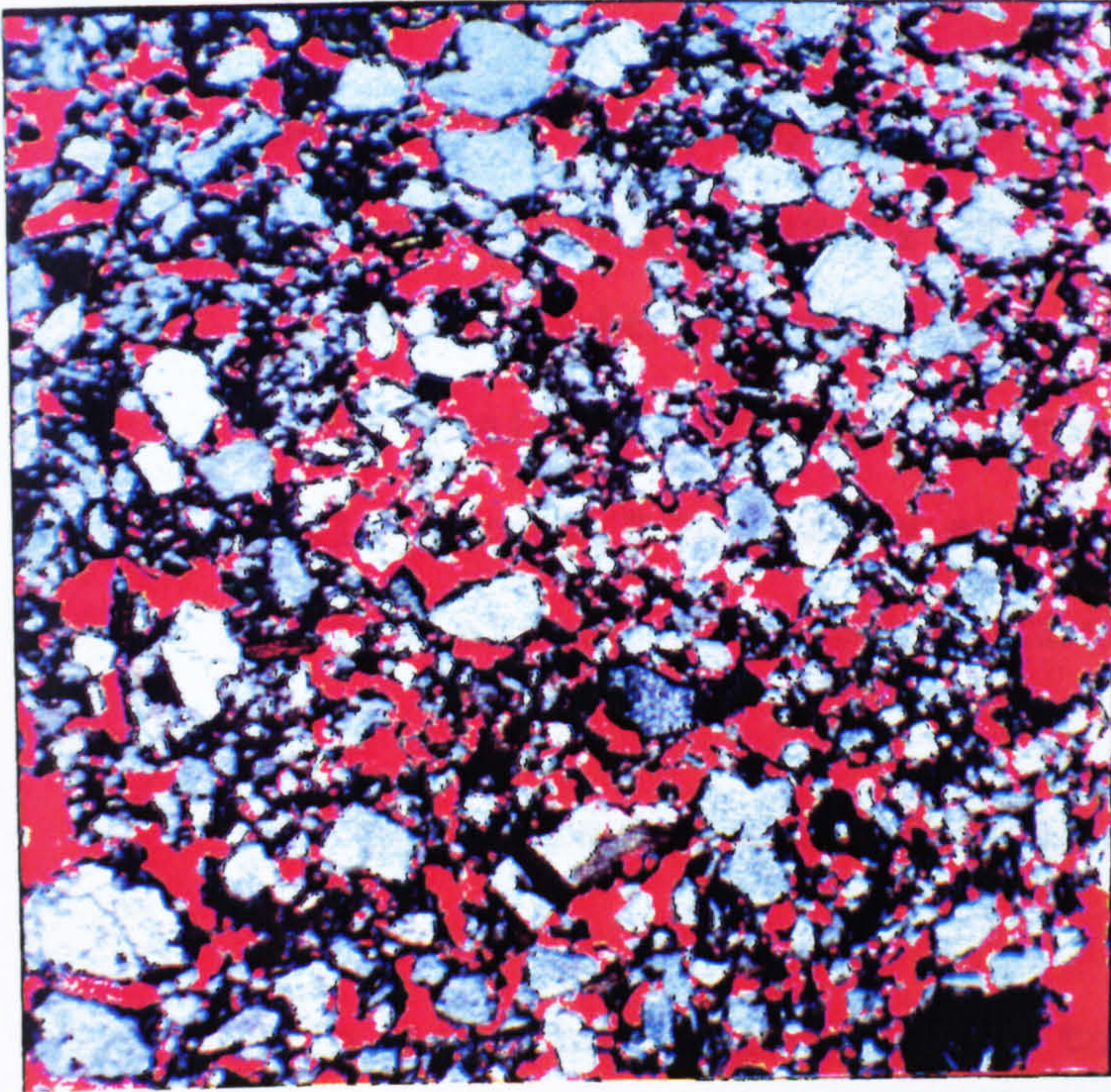


Fig. 8.13 M5042, PTL, red 66-157, green 45-154, blue 67-189, voids are covered by a red overlay, FL 3.8mm

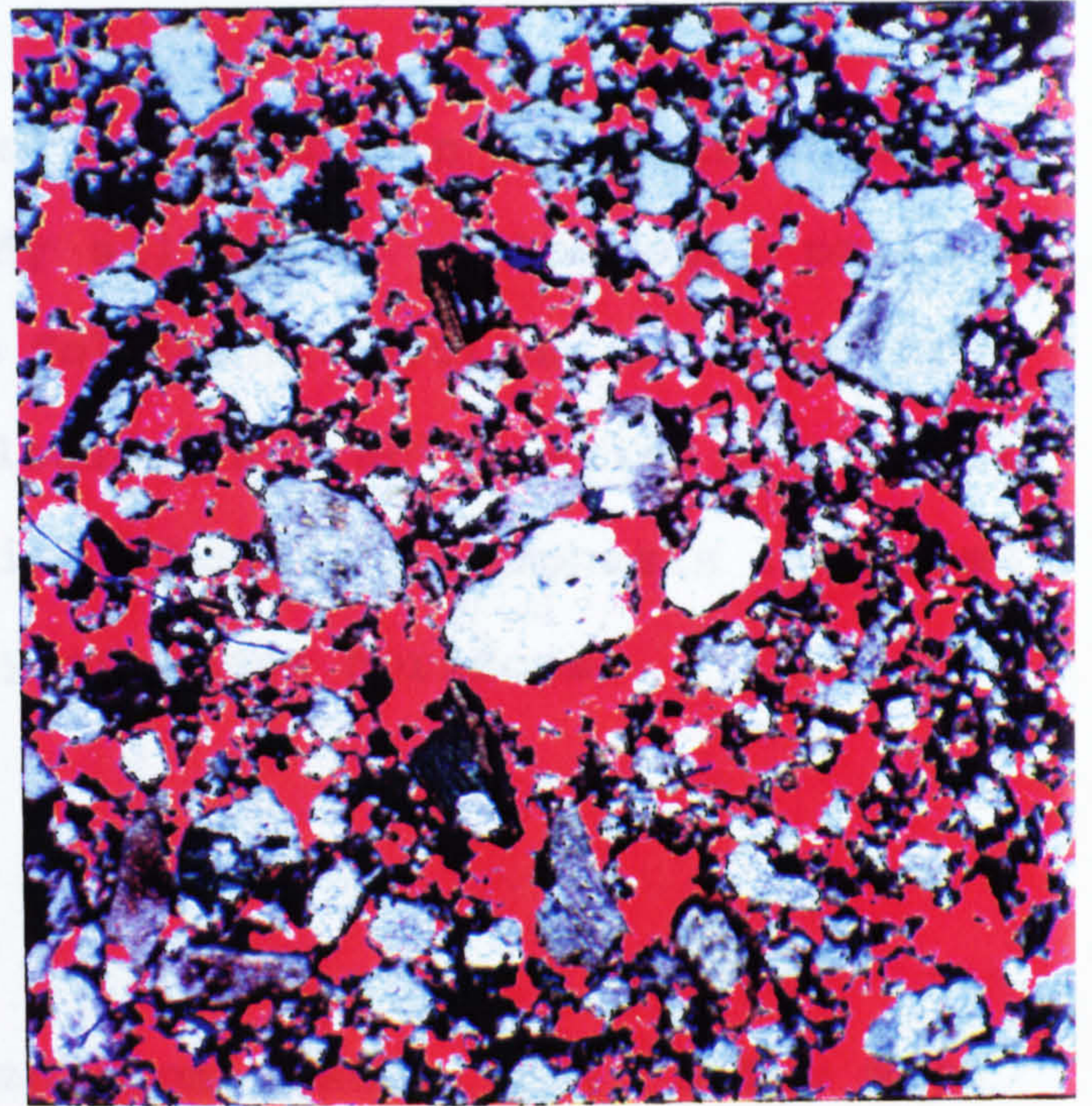


Fig. 8.14 M5043, PTL, red 66-157, green 45-154, blue 67-189, voids are covered by a red overlay, FL 3.8mm

## **Chapter 9**

### **Interpretation of the thin section analysis and conclusion applying image analysis to soil micromorphology**

#### **9.1 Introduction**

Chapters 5, 6 and 7 present the field results and thin section analysis of monuments in groups A, B and C. Chapter 8 discusses the results of an analysis of voids, coarse material and fine material from three buried soils. This chapter describes the conclusions of thin section analysis and evaluates the usefulness of the image analysis techniques, described in chapter 2, to the soil micromorphological study carried out at Lairg.

The number of samples taken for thin section analysis at Lairg offered an opportunity to study all parts of the soil profile using soil micromorphology. The following sections are based upon a discussion of the micromorphological characteristics of glacial till, buried B horizons and buried A horizons, emphasis is placed on the effect of human activity on these horizons.

#### **9.2 Analysis of glacial till.**

Thin section samples were taken from glacial till below M504, M505 and M975. The characteristic feature of the glacial till at Lairg is the abundance of cappings observed in thin sections.

These are present on the tops of rock fragments or form link cappings within the groundmass (figs. 9.1 and 9.2).

The formation and interpretation of cappings is discussed by Van Vliet-Lanoe (1985), Courty et al (1989) and Fitzpatrick (1983). When cappings are found at depth in the profile, for instance in glacial till, they form as a result of periglacial conditions and are typical of freeze thaw activity. Mechanisms including electrophoresis and cryo-suction are believed to contribute to their formation. The percolation of snow meltwater into the soil profile promotes the sorting of coarse and fine material. The meltwater has high dielectric properties allowing dispersion of weakly stabilised aggregates. This can cause internal macro and micro erosion within the soil. Van Vliet-Lanoe (1985, pg. 131) calls the process of movement of fine particles within the soil internal colluviation. Catt (1991) suggests that silty cappings on stones and particles are among the most reliable climatic indicators found in the soil.

Cappings are a common feature of soil that has been affected by periglacial action. Cappings have been identified in Scotland in soils of the Ettrick association (Romans and Robertson 1975a) and in the Alpine soils of North East Scotland (Romans et al. 1966, Romans and Robertson 1974). Romans and Robertson (1974) examined the relationship between depths of cappings and altitude of sites. They concluded that development is strongly related to latitude and altitude. There is some discrepancy with their results and other published data. Romans and Robertson (1974)



Fig. 9.2 Undisturbed link capping within groundmass,  
M504, S5, PPL FL8mm

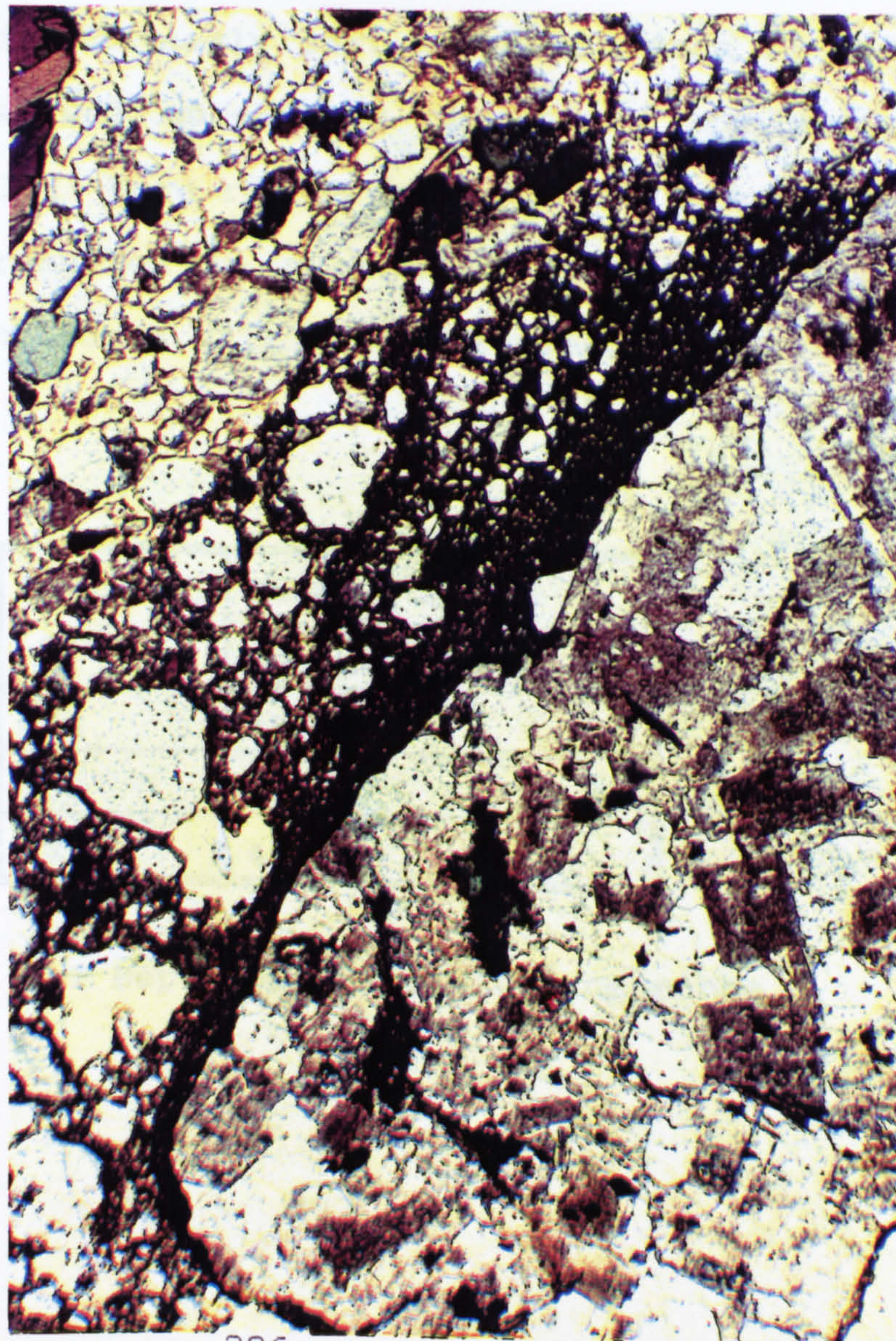
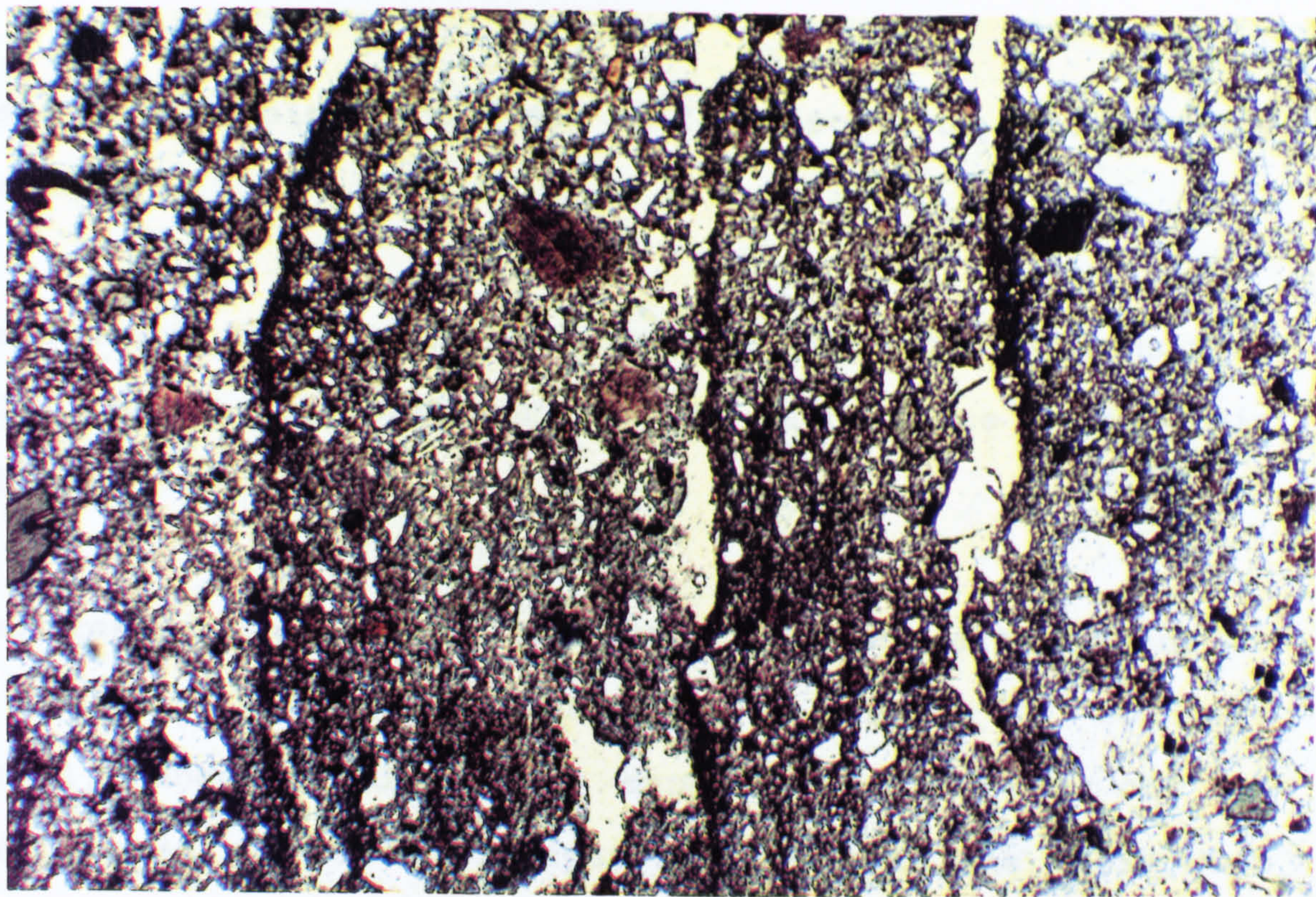


Fig. 9.1 Undisturbed capping overlying a  
rock fragment M504, S5, PPL, FL8mm

suggests that cappings would not be found south of latitude 50°N and report;

"The absence of the silt droplet form in soil thin sections from profiles sited on Dartmoor is in accordance with this expectation" (pg. 501).

However research now shows that silt cappings are present on sites as far south as Chysauster, Penzance, in Cornwall (Macphail, unpublished). Silt cappings form part of the microfabric in subsoils (fragipan horizons) at the Chysauster site. Strongly formed examples are present but fragmentation had often occurred. Their formation is attributed to annual freeze thaw conditions in the early part of pollen zone II and their disruption to renewed sub-arctic conditions and periglacial activity in zone III. More recent annual freezing and thawing in pollen zone IV resulted in a generally massive fabric, with weakly formed continuous silt and clay pans, developing in all the subsoils.

| Monument | Depth (cm) to cappings from old ground surface |
|----------|--|
| 504      | 45   |
| 505      | 40   |
| 975      | 45   |

Table 9.1 Depth of undisturbed cappings

The subsoils at Lairg have been subject to periglacial activity resulting in the formation of undisturbed cappings and link cappings in the glacial till (figs. 9.1 and 9.2). The depths of undisturbed cappings, observed at the Lairg site, is similar under the three monuments sampled (table 9.1). The average depth is approximately 43cm.

Cappings are fairly robust features in the soil and can persist even when the soil is disturbed. Fragmented cappings are present throughout some B horizons and have sometimes been incorporated into A horizons. The presence of disturbed cappings in B horizons is thought to represent biological processes rather than anthropogenic disturbance (section 9.5). The presence of fragmented cappings in A horizons is thought to be the result of intensive agricultural activity (section 9.5).

Coatings are only present in the glacial till where amorphous material, probably sesquioxides, have been translocated from surface horizons. Under M504 the top of the glacial till is impregnated with ferruginous compounds forming an indurated sub-surface horizon. Thin section analysis shows that the ferruginous coatings are most abundant in the top of the glacial till where there are undisturbed cappings present. It is possible that the concentration of fine sediment, which forms the cappings, effects the downward movement of sesquioxides. Similar undisturbed cappings and translocated ferruginous material is present under M505 and M975.

Cappings are useful features to help determine the origin of deposits. For instance the orange material that forms part of the LP hut circle wall (M64) was identified as originating from a Bs horizon on the basis of the abundant fragmented cappings and the pelley microstructure (section 5.2.8).

### 9.3 Development of Bs horizons

The analysis of thin sections, from various parts of the site, show there is considerable micromorphological variation in Bs horizons. This variation appears to be caused by external and internal processes effecting the soil system creating polygenetic soils. To summarise 4 different types of sesquioxide enrichment can be identified at Lairg;

1. Poorly sorted friable Bs horizons buried by prehistoric monuments.
2. Bs horizons where sesquioxide enrichment results in the formation of amorphous (possibly monomorphic) coatings.
3. Well sorted friable Bs horizon buried by Post Medieval monuments.
4. Sesquioxide enrichment at the base of a partially gleyed A horizon.

This section discusses the significance of the different types of Bs horizon to the genesis of the soils at Lairg. Firstly the literature is reviewed and different arguments for the formation of Bs horizons is presented. This is followed by an account of the evidence from Lairg and a discussion of the results.

### 9.3.1 Morphology of Bs horizons

De Connick and Righi (1983) use two terms to describe organic material found in spodic horizons. Monomorphic organic material forms continuous coatings, bridges spaces between coarser material, and has a uniform appearance. Polymorphic organic material is present in the form of pellets.

Various types of spodic horizon can be distinguished by micromorphological characteristics, two of these include friable and cemented horizons. Friable spodic horizons are characterised by pellets consisting of polymorphic organic material often forming parts of aggregates. Scanning electron (SEM) images (De Connick and Righi 1983) indicate that the morphology of the aggregates is heterogenous, composed of mineral material, silt particles and phytoliths, and organic compounds. Cemented horizons are characterised by coatings of monomorphic organic material (*ibid.*). Sometimes regions of the cemented horizons are friable and contain roots. If this occurs, then polymorphic organic material can also be present.

There have been a number of theories to explain the origin of pellets in friable Bs horizons. Firstly the pellets might be the result of biological activity. This might involve either, ingestion of organic material by soil fauna and subsequent excretion of material with a pelley morphology, or organic material being comminuted into small pieces and transformed into dark pellets (*ibid.*). In support of this theory De Connick and Righi (1983) point out that indications of animals in Bs horizons are numerous. Roots are commonly found in Bs horizons but it is rare for there to be any macro sized residues. Faunal reworking of the roots is suggested. The presence of small angular plant remains mixed with polymorphic organic material and a fine mineral fraction might be produced by an active microfauna (Babel 1975).

Other hypotheses concerning the formation of a pelley microstructure include physico-chemical adsorption of soluble organic compounds on Fe and Al hydroxides (Boudot and Bruckert 1978, Bruckert and Selino 1978). De Connick and Righi (1983 pg 407) state that " this theory fails to explain the presence of the large amount of small discrete plant remains in B horizons and the fate of the roots present. It also does not explain the low MRT of the organic carbon ".

Fitzpatrick (1983) suggests that activity of arthropods is unlikely to have caused the pelley microstructure because it would require a high level of biological activity for which there

would not be enough food. The precipitation and flocculation of oxides and humus in a porous medium might be responsible (ibid.).

### 9.3.2 Morphology of Bs horizons at Lairg

Thin section samples from Bs horizons were taken from 5 monuments at the Lairg site, M62, M504, M505, M975 and M1069. One sample was also taken from the lower part of the A horizon (C.8027, section 5.9.3) buried by M75/4. Context 8027 was interpreted in the field as showing some indications of localised accumulation of sesquioxides. In thin section a characteristic feature of this context is numerous channel infillings strongly orientated perpendicular to the surface. The internal fabric of these infillings consists of many orange ovoid pellets measuring approximately  $40\mu\text{m}$  across (fig. 9.3). These pellets are also present in the groundmass (fig. 9.4). The pellets that form channel infillings are the result of reworking of roots. The pellets that form part of the groundmass are either the result of organic rich parts of the soil being reworked or decomposing roots being incorporated into the groundmass. A characteristic feature of the pellets is their strong orange colour. This gives them a similar appearance to pellets observed in Bs horizons on the site and to pellets forming friable structures of Bs horizons described in the literature.

The results from M75/4 suggest that where there is a supply of organic material orange polymorphic pellets can form by biological activity. The orange colour is probably caused by

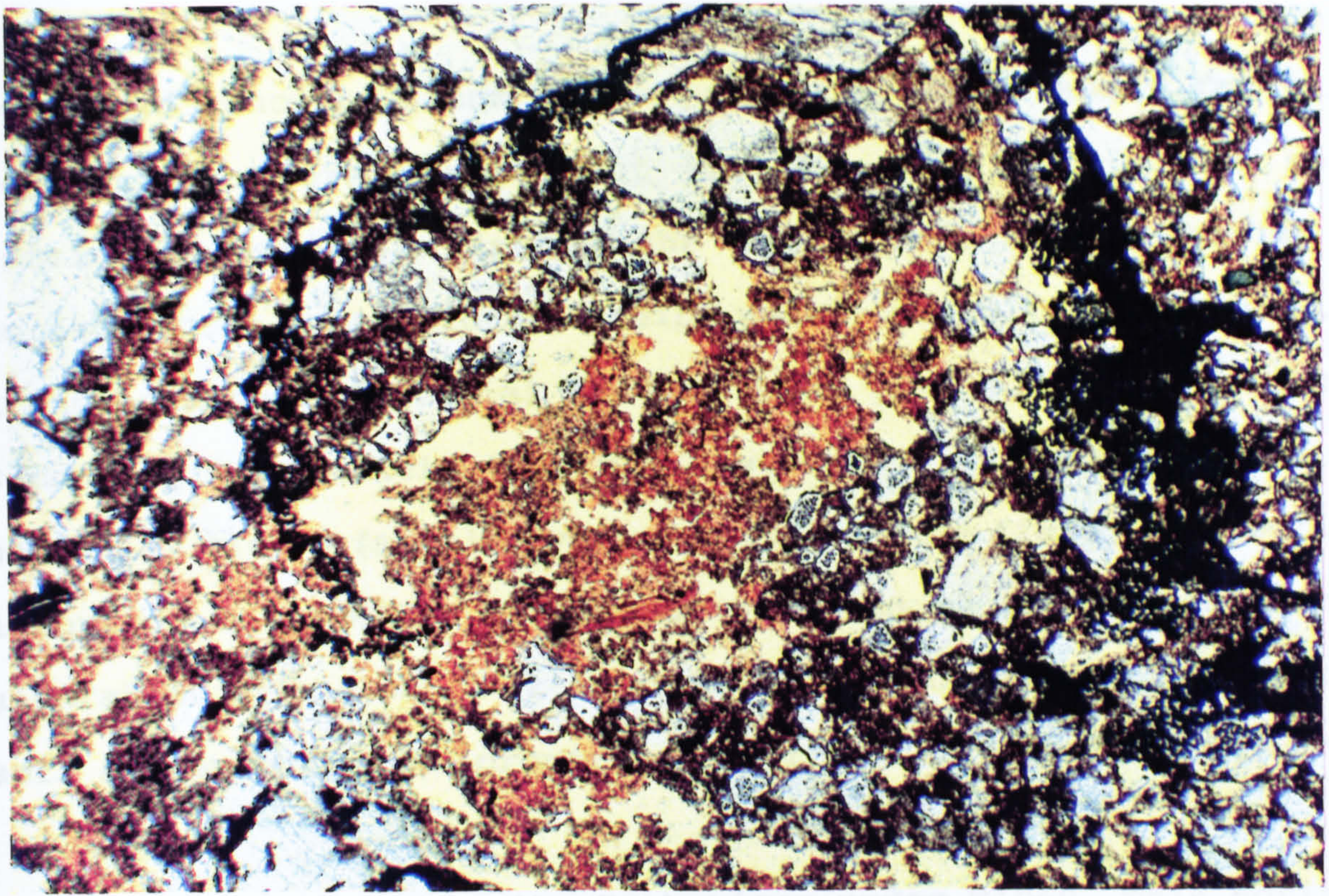


Fig. 9.3 Orange pellets forming the infill of a channel, M75/4, S4, PPL, FL 8mm

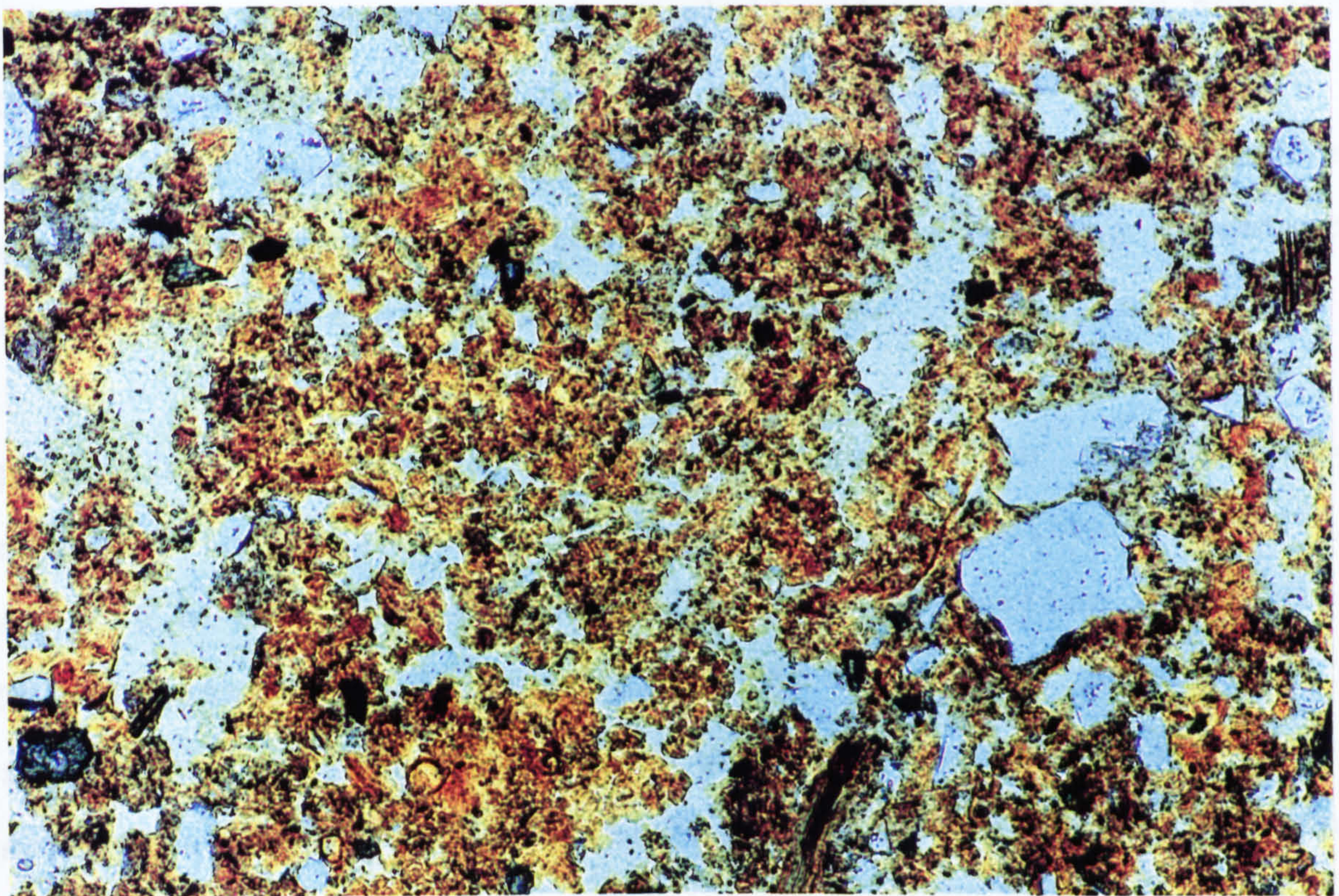


Fig. 9.4 Orange pellets forming areas of the groundmass, M75/4, S4, PPL, FL2mm



localised concentrations of sesquioxides. The reasons for this concentration are unknown but probably result from two soil forming mechanisms. Firstly the upper part of the buried A horizon shows indications of being weakly podzolised, suggesting translocation of material to the lower part of the A horizon. Secondly it is likely that the lower part of the A horizon is partially gleyed (mottles were observed in the field). The buried A horizon below M75/4 is clearly affected by post depositional alteration of the soil. It is an example of dynamic change in the soil system where the properties of the A horizon are altering.

A sample was taken from the Bs horizon under M1069. This horizon is composed entirely of orange pellety material (fig. 9.5). This is the only micromorphological similarity to other Bs horizons. The Bs horizon from M1069 is well sorted and there are no examples of fragmented cappings. Elsewhere, (M62, M504, M505 and M975) Bs horizons are characterised by poor sorting of material and an abundance of fragmented cappings.

There is considerable similarity between the orange pellets observed in the lower part of the buried A horizon under M75/4, and the orange pellets observed in the Bs horizon under M1069. This suggests that it is possible the Bs horizon under M1069 has formed in what was once an A horizon. This would explain the well sorted nature of the material and the absence of any fragmented cappings. Similar micromorphological characteristics are present in Post Medieval buried A horizons. The presence of one or two charcoal fragments in the Bs horizon under M1069 supports this

hypothesis although there are no fine carbonised residues present.

Samples were taken from two types of B horizons dating to the prehistoric period. The Bs horizon below M62 consists of numerous orange ovoid pellets which are in various stages of coalescence (fig. 9.6). The Bs horizon from M504 is composed of a similar material (fig. 9.7). There is no indication of monomorphic coatings in the Bs horizon from M62. In the upper part of the Bs horizon under M504 there are only polymorphic pellets present but at the interface of the Bs horizon and the glacial till amorphous translocated material is present. This material is isotropic, orange (PPL) and dark grey (OIL). This translocated amorphous material closely corresponds to the monomorphic coatings described by De Connick (1980).

The Bs horizon under M505 has a different micromorphology to the other Bs horizons sampled on the site. Translocated material is present in the form of coatings (possibly monomorphic) forming a pellicular grain microstructure. These coatings are similar to the coatings at the interface of the buried Bs horizon and glacial till under M504. The most reflective material (OIL), in the sample from M505, is the fine fraction which forms part of the cappings. This indicates a greater concentration of sesquioxide in areas with a greater abundance of fine material.

The presence or absence of a pellety structure in Bs horizons appears to be correlated with abundance of organic material.

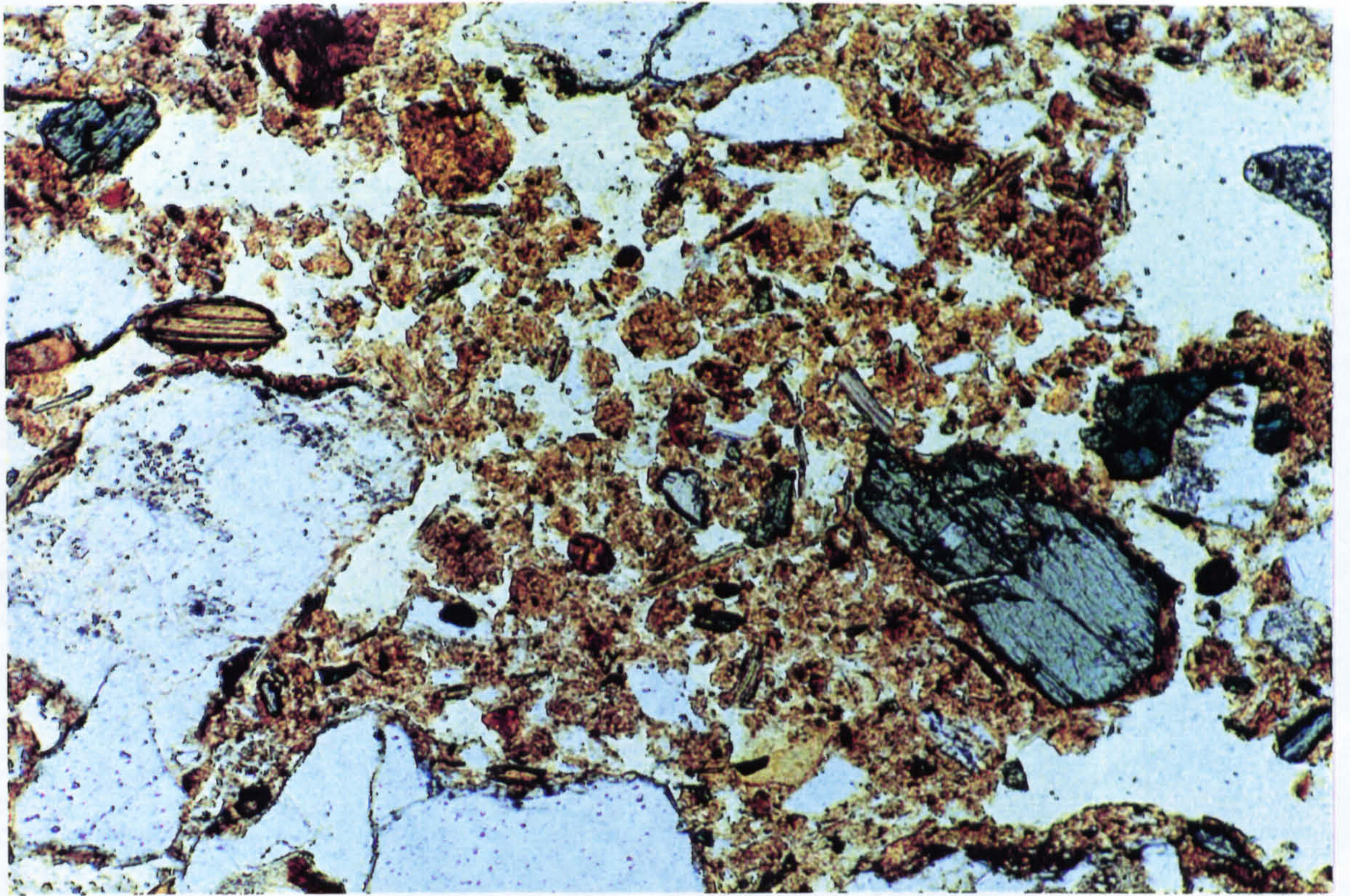


Fig. 9.5 Pelley microstructure in Bs horizon, M1069, S3, PPL, FL 2mm

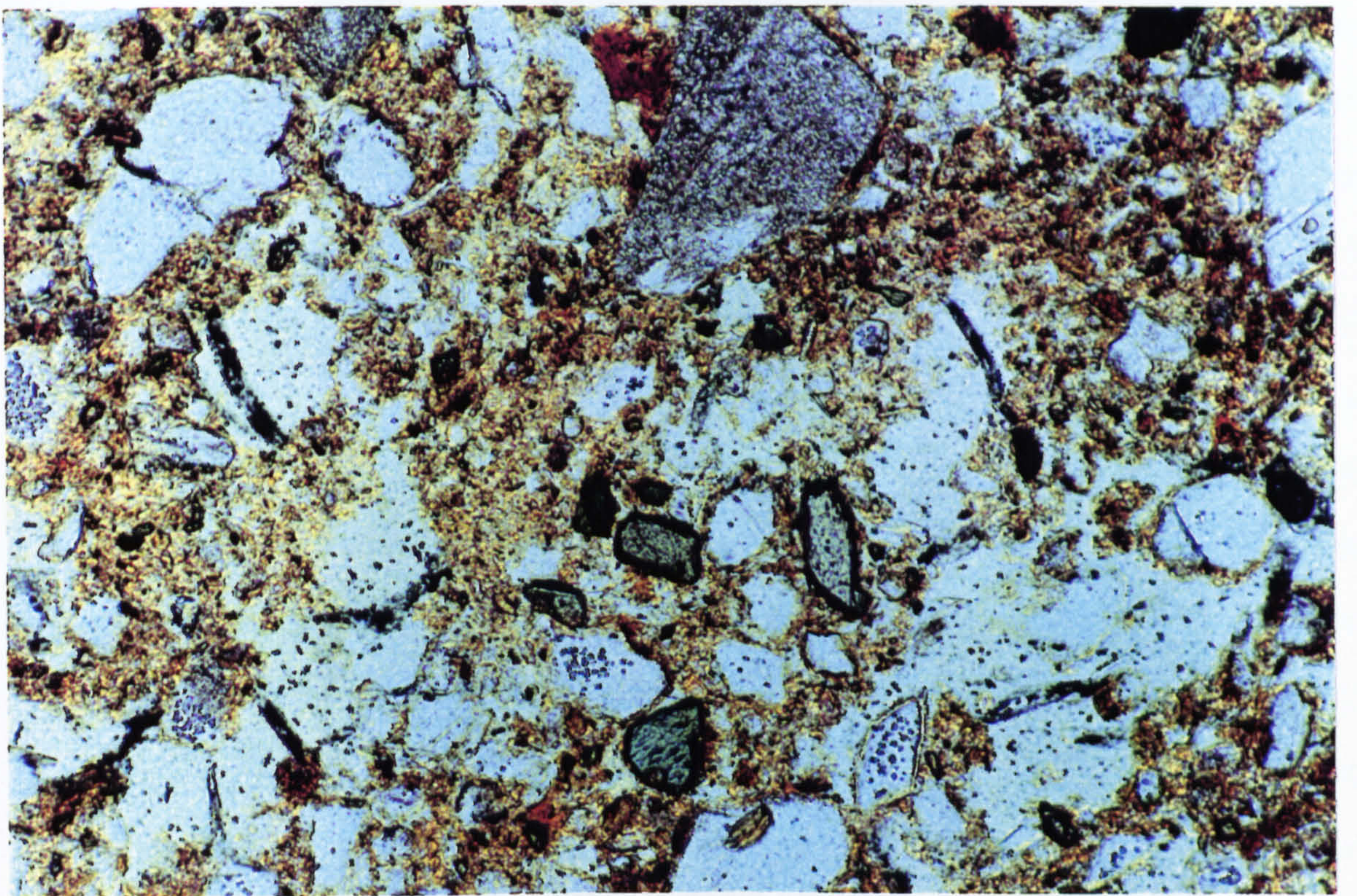


Fig. 9.6 Pelley microstructure from Bs horizon, M62, S5, PPL, FL 2mm

Fig. 9.8 Thin iron pan below M127, S1, PPL,  
FL 8mm

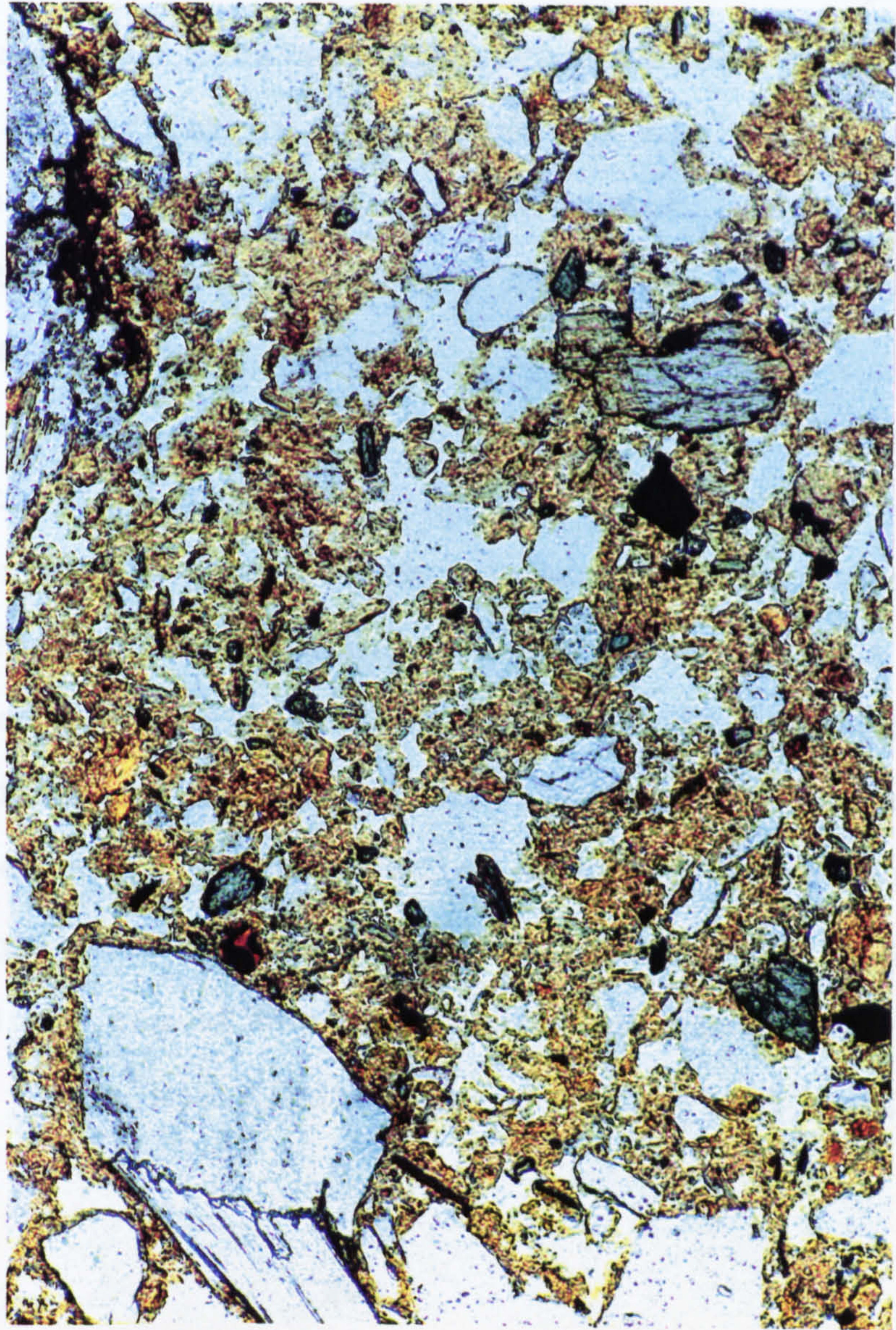
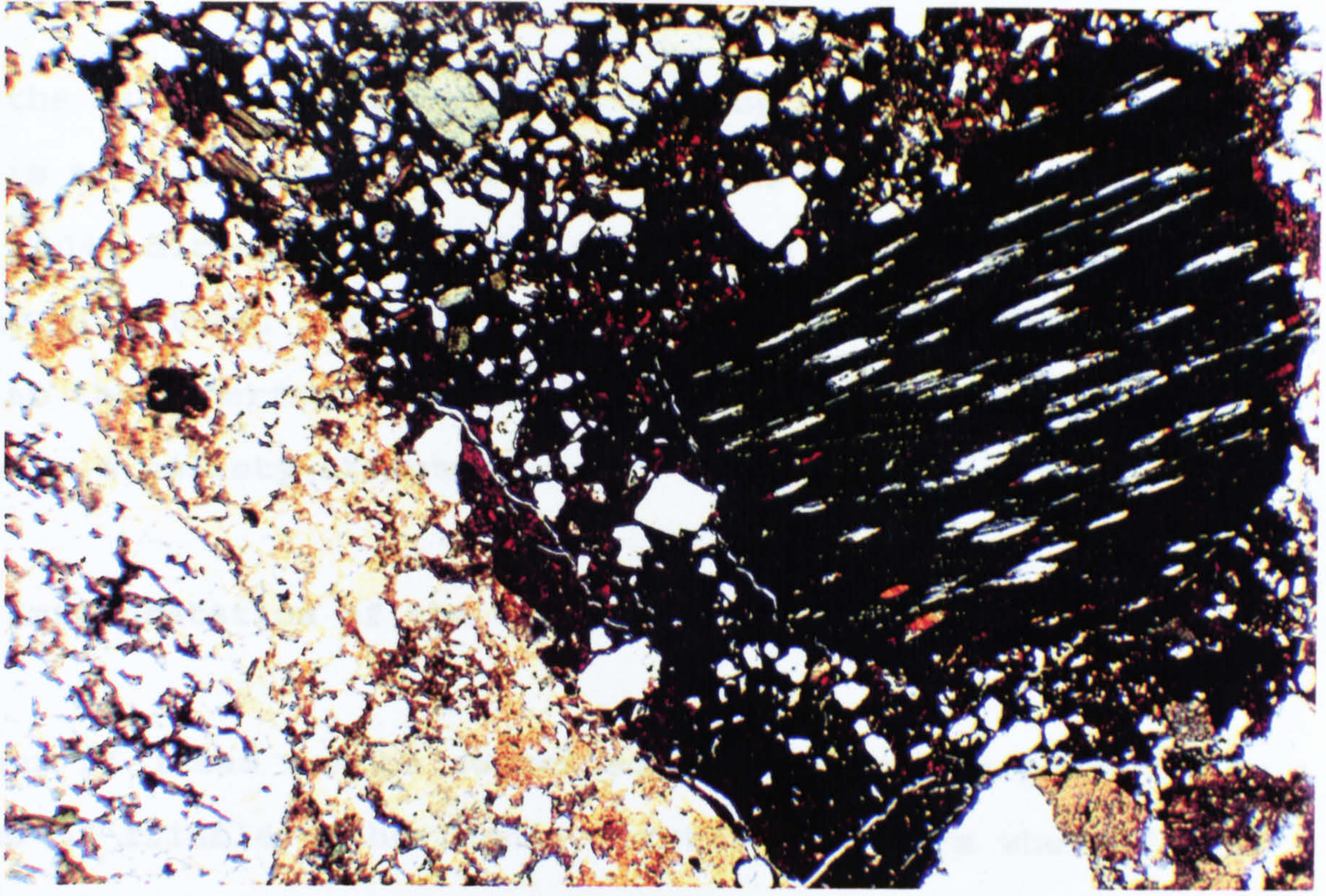


Fig. 9.7 Pellety microstructure in Bs horizon, M504,  
S3, PPL, FL 2mm

Where the Bs horizon has formed in the top of glacial till (M505) there is no pelley microstructure. At the base of the Bs horizon under M504, directly above the glacial till, there is still no pelley structure. However at the top of the Bs horizon under M504, at the interface with the buried A horizon, the Bs horizon does have a pelley structure.

### **9.3.3 Interpretation of the formation of Bs horizons**

A number of ideas can be suggested to explain the presence or absence of friable Bs horizons. Firstly they form where faunal activity is reworking roots. This does not seem to explain the presence and absence in M504 and M505. There seems no reason why there should be significantly more roots and biological activity in one of these contexts than in the other. An alternative explanation is to consider the supply of organic material prior to the formation of a Bs horizon.

It is possible that under M504 the Bs horizon formed in what was once an A horizon. It is possible that podzolisation occurred and sesquioxides were concentrated in the lower part of the A horizon which impregnated the pellets that were already present in the profile. Biological activity continued as long as there was an abundant supply of roots. Translocation of sesquioxides continued downwards through the profile, below the base of the A horizon, until it reached the top of the undisturbed glacial till. At this position, where there was limited or no biological activity or

organic material, the sesquioxides were precipitated as amorphous coatings.

This hypothesis is consistent with the observations under M505. Sesquioxide enrichment occurs as amorphous coatings in the glacial till and in areas where there is no pelley structure. If the hypothesis is correct then it is possible that a friable Bs horizon once existed under M505 but has been removed by profile truncation.

The process responsible for disturbance of the cappings and mixing throughout the profile is not known. Ard marks are cut into the top of the existing Bs horizon showing that the soil was podzolised when it was cultivated. There are no indications of human activity preserved in the Bs horizon. It is more likely that the disruption of the glacial till to form fragmented cappings was caused by the continual growth of roots over the millennia. Anthropogenic activity could have had an indirect impact on this process by initiating the removal of trees.

In conclusion the evidence from Lairg indicates the possibility that the type of Bs horizon present, i.e. friable or cemented, is affected by conditions in the profile prior to illuviation of sesquioxides. Where there is an organic component to the soil, and faunal activity, a friable Bs horizon can develop. Where the soil is composed of mineral material cemented horizons can develop.

#### 9.4 Formation of fragmented nodules and thin iron pans

In all the samples taken from Lairg there is minimal clay sized material present. Coatings are mainly amorphous, isotropic and located in Bs horizons or thin iron pans. The identification of the coatings is not possible using the optical microscope. However the spectral characteristics are qualitatively described and compared to published descriptions from similar soil contexts.

The development of iron pans is well illustrated at the Lairg site. Figures 9.8 to 9.12 show examples of thin iron pans from below M127 and M88. Fragmented nodules, morphologically similar to fragmented iron pans are found throughout buried A horizons under M64 (fig. 9.13) and M505 (fig. 9.14), both monuments are later prehistoric. Similar features are found in undated buried colluvial deposits under M88 (fig 9.15) and M86 (fig 9.16). The nodules under these two monuments are morphologically similar to the ones from M64 and M505 but they are found at the base of the buried A horizon rather than distributed throughout it. The micromorphology of fragmented nodules can be compared to in situ iron pans from M88 (fig 9.8) and M127 (fig 9.11).

The internal composition of the nodules is variable. Figures 9.17 to 9.19 show a detail of one fragmented nodules in M505, sample 1. The groundmass is impregnated by amorphous material which is highly reflective using OIL. Using PPL the colour of the nodule is generally red to dark brownish red. The darker material tends

to be situated in old voids (fig. 9.19). The material which fills the voids is dark brown using OIL and sometimes anisotropic. There is variation between the morphology of the nodules, sometimes lighter yellow colours are present. The material that forms the matrix of the in situ iron pan, associated with monument 86, is isotropic but Farmer et al. (1984, in Farmer 1985) and Farmer et al. (1985) state that weakly anisotropic coatings are also present in placic horizons in Scottish podzols. It is not possible to know the elemental composition of the nodules without the use of microprobe analysis or sub-microscopic techniques. However the darker less reflective material in the old void areas suggests a greater concentration of organic material. Farmer et al. (1984) describes dark organic enriched crusts from allophanic gel deposits in an iron pan from the Tarbothill soil series. It has already been noted (section 9.2) that areas with the highest concentrations of fine material concentrates sesquioxide enrichment. Farmer et al. (1984) state there is no micromorphological evidence for the migration of organic complexes of Fe and Al in podzols but translocation of organic solutions and colloids do migrate through E horizons.

The presence of a sesquioxide rich groundmass surrounding darker organic rich voids can be interpreted in two ways. Firstly the organic solution and Fe and Al compounds do migrate through the soil as single complexes, the Fe and Al is then precipitated in the surrounding groundmass at a point where the oxidation status of the soil is sufficient to cause the precipitation of the sesquioxides. Secondly the deposition of sesquioxides happens



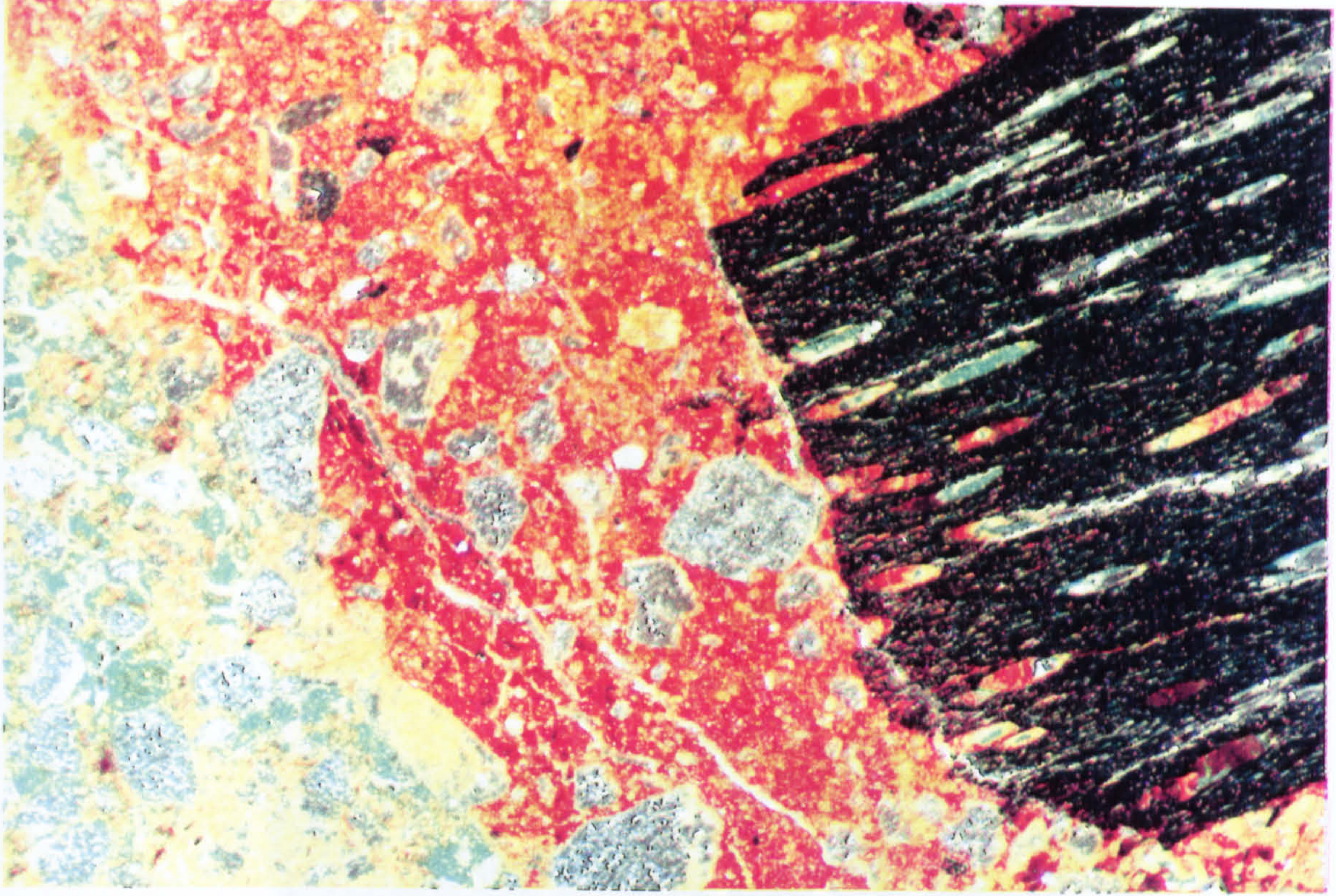


Fig. 9.10 As fig. 9.9 except using OIL

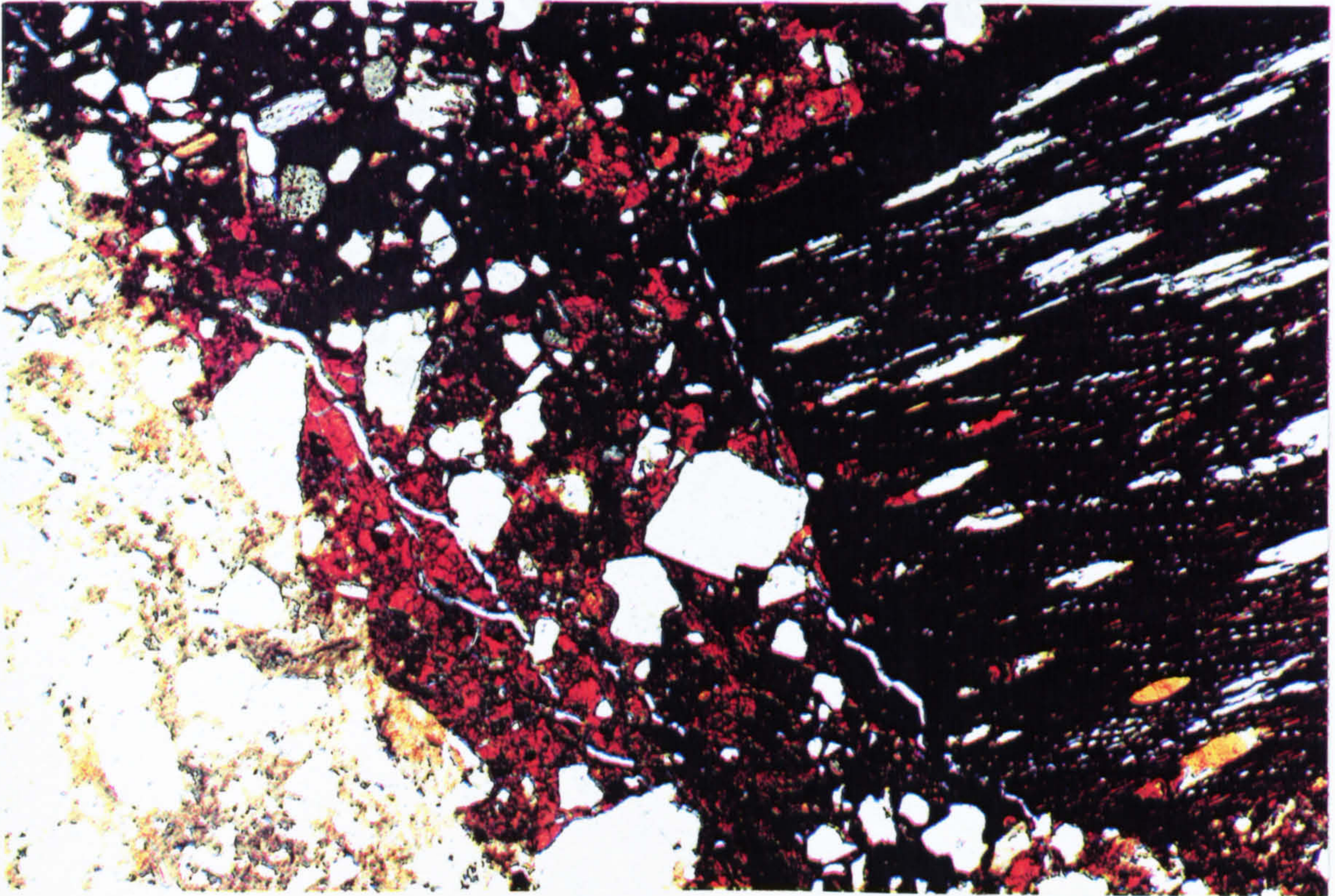


Fig. 9.9 Detail of fig. 9.8, PPL, FL 4mm

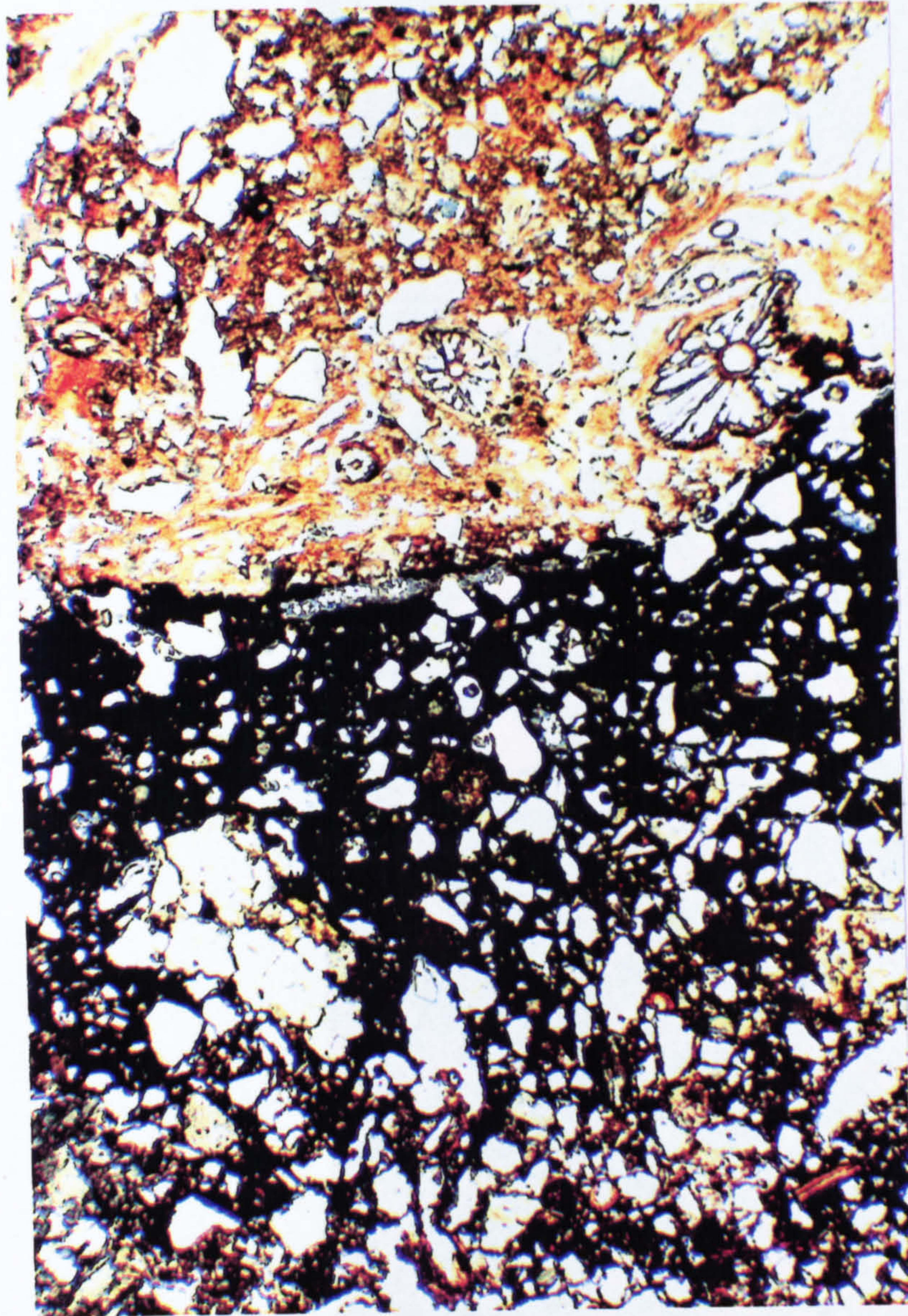
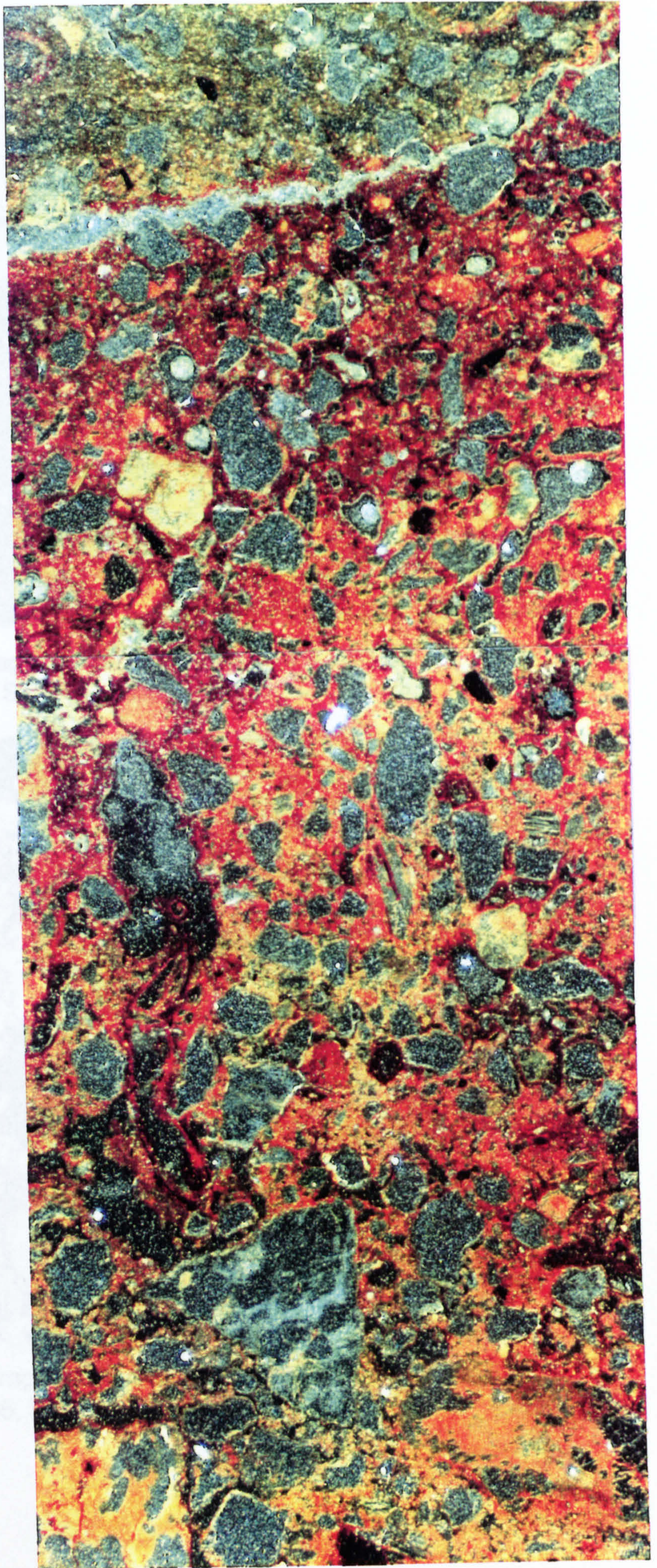


Fig. 9.11 Thin iron pan below M88, S162, PPL,  
FL 8mm

Fig. 9.12 Thin iron pan  
below M88, S162, OIL,  
FL 7mm



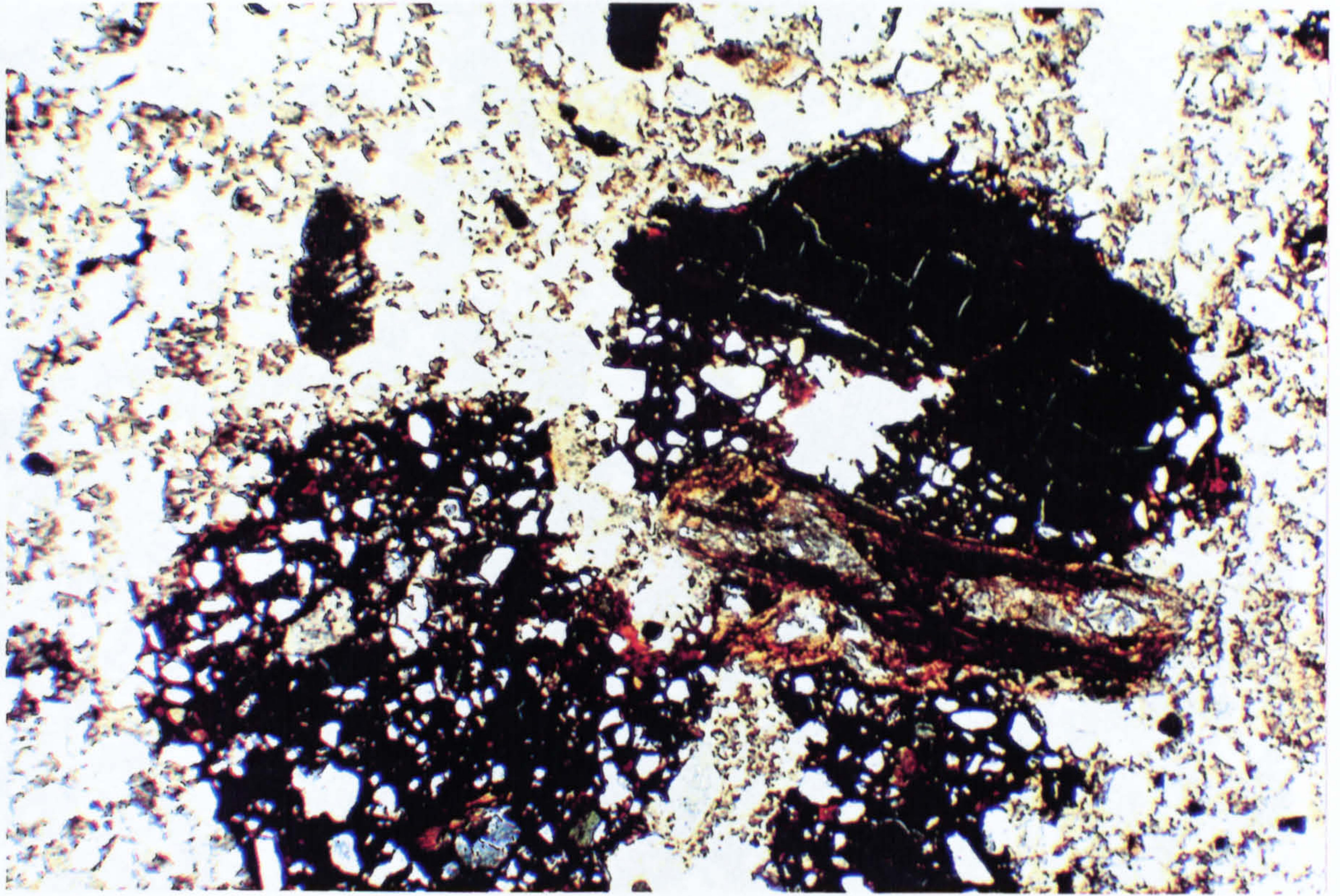


Fig. 9.13 Fragmented nodule in buried A horizon  
below M64, S1, PPL, FL 8mm

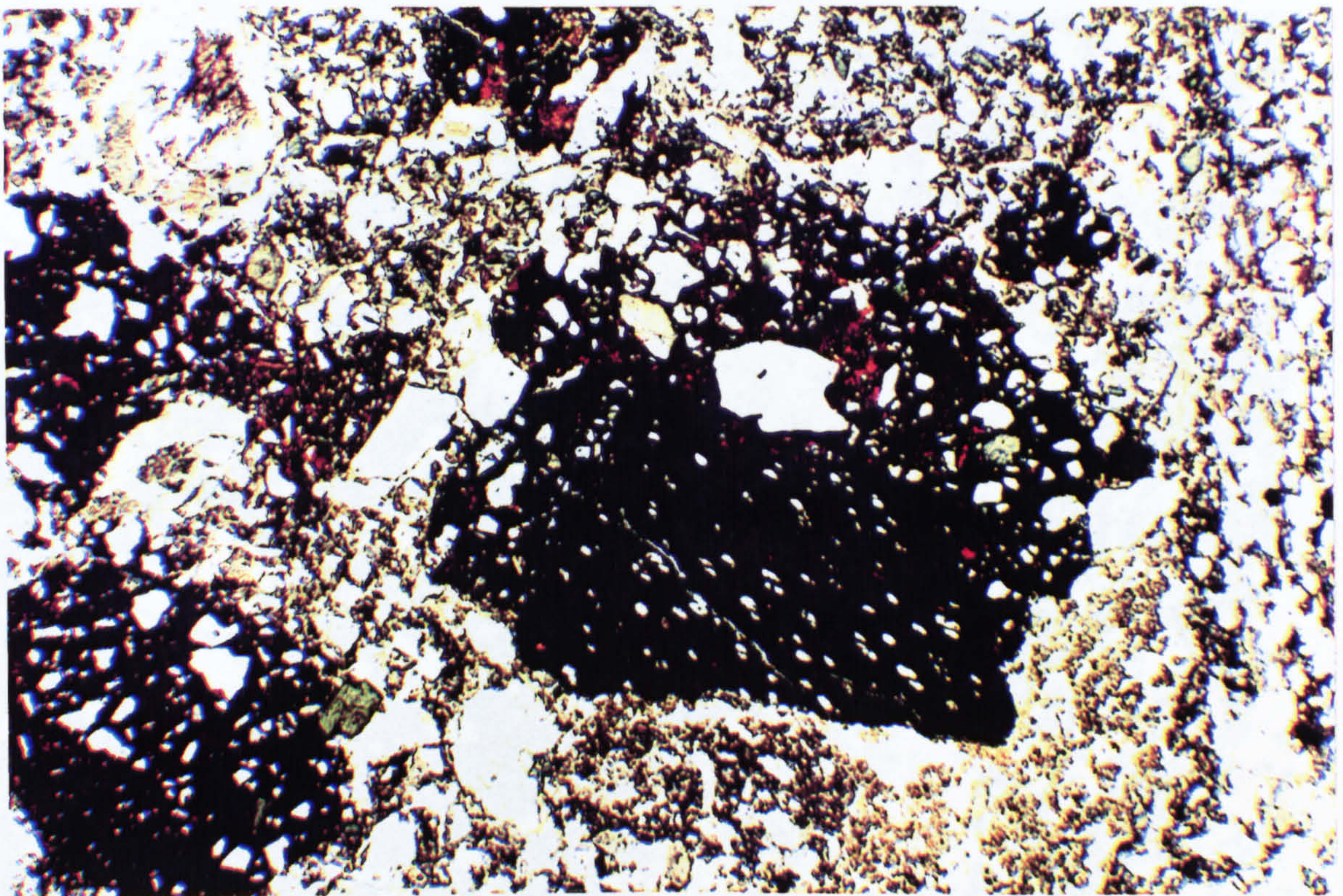


Fig. 9.14 Fragmented nodule in buried A horizon  
below M505, S1, PPL, FL 8mm

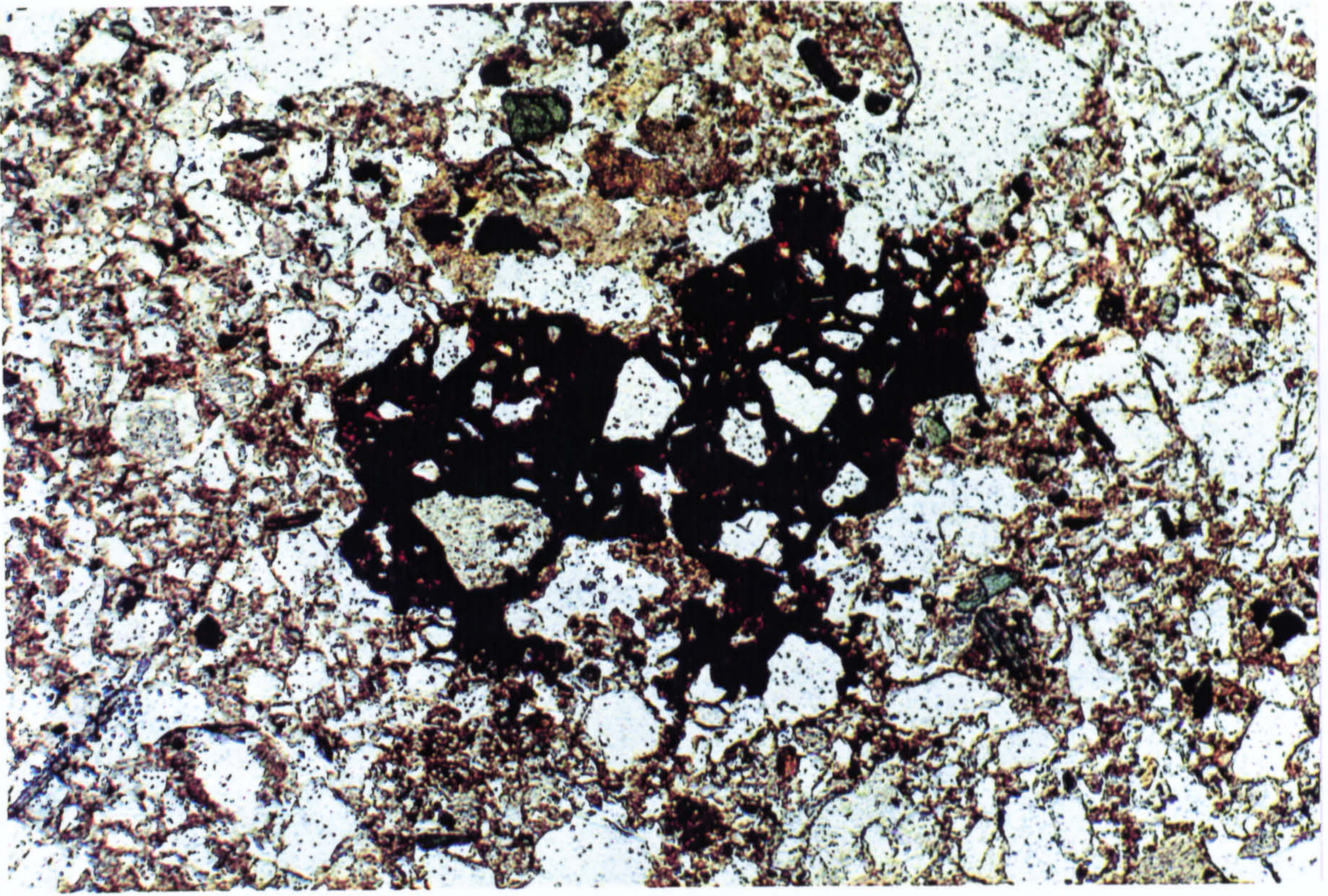


Fig. 9.15 Fragmented nodule at base of buried A horizon, M88, S159, PPL, FL 4mm

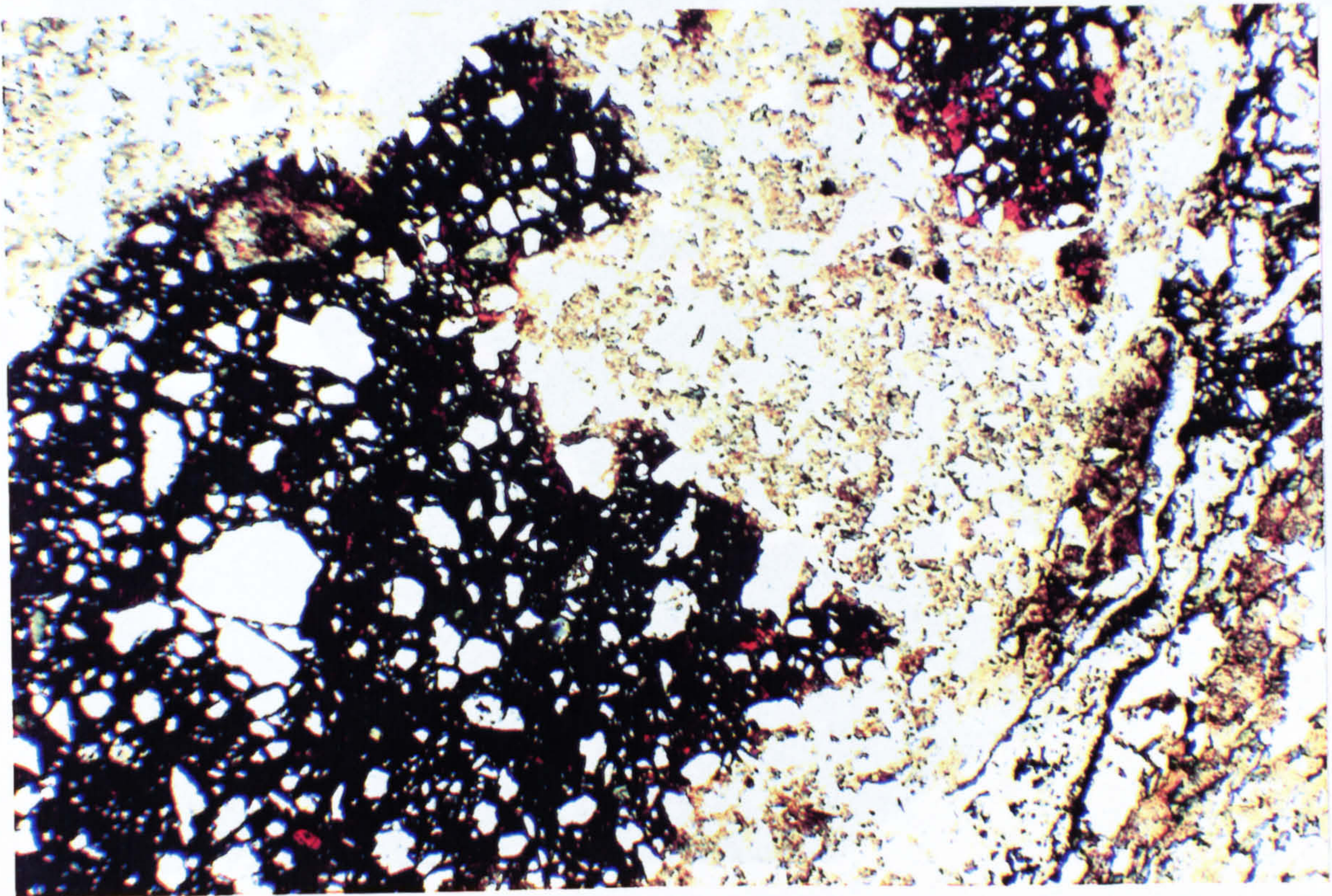


Fig. 9.16 Fragmented nodule at base of buried A horizon, M86, S161, PPL, FL 8mm

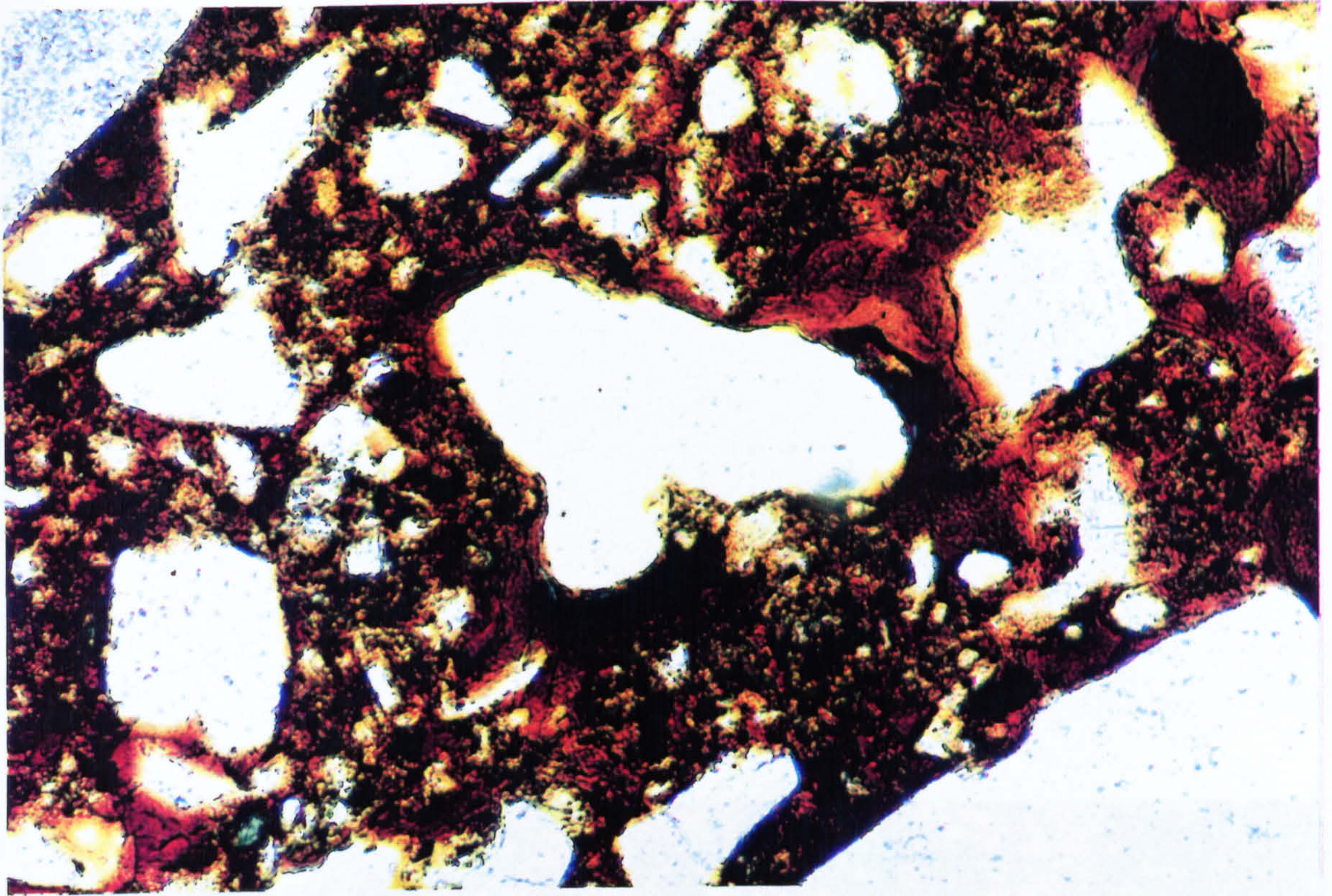


Fig. 9.17 Detail of a fragmented nodule in a buried A horizon under M505, S1, PPL, FL 0.8mm

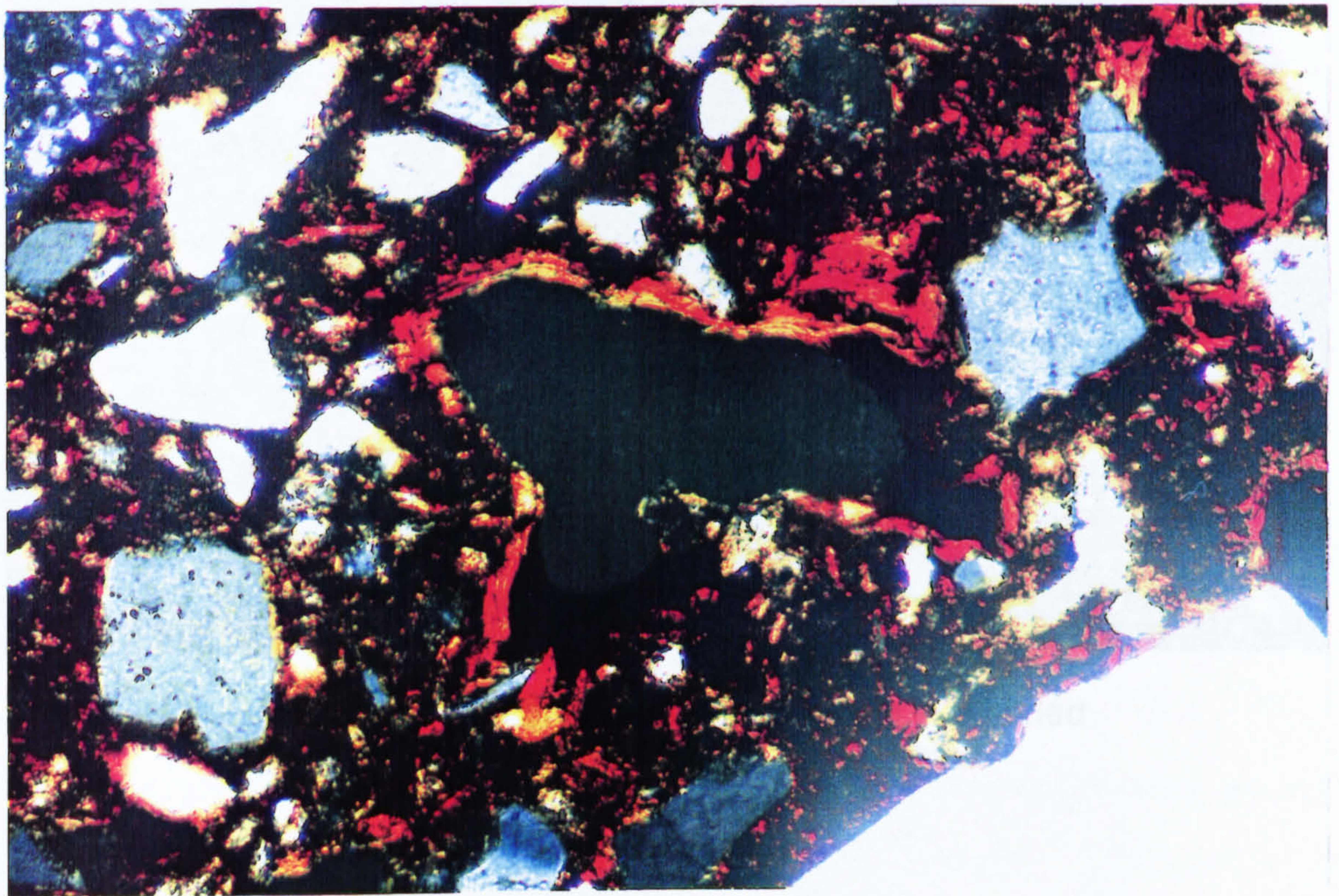


Fig. 9.18 Detail of a fragmented nodule in a buried A horizon below M505, S1, XPL, FL 0.8mm

independently of the...  
voids. The use of microprobe analysis...  
would help to quantify the...  
within and surrounding the...  
that the interpretation...

An issue of particular...  
fragmented nodules...  
A horizon. Two hypotheses...

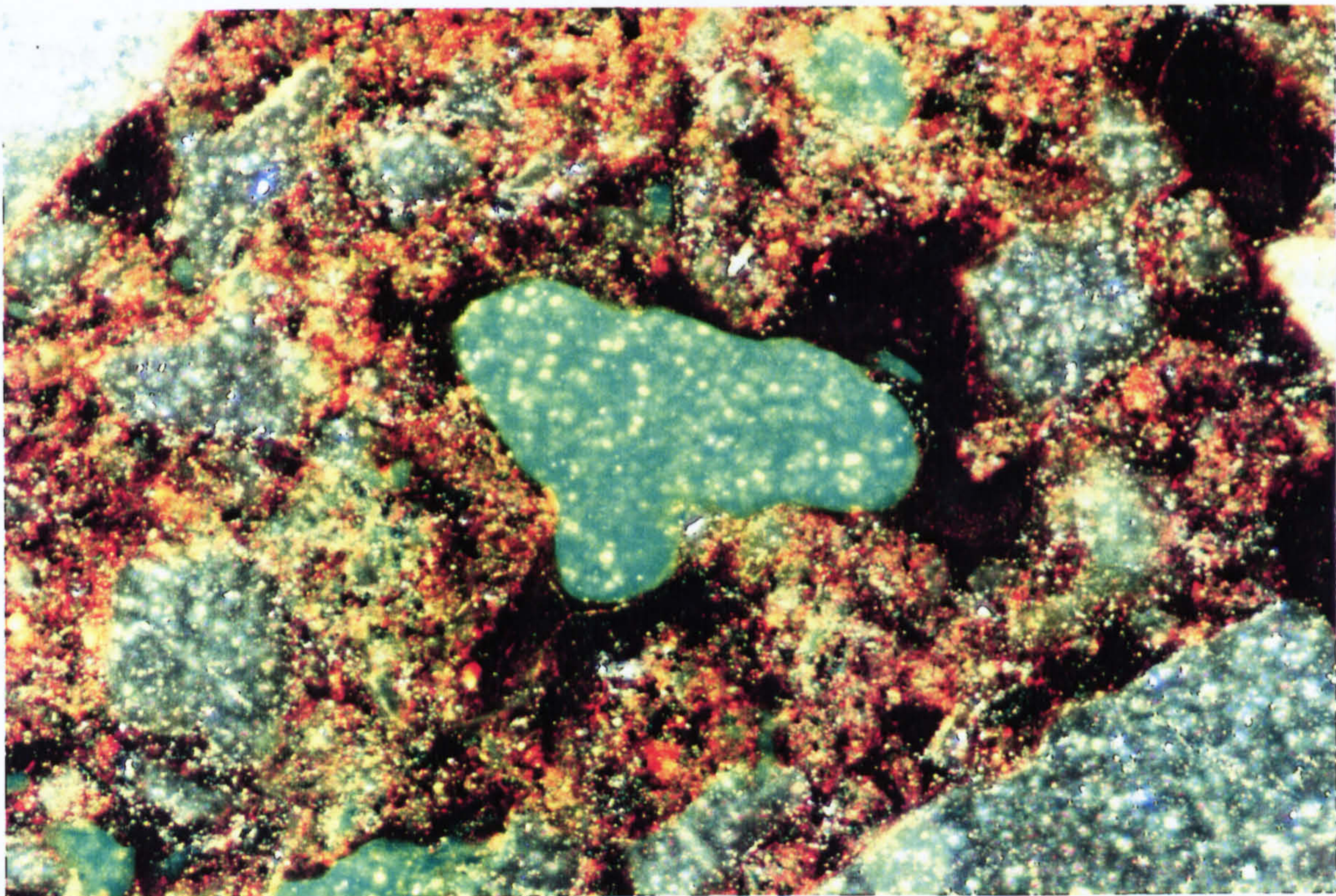


Fig. 9.19 Detail of a fragmented nodule in a buried  
A horizon below M505, S1, OIL, FL 0.8mm

The nodules...  
Pedroff et al. (1990) report...  
frequently preserved...  
oxides. Evans (1985) reports...  
nodules and concretions...

independently of the translocation of organic compounds in the voids. The use of microprobe analysis and spectral classification would help to quantify the relationship between the material within and surrounding the old void spaces. It is likely however that the interpretation would still be unresolved.

An issue of particular importance at Lairg is the genesis of the fragmented nodules seen in some of the early prehistoric buried A horizons. Two hypotheses for their formation are considered;

1. The nodules once formed part of a iron pan which has been fragmented.

This fragmentation might have been the result of soil disturbance caused by anthropogenic activity or biological processes. If the iron pan had developed while there were still trees on the site fragmentation might have been caused by tree throw. Another possibility is importation of the nodules if peaty turf was being cut from stagnopodzol profiles and used as manure.

2. The nodules are the result of periodic gleying of the soil profile.

The nodules might not have been formed by fragmented pan at all. Federoff et al. (1990) report that charcoal fragments are frequently preserved from decay by an impregnation of iron oxides. Romans (1986) reports the presence of iron and manganese mottles and concretions from various contexts, including buried



soils, from Scord of Brouster on Shetland. The formation of these features is attributed to movement of the water table interacting with pedological features in the soil. This second hypothesis is a strong possibility at Lairg given the waterlogged conditions observed in many of the sites excavated.

The second hypothesis does not explain two important features of the nodules observed at Lairg. Firstly it does not account for their fragmented shape. It is possible that ferruginous compounds impregnated features already present in the soil which were then disturbed causing fragmentation. Secondly, and perhaps more importantly, these features are only observed in contexts dating to the prehistoric or in undated soils that are believed to be early. This suggests that the reason for their formation is not just localised environmental conditions in one particular trench, but includes a temporal aspect.

With the data available it is not possible to resolve the origin of the fragmented nodules. The similar morphology of features from buried A horizons under M64, M88, M86 in group A and M505 in group B does suggest a link between these contexts. Perhaps these are remnants of a contemporary buried landscape, without further excavation and analysis this suggestion is only be speculative.

## 9.5 Evidence for landuse and soil development at Lairg from prehistoric to recent times.

Soil development is often considered in terms of the five soil forming factors (Jenny 1941). The impact of humans, on soil development, is often not given as much emphasis as other environmental factors. The intensive thin section sampling of soils at the Lairg site allows soil development and human activity, during different cultural periods to be studied. This section discusses the results and interpretation of the thin section analysis carried out at the Lairg site. In the future the interpretations presented here will be combined with results from other studies, also being carried out on the site, forming a comprehensive study investigating landscape change and human activity at Lairg.

This section begins with a statement of morphological differences between prehistoric buried soils and Post Medieval buried soils that are identified using field observations. The evidence from the thin section analysis of these soils is then presented. The final part of this section discusses the interpretation of the results.

**9.5.1 Effect of human activity on the soils at Lairg based on field observations**

Anthropogenic activity during the prehistoric and the Post Medieval period can be evaluated using field and micromorphological observations of buried profiles.

The depth of the buried A horizon, found on level ground, in different parts of the site can be correlated with the age of overlying monuments. The average depth of A horizons sealed by prehistoric monuments is 12.9cm (Table 9.2).

|                                      |        | Depth of buried A horizon (cm). |
|--------------------------------------|--------|---------------------------------|
| Prehistoric monuments                | 62     | 10-15                           |
|                                      | 64     | 15                              |
|                                      | 505    | 5-15                            |
|                                      | 659    | 5-10                            |
|                                      | 648    | 20                              |
|                                      | 504    | 10-15                           |
| Monuments dated to 2nd millennium AD | 75/4   | 25                              |
|                                      | 127    | 36-44                           |
|                                      | 1069/2 | 26                              |
|                                      | 975/3  | 20                              |
|                                      | 975/2  | 25-30                           |

**Table 9.2 Thickness of Prehistoric and Post Medieval buried A horizons**

The average depth of PM buried A horizons is 27.8cm, approximately 14.9cm deeper than the late prehistoric monuments. The reason for the increase in depth can be explained by

considering the external environmental conditions affecting the soil during prehistoric and Post Medieval periods.

Numerous ard marks are present in the top of the Bs horizon indicating prehistoric agricultural activity. Figure 9.20 shows an aerial view of ard marks around a Bronze Age hut circle. Ploughmarks are found throughout Britain which shows that ards could be used in a wide variety of soils (Rees 1981). Other field evidence indicating prehistoric cultivation at Lairg includes the accumulation of soil against field boundaries (M659 and M505) and the truncation of Bs horizons. For example around the edges of M504, an Iron Age hut circle, soil erosion has truncated the Bs horizon. Similar erosion was observed around other prehistoric monuments and is thought to represent continued landuse around the edges of hut circles. Many of the monuments around group B are thus raised slightly above the surrounding ground. This erosion indicates intensive agricultural activity into at least the Iron Age.

The last type of agriculture activity that can be identified in group B is ridge and furrow. Stagnopodzols have developed in this area and peat has accumulated on top of the ridge and furrow. The basal layers of the peat are dated to the Late Iron Age. The ridge and furrow overlies some of the Bronze Age hut circles. The presence of ard marks in the Bs horizons, underlying hut circles, and the ridge and furrow, overlying hut circles, indicates a long period of cultivation that started in the Bronze Age and finished during the Iron Age.

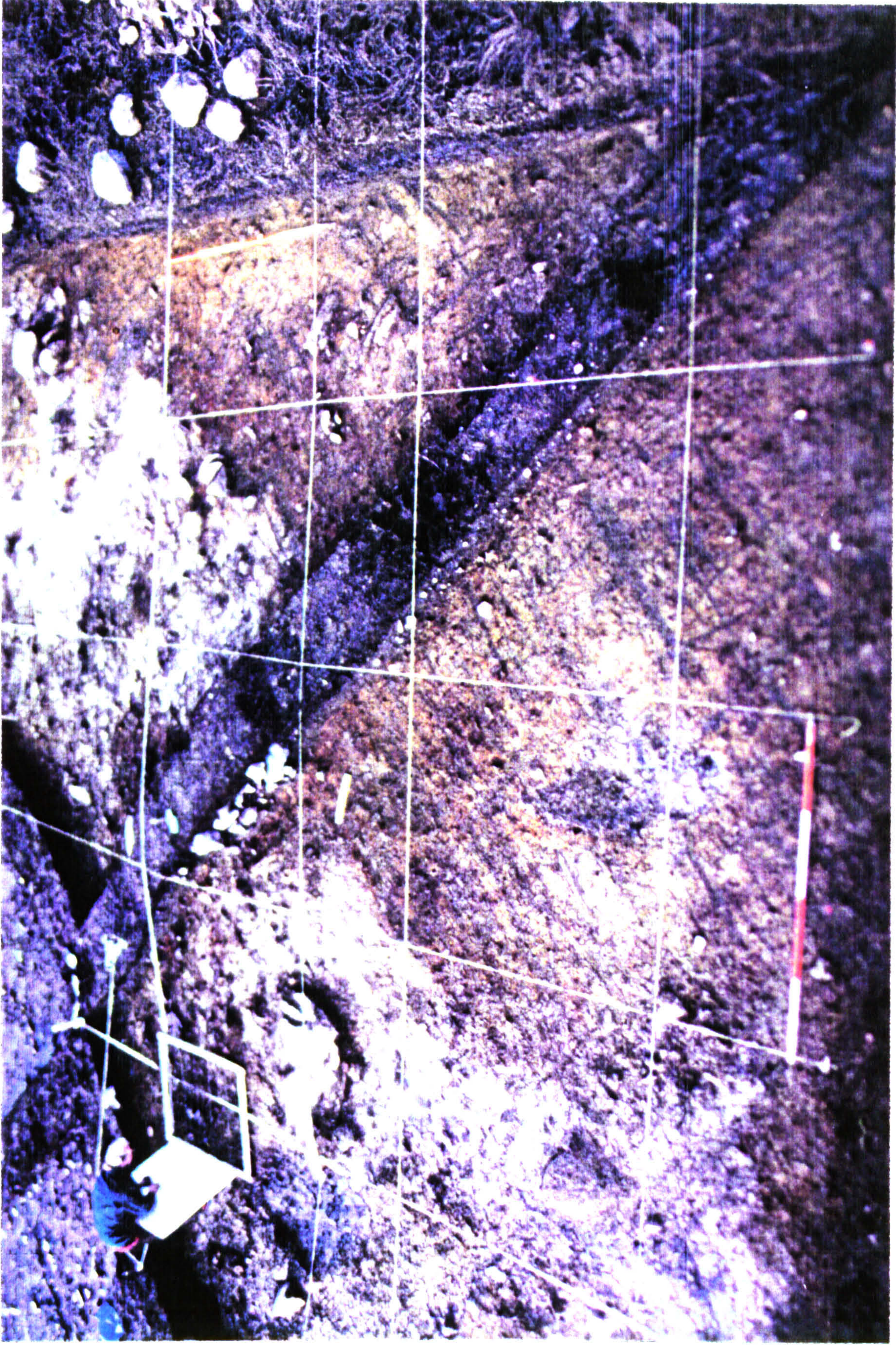


Fig. 9.20 Ard marks in the top of a Bs horizon under an LP hut circle in group B

Buried O horizons (M164, M127) and buried humose A horizons (M75/4) are characteristic of PM monuments in group A. Under both the PM monuments sampled in group C there are buried layers of grey material at the top of the buried A horizon. These are interpreted as gleyed surface humose horizons. The presence of organic layers preserved under the PM monuments suggests that the ground had not been tilled for some period prior to burial. The monuments were not all constructed at exactly the same time so it is possible that the land was being left to pasture for extended periods allowing accumulation of surface organic layers.

#### 9.5.2 Evidence from soil micromorphology

Micromorphology is often used to determine if a soil has been subject to episodes of cultivation at some point in its history. Soil micromorphology can be used to demonstrate cultivation of a soil even where there are no indications in the field (Macphail et al. 1990a). A common micromorphological indicator is the presence of dusty and silty clay coatings in the upper part of a profile (assuming that the profile has not been buried by colluvial material). By calculating the abundance of dusty clay coatings at various depths in the soil profile it is suggested that the type of implement used for cultivation can be inferred (Barclay 1983, Macphail et al. 1987, Romans and Robertson 1983a).

The results of the thin section analysis at Lairg shows the almost complete absence of clay sized material in any of the

slides studied. The reason for this is believed to be the coarse grained nature of the parent material combined with rapid removal of any weathering products. The acidic nature of the soils might also have contributed to the absence of clay sized material. It is not therefore possible to infer cultivation from the presence of dusty clay coatings.

### Disrupted Bs horizon

Intensive cultivation during the Bronze Age and Iron Age in group B is corroborated by thin section evidence indicating mixing of cappings and fragmented Bs horizon throughout the soil profile (table 9.3). As the soils were cultivated fragments of Bs horizon material were incorporated into the tilled A horizon. The cultivation resulted in truncation of the soil profile. M1069 is the only buried A horizon dated to the Post Medieval period to incorporate fragmented Bs horizon.

| Monument                          | Sample number and context          | Feature present       |
|-----------------------------------|------------------------------------|-----------------------|
| M648, LP (Bronze Age) lynchet     | Sample 2, buried A horizon         | Fragmented capping    |
| M505, LP (Bronze Age) lynchet     | Sample 1, buried A horizon         | Fragmented capping    |
| M504, LP (Iron Age) hut circle    | Sample 1, top of buried A horizon  | Fragmented capping    |
|                                   | Sample 2, base of buried A horizon | Fragmented capping    |
|                                   | Sample 3, base of buried A horizon | Fragmented Bs horizon |
| M660, LP (Bronze Age), hut circle | Sample 3, wall of hut circle       | Fragmented Bs horizon |
| M659, LP (Bronze Age), hut circle | Sample 2, buried A horizon         | Fragmented Bs horizon |
| M1069, PM structure               | Sample 2, buried A horizon         | Fragmented Bs horizon |

Table 9.3 Presence of features indicating mixing of Bs horizons and A horizons

## The importance of carbonised fragments in buried A horizons

There are considerable differences in the abundance of charcoal in different soil profiles located on the Lairg site. It would be useful to know if abundance of carbonised residues in the soil profile could be linked with anthropogenic activity. Identification of the charcoal fragments would be the best method to make such an association. For instance the charcoal might be derived from carbonised remains of crops. There was no time to get the charcoal fragments identified. Despite this, the spatial and temporal variability in the distribution of charcoal does suggest an anthropogenic influence.

Thin section samples from Post Medieval monuments show that most of the charcoal is concentrated either near the surface or in layered distributions where organic horizons are preserved. For example, layers of charcoal are present in the organic horizon below M164 and also in the organic part of the turves that form the bank of that structure. This layered distribution suggests that surface burning of vegetation was occurring with no subsequent mixing of the soil. In the prehistoric soils the charcoal is evenly mixed throughout the A horizon. Field evidence already indicates that the prehistoric soils were being intensively cultivated so it is likely that this mixing was the result of tillage.

The abundance of charcoal is variable in different prehistoric contexts. An important question is what abundance of carbonised



fragments would there be present in the soil with no anthropogenic activity? In some buried A horizons, for instance under M86, M505, M648, M659 and slightly to the east of M64 there are occasional to many carbonised fragments. Field evidence and results from the thin section analysis show that these contexts have been cultivated. It is reasonable to suggest that this charcoal was added or mixed into the soil as part of a manuring practice. However in the buried A horizon under M504, which was significantly later than the other soils and was also cultivated, there are only rare carbonised residues. This low abundance indicates important variability that must be considered when trying to interpret carbonised residues. There is no coarse charcoal and rare black particles in the buried A horizon under M62. It is possible that M62 is the remnant of an early podzol profile, the lack of coarse carbonised residues, in this case, is consistent with minimal anthropogenic activity. However the absence of these features cannot be used as categorical evidence that this soil had not been tilled.

To summarise, in the prehistoric contexts occasional to many carbonised residues are generally found in A horizons which have been cultivated during the Bronze Age. There are exceptions to this and lower abundances are also found in contexts that had been cultivated. It seems that high abundances of carbonised residues is generally associated with prehistoric cultivated A horizons although lower abundances, by themselves, do not indicate absence of human activity.

## Sorting of buried A horizons

The later prehistoric buried A horizons are generally poorly sorted while the Post Medieval buried A horizons are moderately to well sorted. C/f ratios in the PM buried A horizons are generally 40:60 while those in the later prehistoric soils are generally 60:40 (table 8.1). This indicates a higher percentage of coarse material in the older soils.

The results from the image analysis results (chapter 8) confirms this trend. Greater amounts of finer material are present in the PM soils. The abundance and shape of voids are affected by the amount of fine material in the soil. The shape of voids in the size range analysed (chap. 8) show that all the voids are irregularly shaped but the voids from M504, the cultivated Iron Age buried A horizon, are significantly more irregular than from M21 or M127.

More research needs to be carried out to compare these results to other physical attributes of the soil, for instance particle size analysis. However it is likely that the shape of the voids is affected by the amount of fine material in the soil and the size distribution of the coarse material. As the abundance of fine material increases a greater proportion of the spaces between mineral grains are filled up. If root growth subsequently occurs regular channel shapes are likely to be left in the soil. The shape of the voids measured, using the formfactor analysis, are likely to reflect the shapes of channels in the soil.

The increased fine fraction in the Post Medieval soils can be explained by considering the environmental conditions in which the soil developed. During the prehistoric period the dominant process acting on the soil was disturbance caused by cultivation. The disturbance promoted the loss of coarse and fine material with the incorporation of dominantly coarser material from the underlying Bs horizon and glacial till. The A horizons buried by Post Medieval monuments are deeper than the prehistoric buried A horizons. This indicates either, a reduction in the amount of erosion was occurring, or greater amounts of material was being added to the soil, or a combination of the two processes.

It is likely that the increase in depth can be attributed, in part, to manuring of the soil. Fenton (1981) identified a number of manuring practices that have been used in Scotland since, at least, the early 1500s. These include converting peat into ashes which were then used as bedding in a byre. This mixture of material ended up being used as fertiliser. Turf could be cut from areas of rough grazing and composted in middens with material like byre manure, seaweed and bracken.

There are no features preserved in any buried A horizon dated to the PM period that can be used as absolute evidence for manuring of the soil. The best evidence is from an unburied soil, M21, which shows that in the most recent history of use burnt and unburnt peat was being added to the soil. The depth of M21, and other PM buried A horizons might be the result of turves being

added to the soil as manure. The c/f ratios show an increase in the fine fraction in these contexts.

### **Vesicular arbuscular mycorrhizae**

Spore cases of vesicular arbuscular mycorrhizae (VA) are more numerous in Post Medieval buried A horizons than in prehistoric buried A horizons. It is suggested that these features, also referred to as bright and dark rings (Romans and Robertson 1983a), might be associated with certain types of grazing. The VA group is part of the endomycorrhiza group and are one of the most widespread types of soil fungi. They are thought to be an important component in helping plants absorb nutrients from relatively infertile soils (Brady 1990). Fungi rely on organic matter in the soil for their energy and carbon. The abundance of bright and dark rings might have increased during the second millennium AD as a result of an increase in organic inputs to the soil.

### **9.6 Conclusion of the thin section and soil study at Lairg**

It seems likely that the changes observed in the soil environment at Lairg since the Bronze Age, have been largely influenced by anthropogenic activity through time. The evidence indicates that intensive cultivation was occurring during the Bronze and Iron Age. The end result of this cultivation is erosion and podzolised soils. The conditions of the soils prior to the Bronze Age are not known but there is some evidence to suggest that podzols had

developed and the brown podzols seen under the prehistoric monuments are truncated profiles.

It is known that the prehistoric soils were being cultivated for a long period of time, at least during the Bronze Age and probably throughout much of the Iron Age. For an agricultural system to have lasted this long it must have been successful in maintaining soil fertility levels. Manuring of the soils must have been occurring although the precise form this took is not clear from the thin sections studied.

By the Post Medieval period the evidence suggests a reduction in the intensity of cultivation combined with areas left as pasture for extended periods. The land was still being tilled and it is likely that turves were being used as manure. The result of this is a deepening of the buried A horizons. In areas where the land has been managed throughout the PM period brown podzols are the dominant soil type. In areas that were abandoned stagnopodzol formation has occurred with groundwater gleying occurring and the accumulation of peat.

An important conclusion from this study is the effect human activity has had on pedogenesis. The original condition of the soils, prior to the Bronze Age is not known. Cultivation during the prehistoric proceeded for a long period but resulted in considerable soil erosion. Where human management stopped the result was stagnopodzol formation. Where human activity continued podzol profiles did not develop and brown podzols are maintained.

Thus to consider the effect of anthropogenic activity as unidirectional, towards waterlogging, gleying and podzolisation, is too simplistic.

To conclude the thin section analysis it is possible to answer the original questions formulated in chapter 3.

### **9.7 Summary of results from an analysis of buried soils**

1. Do buried soils with a temporal distribution exhibit specific characteristics? Yes, the morphology of buried soils from different periods is different. The differences are expressed in variations in the c/f ratio, sorting and void area and morphology. Differences between A horizons are small and not easy to distinguish using qualitative thin section analysis. Accurate measuring using the image analysis techniques described in chapter 2 allow statistical differences to be established.

2. Can temporal variation be isolated from spatial variation? Features present in buried A horizons, including presence or absence of cappings, position and quantity of charcoal, depth of soil correspond to soils dated to different periods. The occurrence of these features is related to the age of the overlying monument rather than their spatial location.

Factors causing post depositional alteration of the soil, including structural modifications by bracken growth and gleying caused by waterlogging, could be distinguished. There was some

doubt about the genesis of the fragmented nodules found in some horizons. The ability to distinguish features caused by post depositional change from features associated with the age of monuments meant that temporal and spatial variation could be separated in most cases.

3. Can former land use be inferred from buried soils? There is no one feature that could be used to determine the type of landuse associated with a buried soil. However using evidence from all the sites sampled, it is possible generalise about the influence of humans on the soil system at different periods in time.

4. Can changes in landuse be identified in buried soils? Different intensities of agricultural activity were associated with the prehistoric and PM periods.

5. Can differences in landuse be observed in buried soils of the same age? There are no discernible differences between buried A horizons of the same age that could be related to landuse. There are deeper than average A horizons observed in the prehistoric period but these could be attributed to topographic position. Samples were taken from two buried A horizons where the field evidence indicated ridge and furrow technique in one sample and ard cultivation in another sample. There were no significant micromorphological differences between these samples suggesting a continuation of the same cultivation techniques.

6. Can differences in land use be observed in buried soils of different ages? The main type of land use associated with the prehistoric period was cultivation. The major effect of this was erosion of soils. In places it appears that erosion was intensive enough to completely remove Bs horizons. By the Post Medieval period agricultural practices had altered. Evidence suggests better management of the soil combined with pasture and burning of surface vegetation.

7. Can specific pedogenetic/sedimentary events be established from a chronological sequence of buried soils? Evaluating the precise pedogenetic history of the site is difficult owing to the complex natural variation in soil types, post depositional change and continued human use of the land since at least the Bronze Age. However a hypothesis can be postulated.

Podzolisation of the soil had occurred by the Bronze Age. Brown podzols or podzols were present under all the prehistoric monuments excavated. The Bronze Age soils had been subjected to intensive cultivation. This caused severe erosion of the soil sometimes removing all material down to the level of the glacial till. There are no monuments at Lairg which bury examples of buried soils dated to the Neolithic or earlier. Soils were podzolised by the Bronze Age but cultivation during this period resulted in profile truncation. There was one profile studied (M62) that might have been a podzol developed prior to the Bronze Age. Further work and excavation needs to be done to confirm the date of the earliest podzol development at the Lairg site.



The soils buried by Post Medieval monuments are all brown podzols. Stagnopodzols have developed in areas where human activity had stopped. Where management continues there has been no reformation of completely podzolic profiles.

It seems that long term effect of human activity since the Bronze Age was one of degradation during the Prehistoric followed by regeneration by Post Medieval period where human activity continued. In this limited geographic area, soil development is closely linked to anthropogenic activity. The path of pedogenesis is not unidirectional, but a continued response to environmental variables of which humans are an important component.

8. Can types of vegetation be identified from the remains of organic matter in buried soils? There are minimal macroscopic remains of organic material in any of the thin section samples studied so no palaeoenvironmental reconstruction is possible.

9. Can specific palaeoenvironmental information be derived from the study of pollen, diatoms, phytoliths etc. in a buried soil? Although there are diatoms and phytoliths present in many of the buried A horizons they are extremely fragmented. The best preservation occurred in buried organic rich horizons and in the remnants of turf layers from the walls of structures. However there was not time to try and obtain precise taxonomic identification.

## 9.8 Summary of results from the analysis of soil accumulations

1. Can the source of the accumulations be identified i.e. natural or anthropogenic? Anthropogenic deposits were distinguished from cultivated soils on the basis of preservation of stratigraphy. The best example is below M127 where anthropogenic activity had created a layered deposit prior to the construction of the house. In the most recent soil accumulations, remains of manuring material could be recognised in thin section. However all the deposits had undergone some biological reworking so it is unlikely that organic material would have persisted in the soil for any long period of time.

2. Can the type of deposit be identified, for instance hillwash or fluvial sediments? Sediment accumulating as a result of disturbance caused by cultivation could be recognised in the field. Micromorphological examination added little to the interpretation of these sediments owing to the amount of biological reworking. Burnt peat could be recognised at the top of a recent soil accumulation (M21).

3. Can different sedimentary and pedogenic phases be identified in the soil accumulations? Can these be correlated with pedogenic sequences observed in buried soils? The deep soil accumulations studied showed no evidence of stratigraphy. The homogeneity of the accumulations might reflect biological reworking.

4. If separate land use phases can be identified what palaeoenvironmental information can be determined from the biological remains? No separate landuse phases could be identified.

5. Can a sequence of landuse change be identified in the soil accumulations? No temporal sequence of events could be inferred from these accumulations.

### 9.9 The applicability of image analysis techniques to the description of soil thin sections

All the image analysis techniques described in chapter 2 were available for use during the thin section analysis of samples from the Lairg. This section evaluates the usefulness of these techniques.

The image analysis process is summarised in fig 9.21. The end result of the analysis depends on the purposes of the investigation. Image enhancement techniques help the analyst to qualitatively divide a thin section slide into regions in preparation for more detailed description. The most useful enhancement technique used was contrast stretch. There is no quantitative measure of the usefulness of this technique but it was found to aid the description of certain thin sections,

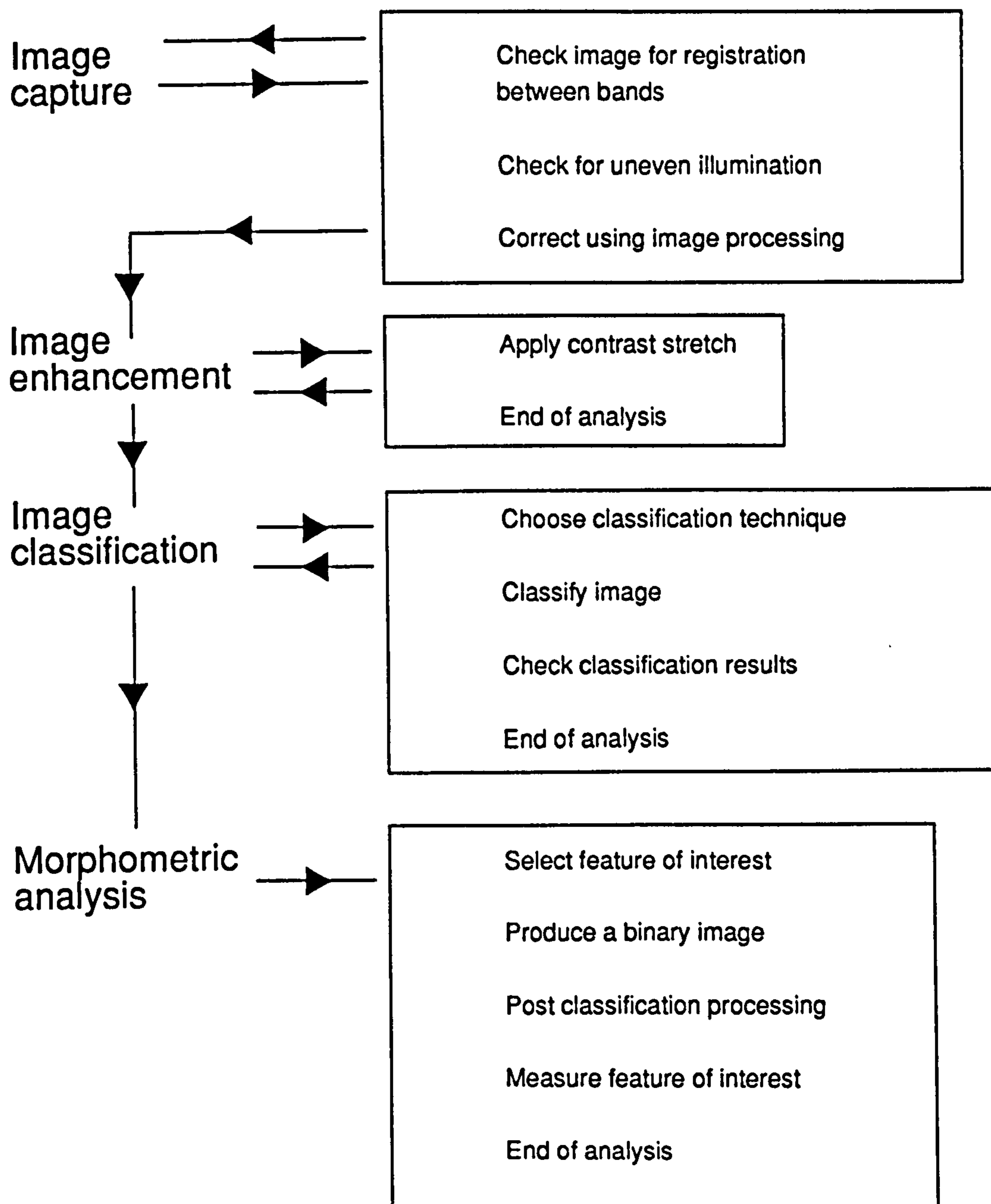


Fig. 9.21 Summary of image analysis techniques used to study soil thin sections

particularly where features were faint or heterogeneity of the slide made it difficult to divide into regions.

Contrast stretching was the main method used to enhance features in thin sections. The transformations were executed in video RAM allowing the final result to be viewed in a matter of seconds. The speed of these operations meant the technique was suitable for interactive use. If the results had taken a number of hours to produce, the technique would not have been used. The slowest part of the process was image capture.

Image enhancement did not add any new results to the analysis. There must be information present in the original image for an enhancement procedure to be successful. Although contrast stretching is capable of enhancing very small differences in grey levels it was found that most features could be observed without their use. The main benefit was a reduction in the uncertainty about the existence of features that were difficult to observe using conventional techniques. If the technique was speeded up then contrast stretching could be used on a routine basis.

The enhancement of images might be the end result of the analysis. However a second level of operation was the multispectral classification of images (fig 9.21). This allowed spectral signatures of features in thin sections to be described and images classified. Of the classification techniques used the unsupervised maximum likelihood method proved to be the most successful for discriminating features of interest.

Based on the results in chapter 2 it was evident that classification techniques could be used in one of two ways. Firstly, the results of analysing L1644 show that classification techniques can be used to find features in the slide that are not easily recognisable. The classification procedure produces a number of spectral classes, determined by the analyst, which are then individually assigned to informational groups. During this process indistinct features can be highlighted.

If classification techniques are to be routinely used for this purpose they would have to operate at greater speeds. The classification techniques used in this study took anything from one hour to many hours depending on the reliability of the software, the number of people using the computing resources and the number of bands submitted to the classifier. When examining a thin section slide the analyst is constantly studying many fields of view at different magnifications. Given the length of time taken to run a classification routine it was not practical to use this technique for the routine inspection of a large number of thin sections.

Secondly classification techniques were used to isolate specific features of interest which were then submitted for further morphometric analysis. The practical example used during this study was the isolation of fine material, coarse material and void area. The benefits of being able to describe statistical relationships between three of the A horizons studied added weight to the observations. This relationship was suspected

during the standard thin section analysis but could not be categorically stated. The interpretational value was mitigated to some extent because there was not time to see if this relationship was true for other buried soils on the site.

Assigning empirical values to features raises the question about how statistically verifiable are results in terms of the rest of the slide, other parts of the horizon which were not sampled, and measurements carried out at different scales of observation. Questions such as this validate the empirical approach rather than invalidate it. The amount of sampling necessary to produce statistically verifiable results should be known, particularly when trying to make assumptions about landscape processes from microscopic sized features seen in thin sections. A problem with this approach is that the amount of sampling required to produce results of this nature would probably not be financially possible on most archaeological sites. This should be considered when deciding on the applicability of using a quantitative technique rather than a traditional qualitative approach.

The difficulties associated with quantitative image analysis, discussed by Thompson et al. (1992, section 2.3) are also evident in this study. Although the use of unsupervised classification is an attempt to increase the quantitative aspect of studying thin sections, the analyst still has to subjectively assign spectral categories to informational groups and decide on appropriate methods for correcting classified images. Both of these represent potential sources of error. There is clearly a

need for research to investigate the amount of error involved in greater detail.

It is hoped in the future that the image analysis processes can be standardised enabling analysts in different laboratories to share information about spectral signatures of features and error levels associated with morphometric analysis. If all variables during the capture of images are kept equal and thin sections are kept the same thickness it should be possible to transfer spectral signatures of features between laboratories for use in classification. The following components of the image capture process would need to be standardised for this to be possible;

- Intensity of light source
- Diffusion of light source
- Sensitivity of digitiser
- Correction for uneven illumination
- Filtration used to select wavelength
- Algorithms used for classification
- Thickness of thin section

Given the continued price reduction of computing facilities it should not be beyond the budgets of most laboratories to afford the basic equipment for image analysis. An optimal equipment list at the present time would be as follows;

486 DX2 (66MHz) IBM compatible PC (or an IBM compatible PC fitted with a Pentium microprocessor which will be available in the



early part of 1993), Windows accelerator card, 1GB hard disk, 32MG RAM, high resolution monitor capable of displaying images as 3 band colour composites and up to 8 overlay planes, A W.O.R.M. or rewritable optical disk for storage of images (or similar medium), software for image enhancement, multispectral classification and morphometric analysis, high quality colour digitiser sensitive to low levels of illumination (or high quality colour filters that do not cause diffraction light), 2 high quality polarising filters and 2 mica plates, a stable and bright illumination source and an optical microscope.

Most of the processing done during this study was carried out on PCs. The processor speed of PCs, the improved internal architecture, the increased amount of RAM available to programs and the size of hard disks now being produced make personal computers as powerful as mainframes which were used a few years ago. This is a trend that looks likely to continue with the release of Intels new Pentium chip during 1993 and the establishment of new 32 bit operating systems including Microsofts NT, IBMs OS/2 and Novels Unix for PCs. As the availability of the equipment listed above increases, and prices decrease, it is hoped that the use of image analysis in soil micromorphological studies will be encouraged.

For many years personal computers have been used for little more than glorified type writers or calculators. As technology changes, PCs are becoming more orientated towards graphic operations. This has been stimulated mainly by the increase in

use of a Graphical User Interface (GUI), in particular Microsoft Windows, and also by the development of computer games and virtual reality equipment. Image analysis can make use of the advantages in hardware that other graphically intensive applications need. For instance dedicated microchips, like the new S3 range of chips, that are designed to carry out the computations needed for graphical displays freeing the main CPU for other operations.

The equipment is already available to have a standard PC set up next to a microscope linked to a digitising camera. Using the multitask facilities of a programs like Windows 3.1, OS/2 or Unix, the operator could use image analysis to aid his description of the thin sections while using a data base facility to store all the results. The data base could also be set up to store results from a conventional description. This would be particularly useful in a study such as the one at Lairg where it was difficult keeping track of the large amount of data generated from the thin section descriptions.

## **Conclusion**

It is hoped that this thesis has indicated ways in which the use of different types of image analysis techniques can be applied to soil micromorphological studies. Emphasis has been placed on the benefits of using techniques interactively, particularly if they are going to be routinely applied to thin section descriptions. There is considerable scope for future research

both in spectral and morphological quantification of soil features. Spectral quantification will benefit from standardised equipment being used and the incorporation of non spectral data in the classification process. The application of neural networks for the pattern recognition of soil features is also a possibility.

## **Appendix 1**

### **List of monuments sampled for thin section analysis from the Lairg site.**

#### **Group A monuments**

##### **M64, LP, hut circle**

Sample 1, buried A horizon, described context 8013.

Sample 2, buried A horizon, impregnated but not made.

Sample 3, wall of structure, impregnated but not made.

Sample 4, wall of structure, impregnated but not made.

Sample 5, buried A horizon, described context 8013.

Sample 6, wall of structure, described c.8008

Sample 7, buried A horizon to east of monument, described c.8006, c.8014 lost during sample preparation.

Sample 8, soil accumulation to east of monument, described c.8008.

##### **M62, EP, cross contour dyke**

Sample 1, impregnated but not made, c.8032, c.8034, c.8035.

Sample 2, buried A horizon, described c.8035 and c.8037.

Sample 3, impregnated but not made, interface between buried E and Bs horizon, c.8037, c.8038, c.8039.

Sample 4, impregnated but not made, buried A horizon to south of monument, c.8036.

Sample 5, buried B horizon, described c.8038.

##### **M86, EP, lynchet**

Sample 162, soil accumulation behind lynchet, described c.5024, 5025 and thin iron pan.

Sample 161, interface between buried A horizon and buried B horizon, described c5026 and c.5027.

**M88, EP, clearance cairn**

Sample 161, buried A horizon to east of clearance cairn, described c.5020.

Sample 159, interface of buried A and buried B horizon, described c.5020 and 5021.

**M87, EP, clearance cairn**

Sample 1, impregnated but not made, soil accumulation behind clearance cairn, c.8021.

Sample 2, impregnated but not made, soil accumulation behind clearance cairn, c.8021.

Sample 3, impregnated but not made, buried B horizon, c.8022.

Sample 4, impregnated but not made, buried B horizon, c.8022.

Sample 5, impregnated but not made, glacial till, c.8023.

**M127, PM, rectangular structure**

Sample 1, stony anthropogenic layer, described c.8045.

Sample 2, buried A horizon, described c.8046 and c.8047.

Sample 3, lower part of buried A horizon, c. 8046.

Sample 4, lower part of buried A horizon, c.8046.

Two samples were taken from the wall of the structure, these were impregnated but not made.

**M75/4, PM, enclosure dyke**

Sample 1, buried humose and non humose A horizon, described c.8029, c.8030 and c.8026.

Sample 2, buried A horizon, impregnated but not described c.8026.

Sample 3, wall of structure, impregnated but not described, c.8025.

Sample 4, base of buried A horizon, described c.8027.

### **M164, PM, dyke**

Sample 1, wall of monument, described c.3032.

Sample 2, wall of monument, described c.3032.

Sample 3, wall of monument, described c.3032.

Sample 4, base of dyke wall, buried organic layer, top of buried A horizon, described O horizon and c.3034.

### **M21, unburied soil accumulation**

Sample 1, soil accumulation, described c.8000.

Sample 2, soil accumulation, described c.8000.

Sample 3, soil accumulation, described c.8000.

Sample 4, soil accumulation, described c.8000.

Sample 5, soil accumulation, described c.8000.

Sample 6, soil accumulation, described c.8000.

Sample 7, buried A horizon, described c.8002.

Sample 8, buried A horizon, described c.8003.

### **Group B monuments**

#### **M648, EP, field boundary**

Sample 1, buried A horizon, described c.7004.

Sample 2, buried A horizon, described c.7004.

Sample 3, soil accumulation to east of monument, described c.7007.

#### **Transect 7000**

One sample was taken from midway between two field boundaries, M648 and M505. The sample was made into a thin section and described.

**M505, EP, field boundary**

Sample 1, buried A horizon, described c.8064.

Sample 2, interface of buried A horizon and buried E horizon, c.8064 and c.8065.

Sample 3, buried Bsg horizon merging into top of glacial till, c.8067.

**M504, LP, hut circle**

Sample 1, buried floor deposits and underlying buried soil, described c.8071 and c.8072.

Sample 2, interface of buried A horizon and buried Bs horizon, described c.8072 and c.8074.

Sample 3, interface of buried A horizon and buried Bs horizon, described c.8076 and c.8074.

Sample 4, interface of buried A horizon, Bs horizon and glacial till, described c.8076, c.8074 and c.8075.

Sample 5, interface of Bs horizon and glacial till, described c.8074 and c.8075.

**M659, EP, hut circle**

Sample 1, Buried A horizon, described c.f2300.

Sample 2, Base of monument wall, not described, f2117 and f2300

**M660, EP, hut circle**

Sample 1, interface between buried A horizon and buried Bs horizon, described c.2132 and c.2184.

Sample 2, three contexts spanning 3 contexts, described base of hut circle wall, c.2099, ash layer, c.2136, and the buried A horizon, c.2132.

Sample 3, hut circle wall, described c.2099.

## **Group C monuments**

### **M975, PM, enclosure dyke**

Sample 1, impregnated but not described, derived from the same context as sample 2.

Sample 2, grey layer at the top of the buried A horizon, described, c.8103, top of the buried A horizon. Context 8101 was the base of the hut circle wall and was not described.

Sample 3, buried A horizon, described c.8103.

Sample 4, interface of buried A horizon and buried Bs horizon, impregnated but not described.

Sample 5, taken from stratigraphy to west of monument, a thin section slide was made but not described.

Sample 6, glacial till, described c.8105.

### **M1069, PM, rectangular house**

Sample 1, grey layer located at the top of the buried A horizon, described c.8111.

Sample 2, buried A horizon, described c.8112.

Sample 3, buried Bs horizon, described c.8113.



## Appendix II

### Field descriptions of selected soil pits excavated during 1989 and 1990 at Lairg

#### M64, LP, hut circle.

Context 8004. Modern A horizon, colour 7.5YR 3/2 dark brown, humose, few medium subangular stones, loamy sand, fine to medium moderately developed granular structure, medium packing density, many medium to coarse fibrous, fleshy bracken roots, many very fine fibrous grass roots. Some earthworms seen, lower boundary was clear and wavy.

Context 8005. Stony material below topsoil at the eastern end of the trench. Probably not archaeological but more likely a naturally stony soil buried by colluvial material. Stones may have been the result of clearance or might have been derived from the bank of the hut circle. Colour 10YR 3/2 very dark greyish brown, humose, abundant subangular medium sized stones, sandy loam, apedal massive, medium packing density, 1 or 2 bracken roots penetrating from the layer above, few fine fibrous grass roots, earthworms present, common manganese nodules, lower boundary wavy and clear with the buried soil below.

Context 8006. Buried soil to the east of the cut. Poorly preserved by colluvial material above it. Colour 10YR 3/2, very dark greyish brown, non humose, abundant medium to large subangular/subrounded stones, few small subangular stones, apedal massive, medium packing density, common fine fibrous grass roots, lower boundary abrupt with the top of the weathered glacial till.

Context 8007. The fill of cut 8015. Loosely packed large and very large boulders with very little matrix towards the base. The bottom of this feature was not reached. Colour 10YR 2/2 very dark brown, non humose, very abundant subangular to subrounded large (approx 20cm diameter) stones, sandy loam, weakly developed fine/medium granular structure, medium packing density, few bracken roots penetrating from the layer above, common very fine/fine grass roots, small flecks of charcoal present, black coatings over the large rocks are possibly Mg or Fe compounds caused by waterlogging. The lower boundary with 8008 is clear and wavy, with 8013 clear and wavy.

Context 8008. Material comprising the bank of the hut circle, probably derived from a Bs horizon. Colour 7.5YR 3/4 dark brown, non humose, abundant subangular/angular stones, few angular large stones, common small subangular stones, loamy sand, weakly developed fine granular structure, medium to loose packing density, few bracken roots penetrating from above, common very fine fibrous grass roots, lower boundary abrupt and wavy with the buried soil (context 8013).

Context 8009. Layer of material within the bank of the hut circle. Colour 10YR 2/1 black, non humose, 1 large subangular stone, sandy loam, weakly developed fine granular, medium packing density, few bracken roots penetrating from above, few very fine fibrous grass roots, charcoal present, lower boundary abrupt and wavy with 8010.

Context 8010. Cell of material within the bank of the hut circle. Colour 10YR 2/2 very dark brown, few small subangular stones, sandy loam, apedal massive, medium packing density, few very fine fibrous grass roots, charcoal present, earthworms seen, lower boundary sharp and irregular with stones.

Context 8011. Layer of stony material at the west end of the trench. Forming an unknown archaeological layer. Possibly represents a later period of activity, possibly a clearance cairn. Colour 10YR 2/2 very dark brown, humose, Extremely abundant large to very large subangular stones, sandy loam, moderately developed fine to medium granular structure, medium packing density, common coarse bracken roots, many very fine fibrous roots, few fine fleshy roots, earthworms present, lower boundary gradual and wavy with 8009.

Context 8012. This is part of the hut circle bank. It consists of a layer of large stones immediately over the top of the buried soil.

Context 8013. Buried A horizon beneath the main section of the hut circle. Colour 10YR 3/2 very dark greyish brown, non humose, many medium subangular stones, loamy sand, apedal massive, medium packing density, few very fine fibrous roots, charcoal present, lower boundary sharp and wavy with the glacial till.

Context 8014. No clear B horizon but the top 10cms of this layer is loose and possibly represents a shallow Bg horizon. Colour 10YR 4/4 dark yellowish brown, non humose, abundant large to very large subangular stone, common small subangular stones, sand to loamy sand, apedal massive, medium packing density, few very fine fibrous roots.

Context 8015. A steep sided ditch or gully cut through the back of the hut circle into the glacial till. Possibly a drainage gully added late in the life of the hut circle. The lower part of the feature was not revealed but it was at least 0.7cms deep.

#### **M62, EP, cross contour dyke**

Context 8031. Topsoil. 7.5YR 3/4 dark brown, humose, sandy loam, few large subrounded stones, weakly developed medium granular structure, medium packing density, many very fine fibrous roots, lower boundary with 8032 abrupt and irregular, with 8033 abrupt and wavy.

Context 8032. Matrix of the monument. Colour 10YR 3/2 dark brown, humose, loamy sand, very abundant large to very large subangular to subrounded stones, weakly to moderately developed medium granular structure, medium packing density, many very fine fibrous roots, common fine fibrous roots, many coarse bracken roots, lower boundary with 8034 sharp and wavy, with 8035 abrupt and wavy.

Context 8033. Soil accumulation to the south of the monument. Colour 10YR 3/3 dark brown, humose, loamy sand, few medium subangular stones, common very small subrounded stones, apedal massive, medium packing density, many coarse bracken roots, lower boundary with 8036 gradual and wavy.

Context 8034. Dark organic layer. Colour 7.5YR 2/0 black, humose, sandy loam, no stones, apedal massive, medium packing density, few fine and very fine fibrous roots, charcoal present, lower boundary with 8035 sharp and wavy.

Context 8035. Buried A horizon. Colour varies between 10YR 3/3 dark brown and 7.5YR 3/4 dark brown, non humose, loamy sand, apedal massive, common very small to small subangular to subrounded stones, medium packing density, few very fine fibrous roots, lower boundary with 8037 sharp and wavy, with 8038 abrupt and wavy.

Context 8036. Buried A horizon not sealed by the monument. Colour 10YR 3/3 dark brown, non humose, loamy sand, few medium subangular stones, few large subangular stones not measuring greater than 10cms, apedal massive, medium packing density, common very fine fibrous roots and few coarse bracken roots, lower boundary abrupt irregular with 8038.

Context 8037. Buried E horizon. Colour 10YR 3/3 pale brown, non humose, loamy sand, common small to medium subangular stones, apedal massive, medium packing density, few very fine fibrous roots, lower boundary with 8038 and 8039 abrupt and wavy.

Context 8038. Bs horizon showing horizontal variations in colour. Colour 7.5YR 4/6 strong brown outside the monument, 7.5YR 4/4 strong brown where buried by the monument, non humose, sand, many small to medium subangular stones, few large to very large subangular stones, apedal massive, medium packing density, few very fine fibrous roots, lower boundary with 8040 clear.

Context 8039. Cell of material below 8037 within the Bs horizon. Colour 7.5YR 3/4 dark brown, non humose, sand, many small to medium subangular stones, few medium to large subangular stones, apedal massive, medium to high packing density, no roots, lower boundary with 8040 clear.

Context 8040. Glacial till. The colour varies between 10YR 3/4 yellowish brown and 10YR 4/6 dark yellowish brown, non humose, sand, common very large subangular stones, apedal massive, high to medium packing density.

## **M86, EP, lynchet**

Lynchet to the north of the head dyke, M75, in an area of stagnopodzols.

Context 5022. Modern peaty topsoil. 5YR 3/2 dark reddish brown, amorphous peat, stoneless, abundant very fine and fine fibrous roots, many medium to coarse woody heather roots, lower boundary abrupt and smooth with 5023, abrupt and smooth with 5024.

Context 5023. Pale mineral horizon beneath the peat. 10YR 3/2 very dark greyish brown, humose, loamy sand, few small to medium subangular stones, apedal massive, medium packing density, common very fine to fine fibrous roots, many medium woody heather roots, lower boundary abrupt and smooth with 5024.

Context 5024. Soil accumulation above iron pan. 10YR 2/2 very dark brown, non humose, sandy loam, few small to medium subangular stones, apedal massive, medium packing density, common very fine to fibrous roots and many medium woody heather roots, thin continuous iron pan at the base of the horizon, lower boundary sharp and smooth with 5025 (formed by iron pan).

Context 5025. Soil accumulation below iron pan. 10YR 4/2 dark greyish brown, non humose, loamy sand, few small to large subangular stones, apedal massive, medium packing density, few fine fibrous heather roots, lower boundary abrupt and smooth with 5026

Context 5026. Buried A horizon. 10YR 3/2 very dark greyish brown, non humose, loamy sand, few small to medium sub-angular stones, apedal massive, medium packing density, few fine fibrous heather roots, lower boundary sharp and smooth.

Context 5027. Shallow B horizon and top of glacial till. 7.5YR 6/6 reddish yellow, many 7.5YR 5/6 strong brown, coarse, faint, diffuse, mottles. Non-humose, loamy sand, many small to large subangular to angular stones, apedal massive, high packing density, few very fine and fine fibrous roots, lower boundary clear and irregular with glacial till or bedrock.

## **M88, EP, clearance cairn**

Clearance cairn to the north of M75, the medieval head dyke, located in an area of stagnopodzols.

Context 5016. Modern peaty topsoil. 5YR 2.5/2 dark reddish brown, semi fibrous peat, stoneless, abundant very fine and fine fibrous roots, many medium and coarse woody heather roots, lower boundary abrupt and smooth with 5017, abrupt and smooth with 5028.

Context 5017. Pale mineral horizon beneath peat. 10YR 3/1 very dark grey, humose, loamy sand, few medium sub-rounded to sub-

angular stones, apedal single grain, medium packing density, abundant very fine and fine fibrous roots, many medium woody heather roots, lower boundary gradual and irregular with 5018, clear and smooth with 5028.

Context 5018. Clearance cairn consisting of vacuous large rubble. Organic matrix only present towards base of context. 5YR 2.5/1 black, amorphous peat, extremely abundant large to boulder sized sub-rounded stones, few very fine to medium fibrous heather roots, lower boundary abrupt and smooth with 5021.

Context 5019. Soil accumulation, 10YR 4/4 dark yellowish brown, non-humose, loamy sand, few small to medium sub-angular stones, apedal massive, medium packing density, few very fine to fine fibrous roots, occasional charcoal, lower boundary clear and smooth with 5020.

Context 5020. Buried A horizon, 10YR 4/2 dark greyish brown, non-humose, loamy sand, few small to medium sub-rounded stones, apedal massive, medium to high packing density, few very fine fibrous roots, occasional charcoal, lower boundary sharp and smooth with 5021.

Context 5021. Mixed B and C horizon material overlying glacial till, 10YR 4/3 brown, and 7.5YR 5/6 strong brown, non-humose, loamy sand, common small to large sub-angular blocky, platy stones, apedal massive, medium packing density, few very fine fibrous roots, charcoal present in pockets of brown material, lower boundary abrupt and irregular with glacial till.

Context 5028. Mineral horizon with Fe pan at base. 10YR 2/2 very dark brown, humose, sandy loam, few small to large sub-rounded blocky stones, apedal massive, medium packing density, abundant very fine to fine fibrous roots, thin continuous Fe pan at the base of the layer, lower boundary with 5019 sharp and smooth, with 5018 sharp and irregular, with 5021 sharp and smooth.

#### **M87, EP, clearance cairn**

Context 8016. Modern peaty topsoil. 5YR 2.5/2 dark reddish brown, semi fibrous peat, stoneless, many very fine fibrous roots, few medium fleshy roots, few fine fleshy roots, lower boundary abrupt and wavy with 8017.

Context 8017. Grey layer below peat. 10YR 3/1 very dark grey, non humose, loamy sand, few medium subangular stones, apedal massive, medium packing density, many very fine fibrous roots, few fine fleshy roots, lower boundary abrupt and wavy above all contexts.

Context 8018. Scattered large stones in a mineral soil matrix situated above a mineral soil which abutts the cairn. Non humose, loamy sand, few medium subangular stones, abundant large subangular stones, medium packing density, common fine fleshy

roots, thin continuous iron pan, lower boundary with 8021 sharp and wavy, with 8019 diffuse.

Context 8019. Monument consisting of large stones and amorphous organic matter. The organic material probably formed as a result of the decomposition of the matted root material around the large stones. 10YR 2/1 black, amorphous organic matter, very abundant large to very large subangular stones, variable root content forming mats around the rocks, abundant very fine fibrous roots, common fine fleshy roots, lower boundary sharp and wavy with 8020.

Context 8020. Mottled layer below monument. 10YR 2/2 very dark brown, many, coarse, prominent, sharp, clear, 10YR 5/8 yellowish brown mottles. Generally non humose but lenses of material have a more humose feel, loamy sand, many medium subangular stones, apedal massive, medium packing density, few very fine fibrous roots, thin continuous iron pan at the base of the context, lower boundary sharp.

Context 8021. Soil accumulation to the east of the monument. Generally 10YR 4/3 dark brown but there is a slight colour change down the profile to 10YR 3/3. Non-humose, loamy sand, common medium to large subangular to subrounded stones, apedal massive, medium packing density, few very fine fibrous roots, occasional charcoal, lower boundary clear and wavy with 8022.

Context 8022. Bs horizon. 7.5YR 4/4 dark brown, non humose, loamy sand, many medium subrounded stones, small angular stones also present, apedal massive, medium packing density, few very fine fibrous roots, lower boundary abrupt and wavy with 8023.

Context 8023. Top of weathered glacial till. 10YR dark yellowish brown, loamy sand, abundant small to medium subangular stones, apedal massive, medium packing density, few to common very fine fibrous roots. At the west end of the trench where the Fe pan rises fine concretions are present.

#### **M127, PM, rectangular structure**

Context 8041. Modern topsoil. The grass on top forms mat of undecomposed remains 3-4cms thick lying directly on top of the monument.

Context 8042. Turf wall with a revetment of stone on its west face. The matrix of the monument consists of cells of material. This appears to be a result of decomposing turves and the addition of material derived from the B horizon. The colour varies between 10YR 3/3 dark brown, where the texture is loamy sand, and 10YR 2/1 black where there is greater amounts of organic material. Organic matter content varies between amorphous organic and humose, loamy sand where there is less organic material, few medium subrounded stones, apedal massive with weakly developed fine granular structure in places, medium

packing density, many fine fibrous roots, earthworms present, lower boundary sharp and wavy with the insitu. turf line.

Context 8043. Cells of orange loamy sand material within the matrix of the monument. Possibly represents material from the B horizon. Colour 7.5YR 3/4 dark brown, non humose, loamy sand, few very small subrounded stones, weakly developed fine granular structure, low to medium packing density, many very fine fibrous roots, lower boundary abrupt and wavy.

Context 8044. Dark black band below the monument interpreted as an O horizon. This feature appears most substantial underneath the revetment. Colour 10YR 2/1 black, amorphous organic, few medium subangular stones, few very fine fibrous roots, lower boundary abrupt and wavy.

Context 8045. Stony layer below the insitu turf with an iron pan running through it. Colour 10YR 2/2 very dark brown, few medium, distinct, clear, 7.5YR 5/6 strong brown mottles. Non humose, sandy loam, many small to medium subangular stones, apedal massive, common very fine fibrous roots. A thin discontinuous iron pan is present, lower boundary abrupt and irregular.

Context 8046. Buried A horizon. Colour 10YR 3/3 dark brown, non humose, sandy loam, common medium subangular stones, apedal massive, medium packing density, few very fine fibrous roots, charcoal present. Lower boundary clear and wavy with 8047, sharp and wavy with Bs horizon.

Context 8047. Cell of material within the 8046. Indistinct and difficult to estimate the position of the boundaries. Colour 10YR 3/2 very dark greyish brown, non humose, sandy loam, common medium subangular stones, apedal massive, medium packing density, few very fine fibrous roots, lower boundary clear and wavy.

Context 8048. Bs Horizon, colour 7.5YR 4/6 strong brown, non humose, loamy sand, many medium to large subangular stones, apedal massive, apedal massive, packing density medium to high, few fine fibrous roots, lower boundary clear with glacial till.

Context 8049. Glacial till, no soil description completed.

#### **M75/4, PM, enclosure dyke**

Context 8024. A layer of topsoil 5cms thick overlying the monument. In places underlying rocks could be seen. Colour 10YR 2/2 very dark brown, humose, sandy loam, few small angular to subangular stones, some tabular, also some large subangular stones protruding from the monument. Weakly developed fine granular structure, loose to medium packing density, abundant very fine fibrous roots and common fine fleshy roots, lower boundary abrupt and irregular with the stones of the monument. Flora on top included predominantly rushes, grasses and mosses.

Context 8025. Turf and stone dyke. Lenses of black organic matter can be seen within the matrix. These might be the result of decomposing turves which had been used to construct the dyke. However mats of organic material had formed around the stones which could have also resulted in this feature. Colour 10YR 2/1 black, humose with lenses of amorphous organic material, sandy loam, many large subangular to subrounded stones, weakly developed granular structure around stones apedal massive elsewhere, medium packing density. Abundant very fine fibrous roots forming mats around stones, common fine fleshy and common very fine fibrous roots found elsewhere in the matrix. Lower boundary sharp and smooth onto a black organic layer (context 8029).

Context 8026. Buried A horizon, upper. Colour 10YR 3/2 very dark brown (N.B Colour difference with 8027 might be caused by eluviation from 8030). Non humose, loamy sand, few small subangular stones, many medium subrounded stones, apedal massive, medium packing density, few very fine fibrous roots, lower boundary clear with lower buried A horizon.

Context 8027. Buried A horizon, lower. Orange colours in the field were interpreted as localised concentrations of sesquioxides. Colour 10YR 3/3 dark brown, few, fine, prominent, sharp, 7.5YR 5/8 strong brown mottles. Non humose, loamy sand, common very small, subangular stones, common small subangular stones, apedal massive, medium packing density, few very fine fibrous roots, lower boundary sharp and smooth with c.8028.

Context 8028. Buried B horizon. Colour 10YR 5/3 brown, common fine prominent, clear 7.5YR 5/8 strong brown mottles, non humose, sand to loamy sand, abundant large stones, apedal massive, medium packing density, no roots.

Context 8029. Buried humose A horizon. Colour 10YR 3/1 very dark grey, non humose/humose, loamy sand, common medium subangular stones protruding from above and below, apedal massive, medium packing density, few very fine fibrous roots, lower boundary abrupt and wavy.

Context 8030. Grey layer below humose horizon, possibly represents a weakly developed E horizon. Colour 10YR 4/2 dark greyish brown, non humose, sandy loam, common medium subangular stones, apedal massive, medium packing density, few very fine fibrous roots, lower boundary clear.

#### **M164, PM, dyke**

Context 3031. Modern A horizon. 5YR 2.5/2 dark reddish brown, semi amorphous peat on top of monument humose elsewhere, few very small subangular blocky stones, apedal massive, medium packing density, abundant very fine fibrous roots, lower boundary smooth and clear.



Context 3032. Dyke or field boundary constructed with an outer cladding of large stones over a generally stone free turf core. A soil matrix is present behind the large stones in the east facing section. Bands of horizontally aligned dark organic material are present where the organic component of the turves used to build the dyke has decomposed. Turf lenses 10YR 2/1 black, amorphous peat. Mineral layers 7.5YR 3/2 dark brown, non-humose, sand, common medium sub-angular blocky stones, abundant very large subangular stones, apedal massive, medium packing density, common very fine fibrous roots, ants nest 12cms in diameter, beetles, lower boundary smooth and sharp.

Context 3033. Buried A horizon. The top of this horizon is sealed by a dark band of amorphous organic material, this is considered to be the insitu O horizon. Insitu O horizon 10YR 2/1 black, amorphous peat. Buried A horizon 7.5 YR 3/2 dark brown, humose, sand, many medium blocky angular stones, few small angular blocky stones, apedal massive, medium packing density, few very fine fibrous roots, thin continuous iron pan beneath 3033, lower boundary sharp and wavy.

Context 3034. Buried B horizon 7.5YR 3/4 dark brown at top changing to 10 YR 3/4 dark yellowish brown at bottom, non-humose, sand, common medium angular blocky platy stones, few very small angular blocky stones, apedal massive, few very fine fibrous roots, lower boundary smooth and clear.

Context 3035. Modern A horizon. 7.5 YR 4/4 brown, non-humose, sand, common medium subangular blocky tabular stones, few very small to small subangular blocky tabular stones, apedal massive, medium packing density, common very fine fibrous roots, lower boundary smooth and clear with 3034, smooth and clear with 3033.

#### **M21, unburied soil accumulation**

Context 8000. Deep accumulation of soil burying a layer with abundant large stones. The deposit is homogenous with no apparent stratigraphy. Colour 5 YR 3/2 dark reddish brown, humose, few small angular/subangular stones, few medium to large subangular stones, loamy sand, apedal massive, medium packing density, many very fine fibrous grass roots in the top 5-10cms, few fine fibrous roots below this, earthworms and unidentified beetles seen. The lower boundary is sharp irregular. The vegetation growing above includes grass on top changing to rushes at the break of the slope.

Context 8001. Concentration of large and very large stones forming a revetment or wall possibly fronting the original field. 10YR 3/3 dark brown, humose, loamy sand, apedal massive but also well developed granular structure between some of the stones, medium packing density, common very fine fibrous grass roots. Lower boundary sharp irregular.

Context 8002. Buried pre-revetment soil, possibly a buried A horizon. 10YR 4/2 dark greyish brown, non humose, sandy loam (gritty), abundant small to large subrounded to angular equidimensional stones, apedal single grain, medium packing density, few very fine fibrous roots. Lower boundary clear and wavy.

Context 8003. Buried A/Bg horizon. Abundant ferruginous mottles and grey colour of overlying horizon implies waterlogging. 10YR 4/3 brown, many, fine, distinct, clear, mottles, 7.5YR 4/4 brown, non-humose, loamy sand, abundant small to very large subangular and angular equidimensional stones, apedal single grain, packing density medium to high, lower boundary not seen.

#### **M505, EP, field boundary**

Context 8061. Layer of turf capping overlying the monument and extending beyond it. To the east of the monument are patches of heather interspersed with areas of grass. At the field boundary edge the predominant vegetation is heather. Colour 10YR 2/1 black, amorphous organic, no stones, many very fine fibrous roots, common fine fleshy roots, lower boundary abrupt irregular.

Context 8062. A horizon to west of monument. Colour 10YR 2/2 very dark brown, humose, sandy loam, common small to medium subangular stones, apedal massive, medium packing density, many very fine fibrous roots, lower boundary sharp and wavy.

Context 8063. Context below the peat including the monument stones and a thin discontinuous Fe pan. Colour 10YR 2/2 very dark brown to 10YR 3/3 dark brown, humose, sandy loam, common medium to large subangular stones, apedal massive, medium packing density, common very fine fibrous roots, charcoal present, thin discontinuous Fe pan, lower boundary clear.

Context 8064. Buried A horizon. Many fragments of charcoal. Colour 10YR 3/2 very dark greyish brown, non humose, loamy sand, common medium subangular stones, apedal massive, medium packing density, common very fine fibrous roots, abundant charcoal fragments, fine equidimensional manganese nodules, lower boundary sharp irregular.

Context 8065. Buried E horizon. Colour 10YR 6/2 light brownish grey, non humose, sand to loamy sand, apedal single grain, common small subangular stones, few medium to large subangular stones, low to medium packing density, few very fine fibrous roots, some charcoal at boundary with 8064. Common very fine rounded nodules (probably manganese), lower boundary abrupt.

Context 8066. Pale layer to west of monument. Colour 10YR 4/3 brown, non humose, sand loamy sand, common medium subangular stones, apedal massive, medium packing density, common very fine fibrous roots, lower boundary abrupt.

Context 8067. B horizon, strong orange mottles present, depth unknown appears to merge into the top of the weathered glacial till. Colour 10YR 5/3 brown, many plate like coarse mottles, 7.5YR 5/8 strong brown to 10YR 5/8 greyish brown, non humose, sand, common small to medium subangular stones, common large subangular to subrounded stones, high packing density, few very fine fibrous roots, lower boundary not seen.

#### M504, LP, hut circle

Context 8068. Topsoil overlying the monument. Colour 10YR 2/1 black, humose, few medium subrounded stones, many very fine fibrous roots, common fine fleshy roots, few coarse woody roots, lower boundary sharp irregular with monument stones, abrupt wavy to south of monument stones.

Context 8069. Matrix of monument stones where they were tightly sealed to the northern end of the trench. Colour 10YR 2/2 very dark brown, lenses of 10YR 5/8 yellowish brown material could also be seen, non humose, sandy loam, abundant large to very large subangular to subrounded stones, apedal massive, medium packing density, common very fine fibrous roots, common fine fleshy roots, some charcoal present, lower boundary sharp wavy with charcoal rich layer, abrupt wavy with buried soil.

Context 8070. Matrix of the monument stones to the south of the well sealed layer. Colour 10YR 2/2 very dark brown, non humose, sandy loam, many large subangular to subrounded stones, few small to medium subangular stones, apedal massive, medium packing density, many very fine fibrous roots, common fine fleshy roots, mycelium present, lower boundary abrupt wavy with the buried soil.

Context 8071. Dark layer between the buried soil and the monument at the north end of the trench (floor deposits). After a more complete excavation had been completed this was found to represent floor deposits. Colour 10YR 2/1 black, humose, sandy loam, few medium to large subangular stones, apedal massive, medium packing density, few very fine fibrous roots, few fine fleshy roots, charcoal present, lower boundary sharp with buried soil.

Context 8072. Buried A horizon underlying the well sealed section at the northern end of the trench. Colour 10YR 3/3 dark brown, non humose, loamy sand, few small to medium subangular stones, few large subangular stones, apedal massive, medium packing density, few very fine fibrous roots, flecks of charcoal present, lower boundary abrupt irregular with Bs horizon.

Context 8073. Lens of material in the west facing section lying within the buried soil. Colour 10YR 3/1 dark grey, non humose, sandy loam, no stones, apedal massive, medium packing density, few very fine fibrous roots, flecks of charcoal seen, lower boundary sharp and wavy.

Context 8074. Buried Bs horizon. Colour 2.5YR 5/4 reddish brown, abundant coarse irregular 10YR 4/6 dark yellowish brown mottles, non humose, sand to loamy sand, many medium subangular stones, common large subrounded stones, apedal single grain, high packing density, few very fine fibrous roots, lower boundary clear and wavy with glacial till.

Context 8075. Glacial till. Colour 2.5YR 6/2 light yellowish brown, common medium to coarse irregular 7.5YR 4/4 dark brown prominent clear mottles, non humose, common large subangular stones, apedal massive, medium packing density, no roots, lower boundary not seen.

Context 8076. Buried A horizon to the south of the tightly packed stones. Colour 10YR 3/3 dark brown, non humose, loamy sand, common medium subangular to subrounded stones, apedal massive, medium packing density, many very fine fibrous roots, lower boundary abrupt and wavy with Bs horizon.

#### **M975, PM, enclosure dyke**

Context 8098. Topsoil. 10YR 2/2 very dark brown, humose, loamy sand, few small to medium subangular to subrounded stones, moderately developed fine to medium granular, medium packing density, many very fine fibrous roots, common fine fleshy roots, common coarse woody bracken roots, earthworms present, lower boundary clear and wavy.

Context 8099. Brown lenses of material within the monument. 10YR 3/2 very dark greyish brown, humose, sandy loam, few small to medium subangular to subrounded stones, poorly developed fine granular, medium packing density, common very fine fibrous roots, few fine fleshy roots, few coarse woody bracken roots, lower boundary abrupt wavy.

Context 8100. Matrix of monument above stony layer. 10YR 3/1 very dark grey, humose, sandy loam, few small medium stones, weakly developed fine to medium granular structure, medium packing density, many coarse woody bracken roots, common very fine fibrous roots, common very fine fleshy roots, lower boundary abrupt irregular.

Context 8101. Context with high stone content within monument. 10YR 3/2 very dark greyish brown, non humose, sandy loam, abundant large subangular to subrounded stones, moderately developed fine granular structure, low to medium packing density, many common woody coarse bracken roots, lower boundary sharp wavy above Fe pan, clear wavy above buried soil.

Context 8102. Discontinuous band of grey material running over buried soil. In places a double iron pan has formed on either side of the layer. 10YR 3/2 very dark greyish brown, common fine distinct sharp equidimensional 7.5YR 4/4 dark brown mottles, non humose, sandy loam, common small to medium subangular to

subrounded stones, apedal massive, medium packing density, few very fine fibrous roots, thin discontinuous iron pan above and below, lower boundary sharp and wavy where iron pan present.

Context 8103. Buried A horizon. Colour varies from 10YR 3/3 dark yellowish brown at the top of the context to 10YR 3/3 dark brown at the bottom. Non humose, loamy sand, common small to medium subangular to subrounded stones, apedal massive, medium packing density, few very fine fibrous roots, fragments of charcoal, lower boundary abrupt and wavy with B horizon.

Context 8104. Buried Bs horizon. Colour varies between 10YR 5/8 yellowish brown to 7.5YR 4/6 strong brown, non humose, loamy sand, many small to medium subangular to subrounded stones, common large subangular to subrounded stones, apedal massive, medium packing density, few very fine fibrous roots, lower boundary abrupt and wavy with glacial till.

Context 8105. Glacial till. 10YR 4/4 dark yellowish brown (section very wet), non humose, sand to loamy sand, many small to large subangular to subrounded stones, apedal massive, medium to high packing density, no roots, lower boundary not seen.

Context 8106. Dark charcoal rich layer at the west end of the trench, possibly associated with the hut circle and represents an earlier phase of landuse. 10YR 3/2 very dark greyish brown, non humose, sandy loam, few medium to large subangular to subrounded stones, apedal massive, medium packing density, few very fine fibrous roots, abundant charcoal present, lower boundary abrupt wavy with 8107.

Context 8107. Grey layer below charcoal rich soil, possibly representing a buried soil of an earlier phase of landuse. 10YR 4/2 dark greyish brown, non humose, sandy loam, many very small subangular to subrounded stones, common medium subangular to subrounded stones, apedal massive, medium packing density, few very fine fibrous roots, some charcoal fragments, lower boundary abrupt wavy.

Context 8108. Lens of amorphous organic material. 7.5YR 2/0 black, amorphous organic, no stones, few very fine fibrous roots, lower boundary sharp and wavy.

#### **M1069, PM, rectangular house**

Context 8109. Modern topsoil. 10YR 3/2 very dark greyish brown, humose, sandy loam, few small to medium subrounded to subangular equidimensional stones, moderately developed medium granular structure, low packing density, abundant very fine and fine fibrous roots, common coarse fleshy roots (grass and bracken), lower boundary clear and irregular to 8110, clear and smooth to 8113.

Context 8110. Remains of cross wall of rectangular structure, very badly collapsed and spread. Composed of a loose collection of large stones in the topsoil matrix. A small lump of slag was found at the base of the layer. 10YR 3/2 very dark greyish brown, humose, sandy loam, abundant medium to large subangular equidimensional stones, weakly developed medium granular structure, medium packing density, many very fine and fine fibrous roots, many coarse fleshy grass and bracken roots, lower boundary abrupt and smooth with 8111.

Context 8111. Grey layer with double iron pan, 10YR 4/1 to 4/2 dark grey to dark greyish brown, non humose, sandy loam, common small to medium stones, apedal single grain, medium packing density, common very fine and fine fibrous roots, few coarse fleshy roots, thin continuous iron pan above and below this layer, lower boundary sharp and wavy to 8112.

Context 8112. Buried A horizon. 10YR 4/2 dark greyish brown, non humose, sandy loam, common small to large subrounded to subangular stones, apedal massive, medium packing density, few very fine and fine fibrous grass roots, charcoal present, lower boundary clear and wavy to 8113.

Context 8113. Bs horizon over bedrock or very stony glacial till. 10YR 4/4 dark yellowish brown, non humose, loamy sand, abundant small to large subrounded to angular stones, apedal massive, high packing density, few very fine fibrous roots, lower boundary abrupt and irregular to bedrock or large stones in the glacial till.

## References

- Altmuller, H.J., and Van Vliet-Lancee, 1990, Soil thin section fluorescence microscopy, in Douglas, L.A., (ed.), Soil micromorphology, a basic and applied science, Elsevier, Amsterdam, 565-579.
- Askew, G.P., Payton, R.W. and Shiel, R.S., 1985, Upland soils and land clearance in Britain during the second millennium BC, in Spratt, D. and Burgess, C., 1985, Upland settlement in Britain, the second millennium BC and after, BAR British Series 143, 5-33.
- Babel, U., 1975, Micromorphology of soil organic matter, in Gieseking, J.E., (ed.), Soil components, vol. I, organic components, Springer-Verlag, Berlin, New York.
- Ball, D.F., 1975, Processes of soil degradation: a pedological point of view, in : Evans, J.G. et al (eds.), The effect of man on the landscape: the highland zone, CBA Res. Rept. No.11, 20-27.
- Barber, J. and Brown, M.M., 1984, An Sithean, Islay, Proc. Soc. Antiq. Scot., 161-188.
- Barclay, G.T., 1983, Sites of the third millennium BC to the first millennium AD at North Mains, Strathallan, Perthshire. Proc. Soc. Anti. Scotland 113, 122-281.
- Barrett, J., Hill, P and Stephenson, J.B., 1976, Second millennium BC banks in the Black Moss of Achnacree; some problems of prehistoric land use, in Burgess C. and Miket, R, (eds), Settlement and economy in the third and second millennium BC, Oxford, 283-287, Brit. Arch. Rep., 33.
- Bell, M. and Walker, M.J.C., 1992, Late Quaternary environmental change, physical and human perspectives, Longman Scientific and Technical.
- Beucher, S. and Lantuejoul, Ch., (1979), Use of watersheds in contour detection. Int. Workshop on image processing, CCETT, Rennes, France.
- Bidwell, D.W., and Hole, F.D., 1965, Man as a factor of soil formation, Soil Sci., 99, 65-72.
- Blackburn, M., Caillier, M., Bourbeau, G.A. and Richard, G., 1988, Use of sodium chloride to replace water in specimens of heavy clay prior to resin impregnation, Geoderma, 41, 369-373.
- Boudot, J.P. and Brucket, S., 1978, Complexes organo-metalliques et structures microagregées des sols chloriteux du système schistograuwaqueux Vosgien, Sci. du Sol, 1, 31-40.
- Bouma, J., Jongerius, A., Boersma, O., Jager, A., Schoonderbeek, D., 1977, The function of different types of macropores during saturated flow through four swelling soil horizons, Soil Sci. Soc. Am. J., 41, 945-951.

- Bradley, R., 1978, The prehistoric settlement of Britain, London.
- Brady, N.C., 1990, The nature and properties of soils, Macmillan.
- Bridges, E.M., 1978, Interaction of soil and mankind in Britain, J. Soil Sci., 29, 125-139.
- Bruckert, S. and Selino, D., 1978, Mise en evidence de l'origine biologique ou chimique des structures microagregées foisonnantes des sols bruns ocreux, Pedologie, 28, 46-59.
- Bui, E. N., 1991, Applications of image analysis to soil micromorphology, Agriculture, Ecosystems and Environment, 34, 305-313.
- Bullock, P., Fedoroff, N., Jongerius, A., Stoops, G. and Tursina, T., 1985, Handbook for soil thin section description, Waine Research Publications, Wolverhampton.
- Bullock, P., and Murphy, C.P., 1980, Towards the quantification of soil structure, Journal of Microscopy, vol. 120, 3, 317-328.
- Bullock, P., and Thomasson, A. J., 1979, Rothamsted studies of soil structure II. Measurement and characterisation of macroporosity by image analysis and comparison with data from water retention measurements, J. Soil Sci., 30, 391-413.
- Butzer, K.W., 1982, Archaeology as human ecology, C.U.P., Cambridge.
- Campbell, J.B., 1987, Introduction to remote sensing, The Guildford Press, N. York, London.
- Catt, J.A., 1991, Soils as indicators of Quaternary climatic change in mid-latitude regions, Geoderma, 51, 167-187.
- Chartres, C.J., Ringrose-Voase, A.J. and Raupach, M., 1989, A comparison between acetone and dioxane and explanation of their role in water replacement in undisturbed soil samples, J. Soil Sci., 40, 849-863.
- Coles, J.M. and Harding, A.F., 1979, The Bronze Age in Europe, London.
- Cornwall, I.W., 1963, The excavation of the Willerby Wold long barrow, in Manby, T.G., Proc. Prehist. Soc., 29, 173-203.
- Courty, M.A., and Fedoroff, N., 1982, Micromorphology of a Holocene dwelling, in Proceedings of the 2nd Nordic Conference on the application of Scientific Methods in Archaeology, Helsingor (Elsinore), Denmark, 17-19th August 1981, 2, 7, II, 257-277.



Courty, M.A., Goldberg, P., and Macphail, R.I., 1989, Soils and Micromorphology in Archaeology. Cambridge: Cambridge University Press.

Dalrymple, J.B., 1958, The application of soil micromorphology to fossil soils and other deposits from archaeological sites, J. Soil Sci., 9, 2, 199-205.

Davidson, D.A., 1982, Soils and man in the past, pgs 1-27, in Bridges, E.M. and Davidson, D.A., (eds.), 1982, Principles and applications of soil geography, Longman.

Davidson, D.A., Carter, S.P., Quine, T.A., 1992, An evaluation of micromorphology as an aid to archaeological interpretation, Geoarchaeology, 7, 1, pgs. 55-65.

De Coninck, F., 1980, Major mechanisms in the formation of spodic horizon, Geoderma 24 : 101-128.

De Connick, F. and Righi, D., 1983, Podzolisation and the spodic horizon, in : Bullock, P., and Murphy, C.P., (ed.), Soil Micromorphology, Vol. 2, Berkhamstead, AB Academic Publisher, pg 389-416.

De Coninck, F., Righi, D., Maucorps, J. and Robin, A.M., 1974, Origin and micromorphological nomenclature of organic matter in sandy Spodosols, in Rutherford, G.K. (ed.), Soil microscopy, The Limestone Press, Kingston, Ontario, 263-280.

Dimbleby, G.W., 1962, The development of British heathlands and their soils, Oxford, Clarendon Press.

Duchaufour, P., 1982, Pedology, Allen and Unwin, London.

Evans, J.G., 1975, The environment of early man in the British Isles, London, Elek.

Fairhurst, H. and Tatlor, D.B., 1970-71, A hut-circle settlement at Kilphedir, Sutherland, Proc. Soc. Antiq. Scot., 103, 65-99.

Farmer, V.C., Fraser, A.R., Robertson, L. and Sleeman, J.R., 1984, Proto-imogolite allophane in podzol concretions in Australia: possible relationship to aluminous ferrallitic (lateritic) cementation, J. Soil Sci. 35, 333-340.

Farmer, V. C., McHardey, W.J., Robertson, L., Walker, A. and Wilson, M.J., 1985, Micromorphology and sub-microscopy of allophane and imogolite in a podzol Bs horizon: evidence for translocation and origin, J. Soil, Sci. 36, 87-95.

Fenton, A.J., 1981, Early manuring techniques, in Mercer, R., Farming practise in British Prehistory, Edin. Uni. Press.

Fedoroff. N., Courty, M.A. and Thompson, M.L., 1990, Micromorphological evidence of palaeoenvironmental change in Pleistocene and Holocene Palaeosols, in Douglas, L.A. (ed.), Soil

micromorphology, a basic and applied science, Developments in soil science, 19.

Fedoroff, N. and Goldberg, P., 1982, Comparative micromorphology of two late Pleistocene palaeosols (in the Paris basin), Catena, 9, 227-251

Fisher, P.J. and Macphail, R.I., 1985, The study of archaeological soils and deposits, in Gilbertson, D.D. and Ralph, N.G.A. (eds.), Palaeoenvironmental Investigations, BAR Int, series 258.

Fitzner, B., 1990, Porosity analysis - A method for the characterisation of building stones in different weathering states, 2031-2037, Marinos and Koukis (eds.), Engineering Geology of Ancient Works, Monuments and Historical sites, Balkema, Rotterdam.

Fitzpatrick, E.A., 1983, Soils: Their formation, classification and distribution, Longman Scientific and technical.

Fitzpatrick, E.A., 1984, Micromorphology of Soils. Chapman and Hall.

Fitzpatrick, E.A. and Gudmundsson, T., 1977, The impregnation of wet peat for the production of thin sections, J. Soil Sci., 29, 585-587.

Futty, D.W., and Towers, W., 1982, Soil and landuse capability for agriculture, northern Scotland, The Macaulay Institute for Soil Research, Aberdeen.

Gleick, J., 1987, Chaos, Cardinal.

Goldberg, P., 1983, Applications of micromorphology in archaeology, pgs. 139-150, in : Bullock, P., Murphy C.P., (eds), Soil micromorphology, Berkhamstead: AB Academic Publishers.

Inversen, J., 1958, The bearing of glacial and interglacial epochs on the formation and extinction of plant taxa, Uppsala Universiteit Arssk, 6, 210-15.

Janssen, C., Bankwitz, E., Bankwitz, P. and Harnisch, G., 1991, Application of digital image analysis in modelling recrystallization processes, Journal of Structural Geology, 13, 7, 851-858.

Jenny, H., 1941, Factors of soil formation, McGraw-Hill Book Co., Inc..

Jensen. J.R., 1986. Digital image processing: A remote sensing perspective. Prentice-Hall.

Jongerius, A. and Heintzberger, G., 1975, Methods in soil micromorphology. A technique for the production of large thin

sections, Soil Survey Papers N° 10, Netherlands Soil Survey Institute, Wageningen.

Jongerius, A., Schoonderbeek, D. and Jager, A., 1972, The application of the Quantimat 720 in soil micromorphometry, The Microscope. 20, 243-254.

Keely, C.M., 1982, Pedogenesis during the later prehistoric period in Britain, 114-126, in Harding, A.F. (ed.), Climate change in later prehistory, Edin. Uni. Press.

Lantuejoul, Ch., 1978, La Squillettisation et son application aux mesures topologiques des mosaïques polycristallines, unpublished Ph.D. thesis, Paris, School of Mines.

Lautridou, J.P., 1977, Loess et sables de la Basse-Seine: lithostratigraphie et chronostratigraphie, Bull. Soc. Geol. Normandie, 64, 81-91.

Limbrey, S., 1975, Soil science and archaeology, Academic press.

Lynch, A., 1981, Man and environment in SW Ireland, BAR 85, Oxford.

Macphail, R.I., 1981, Soil and botanical studies of "dark earth", in Jones, M. and Dimbleby, G.W., (eds.), The environment of man in the Iron Age to the Anglo Saxon period, BAR, Brit. Ser., 87, 309-331.

Macphail, R.I., 1983, The micromorphology of dark earth from Gloucester, London and Norwich: An analysis of urban anthropogenic deposits from the late Roman to early medieval periods in England, in Bullock, P. and Murphy, C.P., (eds), Soil micromorphology Berkhamstead: AB Academic Publishers.

Macphail, R.I., 1986, Paleosols in Archaeology, Chap 9, 263-289 in Wright, V.P., (ed.), Paleosols, Princetown Uni. and Blackwells Press.

Macphail, R.I., (unpublished), Soil report on the cairn and field system at Chysauster, Penzance, Cornwall, Ancient Monuments Laboratory Report 111/87, Historic Buildings and Monuments Commission for England.

Macphail, R.I. and Courty, M.A., 1985, Interpretation and significance of urban deposits, in Proc. of the third Nordic conference in the application of scientific methods, Edgren, T., (ed.), (= ISKOS, 5), 71-83.

Macphail, R.I., Courty, M.A. and Gebhardt, A., 1990a, Soil micromorphological evidence of agriculture in north-west Europe, World Archaeology, 22, 53-69.

Macphail, R.I., Courty, M.A. and Goldberg, P., 1990b, Soil micromorphology in archaeology, Endeavour, 14, 163-171.

- Macphail, R.I. and Goldberg, P., 1990, The micromorphology of tree subsoil hollows; their significance to soil science and archaeology, in Douglas, L.A., (ed.), Soil micromorphology, a basic and applied science, Elsevier Press, Amsterdam, 425-429.
- Macphail, R.I., Romans, J.C.C. and Robertson, L., 1987, The application of soil micromorphology to the understanding of Holocene soil development in the British Isle: with special reference to early cultivation, in Fedoroff, N., Bresson, L. M. and Courty, M. A., (eds.), Soil micromorphology, Plaisir: AFES, 647-656.
- Mackie, E.W., 1963-64, New excavations on the Monomere neolithic chambered cairn, Lamash, Isle of Arran, Proc. Soc. Antiq. Scot., 97, 1-34.
- Marsden, C., 1963, Marsden solvents guide, 2nd ed., Cleaver-Hume Press Ltd., London.
- Mather, P.M., 1984, Computer Processing of Remotely-Sensed Images. John Wiley & Sons.
- McBratney, A. B. and Moran, C. J., 1990, A rapid method of analysis for soil macropore structure II. Stereological model, Statistical analysis and interpretation, Soil Sci. Soc. Am. J., 54, 509-515.
- McKeague, J.A., Fox, C.A., Stone, J.A. and Protz, R., 1987, Effects of cropping system on structure of Brookston clay loam in long-term experimental plots at Woodslee, Ontario, Can. J. Soil Sci., 67, 571-584.
- Meng, B., 1990, Damage diagnosis on building material specimens by means of thin-section microscopy and image analysis, Inst. Phys. Conf. Ser., 98, Chapter 13, 593-596.
- Moore, P.D., 1988, The development of moorlands and upland mires, in Jones, M., (ed.), Archaeology and the flora of the British Isle, Oxford Uni. Committee for Arch. Monograph N° 14.
- Moran, C.J. and McBratney, A.B., 1988, A method for the dehydration and impregnation of clay soil, CSIRO Division of soils, Technical Memorandum 13/88.
- Moran, C.J., McBratney, A.B., Ringrose-Voase, A.J. and Chartres, C.J., 1989a, A method for the dehydration and impregnation of clay soil, J. Soil Sci., 40, 569-575.
- Moran, C.J., McBratney, A.B. and Koppi, A.J., 1989b, A rapid method for analysis of soil macropore structure. I. Specimen preparation and digital image production, Soil Sci. Soc. Am. J., 53, 921-928
- Moran, C.J., McBratney, A.B. and Koppi, A.J., 1990, The solicon imaging system: a description of the software, CSIRO Aust. Div. Soils Rep. N° 110.

Morgan, P., Cooper, C.J., Battersby, N.S., Lee, S.A. Lewis, S.T., Machin, T.M., Graham, S. C. and Watkinson, R. J., 1991, Automated image analysis method to determine fungal biomass in soils and on solid matrices, Soil Biol. Biochem., 23, 7, 609-616.

Murphy, C.P, 1985, Faster methods of liquid-phase acetone replacement of water from soils and sediments prior to resin impregnation, Geoderma, 35, 39-45.

Murphy, C.P, 1986, Thin section preparation of soils and sediments, AB Academic Publishers.

Murphy, C.P., Bullock, P., and Turner, R.H., 1977a, The measurement and characterisation of voids in soil thin sections by image analysis. Part I. Principals and techniques, J. Soil Sci, 28, 498-508.

Murphy, C.P., Bullock, P. and Biswell, K.J., 1977b, The measurement and characterisation of voids in soil thin sections by image analysis. Part II. Applications, J. Soil Sci, 28, 509-518.

Pape, Th. 1974, The application of circular polarized light in soil micromorphology, Neth. J. agric. Sci., 22, 31-36.

Pawluk, S., 1987, Faunal micromorphological features in moder humus of some western Canadian soils, Geoderma, 40, 3-16.

Pepper, D., 1990, The roots of modern environmentalism, Routledge.

Protz, R., Sweeney, S. J., and Fox, C. A., 1992, Applications of spectral analysis to soil micromorphology, I. Methods of analysis, Geoderma, 53, 275-287.

Rees, S., 1981, Agricultural tools: Function and use, in Mercer, R., Farming practise in British Prehistory, Edin. Uni. Press.

Ringroase-Voase, A.J., 1987, A scheme for the quantitative description of soil macrostructure by image analysis, J. Soil Sci., 38, 343-56.

Ringroase-Voase, A.J., 1990, One dimensional image analysis of soil structure I. Principals, J. Soil Sci., 41, 499-512.

Ringroase-Voase, A.J., 1991, Micromorphology of Soil Structure: Description, Quantification, Application, Aust. J. Soil Res., 29, 777-813.

Ringroase-Voase, A.J., and Bullock, P., 1984, The automatic recognition and measurement of soil pore types by image analysis and computer programs, J. Soil Sci., 35, 673-684.

Ringrose-Voase, A.J. and Nys, C., 1990, One-dimensional image analysis of soil structure. II. Interpretation of parameters with respect to four forest soil profiles. J. Soil Sci., 41, 513-527.

Ritchie, G., Ritchie, A., 1981, Scotland, archaeology and early history, Thames and Hudson Ltd. London.

Roberts, N., 1991, The Holocene, an environmental history, Blackwell.

Romans, J.C.C., 1962, The origin of the indurated B<sub>3</sub> horizon of podzolic soils in north-east Scotland, J. Soil Sci., 13., 141-147.

Romans, J.C.C., 1970, Podzolisation in a zonal and altitudinal context in Scotland, Welsh soils discussion group papers, 11, 88-101.

Romans, J.C.C., 1986, Some notes on the soils at Scord of Brouster, Shetland, in Whittle, A., Keith-Lucus, M., Milles, A., Noddle, B., Rees, S. and Romans, J.C.C., Scord of Brouster, an early agricultural settlement on Shetland, Oxford Uni. Comm. for Arch., Monograph N° 9, 125-133.

Romans, J.C.C., and Robertson, L., 1974. Some aspects of the genesis of alpine and upland soils in the British Isle, 498-510, in G.K. Rutherford ed., Soil Microscopy, Kingston, Canada, Limestone press.

Romans, J.C.C., and Robertson, L., 1975a, Some genetic characteristics of the freely drained soils of the Ettrick Association in east Scotland, Geoderma 14, 297-317.

Romans, J.C.C., and Robertson, L., 1975b, Soils and archaeology in Scotland, in Evans, J.G., Limbrey, S. and Cleere, H., (eds.), The effect of man on the landscape: the Highland zone, CBA Research Report 11, 37-39.

Romans, J.C.C. and Robertson, L., 1983a, The environment of north Britain: Soils, pgs 55-80, in Chapman, J.C., and Mytum, H.C. (eds), 1983 Settlement in north Britain 1000 BC - AD 1000, BAR British Series 118.

Romans, J.C.C. and Robertson, L., 1983b, The general effect of early agriculture on the soil profile, 136-141, in Maxwell, G.S., (ed.), The impact of aerial reconnaissance on archaeology. CBA Res. Report 49.

Romans, J.C.C., Stevens, J.H. and Robertson, L., 1966, Alpine soils of north east Scotland, J. Soil Sci., 17, 184-199.

Russ, J.C., 1990, Computer-assisted microscopy. The measurement and analysis of images, Plenum Press, New York.

Sadowski, F., and Sarno, J., 1976, Forest classification accuracy as influenced by multispectral scanner spatial resolution, Report for Contract NAS9-14123:NASA Houston, TX: LBJ Space Centre-Assessment of effects of different resolutions upon accuracy.

- Scaife, R.G., and Macphail, R.I., 1983, The post-Devensian development of heathland soils and vegetation, 70-99, in Burnham, P., (ed.), Soils of the heathlands and chalklands. Seesoil.
- Shipitalo, M. J. and Protz. R., 1987, Comparison of morphology and porosity of a soil under conventional and zero tillage, Can. J. Soil Sci., 67, 445-456.
- Simmons, I.G. and Tooley, M.J., (eds.), 1981, The environment in British Prehistory, Duckworth, London.
- Simpson, I.A., 1985, Anthropogenic sedimentation in Orkney: The formation of deep top soils and farm mounds, vol. I, unpublished Ph.D. thesis, Dept. of Geography, Uni. of Strathclyde, Glasgow.
- Slager, S. and Van Der Wetering, H.T.J., 1977, Soil formation in archaeological pits and adjacent soils in southern Germany, J. Arch. Sci., 4, 259-267.
- Stewart, I., 1990, Does God play dice, the new mathematics of chaos, Penguin.
- Stewart, M.E.C., 1961-62, The excavation of two circular enclosures at Dalnagler, Perthshire, Proc. Soc. Antiq. Scot., 95, 134-158.
- Terribile, F. and Fitzpatrick, E. A., 1992, The application of multilayer digital image processing techniques to the description of soil thin sections, Geoderma, 55, 159-174.
- Thomas, I.L., Benning, V.M. and Ching, N.P., 1987, Classification of remotely sensed images, Higler, Bristol.
- Thompson, M.J., McBride, J.F. and Horton, R., 1985, Effects of drying treatments on porosity of soil materials, Soil Sci. Soc. of Am. J., 49, 1360-1364.
- Thompson, M. L., Singh, P., Corak, S. and Warren, S. E., 1992, Cautionary notes for the automated analysis of soil pore-space images, Geoderma, 53, 399-415.
- Tippkotter, R., (1990), Staining of soil microorganisms and related material with flurochromes, in Douglas, L.A., (ed.), Soil micromorphology, a basic and applied science, Developments in soil science, Elsevier Press, Amsterdam, 605-665.
- Turner, J., 1981, The vegetation, in Jones, M. and Dimbleby, G., (eds.), The environment of man: The Iron Age to the Anglo Saxon period, BAR 87, 67-73, Oxford.
- U.S.D.A., 1975, Soil Taxonomy, Soil Conservation Services, U.S. Dept. of Agric.
- Van Vliet-Lanoe, B., 1985, Frost effects in soils, in Boardman, J. (ed.), Soils and Quaternary landscape evolution, John Wiley and Sons, Ltd., Chichester, 117-138.

Van Vliet-Lanoe, B., Faivre, P., Andreux, F., Robin, A.M. and Portal, J.M., 1983, Behaviour of some organic components in blue ultra violet light: application to the micromorphology of podzols, andosol and planosols, in Bullock, P. and Murphy, C.P., (eds.), Soil micromorphology, vol I, techniques and applications, AB Academic Publishers, 91-99.

Walker, P. J. C. and Trudgell, S. T., 1983, Quantimat image analysis of soil pore geometry: comparison with tracer breakthrough curves, Earth Surface Processes and Landforms, 8, 465-472.

Watson, A.I., 1987, A new method of classification for Landsat data using the 'watershed' algorithm, Pattern Recognition Letters, 6, 15-19.

Watson, A.I., 1990, The application of pattern recognition to geological and soil thin sections, in Vaughab, R.A. (ed.), Proceedings of the 37th Scottish Universities Summer School in Physics, Hilger, 329-337.

Wattez, J., Courty, M.A., and Macphail, R.I., 1990, Burnt organo-mineral deposits related to animal and human activities in prehistoric caves, in Douglas, L.A., (ed.), Soil micromorphology, a basic and applied science, Elsevier Press, Amsterdam, 431-439.

West. L.T., Hendrix, P.F. and Bruce, R.R., 1991, Micromorphic observations of soil alteration by earthworms, Agric. Eco. and Env., 34, 363-370.

Whittington, G., 1980, Prehistoric activity and its effect on the Scottish landscape, in Parry, M.L. and Slater, T.R., The making of the Scottish countryside, Croom Helm, London.

Whittle, A., Keith-Lucus, M., Milles, A., Noddle, B., Rees, S. and Romans, J.C.C., 1986, Scord of Brouster, an early agricultural settlement on Shetland, Oxford Uni. Comm. for Arch., Monograph N° 9, 125-133.